volume 14

Developments in Mineral Processing

D.W. Fuerstenau / advisory editor

Coal Flotation and Fine Coal Utilization

J.S. Laskowski

Developments in Mineral Processing 14

COAL FLOTATION AND FINE COAL UTILIZATION

This Page Intentionally Left Blank

COAL FLOTATION
AND FINE COAL
UTILIZATION

Janusz S. Laskowski
Department of Mining and Mineral Process Engineering
The University of British Columbia
Vancouver, B.C., Canada

2001

To my professors

Tadeusz Laskowski

Willy Ivanovich Klassen

Joseph A. Kitchener

This Page Intentionally Left Blank

PREFACE

Modern civilization cannot exist without sources of power. Coal is an energy resource of great abundance, and population growth and technological development intensify its use. The increasing use of coal on one hand, and the need for decreasing environmental pollution on the other, place ever-growing demands on clean coal technologies, a task impossible to achieve without a clear understanding of coal beneficiation and utilization principles.

Coal, an organic sedimentary rock, is upgraded in coal preparation unit operations which reduce its content of impurities. Traditionally, in designing coal preparation plants, crushing was eliminated as much as possible to reduce the yield of fines and the cost of fine coal processing, dewatering and handling. However, separation results depend directly on the degree of liberation which is improved with a decrease in particle size. This and intensifying mechanization continuously increase the yield of fines in the coal preparation plant feed that end up in flotation circuits. The utilization of fine coal in the form of coal–water slurries eliminates the necessity of dewatering and drying it, and makes fine coal's transport possible without dusting, storage and spontaneous combustion problems by pipelining or shipping it in tankers.

Almost all coal cleaning processes are carried out using water as a medium, so an understanding of the coal/water interface is of utmost importance in dealing with fine coal cleaning and utilization. Surface chemistry plays a very important role in all unit operations handling fine coal; the finer the particles, the more profound the effect of their surface properties on the behavior of fine particle systems. The main objective of this book has been to combine in a single volume the engineering aspects of coal flotation and fine coal utilization with the fundamental principles of colloid and surface chemistry and coal surface chemistry, the fundamentals on which coal flotation technology and fine coal utilization are based.

This book is a result of copious notes employed in teaching short courses on fine coal flotation and utilization in Poland, Canada, Brazil and South Africa, as well as various undergraduate courses taught at the Silesian University of Technology in Poland and at the University of British Columbia in Canada. The author had the opportunity to spend one year as a post-graduate student in Professor Klassen's laboratories at the Mining Institute in Moscow during which he translated his monograph on coal flotation from Russian into Polish (which appeared in Poland in 1966), and since then has been collecting data for his own monograph on the subject. One year with the University of California, Berkeley, in 1981 and participation in the coal surface chemistry-related research projects carried out at that time by prof. D.W. Fuerstenau made it clear that a new monograph on this topic would be very useful for many research centers around the world.

The unit operations, fine and coarse coal processing circuits, and the role of surface chemistry in fine coal processing and utilization are defined in Chapter 1. Coal

classification, petrography, mineral matter chemistry and distribution, and the liberation of mineral matter are discussed in Chapter 2. Chapter 3 considers those aspects of the coal surface and its interactions with water that determine coal surface wettability. The relevant theoretical and practical aspects of electrical phenomena associated with the coal/water interface, as well as experimental methods, including those used to characterize wettability of heterogeneous solid surfaces, are discussed in Chapter 3. Coal floatability and experimental techniques used to characterize it are dealt with in Chapter 4. Flotation cannot exist without reagents, and the chemistry of reagents utilized in coal flotation and the mode of their action are described in Chapter 5. Coal flotation technology is addressed in Chapter 6, and fine coal cleaning circuits in Chapter 7. Chapter 8 surveys flotation machines utilized in coal preparation plants. While decreasing the size of particles improves coal/mineral matter liberation (and thus separation results), dewatering, handling, transportation and storage are much more difficult for fine particles. Therefore, particle size enlargement is an important issue in coal utilization. The principles of these processes are also based on coal surface chemistry and are discussed in Chapter 9. The final chapter is concerned with traditional dewatering-utilization schemes, and with utilization of fine coal in the form of coal–water slurries. The latter, an exciting application of colloid chemistry, is going to entirely revolutionize many facets of coal technology as we know it today.

It is hoped that this book will be used by many groups of readers: those practicing mineral processing, chemical engineering, mining and metallurgical engineering; technical personnel working for reagent suppliers; and scientists researching the field of coal surface chemistry, flotation and fine coal utilization. The book was intended to be written as a text which could also be used in teaching graduate and specialized undergraduate courses, as well as the short courses which are so popular today. For those readers who may require more detail in some of these subject areas, bibliographies have been appended to each chapter.

Thanks are due to a number of people. I am particularly grateful to the late Professor V.I. Klassen who stimulated my early interests in flotation theory and in coal flotation in particular, and to whom I owe much of my conceptual understanding of the subject. I would like to thank all my students and post-docs for the stimulating discussions and for their hard and not always acknowledged work. I am indebted to many colleagues who have been very generous in providing detailed criticism. The whole book was read by Professor Jan Leja; Professor Jerry Luttrell's constructive comments have been particularly helpful. Chapter 3 was critically reviewed by Dr. Jaroslaw Drelich. I thank Mrs. Sally Finora for her ability to deal with what appeared to be an endless sequence of revisions of figures; without her computer touch this book would probably have never materialized. The help offered by Mrs. Elizabeth Fedyczkowski in drawing some figures is also gratefully acknowledged.

Another debt is owed to several persons who worked hard to ease my "Polishisms". Cameron Lilly's help, and my sons' Cyprian's and Kornel's assistance in this respect have been invaluable.

This text was started many years ago. Parts of this book were written when I was on sabbatical leaves with École National Supérieure de Geologié, Nancy, France, and with the University of Cape Town in South Africa. This note of appreciation would be

incomplete without acknowledging the patience of my wife, Barbara, during these long years abroad and at home.

Janusz S. Laskowski

Vancouver, November 2000.

This Page Intentionally Left Blank

CONTENTS

Chapter 1

COAL PREPARATION

1.1. Unit operations

Coal preparation is the stage in coal production at which the run-of-mine (ROM) coal is made into a clean, graded, and consistent product suitable for the market. This precedes the end use as a fuel, reductant, or conversion plant feed. Coal preparation includes physical processes that upgrade the quality of coal by regulating its size and reducing the content of mineral matter (expressed as ash, sulfur, etc.). The major unit operations are classification (screening), cleaning (washing, beneficiation), crushing, and solid/liquid separation which also includes dewatering by drying.

Coal preparation plants may consist of nothing more than a simple crushing/sizing operation but commonly involve complex circuits cleaning the entire size range of feed coal to reject the majority of impurities associated with ROM material. While gravity concentration (dense-medium baths, jigs, dense-medium cyclones, etc.) is the dominant cleaning method for coarse and intermediate coal size fractions, flotation is the dominant cleaning method for fine size fractions.

Fig. 1.1 shows the flowsheet of a typical coal preparation plant treating metallurgical coal. In coal preparation plant classifications based on the extent to which coal is cleaned, the plant cleaning full size range of raw coal is classified as type 4 [1,2]. The first stage, precrushing, which is needed to reduce the top size of the material, is commonly carried out with the use of rotary breakers. These are autogenous size-reduction devices which serve two functions, namely, reduction in top size of ROM and rejection
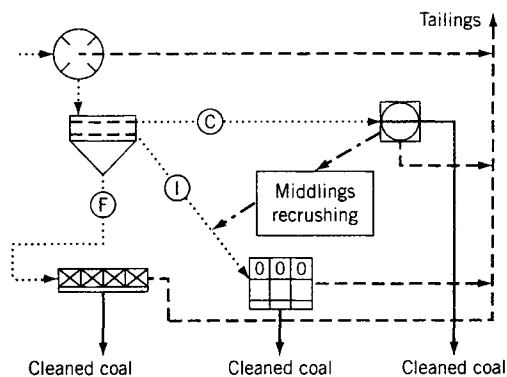
Fig. 1.1. Typical flowsheet of the coal preparation plant treating metallurgical coal.

of oversize inorganic rock. The precrushing is followed by screening into coarse, inter-mediate and fine size fractions which are then cleaned in different processes. The flow-sheet depicted in Fig. 1.1 includes dense-medium bath for coarse coal and jigs for inter-mediate fractions. This is only one of the options. Plants may include a dense-medium bath and dense-medium cyclones, or jigs for both size ranges, etc. Such plants treat the full size-range of raw coal and produce different saleable products that vary in quality.

As a general rule the most efficient circuits are also the most expensive. However, while for a difficult-to-wash coal, selection of very efficient cleaning equipment is necessary (e.g. dense-medium separators), it is often assumed that such equipment is not needed for easy-to-wash coals (in the latter case, a less efficient device such as a jig may produce practically the same yield of clean coal as the most efficient separators). However, because dense-medium circuits offer increased plant efficiency they always offer a better payback than jigs. It is then not surprising to see that coal production statistics indicate the changing patterns in coal preparation methods with decrease in jigs and other less efficient separators and increase in the use of magnetite dense-medium processes [3]. General guidelines can be followed to select cleaning equipment [1].

1.2. Coarse-coal vs. fine-coal circuits

A jig's simplicity and ability to deal with wide size ranges makes it a prime choice for coarse and intermediate size fractions. As Fig. 1.2 indicates, the particle sizes that can be dealt with by a jig range from 0.5 mm to 100 mm. Jigs usually operate at cut point densities (separation density) within a relative density range of 1.6–1.8 (Fig. 1.3). That means that a jig is very efficient in separating high-density gangue from coal, but
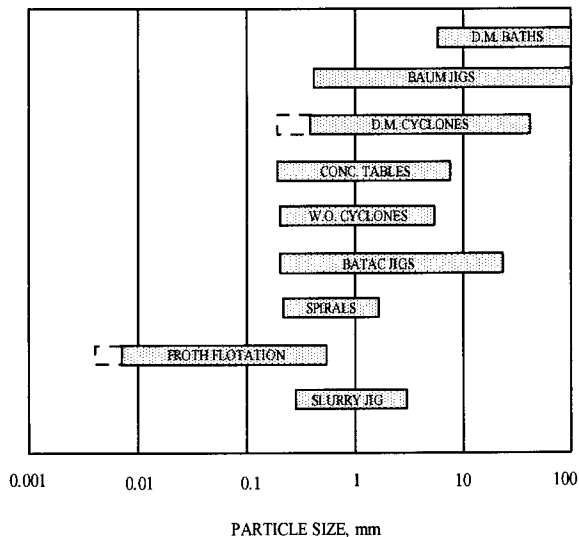
Fig. 1.2. Operating size ranges of major coal cleaning devices.

RELATIVE DENSITY
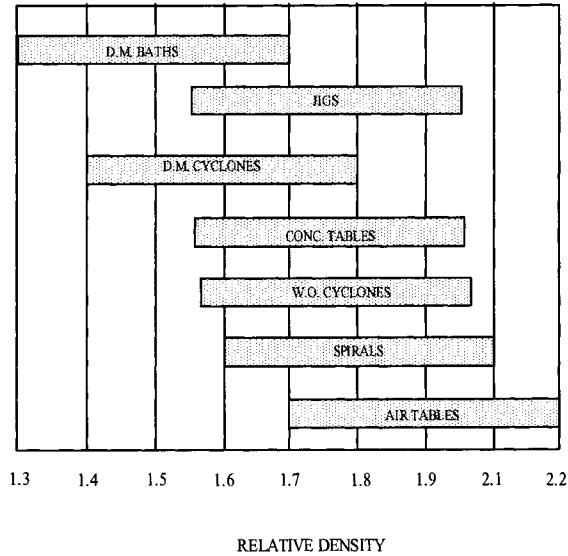
Fig. 1.3. Typical separation density ranges for commercial separators.

not in producing a clean concentrate. However, cleaning depends on the particle size, too, and when a very wide size range is cleaned in a jig, the separation density varies for various sizes; it increases for finer size fractions.

As Fig. 1.3 demonstrates, spirals, tables and water-only cyclones are also characterized by high separation densities.

Separation efficiency of gravity separators is characterized by a value of the probable error, E_p. As seen from Fig. 1.4 [4], these numbers are small for very efficient dense-medium separators but are much larger for other gravity separators. The efficiency of gravity separators strongly depends on the size of treated particles and falls off rapidly for sizes finer than half of a millimeter. This explains a well established strategy in coal preparation: treat as coarse a material as possible without unnecessary comminution.

Flotation depends on coal size, too, and its efficiency drops significantly for coarser fractions (-0.5 $+0.150$ mm). These size fractions generally contain the best quality coal and, since the efficiency of gravity methods falls off rapidly for sizes finer than -0.5 mm, and flotation is not very efficient for coal sizes coarser than about 0.150 mm, various flowsheets have been developed that incorporate gravity separation and flotation in the fine coal cleaning circuits (Chapter 7). Such flowsheets may include either water-only cyclones or spirals, and flotation. The fine-coal cleaning circuits may also include classifying cyclones. Dense-medium cyclones also have been applied to clean -0.5 $+0.1$ mm fine coal [5–7].

A coal preparation plant, or any mineral processing plant for that matter, has to produce final products of appropriate quality. But since most unit operations are wet, the final products must be dewatered before they are shipped to the end user. Therefore, as Fig. 1.5 shows, the flowsheet must also include dewatering of the products, commonly by thickening and filtration, and water clarification since water must be recycled and
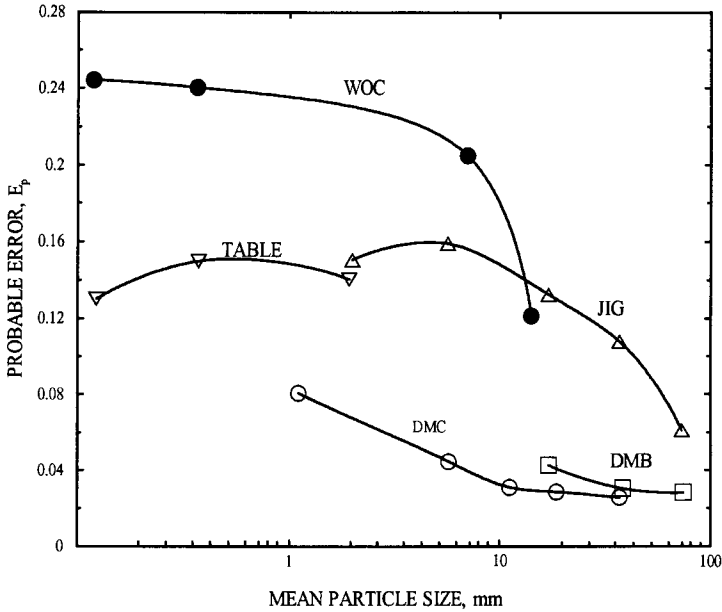
Fig. 1.4. Probable error (E_p) vs. mean particle size of the treated coal for dense-medium bath (DMB), dense-medium cyclone (DMC), jig, concentrating table, and water-only cyclone (WOC). (After Mikhail et al. [4]).

re-used. The efficiency of dewatering falls off rapidly as particle size decreases, and may become so low that thermal drying may be required to dewater fine products. Thus, it is not only the separation efficiency which falls off quickly with decreasing particle size, but thickening and filtration efficiency too. This explains the strategy behind the plant design and equipment selection that states that any size reduction (by crushing and grinding) should be avoided.

Fig. 1.6 shows the most common fine-coal dewatering and water clarification unit operations in coal preparation. While tailings disposal in tailings ponds is still quite common, the use of belt filters and filter presses to dewater flotation tailings continually increases. Of course, such solid/liquid separation processes require flocculants. The macromolecules of the polyelectrolytes utilized as flocculants are highly hydrophilic and traces of such substances in the recycled water may affect the flotation process (Sections 6.5 and 9.1).

Recent environmental restrictions which require efficient cleaning will inevitably force coal preparation technology into implementing crushing and grinding as a means of liberation before deep cleaning. Of course, the cost of dewatering the fine cleaning products would be prohibitive if the traditional solid/liquid separation techniques were utilized. But when the fine clean coal is only partially dewatered and then is converted into a coal/water fuel (coal/water slurry), then dewatering costs can be reduced and the transportation of such a product by pipelining it directly to a power generating station can be further simplified.
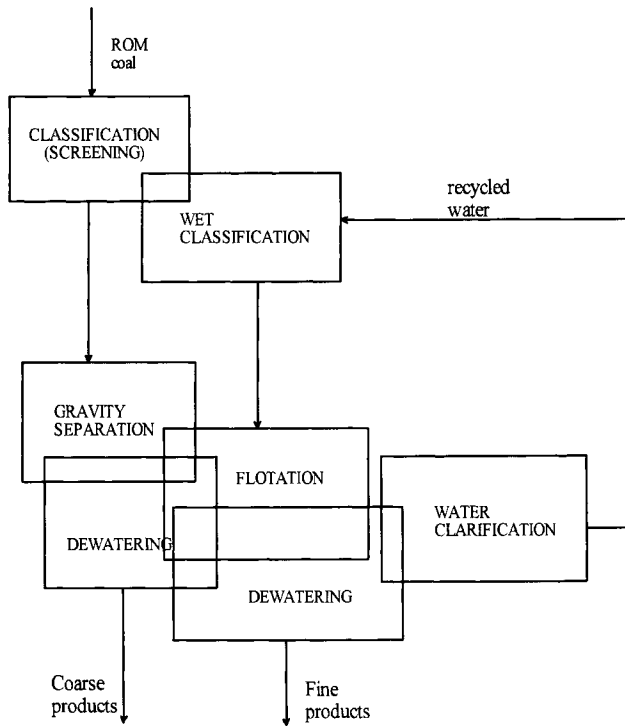
Fig. 1.5. Closed water circuit of coal preparation plant.

1.3. Seam-to-steam strategy

In the seam-to-steam strategy, fine coal is utilized in the form of coal-water fuel (CWF) also referred to as coal-water slurry (CWS). This concentrated suspension of fine coal in water is required to contain about 65–70% coal, and not exceed a viscosity of approximately 41 Pa s. A final requirement for CWF is that it should be stable with respect to sedimentation (see Section 10.3).

As Fig. 1.7 shows, the whole idea includes a deep coal cleaning plant producing concentrates that contain not more than 3–4% ash, coal-water fuel preparation, pipelining over long distances, and combustion in power generating plants [8]. Deep cleaning requires crushing and grinding to achieve good liberation.

As shown in Fig. 1.8, in deep coal cleaning (this flowsheet is also referred to as type 6 [2]) coarse and intermediate coal cleaning is designed to reject liberated gangue, with middlings going to further crushing and subsequent concentration. This approach is very different from a traditional one (Fig. 1.1) characterized by as little crushing as possible and with fines that have to be dewatered before transportation and combustion. In the traditional approach, clean coal (mostly coarse) shipped to power generating plants has then to be crushed and ground before combustion. In the new strategy this operation precedes coal cleaning, and since it assures better liberation it also leads to better separation results. In the traditional preparation plants, the high costs of fine-coal
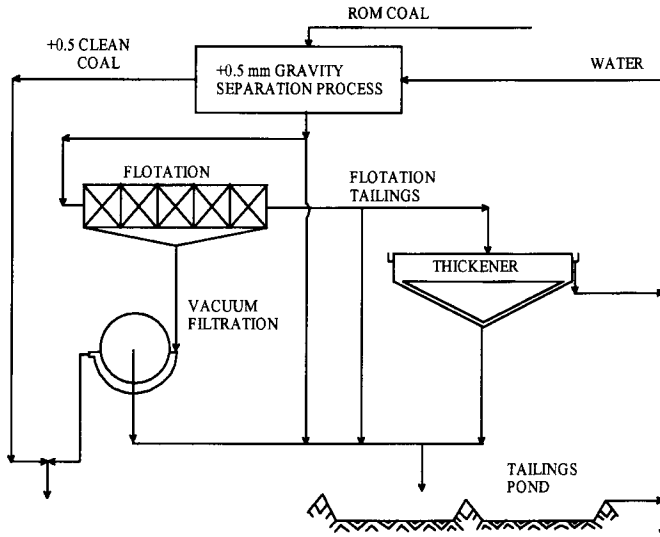
Fig. 1.6. Typical unit operations in the water circuit of coal preparation plant.
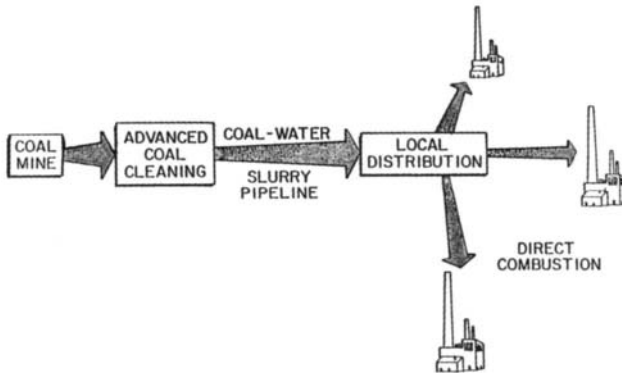
Fig. 1.7. Seam-to-steam strategy. (After Marnell et al. [8].)

dewatering followed by the difficult transportation of the dry fines dictated avoidance of any unnecessary comminution. In the new strategy, the coal preparation fines are converted into a slurry fuel that can be easily handled and efficiently combusted, eliminating an expensive fine-coal dewatering by filtration and thermal drying.

Comparison of simple flowsheets of petrochemical processing and power generating plants, with coal preparation–power generating plant combinations characterized by extensive storage and blending, and complicated solid handling and transportation facilities, reveals nothing but advantages of the new strategy. The former handles liquids and can easily be entirely contained, while the latter's with wide open storage, handling and transportation facilities are more expensive, cannot be contained and pose severe environmental hazards. Conversion of fine coal into a slurry fuel
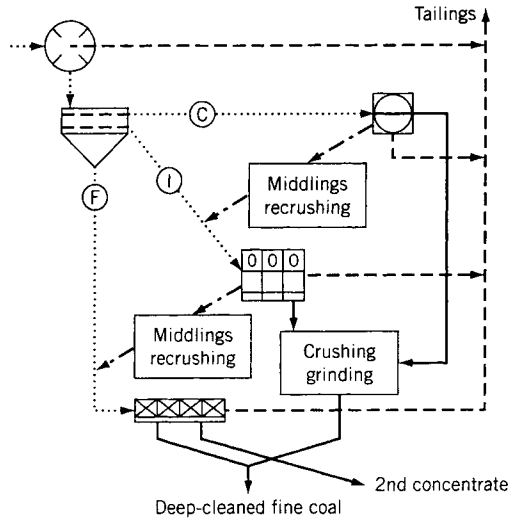
Fig. 1.8. Coal preparation plant flowsheet incorporating deep-cleaning idea.

makes it possible to eliminate all the problems that characterize handling of fine-solid products.

1.4. Role of coal surface properties in fine-coal processing

As Fig. 1.9 shows [9], coal surface chemistry plays a very important role in many unit operations in coal processing and even in mining. A glance at this figure reveals that those unit operations that handle fine coal depend on coal surface properties; the finer the particles the more profound the effect of their surface properties on the behavior of such fine-particle systems.
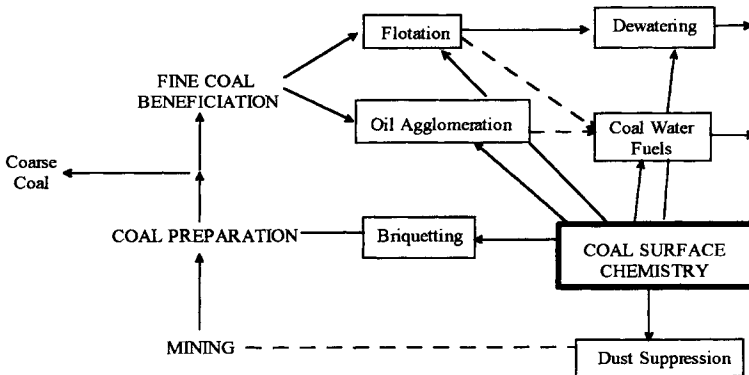
Fig. 1.9. Schematic representation of unit operations based on coal surface properties.

The most important unit operation which relies entirely on coal surface properties is flotation. Oil agglomeration belongs to the same category of surface-based beneficiation processes; so far its commercial applications are limited though. Also, particle size enlargement methods, and fine-coal handleability depend on coal surface properties. Coal-water fuels (or coal-water slurries) constitute probably the most interesting industrial application of colloid chemistry. Coal flotation and coal-water slurries constitute the two most important unit operations in the seam-to-steam strategy. Both coal flotation and coal-water slurry rely heavily on coal surface properties, and are the leading topics of this monograph.

1.5. References

[1] D.F. Symonds, Preliminary design considerations. In: J.W. Leonard and B.C. Hardinge (eds), Coal Preparation. SME, Littleton, CO, 1991, pp. 95–126.
[2] J.S. Laskowski and M. Klima, Coal Preparation. In: R.A. Meyers (ed.), Encyclopedia of Environmental Analysis and Remediation. Wiley, New York, 1998, pp. 1256–1284.
[3] F.F. Aplan, Fine coal preparation — its present status and future. In: S.K. Mishra and R.R. Klimpel (eds), Fine Coal Processing. Noyes Publications, Park Ridge, NJ, 1987, pp. 1–18.
[4] M.W. Mikhail, J.L. Picard and O.E. Homeniuk, Performance evaluation of gravity separators in Canadian washeries. 2nd Tech. Conf. Western Canadian Coals, Edmonton, June 1982.
[5] P.J. van der Walt, L.M. Falcon and P.J.F. Fourie, Dense medium separation of minus 0.5 mm coal fines. In: A.R. Swanson (ed.), Proceedings of the 1st Australian Coal Preparation Conference. Coal Preparation Societies of New South Wales and Queensland, Newcastle, 1981, pp. 207–219.
[6] R. Kempnich, S. van Barneveld and A. Luscan, Dense medium cyclones on fine coal — the Australian experience. In: J.J. Davis (ed.), Proceedings of the 6th Australian Coal Preparation Conference. Australian Coal Preparation Society, Mackay, 1993, pp. 272–288.
[7] R.J. Kempnich, S. van Barneveld and A. Lusan, Dense medium cyclones on fine coal — the Australian experience. In: W. Blaschke (ed.), New Trends in Coal Preparation Technologies and Equipment. Proc. 12th Int. Coal Preparation Congr., Cracow, 1994, Gordon and Breach, London, 1996, pp. 843–850.
[8] P. Marnell, W.N. Poundstone and W. Halvorsen, Coal-water slurries: a seam-to-steam strategy. 5th Annu. Symp. Industrial Coal Utilization, Pennsylvania, June 1983.
[9] J.S. Laskowski, Coal surface chemistry and its effect on fine coal processing. In: S.K. Kawatra (ed.), High Efficiency Coal Preparation. SME, Littleton, CO, 1994, pp. 163–176.

Chapter 2

COAL CHARACTERISTICS RELATED TO COAL PREPARATION

2.1. Introduction

Coal is an organic sedimentary rock whose chemical composition changes with coalification. Since metamorphic development of coal, also referred to as coalification, is synonymous in chemical terms with progressive enrichment of the coal substance in organically bound carbon, all coals, regardless of their origin or type, can be arranged in an ascending order of carbon content (Fig. 2.1) [1]. As this figure shows, coal is a highly cross-linked polymer, which consists of a number of stable fragments connected
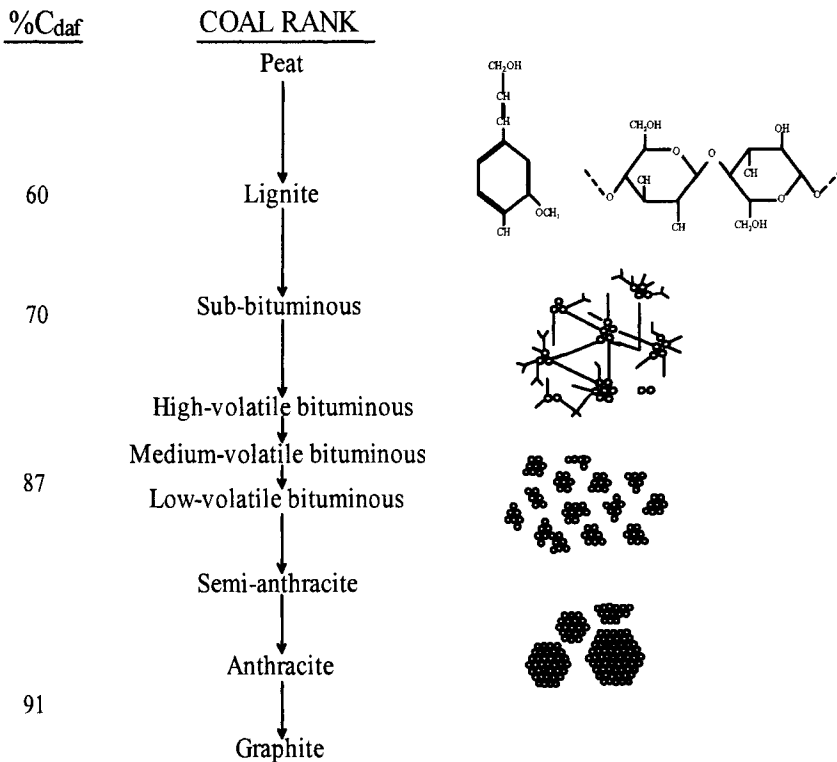
Fig. 2.1. Variation in coal structure and carbon content with coal rank. (After Barnes et al. [1]; by permission of the Geological Association of Canada.)

9
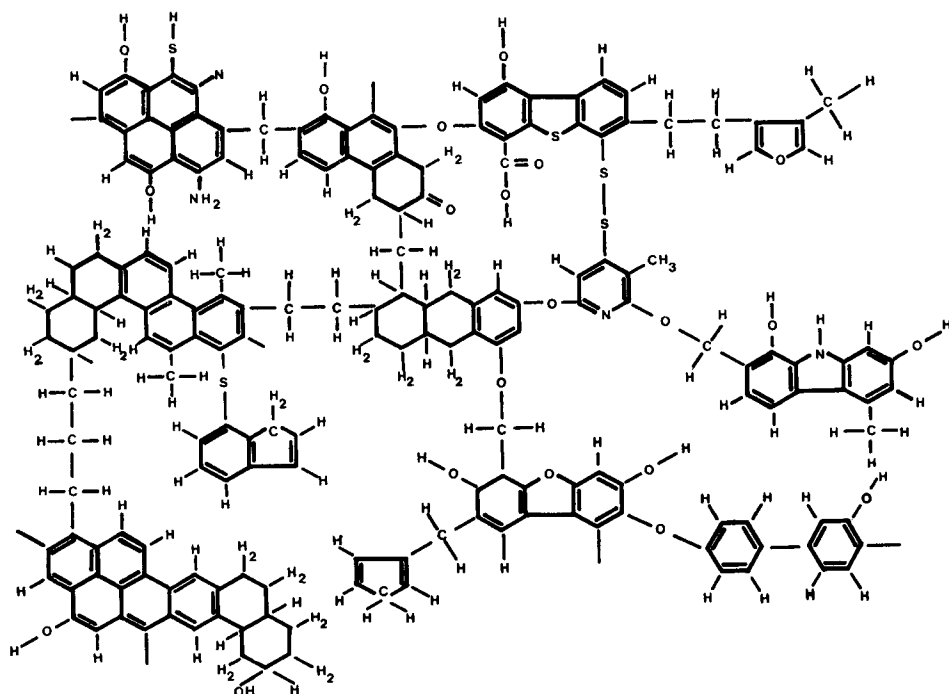
Fig. 2.2. The Wieser model of structural groups and connecting bridges in bituminous coals.

by relatively weak cross-links. This is also shown in Wiser's model (Fig. 2.2) [2] which indicates predominantly aromatic structures.

Coal chemists distinguish: first-order structure, which gives the size distribution of the macromolecules and molecules in coal and the degree of cross-linking; second-order structure, which details the cross-links and the structure of the carbon skeleton; and third-order structure, which is the nature and distribution of the functional groups [3]. Such an approach leads to the conclusion that the number-average molecular weight per cross-link increases from low to high rank (excluding anthracites). This can be ascribed to the presence of larger molecules assembled together to form the macromolecules or to fewer cross-links in the higher-rank coals. The change of chemical composition of coals with rank was summarized by Whitehurst et al. [4] as shown in Fig. 2.3. As this figure reveals, the aromatic carbon content increases with the rank from about 50% for subbituminous coals to over 90% for anthracite.

Coal also contains heteroatoms and functional groups (e.g. see Wiser's model, Fig. 2.2), and their presence in coal structure strongly affects coal surface properties. As shown by Ihnatowicz [5] and Blom et al. [6], oxygen in coals occurs predominantly as phenolic or etheric groups with a lesser amount of carboxylic. It appears that carboxy- and metoxy-groups are of little importance at greater than 80% carbon. The phenolic group content, when expressed as a fraction of the total organic matter in the coal, shows a strong correlation with the carbon content (dry-mineral-matter-free) [7].
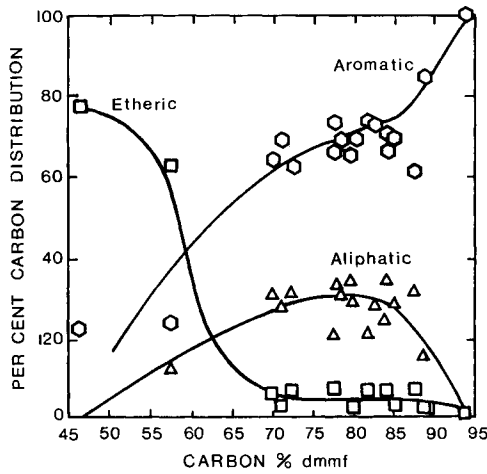
Fig. 2.3. Carbon distribution in coals varying in rank. (After Whitehurst et al. [4]; by permission of Academic Press.)

The content of oxygen functional groups is much higher than the content of all other functional groups combined; organic sulfur content never exceeds a few percent, and nitrogen content is in the range of 0.5–2.0%.

2.2. Coal classification

In all coal classification systems by rank, volatile matter content and calorific value (heating value) are the most important indices. In the American System (ASTM D-388-77), classification is according to fixed carbon content and calorific value calculated on a mineral-matter-free basis. Lower-rank coals are classed according to their calorific values calculated on a moist basis. Fig. 2.4 shows moisture [8], volatile matter and fixed carbon contents of coals varying in rank as calculated on a mineral-matter-free basis. For dry-mineral-matter-free conditions, $FC_{dmmf} = 100 - VM_{dmmf}$, and so FC_{dmmf} is directly interrelated with the volatile matter. As Fig. 2.4 shows, for the ranks from High Volatile B Bituminous to Anthracites there is a good correlation between the volatile matter content and the rank; for lower-rank coals, an additional parameter such as heating value is needed to classify the coal. As the upper part of Fig. 2.4 indicates, the calorific value increases steadily from Lignites up to High Volatile B Bituminous Coals.

2.3. Coal petrography

Coal, an organic sedimentary rock, is very heterogeneous; it contains organic matter which consists of various components with distinct chemical and physical properties referred to as macerals, and inorganic matter mostly in the form of minerals. While
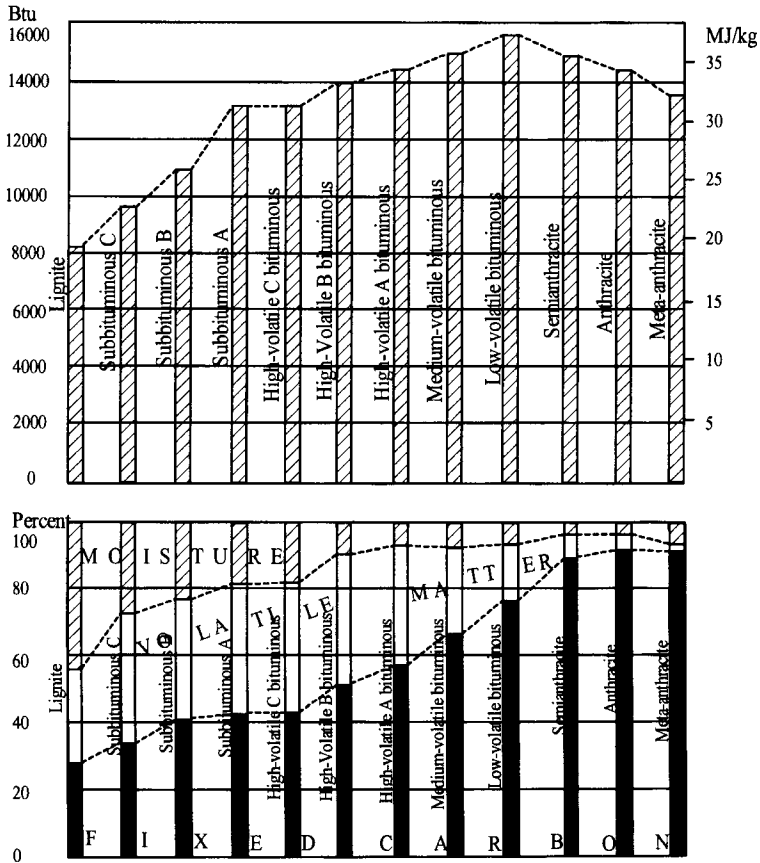
Fig. 2.4. Fixed carbon, volatile matter and moisture contents, and calorific value plotted vs. coal rank on a mineral-matter-free basis. (After Baughman [8].)

coal rank is determined by the thermal history (temperature and time) which the coal has been exposed to (the higher temperature and older the coal generally the higher the rank), the macerals are a product of the parent organic material, the degree of degradation of the parent organic material, and to a lesser extent, the thermal history of the strata. The definition of the macerals is based on microscopic examination [9].

The macerals are classified into three groups: vitrinite, exinite (liptinite) and inertinite, either because of similar origin (exinite group), or because of differences in preservation (macerals of vitrinite and inertinite groups). Chemical and physical properties of the macerals such as elemental composition (Fig. 2.5) [10], moisture content, hardness, density and petrographic features differ widely and change during the course of coalification.

The vitrinite group comprises the most abundant macerals in coal. Measurement of vitrinite reflection is commonly used to determine coal rank. These macerals are
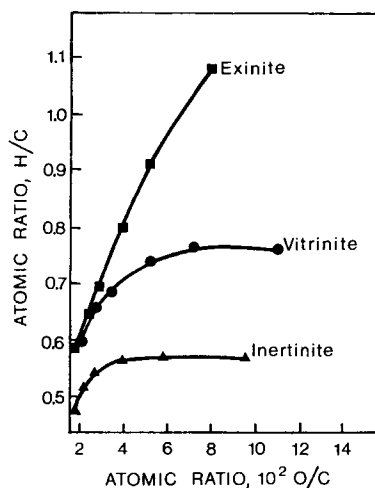
Fig. 2.5. Diagram of atomic H/C vs. O/C ratio. (After Kessler [10]; by permission of Elsevier Science.)

derived from the woody tissue and bark of trees. As the rank increases, so does the homogenization of the macerals of the vitrinite group.

The exinite (liptinite) group macerals are subdivided into two subgroups. Macerals of the first subgroup (sporinite, resinite, cutinite, alginite) can be distinguished in normal reflected light microscopy supplemented by observations of the fluorescent properties. Macerals of the second group can only be detected and distinguished from mineral matter by fluorescent-light observations.

The inertinite group comprises macerals which are characterized by higher reflectance than vitrinite of the same rank (Fig. 2.6) [11]. The inertinite macerals for the most part originate as a result of fires or fungal attack of the same parent material; as coalification proceeds the petrographic properties of the inertinites change little as a result of the high degree of aromatization that took place before or at a very early stage after deposition (charring, oxidation, mouldering, fungal attack). Exceptions are the maceral semifusinite, which represents an intermediate stage between vitrinite and fusinite and whose properties may change considerably during coalification, and micrinite. The fusinite-to-semi-fusinite ratio is used to quantify differences between high-, medium- and low-volatile bituminous coals.

With increasing rank, the coal macerals become chemically more similar and petrographically less distinct.

Macerals do not occur in isolation but occur in associations in various proportions and with variable amounts of mineral matter to give rise to the characteristic banded or layered character of most coals. These associations are referred to as lithotypes and microlithotypes. Lithotypes are distinguished macroscopically, whereas microlithotypes are identified microscopically. The application of the lithotype approach to the description of coal has always been accompanied by problems. One of the most important of these involves the relation between lithotype description and maceral or microlithotype composition as determined microscopically. A brief description of four lithotypes follows.
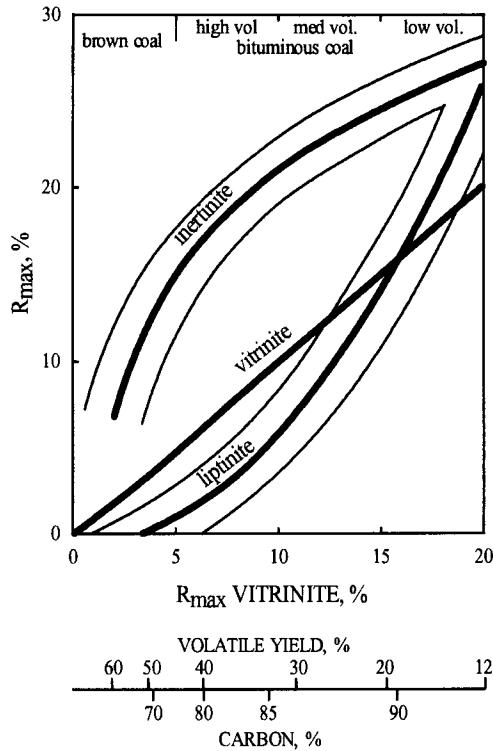
Fig. 2.6. Coalification tracks of the three maceral groups. (After Cook [11]; by permission of Marcel Dekker Inc.)

Vitrain refers to the macroscopically recognizable bright bands in coal. In the macroscopic description of seams, only the bands of vitrain having a thickness of several millimeters are considered.

Clarain is a macroscopically recognizable bright, lustrous constituent of coal, which, in contrast to vitrain, is finely striated by dull intercalations and thus has an appearance intermediate between vitrain and durain. It is the most common lithotype of coal, and has the most variable maceral composition of all four groups.

Durain is characterized by a grey to brownish black color and rough surface with a dull or faintly greasy luster. Durain is less fissured than vitrain and generally shows granular fracture. Microscopically, durain consists of microlithotypes rich in exinite and inertinite.

Fusain is recognized macroscopically by its black or grey-black color, its silky luster, its fibrous structure and its extreme friability. It is the only constituent of coal which blackens objects (like charcoal) it contacts. It may include a high percentage of mineral matter, which strengthens and reduces its friability.

Macerals are characterized by different chemical compositions (Fig. 2.5) and their surface and flotation properties also vary significantly.

2.4. Inorganic matter in coal

Coal preparation upgrades raw coal by reducing its content of inorganic impurities (the mineral matter). The most common criterion of processing quality is that of ash, which is not removed as such from coal during beneficiation processes; instead particles with a lower inorganic matter content are separated from those with a higher inorganic matter content. The constituents of ash do not occur as such in coal but are formed as a result of chemical changes that take place in mineral matter during the combustion process. The ash is sometimes defined as all elements in coal except carbon, hydrogen, nitrogen, oxygen, and sulfur. The list of minerals frequently occurring in coals is given in Table 2.1 [12].

Mineral matter content in coal can be calculated from one of the empirical relationships between mineral matter and ash contents. The best known is Parr's formula. It is used in different forms in major coal-producing countries.

$$\text{MM \%} = 1.08[\text{\% ash}] + 0.55[\text{\% sulfur}] \quad \text{(for US coals)}$$
$$\text{MM} = 1.1[\text{\% ash}] \quad \text{(in Australia)} \tag{2.1}$$

Coal is heterogeneous at a number of levels. At the simplest level it is a mixture of organic and inorganic phases. However, its textures and liberation characteristics differ because the mineral matter of coal comes from the inorganic constituents of the precursor plant, from other organic materials, and from the inorganic components transported to the coal bed. The levels of heterogeneity can then be set out as follows [11].

(1) At the seam level, a large proportion of mineral matter in coal arises from its inclusion during mining of roof and floor rock.

(2) At the ply and lithotype level, the mineral matter may occur as deposits in cracks and cleats or as veins.

(3) At the macerals level, the mineral matter may be present in the form of very finely disseminated discrete mineral matter particles.

(4) At the submicroscopic level, the mineral matter may be present as strongly, chemically bonded elements.

Even in the ROM coal, a large portion of both coal and shale is already liberated to permit immediate concentration. This is so with heterogeneity level 1 and to some extent with level 2; at heterogeneity level 3 only crushing and very fine grinding can liberate mineral matter, while at level 4, which includes chemically bonded elements and probably syngenetic mineral matter (Table 2.2), separation is possible only by chemical methods.

The terms *extraneous mineral matter* and *inherent mineral matter* were usually used to describe an ash-forming material, separable and nonseparable from coal by physical methods. Traditionally, in coal preparation processes only the mineral matter at the first and, to some extent, the second levels of heterogeneity was liberated; the rest remained unliberated and, left with the clean coal, contributed to the inherent mineral matter. Very fine grinding, which also liberates the mineral matter at the third level of heterogeneity, has changed the old meaning of the terms *inherent* and *extraneous*. The content of the "true" inherent part of ash-forming material (i.e. the part left in coal after liberating and

Table 2.1
Minerals frequently occurring in coals, their stoichiometric compositions, relative abundances, and modes of occurrences

Mineral	Composition	Common minor and trace element associations	Frequency of occurrence in coal seams	Concentration in mineral matter	Physical chief occurrences [a]
Clay minerals					
Illite (sericite)	$KAl_2(AlSi_3O_{10})(OH)_2$	Na, Ca, Fe, Li, Ti, Mn, F and other lithophile elements	Common	Abundant	D, L
Smectite (incl. mixed layered)	$Al_2Si_4O_{10}(OH)_{2x}H_2O$		Common	Abundant	D, L
Kaolinite group	$Al_2Si_2O_5(OH)_4$		Common	Abundant	L, F
Chlorite	$Mg_5Al_2(AlSi_3O_{10})(OH)_8$		Rare	Moderate	L, F
Sulfides					
Pyrite	FeS_2 (isometric)	As, Co, Cu, and other chalcophile elements	Rare–common	Variable	D, N, F
Marcasite	FeS_2 (orthorhombic)		Rare–moderate	Trace	D(?)
Pyrrhotite	$Fe_{1-x}S$		Rare	Trace	D
Shalerite	ZnS		Rare	Minor–trace	F
Galena/chalcopyrite	$PbS/CuFeS_2$		Rare	Trace	F
Carbonates					
Calcite	$CaCO_3$		Rare–common	Abundant	N, F
Dolomite (ankerite)	$CaMg(CO_3)_2$	Mn, Zn, Sr	Moderate	Trace	N, L
Siderite	$FeCO_3$		Rare	Minor	N
Oxides					
Quartz	SiO_2	–	Common	Abundant	D, L, N
Magnetite/hematite	Fe_3O_4/Fe_2O_3	Mn, Ti	Common	Minor–trace	N
Rutile and anatase	TiO_2	–	Common	Trace	D
Others					
Goethite/limonite	FeOOH	Mn, Ti	Common	Trace	N
Feldspar	$KAlSi_3O_8$	Ca	Moderate	Trace	D, L
Zircon	$ZrSiO_4$	–	Moderate	Trace	D
Sulfates: gypsum	$CaSO_4 \cdot 2H_2O$	–	Moderate	Minor	D, F
Barite	$BaSO_4$	Na, Sr, Pb	Rare	Minor	F
Szomolnokite	$FeSO_4 \cdot H_2O$	–	Rare	Trace	D
Apatite	$Ca_5(PO_4)f,Cl,OH)3$	Mn, Ce, Sr, U	Moderate	Trace	D
Halite	NaCl	K, Mg	Rare	Trace	D

[a] D = disseminated; L = layers (partings); N = nodules; F = fissures (cleat). First listed is the most common occurrence.

Table 2.2
Coal inorganic impurities

Type	Origin	Examples	Physical separation
Strongly chemically bonded elements	From coal-forming organic tissue material	Organic sulfur, nitrogen	None
Absorbed and weakly bonded	Ash-forming components in pure water, adsorbed on the coal surface	Various salts	Very limited
Mineral matter:			
(a) epiclastic	Minerals washed or blown in the peat during its formation	Clays, quartz	Partly separable by physical methods
(b) syngenetic	Incorporated into coal from the very earliest peat-accumulation stage	Pyrite, siderite, some clay minerals	Intimately intergrown with coal macerals
(c) epigenetic	Stage subsequent to syngenetic; migration of the mineral-forming solutions through coal fractures	Carbonates, pyrite, kaolinite	Vein type mineralization; epigenetic minerals concentrated along cleats, preferentially exposed during breakage; separable by physical methods

removing the mineral matter at the first, second, and third levels of heterogeneity) is usually less than 1%.

Recent findings indicate that most of the mineral matter in coal down to the micron particle size range is indeed a distinct separable phase that can be liberated by fine crushing and grinding. Keller [13] measured the particle size distribution of the mineral matter obtained by low-temperature ashing of a few samples of coal from the Pittsburgh seam. The measurements he carried out on mineral matter obtained from 5-cm lumps of raw coal indicate a bimodal particle size distribution, with most mineral particles falling in the range from about 1 to 10 μm, while the rest are coarser than 100 μm. In coal ground below 250 μm, the mineral-matter particle size distribution was skewed toward the fine range. As a result, when finally ground coal was cleaned by the Otisca-T oil agglomeration process, a very good correlation between the clean coal ash content and the mode of the particle size distribution of the feed coal was observed (Fig. 2.7) [13]. This indicates that the inherent ash content may be as low as about 1% if coal is finely ground to obtain proper liberation and then concentrated using a selective method.

2.5. Sulfur in coal

Sulfur is probably the one constituent of coal that most affects coal marketing. Virtually every coal contract includes specifications for coal sulfur and penalties if the sulfur content is exceeded.
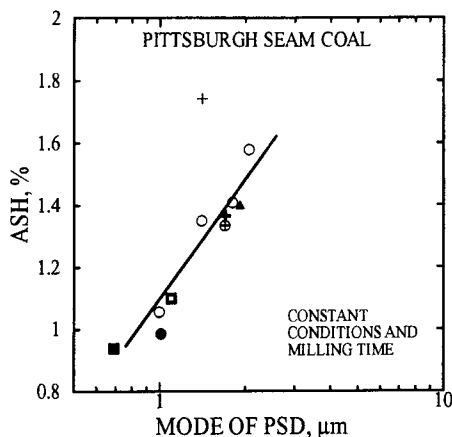
Fig. 2.7. Ash content in the clean coal concentrates versus the mode of the particle size distribution of the feed coal. (After Keller [13].)

Three types of sulfur in coal may be distinguished by chemical analysis. Extraction with hot dilute HCl solution allows determination of sulfates which are easily soluble, while extraction with hot and more concentrated HNO_3 allows determination of pyritic sulfur. Since the Eschka method gives the total sulfur content in coal, the organic sulfur content can be calculated by subtracting the first two (sulfate and pyritic sulfur) from the total sulfur. Direct methods to measure organic sulfur content are also available [14,15]. The routine method for measuring total sulfur is thermal decomposition followed by spectroscopic analysis (IR) of the gas stream (e.g. LECO SC 132 Sulfur Analyzer). The sulfate sulfur is usually of only minor importance and occurs in combination either with calcium (mainly gypsum) or iron (melanterite, jarosite). The sulfate sulfur content of U.S. coals is generally less than 0.3% and in most cases less than 0.01% [16]. The term pyritic sulfur includes both iron sulfides, pyrite and marcasite. Organic sulfur is present as a part of the coal organic matter.

According to Whelan [17], sulfate sulfur in British coals is small, a few tenths of 1%, while organic sulfur is generally of the order of 1%. It is in sulfide sulfur that the wide variation occurs. Whereas in most seams the content of pyritic sulfur lies in the range from 0.5 to 1%, there are large areas in which it runs from 1.5% to 3%. As reported by Wandless [18], high-volatile bituminous coals are appreciably higher in sulfur content than the average.

Typical sulfur analyses of coals from different regions throughout the world set out by Meyers [19] varied from 0.38% to a high 5.32%. The pyritic sulfur content of these selected coals varied from a low of 0.09% to a high of 3.97%, while the organic sulfur content varied from a low of 0.29% to a high of 2.04%. Generally speaking, organic sulfur levels greater than 2% or much less than 0.3% are almost never encountered, and pyritic sulfur levels greater than 4% are also uncommon.

The sulfur content and sulfur distribution in major operating mines representative of the three most important U.S. coal regions are shown in Fig. 2.8. As seen, the overall sulfur content of western coals is low, generally below 1%, and the major sulfur content
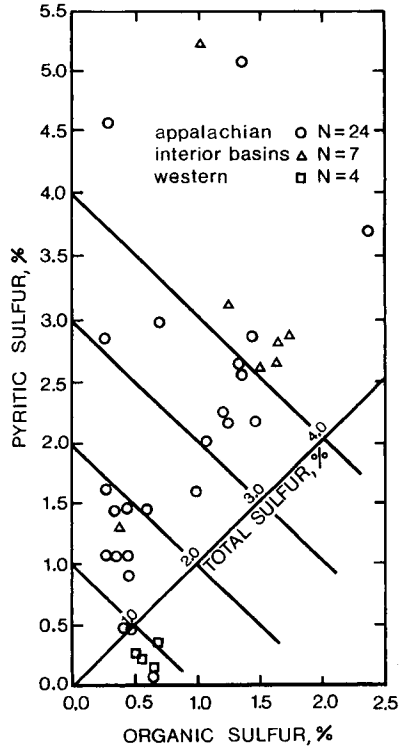
Fig. 2.8. Distribution of sulfur forms (dry-moisture-free basis) in run-of-mine U.S. coals. (After Meyers [19]; by permission of Marcel Dekker Inc.)

is organic. Interior Basin coals generally have a sulfur content of about 4%, with about 30–50% of the sulfur being organic. Appalachian coals tend to have a lower content of organic sulfur with the content of pyritic sulfur being as high as 3%. The geographical trend in sulfur content from east to west is high sulfur to low sulfur, and a similar situation exists in Canada. While coals from the western provinces (British Columbia, Alberta) are low in sulfur, high-volatile bituminous coals from the Atlantic provinces are high in sulfur.

Coal organic sulfur forms are shown in Fig. 2.9 after Given and Wyss [20].

According to Attar [21], the majority of the organic sulfur in high-ranked coals is thiophenic, and during the coalification processes the sulfur-containing organic compounds transform as follows:

thiols → aliphatic sulfides → aromatic sulfides → thiophenes

R–SH → R–S–R → ϕ–S–ϕ →
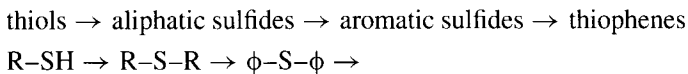
Attar and Dupuis [22] claim that 15–30% of the organic sulfur in all coals is sulfidic. About 30–40% of the organic sulfur in lignite is thiolic, while in bituminous coals 40–60% of the organic sulfur is thiophenic. Attar and Dupuis' data show that the thiolic

THIOLS

R-SH   SH

ALIPHATIC   AROMATIC

SULFIDES

R - S -R'   S - R

ALIPHATIC   AROMATIC   MIXED

THIOPHENES

SINGLE RING   CONDENSED

γ - THIOPYRONES

SINGLE RING   CONDENSED
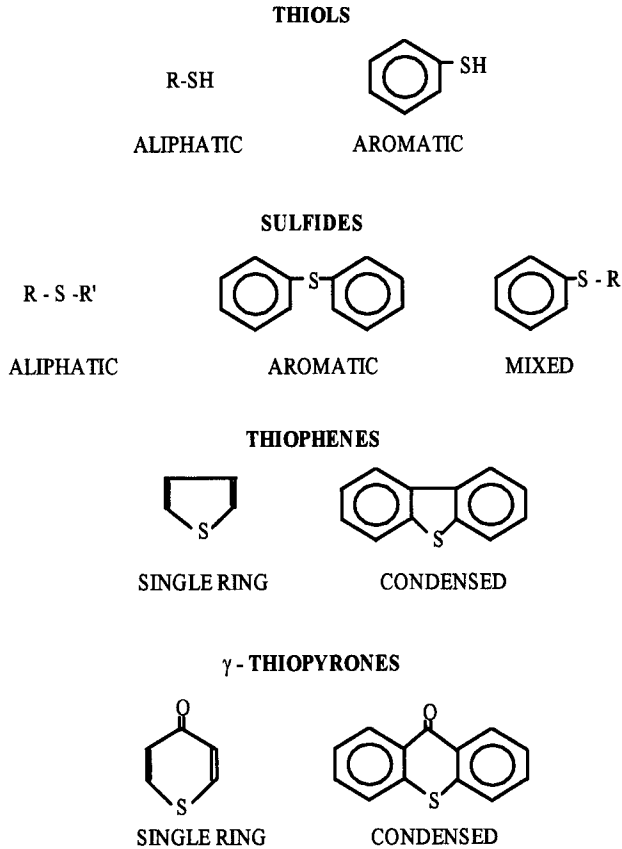
Fig. 2.9. Sulfur forms in coal. (After Given and Wyss [20].)

sulfur and part of the sulfidic sulfur can be easily removed from coal by mild chemical desulfurization.

Stock et al. [23] reviewed the research on sulfur distribution in American bituminous coals and concluded that while the macerals from low-sulfur bituminous coals contain comparable amounts of organic sulfur, the macerals of high-sulfur coals contain significantly different amounts of these substances. It was, for example, reported that exinites are somewhat richer and inertinites somewhat poorer in organic sulfur than the associated vitrinites.

It is well known that hydrogen bonding to sulfur groups is very weak, and compounds containing such groups have little affinity for water. For example, the solubility of simple sulfur compounds is less than that of their oxygen analogues. In line with this type of reasoning, Brooks [24] reported that the moisture content of high-sulfur coals is less than that of normal coals of the same carbon content.

Distinction between inorganic and organic sulfur is of great importance. The inorganic sulfur content in coals can be reduced by physical separation methods, and since the content of sulfates is negligible, the pyritic sulfur content can also be

determined from a linear function between total sulfur and ash contents (see also [25]).

Pyrite density is 5.2 and with coal density being in the range from 1.3 to 1.5, gravity separation methods are quite efficient in separating coal particles from pyrite particles. Due to the very high density of pyrite, even small amounts of pyrite are sufficient to increase the density to a point when the coal particle can be rejected. Therefore, particles containing small amounts of pyrite are more easily rejected by density processes than surface-based processes such as flotation. However, the efficiency of separation by gravity methods falls rapidly for particles finer than 100 μm. While separation of pyrite from other sulfides is commonly carried out by flotation and several selective pyrite depressing agents have been developed to aid selectivity in such differential flotation processes, these agents were found inefficient when used in coal flotation. As a result, coal desulfurization depends critically on pyrite particle size, and hence on dissemination of pyrite in coal. It is worth noting that the degree of required liberation will vary depending on (i) the type of utilized separation process and (ii) the type of mineral to be rejected (e.g. pyrite vs. shale).

It is well documented that a significant portion of the sulfur in coal occurs as pyrite in the form of individual crystals, or as assemblies of crystals forming framboids [26]. A complete chemical and structural analysis for channel samples from three mines revealed that while the proportion of pyrite appearing in the form of framboids varied only from 6 to 12%, the proportions appearing either as single crystals or as larger massive forms were quite different for the three studied coals. Fig. 2.10 shows pyrite crystals, and both individual crystal as well as framboid assemblies.

Only pyrite that is liberated can be separated from coal. Pyrite dissemination and liberation were, therefore, studied by many researchers. Whelan [17] found that iron sulfides appear in British coals as: (a) minute discrete grains disseminated throughout the coal (size −40 μm +0.5 μm); (b) small concretions (usually between 20 and 100
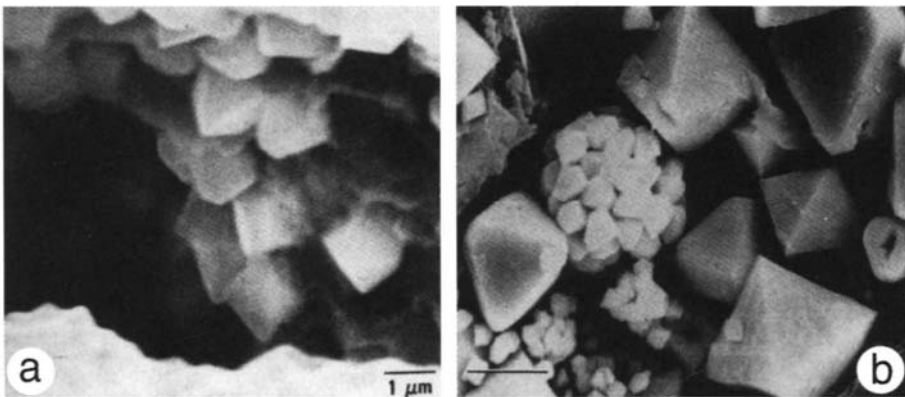
Fig. 2.10. (a) Pyrite crystals attached to upper surface of a horizontal opening in the coal. ICO mine. Scale bar 1 μm. (b) Pyrite crystals occurring as a cavity filling. Both individual crystals and a spherical crystal assembly (a framboid) are seen. Otley mine. Scale bar 5 μm. (After Greer [26]; by permission of American Chemical Society.)

μm); (c) infillings of tension cracks (10 to 15 μm); (d) ramifying veins (20 to 200 μm); (e) surroundings of primary concretions; (f) veinless crossing assemblies of primary concretions; (g) infilling fractured coal structures; (h) cementing fragments of broken fusain cells; and (i) filling fusain cell cavities.

The majority of pyrites was found to occur as the first two types. Whelan concluded that two-sevenths of the sulfur in British coals (0.8%) is organic. One-seventh exists as crystalline, secondary pyrite substantially free from carbon and parting readily from the coal organic matter. Formation of this secondary pyrite occurs in tension cracks and other areas of weakness. Such pyrite remains in flotation tailings when the coal has been finely ground. Between these two lies primary marcasite, containing four-sevenths (1.6%) of the total sulfur, and which occurs in the form of finely disseminated small grains or concretions always impregnated with carbon. Large grains of primary marcasite tend to report to tailings, while small grains, often completely encased in coal, report to the froth product. However, even a large concretion of primary marcasite enters the froth if its extent of coal impregnation is considerable.

These conclusions agree very well with some more recent studies. Wang et al. [27] have recently concluded that although the amount of nearly liberated pyrite in the −28 mesh sample was substantial, the content of truly liberated pyrite of any size appeared to be negligible.

Zitterbart et al. [28] presented statistical analyses of the data which showed that the percentage of pyrite liberated was inversely correlated to the mean grind size for several seams. The correlation for the Pittsburgh seam coal is given in Fig. 2.11. Their overall data shows that more pyrite is liberated upon finer grinding of coal samples, and that coal samples from different seams possess distinct pyrite liberation characteristics. They reported that both pyrite and ash removals increased when coal samples were ground from −8 down to −28 mesh, and that very little improvement in the pyrite/ash reduction was achieved by the additional grinding to −100 mesh.
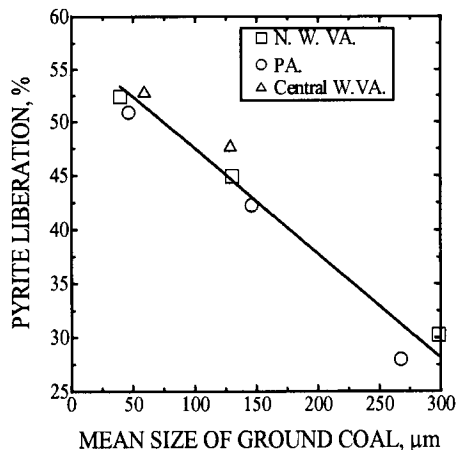
Fig. 2.11. Inverse relationship between pyrite liberation and mean grind size for Pittsburgh seam coals. (After Zitterbart et al. [28].)

Our own data [29] for raw coal from Eastern Canada indicates a bimodal particle size distribution of pyrite grains (the coarser pyrite grains, greater than 5 μm, were mostly of massive subhedral and anhedral forms, while the fine fractions contained framboidal pyrite and fine singular pyrite grains). For the most part, pyrite in most samples not ground below 53 μm had a bimodal distribution inherited from the raw coal; samples crushed below 53 μm generally had a unimodal pyrite distribution with a mode between 3 and 7 μm. The amount of liberated pyrite increased with increased grinding time but even after prolonged grinding time the finest pyrite particles (less than 2 μm) were not liberated. Wet grinding was found to be more efficient in pyrite liberation than dry grinding.

Our data also indicate that in the particular coal studied, all forms of pyrite were predominantly associated with and intergrown with vitrinite. In some vitrinite particles, pyrite infills cell lumens but in most particles the pyrite was randomly distributed. Pyrite was rarely associated with exinite, inertinite or semi-inertinite macerals.

Raymond [14] showed that a general relationship exists in most coals with respect to organic sulfur contents of the macerals: sporinite, resinite > micrinite, vitrinite > pseudo-vitrinite > semi-fusinite > macrinite > fusinite. But since the vitrinite macerals dominate in coal, he also showed that when plotting organic sulfur content of the coals vs. organic sulfur content of respective vitrinite components, the best linear fit of the data has a correlation coefficient of 0.99, a slope of 0.98 and a y-intercept of -0.03. Thus, empirically, the organic sulfur content of a coal (dmmf) equals the organic sulfur content of its vitrinite.

It is also important to point out, however, that while the organic sulfur contents of intertinite macerals is generally reported to be very low, the pyrite content may be high since pyrite impregnations in cell openings in fusinite and semi-fusinite are quite common.

2.6. Liberation

The most important factor that determines coal cleaning efficiency is liberation of organic matter from mineral matter, the two main coal constituents. Since density of "clean" coal particles that mostly contain organic matter is in a range from 1.2 to 1.5 and the densities of most common coal minerals are much above 2.0 (density of pyrite is 5.2), the separation of coal particles into various density fractions can easily be performed in dense liquids. This is the so-called float–sink analysis, the results of which are presented graphically in the form of washability curves (see pp. 95–99).

Fig. 2.12 shows separation results as a function of particle size after Teh et al. [30]. These curves indicate that the separation obtained under the ideal conditions of the float–sink test clearly depends on the particle size; it is possible to obtain cleaner products at the same clean coal yield by grinding coal finer.

Similar conclusions can be drawn from floatability curves as shown in Fig. 2.13 [31]. These curves were obtained following the tree procedure (see Chapter 4) for a coal ground to progressively finer sizes as shown by the reduction in d_{50} from 85 μm to 5 μm. Better separation for finer material obviously results from better liberation.
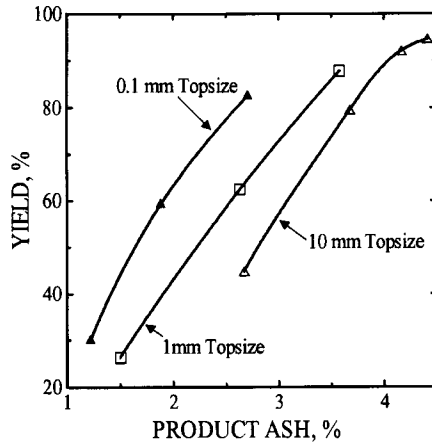
Fig. 2.12. Fine-coal washability as a function of particle size. (After Teh et al. [30]; by permission of the Australasian Institute of Mining and Metallurgy.)
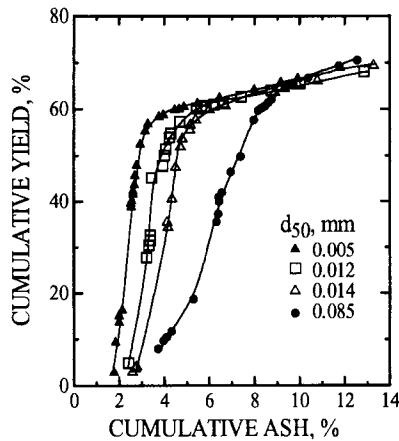
Fig. 2.13. Use of the tree procedure to characterize increased liberation by finer grinding of a coal sample. (After Nicol et al. [31].)

The shape of the M-value curve, or the primary washability curve, indicates the degree of liberation and it is obvious that the shape of such curves can be used to characterize liberation [32]; float–sink data can also be used to derive a liberation function, as discussed by Austin [33].

In the float-and-sink tests a raw coal is fractioned into n density fractions. In Dell's release analysis, a sample of raw coal is separated into n fractions in a series of batch flotation experiments (for details see Chapter 4).

Feed = Product 1 + Product 2 + ... Product n

$$F = P_1 + P_2 + \ldots P_n \qquad (2.2)$$
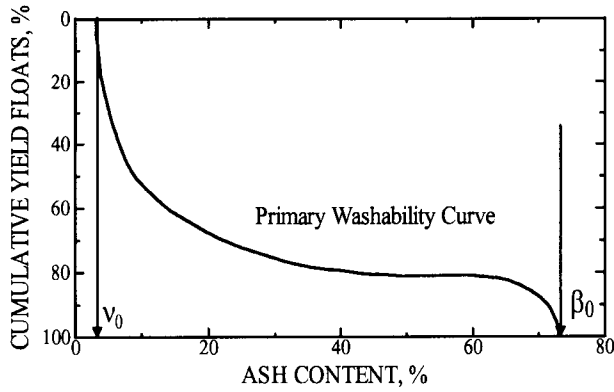
Fig. 2.14. Primary washability curve and estimation of v_o and β_o.

On percent basis:

$$100 = \gamma_1 + \gamma_2 + \dots \gamma_n \tag{2.3}$$

where γ is the product yield (wt.%); $\gamma = (P_i/F)100$

Ash balance can be expressed as follows:

$$F\alpha = P_1\lambda_1 + P_2\lambda_2 + \dots P_n\lambda_n \tag{2.4}$$

$$100\alpha = \gamma_1\lambda_1 + \gamma_2\lambda_2 + \dots \gamma_n\lambda_n \tag{2.5}$$

where α is the ash content in the raw coal, and λ_1, λ_2, and λ_n are the ash contents in the respective fractions (products).

Coal is made up from organic matter and mineral matter, and since their densities are different, a sample of coal particles varying in degree of liberation can be fractionated into various density fractions in a float–sink test in which different-density heavy liquids are utilized. Such separation results give a primary washability curve when plotted graphically as shown in Fig. 2.14.

For floats, at $\sum \gamma_f \to 0$, $\lambda \to v_o$, where v_o is the ash content of the coal organic matter.

For sinks, at $\sum \gamma_s \to 0$, $\lambda \to \beta_o$, where β_o is the ash content of the coal mineral matter.

This is consistent with the assumption that the lowest-density fraction contains only liberated organic matter, while the highest-density fraction contains only liberated mineral matter [34].

Since

$$\text{Coal} = \text{Organic Matter} + \text{Mineral Matter} = \text{OM} + \text{MM} \tag{2.6}$$

and putting that coal ash content is α, and organic matter and mineral matter ash contents are v_o and α_o, respectively, one can write

$$F \cdot \alpha = \text{OM} \cdot v_o + \text{MM} \cdot \beta_o \tag{2.7}$$
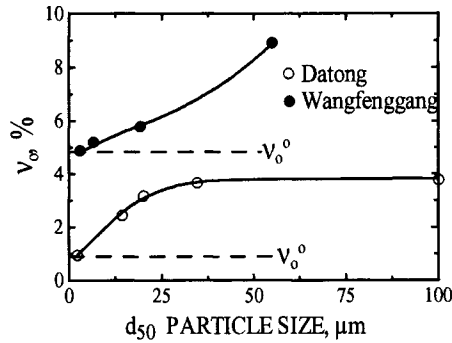
Fig. 2.15. Effect of average particle diameter of coal on v_o. (After Tsunekava et al. [35]; by permission of the Australian Coal Preparation Society.)

If it is assumed that in float–sink tests the fraction with the lowest density contains only well liberated organic matter, and that only well liberated mineral matter appears in the heaviest fraction, then it is possible to determine the ash content of organic matter, v_o, and the ash content of mineral matter, β_o. If it is further assumed that only locked particles appear in the intermediate fractions, then the liberation function gives an estimation of how much of the total mineral matter in coal has been recovered in liberated form in the cumulative sinks, or may estimate the liberation of organic matter in the sample [34].

Fig. 2.15 shows the effect of grinding on the v_o ash content for two coals; the results were obtained from the release analysis [35]. As these curves reveal, the v_o values determined for $\sum \gamma \rightarrow 0$ also depend on particle size, and so the true v_o° value can only be obtained by extrapolating $v_o \rightarrow v_o^\circ$ for $d \rightarrow 0$. Thus, v_o° is the inherent ash content of the coal organic matter.

Based on the washability index of Govindarajan and Rao [36], Mohanty et al. [37] have recently developed the flotation index, FI. It is determined by the shaded area divided by the triangular area ABC when floatability results are plotted as $100 -$ combustible recovery $= f(100 -$ ash rejection) (Fig. 2.16).

$$\text{FI}_{\text{ash}} = \frac{(\text{area of the triangle } ABC) - (\text{area under the curve } CDB)}{\text{area of the triangle } ABC}$$

Since the *CDB* washability curve consists of two distinct regions having different slopes, it is possible to find the inflection point. It usually occurs at about the 75–80% ash rejection level. It is thus possible to generate two different flotation indices, FI_1 and FI_2 (see Fig. 2.16). FI_1 characterizes the area where most of the pure ash particles will be rejected at a minimal loss of combustible recovery, whereas FI_2 represents the area where most of the middling particles will be rejected with a considerable loss of combustible recovery and so characterizes difficulty in cleaning the middling particles. The effect of particle size on the FI index as determined for the Illinois No. 6 coal sample is shown in Fig. 2.17 [37].
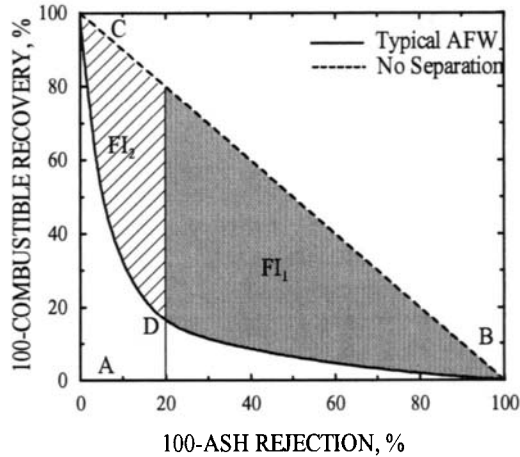
Fig. 2.16. An illustration of the concept of multiple flotation indices. (After Mohanty et al. [37]; by permission of Elsevier Science.)
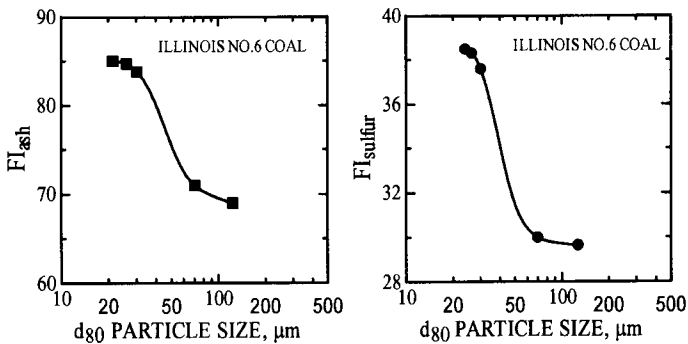
Fig. 2.17. An illustration of the effect of particle size on the flotation index values, both FI_{ash} and FI_{sulfur}, for an Illinois No. 6 coal sample. (After Mohanty et al. [37]; by permission of Elsevier Science.)

2.7. References

[1] M.A. Barnes, W.C. Barnes and R.M. Bustin, Chemistry and evolution of organic material. Geosci. Can., 11 (3) (1984) 103.

[2] R.M. Davidson, Molecular structure of coal. In: M.L. Gorbaty, J.W. Larsen and I. Wender (eds), Coal Science. Academic Press, New York, 1982, Vol. 1, pp. 84–160.

[3] J.W. Larsen and J. Kovac, Polymer structure of bituminous coal. In: J.W. Larsen (ed.), Organic Chemistry of Coal. ACS Symp. Series, Vol. 71, Washington, DC, 1978, pp. 36–49.

[4] D.D. Whitehurst, T.O. Mitchell and M. Farcasiu, Coal Liquefaction. Academic Press, New York, 1980.

[5] A. Ihnatowicz, Studies of oxygen groups in bituminous coals. Bulletin of the Central Mining Research Institute (GIG), Katowice, 1952, No. 125 (in Polish).

[6] L. Blom, L. Edelhausen and D.W. van Krevelen, Chemical structure and properties of coal, XVIII. Oxygen groups in coal and related products. Fuel, 36 (1957) 135.

[7] Z. Abdel-Baset, P.H. Given and R.F. Yarzab, Re-examination of the phenolic hydroxyl content of coals. Fuel, 57 (1978) 95.

[8]   G.L. Baughman, Synthetic Fuels Data Handbook. Cameron Engineers, Denver, CO, p. 175.
[9]   R.M. Bustin, A.R. Cameron, D.A. Grieve and W.D. Kalkreuth, Coal Petrology, Its Principles, Methods
      and Applications. Canadian Geological Association, St. Johns, 1983.
[10] M.F. Kessler, Interpretation of the chemical composition of bituminous coal macerals. Fuel, 52 (1973)
      191.
[11] A.C. Cook, What are we trying to separate? Sep. Sci. Technol., 16 (1981) 1545.
[12] R.D. Harvey and R.R. Ruch, Mineral matter in Illinois and other US coals. In: K.S. Vorres (ed.),
      Mineral Matter and Ash in Coal. ACS Symp. 301, American Chemical Society, Washington, DC, 1986,
      pp. 10–40.
[13] D.V. Keller, The separation of mineral matter from Pittsburgh coal by wet milling. In: Chemistry of
      Mineral Matter and Ash in Coal. Am. Chem. Soc. Div. Fuel Chem., 29 (4) 1984, pp. 326–336.
[14] R. Raymond, Electron probe microanalysis: a means of direct determination of organic sulfur in coal.
      In: E.L. Fuller (ed.), Coal and Coal Products: Analytical Characterization Techniques. ACS Symp. 205,
      American Chemical Society, Washington, DC, 1982, pp. 191–204.
[15] W.E. Straszheim, R.T. Greer and R. Markuszewski, Direct determination of organic sulphur in raw and
      chemically desulphurized coals. Fuel, 62 (1983) 1070.
[16] D.J. Casagrande, Sulphur in peat and coal. In: A.C. Scott (ed.), Coal and Coal-Bearing Strata: Recent
      Advances. Geological Society, London, 1987, pp. 87–106.
[17] P.F. Whelan, Finely disseminated sulphur compounds in British coals. J. Inst. Fuel, 27 (1954) 455.
[18] A.M. Wandless, The occurrence of sulphur in British coals. J. Inst. Fuel, 32 (1959) 258.
[19] R.A. Meyers, Coal Desulfurization. Marcel Dekker, New York, 1977.
[20] P.H. Given and W.F. Wyss, The chemistry of sulfur in coal. Br. Coal Util. Res. Assoc. Mon. Bull., 25
      (1961) 165.
[21] A. Attar, Sulfur groups in coal and their determination. In: C. Karr (ed.), Analytical Methods for Coal
      and Coal Products, Academic Press, New York, 1979, Vol. 3, p. 585.
[22] A. Attar and F. Dupuis, Data on the distribution of organic sulfur functional groups in coals. In:
      M.L. Gorbaty and K. Ouchi (eds), Coal Structure. Adv. Chem. Ser. 192, American Chemical Society,
      Washington, DC, 1981, pp. 239–256.
[23] L.M. Stock, R. Wolny and B. Bal, Sulfur distribution in American bituminous coals. Energy Fuels, 3
      (1989) 651.
[24] J.D. Brooks, Organic sulfur in coal. J. Inst. Fuel, 29 (1956) 82.
[25] D.W. Fuerstenau, J.S. Hanson and J. Diao, A simple procedure for the determination of pyritic sulfur
      content in coals. Fuel, 73 (1994) 123.
[26] R.T. Greer, Coal microstructure and pyrite distribution. In: T.D. Wheelock (ed.), Coal Desulfurization
      — Chemical and Physical Methods. ACS Symp. Ser. 64, American Chemical Society, Washington DC,
      1977, pp. 1–15.
[27] D. Wang, G.T. Adel and R.H. Yoon, Image analysis characterization of pyrite in fine coal flotation.
      Miner. Metall. Proc., 10 (1993) 154.
[28] M.T. Zitterbart, D.G. Nichols and D.E. Lovenhaupt, Pyrite and ash liberation from selected coals.
      In: Y.A. Attia (ed.), Processing and Utilization of High Sulfur Coals. Elsevier, Amsterdam, 1985, pp.
      19–30.
[29] J.S. Laskowski, R.M. Bustin, K.S. Moon and L.L. Sirois, Desulfurizing flotation of Eastern Canadian
      high sulfur coal. In: Y.A. Attia (ed.), Processing and Utilization of High Sulfur Coals. Elsevier,
      Amsterdam, 1985, pp. 247–266.
[30] C.N. Teh, R. Keast-Jones and J.B. Smithan, The preparation of ultra-low ash coals. Proc. AIMM, 292
      (1987) 61.
[31] S.K. Nicol, J.B. Smitham and J.T. Hinkley, Problems relating to the measurement of ideal flotation
      response. In: G.E. Agar, B.J. Hukls and D.B. Hudyma (eds), Column '91. CIB, Sudbury, 1991, Vol. 1,
      pp. 99–107.
[32] E.T. Oliver, J. Abbott and N.J. Miles, Liberation characteristics of a coal middlings. Coal Preparation,
      16 (1995) 167.
[33] L.G. Austin, Patterns of liberation of ash from coal. Min. Metall. Process., 11 (1994) 148.
[34] A.B. Holland-Batt, Estimating liberation in coals. Coal Preparation, 15 (1994) 1.
[35] M. Tsunekava, Y. Kon, T. Hirajima, M. Ito and N. Hiroyoshi, A new method to characterize the

flotation performance of coal. In: A.C. Partridge and I.R. Partridge (eds), Proceedings of the 13th International Coal Preparation Congress. Australian Coal Preparation Society, Brisbane, 1998, Vol. 1, pp. 397–406.

[36] B. Govindarajan and T.C. Rao, Indexing the washability of coal. Int. J. Miner. Process., 42 (1994) 285.

[37] M.K. Mohanty, R.Q. Honaker and B. Govindarajan, Development of a characteristic flotation cleaning index for fine coal. Int. J. Miner. Process., 55 (1999) 231.

This Page Intentionally Left Blank

Chapter 3

COAL SURFACE PROPERTIES

3.1. Introduction

Coal is very heterogeneous. In simple terms it is a mixture of organic matter (macerals) and inorganic matter (minerals). Organic matter was formed through the accumulation of plant material which has undergone biochemical and metamorphic changes, referred to as coalification. Depending on the coalification (rank), composition of the coal organic matter (Fig. 2.1) and the coal properties vary.

As shown in Fig. 3.1, the surface of coal is heterogeneous at different levels. At the molecular level it can be depicted as a hydrocarbon matrix that contains various functional groups (as shown in Fig. 2.2). The composition of the matrix varies with the coalification (Fig. 2.3). It can be inferred from what has been said about coal petrography in Section 2.3, that maceral make-up, inorganic matter inclusions and porosity determine heterogeneity at the microscopic level. Various associations of macerals with each other and with minerals are referred to as lithotypes and it is known that many coal physical properties can be predicted from lithotype characteristics. The heterogeneity at the macroscopic level is then determined by lithotypes and mineral matter. This picture of a coal surface is obviously very complicated and it will have to be simplified in order to describe the relationship between the coal rank and composition, and the coal's surface properties.

This book is primarily on flotation and since this process relies on the surface properties of the treated minerals, first we will have to define what is meant here by surface properties. Although the relationship between wettability and floatability is not straightforward [1–4], only those particles of which the wettability is characterized by a contact angle larger than zero ($\Theta > 0$) can float, so it is generally assumed that wettability as expressed by contact angle is the most fundamental of flotation-related surface property. While low-rank coals which are not very hydrophobic float poorly,
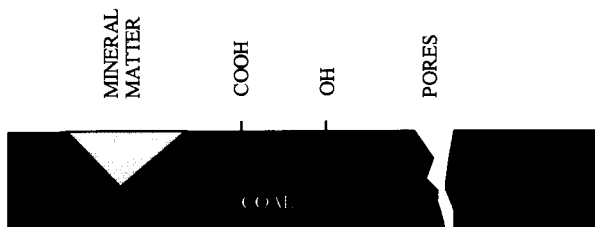
Fig. 3.1. Schematic representation of coal surface.

bituminous coals, if not oxidized, are hydrophobic and are easy to float. Following this line of reasoning, coal surface wettability will be the primary subject of this chapter.

In one of the attempts at describing the coal flotation properties it was postulated [5] that coal surface properties are determined by (i) the hydrocarbon skeleton of coal (related to coal rank), (ii) the number and type of oxygen functional groups, and (iii) mineral matter impurities.

In such an approach the coal matrix is assumed to be hydrophobic (to a varying degree), and this hydrophobicity is further modified by the presence of hydrophilic functional groups on the coal surface, and by mineral matter impurities which are also hydrophilic. Coal is also porous, and this, if the pores are filled up with water, may make the coal surface more hydrophilic [6] or, if the pores are filled with air, may make the coal more hydrophobic.

Since coal wettability by water is determined by the interactions at the coal/water interface, the analysis introduced by Fowkes [7] and Good [8] can be used to study these relationships further.

3.2. Coal surface wettability

3.2.1. Contact angles

The work of adhesion of liquid to solid (W_{SL}) can be split [9] into van der Waals dispersive forces contribution (W_{SL}^d) and several other contributions among which the most important are a hydrogen bond contribution (W_{SL}^h) and, if the solid surface is charged, an electrical forces contribution (W_{SL}^e).

$$W_{SL} = W_{SL}^d + W_{SL}^h + W_{SL}^e \tag{3.1}$$

Recently, all the contributions except the dispersion forces have been grouped into an acid–base contribution (W_{SL}^{AB}) [10,11], and so Eq. (3.1) becomes

$$W_{SL} = W_{SL}^{LW} + W_{SL}^{LW} + W_{SL}^{AB} \tag{3.2}$$

where superscript LW now denotes Lifshits–van der Waals [12].

$$W_{SL} = W_{SL}^d = 2(\gamma_l^d + \gamma_s^d)^{1/2} \tag{3.3}$$

and

$$W_{SL} = \gamma_{SV} + \gamma_{LV} - \gamma_{SL} \tag{3.4}$$

By combining with Young's equation (Eq. 3.26) one obtains [1]

$$W_{SL} = \gamma_{LV}(\cos\Theta + 1) \tag{3.5}$$

where γ_{SV}, γ_{LV} and γ_{SL} are solid–gas, liquid–gas and solid–liquid interfacial tensions, respectively, and γ_l^d and γ_s^d stand for dispersive forces contributions to the liquid and solid surface tensions.

---

[1] A complete Young equation for a liquid droplet resting on a smooth solid surface is usually written as $\pi_e + \gamma_{SV} = \gamma_{SL} + \gamma_{LV}\cos\Theta$. The term π_e (equilibrium surface pressure of water vapors adsorbed on the solid surface) is usually omitted for hydrophobic surfaces.
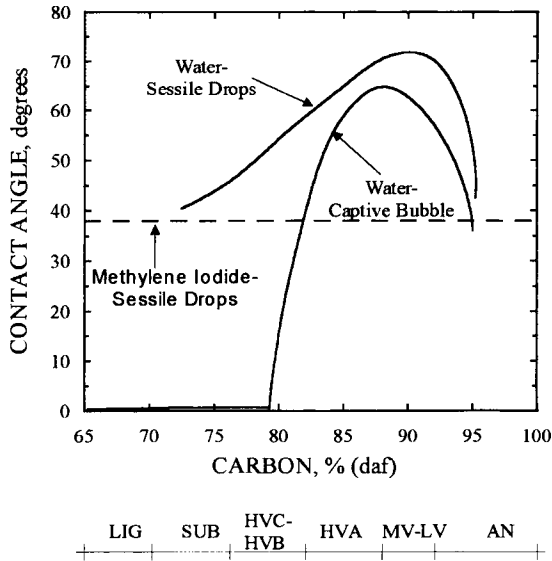
Fig. 3.2. Relationship between coal rank and its wettability by water as measured by the captive-bubble and sessile-drop methods. Dashed line is for methylene iodide-sessile drop measurements. (After Gutierrez-Rodriguez et al. [13]; by permission of Elsevier Science.)

In order to evaluate the dispersion forces contribution to the wettability of coals, Gutierres-Rodriquez et al. [13] in accordance with well established procedures used methylene iodide and showed that the values of the contact angle measured with this compound do not depend on coal rank, nor on its oxidation (Fig. 3.2). These contact angle values for various coals were in the range of $28 \pm 9°$ irrespective of the experimental technique used (captive bubble or sessile drop); along with $\gamma_{LV} = \gamma_l^d = 50.8 mJ/m^2$ for methylene iodide, it gives for coals $\gamma_s^d = 45 \pm 4$ mJ/m^2, which is in very good agreement with previous measurements [14]. Good et al. [15], obtained $\Theta_{adv} = 39.7 \pm 1.9°$ [2] for Upper Freeport coal ($85.95\% C_{daf}$) and this gives $\gamma_s^d = 39.8 \pm 1.0 mJ/m^2$.

From Eqs. (3.2), (3.4) and (3.5) one obtains

$$W_{SL}^{AB} = W_{SL} - W_{SL}^d = \gamma_{LV}(1 + \cos \Theta) - 2(\gamma_l^d \gamma_s^d)^{1/2} \tag{3.6}$$

Since $\gamma_{H_2O}^d = 22 mJ/m^2$ [7] and if, for coal, 40 mJ/m² is used for γ_s^d

$$W_{SL}^d = 2(22 \cdot 40)^{1/2} = 59.3 \simeq 59 mJ/m^2$$

Then for coal [16]

$$W_{SL}^{AB} = \gamma_{LV}(1 + \cos \Theta) - 59 \tag{3.7}$$

---

[2] It is a common practice to use advancing contact angles in this type of analysis. Fig. 3.26 explains conceptual differences between advancing and receding contact angles, and Fig. 3.27 shows how they can be measured. The confusion arises from the fact that on a heterogeneous surface, depending on the experimental procedure, the measured contact angle may be very different.

If the sessile drop contact angles of water on coal are used (Fig. 3.2), they range from about 40° for subbituminous coal to about 70° for medium-volatile bituminous coal; the calculated values for W_{SL}^{AB} for these contact angles are 64 mJ/m^2 and 33.6 mJ/m^2, respectively. For a low-rank coal, the acid–base contribution to the energy of water adhesion is practically the same as the dispersion forces (Lifshits–van der Waals) contribution; for higher-rank metallurgical coals, the dispersive forces' interactions constitute the main contribution. Of course, such an averaging interpretation assumes that the coal surface is homogeneous, which is known not to be the case.

Finally, with this information it is possible to calculate the value of the contact angle of a water droplet on a smooth, unoxidized, homogeneous surface of a coal hydrocarbon matrix. For this, the following equation will be used:

$$\cos \Theta = -1 + \frac{2(\gamma_s^d \gamma_l^d)^{1/2}}{\gamma_{LV}} \tag{3.8}$$

It gives $\Theta = 100.5°$. Any smooth coal surface having a water contact angle of less than 100.5° contains, therefore, various hydrophilic areas (polar functional groups, mineral impurities, etc.) on the hydrophobic hydrocarbon matrix.

In the 1940s, Brady and Gauger [17] observed that the contact angle values measured on Pennsylvania bituminous coals were larger than on anthracite, while North Dakota lignites were completely hydrophilic. The results of comprehensive wettability studies on coals from the Donbass Basin (Ukraine) were published by Elyashevitch [18] while further details were provided by Horsley and Smith [19] in the 1950s. But the first complete analysis of the wettability of coals as a function of coal rank was offered by Klassen in his monograph on coal flotation [20] in which he analyzed Elyashevitch's data [18]. Fig. 3.3 shows contact angle values plotted vs. coal rank taken from the paper published by Elyashevitch et al. in 1967 [21], the C/H ratio from Klassen's plot, and the inherent moisture vs. volatile matter from another Elyashevitch's publication [22]. As can be seen, the contact angle vs. rank curve exhibits a maximum, with decreasing contact angles as volatile matter content (or C%) either decreases or increases from that maximum.

Coal also contains heteroatoms and functional groups (see Wiser's model, Fig. 2.2). As shown by Ihnatowicz [23], and Blom et al. [24], oxygen in coals occurs predominantly as phenolic and etheric groups with a lesser amount of carboxyl (Fig. 3.4). It appears that the carboxy and metoxy groups are of little importance at greater than 80% carbon. The phenolic group content, when expressed as a fraction of the total organic matter in the coal, shows a strong correlation with the carbon content (dry-mineral-matter-free) [25].

These facts were taken into account by Klassen who explained low values of contact angle in the low-rank range by the high oxygen content (see also Fig. 6.1). The sharp increase in coal aromaticity (as indicated by the C/H ratio, see also Fig. 2.3) and increased porosity were suggested as the main reason for the lower hydrophobicity of anthracites (see Section 3.4).

Comparison of the experimental contact angle values obtained while working with real coal samples (Figs. 3.2 and 3.3) confirm that the maximum contact angle values are
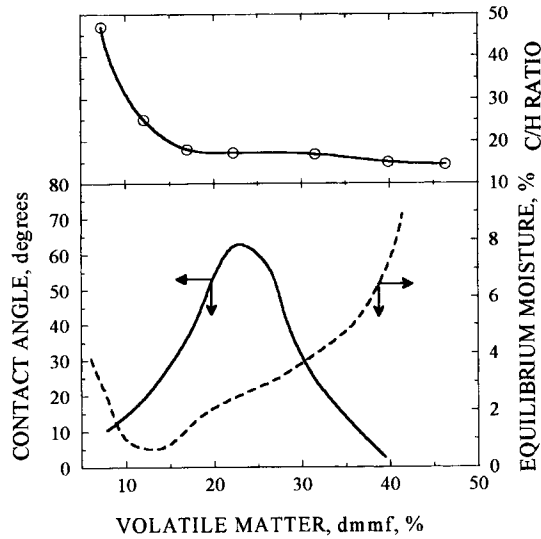
Fig. 3.3. Effect of coal rank on coal wettability by water. (After Klassen [20].) The contact angle vs. volatile matter content (% dmmf) curve is after Elyashevitch et al. [21], and the inherent moisture vs. volatile matter is from another Elyashevitch's publication [22].
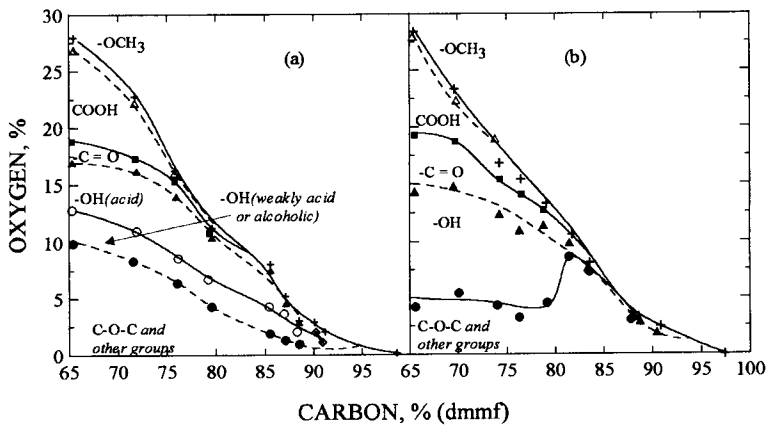
Fig. 3.4. Functional oxygen groups in coal: (a) after Bloom et al. [24] (by permission of Elsevier Science); (b) after Ihnatowicz [23].

always much lower than the theoretical value $\Theta = 100°$ obtained under the assumptions discussed above.

3.2.2. *Electrical charge at coal/water interface*

Electrokinetic measurements provide valuable information on the properties of coal aqueous suspensions that depend on the charge of the particles. Examples include coal

particles' wettability and floatability, coal suspensions' stability and rheology, and coal fines' filterability, etc. Such measurements reveal the relationship of charge to the nature of coal and how the charge is affected by the liquid phase composition. It may also serve as an additional tool in the studies of coal surface composition.

It should also be pointed out that the electrical charge has a pronounced effect on wettability.

The classical boundary condition for the hydrophilic–hydrophobic transition is equality of W_{SL}, the work of adhesion of liquid to solid, and W_{LL} the work of cohesion of the liquid. Since

$$W_{LL} = 2\gamma_{LV} \tag{3.9}$$

From Eqs. (3.5) and (3.9) one obtains

$$\frac{W_{SL}}{W_{LL}} = \frac{\gamma_{LV}(1 + \cos\Theta)}{2\gamma_{LV}} \tag{3.10}$$

which gives

$$\cos\Theta = 2\frac{W_{SL}}{W_{LL}} - 1 \tag{3.11}$$

The condition of hydrophobicity follows from Eq. (3.11): only for $W_{SL} < W_{LL}$ $\Theta \neq 0$ [26].

Fig. 3.5 depicts a sessile liquid droplet resting on a flat surface; the values of the work of cohesion of the liquid, and the work of adhesion of the liquid to the solid determine the contact angle at the solid/liquid/gas interface.

Since, as given by Eq. (3.1), W_{SL} also depends on W_{SL}^e (W_{SL}^e is the contribution from the electrical charge at the interface), the contact angle depends on the solid electrical charge as well [1,27,28]. As Eqs. (3.11) and (3.1) explain, the contact angle reaches maximum value, $\Theta \to \Theta_{max}$, when $W_{SL}^e \to 0$, as confirmed by the electrocapillary curves.

The electrical charge at a solid/liquid interface can be directly determined by titration. In this method a relatively large amount (in terms of surface area) of an insoluble material is suspended in solution and is titrated with potential determining ions. For coals, as well as for oxide minerals, hydroxyl and hydrogen ions are potential
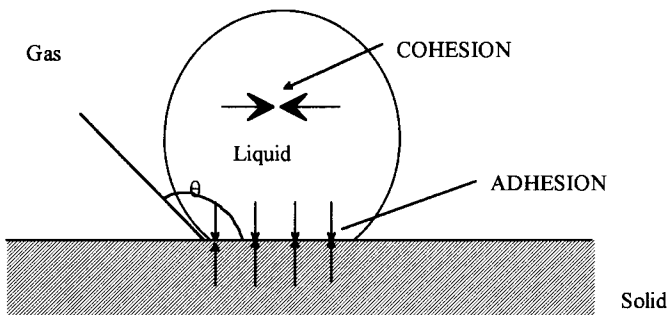
Fig. 3.5. Illustration of the effect of the work of cohesion of liquid and the work of adhesion of liquid to solid on the solid wettability.

determining. The charge can also be determined indirectly using electrokinetic methods. The latter experiment is much easier to carry out and commercial equipment is widely available; therefore, the electrokinetic methods are much more common.

Electrokinetic (zeta) potential. The theory of the electrical double layer associated with a charged particle in an aqueous electrolyte solution has been well documented in textbooks [29–31] and will not be repeated in detail here. Essentially, the charge is assumed to be smeared out uniformly over the particle surface, and this is balanced by ions regarded as point charges, which are of opposite sign and distributed in the medium around the particle. The surface has an electrostatic potential $\psi_\circ$, and on moving away from the surface the potential decays exponentially to zero in the bulk liquid. At low potentials

$$\psi = \psi_\circ \exp[-\kappa x] \tag{3.12}$$

where κ is a function of the electrolyte concentration, and x is the distance from the solid/liquid interface (it is customary to refer to $1/\kappa$ as the thickness of the diffuse double layer).

For aqueous solutions at 25°

$$\kappa = 3.288\sqrt{I} \ \text{nm}^{-1} \tag{3.13}$$

where I is the ionic strength of the solution.

Account is taken of specific adsorption at the solid/liquid interface by assuming that the diffuse part of the double layer starts at a distance d from the surface. The plane is considered to run through the centers of hydrated adsorbed ions. This layer is usually referred to as the Stern layer, and the potential at the boundary of this layer is the Stern potential ψ_d. Across the Stern layer, the potential decays linearly and the Stern potential becomes the origin of the diffuse layer and its exponential decay of potential.

The shear plane (also called the slipping plane), which corresponds to the boundary of the layer of bond solvent, is the location of the zeta potential. There is a considerable body of evidence that suggests that the shear plane lies very close to the Stern layer. Hence it has become common practice to use the zeta potential in theoretical predictions relating the stability of colloidal dispersion to coagulation. Fig. 3.6 illustrates the potential distribution in the double layer and includes reversal of surface charge due to specific adsorption (for details see Hunter's book [29]).

Of the four electrokinetic phenomena, electrophoresis is by far the most commonly used to determine the zeta potential. This is a study of the movement of charged particles dispersed in a medium containing electrolyte under the influence of an electric field. In most cases the microelectrophoretic technique is used and the movement of particles in a dilute dispersion is followed microscopically. A number of commercial instruments are available, some of which involve direct measurements of the electrophoretic mobility, and others of which are designed to reduce the tedium by using sophisticated optics and electronics to give average electrophoretic mobility and even mobility distribution.

The electrophoresis data are commonly expressed in terms of the particle electrophoretic mobility (u_E), i.e. the velocity divided by the potential gradient across the cell and quoted in units of μm s^{-1}/volt cm^{-1}. According to Henry, the relation between
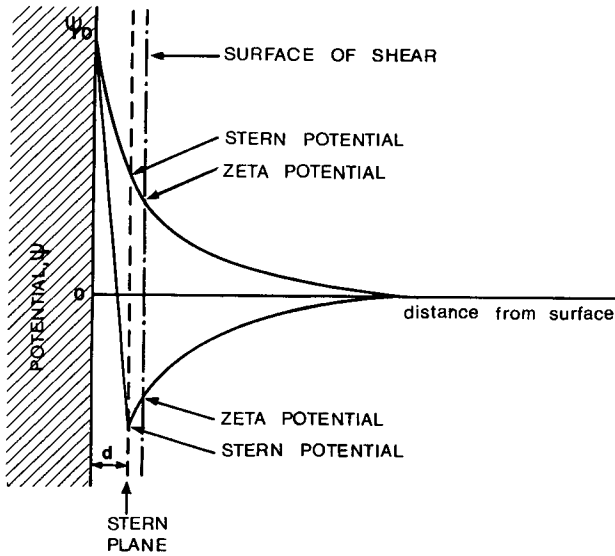
Fig. 3.6. Potential distribution in electrical double layer (lower curve shows charge reversal due to specific adsorption in the Stern layer).

electrophoretic mobility and zeta potential depends on the particle radius (a) and the thickness of the double layer surrounding the particle ($1/\kappa$) expressed in the product κa, as given by:

$$u_{\mathrm{E}} = \frac{\zeta \varepsilon}{1.5 \eta} f(\kappa a) \tag{3.14}$$

In this equation ζ is the zeta potential of solid particles, ε is the permittivity of the medium in which these particles are immersed (the dielectric constant of a material is equal to the ratio between its permittivity and the permittivity of a vacuum), and η is the viscosity of the medium.

For very small particles in dilute solution where the thickness of the double layer ($1/\kappa$) is large, $\kappa a \ll 1$ and the correction factor $f(\kappa a) = 1$ (Huckel equation). For large particles in more concentrated solution $\kappa a \gg 1$ and $f(\kappa a) = 1.5$ (Smoluchowski equation).

Electrokinetic measurements should be made at constant ionic strength. For example, in a study of the effect of pH on the electrophoretic mobility of particles whose surface charge is determined by H^+ and OH^- ions, both the surface and zeta potential change with pH. However, the rate of decay of potential from the surface is also a function of the ionic strength (Eq. (3.12)); hence the zeta potential is dependent on both ψ_o and κ. To measure the true effect of pH on zeta potential requires that κ be maintained as a constant and this is achieved by conducting the measurements in a solution of indifferent electrolyte. For example, if this is a symmetrical electrolyte (say with ions of valency 1, such as KCl or KNO_3), then since in Eq. (3.13)

$$I = \tfrac{1}{2} \sum c_i z_i^2 \tag{3.15}$$

where c_i is the concentration of ion i in mol dm^{-3}, and z is the ion valency, then for the case of KCl

$$I = \tfrac{1}{2}([K^+](1)^2 + [Cl^{-1}](-1)^2)$$

Since $[K^+] = [Cl^-] = c$, the concentration of the salt, one obtains $I = c$. So, if a 1-1 symmetrical salt is used as a supporting electrolyte in electrokinetic experiments, then from Eq. (3.13) one calculates that at a concentration of 10^{-3} mol dm^{-3}, κ has a value of approximately 0.1 nm^{-1}. Hence for particles of radius 1 μm, $\kappa a \approx 100$. Increasing the electrolyte concentration to 10^{-3} mol dm^{-3} increases $\kappa a \approx 1000$. Thus, for such cases the Smoluchowski equation is applicable to calculate the zeta potential values from the experimentally determined electrophoretic mobility.

As already stated, the coal surface properties depend on its hydrocarbon skeleton, its number and type of polar functional groups, and its inorganic impurities.

As Fig. 3.7 shows [32], for nonpolar hydrocarbons such as Nujol medical paraffin [33,34], the zeta potential–pH curve assumes negative values over the entire pH range. Perreira and Schulman [35] found pure paraffin wax to be negatively charged above pH 5.0 and positively below. Zeta potential values for paraffin wax reported by Arbiter et al. [36] were negative in the pH range 3 to 10. Pure hydrocarbon droplets from hexane to octadecane have also been shown to be negatively charged, with the negative zeta potential rising continuously over the pH range 2 to 11 [37]. This type of behavior is believed to represent the adsorption of anions and/or desorption of protons with an increase of pH.

By comparing a hydrophilic solid/water and a hydrophobic solid/water interface, Arbiter et al. [36] concluded that a hydrophobic wall in the extreme has little or no effect on the liquidity of water, and that the electrokinetic properties of the strongly hydrophobic solids are primarily or completely determined by the aqueous phase. Because the solid does not specifically adsorb ions, it does not participate in determining the potential, and for hydrophobic solids, the electrical double layer is then analogous to that at the water/air interface. Chander et al. [38] provide some additional
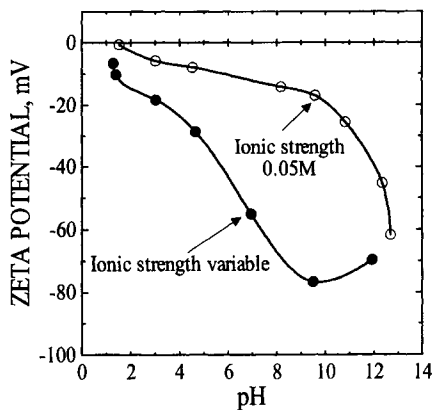
Fig. 3.7. Zeta potential of droplets of Nujol medical paraffin oil. (After Mackenzie [34]; by permission of the American Institute of Mining, Metallurgical, and Petroleum Engineers.)

data showing that the shape of the zeta potential vs. pH curve for other hydrophobic solids such as talc, sulfur, and molybdenite is similar to that of graphite and paraffin wax.

In order to study the effect of coal rank on the zeta potential it is necessary to understand, and if possible eliminate, the effect of inorganic impurities on the measurement as mineral matter may entirely mask coal surface properties (for example, as discussed in Section 3.7, the effect of petrographic composition on coal floatability is clearly visible only when the ash content is below 15%).

The task is extremely difficult. The mineral matter strongly affects coal wettability [39]. One of the first papers on coal electrokinetics, by Sun and Campbell [40], demonstrates that the zeta potential versus pH curves for high-ash petrographic constituents (durain 40.8% ash, fusain 52.4% ash) were quite different from the curves obtained for vitrain (3.2% ash) and whole coal (9.7% ash). This simple fact is often overlooked, and that is why many sets of electrokinetic data for coals are not very reliable.

It is well established that inorganic impurities do contribute to and affect coal electrokinetic measurements. Siffert and Hamieh [41] claim that the electrical charge of coal particles is a function of a molar ratio of SiO_2/Al_2O_3 contained in a coal. But, can the limiting ash content in coal be precisely defined? Is it possible to give a number indicating the maximum ash content above which electrokinetic measurements should be treated as unreliable? As discussed in Section 2.4, inorganic impurities in coal may appear in different forms. Crushing and fine grinding may liberate mineral matter at heterogeneity levels 1, 2 and to some extent 3; inorganic impurities at heterogeneity level 4 cannot be liberated by physical means at all. These impurities form the so-called inherent ash, and so, coal always contains some amount of ash. Careful cleaning of coal by physical means down to a few percent ash is commonly sufficient for meaningful electrokinetic measurements. Fig. 3.8 shows the zeta potential–pH curve for raw (11.5% ash) and demineralized Somerset mine coal [5]. Demineralization was carried out at 50°C first with 40% HF for 45 min and then with 10 M HCl for an additional 45 min, followed by prolonged washing with distilled water so that it finally contained less than 0.5% ash. Such a treatment was shown to have little effect on the chemistry of the coal organic matter [42], and is also commonly used before determination of coal oxygen functional groups by titration [43–45]. For comparison, Fig. 3.9 shows zeta potential–pH curves for a few common oxides. As Fig. 3.8 reveals, 11.5% ash may still be too high and the zeta potential vs. pH curve for such a sample may resemble the mineral matter (silica in this case) more than the coal.

Coal's iso-electric points (concentration of potential-determining ions at which the electrokinetic potential is equal zero; since potential-determining ions for coal are H^+ and OH^- ions, i.e.p. $= (pH)_{\zeta=0}$) plotted versus volatile matter content were shown to depend on coal rank [46]. These results were obtained by Blaszczynski [47] and replotted vs. carbon content are shown in Fig. 3.10. In order to eliminate the effect of mineral matter, the samples from various mines in Poland were crushed below 6 mm, de-slimed on a 0.5-mm screen and were subjected to cleaning in 1.4 g/cm^3 aqueous solution of $ZnCl_2$. The floating fractions were washed with distilled water, dried, and ground below 33 μm in an agate mortar. Such cleaned coal samples contained from 2.8% to 7.3% ash. Electrokinetic measurements were carried out using
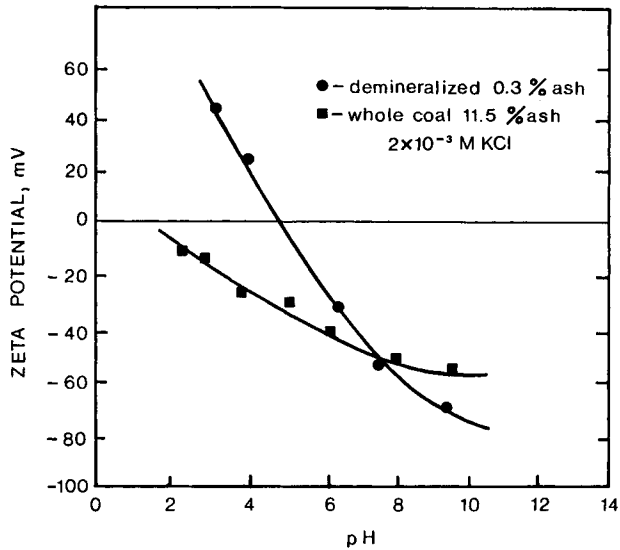
Fig. 3.8. Zeta potential vs. pH curves for raw and demineralized Somerset mine coal. (After Fuerstenau et al. [5]; by permission of Elsevier Science.)
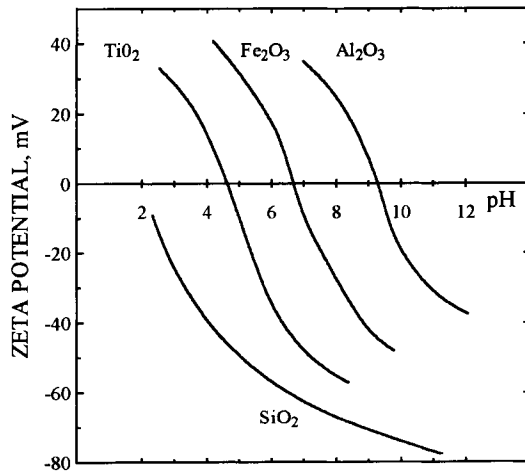
Fig. 3.9. Schematic illustration of the effect of pH on zeta potential of various oxides.

Gortikhov's electroosmosis apparatus (its description can also be found in Yarar's paper [48]).

As Fig. 3.10 reveals, the iso-electric point (i.e.p.) vs. percent C curve has a clear maximum around 86–88% C and then falls off rapidly for higher-rank coals. The measurements gave the i.e.p. for anthracites a value of around 4.5, for low-volatile bituminous coal between 6 and 7, and for high-volatile bituminous coals between 3.5
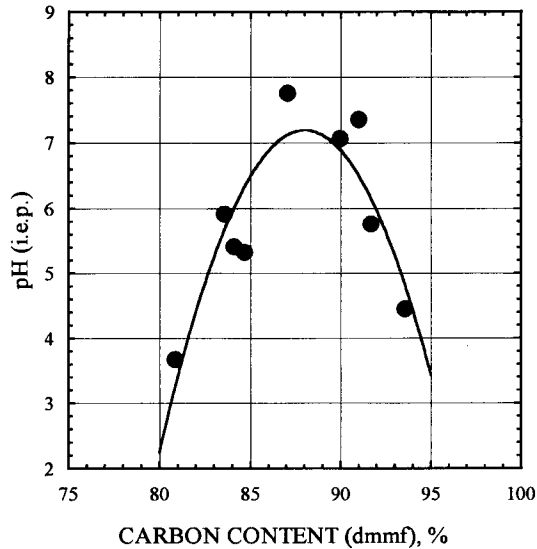
Fig. 3.10. Relationship between iso-electric point and coal rank.

and 5. Campbell and Sun [49] found that the i.e.p. of bituminous coal occurred between 3.5 and 4.6 and for various anthracites between 2 and 4.5. Jessop and Stretton [50] report iso-electric points between 3.5 to 4.8 for low-ash coal samples. Prasad [51] reported low i.e.p. values for anthracite and bituminous coal and a comparatively high i.e.p. (6.3) for coking coal. Marganaski and Rowell [52] found the i.e.p. for bituminous coal to be 6. All these data agree reasonably well. As seen from Fig. 3.10, the i.e.p. of low-rank coals that contain a higher amount of oxygen are shifted toward more acidic pH values. Wen and Sun [53] proved that the i.e.p. of bituminous vitrains decreases from 4.5 for an unoxidized sample to pH 3.4 for a sample oxidized for 24 h at 125°C. This is also clearly seen from Yarar and Leja's paper [54], Kelebek et al. [55], and Al-Taweel et al. [56].

Data extracted from Yarar and Leja's paper [54] on the i.e.p. supplemented by other data of Leja [45] on the carboxylic group content in the same coal samples are shown in Figs. 3.11 and 3.12.

Two curves result from two procedures in the titration experiment used to determine the coal carboxylic group content. In such experiments coal is used either directly as is or after demineralization with strong acids. The pretreatment is usually necessary to free carboxylate groups present as metallic salts [57]. While such a treatment is common before the titration to determine coal carboxylic and phenolic groups, generally it is not used before electrokinetic measurements.

Because of the contribution from acidic (carboxylic and phenolic) groups, the iso-electric points of low-rank, or oxidized coals, are shifted toward the acidic pH range (Figs. 3.11 and 3.12). Measurements reported in this chapter also indicate that the i.e.p. of anthracite, the high-rank coal, is situated in the same pH range. The i.e.p. of metallurgical (coking) coals, which as far as coalification is concerned occupy an
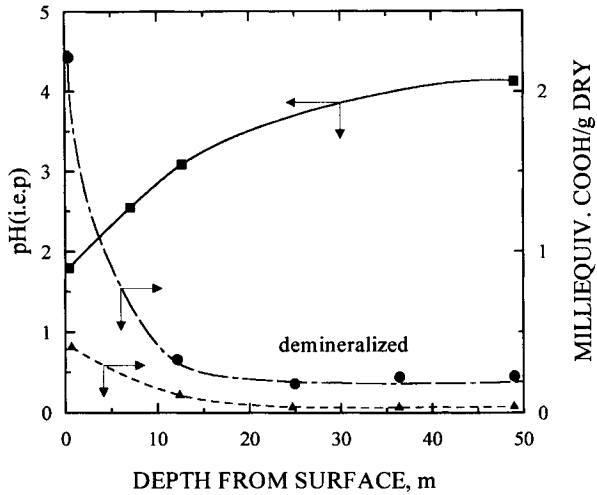
Fig. 3.11. Iso-electric points and carboxylic group content of coal sample collected from seam No. 7 of the Fording River Deposit, BC, at various distances from the surface. (After Laskowski and Parfitt [57]; by permission of Marcel Dekker Inc.)
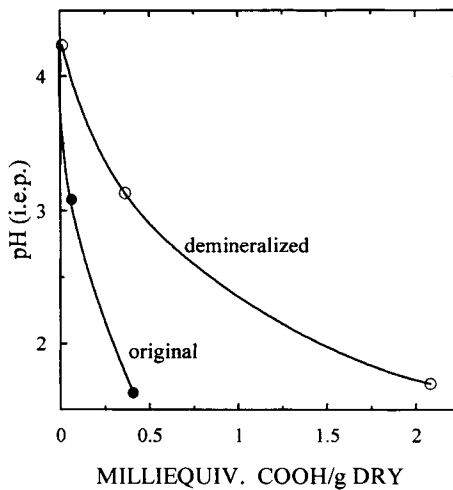
Fig. 3.12. Iso-electric points plotted versus carboxylic groups' concentration for the Fording River Deposit coal (replotted from Fig. 3.11).

intermediate position between high-volatile bituminous and anthracite coals, seem to be situated close to the neutral pH range.

Fig. 3.13 shows zeta potential vs. pH curves for different coals [57]. Deviations from linearity are attributed to the presence of acidic oxygen functional groups, mostly carboxylic.
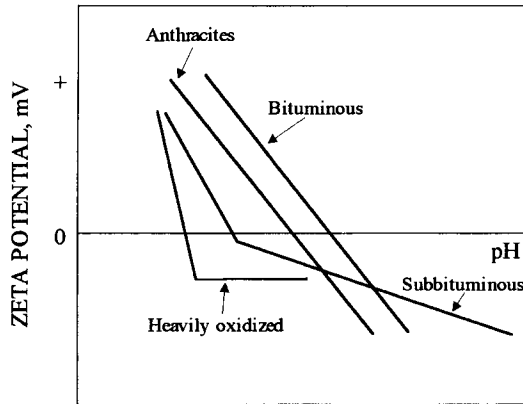
Fig. 3.13. Generalized zeta potential vs. pH diagram for coals of various rank (After Laskowski and Parfitt [57]; by permission of Marcel Dekker Inc.)

3.3. Coal porosity and moisture

Low-rank coals such as brown and lignites can have moisture contents in a range from 30% to 70%, while bituminous coals have relatively low moisture contents of 10% or less. The elimination of water is then an integral part of the coalification process. Coal water content also has a significant effect on the coal's utilization (high moisture contents of low-rank coals is a serious limitation to their exploitation).

The amount of equilibrium moisture held by a coal depends on the vapor pressure in the atmosphere to which it is exposed. The usual method of studying the water in
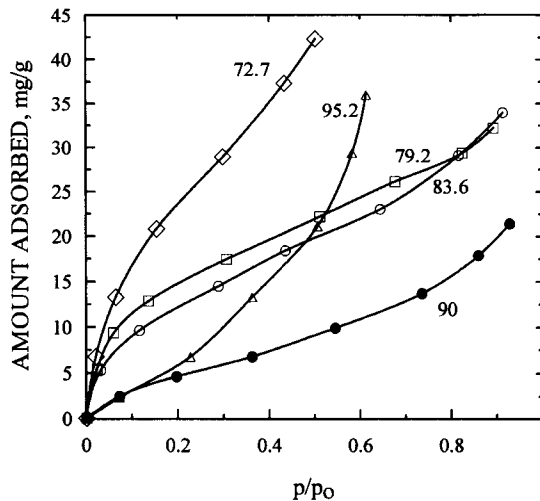
Fig. 3.14. Water vapor adsorption onto coals (at 20°C) as a function of relative pressure. Numbers show carbon content (% daf) in the tested coal samples. (After Mahajan and Walker [58]; by permission of Elsevier Science.)

coal is to measure a water sorption isotherm, which depicts the moisture content of the coal as a function of relative humidity (relative vapor pressure). Fig. 3.14 shows the moisture sorption isotherms measured at 20°C on different coal samples [58]. In this figure the pressure is expressed on a relative vapor pressure basis (p/p_o), which is the ratio of the water pressure to the saturation vapor pressure of water at the isotherm temperature.

The generally accepted [59] interpretation of sigmoid-shaped isotherms with water as sorbate is as follows.

(a) The water removed at close to the saturation vapor pressure (above 0.96 p/p_o) in the nearly vertical part of the isotherm is free or bulk water admixed with the coal and contained in macropores and interstices.

(b) In the convex part of the curve from about 0.96 to 0.5 p/p_o the water is desorbed from capillaries, and the depression in vapor pressure can be explained by a capillary meniscus effect.

(c) Below relative vapor pressure of 0.5, the Kelvin equation predicts pore sizes on the order of a few molecular diameters.

The moisture content of the coal in equilibrium with a relative humidity of 96% at 30°C is referred to as the equilibrium moisture (moisture-holding capacity of a coal, bed moisture) [3].

While moisture contents at high humidities are consistent with coal porosity, the shape of the sorption isotherms, especially at low relative pressures, characterizes interactions between solid and vapor molecules. As seen from Fig. 3.14, sorption on bituminous coals is characterized by Type II isotherms; the isotherm for anthracite more closely resembles Type III. Blom et al. [24] found a very good correlation between the moisture content (determined at 70% relative humidity at 23°C) and the total hydroxylic (phenolic and carboxylic) group content in coal. Iyenger and Lahiri [62] suggested that the calculated BET monolayer adsorption of water onto coal is a measure of the content of the oxygen functional groups of coal. This has been confirmed by Lason et al. [63] who reported an excellent correlation between oxygen content in coal and water sorption.

---

[3] Total moisture is the moisture in the coal, as sampled, determined under standardized conditions (ASTM D3302). The coal samples collected from a freshly exposed coal seam face with no visible surface moisture are considered to be at inherent moisture. When a coal sample is left in a lab it will lose some moisture (this is the air-dry loss (ASTM) or free moisture (ISO)). The moisture remaining in the sample after it has attained equilibrium with the atmosphere to which it was exposed is the residual moisture. Equilibrium moisture (ASTM) and moisture-holding capacity (ISO) are equivalent in principle and represent a coal's moisture when at equilibrium with an atmosphere of 96–97% relative humidity and 30°C. Equilibrium moisture results provide a reasonable approximation of inherent moisture for bituminous and some subbituminous coals [64].

The method for measuring the equilibrium moisture is to equilibrate a coal sample saturated with water in a desiccator containing an aqueous solution of potassium sulfate at 30°C (relative humidity of 96%). For example, the moisture immediately after filtration will give the total moisture of the filter cake, while the moisture determined in the cake placed in a desiccator at 30°C over a saturated solution of potassium sulfate (96% relative humidity) for 2–3 days will give an equilibrium moisture content. In all these cases the content of moisture is determined after drying at 105–110°C following ASTM D 388 (see also ASTM D1412) standards.
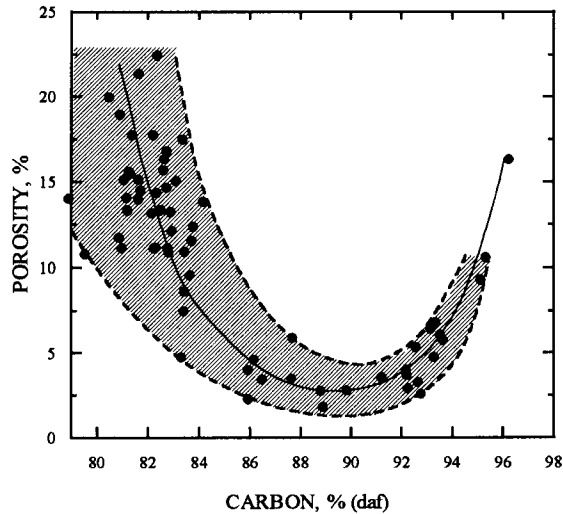
Fig. 3.15. Variation of coal porosity with rank. (After King and Wilkins [60].)

The moisture contents at p/p_o close to unity are in the order of the porosities of the coals. Such a porosity plotted versus carbon content is shown in Fig. 3.15 [60]. Coal rank has a very pronounced effect on porosity. When Gan et al. [61] examined a number of American coals ranging from lignite to anthracite they concluded that the abundance of pores and their size is related to the coal rank. In the lower-rank coals (C content below 75%), porosity is primarily due to the presence of macropores (300–30,000 Å). In coals having a carbon content in the range of 76 to 84%, about 80% of the total open pore volume is due to the transitional pores (12–300 Å) and micropores, while micropores predominate in coals of higher carbon content.

The concept of using the BET model with the sorption isotherms measured on coal requires an additional comment. As Fig. 3.1 shows, coal surfaces are very heterogeneous. They are heterogeneous because hydrophobic coal organic matrix contains different hydrophilic groups and mineral matter inclusions. Pierce et al. [65] proposed that sorption of water on active carbons initially involves adsorption onto oxygen sites. These adsorbed water molecules then serve as secondary sites for the adsorption of additional water. The clusters formed around active sites grow in size with increasing surface coverage and they merge at some stage to cover the rest of the hydrophobic surface with a film. This explains Type III adsorption isotherms for high-rank coals (Fig. 3.14).

The surface properties of hydrophobic solids such as graphite and Teflon were described in a series of papers by Zettlemoyer et al. [66–68]. These solids, while generally considered homogeneous, were found to possess a small fraction of heterogeneous sites. The vast majority of the surface sites on these solids are hydrophobic with a graphite-like array of carbon atoms; these sites showed no tendency to adsorb water up to pressures close to saturation, as indicated by the isotherm for the adsorption of water on graphon which has predominantly a Type III character. The hydrophilic
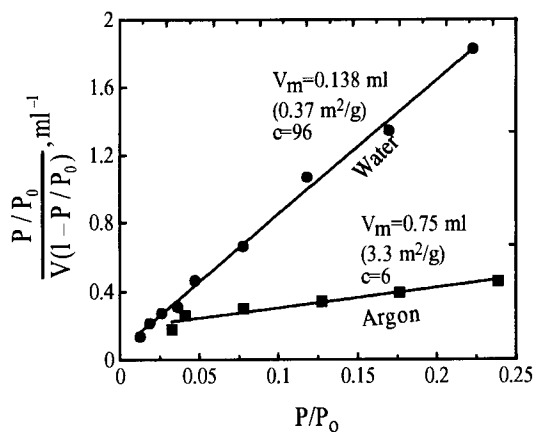
Fig. 3.16. BET plots for the adsorption of argon and of water on the sample of duPont Teflon powder, showing water adsorbed strongly to 11% of the area. (After Fowkes et al. [69]; by permission of Academic Press.)

sites were few in number and they accounted for the initial Type II character of the water adsorption isotherm. After adsorption of water molecules onto these sites, the molecules build up additional layers on and around these sites rather than adsorb on the adjacent hydrophobic area. Based on these results and assuming that the surface area calculated from the water adsorption represents adsorption on the hydrophilic sites only, Zettlemoyer et al. [67] calculated the ratio of the water area to the nitrogen area times 100 as the surface hydrophilicity. This index was determined to be 0.75% for Teflon and 0.15% for graphon; the surface hydrophilicity of aerosol, which is only weakly polar, was found to be 25% [66]. Fowkes et al. [69] measured water vapor adsorption and nitrogen adsorption on a sample of duPont Teflon contaminated with silica. The BET adsorption plots for these two are shown in Fig. 3.16. The water adsorbed on only 11% of the area on which argon adsorbed, but it was held strongly on such sites ($c = 96$, see Adamson's monograph for details [70]); these impurities strongly affected the wettability of the tested hydrophobic surfaces. Since a coal surface is a heterogeneous hydrophobic surface, all the conclusions drawn by the quoted authors apply to coal.

Since at low pressures, water will adsorb onto the polar functional groups only, the BET surface areas determined from water adsorption isotherms and from, for example, N_2 adsorption isotherms are different. Mahajan and Walker [71] determined surface areas of six -75 μm $+45$ μm coal samples (varying in carbon content from 72.7% to 95.2%) from water adsorption isotherms and CO_2 adsorption at 20°C. In all cases the water areas were much lower than the CO_2 areas [4]. It is worth pointing out that the coal

---

[4] The BET surface areas of porous and nonporous solids are conventionally determined from N_2 adsorption isotherms measured at -196°C. The N_2 surface areas of coals are considerably lower than those expected. It is believed that the micropore system in coals is not completely accessible to N_2 molecules owing to an activated diffusion process and/or shrinkage of pores at -196°C. Walker and Kini [72] showed that surface areas of coals measured by Xe adsorption at 0°C and those measured by CO_2 adsorption at -78°C and 25°C are in reasonably good agreement.

industry standard for reporting coal surface area is based on CO_2 gas adsorption near room temperature. The relevance of such data to the flotation reagent accessible portions of coal surface areas in water is, however, questionable [73].

Because interaction between adsorbing gas and porous solid (such as coal) results also from solid's porosity, the shape of the sorption isotherm also depends on the porosity and capillary condensation. While the shape of the isotherm at low p/p_o values characterizes adsorbate–adsorbent interactions, the sorption at high vapor pressures can also be used to determine porosity. If coal's surface properties are to be characterized, penetration of adsorbed molecules into the bulk must be avoided during the experiment. This can be achieved only by working at extremely low gas pressures. An experiment carried out with the use of inverse gas chromatography has recently been shown to meet such conditions. In gas chromatography (GC), the mixture to be separated is vaporized and swept over a relatively large adsorbent surface inside a long narrow tube (column). The sweeping is done by a steady stream of inert carrier gas, which serves only to move the solute vapors along the column. The different components move along the column at different rates and are separated. Inverse gas chromatography (IGC) is an extension of conventional gas chromatography in which a solid to be investigated is a stationary phase in a GC column. This stationary phase is then characterized by monitoring the passage of volatile probe molecules with known properties as they are carried out through the column via an inert gas [74]. When the measurements are carried out at infinite dilution of the solutes or at zero surface coverage of the adsorbent (coal) and when adsorption is the dominant retention mechanism, all thermodynamic parameters derived from the experiment exclusively reflect the interaction between adsorbent and adsorbate. Glass and Larsen recently described [75,76] the use of IGC to determine the specific (acid–base) and nonspecific (dispersive) interactions of polar molecules and hydrocarbons with Illinois No. 6 coal.

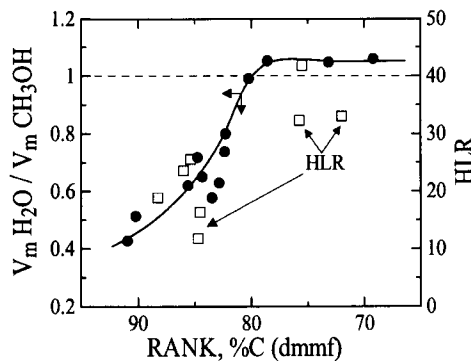Apparently this method was used by Al-Taweel et al. [77] to characterize coal surface properties in the 80s. Fig. 3.17 shows the $V_m(H_2O)/V_m(CH_3OH)$ ratio for

Fig. 3.17. $V_m(H_2O)/V_m(CH_3OH)$ ratio for coals varying in rank plotted after Lason et al. [63] (by permission of Elsevier Science), and the HLR values as determined from adsorption of water and *n*-heptane vapors. (After Al-Taweel et al. [77]; by permission of Elsevier Science.)

various coals plotted vs. carbon content after Lason et al. [63][5], and the HLR values ($\text{HLR} = N_{H_2O}/N_{n-C_7H_{16}}$) determined from adsorption of water and *n*-heptane vapors on coals using IGC [78]. Note that while the ratio of the BET monolayer adsorptions for water and methanol change little with coal rank, the change of the HLR number over the same range of coal rank is very large. Since the HLR number gives the ratio of hydrophilic-to-hydrophobic sites on the coal surfaces, this figure indicates a dramatic change in the coal's surface wettability when the carbon content of the coal changes from about 76% to 84%. It is worth noting a very good agreement with Fig. 3.2.

Since (rank-dependent) oxygen functional groups on coal surface are the primary sites for water molecule adsorption, the moisture content of coal is also related to the coal rank (see Figs. 2.4 and 3.2). However, the correlation between wettability and moisture content is complicated by the capillary condensation phenomena which also affect coal moisture content. Kaji et al. [79] showed a linear correlation between the coal water-holding capacity (measured at 100% relative humidity) and product of coal oxygen content (expressed as the weight fraction of oxygen in the coal) and the coal specific surface area obtained from mercury porosimetry.

3.4. Surface components hypothesis

In order to explain the change in coal wettability and floatability with rank, Sun proposed the surface components hypothesis in 1954 [80]. The equation that Sun derived allows one to calculate the floatability index (FL) using the results of coal proximate and ultimate analyses. The formula in the condensed form is as follows:

$$\text{FL} = x \left(\frac{H}{2.0796} \right) + y \left(\frac{C}{12} - \frac{H}{2.0796} \right) + 0.4 \left(\frac{S}{32.06} \right) - z \left(\frac{M}{18} \right)$$
$$- 3.4 \left(\frac{O}{16} \right) - \left(\frac{N}{14} \right) \tag{3.16}$$

where H, C, S, O and N are the percent contents of hydrogen, carbon, sulfur, oxygen and nitrogen taken from the ultimate analysis, and M is the moisture content on the as-received basis; x depends on the ash content and is equal 3.5 when the ash content is below 8.9%, is equal 3 for the 9–13.0% ash range, and 2.5 if the ash content is higher than 13%. Sun provided complete proximate and ultimate analyses for more than 50 coal samples, various hydrocarbons, and wood-derived substances. To calculate the floatability index for various coals y was assumed to equal 0.6. z is a function of moisture content; when moisture content is below 14.1% (bituminous coal) z is 4, when moisture content is above 14.1% (subbituminous coals and lignites), z is 3.

Since the nitrogen content in coal varies between 0.5% and 2%, the term on the right hand side that includes nitrogen is about 0.1, and since the sulfur content is never higher than 5%, the contribution from the term that includes sulfur is never larger than about

---

[5] V_m calculated from the BET equation gives the amount of sorbate (in moles) required to form a monomolecular layer, but for solids such as coal it is rather a measure of the number of reactive polar groups.
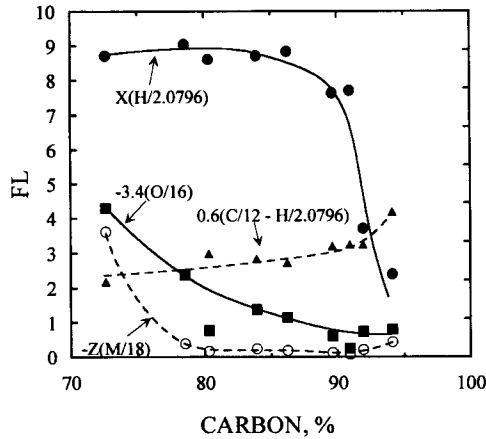
Fig. 3.18. Four contributing terms in Eqs. (3.) and (3.16) plotted versus carbon content for various coals.

0.06. These two terms can then be entirely eliminated from the equation without affecting the final calculations. Fig. 3.18 shows in graphical form the four contributing terms from Eq. (3.16) plotted versus the carbon content as calculated from Sun's data [80].

As can be seen, the first term of the equation drastically decreases for anthracites, which reflects a sudden decrease in hydrogen content (see Fig. 2.3, and the C/H curve in Fig. 3.3) for high-rank coals, and a steady increase of the second term with rank. Obviously, both negative terms, which are calculated from the moisture and oxygen content, assume much higher values for low-rank coals. If both of the positive terms and both of the negative terms are combined, the final result is quite clear (Fig. 3.19). The difference between the two terms, which is equal to the floatability index, is also shown. It correlates quite nicely with Figs. 3.2 and 3.3 and exhibits a maximum.

It is tempting to analyze these results further in terms of Eqs. (3.1) and (3.2). The W_{SL}^d term (Eqs. (3.1) and (3.2)) can be identified with a more or less constant value of the dispersion forces' contribution irrespective of the rank (see the methylene iodide contact
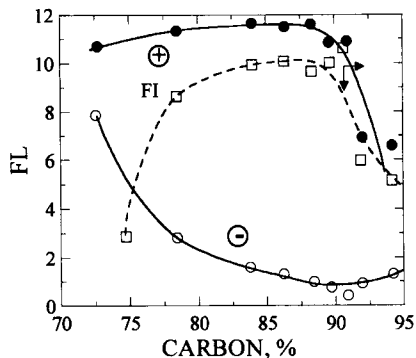
Fig. 3.19. The positive and negative terms in Eq. (3.16), and FL values as plotted vs. carbon content.

angle in Fig. 3.2). The positive term in Fig. 3.19 seems to include both dispersion and some acid–base forces, which is especially clear for the more aromatic anthracites. The negative term in Fig. 3.19 includes a large variety of acid–base interactions, which are primarily between the oxygen functional groups and water. It is intriguing that the i.e.p. curve for bituminous coals plotted vs. carbon content (Fig. 3.10) also shows a maximum around 86–88% C.

3.5. Patchwork assembly model of coal surface

As seen from Figs. 3.2 and 3.3, the contact angle measured on a coal surface and plotted versus rank passes through a maximum (around medium-volatile bituminous coal) and again assumes much lower values for anthracites. In the low-rank range, Klassen [20] explained this trend by the high oxygen content. The variation in the C/H ratio with rank (the concept put forward by Taggart in 1939 [81]) and higher porosity were used to explain the lower hydrophobicity of anthracites. Horsley and Smith [19] observed that some petrographic constituents (e.g. fusain), lose good natural floatability after prolonged immersion in water and hypothesized that this may be the result of porosity.

As Fig. 3.1 shows, coal is heterogeneous. A hydrophobic hydrocarbon matrix contains hydrophilic functional groups, a hydrophilic mineral matter, and is porous. In their explanation, Rosenbaum and Fuerstenau [82] assumed that coal may be modeled as a composite material, the nonwettable portions of which are made up of paraffins and aromatic hydrocarbons, and whose wettable portions are represented by functional groups and mineral matter. To calculate the contact angle on such a composite surface, they used the Cassie–Baxter equation [83,84] in the way described by Philippoff et al. [85]. The maximum values for contact angles on paraffinic hydrocarbons can be as high as 110°, while those for aromatic hydrocarbons are only 85°, and since the composition of coal organic matter varies as shown in Fig. 2.3, Rosenbaum and Fuerstenau were able to demonstrate that their model is able to explain the maximum on the contact angle vs. rank curve.

By extending this model, Keller developed the patchwork assembly model [86].

Upon writing the Cassie equation for a composite material that contains organic matter and mineral matter, Keller obtained

$$\cos(\Theta_c) = m \cos(\Theta_m) + (1 - m) \cos(C') \tag{3.17}$$

But the organic matter is porous,

$$\cos(C') = p \cos(\Theta_{por}) + (1 - p) \cos(C'') \tag{3.18}$$

contains hydrophilic functional groups,

$$\cos(C'') = o \cos(\Theta_o) + (1 - o) \cos(C''') \tag{3.19}$$

and also contains aromatic and paraffinic hydrocarbons,

$$\cos(C''') = A \cos(\Theta_a) + (1 - A) \cos(\Theta_p) \tag{3.20}$$

where Θ_c is the contact angle of water on the coal, Θ_m is the contact angle on the mineral matter inclusions, Θ_{por} is the contact angle on pores, Θ_o is the contact angle on
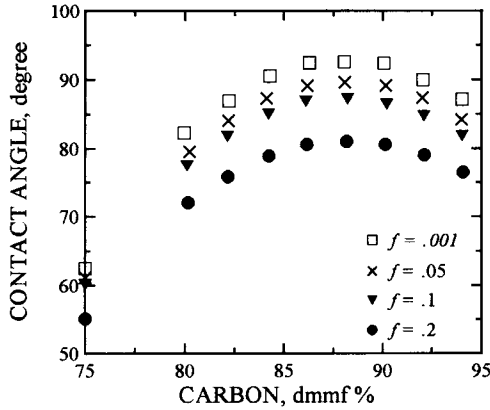
Fig. 3.20. The calculated results for the contact angle of water on coal with no surface oxidation ($h = 0$), and mineral matter varying as ($\square$) 0.1%, $f = 0.001$; ($\times$) 5%, $f = 0.05$; ($\triangledown$) 10%, $f = 0.1$. The lower curve ($\bullet$) shows the results of the calculation for the conditions of 0.1% mineral matter and 20% surface oxidation ($h = 0.2$). (After Keller [86]; by permission of Elsevier Science.)

oxygen polar sites, Θ_a is the contact angle on aromatic hydrocarbons, Θ_p is the contact angle on paraffinic hydrocarbons, m is the fraction of surface occupied by mineral matter, p is the fraction of surface occupied by pores (equal to the equilibrium moisture content in volume percent), o is the weight fraction of oxygen and A is the fraction of surface area occupied by aromatic molecules.

By inserting Eqs. (3.18)–(3.20) into Eq. (3.17), by assuming $\Theta_a = 88°$, $\Theta_p = 110°$, $\Theta_o = 0°$, $\Theta_{por} = 0°$ and $\Theta_m = 0°$, and by assuming functional relationships between oxygen content and carbon content (rank), aromatic hydrocarbons content and carbon content, and porosity and carbon content, Keller was able to predict the values of contact angles for various coals. An example of such calculation is shown in Fig. 3.20.

It is worth pointing out that in Keller's model, porosity is assumed to play a very important role in determining coal surface wettability. Keller assumes that pores are filled with water and so they increase wettability of the coal surface. It is easy to show that this effect must depend on coal wettability [6]. For hydrophobic coals, water will not be able to displace air from pores so these will rather increase coal hydrophobicity. The pores will, however, quickly be filled with water in hydrophilic coals and will definitely increase their overall wettability. This phenomenon has a very important bearing on the properties of coal water slurries.

As discussed in Section 3.2.1, the contact angle on a smooth unoxidized surface of a bituminous coal should be about 100°. The maximum measured values are not larger than about 70° (Figs. 3.2 and 3.3). If it is assumed in accordance with Fig. 2.3 that the ratio of aromatic to aliphatic hydrocarbons in a low-volatile bituminous coal is about 80 : 20 then Eqs. (3.19) and (3.20) can be written as follows:

$$\cos \Theta_c = x \cos \Theta_o + (1 - x) \cos \Theta_h \tag{3.21}$$

where x is the fraction area of hydrophilic sites, $\cos \Theta_o$ is the contact angle on the hydrophilic sites ($\cos \Theta_o = 0$), and $\cos \Theta_h$ is the contact angle on the coal hydrocarbon

matrix. And

$$\cos \Theta_h = a \cos \Theta_{ar} + (1 - a) \cos \Theta_{al} \tag{3.22}$$

where a is the aromatic fraction area on coal hydrocarbon matrix (in this case $a = 0.8$), $\cos \Theta_{ar}$ is the contact angle on the aromatic hydrocarbon sites ($\Theta_{ar} = 85°$), and Θ_{al} is the contact angle on the aliphatic hydrocarbon sites ($\Theta_{al} = 110°$).

Eq. (3.22) gives $\Theta_h = 89.9°$ and from Eq. (3.21) one can get that $x = 0.34$. The answer then is that at least about one third of the bituminous coal surface is occupied by hydrophilic sites (that also includes mineral inclusions and pores filled with water). For a very hydrophobic surface for which $\Theta_h = 89°$ the overall result at $x = 0.34$ is $\Theta_c = 70°$.[6]

It is to be borne in mind that a fundamental assumption in the use of Cassie–Baxter's approach is that the hydrophilic and hydrophobic areas are small and evenly distributed on the composite surface. As in Keller's model, the pores were assumed to be filled up with water and thus also provided hydrophilic sites, which for a very hydrophobic bituminous coal does not have to hold true.

The method (based on Zisman's critical surface tension concept) of estimating the content of hydrophilic sites on a heterogeneous hydrophobic surface can be found in Kelebek's paper [89].

While Keller's model brings us much closer to an understanding of coal surface properties, it is to be kept in mind that in all practical situations coal composition is usually determined by petrographic analysis which is not utilized in the calculations as shown above. Petrographic analysis is used in many other areas; for instance, it is commonly used to predict coal coking properties and the properties of the coke. This subject will further be discussed in the chapter dealing with coal floatability (see pp. 54–57 and 99–109).

3.6. Effect of coal rank on floatability

As Figs. 3.2 and 3.3 demonstrate, medium-volatile bituminous coals are most hydrophobic. Flotation tests carried out under some standardized conditions with different coals confirm such conclusions.

Fig. 3.21 shows flotation results [90] for coals varying in rank using light fuel oil. At the time of these tests (1961), fuel oils produced from coal tars were commonly utilized in coal flotation as a universal collector–frother. These products are characterized by a high content of phenols and other toxic aromatic compounds and are no longer used in coal flotation.

In 1951, Horsley and Smith [19] concluded that in order to obtain equal recoveries a larger quantity of reagents were required for anthracites and lignites than for bituminous coals. Fig. 3.22 shows Brown's results [91] in which the amount of reagent needed for

---

[6] It is worth noting that recent reexamination of advancing contact angles on coal with the use of the improved methodology of coal sample preparation [87,88] indicate that these contact angles may reach values larger than 85°.
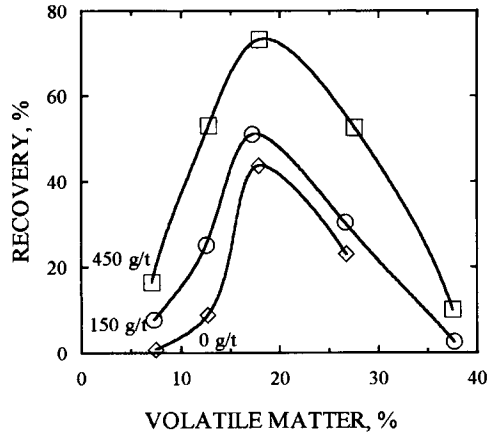
Fig. 3.21. Flotation of coals varying in rank using light tar oil. (After Shebanov [90].)
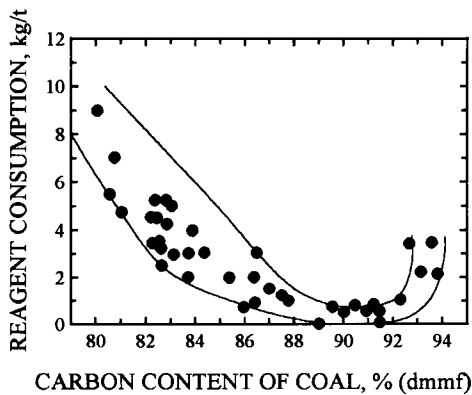
Fig. 3.22. Variation of reagent consumption (cresols) with carbon content of coal. (After Brown [91]; by permission of the American Institute of Mining, Metallurgical and Petroleum Engineers.)

flotation is plotted versus the coal carbon content. Both Figs. 3.21 and 3.22 indicate that bituminous medium- and low-volatile coals float the best.

Fig. 3.23 is taken from a more recent publication [92]. In this Fig. 3.10u and Aplan demonstrate that while MIBC alone is sufficient to float the very hydrophobic bituminous coals, a combination of MIBC (frother) and an oil (collector) is needed to float lower-rank coals. Aplan [93] noted a semi-logarithmic relationship between the fuel oil collector and the carbon content in coal.

3.7. Floatability of coal macerals

As Fig. 3.24 taken from Klassen's monograph [20] shows, coal particles varying in size and petrographic composition behave differently in the process. As this figure
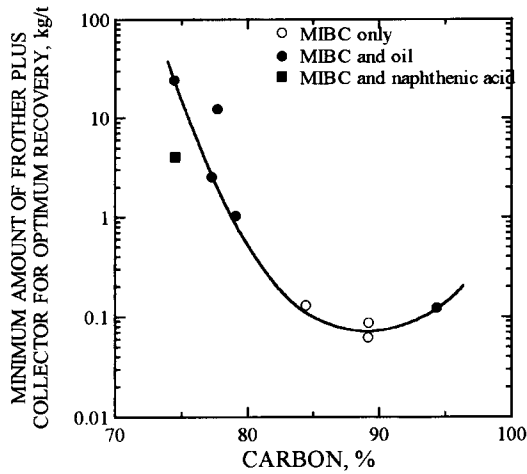
Fig. 3.23. Minimum amount of frother and collector for optimum recovery of coals of various carbon contents (After Xu and Aplan [92].)
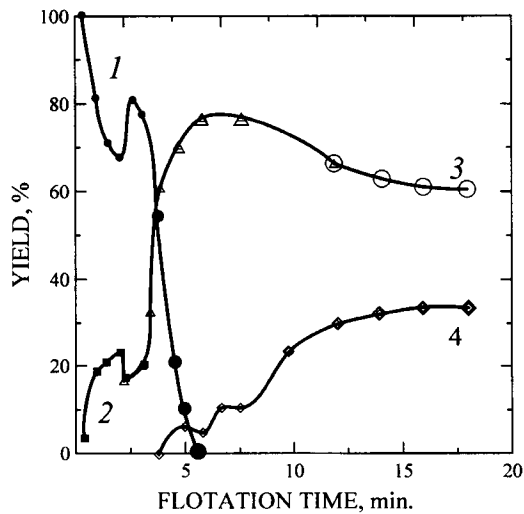
Fig. 3.24. Effect of petrographic composition and particle size on coal flotation kinetics. 1, bright coal; 2, dull coal; 3, shale interlocked with dull constituents; 4, gangue. The size of the points represents the particle size. (After Klassen [20].)

indicates, fine bright particles dominate in the first products and only with time coarser particles and dull constituents start floating. Large particles, including particles which are not liberated, float only when the fine particles are removed from the cell. These data correlate very well with Horsley and Smith's observations [19] which indicate that bright petrographic components (vitrain) are more hydrophobic and float better than dull components (durain). As Table 3.1 [91] shows, vitrinite dominated

Table 3.1
Flotation of coal lithotypes [91]

Concentrate drawn from:	Recovery, % of feed	Coal type (%)		
		Brights (vitrain)	Fusain	Dull (clarain, durain)
First 4 cells	65	80	20	–
Middle 4 cells	30	2	28	70
Last 4 cells	5	2	33	65
Total concentrate	100	52.6	23	24.4

in the froth products collected from the first cells in one of the British commercial plants. All of these results point to different response of petrographic constituents to flotation.

This is a complicated matter because on one hand coal macerals differ in chemical composition and properties (Fig. 2.5), but on the other, with increasing rank they become chemically similar and are less petrographically distinct. Vitrinites exhibit a decrease in aliphatic H content from the high-volatile bituminous to anthracite, and a general increase in aromatic H values with increasing C content [94]. Aliphatic H content decreases systematically with decreasing total H content after high-volatile bituminous rank, whereas there is a general progressive increase in aromatic H as the total H content decreases. Sporinites (exinite maceral group) from subbituminous and high-volatile bituminous coals were found to contain more aliphatic H than vitrinites, and less oxygen. In medium-volatile bituminous coal, differences in maceral chemistry are of much lower magnitude than in high-volatile bituminous coal.

In rather good agreement with these conclusions, Arnold and Aplan [95] found that hydrophobicity of coal macerals follows the pattern: exinite > vitrinite > inertinite.

Bujnowska [96] tested flotation properties of different petrographic constituents separated from a subbituminous coal which did not float at all without flotation reagents.

Flotation was possible with the addition of some heteropolar reagents, such as diacetone alcohol, and under such conditions inertinite floated the best, then vitrinite, followed by exinite. Horsley and Smith [19] observed that the floatability of fusinite (inertinite group of macerals), which floated quite well, was very much affected by prolonged immersion in water (under these conditions vitrinite particles were not affected by immersion in water at all) and this probably explains the differences observed by some authors.

Klassen [20] was also of the opinion that as a result of high porosity, inertinite macerals become quite hydrophilic in water and float poorly. However, in the case of oxidized coals, inertinite macerals may float better than vitrinite as they are more resistant to oxidation than vitrinite. In general, Klassen points out that better flotation of bright petrographic constituents (vitrinite) results from oriented adsorption of heteropolar molecules (e.g. frothers) on their surface.

The conclusions regarding the behavior of coal macerals in flotation are further complicated by mineral matter content. It was shown [97] that the effect of petrographic composition of coal particles on their flotation properties can be studied only for fresh

(unoxidized) and low ash samples. The -1.3 g/cm^3 density fraction of a high-volatile bituminous coal (which is a concentrate of well-liberated vitrinite macerals), was the most hydrophobic, while the $1.3–1.35$ density fraction (which was a concentrate of interlocked vitrinite with inertinite) was much less hydrophobic. For samples containing more than 15% ash, the surface properties were predominantly determined by mineral matter.

3.8. Experimental methods of characterizing coal wettability

As Fig. 3.5 and Eq. (3.11) show, solid wettability is determined by the balance between the energy of solid/liquid adhesion and liquid cohesion. Although high surface tension liquids (high cohesive energy) mostly give a finite contact angle, measurements with a high-tension liquid such as water demonstrate that the whole range of contact angles from zero to large values is possible depending on the interaction across the solid/water interface.

Eq. (3.11) can be written [7,27]

$$\cos \Theta = 2 \frac{W_{SL}}{W_{LL}} - 1 = 2 \frac{W_{SL}^{LW} + W_{SL}^{AB}}{W_{LL}} - 1 \tag{3.23}$$

Since $W_{SL}^{LW} = W_{SL}^d$, after Fowkes [7] it can be calculated from

$$W_{SL}^d = 2(\gamma_{H_2O}^d \cdot \gamma_s^d)^{1/2} \tag{3.24}$$

where the dispersion forces contribution to the surface tension of water is $\gamma_{H_2O}^d \cong 22$ mJ/m^2.

Then for $W_{SL}^{AB} \cong 0$ one can get

$$\cos \Theta \cong 2 \frac{W_{SL}^{LW}}{W_{LL}} - 1 \tag{3.25}$$

Since for all solids $W_{SL}^{LW} < W_{LL}$ Eq. (3.25) indicates the solid is always hydrophobic, $\Theta > 0°$, whenever $W_{SL} \cong W_{SL}^{LW}$. All solids would then be hydrophobic if they did not carry polar or ionic groups that can strongly interact with water molecules [26]. It is thus obvious that since coals may contain many different polar groups, their wettability by water must strongly depend on the content of such groups (or coal rank, oxidation and inorganic impurities).

Although the procedure for measuring contact angles is simple, it is not easy to obtain reproducible results. The measurements on flat polished surfaces will be discussed first, and these will be followed by the methods used to measure contact angles on granular materials.

3.8.1. Contact angle measurements on flat surfaces

The thermodynamic equilibrium contact angle, Θ_Y, is a unique function of the interfacial tensions γ_{SV}, γ_{SL}, and γ_{LV} given by the Young equation (SV, SL and LV stand for solid/vapor, solid/liquid and liquid/vapor interfaces) (Fig. 3.25).
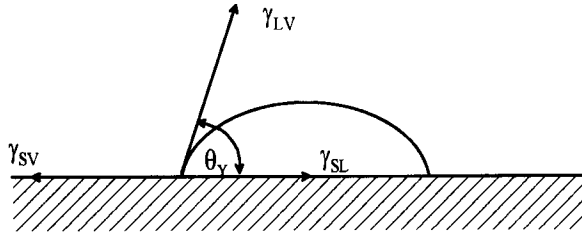
Fig. 3.25. Wettability of hydrophobic solid by water.

$$\gamma_{SV} = \gamma_{SL} + \gamma_{LV} \cos \Theta_Y \qquad (3.26)$$

The Young equation was developed for an ideal solid surface, namely a perfectly smooth, chemically homogeneous, rigid, insoluble and non-reactive surface [98]. For such a surface, the contact angle is the same at each point along the contact line. Since real solid surfaces are rough and chemically heterogeneous to some extent, the contact angle may change from one point to another along the contact line, a fact well known to all carrying out such measurements.

The usual optical methods for measuring contact angles yield the apparent contact angle. This is the angle between the line which is tangent to the bubble/droplet at the point of three-phase contact and the line described by the solid surface. The apparent contact angles on real surfaces exhibit hysteresis. A simple experiment with a droplet placed on a plate tilted to the point of incipient motion will reveal that there is a large difference between the contact angle at the leading edge and the contact angle at the trailing edge (Fig. 3.26). The difference between the advancing contact angle (Θ_A) and receding angle (Θ_R) is referred to as hysteresis. It is large for heterogeneous solid surfaces. According to Good [99], on a patch-wise heterogeneous surface, the advancing angle is related to — and may be equal to — the equilibrium angle that would be

Fig. 3.26. Shape of liquid droplet on inclined solid surface.

Fig. 3.27. Examples of captive droplet (a) and captive bubble (b and c) methods of contact angle measurements.

observed on a homogeneous, flat surface composed of the lower-energy (hydrophobic) component. Similarly, the receding angle may be considered to characterize the higher-energy (more hydrophilic) component.

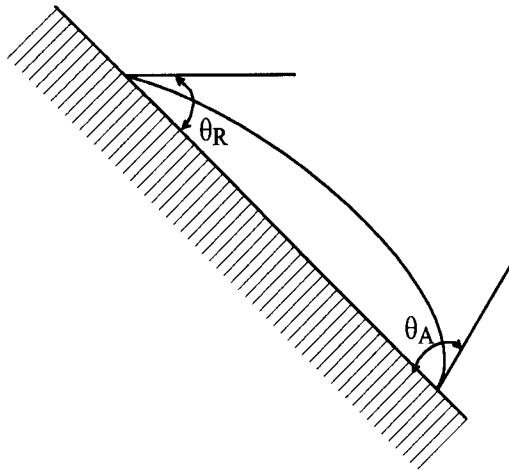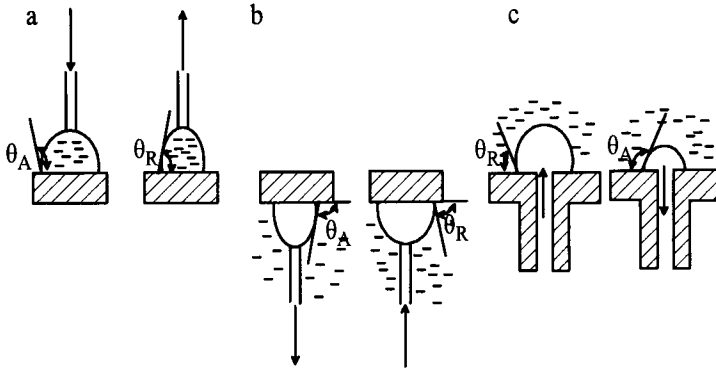Only certain methods allow measurement of both advancing and receding contact angles. According to Good [15,16], a sessile drop measurement where the drop is allowed to fall on the solid, tends to yield contact angle values that approximate (but are less than) the advancing values. The sessile bubble method which utilizes bubbles that are not retired on the bubbling tip yields an angle that is approximately equal to (but greater than) the receding angle. Especially recommended are the captive bubble and captive drop methods. Fig. 3.27 taken from the paper by Drelich et al. [100] illustrates the principles of the methods which were adapted following some previous publications [101,102].

Both techniques require a goniometer (such as, for instance, a Rame-Hart Inc. goniometer). The optical system of the goniometer has independently rotatable cross-hairs and an internal protractor readout calibrated in 1° increments. The supporting stage of the instrument is calibrated on both the horizontal and vertical axes in 0.02 mm divisions to accurately measure the drop (bubble) base diameter. A controlled-atmosphere chamber can also be used if required. Modern version of this instrument allows for automatic imaging of the drop (bubble) shape and analysis of the drop (bubble) shape using the Young–Laplace equation. The contact angle is determined by the slope of the contour line at the three-phase boundary point.

As Fig. 3.27 shows, in both techniques a microsyringe is used with a stainless steel needle (0.5 mm in diameter) which remains in contact with either the drop (captive-drop method), or the bubble (captive-bubble method). Precautions are needed to avoid distortion of the drop shape by the needle. The outer surface of the needle should be coated with paraffin to stop the liquid from climbing up the needle and to protect against the formation of a concave meniscus [100]. The tip of the needle should always be kept at the top of the captive drop/captive bubble to avoid distortion of a shape of the liquid drop/gas bubble (for more details see Drelich et al. [103]).

The captive-bubble technique involves a small air bubble at the tip of a U-shaped needle supplied via a microsyringe; by moving it up the bubble touches the coal surface. The three-phase contact line of the gas bubble is made to retreat or advance by increasing or decreasing the volume of the bubble, and the receding and advancing contact angles are measured with a goniometer within 30–60 s on both sides of the air bubble. The advancing and receding contact angles are measured varying the bubble size.

In the captive-drop technique, a water drop is introduced onto a coal specimen equilibrated in the chamber with water vapors and either advancing (when droplet volume is increased) or receding contact angle (when droplet volume is reduced) is measured.

Coal is porous and its moisture content depends on the humidity of the surrounding environment. Elyashevitch [18] showed that the coal moisture content strongly affects the value of the measured contact angle; this effect was claimed to be particularly strong for low-rank coals. Also Gutierrez-Rodriquez et al. [13] confirmed that humidity affects the sessile-drop contact angles and showed that increased humidity during contact angle measurements reduced the advancing contact angles. This is not surprising, and in Keller's patchwork assembly model of coal surface [86], porosity and humidity play an important role in determining contact angle values. The measurements then require a constant and defined humidity, and this is easier to maintain during contact angle measurements with the captive-bubble technique, since both the coal specimen and air bubble become saturated with water after several minutes of contact. This technique is recommended to characterize coal wettability in coal-related research [87,88].

Surface preparation. The wetting of a surface by a liquid is affected by the roughness of the surface. The value of the equilibrium contact angle (intrinsic angle) is related to the apparent contact angle measured on a rough surface by Wenzel's equation

$$\cos \Theta_a = r \cos \Theta_e \tag{3.27}$$

where Θ_e is the equilibrium contact angle[7], Θ_a is the apparent contact angle and r is the surface roughness ratio ($r = a/A$, a is the actual surface area of the solid, and A is the geometric surface area). This treatment assumes that the surface features of the solid are insignificant compared to the drop dimensions. Measurements on two polytetrafluoroethylene (PTFE) films revealed that nanometer size surface roughness strongly influences the wetting of hydrophobic materials. Both advancing and receding contact angles on the more rough PTFE surface were much larger [105]. Eq. (3.25) is now believed to hold for large droplets/bubbles. For homogeneous and smooth solid surfaces the measured angles do not depend on the radius of the droplet/bubble [98]. The measurements on the PTFE film roughened by polishing with a 600-grit polishing paper showed that the captive-drop receding angle was clearly dependent on the droplet size. The hysteresis was found to depend on the size of droplets: it was large for small (2 mm) bubbles but decreased for larger bubbles (5 mm and more) [100].

Contact angle depends not only on surface roughness, but also on surface heterogeneity. As Eqs. (3.17)–(3.20) show, surface wettability depends on the surface

---

[7] According to some authors [104], the equilibrium contact angle can be calculated from $\cos \Theta_e = (\cos \Theta_A + \cos \Theta_R)/2$.

heterogeneity. According to Cassie's equation, the apparent contact angle measured on a surface that contains two components characterized by the Θ_1 and Θ_2 intrinsic contact angle values, is given by:

$$\cos \Theta_a = f_1 \cdot \cos \Theta_1 + f_2 \cdot \cos \Theta_2 \qquad (3.28)$$

where f_1 is the area fraction of the surface having an intrinsic contact angle Θ_1 and f_2 is the area fraction of the surface having an intrinsic contact angle $\Theta_2 (f_1 + f_2 = 1)$. Drelich's contact angle measurements on fluorite treated in sodium oleate solutions varying in concentration revealed that hysteresis increases with increasing hydrophobicity of fluorite (increasing concentration of sodium oleate) [106,107]. This is in agreement with Rhebinder's data [108] who, using the captive-bubble method, showed that increasing concentration of xanthate increased the hydrophobicity of galena while also substantially increasing the hystereris. Drelich et al. [109] also demonstrated that the dependence of the contact angles measured by the captive-drop method on droplet size, which was insignificant for hydrophilic surfaces, sharply increased with increasing hydrophobicity. These conclusions seem to be very relevant to coal which is very heterogeneous and hydrophobic.

A collaborative research program between the University of British Columbia and the Michigan Technological University [87,88] resulted in a set of recommendations that detailed how a coal surface should be polished for contact angle measurements. This recommended procedure involves the following steps.
(1) Wet coarse polishing of the coal sample with a series of abrasive papers, from 60 grit to at least 600–1200 grit.
(2) Washing of the coal sample with a stream of water in order to remove loose pieces of coal and grit which might have been liberated/loosen during the coarse polishing.
(3) Wet surface polishing using fine alumina powder, 0.05 µm fraction or less, to smooth the roughness left after coarse polishing with abrasive papers.
(4) Repeat (2).
(5) Cleaning of the coal sample in an ultrasonic bath filled with water for about 10 min in order to remove the remaining attached alumina particles. This should be followed by (2).
(6) Wet polishing/cleaning of the coal surface with a polishing cloth, inactive to coal (e.g. Chemomet from Buehler) to remove alumina particles that are strongly attached to the coal.
(7) Additional cleaning of the sample in an ultrasonic bath for a few minutes followed by (2).

The following examples were selected to illustrate how the recommended procedure affects reproducibility of the measurements, and reduces the differences between the advancing and receding contact angles.

Fig. 3.28 shows the advancing and receding contact angles measured on C357 coal from Illinois (5.0% ash, 8.64% moisture, 37.2% V^{dmmf} and $FC^{dmmf} = 62.8\%$) (dmmf = dry-mineral-matter-free). The coal surface was polished with 600-grit abrasive paper and washed with distilled water. As this figure shows, over the range of bubble base diameters from about 1.5 to 5 mm the advancing angle showed a significant change
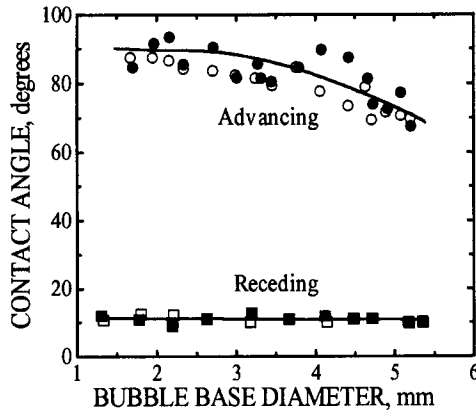
Fig. 3.28. Effect of the bubble size on the water advancing contact angles for a bituminous coal whose surface was polished with the 600-grit abrasive paper. The contact angles were measured at both sides of bubbles. (After Drelich et al. [87]; by permission of VSP.)
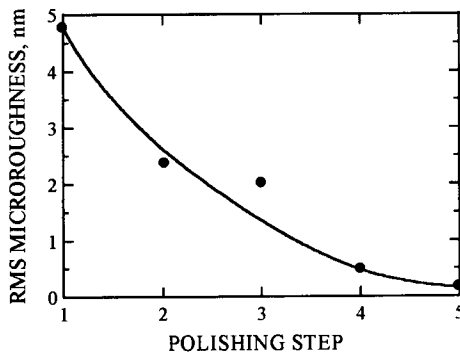

Fig. 3.29. Effect of the polishing stages on the roughness of a bituminous coal sample. The polishing step numbers stand for: (1) polishing with the 600-grit abrasive paper; (2) 5 μm γ-alumina powder; (3) 1 μm γ-alumina powder; (4) 0.06 μm γ-alumina powder; (5) 0.06 μm γ-alumina powder followed by polishing with a CHEMOMET cloth. (After Drelich et al. [87]; by permission of VSP.)

while the receding contact angle remained practically constant. A significant change of the contact angle with bubble size suggests the presence of imperfections on the solid surface. The roughness of the polished surface was studied using an atomic force microscope and electron scanning microscope. Fig. 3.29 shows the effect of the following polishing stages on the roughness of the C357 sample. As seen, the root mean square (RMS) roughness dropped from about 5.8 nm for the surface polished with a 600-grit paper to 0.5 nm for the surface polished with 0.06 μm alumina powder. Since coal contains mineral inclusions with different hardnesses (for example, while on Moh's scale coal hardness is 1–4, quartz is 7, pyrite 6–6.5, and dolomite 3.5–4), polishing with alumina powder produces the surface shown in Fig. 3.30. While polishing with an abrasive paper produces flatter surfaces, such surfaces contain grooves on the order of a
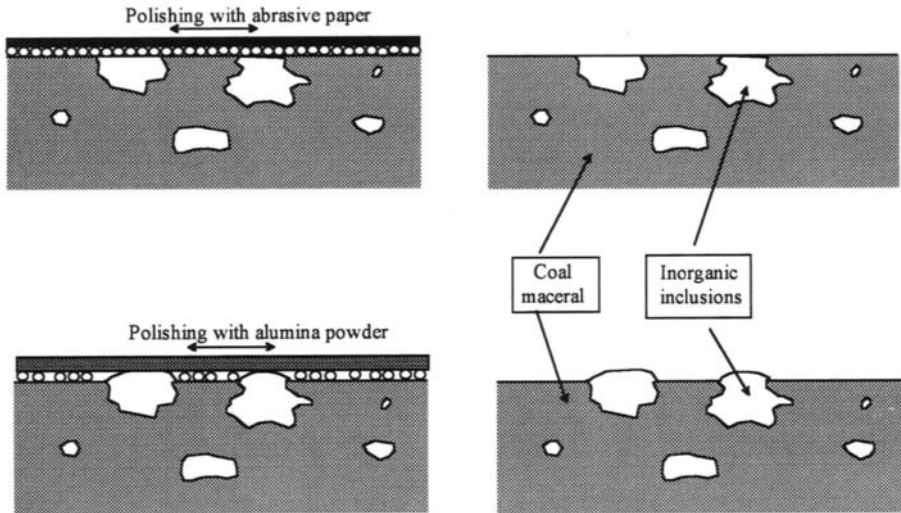
Fig. 3.30. Illustration of the action of the abrasive paper and alumina powder during the polishing of heterogeneous specimen such as coal. (After Drelich et al. [87]; by permission of VSP.)

few micrometers wide [87]. Further polishing with polishing powders is thus necessary, but this in turn requires thorough cleaning to remove the hard powder particles (alumina hardness is 8) from the coal surface. Any irregularities resulting from over-polishing with the polishing powder affect the measured apparent contact angle as shown in Fig. 3.31.

The effect of the various polishing stages on the measured advancing and receding contact angles is shown in Fig. 3.32. Both advancing and receding contact angles decreased on coal surfaces polished with 5 μm and 1 μm alumina powder, compared with those polished with a 600-grit abrasive paper only. The contact angles increased on the coal surfaces polished with 0.06 μm alumina powder, and cleaning with a Chemomet cloth was found to be very important [87].

It is also worthy of mention that the measured advancing and receding contact angles have recently been reported to depend on vibrations; large vibration levels were found to mitigate hysteresis [104].

3.8.2. Contact angle measurements on granular material

Measuring contact angles on powders is more difficult than on flat polished surfaces and various methods have been developed [101].

3.8.2.1. Direct measurements on compressed discs

In this method fine coal particles are compressed into a disc on which the contact angle is measured. Obviously the surface of the disc is porous (Fig. 3.33), and its smoothness is far from being perfect. If it is assumed that the surface is hydrophobic enough so that the capillary forces will not allow filling the pores with water, then the contact angle measured on the disc, Θ', is greater than that on the solid alone, Θ. The
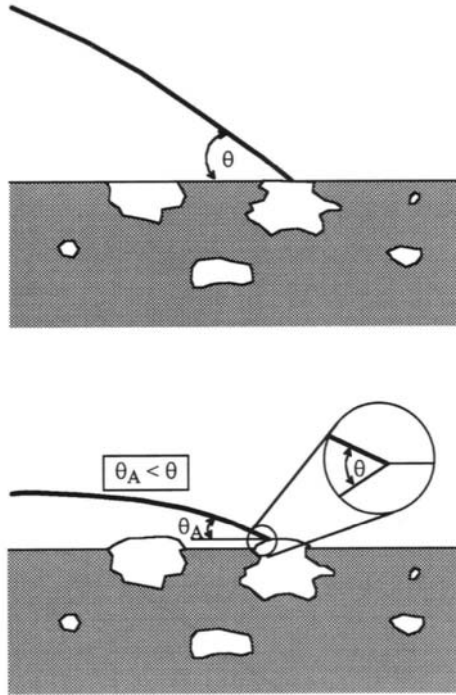
Fig. 3.31. A liquid in contact with a heterogeneous surface after polishing it. (After Drelich et al. [87]; by permission of VSP.)

POLISHING MATERIAL
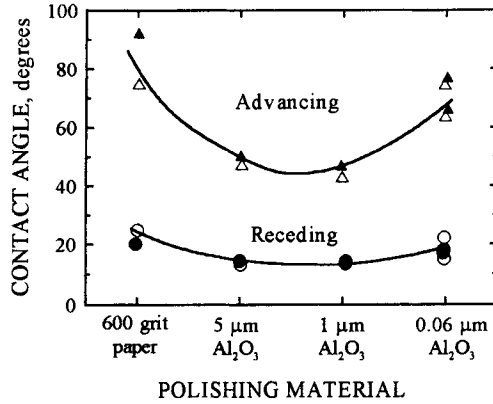
Fig. 3.32. Example of the effect of polishing of coal surface on water advancing and receding contact angles. (After Drelich et al. [87]; by permission of VSP.)

Cassie–Baxter equation for this case gives

$$\cos \Theta' = f_1 \cdot \cos \Theta - f_2 \tag{3.29}$$

f_2 represents the fractional area of pores on the disc surface and it was shown that it can be obtained through the measurement of disk bulk porosity [6].
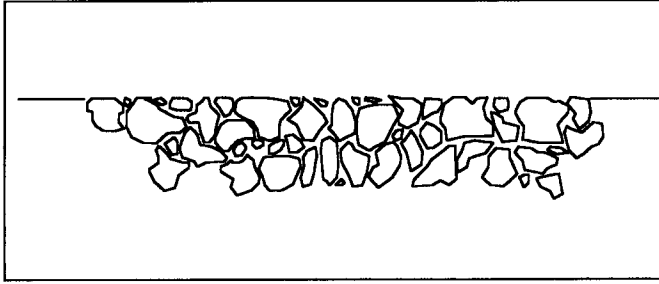
Fig. 3.33. Surface of the disc obtained after compression of fine coal.

As Eq. (3.29) shows, the contact angles measured on discs prepared from fine particles strongly depend on the discs' porosity [6].

Also, since the surface is not quite smooth, and is heterogeneous, the liquid–vapor interface near the solid is highly distorted by local imperfections and this affects the measured values if they are directly read through the goniometer. It was shown that the axisymmetric drop method developed by Rotenberg et al. [110] to calculate the contact angle value from the main profile of the drop instead of the distorted part near the solid surface is more reliable for such measurements [6].

Fig. 3.34 shows the measured and corrected for porosity contact angles for a 1.3 density fraction (2.6% ash content) of bituminous coal (ground 95% below 10 μm and compressed into a disc) [6]. As seen, with the pressure applied to compress the powder into a disc exceeding 25 mPa the contact angle reaches its plateau and does not change with further increase in pressure.

Fig. 3.35 shows another important feature of this technique. The apparent contact angle (measured in a thermostatted chamber saturated with water vapor), if measured

Fig. 3.34. Contact angles measured on the surface of the disc compressed from fine coal plotted vs. the pressure applied in disc preparation. (After He and Laskowski [6]; by permission of Gordon and Breach.)

Fig. 3.35. Effect of the time of contact with water on the contact angle values measured on the discs prepared from −1.3, 1.4–1.5, 1.5–1.6 and 1.6–1.8 density fractions. (After He and Laskowski [6]; by permission of Gordon and Breach.)
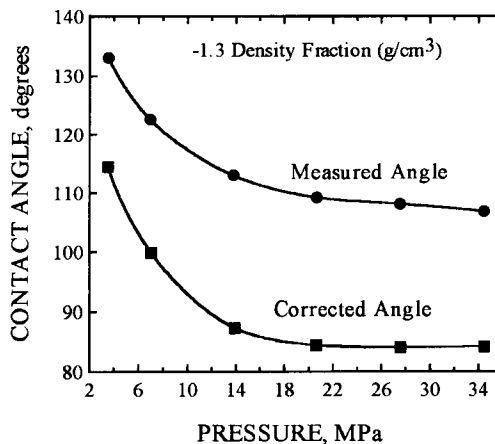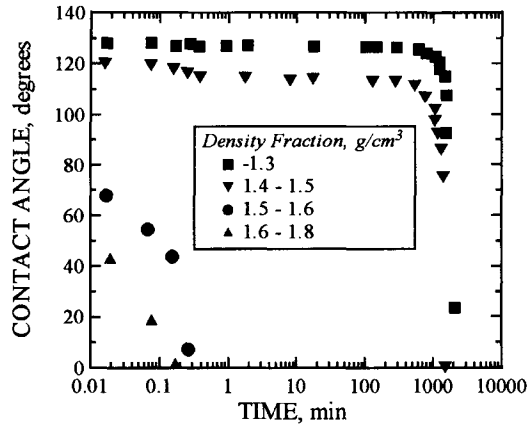
versus time, strongly depends on solid wettability. For hydrophobic discs, the contact angle is stable over a very long period of time (up to 500 min), but quickly decreases for less hydrophobic samples. The various coal density fractions utilized in these measurements contained: −1.3 density fraction 2.6% ash, 1.4–1.5 fraction 18.8% ash, 1.5–1.6 fraction 39.6% ash, and 1.6–1.8 fraction 41.4% ash. It is obvious that high-ash fractions are much less hydrophobic and that any water droplet placed on the surface of such a disc will immediately be sucked into capillaries by a capillary force. Thus, for less hydrophobic coals, pores can quickly be filled with water, and therefore the porosity may lead to smaller measured contact angles [6]. Because the discs produced by compression of fine coal particles are porous, and because it is uncertain how the porosity will affect the measured contact angle value, this technique is not considered very reliable. Using this method, Murata [111] reported contact angle values in the range from 90 to 110° for coals containing 20% to 30% oxygen; these values are much larger than expected. To allow contact angle measurements in cases where the liquid penetrates into the disc, Kossen and Heertjes [112] presoaked the disc with the measuring liquid and showed that droplets placed on such a surface were stable.

3.8.2.2. Maximum particle-to-bubble attachment method

This method, studied by Hanning and Rutter [113], relies simply on determining the largest particle which can be lifted by a captive air bubble as shown in Fig. 3.36.

To calculate the contact angle from the size of the largest particle held by a bubble, Hanning and Rutter used the following formula:

$$R_{max} = \sqrt{\frac{3\gamma_{LV}}{2\Delta\rho g}} \cdot \sin \Theta/2 \qquad (3.30)$$

where R_{max} is the radius of the largest particle which can be raised against gravity, and $\Delta\rho$ is the density difference between the solid and liquid.
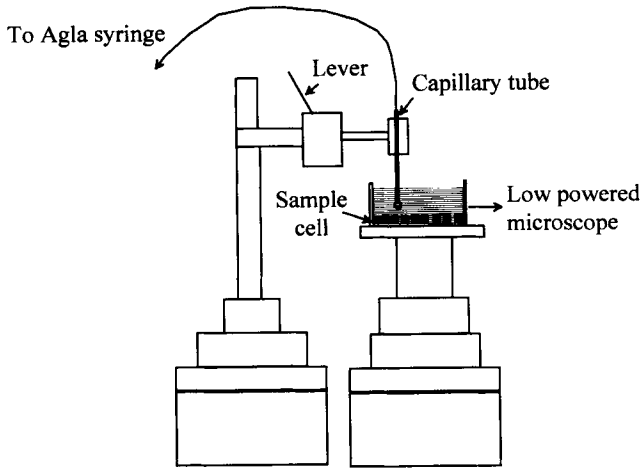
Fig. 3.36. A set-up used by Hanning and Rutter to determine the size of the particles attached to bubbles. (After Hanning and Rutter [113]; by permission of Elsevier Science.)

Using this method they determined the wettability of four coals containing from 67.2% to 76.6% carbon (air-dried basis). The contact angles calculated from the bubble-pickup tests were all in the range from 12° to 29°. A conventional sessile-drop method gave contact angles ranging from 61° to 78° for the same coals. The agreement is quite obviously disappointing.

Drzymala and Lekki's flotometric technique allows determination of the maximum size of the particles floating in a Hallimond tube [114,115]. Using Eq. (3.30), Drzymala calculated [115] the detachment angle [8] from the maximum size of the particles that could be floated and for sulfur, pyrite and paraffin-coated particles obtained 45.6, 49.8 and 92.5±5°, respectively. The results would be quite reasonable if the detachment angles calculated for graphite and molybdenite particles were not 6.2° and 5.9°, respectively, and the corresponding equilibrium contact angles 3.4° and 3.1°.

3.8.2.3. Methods based on the rate of liquid penetration

As is well known, the liquid rises up a narrow capillary if it wets the capillary walls. If the capillary is circular in cross-section and not too large in radius, the meniscus — when the liquid completely wets the capillary walls — will be approximately hemispherical and the pressure gradient, ΔP, across the curved liquid interface will establish.

$$\Delta P = \frac{2\gamma_{LV}}{r} \qquad (3.31)$$

where r is the radius of the capillary.

If h denotes the height of the meniscus above a flat liquid surface in a larger container, then ΔP, which is a driving force for liquid penetration, must also equal the

---

[8] This should not be different from the advancing contact angle.

hydrostatic pressure drop in the column of liquid in the capillary.

$$\Delta P = \frac{2\gamma_{LV}}{r} = \Delta\rho h g \tag{3.32}$$

and this relationship is frequently used to measure the surface tension of liquids.

If the liquid meets the circularly cylindrical capillary wall at some angle, Θ, and the meniscus is still taken to be spherical in shape

$$\Delta\rho h g = \frac{2\gamma_{LV}\cos\Theta}{r} \tag{3.33}$$

this relationship can also be used to determine the contact angle between the walls of the capillary and the wetting liquid.

The penetration rate is given by the Hagen–Poiseuille equation:

$$\frac{d\ell}{dt} = \frac{r^2}{8\eta\ell}\Delta P \tag{3.34}$$

where ℓ is the distance of penetration, r denotes the average radius of the capillary, and h is the viscosity of the liquid. Since the capillary pressure, which drives the liquid into capillary, is given by Eq. (3.32) the penetration rate is then

$$\frac{d\ell}{dt} = \frac{r^2}{8\eta\ell}\frac{2\gamma_{LV}\cos\Theta}{r} \tag{3.35}$$

One thus arrives at the important conclusion that the rate of liquid penetration into a capillary can be related to the wettability of the capillary walls.

3.8.2.4. Penetration rate method

Among various methods used to characterize the wettability of powders, the penetration rate method based on the Washburn equation is frequently used. In this method, the rate of penetration of liquid into a bed of fine particles is measured.

For the case when the tube holding a bed of fine particles is vertical (Fig. 3.37), and the height h through which the liquid has risen is small (initial stage) so that the gravity effects can be neglected, by replacing the length ℓ by h, and integrating assuming that the distance $h = 0$ at $t = 0$ (initial penetration rate), one arrives at the Washburn equation:

$$\frac{h^2}{t} = \frac{r\gamma_{LV}\cos\Theta}{2\eta} \tag{3.36}$$

For a powder packed uniformly into a tube, the system may be considered to consist of a bundle of capillaries, of hypothetical mean radius r. The distance of penetration is (kh), where k is a factor introduced to allow for the tortuous path of the capillaries. The Washburn equation then becomes

$$(kh)^2 = \frac{rt\gamma_{LV}\cos\Theta}{2\eta} \tag{3.37}$$

For a given packing of powder in the column, the values assigned to r and k will be constant, and, hence, by rearrangement of Eq. (3.37) one gets

$$\frac{h^2}{t} = \left(\frac{r}{k^2}\right)\frac{\gamma_{LV}\cos\Theta}{2\eta} \tag{3.38}$$
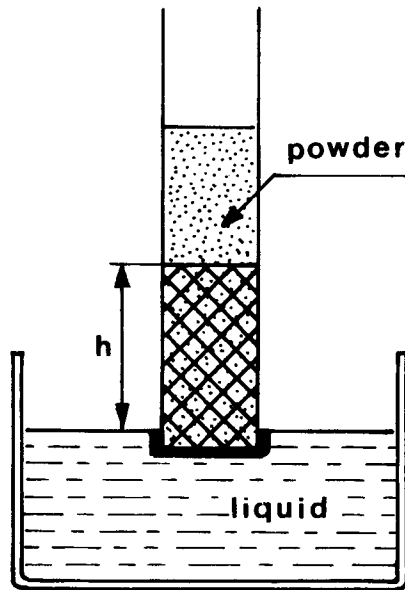
Fig. 3.37. A set-up used for the penetration rate measurements.

Before the contact angle can be determined from Eq. (3.38), r/k^2 must be estimated. This is done by a separate calibration step in which a liquid that wets the particles completely ($\cos \Theta = 1$) is utilized. The method has been used to study the wettability of various powders [116–118]. Fig. 3.37 shows the usual set-up.

This simple technique poses many difficult problems. One concerns packing; a strict and reproducible powder packing is essential since the r/k^2 factor determined in the calibration step must be maintained constant in all the tests. Another problem results from the way in which liquids wet solid particles packed in a tube. The wetting front in some cases is not visible, and in most cases does not reflect accurately the inner progression of the liquid in the bed of packed particles. In cases of very heterogeneous solids such as coal, finding a liquid that completely wets all the particles is practically impossible.

In the procedure described by Tampy et al. [119], the dried coal powder is packed into glass tubes (120 mm long × 10 mm i.d.) having a fritted glass bottom. A standard tapping procedure used to ensure constant packing includes 500 taps, dealt out 50 at a time, interspersed with the addition of more coal to the tube. It was found that after 500 taps, the variation in the final height of the sample in the tube did not change more than 2 mm (by more than 1.7%). In the packing procedure described by Siebold et al. [120], the powder is first introduced stepwise with equivalent subquantities and the column is then dropped about 100 times from a height of 7 to 8 cm. This operation is repeated until the powder reaches a nearly constant value.

To avoid calibration step needed to determine the r/k^2 factor in Eq. (3.36), Tampy et al. [119] introduced the hydraulic radius R which for a circular tube is

$$R = \frac{\pi r^2}{2\pi r} = \frac{r}{2} \tag{3.39}$$

For a bed of fine particles characterized by a bed porosity, ε, and the wetted surface per unit volume of bed, a,

$$R = \frac{\left[\dfrac{\text{void volume}}{\text{bed volume}}\right]}{\left[\dfrac{\text{wetted surface}}{\text{bed volume}}\right]} = \frac{\varepsilon}{a} \tag{3.40}$$

The parameter a is related to the specific surface area of solid particles, a_s, by

$$a = a_s(1 - \varepsilon) \tag{3.41}$$

and for spherical particles, the mean diameter d is related to a_s by

$$d = 6/a_s \tag{3.42}$$

for nonspherical particles, a sphericity factor Φ is introduced, and the hydraulic radius is given by

$$R = d\varepsilon\Phi F/6(1 - \varepsilon) \tag{3.43}$$

To avoid calibration with liquid that does not necessarily perfectly wet the particles, Tampy et al. [119] applied external pressure ΔP_e, which is of the same order of magnitude of the capillary pressure and acts along with it to drive the fluid through the bed. This gives different penetration rates for different applied pressures and allows calculation of the contact angle using the same liquid in all the measurements. The final relationship used to determine the contact angle assumes the following form:

$$\frac{h^2}{t} = \frac{(d\varepsilon\Phi)^2}{75(1 - \varepsilon)\eta}\left[\frac{6(1 - \varepsilon)\gamma_{LV}\cos\Theta}{d\varepsilon\Phi} + \Delta P_e\right] \tag{3.44}$$

A criticism would be that the value of F equal to 0.73 was assumed from the literature for fine coal particles.

The set-up used in the measurements following this modification is shown in Fig. 3.38.

In the procedure as modified by He and Laskowski [121], a fine coal (below 38 μm) is compressed (under high pressure varying from 6.9 MPa to 20.67 MPa) in a MET-A-TEST press with the inner diameter of the mould of 2.54 cm (1″). Following the introduction of the pulverized coal into the press mould, the pressure is slowly increased to a pre-set value and maintained over 5 min. By changing the amount of coal, the height of the column obtained by compressing fine coal is varied from 0.4 to 1.5 cm. Since in this technique no glass tube is required to hold the column, the effect of the tube wettability on the penetration rate of the liquid in the column is eliminated. A porous bed made of degreased cotton is prepared and fitted into a small container of 10 mm in depth and 40 mm in diameter. The bed is saturated with penetrating liquid and the column is placed on the wet cotton bed. Timing is started upon contact. A horizontal penetration borderline along the cylindrical wall, heading slowly upward, can be clearly observed. From each column, only one point is determined: the column height (h) versus the time (t) required for the liquid to penetrate the entire length of the column. The same procedure is repeated for other columns varying in height. A set of experimental data obtained for various density fractions of metallurgical coal from
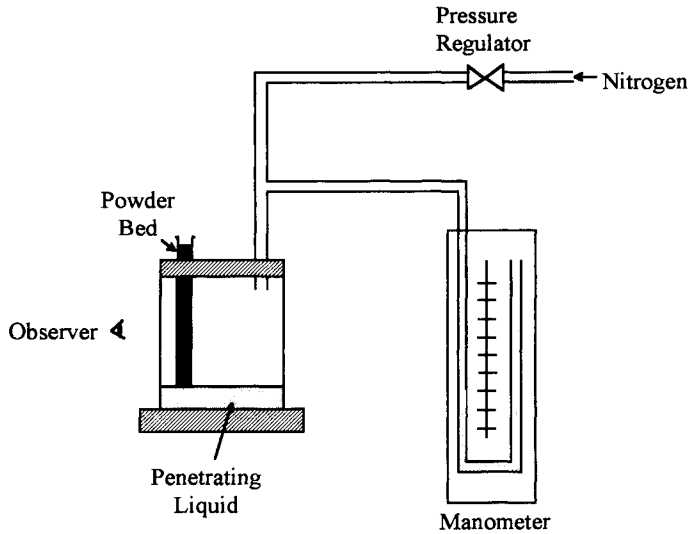
Fig. 3.38. The penetration rate set-up as modified by Tampy et al. (After Tampy et al. [119]; by permission of the American Chemical Society.)
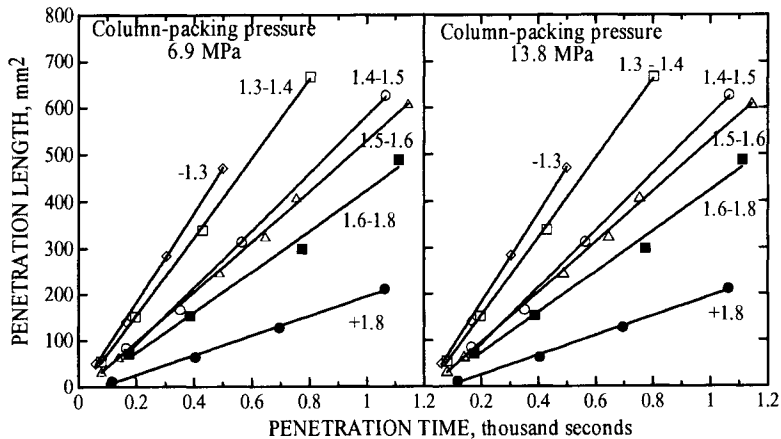
Fig. 3.39. Penetration rate experiments in the columns prepared by compressing different density fractions of fine coal which are characterized by different ash content. (After He and Laskowski [121]; by permission of the Canadian Institute of Mining, Metallurgy and Petroleum.)

Bullmoose mine in British Columbia, and deodorized kerosene (J.T. Baker ChemCo., Philipsburg, NJ) is shown in Fig. 3.39. Ash contents in the density fractions used were as follows: -1.3 g/cm^3 3.8%, 1.3–1.4 g/cm^3 9.2%, 1.4–1.5 g/cm^3 18.5%, 1.5–1.6 g/cm^3 26.9%, 1.6–1.8 g/cm^3 36.3%, and $+1.8$ g/cm^3 78.1%. In this case the radius of the capillaries is so small that as Fig. 3.39 demonstrates, almost perfectly straight lines are obtained, with the penetration rate by kerosene being clearly much higher for more hydrophobic low-ash coal fractions.

Fig. 3.40. A set-up used in the author's laboratory to compact fine powders for the penetration rate measurements.

Since some materials cannot be compressed into columns that are strong enough to withstand handling, a different technique is required for such cases. To measure wettability of talc powders, a column-packing device which is depicted in Fig. 3.40 was devel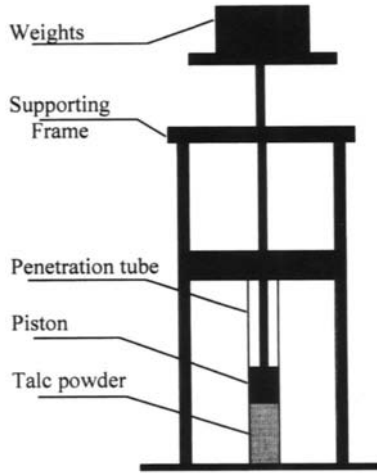oped [122]. In this device, the powder is compacted under controlled pressure (up to 3 MPa) in a tube with an inner diameter of 13.6 mm. Since the distance of penetration h in Eq. (3.36) and the weight of the penetrating liquid, w_l, are interrelated,

$$w_l = \varepsilon A h \rho_l \tag{3.45}$$

to eliminate the problems which visual observation of the wetting front may create, the weight of the column can be monitored on-line using an electronic balance as reported elsewhere [123] (Fig. 3.41). In Eq. (3.45), A stands for the cross-sectional area of the column, and ρ_l stands for the liquid density.

Fig. 3.42 shows the squared weight vs. time for the -400 mesh talc powders compacted in a tube prior to measurement following standard procedures. As seen, the reproducibility is very poor. It was found that whenever the pressure applied to compact the powder exceeded 0.5 MPa, the reproducibility improved remarkably. Fig. 3.43 provides examples of tests with various liquids and two type of tubes: tube A constituted a hydrophilic glass while tube B was made hydrophobic by methylation following the procedure described by Laskowski and Kitchener [26]. As can be seen, the compacting under increased pressure significantly improves the reproducibility of the penetrating tests.

An alternative method was described by Dunstan and White [124]. In this method an external pressure is applied to oppose the capillary pressure and the pressure difference DP which just stops the capillary rise is measured. The equation which was derived to calculate the contact angle is as follows:

$$\Delta P = \frac{\varphi \rho_s a_s}{1 - \varphi} \gamma_{LV} \cos \Theta \tag{3.46}$$
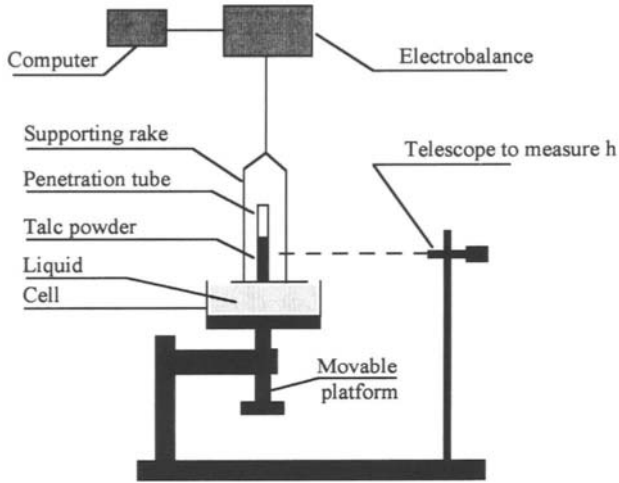
Fig. 3.41. A modified penetration rate set-up in which the weight of the column is monitored on-line versus time.
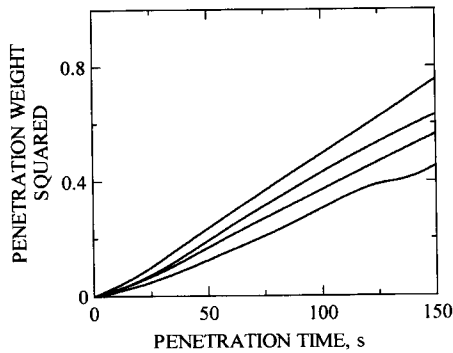
Fig. 3.42. A set of examples of the penetration rate measurements in which fine talc is placed in a tube following standard procedure.

where φ stands for the volume fraction of solid in the packed bed, and ρ_s is the density of the solid.

As can be found from the cited publications [116–120], while the modified experimental procedures are simple enough to be widely used, even for pure liquids the final results are still open to doubt. For example, Siebold et al. [120] reported water contact angles in the range of 50–60° for pure silica particles, and 69 ± 5° for limestone. Thus the use of such methods to study the effect of surfactants on the wettability of solids is very questionable. The capillary penetration of the surfactant solution is characterized by a dependence of surface tension and contact angle on the surfactant concentration near to the meniscus. As shown by Churaev and Zorin [125], three mechanisms of penetration of surfactant solutions into hydrophobic capillaries are possible and at a low surfactant concentration (much below CMC) the rate of

Fig. 3.43. Example of the penetration rate measurements (using the same talc sample as in Fig. 42), following the preparation by compaction with the use of the set-up shown in Fig. 40.

penetration is determined by the surface diffusion of surfactant molecules in front of the meniscus.

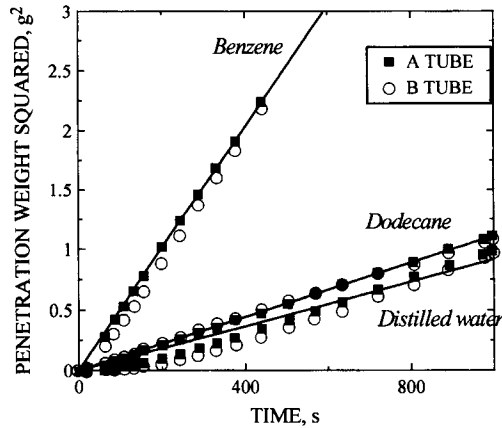A few examples of measurements with surfactant solutions in which the diffusion was neglected follow. Kilau and Pahlman [126] used the liquid penetration method to study the effect of sodium di(e-ethylhexyl) sulfosuccinate on the wettability of fine coal. 0.82% aqueous solutions were employed and deviations from the Washburn equation were noted. Varadaraj et al. [127] used the same experimental procedure to study the effect of various linear and branched surfactants (ethoxylates, sulfates and ethoxysulfates) on the wettability of phenolic resin-coated sand. 0.5% aqueous solutions were utilized. Both the surfactant type and the hydrocarbon chain branching were observed to exert a significant influence on the rate of wetting, but it is not clear whether these effects resulted from the affected solid wettability, or from the diffusion phenomena discussed by Churaev and Zorin [125].

A simple qualitative method of assessing the effect of surfactants on fine-coal wettability was described by Kilau [129]. The schematic diagram that illustrates how this method is applied is shown in Fig. 3.44. In this test, a 40 μm droplet of wetting solution is deposited on a planar bed of −200 mesh dry coal particles. A pure water droplet is shown resting on the coal bed. No coal particles penetrate into the droplet's interior, and instead only coat the droplet's exterior surface. In the case of droplets containing wetting agents, the coal particles are observed to penetrate and migrate into the interior of the droplet rather than the droplet seeping into the interstitial space between the particles. Please note that wetting by water depends on coal wettability (rank) and does not have to mirror the example depicted in Fig. 3.44.

3.8.2.5. Suction potential method

Qiu and Wheelock [129] further modified and used the suction potential method [130,131] to study the wettability of fine coal particles. In this method, a sample of fine coal particles (in Qiu and Wheelock's tests a 35–40 g sample of −210 +149 μm
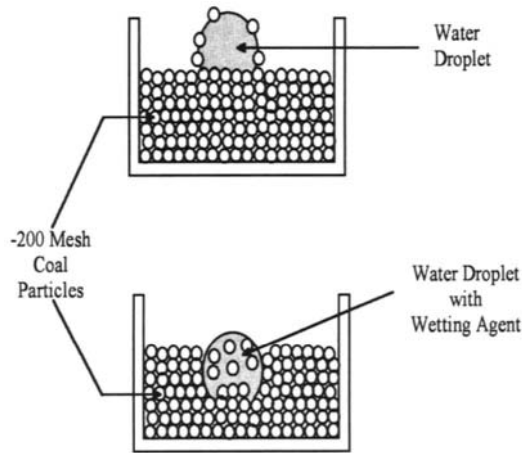
Fig. 3.44. Schematic diagram of the drop penetration test. (After Kilau and Pahlman [128]; by permission of VSP.)

size fraction) is mixed with 250–300 ml of water under vacuum (50 mmHg absolute pressure) for 15–20 min to de-gas the slurry. The slurry is thus transferred into the sample holder where the coal is allowed to settle, and by applying partial vacuum the water surface is drown to within 15–22 mm above the surface of coal bed. Some amount of heptane or hexane (6–8 ml) is then added to the sample holder as shown in Fig. 3.45. Next, water is drained from the sample holder in a series of small increments to measure the volume drained as a function of suction head. The typical result is shown
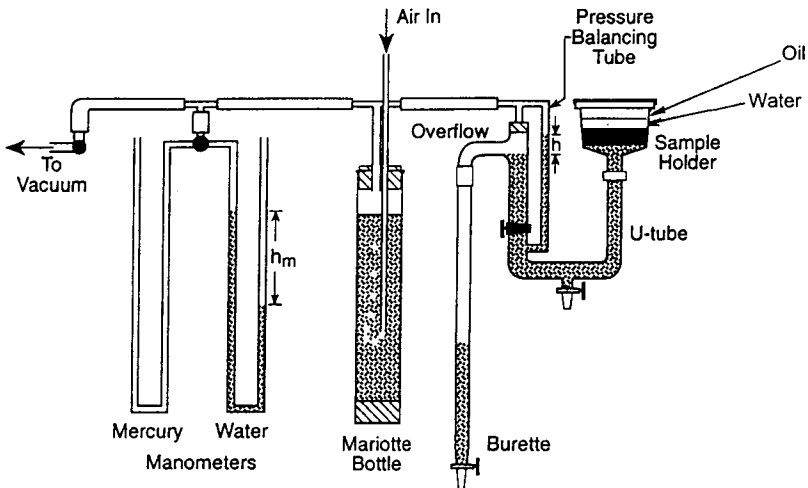
Fig. 3.45. Modified apparatus used by Qiu and Wheelock to measure the three-phase (oil/water/coal) contact angle by suction potential method. (After Qiu and Wheelock [129]; by permission of Gordon and Breach.)

Fig. 3.46. Typical results obtained with the modified suction potential method. (After Qiu and Wheelock [129]; by permission of Gordon and Breach.)

in Fig. 3.46. During the first stage from (a) to (b), the suction pressure is increased and water is drained until the oil/water interface touches the top of the coal bed. During the second stage from (b) to (c), a large increase in the suction is required to draw the oil/water interface into the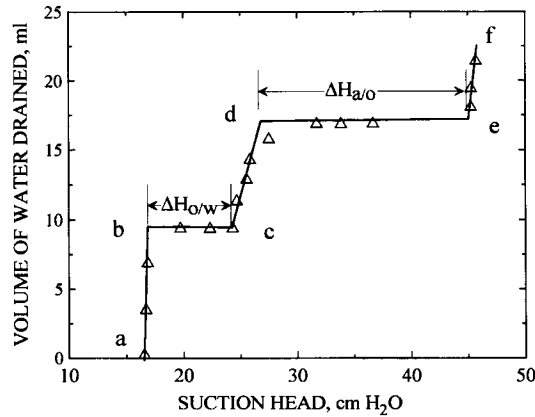 bed while draining the volume of water from the bed. The oil/water/coal contact angle measured through the water phase is calculated as follows:

$$\Delta H_{o/w} = \frac{2\gamma_{o/w} \cos \Theta_{o/w}}{g\rho_w r_{\mathrm{eff}}} \tag{3.47}$$

where $\gamma_{o/w}$ is the oil/water interfacial tension, $\Theta_{o/w}$ is the oil/water/coal contact angle measured through the aqueous phase, g is the acceleration of gravity, and r_{eff} is an effective mean radius of the capillaries in the bed of particles.

During the third stage of (c) to (d), more water is drained from the bed until the air/oil interface just touches the top of the bed. At the same time the oil/water interface is drawn deeper into the bed. During the fourth stage from (d) to (e) (Fig. 3.46) a large increase in suction head is required to draw the air/oil interface into the bed while draining a negligible volume of water from the system. The increase in suction head in this stage is given by

$$\Delta H_{a/o} = \frac{2\gamma_{a/o} \cos \Theta_{a/o}}{g\rho_w r_{\mathrm{eff}}} \tag{3.48}$$

where $\gamma_{a/o}$ is the surface tension of oil and $\Theta_{a/o}$ is the air/oil/coal contact angle.
The oil/water/coal contact angle is calculated from

$$\frac{\Delta H_{o/w}}{\Delta H_{a/o}} = \frac{\gamma_{o/w} \cos \Theta_{o/w}}{\gamma_{a/o} \cos \Theta_{a/o}} \tag{3.49}$$

assuming that oil wets coal completely and hence $\Theta_{a/o}$ is zero.
Using this method, Qiu and Wheelock [129] found excellent correlation between the measured contact angle and oxidation time, heat of immersion, hydrophilicity index (Figs. 3.47 and 3.48) and the oil agglomeration results (Fig. 9.3).
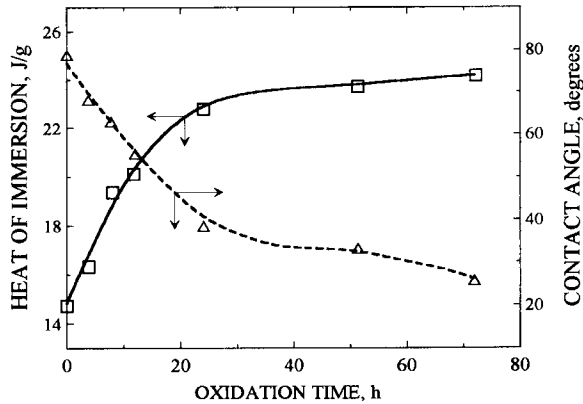
Fig. 3.47. Effect of oxidation time on the three-phase contact angle (measured within water) and heat of immersion. (After Qiu and Wheelock [129]; by permission of Gordon and Breach.)
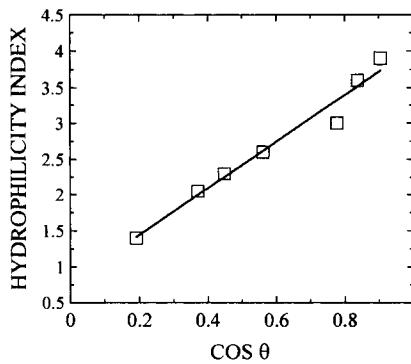
Fig. 3.48. Correlation between the hydrophilicity index and cos Θ for $-210 +149$ μm Colchester seam coal. (After Qiu and Wheelock [129]; by permission of Gordon and Breach.)

3.8.2.6. *Methods based on behavior of solid particles in liquids*

In the penetration rate methods, the liquid penetrates a static bed of particles and the wettability of the solid particles is determined from the rate of penetration. However, it is possible to reverse the experiment and follow the behavior of solid particles in a stagnant liquid. Quite a large variety of methods have been developed based on this principle.

Probably one of the first attempts to develop a more quantitative method was that by Walker et al. [132], who studied wettability by monitoring the surface tension of the solution into which individual particles would be imbibed immediately when dropped from a 1-cm height.

The following analysis of the process that occurs when a solid phase and a liquid phase come into contact so that the solid/air interface is replaced by the solid/liquid interface is taken from Parfitt [133]. The particles are considered to be cubes and Fig. 3.49 illustrates four stages of the process of wetting them completely.

Fig. 3.49. The three stages involved in the complete wetting of a solid cube by a liquid.

Taking the side length as 1 cm, and assuming that before wetting the solid is in equilibrium with the vapor of the liquid, the energy changes that take place are given by
(a) to (b) adhesional wetting:

$$W_a = \gamma_{SL} - (\gamma_{SV} + \gamma_{LV}) = -\gamma_{LV}(\cos \Theta + 1) \tag{3.50}$$

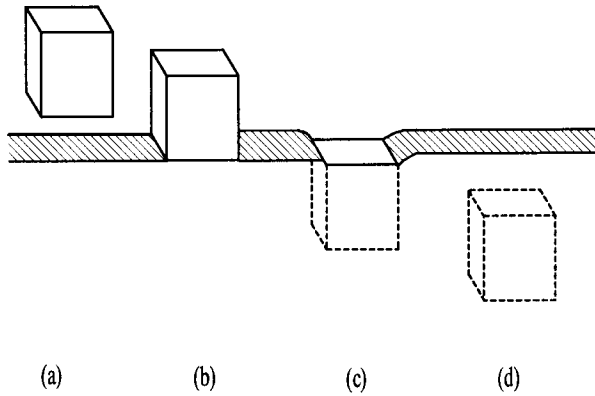Eq. (3.4) describes the energy needed to separate a solid/liquid interface (e.g. to form solid/vapor and liquid/vapor interfaces instead of a solid/liquid interface). When 1 cm^2 of a plane solid (S) is brought into contact with 1 cm^2 of a plane liquid (L) surface, the work involved in this process is equal to W_{SL} from Eq. (3.4).
(b) to (c) immersion-wetting:

$$W_i = 4\gamma_{SL} - 4\gamma_{SV} = -4\gamma_{LV} \cos \Theta \tag{3.51}$$

(c) to (d) spreading wetting:

$$W_s = (\gamma_{SL} + \gamma_{LV}) - \gamma_{SV} = -\gamma_{LV}(\cos \Theta - 1) \tag{3.52}$$

The contact angle is introduced into Eqs. (3.50)–(3.52) by making use of the Young equation.

The powder will wet spontaneously when W is negative. The adhesional wetting is spontaneous if Θ is less than 180°, the immersion-wetting is only spontaneous if Θ is less than 90°, but spreading wetting is spontaneous only when $Q = 0°$. Because the spreading wetting stage requires a contact angle of zero, the powder will tend to float on the liquid surface if the contact angle is not zero. And since Zisman's critical wetting surface tension [134] determines the exact conditions under which the solid is perfectly wetted ($Q = 0$), the use of the powder wetting observations along with the Zisman's concept became one of the important methods of testing the wettability of fine particles. As shown by Diao and Fuerstenau [135], the effect of particle density and particle size on the critical wetting surface tension as determined from the film flotation technique (which will be discussed later) is negligible.

Zisman and his co-workers at the Naval Research Laboratory [136] evaluated the γ_{SV} of low-energy solids ($\gamma_{LV} > \gamma_{SV}$) by measuring contact angles for a series of liquids.
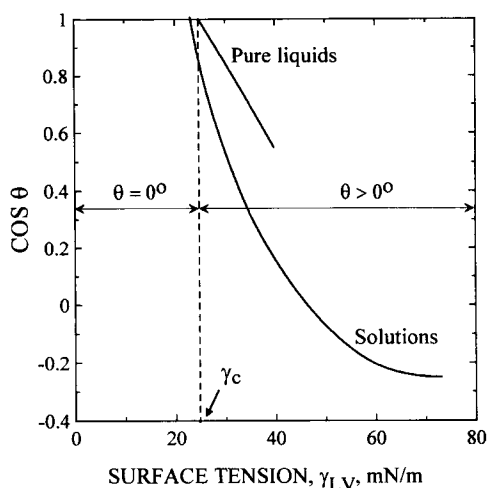
Fig. 3.50. Zisman's plot.

By plotting $\cos \Theta$ vs. the surface tension of the liquid they obtained the value of γ_{LV} at the intercept where $\cos \Theta = 1$. This value is referred to as the critical surface tension of wetting, γ_c, and Fig. 3.50 illustrates the result.

$$\gamma_c = (\gamma_{LV})_{\cos \Theta = 1} \tag{3.53}$$

As Fig. 3.50 shows, a solid characterized by a given γ_c value is completely wettable ($\Theta = 0$) when immersed in liquids of $\gamma_{LV} < \gamma_c$, but becomes lyophobic when immersed in liquids of $\gamma_{LV} > \gamma_c$. When aqueous surfactant solutions are used instead of pure liquids, the relationship $\cos \Theta$ vs. γ_{LV} becomes non-linear [137] but still allows finding the γ_c by extrapolation to $\cos \Theta = 1$. It has become a common practice to use aqueous methanol solutions in such measurements.

The critical surface tensions of wetting have been determined for many solids. A few examples of such measurements follow: 26.9 mJ/m^2 for crystals of sulfur, but 33.3 for discs compressed from fine sulfur; 29.2 for faces of molybdenite crystal, but 41.7 for molybdenite discs and more than 72.5 for molybdenite crystal edges [139]. It is of interest to point out that the conclusion so far is that nonpolar solids are hydrophobic and are not wetted by water, because their surface tension is too low; the values of critical surface tension of wetting are low for very hydrophobic solids and increase for solids which are less hydrophobic. Zisman used contact angle measurements to determine the critical surface tension of wetting, but it is obvious that this value can easily be determined for fine particles and can then be used to characterize solid wettability. Many experimental techniques have been developed following this line of thought. They are all based on observations of the behavior of fine particles in liquids with varying surface tension since such behavior changes abruptly when the liquid surface tensions approach $\gamma_{LV} = \gamma_c$.

In the method as modified by Garshva et al. [139], 150 mg samples of powdered solid are gently placed on the surface of solutions (varying in surface tension) in test tubes of 1.4 cm internal diameter. The time needed for about 3/4 of the powder to sink is taken
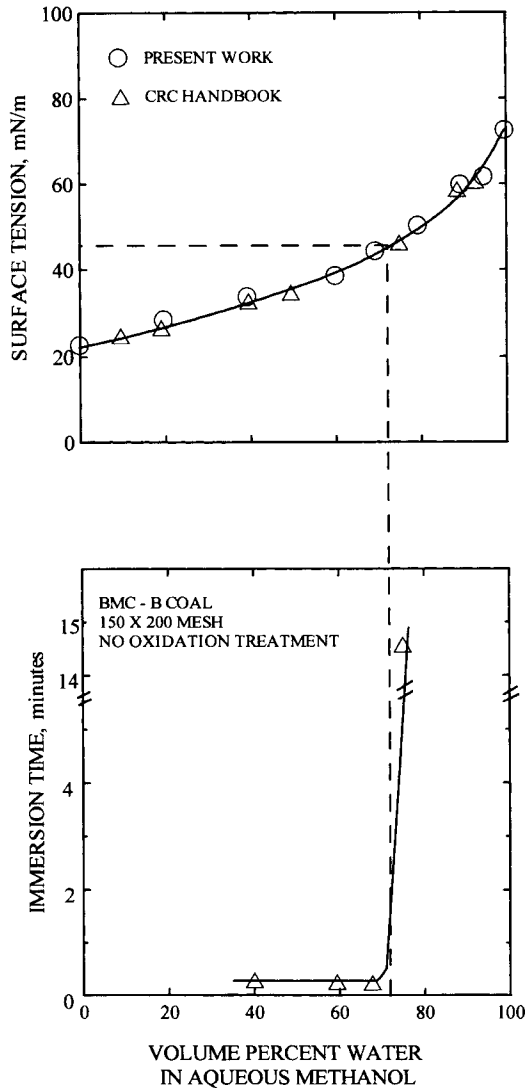
Fig. 3.51. An example illustrating the method to estimate the critical wetting surface tension of Pennsylvania bituminous coal in aqueous methanol solutions. (After Fuerstenau et al. [140]; by permission of Gordon and Breach.)

as the time of immersion. This method was used with methanol aqueous solutions at Berkeley in 1981–82 to characterize the wettability of fine coal particles [140]. Fig. 3.51 provides an example of the results and their interpretation. Mohal and Chander [141] further modified this method by placing the pan of a Cahn electrobalance beneath the liquid surface to monitor the weight of the imbibed coal.

Finch and Smith [142] used a bubble pick-up method and small-scale flotation experiments. In their preliminary tests, Hornsby and Leja [143] evaluated the critical

surface tension of coal by placing samples of fine coal in test tubes filled with water–methanol solutions of successively lower methanol concentrations. These solutions represented a range of surface tensions varying from a low of 23 mJ/m² for pure methanol to a high of 71.5 mJ/m² for pure water. After shaking the tubes and allowing them to sit for several hours the tubes were photographed. The coal was completely wetted in solutions of high methanol concentration (low surface tensions) and sank, but at lower concentrations of methanol the majority of coal particles reported to the froth layer on top of the solution. This identified the range of surface tensions within which the critical surface tension for this coal is situated. In the following tests, Hornsby and Leja [144] used a Partridge–Smith flotation cell and introduced the concept of the critical surface tension of floatability. It is worthy of mention that Yarar et al. [145,146] found an excellent agreement between contact angle, the critical surface tension of wettability values and flotation for many inherently hydrophobic minerals (Fig. 3.52).

As it is known, coal is heterogeneous and fine coal particles may have quite a wide range of surface properties. Such particles are thus characterized by different critical surface tensions of wettability, and different critical surface tensions of floatability. The flotation experiments carried out in aqueous solutions with varying concentrations of methanol would then produce a floatability curve showing the distribution of coal particle wettability. Such a method of testing coal fines in methanol solutions was introduced by Hornsby and Leja [147]. The method is unique in that it provides a distribution of the wettabilities of coal particles in a sample, and can characterize the natural properties of the sample as no other method. In a way, it provides floatability
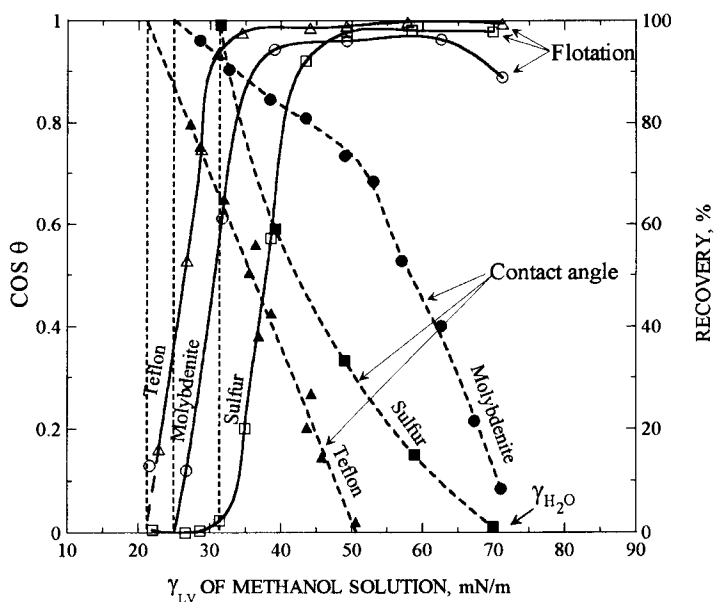

Fig. 3.52. Effect of surface tension of methanol aqueous solutions on floatability and wettability of molybdenite, sulfur and Teflon. (After Yarar and Kaoma [145]; by permission of Elsevier Science.)

curves, which are equivalent of the washability curves that are based on float–sink tests.

To study the effect of surfactants on solid wettability, Lucassen-Reynders [148,149] introduced a diagram in which the adhesion tension ($\gamma_{LV} \cdot \cos \Theta$) is plotted versus γ_{LV}. In such plots, any straight line through the origin is the locus for a particular contact angle value, from 0 degrees to 180 degrees. For short chain alcohol solutions a linear relationship is also obtained between $\gamma_{LV} \cos \Theta$ and γ_{LV} of the form

$$\gamma_{LV} \cos \Theta = b\gamma_{LV} + (1 - b)\gamma_c \tag{3.54}$$

where b is the slope of the wettability line, and γ_c is the intercept with the $\Theta = 0$ degree boundary. As the polarity of the solid surface increases, the parameter which characterizes their wettability in aqueous alcohol solutions is not only the value of γ_c but that of b, the slope of the wettability line; with increasing polarity b becomes less negative while γ_c increases [138,144]. If the γ_c values for two low-energy solids (given by lines A and B in Fig. 3.53) are sufficiently different, then a selective wetting region exists (shaded area) where an aqueous solution of the alcohol with $\gamma_c^A < \gamma_{LV} < \gamma_c^B$ will completely wet solid B, but will only partially wet (form a finite contact angle with) solid A. As demonstrated by Hornsby and Leja [143], a separation of the non-wetted solid particles A from those of solid B can be made using methanol solutions of intermediate surface tension. Yarar coined the term 'gamma flotation' for such a process [146].

As Eq. (5.23) indicates, particle-to-bubble attachment is possible when $\Theta > 0°$. Such thermodynamic considerations concern only dewetting of the solid surface. Flotation processes also depend on the collision probability, which in turn depends on hydrodynamic conditions, particle and bubbles sizes, particle–bubble aggregate stability, etc. Thus, in general, a particle will be floatable if $\gamma_{LV} > \gamma_{cf} > \gamma_c$, where γ_{cf} is the
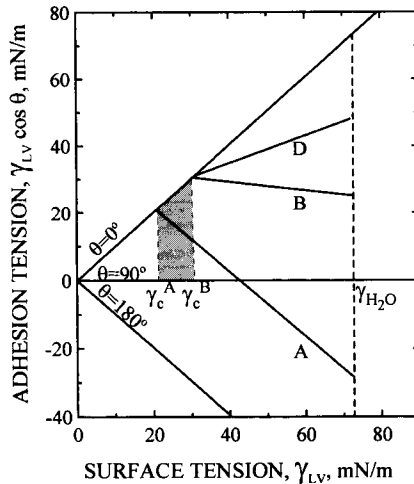

Fig. 3.53. Adhesion tension diagram illustrating wettability lines for three low-energy solids of different hydrophobicity in aqueous solutions of a short-chain *n*-alcohol, and selective wetting region (shaded area) between solids A and B. (After Yarar and Kaoma [145]; by permission of Elsevier Science.)

critical surface tension of floatability. And since — as shown by Hornsby and Leja — wettability of coal particles differs because of differences in petrographic composition and content of mineral matter inclusions, such particles are characterized by different critical surface tensions of floatability. Thus, flotation experiments carried out in aqueous methanol solutions can split the sample of coal into fractions varying in wettability. This method (as will be discussed later) was used to produce yield-ash curves which can be treated as an equivalent to the washability curves.

While Hornsby and Leja [144,147] used flotation experiments in methanol solutions of progressively decreasing surface tension to characterize coal floatability, Williams and Fuerstenau [150] further modified the immersion-time technique which evolved into what is known today as the film flotation method. In this method, a monolayer of about 0.06–0.1 g of closely sized coal particles is placed on the surface of an aqueous solution of methanol. The tests are carried out in a shallow vessel of 8 cm in diameter and 2 to 3 cm in depth. In general, the solids either remain on the liquid surface or are immediately imbibed. Thus, for closely graded monosized coal powder fractions, the times of immersion need not be measured; after the film flotation the lyophobic floating material is separated from the lyophilic sinking fraction, and both are dried and weighed. The floating fraction percentage is plotted versus solution surface tension as shown in Fig. 3.54a. As this figure indicates, the cumulative curve is analogous to a Tromp curve and can also be presented in a form of frequency histogram (Fig. 3.54b). The curves allow determination of the surface tension of the solution that wets all of the particles, γ_c^{min}, the mean surface tension of particles in the distribution, $\bar{\gamma}_c$, and the surface tension of the solution in which none of the particles are wetted, γ_c^{max}. While the range from γ_c^{min} to γ_c^{max} is a measure of coal heterogeneity, the mean surface tension of particles in the sample, $\bar{\gamma}_c$, can be used to compare the wettabilities of different samples.

To show the relationship between coal surface wettability characterized by $\bar{\gamma}_c$ and coal flotation, the same coal samples were floated in a 0.5 M NaCl solution. This is the so-called salt flotation. As discussed in Section 5.3.5, the results of such tests depend on coal wettability and reach a maximum around the pH of the i.e.p. Fig. 3.55 shows the dependence of coal salt flotation on the mean critical surface tension of wetting. Curve No. 1 was obtained from the immersion time tests and was plotted vs. flotation at an optimum pH (pH = i.e.p.) [140], while Curve 2 represents salt flotation results plotted vs. the mean critical surface tension of wettability determined from the film flotation experiments [151]. As can be seen, floatability decreases as the $\bar{\gamma}_c$ value increases and this relationship further confirms that the $\bar{\gamma}_c$ can reliably be used as a parameter characterizing coal wettability. Since in its determination, fine coal particles and not polished specimens (as in the contact angle measurements) are used, and since determination of the mean wetting surface tension is simple, this emerges as the most reliable method of characterizing coal surface wettability.

It is of interest to point out that Fuerstenau et al. [152] used the critical surface tension of wettability data along with the Neumann equation of state [153] to calculate the values of the contact angle. While the use of the equation of state is a very controversial topic (e.g. [154]), this is a very attractive avenue and it allows a distribution of contact angles to be calculated for a sample of fine coal. As we quickly learned [155], it is better to use a modified equation of state [156] for such calculations.
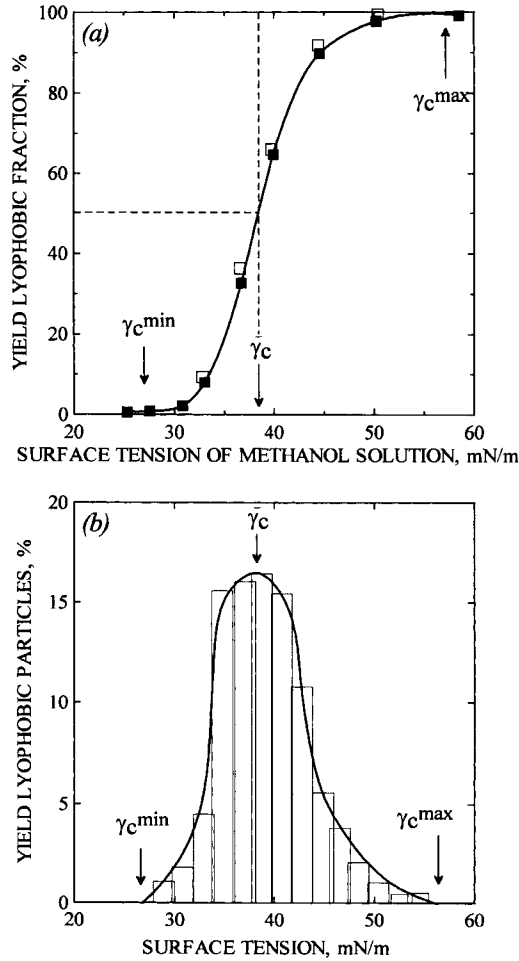
Fig. 3.54. Partition curve (a) and frequency histogram (b) for the film flotation of -150 μm $+100$ μm particles of Dave Johnston subbituminous coal in aqueous methanol solutions. The two sets of data are duplicate runs. (After Williams and Fuerstenau [150]; by permission of Elsevier Science.)

Since solid particles are perfectly wetted only by liquids when $\gamma_{LV} < \gamma_c$, many solids are not wetted by water ($\gamma_{H_2O} \approx 71.5$ mJ/m^2). Thus such particles are not imbibed by water. Ramesh and Somasundaran [157] introduced a method in which the centrifugal force required to wet and immerse particles gently placed on the surface of water is determined. Since this force is related to the particle wettability, its determination allows characterization of the wettability.

3.8.2.7. Miscellaneous methods

Fig. 3.17 gives the relationship between the HLR number determined from the adsorption of water and *n*-heptanol onto coal [77]. The method is not experimentally
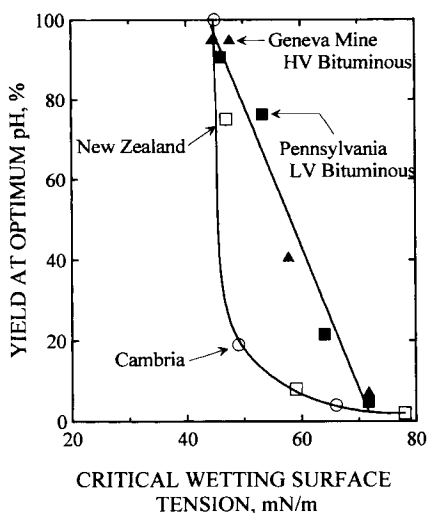
Fig. 3.55. Correlation of the optimum flotation yield with the critical wetting surface tension (solid symbols) as determined from the immersion time measurements (after Fuerstenau et al. [140]; by permission of Gordon and Breach), and of the flotation yield with the mean critical wetting surface tension (open symbols) determined by film flotation (after Fuerstenau and Diao [151]; by permission of Gordon and Breach). Vacuum flotation in 0.5 M NaCl solutions was used to study flotation response; to vary surface properties the tested bituminous coals were oxidized at 150°C, 200°C and 244°C.

easy but it is obvious that it is accurate enough to characterize coal surface properties over a very broad range.

A method described by Adams-Viola et al. [158] classifies coals as hydrophilic or oleophilic (hydrophobic) based on their behavior in an oil/water system. In the 60s Takakuwa and Takamori [159] proposed a phase inversion method to characterize wettability of mineral particles as affected by various collectors. The method developed by Adams-Viola is very similar as the results given in Table 3.2 suggest. In these tests coals are ground 100% below 150 μm. The 5 g samples are prewetted either with water or kerosene (100 ml) by mixing in a Waring blender for 1 min. This is followed by addition of an equal volume of the second liquid and the mixture is blended for an additional 30 s. The type of emulsion, i.e. oil-in-water (O/W) or water-in-oil (W/O) is evaluated either by a dilution test or by a conductivity measurement. As seen from Table 3.2, while bituminous coals form W/O emulsions, O/W emulsion are formed in the presence of low-rank coals, subbituminous and lignites. These tests were followed by oil agglomeration tests (see Section 9.2) in which coal was either suspended in water and agglomerated with 20% addition of oil (forward agglomeration) or was suspended in kerosene and agglomerated with 20% addition of water (reverse agglomeration) under standardized hydrodynamic conditions. The agglomeration results in terms of the agglomeration number are given in Table 3.3. The forward agglomeration number is defined as:

$$N_f = \frac{\bar{D}_o}{\bar{d}} \tag{3.55}$$

Table 3.2
Qualitative characterization of the relative oleophilic/hydrophilic nature of several coal powders [158]

Coal type	Ash (% A.R. coal)	Moisture (% A.R. coal)	Emulsion type	Coal surface
Pocahontas	6.3	1.1	W/O	Oleophilic
Sewell	5.7	1.3	W/O	Oleophilic
Buck Mountain anthracite	3.4	5.8	W/O	Oleophilic
Pennsylvania anthracite	16.3	1.6	W/O	Oleophilic
Brookfield bituminous	4.8	5.3	W/O	Oleophilic
Sewanee bituminous	14.2	1.6	W/O	Oleophilic
Illinois	12.7	11.2	O/W	Hydrophilic
Dietz No. 3 subbituminous	4.0	17.9	O/W	Hydrophilic
Big Dirty subbituminous	18.4	18.2	O/W	Hydrophilic
Darco lignite	6.0	33.2	O/W	Hydrophilic
Zap lignite	8.5	28.9	O/W	Hydrophilic
Baukol-Noonan lignite	8.2	21.6	O/W	Hydrophilic

Table 3.3
Results of forward and reverse agglomeration tests [158]

Coal	Forward agglomeration			Reverse agglomeration	
	d, μm	D_o, μm	N_f	D_w, μm	N_r
(1) Pocahontas bituminous	35	220	6.3	50	1.4
(2) Buck Mountain anthracite	65	310	4.8	70	1.1
(3) Sewanee bituminous	45	200	4.4	150	3.3
(4) Sewell bituminous	35	130	3.7	50	1.7
(5) Pennsylvania anthracite	65	180	2.8	70	1.4
(6) Brookfield bituminous	35	90	2.6	70	2.0
(7) Illinois bituminous	30	70	2.3	290	9.7
(8) Dietz No. 3 subbituminous	50	110	2.2	170	3.4
(9) North Dakota lignite	35	50	1.4	190	5.4
(10) Big Dirty subbituminous	45	60	1.3	390	8.7
(11) Darco lignite	50	60	1.2	100	2.0
(12) Zap lignite	50	60	1.2	200	4.0

where $\bar{D}_o$ is the mean size of the oil agglomerates, and $\bar{d}_o$ is the mean size of the coal particles. Similarly, the definition of the reverse agglomeration number, N_f, is based on the mean size of the water agglomerates and coal particles.

The results displayed in Table 3.3 indeed demonstrate that those coals which formed the W/O emulsions (Table 3.2) are characterized by relatively large forward agglomeration numbers, whereas those forming O/W emulsions are characterized by much larger reverse agglomeration numbers. This is a simple technique and provides quite a large scale for estimation of the relative wettability of various coals. A good correlation between contact angle and agglomeration (Fig. 9.3), obtained by Qiu and Wheelock [130], is perfectly in line with these observations.
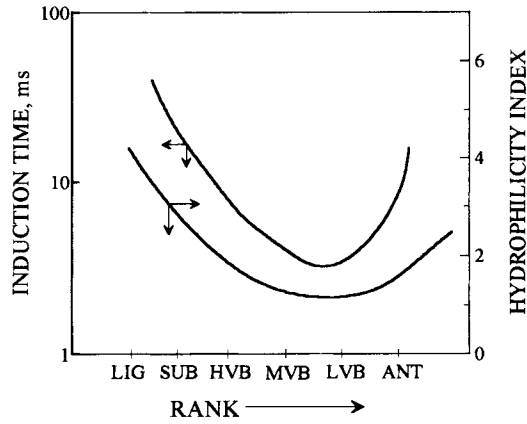
Fig. 3.56. Induction time and the hydrophilicity index for six coals varying in rank. (After Jin and Miller [163]; by permission of Gordon and Breach.)

Ye et al. [160] used the induction time meter [161] to study coal surface wettability[9]. Their results were shown to correlate very well with directly measured contact angles, and with the hydrophilicity index obtained from the infrared measurements [162]. This index is defined as follows:

$$HI = \frac{(-COOH) + 2(-OH)}{(R-H) + (Ar-H)} \tag{3.56}$$

where $(-COOM)$, $(-OH)$, $(R-H)$ and $(Ar-H)$ are the values of the absorption intensity obtained using FTIR and diffuse reflectance technique. Qiu and Wheelock [128] used the peaks at 1710 cm^{-1} for $-C=O$, at 3400 cm^{-1} for $-OH$, at 2965 cm^{-1} for $-C-H$ and at 3030 cm^{-1} for $Ar-H$. Fig. 3.56 shows the correlation between the hydrophilicity index and induction time for different coals varying in rank [163].

Solid–liquid interactions can also be characterized by measuring calorimetrically the heats of immersion of powdered solids in liquids. The free energy of immersion is given by

$$\Delta G_i = \gamma_{SL} - \gamma_S \tag{3.57}$$

where γ_S is the surface tension (surface free energy) of the solid in a vacuum, and the heat of immersion is

$$\Delta H_i = \Delta G_i - T \left(\frac{d\Delta G_i}{dT} \right) \tag{3.58}$$

The heat of immersion for -75 µm coal samples in water are given in Fig. 3.57 [164]. The results confirm that the heat of immersion varies markedly with the rank of the coal. The lower-ranked coals which have quite a large content of oxygen functional groups actively interact with water and this gives high values of the evolved heat. Such measurements are also very sensitive to the specific surface area of the coal particles (particle size) as well as mineral matter contact (ash).

---

[9] More information on the induction time measurements in the coal flotation-related research can be found in the paper by Yordan and Yoon [162].
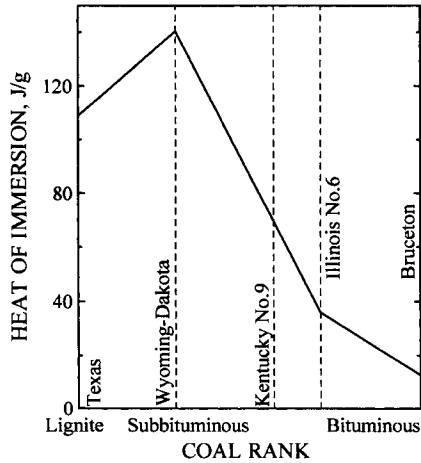
Fig. 3.57. Variation of heat of immersion with coal rank (After Fuller [164]; by permission of Academic Press.)

3.9. References

[1] J.S. Laskowski and J. Iskra, Role of capillary effect in bubble–particle collision in flotation. Trans. IMM, Sect. C, 79 (1970) 5.

[2] J.S. Laskowski, The relationship between floatability and hydrophobicity. In: P. Somasundaran (ed.), Advances in Mineral Processing. SME, Littleton, CO, 1986, pp. 189–208.

[3] J.S. Laskowski, Thermodynamic and kinetic flotation criteria. In: J.S. Laskowski (ed.), Frothing in Flotation. Gordon and Breach, New York, 1989, pp. 25–41.

[4] J.S. Laskowski, Z. Xu and R.H. Yoon, Energy barrier in particle-to-bubble attachment and its effect on flotation kinetics. Proc. 17th Int. Mineral Processing Congress, Dresden, 1991, Vol. 2, pp. 237–249.

[5] D.W. Fuerstenau, J.M. Rosenbaum and J.S. Laskowski, Effect of surface functional groups on the flotation of coal. Coll. Surf., 8 (1983) 153.

[6] Y.B. He and J.S. Laskowski, Contact angle measurements on discs compressed from fine coal. Coal Preparation, 10 (1992) 19.

[7] F.M. Fowkes, Attractive forces at interfaces. Ind. Eng. Chem., 56 (12) (1964) 40.

[8] R.J. Good, Theory for the estimation of surface and interfacial energies. In: R.F. Gould (ed.), Contact Angle — Wettability and Adhesion. Advances in Chemistry Series No. 43, American Chemistry Society, Washington, DC, 1964, pp. 74–87.

[9] F.M. Fowkes, Attractive forces at solid liquid interfaces. In: Wetting — S.C.I. Monograph No. 25. Soc. Chem. Ind., London, 1967, pp. 3–30.

[10] F.M. Fowkes, Donor–acceptor interactions at interfaces. J. Adhesion, 4 (1972) 155.

[11] F.M. Fowkes, M.B.N. Kaczinksy and D.W. Dwight, Surface sites characterization of polymer with contact angles of test solutions. Langmuir, 7 (1991) 2464.

[12] C.J. van Oss, M.K. Chaudhury and R.J. Good, Interfacial Lifshitz–van der Waals and polar interactions in macroscopic systems. Chem. Rev., 88 (1988) 927.

[13] J.A. Gutierrez-Rodriguez, R.J. Purcell and F.F. Aplan, Estimating the hydrophobicity of coal. Coll. Surf., 12 (1984) 1.

[14] B.K. Parekh and F.F. Aplan, The critical surface tension of wetting of coal. In: N.N. Li, R.B. Long, S.A. Stern and P. Somasundaran (eds), Recent Development in Separation Science. Am. Inst. Chem. Eng., 1978, Vol. 4, pp. 107–113.

[15] R.J. Good, N.R. Srivasta, M. Islam, H.T.L. Huang and C.J. van Oss, Theory of the acid–base hydrogen bonding interactions, contact angles, and the hysteresis of wetting: application to coal and

graphite surfaces. J. Adhesion Sci. Technol., 4 (1990) 607.

[16] J.S. Laskowski, Coal surface chemistry and its role in fine coal beneficiation and utilization. Coal Preparation, 14 (1994) 115.

[17] G.A. Brady and A.W. Gauger, Properties of coal surface. Ind. Eng. Chem., 32 (1940) 1599.

[18] M.G. Elyashevich, Contact angles as a criterion of coal floatability. Trans. Donetsk Industrial Inst., Gosgortiekhizdat, 32 (1941) 225–235 (in Russian).

[19] R.M. Horsley and H.G. Smith, Principles of coal flotation. Fuel, 30 (1951) 54.

[20] V.I. Klassen, Coal Flotation. Gosgortiekhizdat, 2nd ed., Moscow, 1963 (in Russian).

[21] M.G. Elyashevitch, J.N. Zubkova, and R.V. Kucher, On hydration and natural floatability of Donbass coals. Khimia Twerdogo Topliva, 3 (1967) 126 (in Russian).

[22] M.G. Elyashevitch, M.E. Ofengenden and J.N. Zubkova, Some physico-chemical surface properties of Donetsk coals affecting their floatability. Rozrabotka Mestorozdeni Polyeznykh Iskopaemykh, Tekhnika, Kiev, 1966, No. 6, 1966, pp. 5–12 (in Russian).

[23] A. Ihnatowicz, Studies of oxygen groups in bituminous coals. Bull. Central Res. Mining Institute, No. 125, Katowice, 1952 (in Polish).

[24] L. Blom, L. Edelhausen and D.W. van Krevelen, Chemical structure and properties of coal oxygen groups in coal and related products. Fuel, 36 (1957) 135.

[25] Z. Abdel-Baset, P.H. Given and R.F. Yarzab, Re-examining of the phenolic hydroxyl content of coals. Fuel, 57 (1978) 95.

[26] J.S. Laskowski and J.A. Kitchener, The hydrophilic–hydrophobic transition on silica. J. Coll. Interf. Sci., 29 (1969) 670.

[27] J. S. Laskowski, An introduction: physicochemical methods of separation. In: J.S. Laskowski and J. Ralston (eds), Colloid Chemistry in Mineral Processing. Elsevier, Amsterdam, 1992, pp. 225–242.

[28] L.G.J. Fokking and J. Ralston, Contact angles on charged surfaces. Coll. Surf., 6 (1989) 69.

[29] R.J. Hunter, Zeta Potential in Colloid Science. Academic Press, New York, 1981.

[30] P.C. Hiemenz, Principles of Colloid and Surface Chemistry. Marcel Dekker, 1977, New York.

[31] D.J. Shaw, Introduction to Colloid and Surface Chemistry, 2nd ed. Butterworths, London, 1970.

[32] A.M. James, Electrophoresis of particles in suspension. In: E. Matijevic (ed.), Surface and Colloid Science. Plenum Press, New York, 1981, Vol. 11, pp. 121–186.

[33] H.W. Douglas and D.J. Shaw, Electrokinetic studies on model particles. Trans. Faraday Soc., 53 (1957) 512.

[34] J.M.W. Mackenzie, Electrokinetic properties of nujol-flotation collector emulsion drops. Trans. AIME, 244 (1969) 393.

[35] H.C. Perreira and J.H. Schulman, Streaming potential measurements on paraffin wax. In: R.F. Gould (ed.), Solid Surfaces. Adv. Chem. Ser. 33, Am. Chem. Soc., Washington, DC, 1961, pp. 160–.171.

[36] N. Arbiter, U. Fujii, B. Hansen and A. Raja, Surface properties of hydrophobic solids. In: P. Somasundaran and R.B. Grieves (eds), Advances in Interfacial Phenomena of Particulate/Solution/Gas Systems; Applications to Flotation Research. Am. Inst. Chem. Eng., Vol. 71, 150, 1975, pp. 176–182.

[37] W.W. Wen and S.C. Sun, An electrokinetic study on the oil flotation of oxidized coal. Separation Sci., 16 (1981) 1491.

[38] S. Chander, J.M. Wie and D.W. Fuerstenau, On native floatability and the surface properties of naturally hydrophobic solids. In: P. Somasundaran and R.B. Grieves (eds), Advances in Interfacial Phenomena of Particulate/Solution/Gas Systems; Applications to Flotation Research. Am. Inst. Chem. Eng., Vol. 71, 150, 1975, pp. 183–188.

[39] S. Kelebek, T. Salman and G.W. Smith, Interfacial phenomena in coal flotation systems. In: A.M. Al-Taweel (ed.), Coal: Phoenix of the 80s. Chem. Eng., Halifax, Vol. 1, 1981, pp. 145–152.

[40] S.C. Sun and J.A.L. Campbell, Anthracite lithology and electrokinetic behavior. In: P. Given (ed.), Coal Science. Adv. Chem. Ser. 55, Am. Chem. Soc., Washington, DC, 1966, pp. 55–63.

[41] B. Siffert and T. Hamieh, Effect of mineral impurities on the charge and surface potential of coal. Coll. Surf., 35 (1989) 27.

[42] R.E. Winans, R.L. McBeth and J.E. Young, The effects of acid demineralization on the sulfur-containing compounds found in an Illinois-Basin high-sulfur coal. In: R. Markuszewski and T.D. Wheelock (eds), Processing and Utilization of High-Sulfur Coals III. Elsevier, Amsterdam, 1990, pp. 53–66.

[43] H.N.S. Schafer, Carboxyl groups and ion exchange in low-rank coals. Fuel, 49 (1970), 197.

[44] H.N.S. Schafer, Determination of the total acidity of low-rank coals. Fuel, 49 (1970), 271.

[45] K.C. Teo, S. Finora and J. Leja, Oxidation states in surface and buried coal from the Fording River deposit. Fuel, 61 (1982) 71.

[46] J.S. Laskowski, Effect of surface properties of coals on their floatability. Proc. 8th Int. Mineral Processing Congress, Leningrad, 1968, Vol. 1, pp. 626–631.

[47] S. Blaszczynski, Effect of Liquid Viscosity on Its Flow Through Porous Material and Dewatering of Coal Fines by Filtration. Ph.D. Thesis, Silesian University of Technology, Gliwice, 1967 (in Polish).

[48] A. Yucesoy and B. Yarar, Zeta-potential measurements in the galena–xanthate–oxygen flotation system. Trans. IMM, Sect. C, 83 (1974) C96.

[49] J.A.L. Campbell and S.C. Sun, Anthracite coal electrokinetics. Trans. AIME, 247 (1970) 120.

[50] R.R. Jessop and J.L. Stretton, Electrokinetic measurements on coal and a criterion for its hydrophobicity. Fuel, 48 (1969) 317.

[51] N. Prasad, Electrokinetics of coal. J. Inst. Fuel, 47 (1974) 174.

[52] R.E. Marganski and E.L. Rowell, Electrophoretic mobility distribution in aqueous bituminous coal dispersions. J. Disp. Sci., 4 (1983) 415.

[53] W.W. Wen and S.C. Sun, An electrokinetic study of the amine flotation of oxidized coal. Trans. AIME, 262 (1977) 174.

[54] B. Yarar and J. Leja, Flotation of weathered coal fines from USA and Western Canada. Proc. 9th Int. Coal Preparation Congress, New Delhi, 1982, Paper C5.

[55] S. Kelebek, T. Salman and G.W. Smith, An electrokinetic study of three coals. Can. Metall. Q., 21 (1982) 205.

[56] A.M. Al-Taweel, O.A. Fadaly, J.C.T. Kwak and H.A. Hamza, Influence of aggregate formation on the rheology and stability of coal/water slurries. Proc. 4th Int. Symp. Agglomeration, Toronto, 1985, pp. 607–615.

[57] J.S. Laskowski and G.D. Parfitt, Electrokinetics of coal–water suspensions. In: G.D. Botsaris and Y.M. Glazman (eds), Interfacial Phenomena in Coal Technology. Marcel Dekker, New York, 1989, pp. 279–327.

[58] O.P. Mahajan and R.L. Walker, Water adsorption on coals. Fuel, 50 (1971) 308.

[59] D.J. Allardice and D.G. Evans, Moisture in coal. In: C. Karr (ed.), Analytical Methods for Coal and Coal Products. Academic Press, New York, 1978, pp. 247–262.

[60] J.G. King and E.T. Wilkins, The internal structure of coal. In: Proceedings of the Conference on Ultra-Fine Structure of Coals and Cokes. British Coal Utilisation Research Association, 1944, pp. 46–56.

[61] G. Gan, S.P. Nandi and P.L. Walker, Nature of the porosity of American coals. Fuel, 51 (1972) 272.

[62] M.S. Iyenger and A. Lahiri, The nature of reactive groups in coal. Fuel, 36 (1957) 286.

[63] M. Lason, L. Czuchajowski and M. Zyla, A note on the sorption of methanol and water vapours on vitrains. Fuel, 39 (1960) 366.

[64] J.A. Lupens and A.P. Heft, Relationship between inherent and equilibrium moisture contents in coals by rank. J. Coal Quality, 10 (1991) 133.

[65] C. Pierce, R.N. Smith, J.W. Wiley and H. Cardes, Adsorption of water by carbon. J. Am. Chem. Soc., 73 (9) (1951) 4551.

[66] A.C. Zettlemoyer, J.J. Chessick and C.M. Hollabauch, Estimations of the surface polarity of solids from heat of wetting measurements. J. Phys. Chem., 62 (1958) 489.

[67] J.J. Chessick, F.H. Healey and A.C. Zettlemoyer, Adsorption and heat of wetting studies of teflon. J. Phys. Chem., 60 (1956) 1345.

[68] G.J. Young, J.J. Chessick, F.H. Healley and A.C. Zettlemoyer, Thermodynamics of the adsorption of water on graphon from heats of immersion and adsorption data. J. Phys. Chem., 58 (1954) 313.

[69] F.M. Fowkes, D.C. McCarthy and M.A. Mostafa, Contact angles and the equilibrium spreading pressures of liquids on hydrophobic solids. J. Coll. Interf. Sci., 78 (1980) 200.

[70] A.W. Adamson, Physical Chemistry of Surfaces, 3rd ed. Wiley, New York, 1976.

[71] O.P. Mahajan and P.L. Walker, Porosity of coals and coal products. In: C. Karr (ed.), Analytical Methods for Coal and Coal Products. Academic Press, New York, 1978, Vol. 1, pp. 125–162.

[72] P.L. Walker and K.A. Kini, Measurement of the ultrafine surface areas of coal. Fuel, 44 (1965) 453.

[73] H.G. Linge, The surface area of coal particles. Fuel, 68 (1989) 111.

[74] H.P. Schreiber and D.R. Lloyd, Overview of inverse gas chromatography. In D.R. Lloyd, T.C. Ward, H.P. Schreiber and C.C. Pizana (eds), Inverse Gas Chromatography. ACS Symp. Ser. 391, Washington, DC, 1989, pp. 1–11.

[75] A.S. Glass and J.W. Larsen, Surface thermodynamics for nonpolar adsorbates on Illinois No. 6 coal by inverse gas chromatography. Energy Fuels, 7 (1993), 994.

[76] A.S. Glass and J.W. Larsen, Coal surface properties. Specific and nonspecific interactions for polar molecules and surface tensions for hydrocarbons at the surface of Illinois No. 6 coal. Energy Fuels, 8 (1994) 629.

[77] A.M. Al-Taweel, B. Delory, J. Wozniczek, M. Stefanski, N. Andersen and H.A. Hamza, Influence of the surface characteristics of coal on its floatability. Coll. Surf., 18 (1986) 9.

[78] A.M. Al-Taweel, B. Delory, A. Doniec and J.J. Wozniczek, Measurement of Coal Wettability and Prediction of the Hydrophobic Nature of Oxidized Coal. Centre for Energy Studies, Technical University of Nova Scotia, Contract No. OST83-00189.

[79] R. Kaji, Y. Muranaka, K. Otsuka and Y. Hishinuma, Water absorption by coals: effects of pore structure and surface oxygen. Fuel, 65 (1986) 288.

[80] S.C. Sun, Hypothesis for different floatabilities of coals, carbons, and hydrocarbon minerals. Trans. AIME, 199 (1954) 67.

[81] A.F. Taggart, G.R. del Giudice, A.M. Sadler and M.D. Hassialis, Oil–air separation of nonsulfide and nonmetal minerals. Trans. AIME, 134 (1939) 180.

[82] J.M. Rosenbaum and D.W. Fuerstenau, On the variation of contact angles with coal rank. Int. J. Miner. Process., 12 (1984) 313.

[83] A.B.D. Cassie and S. Baxter, Wettability of porous surfaces. Trans. Faraday Soc., 40 (1944) 546.

[84] A.B.D. Cassie, Contact angles. Disc. Faraday Soc., 3 (1948) 11.

[85] W. Philippoff, S.R.B. Cooke and D.E. Cadwell, Contact angles and surface coverage. Trans. AIME, 193 (1952) 283.

[86] D.V. Keller, The contact angle of water on coal. Coll. Surf., 22 (1987) 21.

[87] J. Drelich, J.S. Laskowski, M. Pawlik and S. Veeramasuneni, Preparation of a coal surface for contact angle measurements. J. Adhesion Sci. Technol., 11 (1997) 1399.

[88] J. Drelich, J.S. Laskowski and M. Pawlik, Improved sample preparation and surface analysis methodology for contact angle measurements on coal (heterogeneous) surfaces. Coal Preparation, 21 (2000), 247.

[89] S. Kelebek, Wetting behavior, polar characteristics and flotation of inherently hydrophobic minerals. Trans. IMM, Sect. C, 96 (1987) 103.

[90] V.A. Shebanov, Transactions of Kharkhov Mining Institute, 9, 1961 (quoted after V.I. Klassen, Ref. [20])

[91] D.J. Brown, Coal flotation. In: D.W. Fuerstenau (ed.), Froth Flotation. AIME, 1962, pp. 518–538.

[92] D.D. Xu and F.F. Aplan, quoted after Ref. [93].

[93] F.F. Aplan, Coal properties dictate coal flotation strategies. Miner. Eng., 45 (1993) 83.

[94] M. Mastalerz and M. Bustin, Variation in maceral chemistry within and between coals of varying rank: an electron microprobe and micro-Fourier Transform Infra-Red investigation. J. Microsc., 171 (1993) 153.

[95] B.J. Arnold and F.F. Aplan, The hydrophobicity of coal macerals. Fuel, 68 (1989) 651.

[96] B. Bujnowska, Studies on floatability of petrographic constituents of subbituminous coal. Coal Preparation, 1 (1985) 169.

[97] M. Holuszko and J.S. Laskowski, Coal heterogeneity and its effect on coal floatability as derived from flotation tests in methanol solutions. In: J.S. Laskowski and G.W. Poling (eds), Processing of Hydrophobic Minerals and Fine Coal. Proc. 1st UBC–McGill Int. Symp., Metall. Soc. of CIM, Montreal, 1995, pp. 145–164.

[98] A. Marmur, Equilibrium contact angles: theory and measurement. Coll. Surf., 116A (1996) 55.

[99] R.J. Good, Contact angles and the surface free energy of solids. In: R.J. Good and R.R. Stromberg (eds), Surface and Colloid Science. Plenum Press, New York, 1979, Vol. 11, pp. 1–30.

[100] J. Drelich, J.D. Miller and R.J. Good, The effect of drop (bubble) size on advancing and receding contact angles for heterogeneous and rough solid surfaces. J. Coll. Interf. Sci., 179 (1996) 37.

[101] A.W. Neumann and R.J. Good, Techniques of measuring contact angles. In: J.S. Laskowski and G.W.

Poling (eds), Processing of Hydrophobic Minerals and Fine Coal. Proc. 1st UBC–McGill Int. Symp., Metall. Soc. of CIM, Montreal, 1995, pp. 31–92.

[102] R.E. Johnson and R.H. Dettre, Wettability and contact angles. In: E. Matijevic (ed.), Surface and Colloid Science. Wiley, New York, 1969, pp. 85–153.

[103] J. Drelich, J.D. Miller and J. Hupka, The effect of drop size on contact angle over a wide range of drop volumes. J. Coll. Interf. Sci., 155 (1993) 379.

[104] E.L. Decker and S. Garoff, Using vibrational noise to probe energy barriers producing contact angle hysteresis. Langmuir, 12 (1996) 2100.

[105] J.D. Miller, S. Veeramasuneni, J. Drelich and M.R. Yalamanchili, Effect of roughness as determined by atomic force microscopy on the wetting properties of PTFE thin films. Polym. Eng. Sci., 36 (1996) 1849.

[106] J. Drelich, A.A. Atia, M.R. Yalamanchili and J.D. Miller, Formation and wetting characteristics of adsorbed layers of unsaturated carboxylic acids at a fluorite surface, J. Coll. Interf. Sci., 178 (1996) 720.

[107] J. Drelich, Contact angles measured at mineral surfaces covered with adsorbed collector layers. Miner. Metall. Process. (in press).

[108] P.A. Rehbinder, quoted after V.I. Klassen and V.A Mokrousov, An Introduction to the Theory of Flotation. Butterworths, London, 1963, p. 64.

[109] J. Drelich, The effect of drop (bubble) size on contact angle at solid surfaces. J. Adhesion, 63 (1997) 31.

[110] Y. Rotenberg, L. Boruvka and A.W. Neumann, Determination of surface tension and contact angle from the shapes of axisymmetric fluid interfaces. J. Coll. Interf. Sci., 93 (1983) 169.

[111] T. Murata, Wettability of coal estimated from the contact angle. Fuel, 60 (1981) 744.

[112] N.W. F. Kossen and P.M. Heertjes, The determining of the contact angle for systems with a powder. Chem. Eng. Sci., 20 (1965) 593.

[113] R.N. Hanning and P.R. Rutter, A simple method of determining contact angles on particles and their relevance to flotation. Int. J. Miner. Process., 27 (1989) 133.

[114] J. Drzymala and J. Lekki, Flotometric analysis of the collectorless flotation of sulfide minerals. Coll. Surf., 44 (1990) 179.

[115] J. Drzymala, Characterization of materials by Hallimond tube flotation, Part 2. Maximum size of floating particles and contact angle. Int. J. Miner. Process., 42 (1994) 153.

[116] V.T. Crowl and W.D. Wooldridge, A method for the measurements of adhesion tension of liquids in contact with powders. In: Wetting — S.C.I. Monograph No. 25. Soc. Chem. Ind., London, 1967, pp. 200–212.

[117] H.G. Bruil and J.J. von Aasten, The determination of contact angles of aqueous surfactant solutions on powders. Coll. Polym. Sci., 252 (1974) 32.

[118] R. Crawford, L.K. Koopal and J. Ralston, Contact angles on particles and plates. Coll. Surf., 27 (1987) 57.

[119] G.K. Tampy, W.J. Chen, M.E. Prudich and R.L. Savage, Wettability measurements of coal using a modified Washburn technique. Energy Fuels, 2 (1988) 782.

[120] A. Siebold, A. Walliser, M. Nardin, M. Oppliger and J. Schultz, Capillary rise for thermodynamic characterization of solid particle surface. J. Coll. Interf. Sci., 186 (1992) 60.

[121] Y.B. He and J.S. Laskowski, A modified penetration rate technique to characterize wettability of fine coal particles. In: J.S. Laskowski and G.W. Poling (eds), Processing of Hydrophobic Minerals and Fine Coal. Proc. 1st UBC-McGill Int. Symp., Metall. Soc. of CIM, Montreal, 1995, pp. 121–136.

[122] H. Liu and J.S. Laskowski, A Modified Method to Measure the Penetration Rate to Characterize Wettability of Talc Powder. University of British Columbia, Vancouver, 1996 (unpublished).

[123] N. Kaya and M. Koishi, The wetting properties of powders and devices for measuring them. Kona, 6 (1988) 86.

[124] D. Dunstan and L.R. White, A capillary pressure method for measurement of contact angles in powders and porous media. J. Coll. Interf. Sci., 111 (1986) 60.

[125] N.V. Churaev and Z.M. Zorin, Penetration of aqueous surfactant solutions into thin hydrophobized capillaries. Coll. Surf., 100A (1995) 131.

[126] H.W. Kilau and J.E. Pahlman, Coal wetting ability of surfactant solutions and the effect of multivalent anion additives. Coll. Surf., 26 (1987) 217.

[127] R. Varadaraj, J. Bock, N. Brons and S. Zushma, Influence of surfactant structure on wettability modification of hydrophobic granular surfaces. J. Coll. Interf. Sci., 167 (1994) 207.

[128] H.W. Kilau, The wettability of coal and its relevance to the control of dust during coal mining. In: K.L. Mittal (ed.), Contact Angle, Wettability and Adhesion. VSP, Utrecht, 1993, pp. 953–971.

[129] X. Qiu and T.D. Wheelock, A modified suction potential method for measuring the three-phase contact angle. Coal Preparation, 14 (1994) 97.

[130] R. Bailey and V.R. Gray, Contact angle measurements of water on coal. J. Appl. Chem., 8 (1958) 197.

[131] W.C. Clark and G. Mason, Oil on wet coal — measurements of contact angle by a suction method. J. Appl Chem., 18 (1968) 240.

[132] P.C. Walker, E. Peterson and G.C. Wright, Surface active agent phenomena in dust abatement. Ind. Eng. Chem., 44 (1952) 2389.

[133] G.D. Parfitt, Fundamental aspects of dispersion. In: G.D. Parfitt (ed.), Dispersion of Powders in Liquids, 2nd ed. Halsted Press, New York, 1973, pp. 1–43.

[134] W.A. Zisman, Relation of the equilibrium contact angle to liquid and solid constitution. In: K.J. Mysels, C.M. Samour and J.H. Hillster (eds), The Kendal Award Addresses. ACS, Washington, DC, 1973, pp. 109–157.

[135] J. Diao and D.W. Fuerstenau, Characterization of the wettability of solid particles by film flotation, Part 2. Coll. Surf., 60 (1991) 145.

[136] W.A. Zisman, Relation of the equilibrium contact angle to liquid and solid constitution. In: Contact Angle, Wettability and Adhesion. ACS Adv. Chem. Ser. 43, Washington, DC, 1964, pp. 1–51.

[137] M.K. Bernett and W.A. Zisman, Relation of wettability by aqueous solutions to the surface constitution of low-energy solids. J. Phys. Chem., 63 (1959) 1241.

[138] S. Kelebek, Critical surface tension of wetting of floatability of molybdenite and sulfur. J. Coll. Interf. Sci., 124 (1988) 504.

[139] S. Garshva, S. Contreras and J. Goldbarb, Hydrophobic characterization of powders. Coll. Polym. Sci., 256 (1978) 241.

[140] D.W. Fuerstenau, G.C. Yang and J.S. Laskowski, Oxidation phenomena in coal flotation. Coal Preparation, 4 (1987) 161.

[141] B.R. Mohal and S. Chander, A new technique to determine wettability of powders — imbibition time measurements. Coll. Surf., 21 (1986) 193.

[142] J.A. Finch and G.W. Smith, Bubble–solid attachment as a function of bubble surface tension. Can. Metall. Q., 14 (1975) 47.

[143] D.T. Hornsby and J. Leja, Critical surface tension and the selective separation of inherently hydrophobic solids. Coll. Surf., 1 (1980) 425.

[144] D.T. Hornsby and J. Leja, Critical surface tension of floatability. Coll. Surf., 7 (1983) 339.

[145] B. Yarar and J. Kaoma, Estimation of the critical surface tension of wetting of hydrophobic solids by flotation. Coll. Surf. 11 (1984) 429.

[146] B. Yarar, Gamma flotation: a new approach to flotation using liquid–vapor surface tension control. In: S.H. Castro and J. Alvarez (eds), Froth Flotation. Elsevier, Amsterdam, 1988, pp. 41–64.

[147] D.T. Hornsby and J. Leja, A technique for evaluating floatability of coal fines using methanol solutions. Coal Preparation, 1 (1984) 1.

[148] E.H. Lucassen-Reynolds, Contact angles and adsorption on solids. J. Phys. Chem., 67 (1963) 969.

[149] E.H. Lucassen-Reynolds and J. Lucassen, Thin films, contact angles, wetting. In: K.J. Ives (ed.), The Scientific Basis of Flotation. NATO ASI Ser., Martinus Nijhoff, Dordrecht, 1984, pp. 79–109.

[150] M.C. Williams and D.W. Fuerstenau, A simple flotation method for rapidly assessing the hydrophobicity of coal particles. Int. J. Miner. Process., 20 (1987) 153.

[151] D.W. Fuerstenau and J. Diao, Characterization of coal oxidation and coal wetting behavior by film flotation. Coal Preparation, 10 (1992) 1.

[152] D.W. Fuerstenau, J. Diao and J.S. Hansen, Estimation of the distribution of surface sites and contact angles on coal particles from film flotation data. Energy Fuels, 4 (1990) 34.

[153] A.W. Neumann, R.J. Good, C.J. Hope and M.J. Sejpal, An equation-of-state approach to determine surface tensions of low-energy solids from contact angles. J. Coll. Interf. Sci., 49 (1974) 291.
[154] J. Kloubek, Development of methods for surface free energy determination using contact angles of liquids on solids. Adv. Coll. Interf. Sci., 38 (1992) 99.
[155] M. Pawlik and J.S. Laskowski, Direct yield stress measurements as a method of determining contact angle on fine coal particles. Symp. Apparent and Microscopic Contact Angles, 216th National ACS Meeting, Boston, August 24–27, 1998.
[156] D. Li and A.W. Neumann, A reformulation of the equation of state for interfacial tensions. J. Coll. Interf. Sci., 137 (1990) 304.
[157] R. Ramesh and P. Somasundaran, Centrifugal immersion technique for characterizing the wettability of coal particles. J. Coll. Interf. Sci., 139 (1990) 291.
[158] M. Adams-Viola, G.O. Botsaris and Y.M. Glazman, An investigation of the hydrophilic/oleophilic nature of various coals. Coll. Surf., 3 (1981) 159.
[159] T. Takakuwa and T. Takamori, Phase inversion method for flotation study. In: A. Roberts (ed.), Mineral Processing — Proc. 6th Int. Mineral Processing Congress. Pergamon Press, Oxford, 1963, pp. 1–10.
[160] Y. Ye and J.D. Miller, Bubble/particle contact time in the analysis of coal flotation. Coal Preparation, 5 (1988) 147.
[161] J.L. Yordan and R.H. Yoon, Induction time measurements for the quartz–amine flotation systems. 115th SME Annu. Meet., New Orleans, 1985.
[162] J.L. Yordan and R.H. Yoon, Induction time measurements for a coal flotation systems. In: Y.A. Attia, B.M. Moudgil and S. Chander (eds), Interfacial Phenomena in Biotechnology and Materials Processing. Elsevier, Amsterdam, 1988, pp. 333–334.
[163] Y.Ye, R. Jin and J.D. Miller, Thermal treatment of low-rank coal and its relationship to flotation response. Coal Preparation, 6 (1988) 1.
[164] E.L. Fuller, Structure and chemistry of coals: calorimetric analyses. J. Coll. Interf. Sci., 75 (1980) 577.

Chapter 4

COAL FLOATABILITY

4.1. Introduction

Most coal-cleaning processes used to remove mineral impurities from coal are based on the gravity separation of coal from its associated gangue. The differences in density between pure coal particles (1.2–1.5 g/cm^3) and liberated mineral inclusions are sufficient to achieve almost complete separation fairly easily. Generally speaking, the mineral matter content in any coal particle is proportional to its density and inversely proportional to its calorific value.

For the prediction of concentration results (design of flowsheet) and for the control of preparation plant operations, a measure of concentrating operations is needed. The best known means of investigating and predicting theoretical beneficiation results are the so-called washability curves, which graphically represent the experimental separation data obtained under ideal conditions in float–sink tests.

The principle of the float–sink testing procedure is as follows (Fig. 4.1): a weighed amount of a given size fraction is gradually introduced into the heavy liquid of the lowest density. The floating fraction is separated from the fraction that sinks. The procedure is repeated successively with liquids, extending over the desired range of densities (usually from 1.3 to 1.8 g/cm^3, but in some cases densities as high as 2.2 g/cm^3 may be required). The fraction that sinks in the liquid of the highest density is also obtained. The weight and ash contents of each density fraction are determined.

The advanced coal cleaning technologies, which also include flotation, involve finer sizes of coal than previously tested. The U.S. Bureau of Mines developed a procedure in which a centrifuge is used to increase gravimetric force for improving the separation
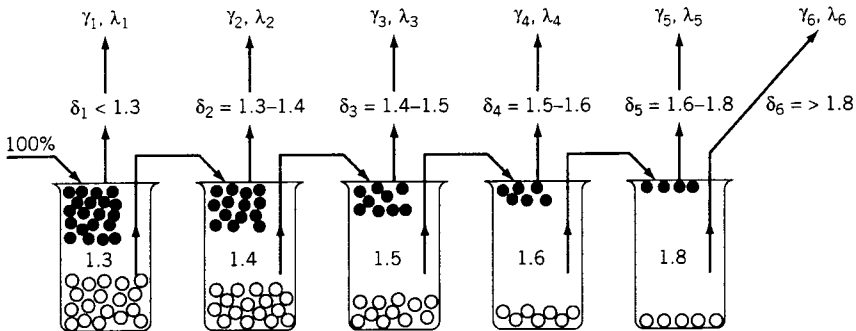
Fig. 4.1. Float–sink analysis procedure.

95

[1]. This method was further modified [2] to test coals ground below 75 μm and 45 μm.

The new methods were shown to provide satisfactory results but require additional precautions when very fine coal fractions are tested (e.g. below 14 μm) [3,4]. For such fine fractions the use of 100-g samples per 600-ml centrifuge bottles is recommended. Organic heavy liquids such as Certigrav can be used for 150 μm × 26 μm coal fractions along with a dispersant (Aerosol OT-100 surfactant at 2% concentration in the fresh medium). To remove OT-100, washing with a 3 : 1 ethanol–water solutions is used. For the 26 μm × 0 material, aqueous solutions of CsCl are recommended along with Brij-35 dispersant (8% addition). To remove CsCl and Brij-35, hot water, cold water and 3 : 1 ethanol–water is used for washing the samples. For subbituminous coals and lignites only organic heavy liquids are recommended. In the case of bituminous coals, the samples are dried at 40–65°C, and subbituminous and lignites are dried at 25–40°C.

It is well known that fine particles tend to form larger aggregates when suspended in water. This is especially true in the case of particles such as coal, which are hydrophobic to some extent. In order to separate such particles into various density fractions, they first must be dispersed. Moisture causes agglomeration of fine fractions in an organic liquid (as oil does in agglomeration of fine coal particles suspended in water). Therefore, fine coal fractions must be dried very well before carrying out the float–sink tests in organic heavy liquids, and, in addition, dispersing agents should also be used.

Table 4.1 shows the washability results, and Fig. 4.2 the washability curves (Henry-Reinhard plot) for a coal which is very easy to clean.

Fig. 4.3 shows the Mean-Value curve, also known as M-curve, for the same coal.

The shape of the primary washability curve and M-curve is an indication of the ease or difficulty of cleaning the coal. Fig. 4.4 illustrates four different cases: ideal separation, easy cleanability, difficult cleanability, and impossible separation. The primary washability curve for the difficult-to-clean coal exhibits only a gradual change in slope revealing a large proportion of middlings. The more the shape approximates the

Table 4.1
Set of float–sink test results

| Relative density	γ (%)	λ (%)	$\gamma\lambda/100$	$\sum\gamma\lambda/100$	Clean coal		Reject		0.1 Density distribution	
					$\sum\gamma_c$	ν	$\sum\gamma_t$ (%)	β (%)	Density	γ (%)
−1.3	43.0	2.0	0.860	0.86	43.0	2.0	57.0	36.5		
1.3–1.4	26.0	5.5	1.430	2.29	69.0	3.3	29.0	66.7	1.3	69
1.4–1.5	3.6	17.0	0.612	2.90	72.6	4.0	25.4	73.8	1.4	29.6
1.5–1.6	3.4	28.0	0.952	3.85	76.0	5.1	24.0	74.0	1.5	7
1.6–1.7	2.3	39.0	0.897	4.75	78.3	6.1	21.7	77.8	1.6	5.7
1.7–1.8	3.0	52.0	1.560	6.31	81.3	7.7	18.7	82.2	1.7	5.3
1.8–2.0	4.7	67.0	3.150	9.46	86.0	11.0	14.0	87.0	1.8	5.35
+2.0	14.0	87.0	12.200	21.64	100.0	21.6	0.0			
	100.0			21.64						
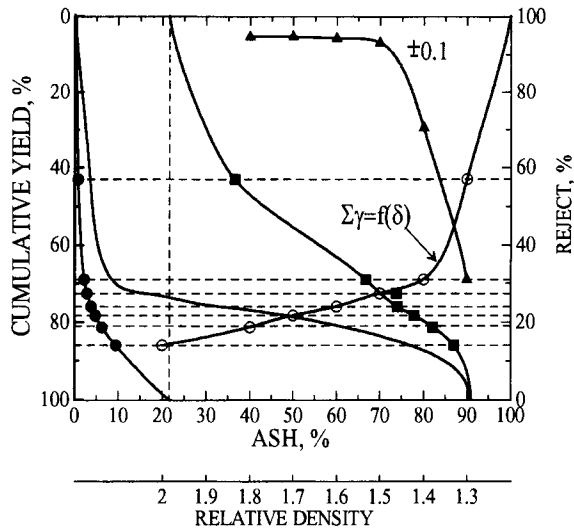
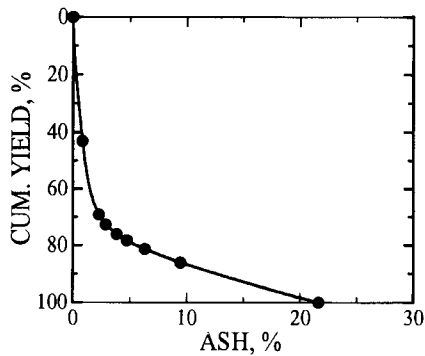Fig. 4.2. Washability curves for the data in Table 4.1.

Fig. 4.3. M-Value curve for the data in Table 4.1.

letter L, the easier the cleaning process. The example shows that the further the M-curve is from the line connecting the zero yield point with a (raw coal ash content) on the λ-axis, the greater the range of variation of ash content in the coal. A more gradual change in the slope of an M-curve indicates more difficult washability characteristics.

Most coal cleaning processes involve different gravity separation methods which are based on differences in density. ROM coal consists of a proportion of both coal and shale particles together with coal particles which include gangue. Clean coal particles have densities ranging from 1.2 to 1.5, while carbonaceous shale density ranges from 2.0 to 2.6 (density of pyrite is 5.0) and poorly liberated particles cover the whole range between these extremes. As always, liberation can be improved by finer crushing and grinding (see Fig. 2.13). Separation of such a mixture of particles varying in density in the float–sink tests leads to construction of washability curves. They are an ideal tool
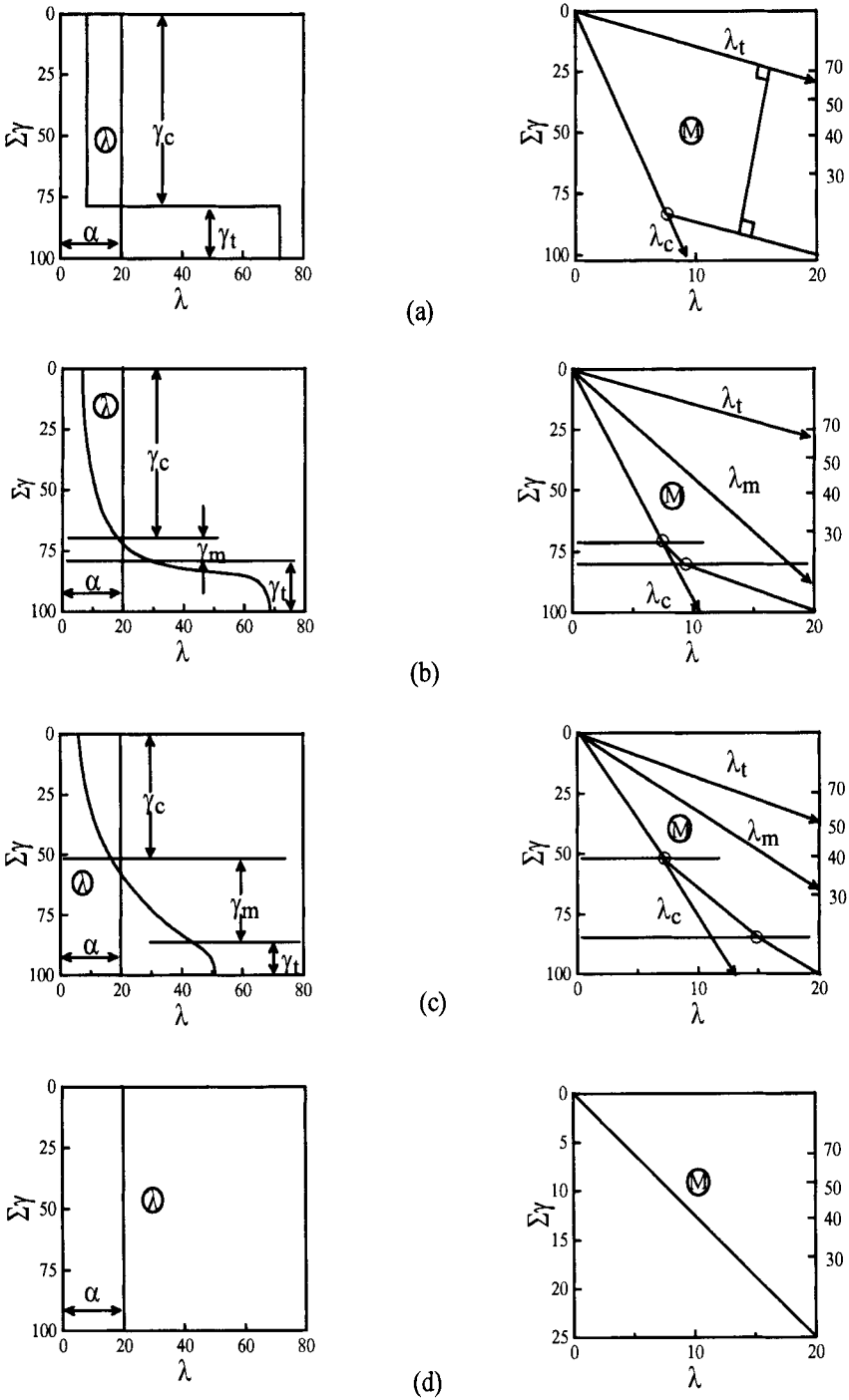
Fig. 4.4. Primary washability and M-value curves for (a) ideal separation, (b) easy-to-clean coal, (c) difficult-to-clean coal, and (d) impossible separation (γ_c stands for the yield of concentrate, γ_t stands for the yield of tailings, γ_m stands for the yield of middlings, λ_c stands for the ash content of concentrate, λ_t stands for the ash content of tailings, and λ_m stands for the ash content of middlings).

to estimate coal amenability to beneficiation by gravity methods, and to estimate the theoretical limits of cleaning for a given coal.

The separation produced by a washability analysis is based on the bulk property of the material (density), while the separation resulting from a flotation process is based on surface properties. The differences between these two types of separation processes can be substantial.

Since the density of coal organic matter is much lower than the density of mineral matter, coal density is proportional to the mineral matter content[1]. Gravitermic separation can therefore easily differentiate between particles varying in ash content. Coal wettability depends not only on the mineral matter content; it depends (see Section 3.5) also on coal rank, oxidation, porosity, etc. For example, low-density particles of subbituminous coal will report to floats in a float–sink analysis, but since such particles are rather hydrophilic they may report to the tailings in a flotation experiment. In general, it can be expected that float-and-sink separation will yield cleaner products than flotation. However, the differences between these two — density based and surface properties based — sets of data are impossible to predict. The effect of liberation on the results of gravity separation and those of flotation can be quite different; a particle containing 95% pyrite and 5% carbonaceous material will report to the sink product while the same particle may be readily floatable. Therefore, the use of washability curves in the prediction and evaluation of flotation results may lead to erroneous conclusions.

4.2. Floatability

4.2.1. Equipment

Several mechanisms are responsible for transferring mineral particles from the slurry to the froth. These include selective transfer by particle-bubble attachment, and non-selective transfer of material by entrainment and entrapment/coatings. In particular, the hydraulic entrainment of fine slimes into the froth launder has a tremendous impact on the froth product quality. This is further aggravated in coal flotation which is characterized by a large amount of floatable material reporting to the froth product, and a large amount of poorly liberated middling particles. Under such conditions, inconsistent froth removal is claimed to be a major reason for poor reproducibility of the flotation tests [5].

Australian Standards (AS2579-1983) recommend the use of the batch flotation cell as modified by Roberts et al. [6]. With this cell, inconsistencies arising from the operator's selection of the area and depth of froth removal are better controlled by means of a perspex cell insert. This insert prevents the stagnation of froth at the back of the cell and near the impeller shaft. The bottom of the insert is sloped at 45° to guide the air/coal aggregates to the front of the cell (Fig. 4.5).

---

[1] The plot of incremental ash (from the float sink data) versus 1/density (for that incremental ash class) is normally a straight line.
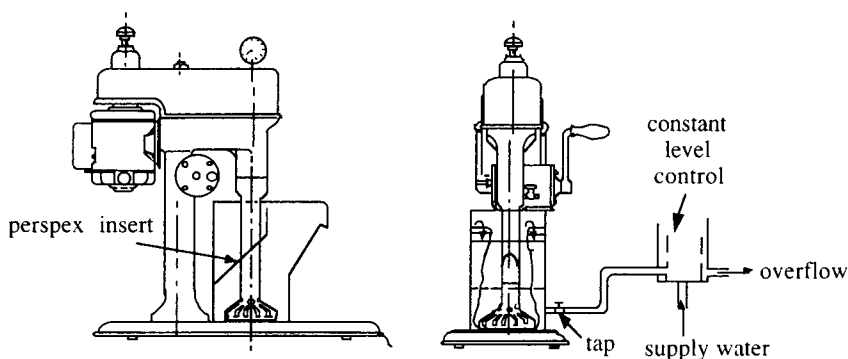
Fig. 4.5. The batch flotation cell, as modified by Roberts et al., recommended by Australian Standards for floatability tests. (After Roberts et al. [6]; by permission of Elsevier Science.)

In tests carried out to obtain the floatability curve, flotation kinetics is not important at all as the tests are carried out as long as the froth contains floatable particles.

Selection of the equipment for such tests is therefore not a critical issue, and the results obtained [7] by using the "tree" procedure on a single coal in cells of different volume indicate that the procedure is unaffected by this consideration.

A comprehensive review of various flotation cells available for lab testing was written by Jameson [8].

It is well established that in conditions approaching those of plug flow, a thick layer of froth and the addition of wash water to a flotation columns results in a sharper separation than would be attainable in a mechanical cell. In 1991, Mular and Musara [9] described a batch flotation column. A similar device is used in the advanced flotation washability procedure developed by Mohanty et al. [10].

4.2.2. Release analysis

A single-batch flotation experiment provides only concentrate yield and concentrate ash content and no indication as to whether concentrates of different quality could be obtained. A yield/ash curve could be constructed by running a number of batch tests under different reagent dosage conditions, but because of the entrainment of gangue and the poor flotation of coarse particles at low reagent dosages, the resulting cumulative yield/cumulative ash curve would not represent a limit of separation.

In the Dell Release Analysis (introduced in 1953 and refined in 1964 [11]), flotation is conducted in two phases in a laboratory Denver flotation cell. In the first phase, the coal is floated to exhaustion to reject all hydrophilic particles from the bulk concentrate. Reagents are added several times to ensure flotation of all particles with some degree of hydrophobicity. In the second stage of the release analysis, the bulk concentrate is separated into products varying in floatability by repeating flotation at increasing aeration rates and impeller speeds. Fig. 4.6 depicts the procedure [12]. In the modification suggested by Cavallero and Deurbrouck [13], the bulk concentrate is split into several products by collecting the concentrates over various time intervals.
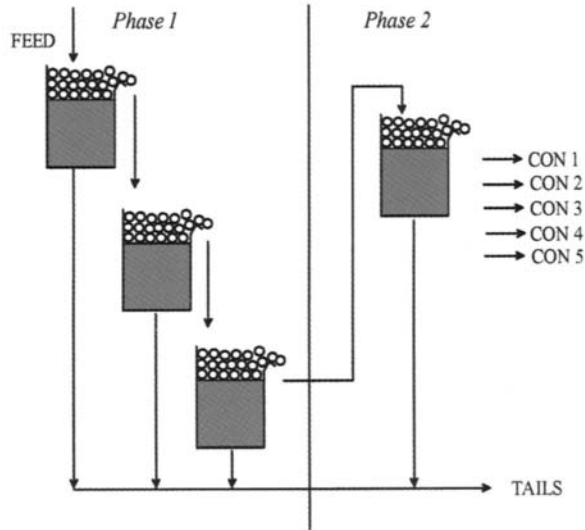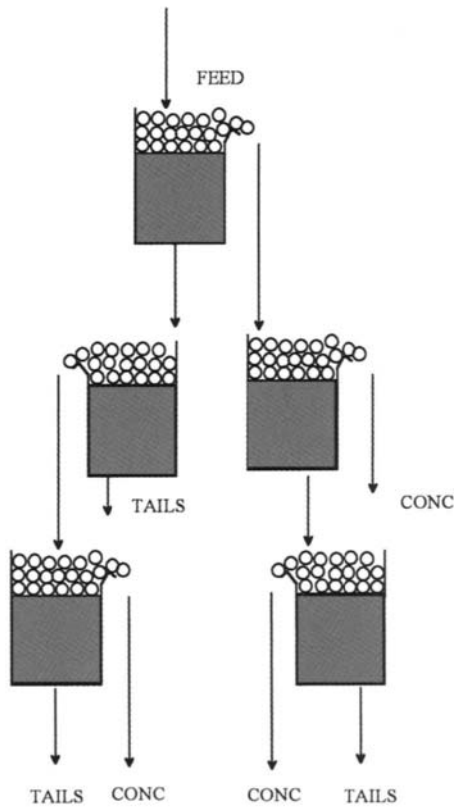
Fig. 4.6. Schematic diagram of the step-by-step procedures for release analysis. (After Mohanty et al. [12]; by permission of Gordon and Breach.)
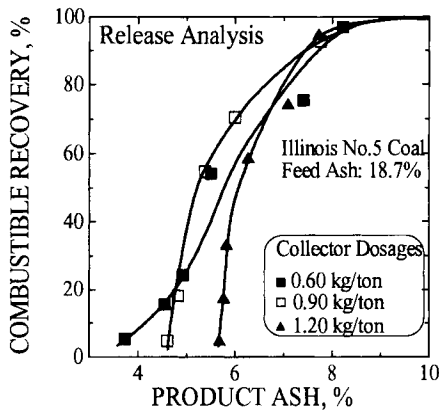
Fig. 4.7. Illustration of the sensitivity of the release performance curve to the collector dosage. (After Mohanty et al. [12]; by permission of Gordon and Breach.)

According to Mohanty et al. [12], the release analysis procedure is sensitive to collector dosages; the curves obtained for different coals all depended on the collector dosage. In all cases the performance deteriorated at excessively high dosages of reagents (Fig. 4.7). It was also noted that higher optimum collector dosages should be expected for coal samples having finer particle size distributions, and/or a higher degree of oxidation. Mohanty et al.'s data also indicate that the release analysis data significantly depend on the solids content of the feed. Fig. 4.8 clearly shows that the performance curves improve sharply with an increase in feed solids content from 8 to 16%, and only slightly with further increase in solids content up to 24%. In terms of the product sulfur
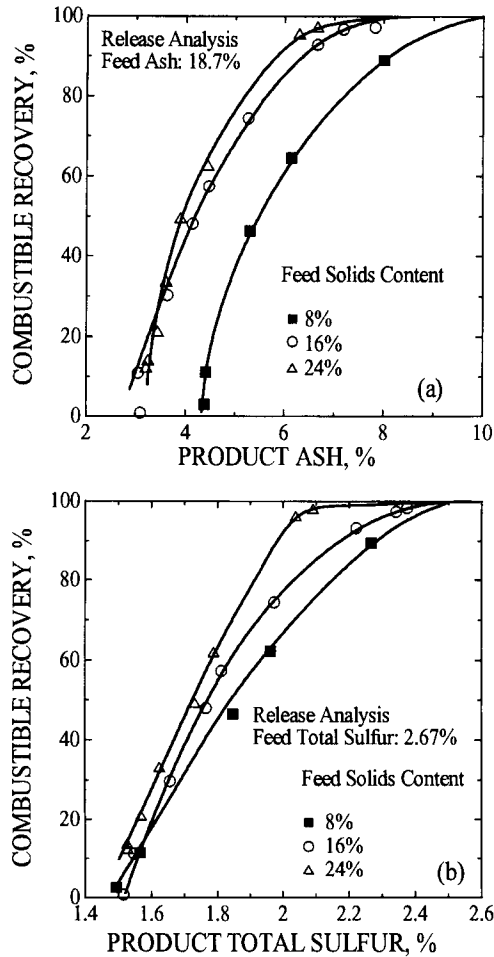
Fig. 4.8. Improvement in the release performance curve obtained with −180 μm Illinois No. 5 coal at high feed solids content on the basis of (a) product ash and (b) product total sulfur contents. (After Mohanty et al. [12]; by permission of Gordon and Breach.)

content, the separation performance continued to improve at each increase in feed solids content as shown in Fig. 4.8.

4.2.3. The tree technique

This procedure, developed by Nicol and his co-workers [5,14,15] involves repeated branching of the flotation steps (Fig. 4.9) in which the resulting concentrate and tailings are subjected to a number of successive scavenger and cleaner flotations in a laboratory batch cell. An initial rougher flotation is conducted at a relatively low reagent dosage and the resulting concentrate and tailings are refloated with an addition of reagents at each step. The accuracy of the overall separation performance can be improved

Fig. 4.9. Schematic diagram of the step-by-step tree analysis procedure. (After Mohanty et al. [12]; by permission of Gordon and Breach.)

by increasing the number of subsequent cleaning and scavenger steps. Pratten et al. [14] compared the release and tree analyses and found that while the release analysis produced different floatability curves depending on reagents consumption, the tree analysis points consistently converged on the same curve.

Mohanty et al. [12] have recently compared the two procedures. Their results indicate that the release procedure provide a superior separation in the high recovery regions, while the tree analysis is superior in the low recovery regions (Fig. 4.10). Mohanty et al. concluded that middling particles are more effectively treated in the release procedure.

4.2.4. The advanced flotation washability (AWF) procedure

This procedure is schematically shown in Fig. 4.11 [10]. The procedure combines the first stage of the release analysis where a "bulk" concentrate is produced, with the separation of this product into approximately seven different fractions according to a decreasing order of hydrophobicity by varying the aeration rate from about 1.5 l/min to 2.5 l/min. The batch flotation column used in the second stage is vertically baffled with
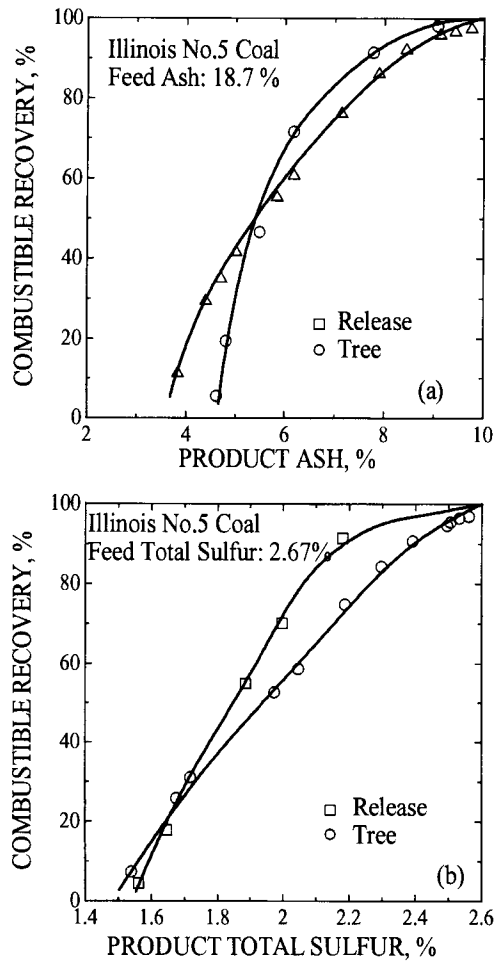
Fig. 4.10. Comparison of the release and tree analyses results. (After Mohanty et al. [12]; by permission of Gordon and Breach.)

stainless steel corrugated packing material similar to that used in the Packed-Column [16].

Fig. 4.12 shows a comparison of the washability curves obtained for Illinois No. 5 coal crushed below 180 μm using different techniques. A kerosene (collector) and Dow Froth M-150 polyglycol frother were utilized. No collector was used in the second cleaning stage, and only a few drops of frother were sometimes necessary to maintain a deep froth of about 90 cm. In the AFW procedure, the froth slowly flows over the column's lip to the product launder without any assistance from an operator. The release analysis procedure was conducted beginning with a feed solid content of about 20% in a batch Denver flotation cell. The centrifugal gravity-based washability analysis was carried out for the +25 μm material.
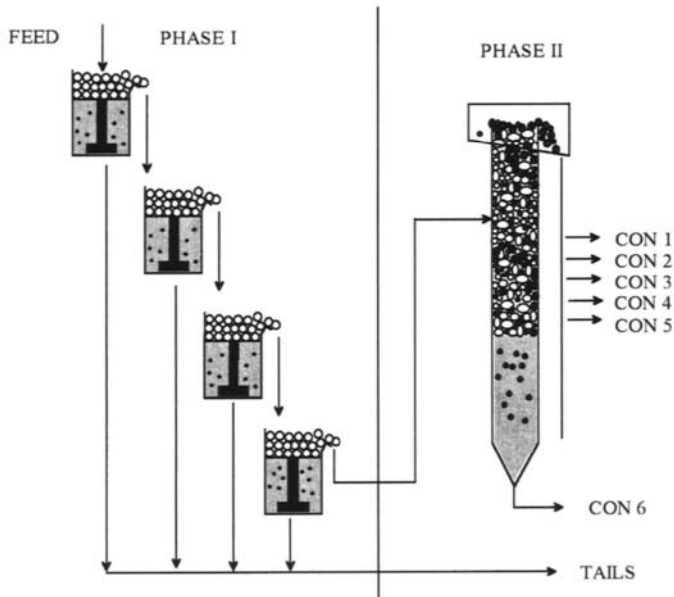
Fig. 4.11. The step-by-step advanced floatability analysis. (After Mohanty et al. [10]; by permission of Gordon and Breach.)

According to the authors [10], the separation curve obtained using the AWF procedure is much superior to that produced by the standard release analysis (Fig. 4.12). As expected, both were substantially inferior to the washability curve obtained using a centrifuge. Also, sulfur contents in the corresponding products were much lower in the products from the AFW procedure in comparison to the release analysis. The separation achieved in the AWF procedure was also superior to multi-stage cleaning in a continuously operated flotation column. Since the apparatus used in the AWF procedure is fully automated, and therefore reduces the possibility of human error, this procedure seems to offer a better way of characterizing coal floatability.

The lack of a standard procedure to determine the optimum floatability of a fine coal has recently prompted the National Energy Technology Laboratory (NETL) to set an interlaboratory test program to compare various techniques that have been in use. The participating laboratories conducted their floatability analysis using a slurry sample of an easy-to-clean Pittsburgh seam coal provided by CONSOL. The results plotted and analyzed by NETL led to interesting conclusions [17]. Several procedures, including Dell's release analysis and the AWF procedure gave comparable results. The best result was provided by the "reverse" release analysis (Fig. 4.13) in which the sample is first floated in a Denver cell to exhaustion, followed by the concentrate being re-floated to exhaustion two more times with the tailings being combined. The concentrate that remains is then placed in a Denver cell and floated at a fairly severe (high aeration and impeller rate) conditions. The tailings are saved separately and the concentrate again placed in a Denver cell. This flotation and saving of the tailings is repeated with each
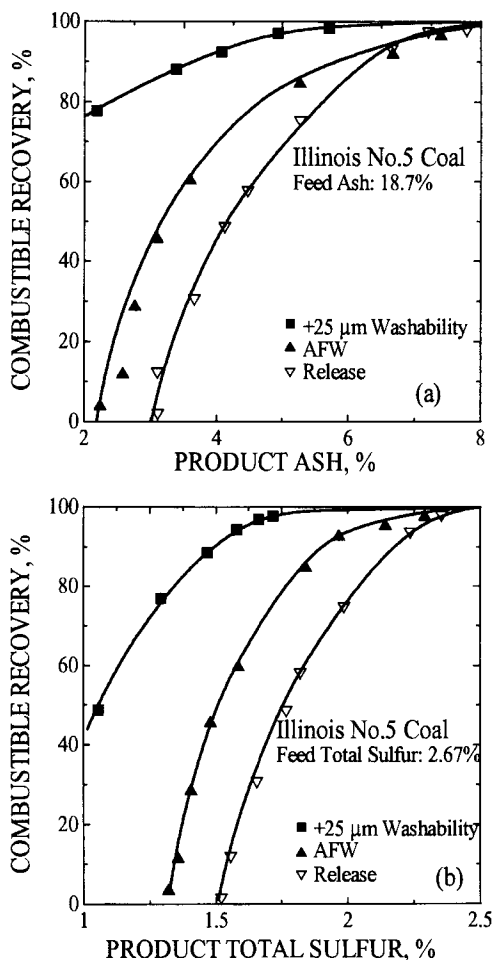
Fig. 4.12. Comparison of the washability curve form sink–float analysis of the +25 μm fraction with the floatability curves obtained following the advanced floatability analysis and the release analysis (After Mohanty et al. [10]; by permission of Gordon and Breach.)

subsequent test being at lower severity conditions (lower aeration and/or impeller rate). This procedure produced six tailing samples and one concentrate sample.

In their summary, Killmeyer et al. [17] concluded that several tested procedures provided fairly similar grade/recovery curves. The study showed that determination of the floatability potential of a coal is not at a level of a standardized procedure. The results can vary depending on the technique and the skill/experience of the personnel.

4.2.5. The use of floatability curves

Washability curves are used to design the flowsheet for a coal preparation plant, and to evaluate the results of the operating unit. The floatability curves can be
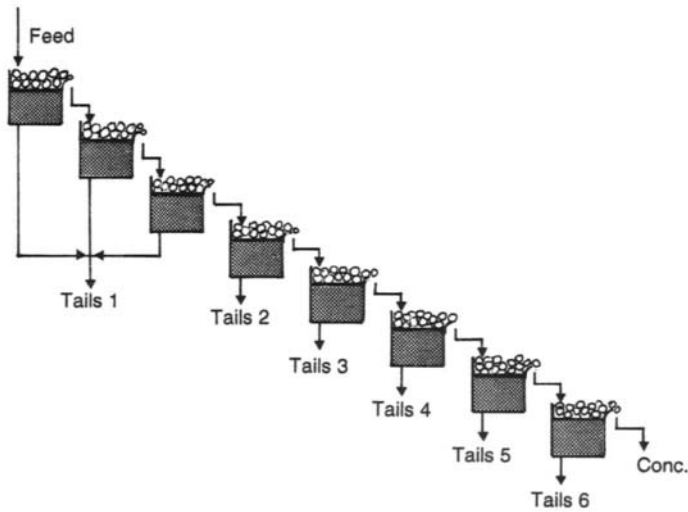
Fig. 4.13. "Reverse" release analysis procedure.

utilized in exactly the same way to design a flotation circuit and to evaluate its performance.

It is clear that the performance of the flotation circuit, expressed by the yield and ash content of the concentrate, can be evaluated by the position (proximity) of this point in relation to the floatability curve. Quantitatively, the proximity of the result to the curve may be measured in terms of organic efficiency as shown in the following example taken from Pratten et al. [14].

Two parallel flotation banks were sampled, each consisting five 14-m^3 cells, and the results are given in Table 4.2. Judging from the higher calculated concentrate yield and much higher ash content in the tailings, Bank A seems to perform better than Bank B, but by how much? However, at the same time it is obvious that the ash content in the feed to Bank A (11.1%) was also much lower than the ash in Bank B (13.3%) and this could also contribute to the differences.

In order to determine which circuit performs better, the feeds of both banks were sampled and the tree procedure was used to obtain the floatability curves for both. These are shown in Fig. 4.14. The calculated concentrate yields and quality are also given. These data sets allow calculation of the organic efficiency for both circuits.

Table 4.2
Measured flotation performance data

	Bank A	Bank B
Feed ash/% (d)	11.1	13.3
Concentrate ash/% (d)	8.0	8.1
Tailings ash/% (d)	66.5	58.7
Concentrate yield/%	95	90
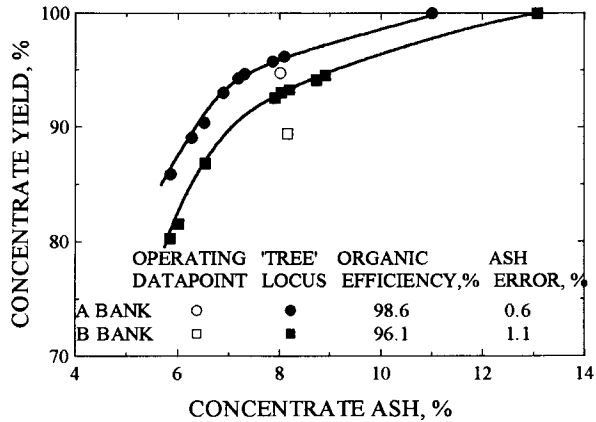
Fig. 4.14. An example of the use of the tree procedure to quantify flotation efficiency. (After Pratten et al. [14]; by permission of Elsevier Science.)

Organic efficiency is defined as

$$E_o = \frac{\gamma \cdot 100}{\gamma_t} \tag{4.1}$$

where E_o is the organic efficiency (%), γ is the actual yield of clean coal (%), is γ_t the theoretical yield of the clean coal from the washability curve at the same ash content (%).

The calculated clean coal yield for Bank A (95%) divided by the clean coal yield for 8% ash content from Fig. 4.14 gives an organic efficiency of 98.6%; the organic efficiency for Bank B is 96.1%. Now, it is obvious that Bank A performs better than Bank B, but only a statistical evaluation of this data could answer the question of how significant the difference is.

Another example which shows how to use floatablity curves is taken from Davis et al. [18].

This paper describes the modification of the Middle Fork plant in the U.S.A. Conventional flotation at this plant performed poorly and from coal containing 45–55% ash (75% below 45 μm) they produced a concentrate containing 14–18% ash at a combustible recovery of 60–70%. The release analysis and testing in a Microcel lab column gave the results shown in Fig. 4.15. These data revealed that for this coal it is possible to obtain 75% combustible recovery at 8% ash content using a flotation column. Based on this information it was decided to replace the mechanical cells by a flotation column. As Fig. 4.16 demonstrates, the plant column performs very well indeed and produces results which are extremely close to the theoretical limits as given by the release analysis results.

In one of the papers presented at the 12th International Coal Preparation Congress, Nicol et al. [15] attempted derivation of the partition (Tromp) curve for flotation equipment. The floatability curves based on the tree (or AWF) procedure, together with the efficiency numbers which like E_p would characterize performance of flotation cells, could then be used to predict complete flotation results as is now possible for gravity
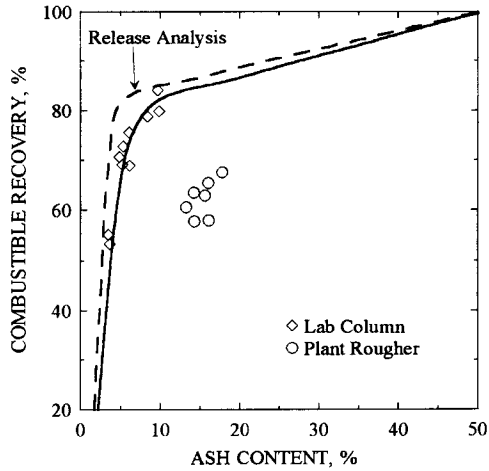
Fig. 4.15. Combustible recovery vs. combustible ash content for the Middle Fork plant conventional flotation cells, laboratory-scale column, and release analysis. (After Davis et al. [18]; by permission of Gordon and Breach.)
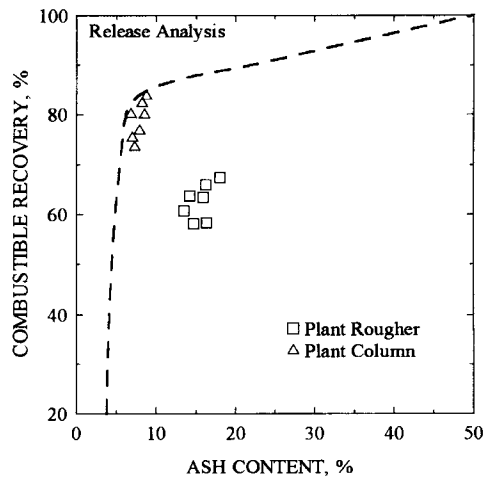
Fig. 4.16. Comparison of full-scale column and conventional flotation performance at the Middle Fork facility. (After Davis et al. [18]; by permission of Gordon and Breach.)

separators. The development work of measuring the partition curve for flotation cells has begun [19].

4.3. References

[1] E.R. Palowitch and T.M. Nasiaka, Using a centrifuge for float-and-sink testing. Fine coal. US Bureau of Mines, RI 5741 (1961).

[2] J.A. Cavallaro and R.P. Killmeyer, Development of a centrifuge float–sink procedure for gravimetric evaluation of ultrafine coals. J. Coal Quality, 7 (1988) 55.

[3] R.P. Killmeyer, R.E. Hucko and P.S. Jacobsen, Centrifugal float–sink testing of fine coal: an interlaboratory test program. Coal Preparation, 10 (1992) 107.

[4] P.J. Suarini, Improving fine-coal washability procedures. In: S.K. Kawatra (ed.), High Efficiency Coal Preparation: An International Symposium, SME, Littleton, CO, 1995, pp. 119–128.

[5] S.K. Nicol, Fine Coal Beneficiation — Advanced Coal Preparation Monograph Series, Vol. IV, Part 9. Australian Coal Preparation Society, 1992.

[6] T. Roberts, B.A. Firth and S.K. Nicol, A modified laboratory cell for the flotation of coal. Int. J. Miner. Process., 9 (1982) 191.

[7] S.K. Nicol, J.B. Smitham and J.T. Hinkley, Problems relating to the measurements of ideal flotation response. In: G.E. Agar, B.J. Huls and D.B. Hudyma (eds), Column '91. Sudbury, 1991, Vol. 1, pp. 99–108.

[8] G.J. Jameson, Experimental techniques in flotation. In: K.J. Ives (ed.), The Scientific Basis of Flotation. NATO ASI Series, Martinus Nijhoff Publishers, Boston, MA, 1984, pp. 193–228.

[9] A.L. Mular and W.T. Musara, Batch column flotation: rate data measurement. In: G.E. Agar, B.J. Huls and D.B. Hudyma (eds), Column '91. Sudbury, 1991, Vol. 1, pp. 63–74.

[10] M.K. Mohanty, R.Q. Honaker and K. Ho, Coal flotation washability: development of an advanced procedure. Coal Preparation, 19 (1998) 51.

[11] C.C. Dell, An improved release analysis procedure for determining coal washability. J. Inst. Fuel, 37 (1964) 149.

[12] M.K. Mohanty, R.Q. Honaker, A. Patwardhan and K. Ho, Coal flotation washability: an evaluation of the traditional procedures. Coal Preparation, 19 (1998) 33.

[13] J.A. Cavallaro and A.W. Deurbrouck, Froth flotation washability data of various Appalachian Coals using the timed release analysis technique. US Bureau of Mines, RI 6652 (1965).

[14] S.J. Pratten, C.N. Bensley and S.K. Nicol, An evaluation of the flotation response of coals. Int. J. Miner. Process., 27 (1989) 243.

[15] S.K. Nicol, J.B. Smitham and J.T. Hinkley, Measurement of coal flotation efficiency using the tree flotation technique. In: W.S. Blaschke (ed.), Proc. 12th Int. Coal Preparation Congress (Cracow, May 1994). Gordon and Breach, New York, 1996, pp. 741–746.

[16] D.C. Yang, Packed-bed column flotation of fine coal. Coal Preparation, 8 (1990) 19.

[17] R.P. Killmeyer, M.V. Ciocco and P.H. Zandhuis, Comparison of procedures for determining the floatability potential of fine coal. 17th International Coal Preparation Exhibition and Conference, Lexington, May 2–4, 2000.

[18] V.L. Davis, F.L. Stanley, P.J. Bethel, G.H. Luttrell and M.J. Mankosa, Column flotation at the Middle Fork Preparation Facility. Coal Preparation, 14 (1994) 133.

[19] J. Smithan, R. Keast-Jones, A. Pickup and B. Leyden, Development and use of the tree flotation technique to measure coal flotation efficiency. In: J. Smitham (ed.), Proc. 7th Australian Coal Preparation Conference. Australian Coal Preparation Society, Mudgee, 1995, pp. 356–370.

Chapter 5

REAGENTS

5.1. Introduction

The behavior of a coal in the flotation process is determined not only by a coal's natural floatability (hydrophobicity), but also by the acquired floatability resulting from the use of flotation reagents.

Coal flotation, just as any other froth flotation process, requires the use of reagents. Since coals, along with graphite, sulfur, talc and molybdenite, are classified into the same group of solids that are hydrophobic by nature [1], their flotation requires similar reagents. The use of hydrocarbons ("oils") as collectors is characteristic for this group of minerals. The first and perhaps most obvious difference between such collectors and the ionic collectors utilized in mineral flotation is that the oily collectors are insoluble in water. The simultaneous use of both water-insoluble oil and water-soluble frother creates a physico-chemical system which is usually poorly understood.

The general classification of reagents for coal flotation is shown in Table 5.1 [2].

Table 5.1
Coal flotation reagents

Type	Flotation use as	Functional group	Examples	Action
Nonpolar (water insoluble)	Collectors	–	Kerosene; fuel oil	Through selective wetting and adhesion of oil drops to coal particles
Surface active (water soluble)	Frothers	Hydroxyl; nitrogenous	Aliphatic alcohols; pyridine cont. tar oils	Frothers with some collecting abilities. Also improve emulsification of oily collectors
Emulsifiers (soluble in oily collector)	Promoters	Hydroxyl; carboxyl; nitrogenous	Polyethoxylated alcohols, fatty acids, etc.	Facilitate collector emulsification and its spreading over coal surface
Inorganic (water soluble salts)	Modifiers	–	NaCl, $CaCl_2$, Na_2SO_4; H_2SO_4, CaO; CaO	Promoters (?); pH regulators; sulfide depressants (?)
Protective colloids	Depressants	Hydroxyl; carboxyl	Polymers: starch, dextrin, carboxymethyl cellulose, etc.	Modifiers; coal depressants

111

5.2. Reagents

5.2.1. Collectors

Two types of hydrocarbons were used in coal flotation as collectors: hydrocarbons produced as coke-oven by-products, and hydrocarbons produced from crude oil (petroleum). The former were very common more than 30 years ago, but since they contain phenols and other toxic aromatic hydrocarbons their use in coal flotation was discontinued. These products were replaced by "oils" produced from crude oil.

According to ASTM D-288, crude petroleum is defined as a naturally occurring mixture, which is removed from the earth in a liquid state, containing predominantly hydrocarbons, and/or sulfur, nitrogen and oxygen derivatives of hydrocarbons.

Table 5.2 [3] provides information on various types of petroleum products; this table also indicates how major types of hydrocarbons accumulate in various fractions.

The light distillate fractions, intermediate fractions and heavy distillate fractions are characterized by the boiling ranges 93–204°, 204–343° and 343–566°C, respectively. The residues, after all the distillates are removed, include residual fuel oils, petrolatum and asphalt. These contain paraffins of very high molecular weight, polycyclic hydrocarbons, condensed polyaromatics and mixed naphteno-aromatics, as well as sulfur-, nitrogen- and oxygen-containing compounds. The oxygen content increases with the boiling point of the fraction, the greater portion of the oxygen-containing constituents are concentrated in the residues, where oxygen contents as high as 8% are reported [4].

Fuel oil No. 2, frequently used in coal flotation, is one of the products within a boiling range of 204–343°C. It consists of paraffins, iso-paraffins, aromatics, naphtenes, and also sulfur-, nitrogen- and oxygen-containing hydrocarbons not removed by refining. Fuel oils also appear among the products listed under the residues. These are high molecular weight paraffinic and cyclic hydrocarbons along with oxygen, sulfur and nitrogen derivatives. Since these oils are characterized by a high viscosity they are mixed with intermediate distillates. The mixtures containing 20–50% of intermediate distillates are referred to as No. 4 and No. 5 fuel oils; the mixture with only 5–20% of the distillate is known as No. 6 fuel oil. No. 6 fuel oil is reported to contain 10–500 ppm vanadium and nickel in the form of porphyrins.

For aliphatic hydrocarbons, the water–hydrocarbon interfacial tension slightly exceeds 50 mJ/m². The water/oil interfacial tension for petroleum products is often in the range from 25–32 mJ/m² to as low as 12 mJ/m² [5]. This indicates that these products also contain hydrocarbons with polar groups. Fig. 5.1, taken from Woods and Diamadopoulos [6], shows oil–water interfacial tension as a function of pH for a few crude oils. This relationship confirms that the crudes contain surface active species. An especially strong effect of pH on the water/oil interfacial tension was reported for heavy crude oil fractions, such as asphaltenes [7].

5.2.2. Frothers

The general list of flotation frothers is given in Table 5.3 [8].

Table 5.2
Chemical compositions of various crude oil distillation fractions

Crude oil products	Paraffins C_nH_{2n+2} $-C-C-C-C-C-$	Isoparaffins C_nH_{2n+2} $-C-C-C-C-C-$ $\overset{\displaystyle |}{-C-}$	Naphtenes C_nH_{2n}	Aromatics C_nH_n	Sulfur containing compounds	Nitrogen compounds	Oxygen compounds
Natural gasoline							
Light distillates			Substituted monocyclic naphtenes and polycyclic naphtenes	Condensed polyaromatic molecules	Mercaptans, thio-ethers, cyclic thio-ethers	Basic nitrogen-containing compounds	
Intermediate distillates							
Heavy distillates							
Residues							
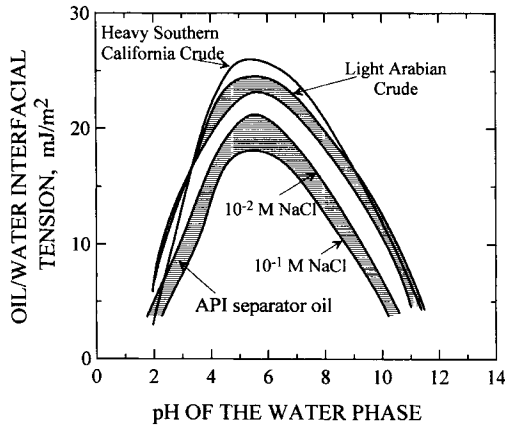
Fig. 5.1. Oil–water interfacial tension as a function of pH for several crude oils. (After Woods and Diamadopoulos [6]; by permission of Marcel Dekker Inc.).

In the past, cresols and xylenols were quite heavily used in coal flotation; today they are replaced by aliphatic alcohols, or polyglycol ethers.

Aliphatic alcohols that contain a single $-OH$ group are generally of limited solubility in water. The frothers which belong to this group have a chain length of 5 to 8 carbon atoms. These include iso-amyl alcohol, hexanol, cyclo-hexanol, and heptanol; probably the best known examples in this group are MIBC (methyl-iso-butyl carbinol) and 2-ethyl hexanol. Several manufacturers now offer MIBC-like commercial products (e.g. Allied Colloids Procol F937, Witco Arosurf F-139 and F-141).

Polyglycol type frothers are polymeric derivatives of ethylene oxide or propylene oxide. This group includes well-known frothers manufactured under the trade name of Dowfroth, the products manufactured by Union Carbide (PPG frothers), Cyanamid (Aerofroth), ICI Australia (Terric 400 series frothers), Huntsman (Unifroth 250), and Witco (Arosurf F-214 and F-215), and others. The frothers classified into this group range from completely miscible with water to partially soluble types. This is achieved by varying the ratio of hydrophobic (e.g. $-CH_2-$ groups) to hydrophilic groups (e.g. $-CH_2CH_2O-$) in the frother molecule.
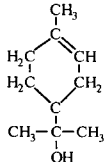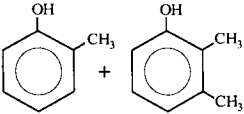
As it will be discussed in Section 5.3, in coal flotation the frothers also exhibit some collecting properties.

5.2.3. Promoters

Because most coal flotation circuits do not provide for collector emulsification and for intense conditioning in spite of the use of water-insoluble collectors, the use of surface-active emulsifiers (promoters) can help to enhance emulsification (dispersion) and abstraction of the oily collector by coal particles. That was the major reason for the development of so-called promoters; some of them are listed in Table 5.4.
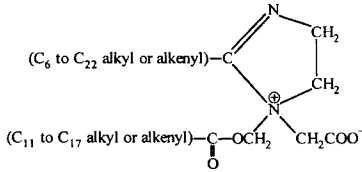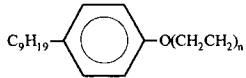
Table 5.3
Flotation frothers

	Name	Formula	Solubility in H$_2$O
(1)	*Aliphatic alcohols*	R—OH	
	Methyl isobutyl carbinol (MIBC)	CH$_3$—CH—CH$_2$—CH—CH$_3$ (with CH$_3$ and OH branches)	Low
	2-ethyl hexanol	CH$_3$—CH$_2$—CH$_2$—CH$_2$—CH—CH$_2$—OH (with CH$_2$—CH$_3$ branch)	Low
	diacetone alcohol	CH$_3$—C(CH$_3$)(OH)—CH$_2$—C(O)—CH$_3$	Very good
	2,2,4-trimethylpentanediol 1,3-monoisobutyrate (TEXANOL)	CH$_3$—CH(CH$_3$)—CH(OH)—C(CH$_3$)—CH$_2$—O—C(O)—CH(CH$_3$)	Insoluble
(2)	*Cyclic alcohols*		
	α-terpineol (active constituent of pine oil)		Low
	Cyclohexanol	C$_6$H$_{11}$OH	Low
(3)	*Aromatic alcohols*		
	cresylic acid (mixture of cresols and xylenols)		Low
(4)	*Alkoxy-type frothers*		
	1,1,3-triethoxybutane (TEB)	CH$_3$—CH(O—C$_2$H$_5$)—CH$_2$—CH(O—C$_2$H$_5$)(O—C$_2$H$_5$)	Low
(5)	*Polyglycol-type frothers*	R(X)$_n$OH, R=H or C$_n$H$_{2n+1}$, X=EO, PO or BO	Very good or total
	DF 250	CH$_3$(PO)$_4$OH	Total
	DF 1012	CH$_3$(PO)$_{6.3}$OH	32%
	Aerofroth 65, DF 400	H(PO)$_{6.5}$OH	Total
	DF 1263	CH$_3$(PO)$_4$(BO)OH	Very good

5.2.4. Coal and pyrite depressants

The function of a depressant is the opposite of that of a collector — it inhibits flotation of a given mineral. Since coals are hydrophobic, their flotation can be depressed only by making them hydrophilic. In a group of coal depressants, Klassen [2] listed organic polymers such as dextrins, starches, tannins and sodium lignosulfonates. These are polymers whose macromolecules contain numerous functional

Table 5.4
Coal flotation promoters

	Contains imidazole or imidazolinium ions	
DOWELL M-210 U.S. Patent 4,450.070	$(C_6$ to C_{22} alkyl or alkenyl)—C … CH$_2$ … CH$_2$ … N … $(C_{11}$ to C_{17} alkyl or alkenyl)—C—OCH$_2$ CH$_2$COO$^-$ ‖ O	Behaves as cationic surfactant at pH < 7.3 and as anionic at pH > 8.8
EKT Polish Patent 104,569/1977	Polyethoxylated fatty acids	Strong emulsifiers
TERIC GN ICI Australia	Polyethoxylated nonyl phenols C$_9$H$_{19}$—⬡—O(CH$_2$CH$_2$)$_n$	GN 4–5 very surface active, least frothing; GN 8–10 least surface active, most frothing
SHEREX Shur Coal Promoters #159 and #168	?	In oil–water systems behave like anionic surfactants
Accoal 4433 American Cyanamid	Mixture of aliphatic alcohols, alkenes, etc.	

groups and are consequently very hydrophilic. Guar gums are used as depressants for talc [9].

The basic structural unit of polysaccharides is D-α-glucose, whose chemical composition is shown schematically in Fig. 5.2a. As indicated in Fig. 5.2b, these basic units can be connected through α-1.6 linkages or α-1.4 linkages. While α-1.6 linkages are present in linear amylose, both α-1.4 and α-1.6 linkages appear in amylopectin with branching occurring approximately every 25 glucose units [10–12]. These two, amylose and amylopectin, are constituents of starch; a typical starch contains about 25% amylose and about 75% amylopectin. Tapioca contains 17–22% amylose, wheat 17–27%, potato 23% and corn 22–28% [13].

Dextrin is derived from starch by thermal degradation under acidic conditions. Depending on the degree of conversion, dextrin may exhibit varying solubility in water.

Both starch and dextrin form colloidal systems in water. The main difference between them is that dextrin is a highly branched smaller molecule with its molecular weight ranging from 800 to 79,000 [14], whereas starch is made up of much larger molecules with amylose molecular weight ranging from 340,000 to 2,500,000 [15], and that of amylopectin reported even up to 10^8 [13].

Dextrins were patented as coal depressants in a two-stage reverse flotation of coal in which, following the first conventional flotation stage, pyrite is floated with xanthates in the second stage while coal is depressed with dextrins [16,17].

a)

Glucose molecule (α-D-(+) glucopyranose)

b)

branch point, (1-6) linkage

(1-4) linkage

Branched structure of amylopectin and dextrin

c)

Carboxymethyl Cellulose

d)
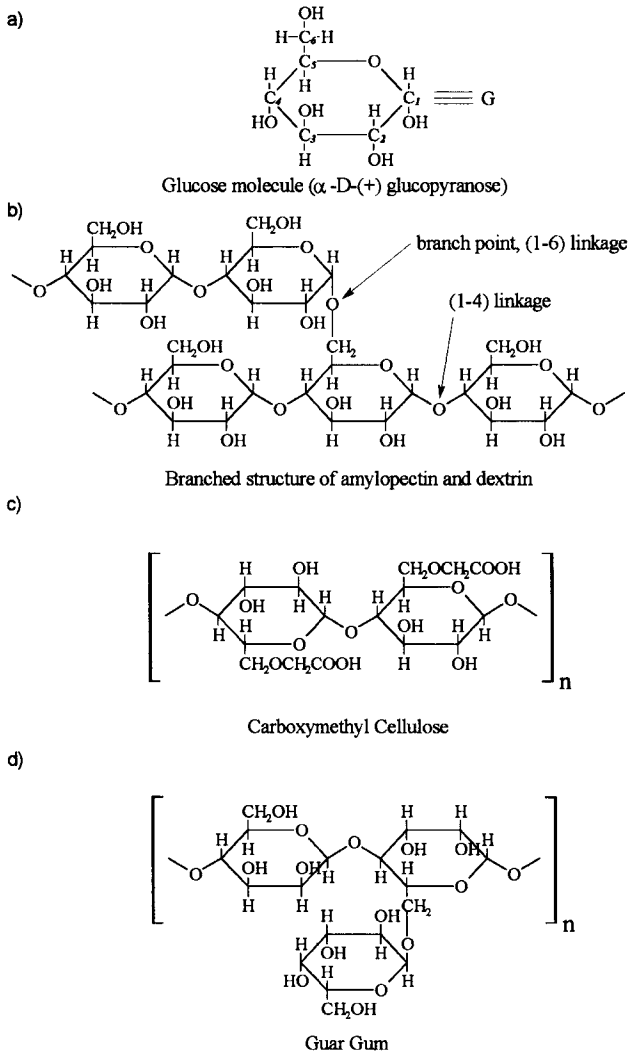
Guar Gum

Fig. 5.2. Molecular structure of glucose unit (a), dextrin (b), carboxymethyl cellulose (c) and guar gum (d).

The structure of carboxymethyl cellulose with the glucose units bonded by β-1.4 links is shown in Fig. 5.2c. The presence of carboxylic groups makes it an anionic polymer, which is fully ionized in alkaline solutions.

Laskowski et al. [18] reported carboxymethyl cellulose's ability to depress pyrite in the flotation of coal. Methocel was shown to depress coal [19] (Section 5.3.6.1). Polyacrylamide flocculants are reported to depress coal (see Fig. 6.18). Perry and Aplan [20] found that starches with a high amylose content (e.g. Hylon VII) exhibited good depressing properties towards pyrite. Starch was apparently successfully used as a pyrite depressant in the selective oil agglomeration of fine coal [21].

Wood consists of about 50% cellulose fibers, about 30% lignin and 20% carbohydrates. Tannis extracts obtained from two types of trees are well-known modifying agents: quebracho and wattle bark. The chemical composition of quebracho is shown below:

$$n = 1 - 200$$
$$MW = 200 - 50,000$$
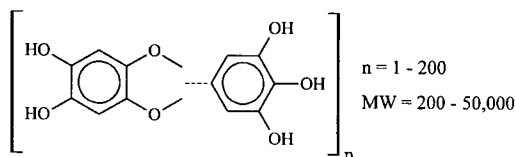
Lignin, which binds together the cellulose fibers of wood, represents an extremely complex mixture of monomeric cyclic species with polymers which are both two- and three-dimensional. A dioxyphenyl propyl unit, which Leja [22] cites as an important repeating unit of most lignin components, is depicted below:

$$-O-\langle\!\!\!\bigcirc\!\!\!\rangle-CH_2-CH_2-CH_2-$$
$$-O$$
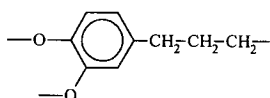
Lignin sulfonates have found broad applications as dispersing agents.

Humic acids will also be classified in this group. These are highly reactive, amorphous, predominantly aromatic complex anionic polyelectrolytes with carboxylic and phenolic groups. Humic acids are present in practically all natural waters and impart a brown or yellow color to them. Humic acids are strong coal flotation depressants.

Humic acids can be readily extracted from oxidized coal with aqueous alkali. The yield of humic acids extracted from coal decreases as the coal rank increases [23] [1]. In the case of alkali-insoluble coals, humic acids may be obtained by oxidation. Molecular weights were reported to range from 500 to 10,000.

As it is known, the initial stages of coal oxidation are characterized by chemisorption of oxygen at readily accessible surface sites and by the formation of acidic functional groups, in particular $-COOH$, $=CO$ and phenolic $-OH$. However, given enough time, the oxidation will gradually reach deeper and begin to degrade the coal substance itself, first converting it into alkali-soluble humic acids and then breaking those substances down into progressively smaller molecular species. According to Berkowitz [24], in air-oxidation, rapid generation of humic acids occurs only at temperatures exceeding 150°C.

Humic acids contain not only carboxylic and phenolic groups with pK_a of 4.5–4.9 and 8–8.9, respectively, but also carboxylic groups ortho to phenolic hydroxyls (as in salicylic acid) with pK_a values for such groups which may be as low as 3. This explains

---

[1] Extraction of humic acids in alkaline solutions from coal was standardized as a method of quantifying the degree of coal oxidation [25,26].

the chelating properties of humic acids and their ability to form complexes with metal ions and clays [27].

In their paper presented at the 11th International Mineral Processing Congress, Attia and Kitchener [28] described a number of water-soluble polymers of high molecular weight, incorporating sulfhydryl ($-SH$) or other groups which complex or chelate heavy metal ions. Following these ideas, Attia and Fuerstenau [29] and Attia [30] described the polyxanthate dispersant (PAAX) as a depressant of pyrite in a selective flocculation. PAAX, which is obtained by reacting low molecular weight polyacrylic acid with xanthate, is structured as shown below:

$$
\left[\left[\begin{array}{c} -CH_2-CH- \\ | \\ C=O \\ | \\ ONa \end{array}\right]_{n-d} - \left[\begin{array}{c} -CH_2-CH- \\ | \\ C=O \\ | \\ O \\ | \\ C=S \\ | \\ SNa \end{array}\right]_d\right]_n
$$
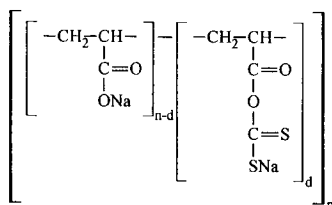
Sotillo et al. [31] described a new reagent, TEPA, as a coal depressant.

Chmielewski and Wheelock [32] studied thioglycolic acid as a pyrite depressant in coal flotation. Drzymala and Wheelock [33] reported that the compounds that contain both a sulfhydryl group ($-SH$) and a carboxyl or sulfonic acid group (e.g. 2-mercaptoethanesulfonic acid, mercaptosuccinic acid, tioglycolic acid, thiolatic acid, 3-mercaptopropionic acid, etc.) exhibit depressing properties towards pyrite in coal oil agglomeration.

Ye et al. [34] reported improved ash and pyrite rejection during fine-coal flotation by preconditioning the coal suspension with potassium monopersulfate ($KHSO_5$). Certain reducing agents such as sodium dithionide, and some dispersants such as Aerosol OT were found to enhance selectivity in the desulfurizing flotation of coal [35].

Several researchers studied the depressing effect of the bacteria *Tiobacillus ferrooxidans* on pyrite depression in coal oil agglomeration and in coal flotation [36–38].

5.2.5. Inorganic modifiers

Hydrophobic solids can be floated at high electrolyte concentrations without any other reagents; this is the so-called salt flotation process [39]. The rate of coal flotation increases dramatically in concentrated electrolyte solutions (e.g. 0.3–0.5 M NaCl), whereas in salt solutions flotation with conventional reagents can be carried out at much lower dosages [40,41]. Flotation tests carried out with different salts revealed that sodium sulfate produced the best results in accordance with the following pattern: sulfates > chlorides > nitrates [2]. Flotation experiments with coal (containing less than 1% of ash) which has been subjected to oxidation under controlled conditions revealed a strong correlation between salt flotation and coal hydrophobicity. At a given degree of oxidation (Fig. 5.3), when the coal surface is not hydrophobic enough, the coal stops floating in salt solutions [42].
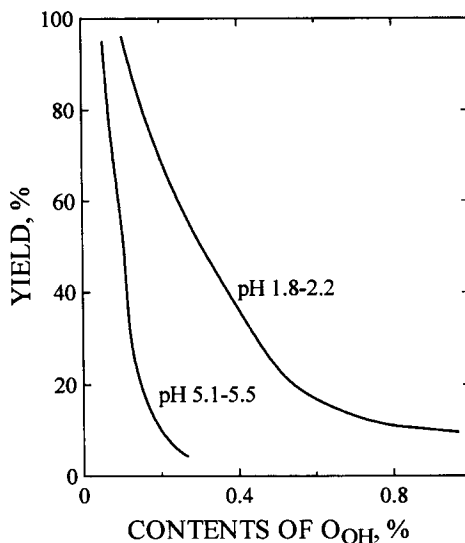
Fig. 5.3. Effect of oxidation of high-volatile bituminous coal on its flotation in 0.5 M NaCl aqueous solution. (Adapted from Iskar and Laskowski [42]; by permission of Elsevier Science.)

5.3. Reagents' mode of action

5.3.1. Water-insoluble oily collectors

5.3.1.1. Introduction

Suspensions and emulsions, or disperse systems in general, are characterized by a large free energy which is given by a product of interfacial area and interfacial tension. Since the interfacial area between the suspended fine particles and liquid, or oil droplets suspended in aqueous phase, is huge, the dispersed system tends to reduce it by particle aggregation (emulsion droplets coalescence). This may be either coagulation or flocculation. When oil is dispersed into fine droplets in an aqueous suspension of hydrophobic particles, the hydrophobic solid particles may be aggregated by oil droplets since oil will preferentially wet the hydrophobic particles (Fig. 5.4) [21]. This process is referred to as *oil agglomeration* and it plays an important role in many separation processes.

Depending on the quantity of the immiscible liquid (oil), the hydrodynamic conditions, and the method used to separate the agglomerates, the final result may be very different as shown in Table 5.5 [43].

The first process in the table, *extender flotation*, utilizes small doses of an oil (up to a few hundred grams per ton of ore) to enhance the collector, and/or to reduce its consumption. Extender oils are frequently used to improve flotation of coarse particles.

In *agglomerate flotation*, which was invented to treat very fine particles that are not recovered efficiently in conventional froth flotation, oil is added to increase the size of particles by agglomerating them. The method involves conditioning at high pulp density
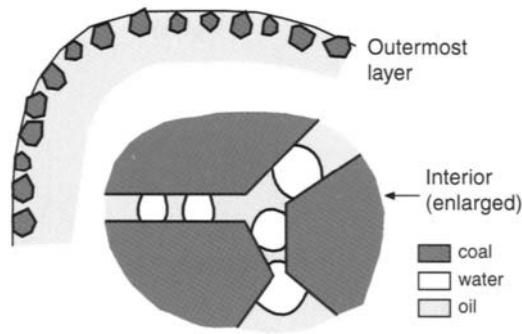
Fig. 5.4. A stable aggregate of hydrophobic coal particles in oil, with water forming liquid bridges. (After Good et al. [21]; by permission of Elsevier Science.)

Table 5.5
Characterization of separation processes in which oil is utilized [43]

Technique	Ionic collector	Oily collector	Oil consumption (kg/t)	Conditioning	Method of separation
Extender flotation	Yes	Yes	0.05–0.5	Regular	Flotation
Agglomeration flotation	Yes	Yes	a few kg/t	Intense	Flotation
Emulsion flotation	No	Yes	up to a few kg/t	Regular	Flotation
Oil agglomeration	Yes	Yes	5–10%	Slow/intense shearing	Sizing
Liquid–liquid extraction	Yes	Yes	N/A	Intense	Phase separation

first with an appropriate collector to render the particles hydrophobic and then with an oil to bridge particles together. Pulp dilution and conventional froth flotation follows.

Emulsion flotation is applied to treat inherently hydrophobic solids (coals, graphite, sulfur, molybdenite, talc). In this process, water-insoluble oil is used as a collector. Both agglomerate flotation and emulsion flotation use larger quantities of oil than extender flotation (up to a few kg/t).

The first three processes in Table 5.5 belong to a family of flotation processes, the following two do not. *Liquid phase agglomeration*, as the process is termed by Capes [44–46], can be used to beneficiate fine coal by separating hydrophobic coal particles from hydrophilic inorganic gangue (see Section 9.2).

In all these processes, the second liquid added under appropriate hydrodynamic conditions must be immiscible with the suspending liquid (water in coal preparation), and be capable of displacing this liquid from the surface of the treated (coal) particles.

5.3.1.2. Emulsion flotation

In the flotation process, collectors are used to render the mineral which is to be floated hydrophobic. Water-soluble collectors adsorb selectively onto a given solid surface, and if the adsorption is oriented (Fig. 5.5), the overall result will be an increased
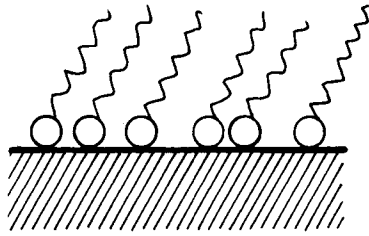
Fig. 5.5. Orientation of a flotation collector at solid/liquid interface.

solid hydrophobicity. The oriented adsorption requires a strong interaction between a functional group of the collector and a mineral surface.

In the following discussion a two-component system containing the solvent as component 1 and the solute as component 2 is considered. In flotation systems the solvent is water, and the solute may be a flotation agent dissolved in water. Since flotation processes are usually carried out at a constant temperature, the Gibbs adsorption equation can be written as

$$-\mathrm{d}\gamma = \Gamma_1 \mathrm{d}\mu_1 + \Gamma_2 \mathrm{d}\mu_2 \tag{5.1}$$

where $\mathrm{d}\gamma$ is the surface free energy change, Γ_1 and Γ_2 are adsorptions of component 1 and 2, respectively, and μ_1 and μ_2 are the chemical potentials of components 1 and 2. If it is assumed that the adsorption of solvent (component 1) is zero, and that Γ_2 is the excess surface concentration, Eq. (5.1) can be written

$$-\mathrm{d}\gamma = \Gamma_i \mathrm{d}\mu_i \tag{5.2}$$

Since

$$\mathrm{d}\mu_i = RT \cdot \mathrm{d}\ln a_i \tag{5.3}$$

where the thermodynamic activity, $a = fc$, where c is the bulk concentration and f is the activity coefficient, and since $f \to 1$, when $c \to 0$. Eq. (5.3) is commonly written

$$\mathrm{d}\mu_i = RT \cdot \mathrm{d}\ln c_i \tag{5.4}$$

Eqs. (5.2) and (5.4) finally give

$$\Gamma = -\frac{c}{RT}\left(\frac{\mathrm{d}\gamma}{\mathrm{d}c}\right)_T = -\frac{1}{RT}\left(\frac{\mathrm{d}\gamma}{\mathrm{d}\ln c}\right)_T = -\frac{1}{2.303RT}\left(\frac{\mathrm{d}\gamma}{\mathrm{d}\log c}\right)_T \tag{5.5}$$

This form of the Gibbs equation shows that the slope of a plot of γ versus the logarithm of concentration can be used to determine adsorption of the solute. For systems for which the surface tension can be measured, this equation provides a method to evaluate the surface excess. At solid surfaces, γ is not directly measurable. However, if the amount of the agent adsorbed onto solid particles can be determined from its initial and final bulk concentrations, this may be related to the reduction of surface free energy through Eq. (5.2).

As the Gibbs adsorption equation indicates, adsorption reduces the surface free energy of the system and this is a driving force for this spontaneous process.

In the adsorption process, solute molecules (or ions) accumulate at the interface. For collector species i, its chemical potential in bulk solution is given by Eq. (5.3) (or Eq. (5.4)). The chemical potential of the same species at the interface is

$$\mu_i^\circ = (\mu_i^\circ)^s + RT \ln a_i^s \tag{5.6}$$

where μ_i° and $(\mu_i^\circ)^s$ are standard chemical potentials of species i in bulk, and at the interface, respectively.

Since at equilibrium $\mu_i = \mu_i^s$

$$\frac{a_i^s}{a_i} = \exp\left(\frac{\mu_i^\circ - (\mu_i^\circ)^s}{RT}\right) \tag{5.7}$$

This relation can be transformed into the well-known Stern–Grahame equation by making the following assumptions:

$$a_i = c(\text{the bulk concentration}) \text{ and } a_i^s = \Gamma_\delta/2r$$

where Γ_δ is the adsorption density in the Stern plane and r is the effective radius of the adsorbed ion (polar group of organic molecule/ion).

The standard free energy of adsorption determined by a free energy difference between the chemical potential of species i in bulk and at the interface is defined as

$$\Delta G_{\text{ads}}^\circ = (\mu_i^\circ)^s - \mu_i^\circ \tag{5.8}$$

This finally yields the Stern–Grahame equation:

$$\Gamma_\delta = 2rc \cdot \exp(-\Delta G_{\text{ads}}^\circ/RT) \tag{5.9}$$

As discussed in numerous publications by D.W. Fuerstenau [47,48], this is a very useful relationship as it allows one to analyze different contributions to the energy of adsorption. In general

$$\Delta G_{\text{ads}}^\circ = \Delta G_{\text{elec}}^\circ + \Delta G_{\text{spec}}^\circ \tag{5.10}$$

where $\Delta G_{\text{elec}}^\circ$ represents electrical interaction effects (e.g. when ion adsorbs trough electrostatic interactions), and $\Delta G_{\text{spec}}^\circ$ represents specific interaction terms.

$$\Delta G_{\text{spec}}^\circ = \Delta G_{\text{chem}}^\circ + \Delta G_{\text{CH}_2}^\circ + \Delta G_{\text{hydroph}}^\circ \tag{5.11}$$

$\Delta G_{\text{chem}}^\circ$ stands for the free energy due to the formation of covalent bonds with the surface (e.g. in chemisorption), $\Delta G_{\text{CH}_2}^\circ$ depicts the interaction due to association of the hydrocarbon chain of the adsorbed molecules at the interface, and $\Delta G_{\text{hydroph}}^\circ$ represents the interaction of the hydrocarbon chain with a hydrophobic surface.

Adsorption of a molecule of aliphatic hydrocarbon on a polar surface from an aqueous solution is impossible because the interaction energy of water molecules (solvent) with the polar surface is much stronger, and therefore the displacement of the water molecules by the hydrophobic molecules at the interface (adsorption) is very unlikely. However, in the case of hydrophobic surfaces, $\Delta G_{\text{hydroph}}^\circ$, the interaction energy between hydrocarbon chains and hydrophobic surfaces could still lead to adsorption.

To answer the question of what the mode of action of hydrocarbons in coal flotation is, Taubman and Yanova [49] studied the behavior of different compounds in coal

flotation. They observed that the flotation yield did not depend on the chemical composition and molecular structure of the tested hydrocarbons (e.g. benzene, cyclohexane, *n*-hexane, *n*-octane, *n*-decane, *m*-xylene, decalin, kerosene, etc.), but directly depended on the solubility (L) of the reagent in water and the saturated vapor pressure (p). For the highest homologous series, for which $L \to 0$ and $p \to 0$, the dosage required for efficient flotation was the lowest. Compounds such as hydrocarbons and their hydroxyl-groups-deprived halogen derivatives were found to possess a considerable flotation activity with respect to coal only if they were used in the form of liquid droplets, but not when they were used in a dissolved state. This indicates that they act not by an adsorption mechanism, but only by selective wetting. With very hydrophobic coal which floated in water without any reagents, depression was observed when volatile reagents were utilized. This can be explained by the fact that when a coal particle carrying droplets of the reagent contacts a bubble, the volatile reagent begins to evaporate from the solid surface into the volume of the bubble and the stability of the particle–bubble aggregate is disturbed. This effect could be eliminated by saturating the air with the vapors of the tested reagent, and by using the reagent in its saturated solution. The effect of solubility of polar flotation agents (aliphatic alcohols, phenols, etc.) was found to be quite different. Such agents strongly adsorb onto the coal surface from aqueous solutions and are characterized by high flotation activity.

Taubman and Yanova's results [49] show in a quite convincing way that only hydrocarbons insoluble in water can be utilized in an emulsion flotation. Since, in general, their action does not result from their adsorption onto a coal surface, there must be another mechanism by which they accumulate at the flotation interfaces and enhance flotation.

It is often assumed that oily droplets at a mineral/water interface spread onto the mineral surface and form a thin film. Let us first analyze such a process.

5.3.1.2.1 Spreading of hydrocarbons at a solid/water interface. As shown in Fig. 5.6, the spreading of organic phase at the solid/water interface will require a change in free energy given by

$$\Delta G_{\text{spread}} = \gamma_{\text{SO}} + \gamma_{\text{OW}} - \gamma_{\text{SW}} \tag{5.12}$$

Substitution of γ_{SW} from Young's equation (Eq. (5.19)) gives

$$\Delta G_{\text{spread}} = \gamma_{\text{OW}}(1 - \cos \Theta_{\text{oil}}) \tag{5.13}$$

But since $\Theta_{\text{oil}} = 180 - \Theta$ (Fig. 5.7)

$$\Delta G_{\text{spread}} = \gamma_{\text{OW}}(1 + \cos \Theta) \tag{5.14}$$
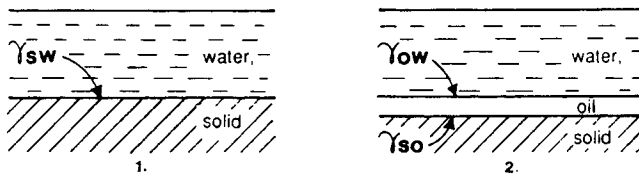
Fig. 5.6. Schematic model of oil spreading at solid/water interface.
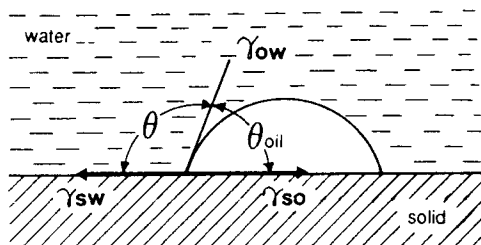
Fig. 5.7. Contact angle at solid–water–oil three-phase contact.
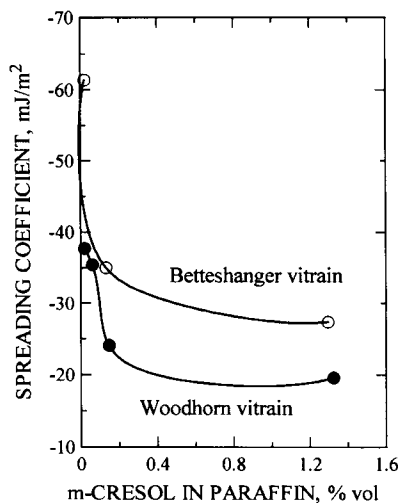
Fig. 5.8. Effect of *m*-cresol addition to paraffin oil on its spreading on two different vitrains. (After Brown et al. [50]; by permission of Socitey of Chemical Industry.)

and $\Delta G_{\mathrm{spread}}$ is always a positive number indicating that thermodynamically the spreading of oil into a thin film at the solid/water interface is always unlikely. $\Delta G_{\mathrm{spread}} = 0$ only if $\cos \Theta = -1$, that is when $\Theta = 180°$, a condition never met in practice[2].

Brown et al. [50] studied wetting of various coals by paraffinic oils in water, also in the presence of surface active agents. Some of their results are given in Fig. 5.8. It is apparent that oils do not spread spontaneously on coal when coal is immersed in water. This is true even when the oil/water interfacial tension is reduced by the addition of surface active compounds. In accordance with these conclusions, Fig. 5.9

---

[2] The spreading process is also analyzed with the use of Harkins' spreading coefficient. For the spreading of oil on a solid immersed in water $S = \gamma_{\mathrm{SW}} - \gamma_{\mathrm{SO}} - \gamma_{\mathrm{OW}}$ Since the spreading coefficient represents the energy gained by spreading, the process may occur spontaneously if S is positive. When S is negative the oil droplet adopts a stable position on the solid surface displaying a contact angle $\Theta_{\mathrm{oil}} > 0$. Applying Young's equation $S = \gamma_{\mathrm{OW}}(\cos \Theta_{\mathrm{oil}} - 1)$ and, therefore, it is always negative for a finite value of Θ_{oil} (see Table 5.10).
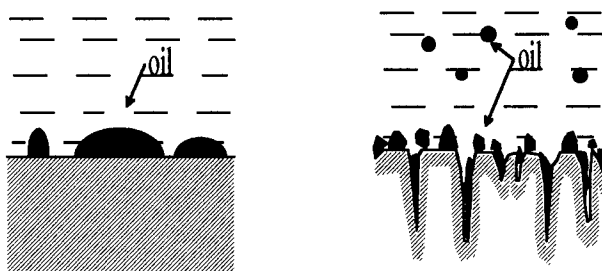
Fig. 5.9. Oil droplets on hydrophobic coal surface in water. (After Klassen [2].)

shows oil droplets on a hydrophobic solid (coal), and also on a porous hydrophobic surface in water [2]. The pores on a coal surface, as shown in Fig. 5.9, are partially filled with oil since the condition for replacement of water (or air) by oil in a capillary, crack, or space between the particles also depends on the coal wettability. Our recent observations [51] indicate that in the case of hydrophobic coal particles immersed in water, the pores may stay filled with air for a very long time, whereas the pores on more hydrophilic particles are quickly filled with water. This further increases the differences in wettability between particles varying for example by ash content, and sets up conditions under which oil (if added to the pulp containing such particles) will easily wet and penetrate into the pores of hydrophobic particles.

5.3.1.2.2 Attachment of oil droplets to mineral surfaces. Fig. 5.10 shows the solid–oil droplet interaction before and after attachment. If an oil droplet is forced isothermally and in a reversible way against a solid particle immersed in water, the work performed is identical to the free energy change of the system

$$\Delta G_{\text{attach}} = G_2^s - G_1^s \tag{5.15}$$

$$G_1^s = A_{\text{SW}}\gamma_{\text{SW}} + A_{\text{OW}}\gamma_{\text{OW}} \tag{5.16}$$

where A_{SW} and A_{OW} stand for the surface areas of the solid particle and oil droplet, respectively, and γ_{SW} and γ_{OW} are solid/water and oil/water interfacial tensions.

If the attachment area A_{SO} is assumed equal to 1 cm^2

$$G_2^s = (A_{\text{SW}} - 1)\gamma_{\text{SW}} + (A_{\text{OW}} - 1)\gamma_{\text{OW}} + 1 \cdot \gamma_{\text{SO}} \tag{5.17}$$
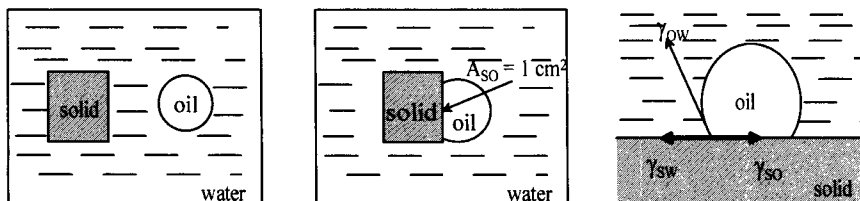
Fig. 5.10. Attachment of oil droplet to solid particle in water.

and

$$\Delta G_{\text{attach}} = G_2^s - G_1^s = \gamma_{\text{SO}} - \gamma_{\text{SW}} - \gamma_{\text{OW}} \tag{5.18}$$

Since from Young's equation

$$\gamma_{\text{SW}} = \gamma_{\text{SO}} + \gamma_{\text{OW}} \cos \Theta \tag{5.19}$$

then

$$\Delta G_{\text{attach}} = \gamma_{\text{OW}}(\cos \Theta - 1) \tag{5.20}$$

The result is that the attachment of an oil droplet to a mineral particle is likely to take place only if $\Theta > 0$; for $\Theta = 0$, $\cos \Theta = 1$ and $\Delta G_{\text{attach}} = 0$, the attachment is impossible. This explains why oily collectors are only used in the flotation of inherently hydrophobic minerals. In the extender flotation process, a collector which will render the mineral surface hydrophobic is needed first before adding oil.

Eq. (5.20) describes the free energy change between states 1 and 2 (Fig. 5.10) without taking into account the intermediate stages; it indicates only the probability of the attachment. While $\Delta G_{\text{attach}} = 0$ indicates that particle–oil droplet attachment is impossible, the condition $\Delta G_{\text{attach}} < 0$ indicates only that it is likely that the attachment will take place, but does not necessarily have to. As discussed by Burkin and Bramley [52], an encounter between an oil droplet and coal particle, both suspended in an aqueous solution, may lead to attachment if their kinetic energy is sufficient to overcome the energy barrier. Burkin and Bramley discuss two energy barriers — one preventing collision and attachment, and the other preventing the spreading of the oil over the coal surface. The barrier to collision depends on the potentials of the approaching surfaces, identified with the electrokinetic potentials of both oil droplets and coal particles and the ionic strength of the aqueous electrolyte. The barrier to spreading is shown by the difference between advancing and receding contact angles; spreading is controlled by the relevant interfacial tensions, solid porosity, surface texture, heterogeneity, among other things.

Fig. 3.13 shows the zeta potential curves plotted vs. pH for various coals. It is obvious that especially lower-rank and/or oxidized coals are characterized by negative electrical charge over the pH ranges in which flotation is commonly carried out (pH is not controlled in coal flotation circuits and is mainly determined by the coal, the mineralogical composition of the gangue, and the water chemistry). Fig. 5.11 shows the zeta potential–pH curves for various hydrocarbons [3]. Comparison of Fig. 3.13 and Fig. 5.11 reveals that in most cases both coal particles and oil droplets carry negative electrical charges and this will result in a repulsion force. According to the DLVO theory (Derjaguin–Landau–Verwey–Overbeek), the interaction energy between two particles can be calculated from the attractive London–van der Waals forces, and if the surface of the particles have the same charge, from coulombic repulsion.

Burkin and Bramley [52,53] analyzed such an attachment process and were able to identify three clear sets of conditions.

(i) At pH 7.9 in 10^{-3} M NaCl solution, the zeta potential of the coal and the oil droplets were -18 and -69 mV, respectively; under such conditions less than 0.5% of the coal floated after conditioning for 4 min and floating for 3 min.
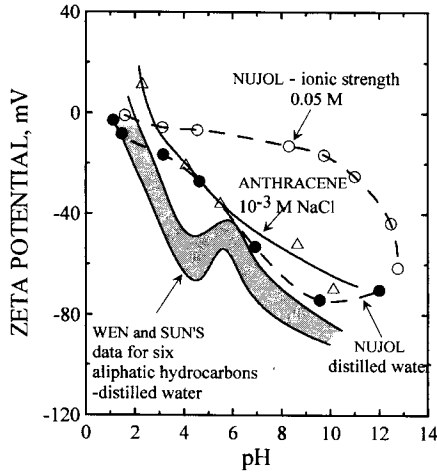
Fig. 5.11. Zeta potential–pH curves for emulsions of different hydrocarbons in water. (After Laskowski [3]; by permission of Elsevier Science.)

(ii) At pH 6.8 in 10^{-3} NaCl solution, the zeta potential of the coal was zero within experimental error, and the system behaved in qualitatively different manner: 7.7% of coal floated and the remaining amount which did float seemed sticky as particles clung together and to the sides of glass vessel.

(iii) At pH 7.9 in 10^{-3} NaCl solution containing 0.1 g/l of the commercial surfactant Lissapol NDB, the zeta potentials of the coal and oil were -4 and -57 mV, respectively, and the whole of the coal floated after conditioning for 4 min and floating for 3 min. The applied concentration of the surfactant in the absence of fuel oil caused only about 10% of the coal to float [53].

The calculated energy barriers to collision were 7.1×10^{-16} J in case (i), much less than 10^{-18} J in case (ii) and 8.6×10^{-18} J in case (iii).

These results clearly show that when the calculated energy of repulsion (energy barrier) is slightly less than the energy of approach between coal particles and oil droplets, the attachment of oil droplets to coal particles does occur. Only when the available kinetic energy exceeds the calculated energy barrier, and an surface active agent which aids the spreading of oil over wet coal surfaces is present, was the flotation efficient.

Fig. 5.12 shows the zeta potential–pH curves for kerosene, fuel oil No. 2, and a mixture of fuel oil No. 2 and No. 6 (4:1 ratio) [54,55]. The figure explains why, as found by Wen and Sun [54], the mixture of fuel oil No. 2 and No. 6 turned out to be a much better collector for difficult-to-float coals than kerosene, or fuel oil No. 2. Apparently, fuel oil No. 6 contains some surface active compounds which shift the iso-electric point of the tested oil to the right. The change of the zeta potential–pH curve for fuel oil No. 2 in the presence of fuel oil No. 6 is very similar to the change of the zeta potential of hydrocarbons in the presence of cationic surfactants (amines), as shown in Fig. 5.13. The curves shift towards the position of the iso-electric point of colloidal dodecyl amine which is situated around pH 11 [56,57].
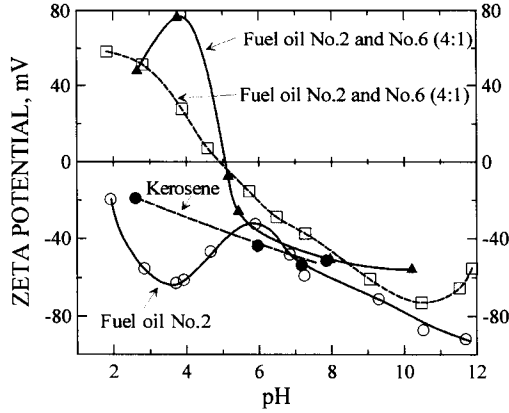
Fig. 5.12. Zeta potential–pH curves for emulsions of kerosene, and fuel oils in water. (□ and ○ after Wen and Sun [54]; by permission of Marcel Dekker Inc.; and solid symbol curves after Laskowski and Miller [55]; by permission of the Institution of Mining and Metallurgy.)
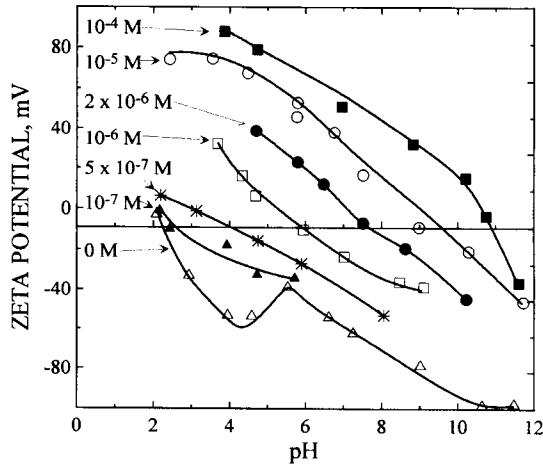
Fig. 5.13. Effect of concentration of dodecylammonium chloride on the electrokinetic potential of hexadecane droplets in water. (After Wen and Sun [54]; by permission of Marcel Dekker Inc.)

In order to enhance emulsion flotation, oil droplets must attach to coal particles. Since the oil remains on the coal surface in the form of droplets (Fig. 5.9), there arises the question of what the mechanism through which the oil improves the flotation is.

In spite of the positive values of ΔG_{spread} (Eq. (5.14)), which indicates that the oil will not displace water, the oil may still displace water if a four-phase solid/oil/water/air interface is established. Since this situation is relevant to flotation, it is further analyzed in Fig. 5.14 which is adapted from Zettlemoyer et al. [58], and Klassen et al. [59,60].

Zettlemoyer et al. [58] used Teflon in their spreading experiments. The spreading coefficient of oil (purified white mineral oil) on teflon in contact with water was
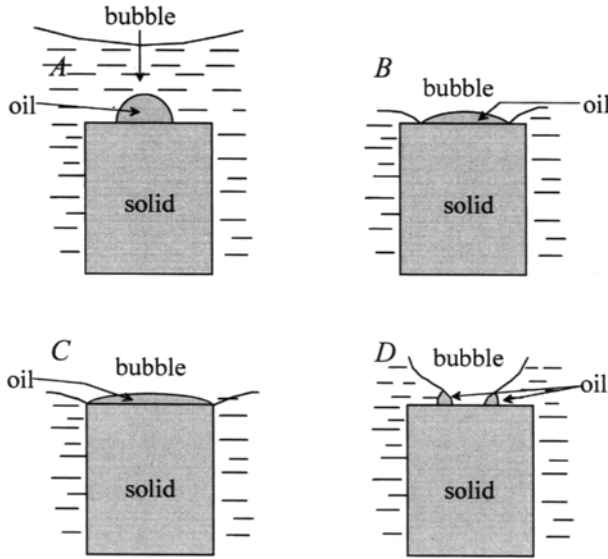
Fig. 5.14. Attachment of bubble to hydrophobic particle in the presence of oil droplet on the solid particle.
(After Laskowski [3]; by permission of Elsevier Science.)

$S_{o/sw} = -2.42$ mJ/m^2 and the process was spontaneous when the spreading coefficient was positive), and the oil exhibited a finite contact angle of 37°. The water recedes down the oil drop when a bubble approaches the particle until the water/oil interface is eliminated. After this, the water dewets the Teflon plate, receding to the edges. This may either be followed by the film breaking into individual droplets with $\Theta_{o/w} = 37°$ or, according to Klassen [59,60], the oil recedes into a thread along the solid/water/air interface (Fig. 5.14D).

One noticeable effect of the oily collector is an increased size of floated particles. As maintained by Melik-Gaykazyan [59–61], because the oily hydrocarbon is located as a thread at the line of contact of the three phases its presence increases the contact angle. Its presence also increases the contact angle hysteresis. Under turbulent conditions prevailing in a flotation cell, an increased hysteresis improves the chance of survival of the particle–bubble aggregate.

5.3.1.2.3 Effect of oily collectors on coal flotation. A very impressive research program, carried out by Klassen and his co-workers in the 1960s [2,62] led to the conclusion that simple pure hydrocarbons are not very efficient collectors. While they improve the floatability of unoxidized metallurgical coal to some extent, they are not useful in the flotation of lower-rank coals. Compounds containing more than eight carbon atoms (octane), and especially cyclic hydrocarbons such as cyclodecane ($C_{10}H_{18}$), were found to be better than shorter chain homologues.

Petukhov et al. [63,64] provided some data on the flotation activity of cyclic acetals. They found that 1.4-dioxane and 1.3-dioxane performed poorly when used as collectors

in the flotation of coal, and graphite.
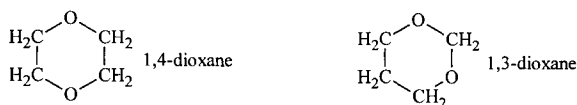
However 1,3-dioxane with some side chains, e.g.
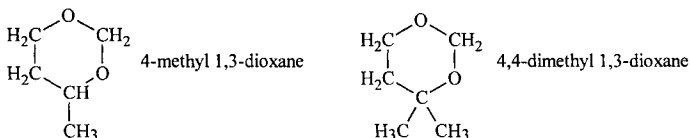
turned out to be an excellent collector for both coal and graphite.

This subject was also studied by Harris et al. [65,66]. In comparative tests, they evaluated coal flotation with dodecane and ethoxylated nonyl phenols and reported that the introduction of a benzene ring into a hydrocarbon significantly increases its effectiveness as a collector for coal flotation. Ethoxylated nonyl phenols were found to be the most effective collectors. To explain these results, they postulated that weak interactions between dodecane and the coal surface is not likely to lead to a displacement of water molecules from the coal surface by dodecane. On the other hand, ethoxylated nonyl phenol can interact both with the graphitic rings in the coal structure as well as through hydrogen bonds between ethoxy groups and the oxygen functional groups on the coal surface (Fig. 5.15).
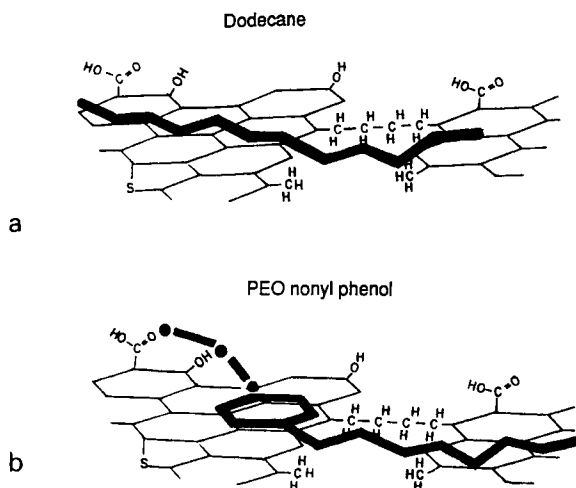
Fig. 5.15. Schematic representation of the adsorption of a collector molecule on the surface of coal: (a) dodecane, (b) ethoxy nonyl phenol. (After Harris et al. [66]; by permission of Gordon and Breach.)

Several authors drew conclusions regarding the effect of oily collectors on flotation [67–69], but since their experiments were always carried out with the simultaneous use of frothers, these results are discussed in the next section.

5.3.2. Frothers — water soluble surface active agents

Frother molecules have an uneven distribution of polar and non-polar groups which enables them to orient preferentially at a water/air interface. In contrast to ionic collectors, the polar groups in frother molecules, hydroxyl (−OH), ether linkages (−O−) and carbonyl (−C=O) do not form stable bonds at mineral surfaces [70]. The case of coal, however, is very different and must be discussed separately. First, it is a heterogeneous solid in which a hydrocarbon matrix contains various polar sites (e.g. phenolic and carboxylic groups, mineral inclusions which may contain hydroxylic and other polar groups, etc.), and second, the hydrocarbon matrix may be highly hydrophobic.

As discussed in Section 3.3, there is a good correlation between the moisture content of coal and the phenolic and carboxylic groups' content. As Fig. 3.17 shows, for lower-rank coals there exists a very good correlation between the amount of water and the amount of methanol vapors adsorbed onto coal. However, for higher-rank coals the adsorption of methanol increases over that of water probably due to the increased dispersive interaction between CH_3 groups and the coal surface [71,72].

Adsorption of frothers onto coal has been extensively studied [73–76]. As Fig. 5.16a shows [74], adsorption of phenol onto coals varying in rank follows the behavior observed when working with methanol. Low-rank coals adsorb more phenol in a short time than anthracite (Fig. 5.16b). This was confirmed by Miller et al. [76] when studying adsorption of MIBC. They reported that the equilibration with a high-volatile bituminous coal was slow, whereas the equilibration with a medium-volatile coal was fast (5 min).

Fig. 5.17 shows adsorption isotherms of α-terpineol and MIBC onto a high-volatile bituminous coal [75]. The scatter of the experimental points was attributed to the difficulties associated with the gas chromatographic technique. The adsorption of MIBC increases linearly with an increase in the equilibrium concentration in solution, but an isotherm more Langmuirian in shape was obtained for α-terpineol. Since coal is heterogeneous it is difficult to identify adsorption sites which may be responsible for the adsorption.

High adsorption of phenol onto low-rank coals (Fig. 5.16) seems to correlate well with the content of oxygen functional groups. But coals are porous, and as pointed out by Gan et al. [77], low-rank coals (less than 75% C) contain mostly macropores (300–30,000 Å), bituminous coals (carbon content ranging from 76 to 84%) contain mostly transitional pores (12–300 Å), and higher-rank coals contain mostly micropores (4–12 Å). The rate of adsorption may then also be explained by the ease with which different adsorbing molecules diffuse into the pores [76].

Vlasova [78] claims that the Freundlich adsorption isotherm describes the adsorption of aliphatic alcohols onto coal quite well. Adsorption of hexyl alcohol was higher than the adsorption of butyl alcohol, and this was higher than the adsorption of benzyl
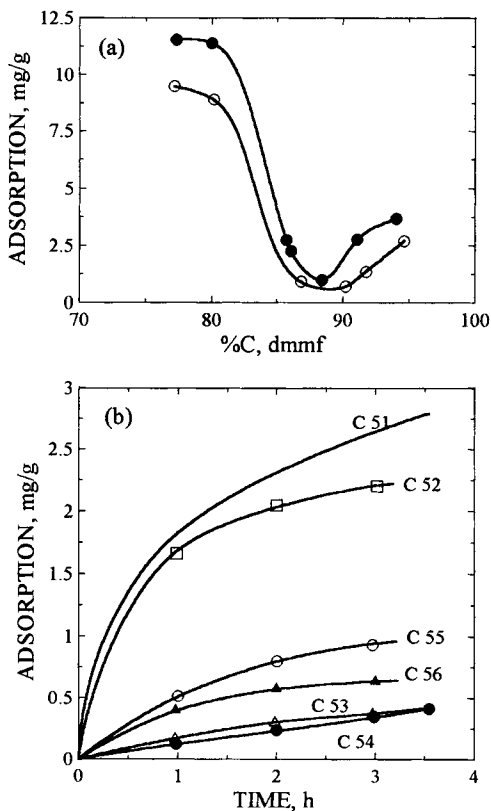
Fig. 5.16. Adsorption of phenol on coals varying in rank: (a) at two initial phenol concentrations of 1.5 mg/l (·) and 0.5 mg/l (○); (b) adsorption rate on various coals at 0.5 mg/l initial phenol concentration. (After Eveson et al. [74]; by permission of the Institute of Energy.)

alcohol. The shape of the obtained adsorption isotherms was similar to the one shown in Fig. 5.17b. for MIBC. Vlasova also reported that the oxidation of coal in air at 200°C, which increased the content of carboxylic and phenolic groups, also increased heptyl alcohol adsorption without however changing the shape of the isotherm. In comparative tests with heptyl alcohol, coal fractions with a higher ash content adsorbed more heptyl alcohol. While this information sheds some light on the nature of the adsorption centers responsible for the adsorption of frothers it does not answer all the questions.

The use of MIBC as a frother is very common in coal flotation. The most interesting data on adsorption of MIBC are that of Aston et al. [79] who studied its adsorption onto hydrophilic silica and methylated hydrophobic silica. The methylated silica can be obtained by reacting dry silica particles with trimethylchlorosilane following the reaction

$$\equiv Si-OH + ClSi(CH_3)_3 \rightarrow \equiv Si-O-Si(CH_3)_3 \tag{5.21}$$
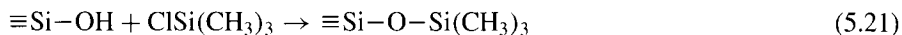
The reaction is known to render silica particles permanently hydrophobic [80].
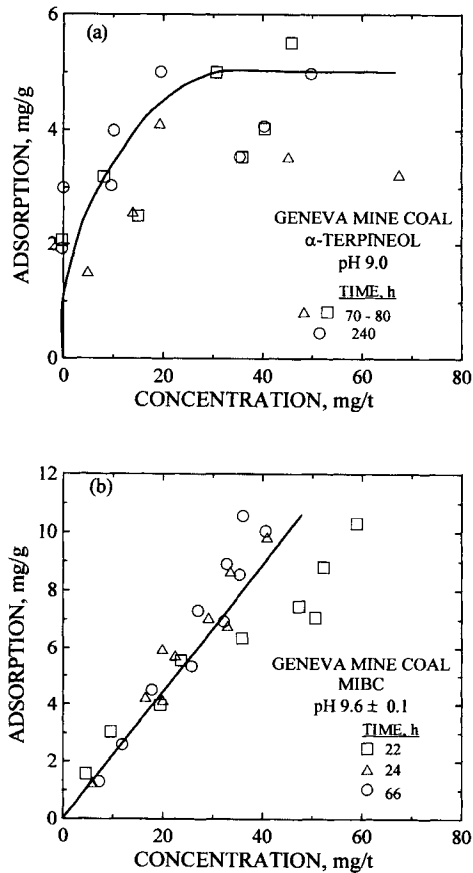
Fig. 5.17. Adsorption isotherms of α-terpineol (a) and MIBC (b) onto a high-volatile bituminous Geneva mine coal. (After Fuerstenau and Pradip [75]; by permission of Elsevier Science.)

Fig. 5.18 shows the adsorption isotherms of MIBC on both hydrophilic and hydrophobic silicas, and Fig. 5.19 shows the effect of the adsorption on the wettability of the treated silica surfaces. Both adsorption isotherms appear to be of a Langmuirian form. The initial slopes of the isotherms indicate that the interaction between MIBC and the hydrophobic methylated silica is stronger than its interaction with the hydrophilic silica.

As seen from Fig. 5.19 [79], both advancing and receding contact angles on methylated silica remain relatively unchanged with an increase in concentration of MIBC up to 10^{-4} mol/l. However, at higher MIBC concentrations the contact angle values decreased to a value of 57° ± 5° and remained constant with further increase in the MIBC concentration up to a solubility limit. The region of greatest reduction in the contact angle coincides with the concentration range in which there is a sharp increase in the adsorption of MIBC. The increase in the contact angle of the hydrophilic surface occurs at a slightly higher MIBC concentration than the decrease in the contact angle for the hydrophobic surface. These conclusions correlate very well with those of Miller
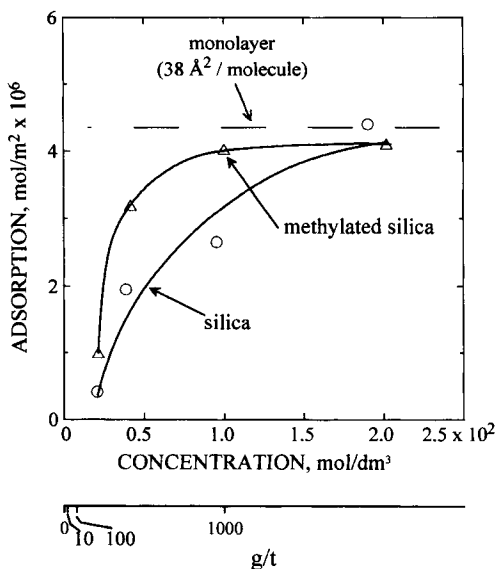
Fig. 5.18. Adsorption isotherms for MIBC on silica and hydrophobic methylated silica (After Aston et al. [79]; by permission of Gordon and Breach.)
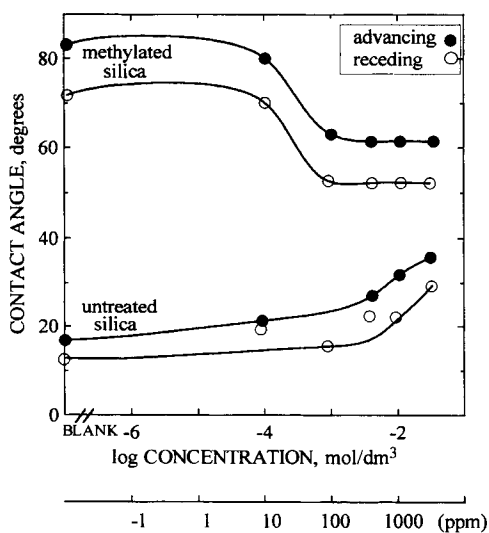
Fig. 5.19. Effect of MIBC concentration on advancing and receding contact angles on quartz and methylated quartz plates. (After Aston et al. [79]; by permission of Gordon and Breach.)

et al. [76] who measured the contact angle on a high-volatile bituminous coal and found that it did not change with the MIBC addition, but at concentrations higher that 0.04 M the induction time increased significantly.

Table 5.6
Percentage recoveries in batch flotation tests

Coal	Recovery, %		
	10 mg frother, 2 min flotation	5 mg frother, 2 min flotation	5 mg frother, 1 min flotation
A	24	8	5
B	99	94	88
C	97	93	85
E	57	26	13
G	10	7	3
H	5	5	3
I	9	2	–

As these experiments indicate, MIBC can adsorb onto both hydrophobic and hydrophilic surfaces (Fig. 5.18). The orientation of the adsorbed MIBC molecule at these interfaces is however quite different. While the molecule seems to be interacting with the hydrophilic surface through its $-OH$ group (hydrogen bonding) and thus slightly increases overall solid hydrophobicity, its orientation at the hydrophobic interface seems to result from the hydrophobic interactions. In the latter case, alcohol $-OH$ groups face an aqueous phase and thus the surface hydrophobicity decreases. Since coal is hydrophobic and, depending on rank and/or oxidation, may contain different number of hydroxylic groups, the molecule of MIBC may easily adsorb onto such a surface with quite different orientations at different surface sites.

Horsley and Smith [67] measured contact angles on various coals and concluded that they were not affected by the addition of MIBC. In line with these findings, their flotation experiments (Table 5.6) showed that while the flotation of very hydrophobic low-volatile bituminous coals (B and C) was slightly improved by MIBC, lignite and subbituminous coals (I and H) did not float in the presence of MIBC, and anthracite (A) did not respond well to MIBC either.

The results of Gutierrez-Rodriquez and Aplan [81] given in Fig. 5.20 confirm a very good correlation between the collectorless flotation of various coals in which MIBC only was utilized, and coal wettability.

Frothers are used in froth flotation to enhance the generation of fine bubbles, to aid particle-to-bubble attachment, and to stabilize the froth. There are many ways of testing the frothing properties of frothers [8]. To examine the effect of frothing on flotation, Malysa et al. [82] carried out experiments in a Denver batch flotation cell using various frothers and a hydrophobic solid (coal) which did not require a collector. Aliphatic alcohols such as *n*-butanol, *n*-pentanol and *n*-hexanol were utilized as frothers. Their results plotted in a conventional way, that is by plotting the yield of the froth product vs. the frother concentration gave the results shown in Fig. 5.21. As seen, the flotation with hexanol alcohol was better than with the other two selected alcohols. However, these differences can result from different frothing and/or different collecting properties of the tested agents. To narrow the possibilities, Malysa et al. [82] replotted their experimental results (Fig. 5.22). This time the yield of the froth product was plotted versus DFI $\times$ *c*
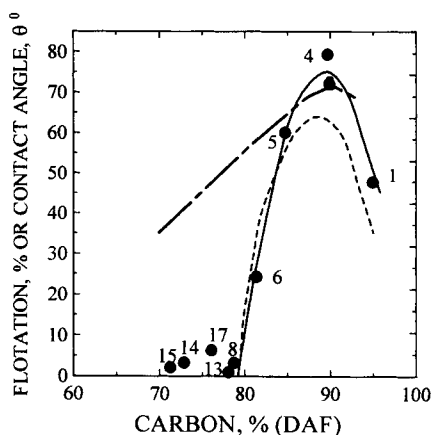
Fig. 5.20. Effect of coal rank (expressed as % carbon content) on wettability and floatability of coal particles; (– – –) microflotation of −500 +380 μm coal fractions with 10 μl of MIBC and no collector; (— – —) sessile-drop contact angle; (•) captive–bubble contact angle data. (After Gutierrez-Rodriguez and Aplan [81]; by permission of Elsevier Science.)
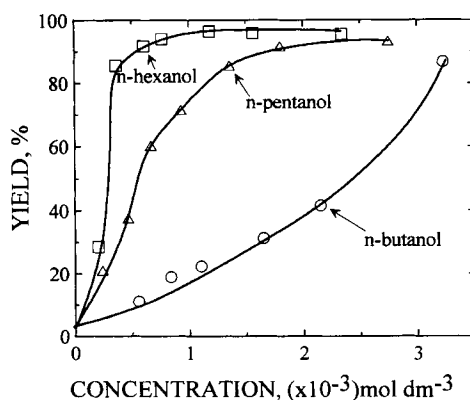
Fig. 5.21. Effect of aliphatic alcohols concentration on flotation of a high-volatile C bituminous coal. (After Maylsa et al. [82]; by permission of Elsevier Science.)

and as can be seen, all the experimental points for the tested frothers converged on the two curves for two different coals. Higher values of the DFI × c were needed for thermal coal (high-volatile C bituminous coal) than for a higher-rank bituminous coal (high-volatile A bituminous coal). Although the wettabilities of these two coals were not determined, it is obvious that the higher-rank bituminous coal was more hydrophobic.

Here DFI stands for the Dynamic Frothability Index [83,84], and it is determined from the retention time, which is defined as the slope of the linear part of the dependence of the total gas volume in the experimental set up on the gas flow rate. The DFI is calculated as the limiting slope of the retention time vs. concentration for $c \rightarrow 0$:
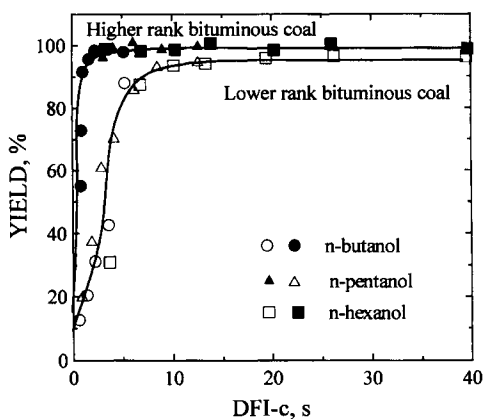
Fig. 5.22. Dependence of the froth product yield on DFI × c for two bituminous coals: high-volatile A (solid symbols) and high-volatile C (open symbols) (After Maylsa et al. [82]; by permission of Elsevier Science.)

$$DFI = \left(\frac{\partial rt}{\partial c}\right)_{C=0} \tag{5.22}$$

The values for n-butanol, n-pentanol and n-hexanol, used in plotting the curves in Fig. 5.22, are given in Table 5.7. Table 5.8 lists DFIc values for many surface active substances measured in the tap water of Cape Town [85].

The fact that all of the experimental points converge on two curves for two coals (Fig. 5.22) indicates that in these experiments the utilized alcohols acted mainly as frothers. Although such alcohols are known to adsorb onto coal [1], the effect of the adsorption on coal wettability may be insignificant (see Fig. 5.19). This, however, does not have to be true for all frothers.

This subject was tackled by Wheeler in his interesting paper on the effect of frothers on coal flotation [86]. Wheeler points out that frothers have by far the largest effect on coal recovery and that they do not only act in their traditionally accepted function of "bubble makers". In his flotation tests he used anthracite, medium volatile bituminous and high-volatile B bituminous coals, and sub-bituminous A coal. All samples were floated with various frothers and the following consumptions of fuel oil: 0.25 kg/t for anthracite, 0.5 kg/t for high-volatile bituminous and 0.75 kg/t for subbituminous coal; no collector was utilized with medium volatile bituminous coal.

Table 5.7
Values of dynamic frothability index [82]

Substance	Ret. time$_\infty$ (s)	k (dm³ mol⁻¹)	DFI	
			(s dm⁻³ mol⁻¹)	(s dm⁻³ g⁻¹)
n-Butanol	16.8	96.3	1.6×10^3	21.6
n-Pentanol	24.9	184.0	4.6×10^3	52.3
n-Hexanol	38.9	437.7	1.7×10^4	166.7

Table 5.8
Dynamic frothability index for solutions of several frothers in tap water of Cape Town [85]

Frother molecule	Ret. time$_\infty$ (s)	k (dm^3 mol^{-1})	DFI (s dm^{-3} mol^{-1})
n-Butanol	20.51	65.27	1339
2-Butanol	12.72	64.98	826
t-Butanol	10.83	146.57	1588
n-Pentanol	22.64	243.68	5517
n-Hexanol	38.27	1116.96	42748
n-Heptanol	82.47	495.56	40867
n-Octanol	87.33	908.54	79338
2-Octanol	61.05	2313.33	141226
2-Ethyl-hexanol	68.29	2066.76	141147
MIBC	13.12	2727.39	35786
α-Terpineol	27.12	5093.93	138171
TEXANOL	31.17	10392.72	323901
TEB	34.70	7279.42	252589
Dowfroth 400	72.75	11025.69	802142
DIBK	21.46	3589.58	77019
n-Butanol (distilled water)	20.82	61.04	1271

For easy-to-float medium volatile bituminous coal the aliphatic alcohols, especially MIBC, were found to be excellent. Going down in the order of natural floatability, medium-volatile bituminous > anthracite > high-volatile B bituminous > sub-bituminous A, MIBC quickly loses its effectiveness, first to 2-ethyl hexanol, then to texanol and glycol frothers (Dowfroth 1012 and Aerofroth 65). On the hvBb coal 2-EH floated 15% more coal than MIBC. Wheeler's results confirm that while short chain aliphatic alcohols possess only frothing properties, other frothers also exhibit collecting properties.

Since coal is porous and its specific surface area may be quite large, the frother concentration in the pulp needed for flotation is quickly depleted. Hindmarch and Waters [87] showed that the high consumption of frothers may be reduced by short conditioning time with a frother prior to flotation.

Klassen [2] claims that the oriented adsorption of alcohols onto coal can take place only if the coals contain polar groups which can interact with adsorbing molecules through hydrogen bonds. Frothers with 6–8 carbon atoms per molecule perform the best because the adsorption of shorter chain molecules does not improve surface hydrophobicity, while molecules with too large a radical are water-insoluble. Klassen and Nevska [88,89] reported that aliphatic alcohols with 6–8 carbon atoms per molecule also exhibit peptizing properties towards clays. This is claimed to be the main reason why such frothers were found to be so beneficial in the flotation of coals from clay-rich pulps.

5.3.3. *Joint use of oily collectors and frothers*

In accordance with Fig. 3.22, Table 5.9 [1] confirms that any agent is good enough to float a medium-volatile bituminous coal. A tar oil (coke-oven byproduct) was commonly

Table 5.9
Flotation of coals varying in rank with the use of different reagents [2]

Coal type	Flotation agents	Concentrate		Tailings	
		Yield (%)	Ash (%)	Yield (%)	Ash (%)
Bituminous medium volatile	tar oil 2.5 kg/t	71.7	4.5	28.3	63.9
Bituminous high-volatile C	tar oil 2.5 kg/t	38.9	3.9	61.1	23.2
Bituminous high-volatile C	kerosene 2 kg/t, nonyl alcohol 0.62 kg/t	79.1	4.1	20.9	62.1

Table 5.10
Effect of added surfactants on spreading coefficient of paraffinic oil on polished Betteshanger vitrain [50]

Concentration (%)	Advancing contact angle, θ_A (°)	Number of readings	Interfacial tension, γ_{OW} (mJ/m^2)	$\Delta G_{spread.}$
Lubrol:				
0	82 ± 4	30	43.8	37.7
0.01	109 ± 2	8	25.0	33.1
0.021	115 ± 2	7	12.1	17.2
0.044	141 ± 4	10	4.1	7.3
0.08	150 ± 1	6	2.7	5.0
m-Cresol:				
0	82 ± 4	30	43.8	37.7
0.052	90 ± 0	6	34.9	34.9
0.132	90 ± 0	7	23.2	23.2
1.320	91 ± 2	7	18.5	18.8

applied in the past. However, the same "universal" reagent is not efficient when floating lower-rank coals. Does this mean that the lower-rank coals cannot be beneficiated by flotation? As Table 5.9 reveals, lower-rank coals can be floated if the reagents are properly selected. A combination of kerosene and nonyl alcohol is shown to float coal which could not be floated using only one universal reagent.

In the system consisting of coal particles and oil droplets, a frother will adsorb not only at the coal/water interface, but also at the oil/water interface. The adsorption at the oil/water interface reduces the oil/water interfacial tension and thus enhances oil emulsification. This by itself will improve emulsion flotation.

The effect of Lubrol MOA surfactant (ethoxylated fatty alcohol) and *m*-cresol on paraffinic oil/water interfacial tensions, and the free energy of spreading of that oil on well polished vitrain (hydrophobic bituminous coal) is shown in Table 5.10 [50]. As seen, in the presence of the tested surfactants, the oil/water interfacial tension decreases (more with Lubrol MOA than with *m*-cresol), Θ_{oil} increases, and ΔG_{spread} decreases from 37.7 down to 5.0 mJ/m^2 for Lubrol, and down to 18.2 mJ/m^2 for *m*-cresol. While decreasing oil/water interfacial tensions indicate an improved emulsification, decreasing values of ΔG_{spread} indicate an easier spreading of the oil over the coal surface. However, since the ΔG_{spread} values are positive, the spreading does not take place spontaneously.
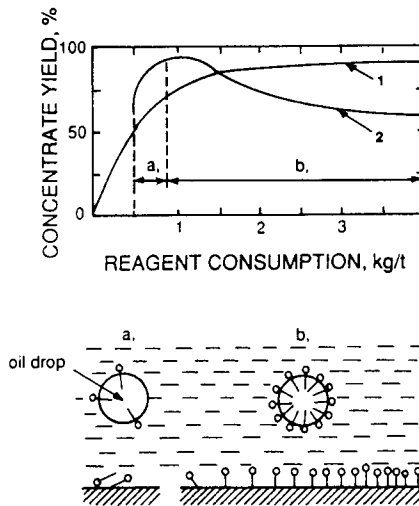
Fig. 5.23. Flotation of coal under various conditions: 1, using only kerosene; 2, using 0.5 kg/t of kerosene and increasing amount of *n*-octyl alcohol. (After Melik-Gaykazian et al. [90].)

While in the case of cresol, decrease in ΔG_{spread} results only from the reduced values of the oil/water interfacial tension and is small; in the case of Lubrol both the oil/water interfacial tension and contact angle are affected and the reduction of ΔG_{spread} is more marked.

The beneficial effect of a frother on flotation with an oily collector was demonstrated and explained by Melik-Gaykazian et al. [90]. Frother adsorbs at the oil/water interface, lowers the interfacial tension and improves emulsification. However, it also adsorbs at the coal/water interface, and provides anchorage for the oil droplets to the coal surface. At higher frother concentrations, as shown in Fig. 5.23, an opposite effect can be expected.

The co-operation between an oily collector and a frother was extensively discussed in Klassen's publications [2,60,62]. Following this line of reasoning, Vlasova [91] used a bituminous coal (87.5% C) with a high content of vitrinite (96%). The coal was ground dry under either nitrogen, air, or oxygen. Titration methods were used to follow the total content of carboxylic and phenolic groups in the ground samples. The following contents were determined: 0.365 mequiv/g (nitrogen), 0.54 mequiv/g (air), and 0.66 mequiv/g (oxygen). Fig. 5.24a [91] shows the effect of the content of phenolic and carboxylic oxygen functional groups on the natural floatability of the tested coal. As expected, an increased content of oxygen functional groups reduced the coal's natural floatability. Floatability was also reduced when 500 g/t of kerosene was used in the flotation experiments (Fig. 5.24b). However, the differences between the flotation of the three samples almost completely disappeared when hexyl alcohol was utilized (250 g/t). These results reveal that while coal oxidation reduced the natural floatability of the tested coal, and also its flotation in the presence of oily collector, the oxidation seemed to improve conditions for hexyl alcohol adsorption, and all the samples responded to flotation with this reagent very well.
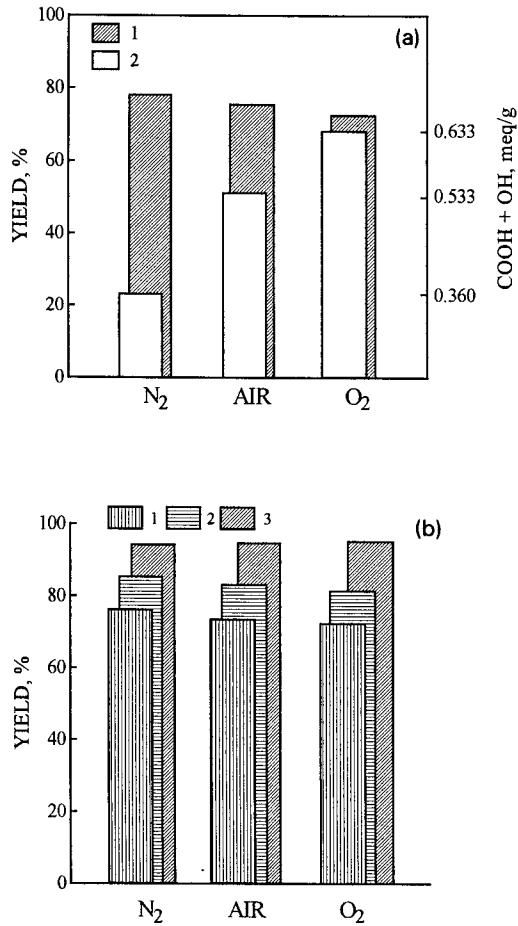
Fig. 5.24. Effect of coal oxidation (expressed as a content of carboxylic and phenolic groups in a bituminous coal) on natural floatability (a): 1, concentrate yield; 2, content of carboxylic and phenolic groups. (b) 1, natural floatability after 15 min; 2, flotation with kerosene (7 min); 3, flotation with *n*-heptyl alcohol (7 min). (After Vlasova [91].)

To improve the oil agglomeration of lower-rank coal, Good et al. [21] added *n*-octanol to oil to restore the coal's hydrophobicity. Since the solubility of octanol in water is very low, it stays almost entirely in an organic phase. Fig. 5.25 shows the effect of *n*-octanol on the decane–water contact angle (measured through water) on coal. It is clear that octanol made the coal appreciably more hydrophobic. Similar effects can be expected whenever a properly selected surface active agent and an oily collector are used.

Fig. 5.26 [92] summarizes in a very clear way the effect of MIBC and increasing doses of fuel oil on the flotation of various coals. These figures confirm that while a frother alone is sufficient to float medium- and low-volatile bituminous coals, a combination of oily collector and frother is required to float high-volatile coals.
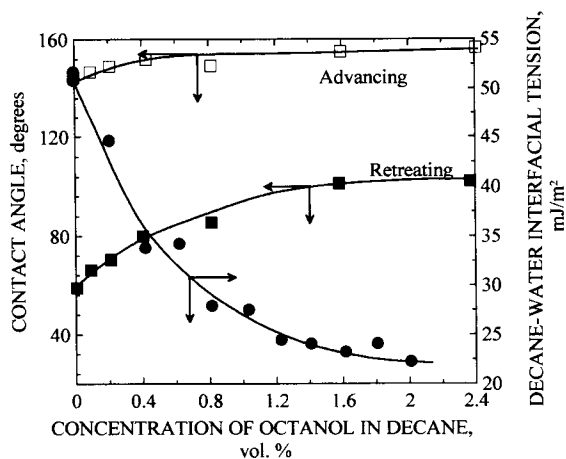
Fig. 5.25. Wettability of coal surface by decane with varying amount of octanol dissolved in decane, and effect of octanol in decane concentration on decane/water interfacial tension (After Good et al. [21]; by permission of Elsevier Science.)

5.3.4. Promoters

In the flotation with water-insoluble oily collectors, a major problem is inefficient mass transfer of the collector to the coal surface. If the collector is insufficiently dispersed, some coal particles will be excessively coated while others will starve. If more oil is added to counteract such a deficiency, selectivity may suffer as more high-in-ash particles will tend to float. Since most coal flotation circuits do not provide for collector emulsification and for intense conditioning, the use of surface active agents as emulsifiers can enhance oil dispersion (emulsification); such agents can also improve the interaction between oil droplets and the coal surface. Chander et al. [93] studied various non-ionic surfactants and concluded that the flotation of coal improved in the presence of the tested additives. The increase in yield was attributed to an increase in the oil droplet–coal particle collisions resulting from an increase in the number of droplets in the presence of surfactants. This is one of the functions of the promoters; a few examples of such agents are listed in Table 5.4.

Burkin and Soane [94] proved experimentally that hydrophilic quartz particles could not be floated with oil. The same quartz could, however, be floated when extremely small amounts of dodecylamine were simultaneously added; these amine quantities were not sufficient to cause the flotation of quartz by themselves.

It has been known since the early publication by Sun [95] that amines can efficiently float oxidized coals. Wen and Sun [54] showed that amines adsorb on oxidized coal and drastically change its zeta potential from initially negative to positive values. The effect of amine on the zeta potential of oxidized coal is very similar to the effect of amines on the zeta potential of quartz. All these results indicate that amines can serve as oxidized coal flotation promoters when used in a small amount together with an oily collector.

Wen and Sun [54] were able to show through electrokinetic measurements that
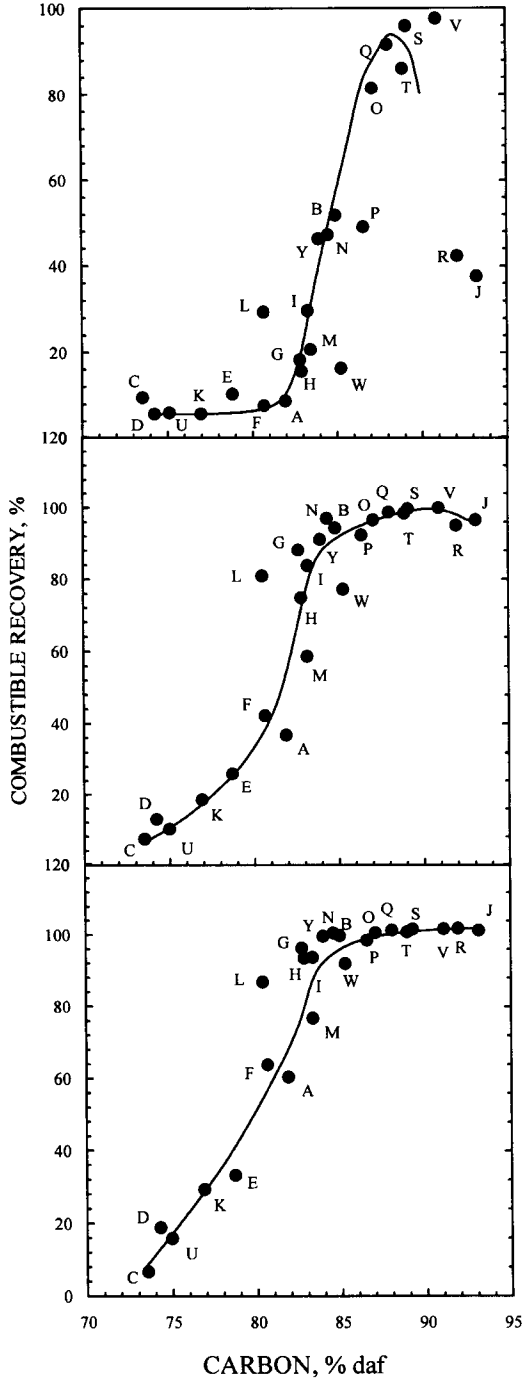
Fig. 5.26. Effect of coal rank on coal flotation, with 0.2 kg/t of MIBC (upper panel), with 0.2 kg/t of MIBC and 0.5 kg/t of fuel oil (middle panel), and with 0.2 kg/t of MIBC and 1 kg/t of fuel oil (bottom panel). (After Agus et al. [92]; by permission of Gordon and Breach.)

kerosene droplets carry a negative electrical charge in water practically over the whole pH range (Fig. 5.12) and therefore kerosene is an inferior collector to the mixture of No. 2 and No. 6 fuel oils.

Aston et al. [79] also investigated the adsorption of ethoxylated nonyl phenols on hydrophobic and hydrophilic surfaces and showed that they can adsorb onto both. Rubio and Kitchener's [96] data on the adsorption of polyethylene oxide on hydrophilic and hydrophobic silicas seem particularly relevant to this discussion. Polyethylene oxide, $-(CH_2CH_2O)_n-$, contains the ether groups which are responsible for the solubility of PEO in water, and $-CH_2CH_2-$ groups which are sufficiently hydrophobic to lead to physical adsorption of PEO at air/water and oil/water interfaces. Rubio and Kitchener's results indicate that PEO strongly adsorbs onto a hydrophobic silica which has only isolated silanol groups on its surface; the adsorption is favored if the regions between such sites are hydrophobic. In other words, their results show that PEO and similar compounds should adsorb well onto hydrophobic surfaces that contain some polar groups, and coal is a very good example of such a surface. In line with these findings, Gochin et al. [97] reported that PEO adsorbs on anthracite through hydrophobic interactions and flocculates anthracite suspensions.

In view of the results reported by various researchers who studied properties of ethoxylated surfactants, it is not surprising to see that such surfactants found applications in emulsion flotation of coal. Ethoxylated fatty acids (EKT promoter) were studied by Sablik [98] as a coal flotation promoter. A mixture containing 76% fuel oil, 20% long-chain aliphatic alcohols and 4% EKT was shown to efficiently float coals which otherwise could not be floated with conventional reagents (Fig. 5.27).
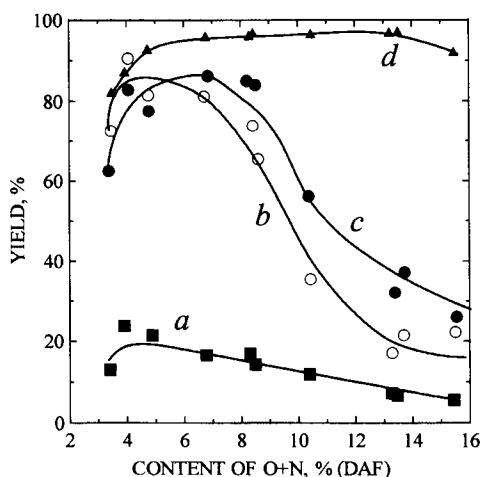
Fig. 5.27. Dependence of concentrate yield on coal rank and flotation conditions: *a*, natural floatability of −0.3 +0.2 mm size fractions in Hallimond tube without reagents; *b*, flotation of −0.3 +0.2 size fractions with 1 kg/t of fuel oil in Hallimond tube; *c*, flotation of −0.5 mm size fractions in a subaeration batch cell with fuel oil and frother (long-chain alcohols) at 9 : 1 collector-to-frother ratio; *d* as *c* but using reagents containing 76% fuel oil, 20% alcohols and 4% EKT promoter. (After Sablik [98]; by permission of Elsevier Science.)

Nimerick et al. [99] reported the results obtained with the use of a blend of Diesel oil collector, M-150 glycol ether frother and M-210 Dowell promoter. The clean coal recovery using 0.3 kg/t of reagents (2 : 1 Diesel oil to M-150 frother) was 63.4%, but a blend of 2 parts of Diesel with 10% M-210 to one part of M-150 frother produced 87% recovery. Dowell M-210 promoter contains imidazoline, which has the following formula [100]:

$$
\begin{array}{c}
\text{(C6 to C12 alkyl or alkenyl)} \\
\text{(C11 to C17 alkyl or alkenyl)}\!-\!\overset{\displaystyle O}{\underset{\displaystyle \|}{C}}\!-\!O\!-\!CH_2
\end{array}
\quad
\begin{array}{c}
N \\
\diagdown CH_2 \\
| \\
N\!-\!CH_2 \\
\diagdown \\
CH_2COO^-
\end{array}
$$
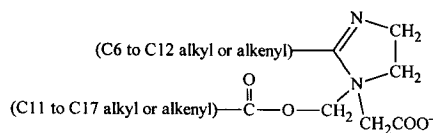
It is an amphoteric surfactant which behaves as a cationic agent at pH < 7.3 and as an anionic at pH > 8.8 [101].

Our electrokinetic measurements revealed that the iso-electric-point of kerosene droplets containing 5% of Dowell M-210 promoter is around pH 6 (Fig. 5.28). With 5% content of Dowell M-210 in kerosene, the kerosene/water interfacial tension was about 0.1 mJ/m^2 (with 5% addition of Sherex Shur 168 to kerosene, the kerosene/water interfacial tension was about 9.6 mJ/m^2). It is obvious then that promoters are very surface-active agents which adsorb at an oil/water interface and very efficiently reduce the oil/water interfacial tension [102]. Fig. 5.29 shows the zeta potential–pH curves for an easy-to-float bituminous coal. Curve 1 shows the effect of pH on the zeta potential of the tested coal, while curve 2 was measured at a constant pH of 5.6–5.9 for the coal samples which were conditioned varying pH in the aqueous solutions of Dowell M-210 [103]. These results indicate (i) that the solubility of M-210 promoter in water apparently increases in more acidic solutions and that it interacts with coal under such conditions, and (ii) that adsorption of this compound onto coal surface must be very strong. Thus, this agent strongly affects the electrokinetic properties of both coal and oil droplets.
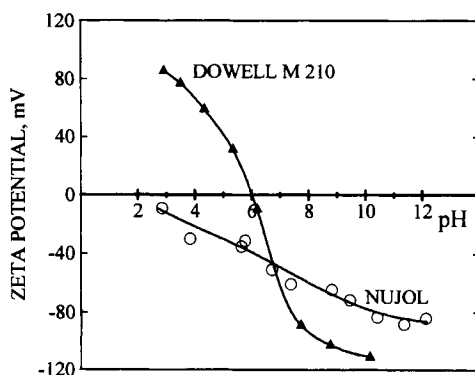
Fig. 5.28. Zeta potential vs. pH for Nujol droplets, and Nujol with 5% addition of Dowell M-210 promoter. (After Laskowski [102].)
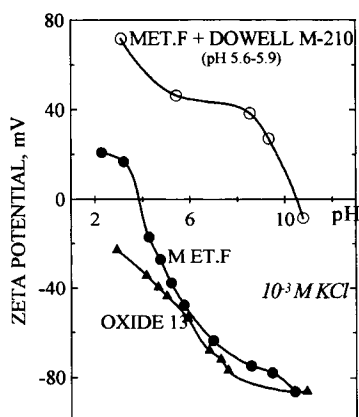
Fig. 5.29. Zeta potential vs. pH curves for Met F bituminous coal and Oxide 13 oxidized bituminous coal in 10^{-3} M KCl; circles, zeta potential of Met F coal measured in M-210 solutions and plotted vs. initial pH of the aqueous solution in which Dowell M-210 was left to equilibrate overnight. (After Laskowski [103]; by permission of Canadian Institute of Mining, Metallurgy and Petroleum.).
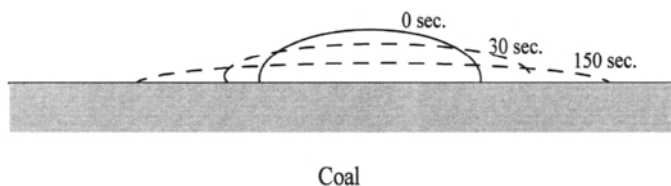
Coal

Fig. 5.30. Dynamic process of spreading of kerosene droplets containing 5% of Dowell M-210 promoter on coal surface in water. (After Laskowski [102].)

It was observed in the contact angle measurements that the kerosene droplets containing 5% promoter spread gradually on the coal surface immersed in water (Fig. 5.30). The contact angles measured with kerosene were quite stable. It is obvious, that intense shearing and turbulence in a flotation cell will speed up such a spreading process.

Fig. 5.31 shows the effect of Dowell M-210 promoter on the flotation of Oxide 13 coal (Fording mine, British Columbia) with kerosene and MIBC. Fig. 5.32 shows the effect of the Dowell M-210 promoter on the flotation of coarse coal ($-600 +212$ μm) with kerosene. Whereas unoxidized bituminous coal floated very well without the promoter, the oxidized coal (Oxide 13) required its addition. The sharp drop of floatability above pH 10 coincides with the zeta potential–pH curve in Fig. 5.29 (curve 2). Because quartz floats very well with cationic collectors, it also floated with M-210 in a very broad pH range in which this agent behaves as a cationic surfactant. Since — as these results indicate — the use of such agents may cause selectivity problems, their concentration must be kept within certain limits.

Scanlon et al. [104] provided some information on Accoal 4433 coal promoter, and Keyes [105] showed how coarse coal flotation can be improved with the use of
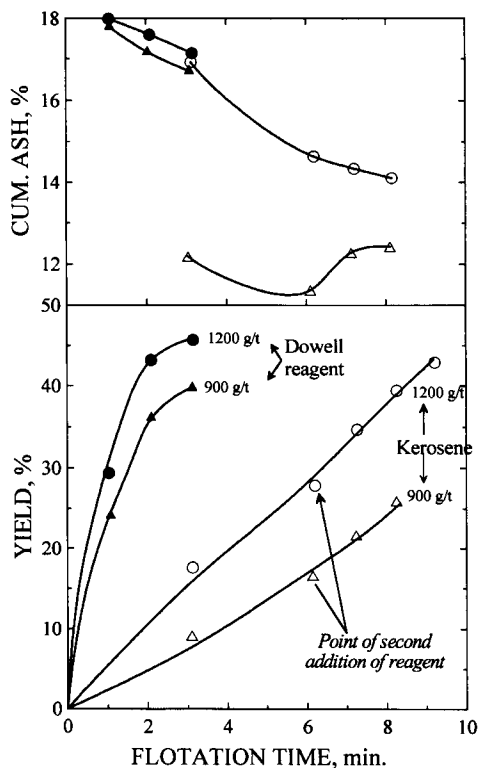
Fig. 5.31. Flotation of −425 μm size fraction of Oxide 13 coal using kerosene, MIBC and Dowell reagent. In the experiments without Dowell reagent, either 900 g/t or 1200 g/t of kerosene emulsified with MIBC (50 g/t or 100 g/t, respectively) was added in the first stage, followed by the same amount of reagents after 6 min of flotation. Dowell reagent contained: 61% No. 2 fuel oil, 29% Dowfroth 250 and 10% Dowell M-210 and was added in one single stage.

Shur-Coal 159 and 168 promoters. These products contain texanol and some other patented additives [3].

5.3.5. Concentrated inorganic salt solutions

As described in Klassen's monographs [2,39], coal can be floated in concentrated inorganic salt solutions without any other agents. The process is referred to as salt flotation.

The solid particle and oil droplet before and after attachment are shown in Fig. 5.3. Replacement of an oil droplet by a bubble in this picture (Fig. 5.33) and the same reasoning (Eqs. (5.15)–(5.20)) leads to the following formula:

$$\Delta G_{\text{flot}} = \gamma_{\text{LV}}(\cos \Theta - 1) \tag{5.23}$$

---

[3] In the group of coal flotation promoters should also be included ethylene oxide, propylene oxide and butylene oxide which additions to oily-collectors can clearly improve coal flotation (V.I. Tyhrnikova and M.E. Nahmov. Improving the Effectiveness of Flotation. Technicopy Ltd, Stonehouse, 1981, pp. 133–164).
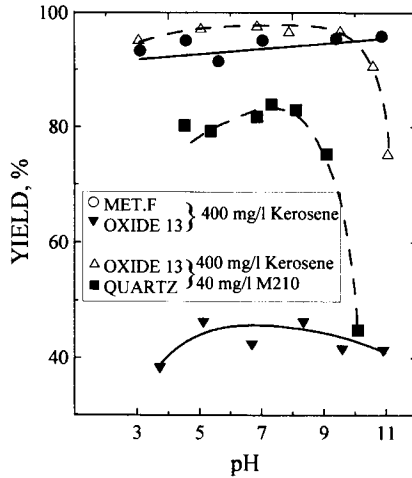
Fig. 5.32. Hallimond flotation of +212 −600 μm fractions of Met F and Oxide 13 coals, and +105 −212 μm quartz size fraction. Flotation was carried out either with kerosene only, or with kerosene containing M-210 promoter. (After Laskowski [102].)

This equation describes the probability of solid-to-bubble attachment, but is often referred to as the thermodynamic criterion of flotation. It simply states that the attachment of a solid particle to a bubble is probable only if $\Theta > 0$. For $\Theta = 0$, $\Delta G_{flot} = 0$ and the attachment process (and therefore flotation) is impossible.

Eq. (5.23) describes only the free energy change between states 1 and 2 (Fig. 5.33) without taking into account the intermediate stages. The disjoining film separating a particle and a bubble in Fig. 5.33 is situated between the solid/liquid and liquid/gas interfaces. The free energy of a column of such a film of unit cross-section can be expressed as [106]

$$G^s(h) = \gamma_{SL} + \gamma_{LV}(h) \tag{5.24}$$

where γ_{SL} is the solid/liquid interfacial tension, and $\gamma_{LV}(h)$ is the surface tension at the liquid/vapor interface expressed as a function of the film thickness, h. For a thickness of the disjoining film $h < h_0$ where h_0 corresponds to the range of surface forces acting across the interface, γ_{LV} also becomes a function of h. According to Frumkin [106], when the film becomes very thin, $h < h_0$, $G^s(h)$ may deviate from $G^s_\infty = \gamma_{SL} + \gamma_{LV}$ in

State I   State 2
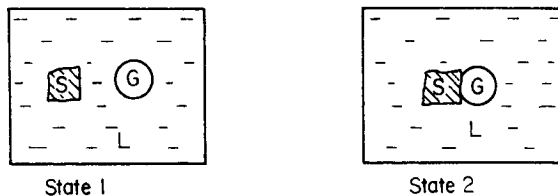
Fig. 5.33. Attachment of solid particle to bubble in flotation process.

either direction. The disjoining film is completely stable when $dG^s(h)/dh < 0$ (curve A, Fig. 5.34). As work is required to reduce the thickness of a stable film (curve A), the system reacts as though an additional force were keeping the interfaces apart; this additional force is referred to as Derjaguin's disjoining pressure

$$\pi(h) = -\frac{dG^s}{dh} \qquad (5.25)$$

Curve B shows the case of a completely unstable film, which when formed, will spontaneously rupture, forming a very thin film (adsorption layer) together with discrete drops.

The disjoining pressure is then positive for curve A (repulsion between interfaces) and a negative disjoining pressure corresponds to attraction. Thus, a negative disjoining pressure must exist in the film C at the film thickness which is just about to rupture and form a contact angle. ΔG (calculated from Eq. (5.23)), which is the difference between the free energy of the system at state 1 (before attachment) and state 2 (after attachment), is also shown in Fig. 5.34. However, if an energy barrier exists between states 1 and 2, then the attachment may not take place in spite of the overall favorable conditions ($\Delta G < 0$) (Eq. (5.24)). Here the energy barrier in the attachment process may be compared to the activation energy in chemical reactions. It is known that in Smoluchowski's kinetic theory of coagulation, the rate of coagulation depends on the energy barrier; the coagulation is fast when the energy barrier is zero and each particle–particle collision leads to attachment, but it may be slow if the energy barrier is large and only some collisions are fruitful.

The DLVO theory of colloidal stability considers the two principal sources of interaction between particles to be attractive dispersion London–van der Waals forces, and the electrical repulsive forces if the interacting particles carry the same electrical charge [107,108].

While working with quartz and methylated hydrophobic quartz (Eq. (5.21)), Laskowski and Kitchener [80] found that both of these samples carried practically
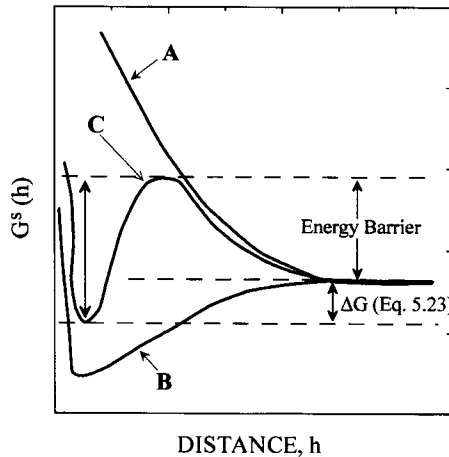
DISTANCE, h

Fig. 5.34. Schematic energy versus distance profiles for wetting films on solids.
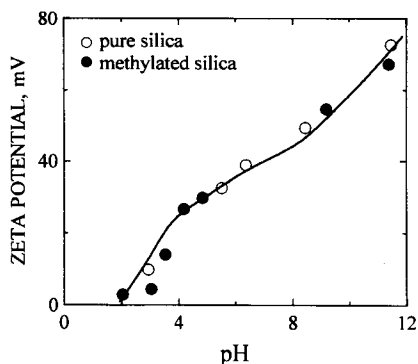
Fig. 5.35. Zeta potential of hydrophilic vitreous silica and methylated hydrophobic silica vs. pH (After Laskowski and Kitchener [80]; by permission of Academic Press.)

the same electrical charge, even though pure quartz was completely hydrophilic and the methylated quartz was very hydrophobic. These results are shown in Fig. 5.35. If the aqueous films on such particles are considered, the repulsive electrical contributions to the disjoining pressure in both cases are identical. The attractive forces for these two cases are not very different, and in both cases the positive values of the disjoining pressure should translate into a good stability of the films. Since an aqueous film on hydrophobic methylated silica is unstable and a large contact angle can be measured, and aqueous films on pure silica are perfectly stable, the hypothesis was put forward that "the instability of water films of a certain thickness on hydrophobic solids is fundamentally due to a deficiency of hydrogen bonding in these films compared with liquid water." Pashley [109] called this one of the most elegant demonstrations of the inadequacy of the DLVO theory. As is known today, the results graphically shown in Fig. 5.35 can only be explained if a third structural component is introduced into the classical DLVO theory [110,111]. In the case of hydrophobic surfaces, the third component is a strongly attractive hydrophobic force.

It is worth illustrating the importance of the hydrophobic forces by recalling the experiments carried out by Xu and Yoon [112,113]. In their coagulation studies they used methylated silica and fine coal. As an example, in Fig. 9.14 their zeta potential and coagulation data for a fresh and oxidized (140°C) bituminous coal are plotted against pH. The fresh coal was coagulating over a wide range of pHs from 3.8 to 8.9. The fact that the fresh coal could coagulate even at high zeta potentials (from +43 to −43 mV) suggests that there exists a highly attractive force which can overcome the strong electrostatic repulsive force. This attractive force is much larger than the London–van der Waals force considered in the classical DLVO theory. As Fig. 9.14 shows, the oxidation of the coal at 140°C did not change the zeta potential vs. pH curve, but the effective pH range for coagulation was significantly reduced. The upper critical coagulation pH limit, pH_c, was lowered to 7.3, at which point the corresponding zeta potential was only −23 mV. The fact that no coagulation was possible at higher zeta potential values suggests that the oxidation significantly reduced the hydrophobic interaction force.

Fig. 9.15 shows various energy interaction terms in the complete DLVO theory as a function of separation distance between two highly hydrophobic particles at the critical pH of coagulation. As this figure explains, for such a case, the hydrophobic interaction term V_H plays a much more important role than the London–van der Waals attractive interaction V_A. The total interaction V_T, ($V_T = V_A + V_R + V_H$) and the energy barrier thus results from the balance between the electrostatic repulsion V_R, and the hydrophobic attraction V_H. In a more recent publication, a relationship between the hydrophobic force and the solid wettability ($\cos \Theta$) was reported [114].

With this information we can now go back to the phenomenon of salt flotation.
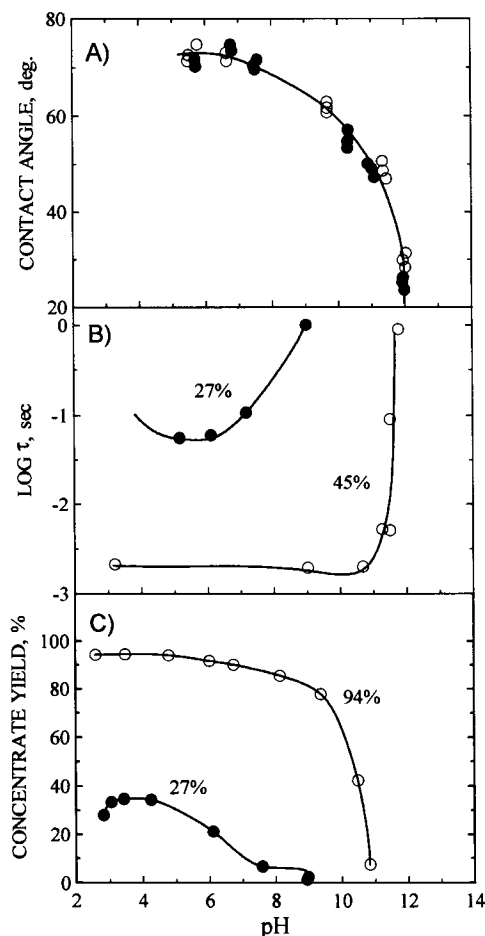
Fig. 5.36. Effect of pH on contact angles measured on methylated silica plate (A), induction time for two methylated quartz samples (B), and flotation of two methylated quartz samples (C). Numbers 27%, 45% and 94% are yields of concentrate in standard flotation tests carried out to characterize hydrophobicity of the methylated silica samples. All experiments conducted at contact ionic strength of 0.5 M KCl. (After Laskowski and Iskra [115]; by permission of The Institution of Mining and Metallurgy.)

Fig. 5.36 shows the effect of pH on the contact angle of methylated silica plates, the induction time of methylated quartz particles, and the flotation of such particles in 0.5 M KCl solution[115,116].

Eq. (3.11) can be further extended following Fowkes' concepts [117] to write

$$\cos \Theta = \frac{2(W_{SL}^d + W_{SL}^h + W_{SL}^e)}{W_{LL}} - 1 \tag{5.26}$$

where W_{SL}^d is the contribution from dispersion forces, W_{SL}^h is the contribution from the hydrogen bonding of water to a solid surface and W_{SL}^e is the contribution from the electrical charge at the interface.

According to Eq. (5.26), contact angles depend on the electrical charge of the solid and should be at maximum when $W_{SL}^e \approx 0$. The contact angle in Fig. 5.36 clearly depends on the pH and rapidly decreases in the pH range in which the electrokinetic potential of the methylated quartz particles becomes very negative (Fig. 5.35). In this pH range the induction time sharply increases and the floatability drops to zero. Fig. 5.37 shows the effect of KCl concentration at pH of 5.5 on contact angle, induction time, and flotation. As seen, the contact angle does not depend on the ionic strength of the solution; however, the induction time decreased with increased KCl concentration and the floatation of the methylated quartz particles also improved at higher KCl concentrations.

At high ionic strength (0.5 M KCl) when the electrical double layers of interacting bodies are compressed, the agreement between contact angle, induction time and flotation is excellent (Fig. 5.36). When pH is kept constant but the ionic strength of the solution is varied (Fig. 5.37), there is no agreement between the measured contact angle and flotation. The solid is hydrophobic, so according to Eq. (5.23) ΔG_{flot} is negative, but in spite of that the flotation is not very efficient. An obvious reason for that is the energy barrier [118] resulting from the negative zeta potentials of the methylated quartz particles. At increased KCl concentrations, the double layers around solid particles are compressed and this reduces the electrical repulsion term. Since the particles are hydrophobic this makes the particle-to-bubble attachment kinetically feasible. These results show that salt flotation is a kinetic phenomenon. They also demonstrate that both thermodynamic ($\Theta > 0°$) and kinetic (induction time < time of particle–bubble contact during collision) criteria must be satisfied for a solid particle to be floatable.

Fig. 5.38 shows salt flotation of coarse coal particles (-600 $+212$ μm) in a Hallimond tube [116]. For solids like coal, H^+ and OH^- ions are potential-determining and the surface electrical charge of coal particles is determined by the pH. As seen from Fig. 5.37, an increase in KCl concentration increased the rate of flotation but the maxima on all curves remained at the same pH. This figure illustrates two effects: (i) a shape of the flotation response curve vs. pH at constant ionic strength; (ii) an increase in the flotation rate with increase in solution ionic strength at constant pH.

Since the solid hydrophobicity should be at maximum when $W_{SL}^e \approx 0$, the maximum on the flotation vs. pH curve at constant ionic strength should coincide with $pH_{i.e.p.}$. An increase in ionic strength which suppresses the electrical forces hindrance under otherwise thermodynamically favorable conditions is reflected by an increase in floatability with increasing salt concentration.
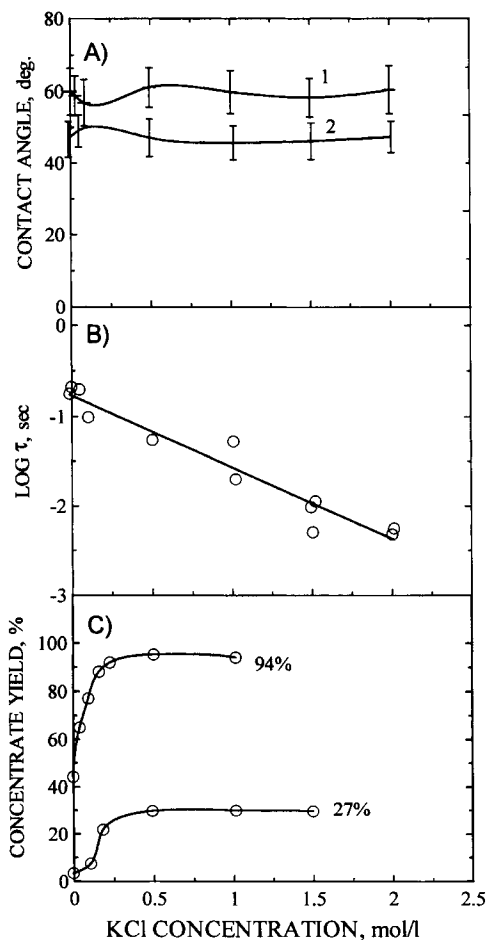
Fig. 5.37. Effect of KCl concentration on contact angle on two methylated silica plates (A), induction time of methylated quartz particles showing 27% yield of concentrate in standard flotation test (B), flotation of two methylated quartz samples (C). All experiments were conducted at natural pH. (After Laskowski and Iskar [115]; by permission of The Institution of Mining and Metallurgy.)

The hydrophobicity of coal particles in the salt flotation cannot be increased, hence this process can only be used to float hydrophobic bituminous coals. The results in Fig. 5.39, which illustrate the relationship between the maximum flotation rate constant (measured at $pH_{i.e.p.}$ in 0.5 M NaCl) and moisture content in western US coals [118], support this conclusion. The relationship between the floatability and the content of phenolic and carboxylic groups is very similar.

As already indicated, coal hydrophobicity is maximized at $pH = pH_{i.e.p.}$, and that should be reflected by a maximum on the salt flotation–pH curve (see Fig. 5.40). The dependence of coal's contact angle on pH was clearly demonstrated by Kelebek et al. [120]. An experimental verification that salt flotation is indeed best at $pH_{i.e.p.}$ is also
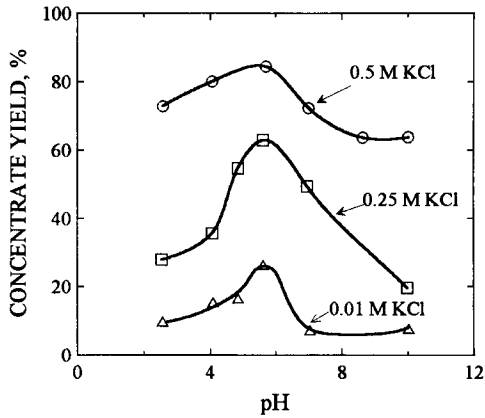
Fig. 5.38. Effect of pH on Hallimond tube flotation of Fording metallurgical coal at various KCl concentra-tions. Coal particle size: $-600 +212$ μm. (After Laskowski [116]; by permission of the Society of Mining Engineers.)
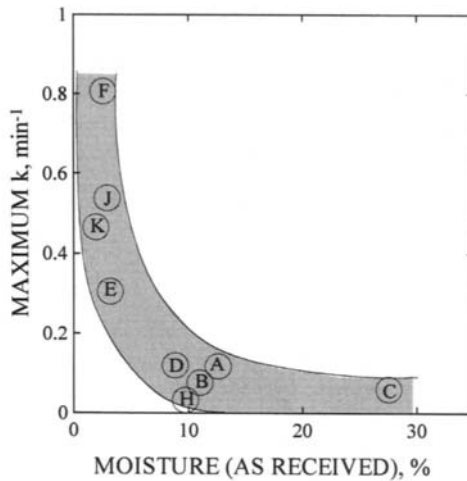
Fig. 5.39. Maximum flotation rate constants (salt flotation in 0.5 M NaCl) versus moisture content for U.S. western coals. (After Fuerstenau et al. [119]; by permission of Elsevier Science.)

available [121–123]. The flotation rate constants calculated for several coals from the salt flotation tests carried out at 0.5 M NaCl are plotted versus the zeta potential values determined from the zeta potential–pH curves (measured at a constant ionic strength of 2×10^{-3} M NaCl) in Fig. 5.40. These results clearly confirm that salt flotation is indeed best at pH = $pH_{i.e.p.}$.

It is worth pointing out that some other phenomena which were discussed to explain the salt flotation mechanism may also play a role in the overall result. Kharlamov [1] found from salt flotation experiments with various coals that in general sodium sulfate provides better results than sodium chloride, which in turn is better than sodium nitrate.
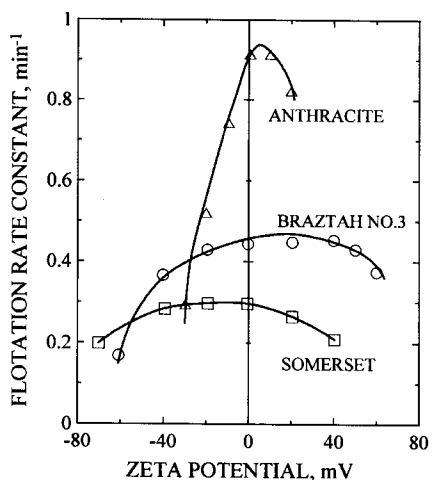
Fig. 5.40. Flotation rate constants in 0.5 M NaCl solutions for three coals vs. the zeta potential of the coal. (After Fuerstenau et al. [119]; by permission of Elsevier Science.)

Foaming properties of the aqueous solutions of these salts follow the same order, and therefore some researchers, as discussed by Klassen [1], claimed this to be the main effect of salts on salt flotation. It is, however, worthy of mention that it is possible to sharply improve salt flotation by only a slight change in pH while maintaining a constant high salt concentration. Under such high ionic strength conditions the frothability of the solution is not affected at all but the flotation may be sharply improved.

As discussed in Section 3.3, the adsorption isotherms of water vapors on coal indicate that water molecules adsorb only onto the polar sites on coal surface, and that these adsorbed water molecules serve as secondary sites for the adsorption of additional water. The clusters formed around the active sites grow in size with increasing surface coverage and they merge at some stage to cover the rest of the hydrophobic surface with a film. Such a peculiar hydration layer is anchored to the coal surface only through hydrophilic sites and the stability of such a layer should critically depend on the electrical double layer structure and thickness. It can be visualized that under high electrolyte concentration, compression of the double layer will destabilize the wetting film by exposing the mosaic of the hydrophobic patches on a heterogeneous coal surface.

Oily collectors are commonly applied to enhance the flotation of coarse particles and the role of such an agent in increasing the adhesive particle–bubble forces is well established. It is surprising then that large coal particles also float very well in concentrated salt solutions. To illustrate this point some results of salt flotation tests on a medium volatile bituminous coal ground below 0.75 mm are shown in Fig. 5.41 [122]. The feed contained 31% ash. The experiments were carried out using a 1.5-l batch flotation cell; flotation time was varied from 6 min in experiments 1–3, to 5 min in exp. 4, 4 min in experiment 5, and 3.5 min in experiments 6 and 7. Experiments 1 and 2 were carried out with kerosene only, experiments 3–5 were carried out with 430 g/t of
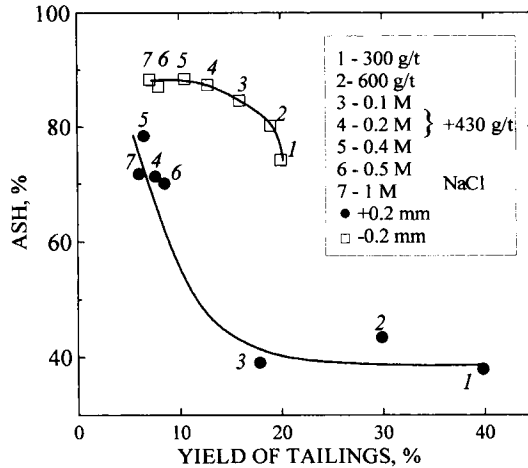
Fig. 5.41. Ash content vs. yield of the −0.2 +0.2 mm size fractions in flotation tailings from batch flotation experiments. Medium-volatile bituminous coal, dosages of kerosene and concentrations of NaCl solutions as shown. (After Laskowski [122].)

kerosene in NaCl solutions, and experiments 6 and 7 were carried out in NaCl solutions without any organic agents. The coal was conditioned in salt solution (or in water), then 60% of the kerosene was added 1 min prior to flotation and two 20% portions were added during the flotation experiment. The tailings from the experiments were screened to obtain +0.2 and −0.2 mm size fractions, and these were analyzed for ash content. The ash content in the −0.2 mm tailings was high in all experiments and did not depend on the experimental conditions very much. However, the ash content in the +0.2 mm fraction of tailings clearly depended on the NaCl concentration. The ash contents in this coarse fraction in the experiments carried out in 0.5 M and 1 M NaCl solutions were as high as the ash contents in the experiments carried out with some kerosene in spite of the fact that the flotation times in the experiments with kerosene were much longer. Apparently, coarse coal particles floated better at higher concentrations of NaCl even with lower dosages of kerosene. In the experiments that followed, the size fraction of low-ash bituminous coal was so selected that it did not float either in 0.4 M NaCl or with kerosene. However, small amounts of kerosene (195–650 g/t) in 0.4 M NaCl solution caused excellent flotation of such particles.

As reported by Sun and Zimmerman [123], coarse particles have to be floated with more than one attached bubble and the salt flotation environment apparently favors such multi-bubble attachments. This also seems to suggest that high electrolyte concentration conditions favor the precipitation of micro-bubbles on the coal surfaces. The presence of micro-bubbles on a solid surface is known to facilitate the attachment of larger bubbles to it [2]. Fig. 5.42 shows the flotation results for the −1.2 +0.6 mm size fraction of a low-ash bituminous coal in a 0.4 M NaCl solution with 325 g/t of kerosene. The flotation experiments conducted in a solution which was deaerated for 4 hours under vacuum gave clearly inferior results to those carried out under usual conditions. This
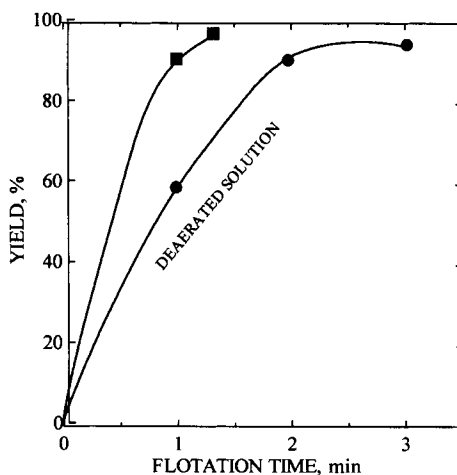
Fig. 5.42. Flotation of a −1.2 +0.6 mm size fraction of low-ash bituminous coal in 0.4 M NaCl solution with 325 g/t of kerosene. The flotation in a deaerated NaCl solution is also shown. (After Laskowski [122].)

observation seems to confirm the role which may be played by micro-bubbles nucleating on coal surface in concentrated salt solutions.

5.3.6. Depressants

The flotation of a given mineral can be depressed either by (a) preventing collector from adsorbing onto this given mineral, or by (b) making the mineral surface hydrophilic. Both these mechanisms require adsorption of the reagent onto the mineral surface.

In general, depressing agents can be classified into inorganic compounds and polymers. The former are used to prevent collector from adsorbing. Although the latter are able to engage in both types of interactions, they are mostly used to render mineral surfaces hydrophilic since they are large hydrophilic macromolecules. Because coal is hydrophobic, only organic polymers are utilized to depress it, but both inorganic and polymeric depressants are used to control flotation of pyrite.

5.3.6.1. Coal depression

The group of organic depressants includes polysaccharides (dextrines, starches, guar gums, carboxymethyl cellose, hydroxylpropyl methylcellulose, etc.), polyphenols (tannin extracts: quebracho and wattle bark, lignin, etc.), and humic acids. It is worthy of mention that some of these polymers (e.g. starches, carboxymethyl cellulose, etc.) and synthetic polyelectrolytes are also used as flocculants. This depends first of all on the polymer's molecular weight. In general, while linear high molecular weight polyelectrolytes are good flocculants, lower weight branched polymers cannot be used as flocculants and are only used as dispersants/depressants. Flocculants are known to strongly depress coal flotation [124]. Moudgil [125] tested unidentified polyacrylamide (PAM) and polyethylene oxide (PEO) and found that depressing effect of PAM on coal flotation was much stronger. This is in line with Pradip and Fuerstenau [19] who
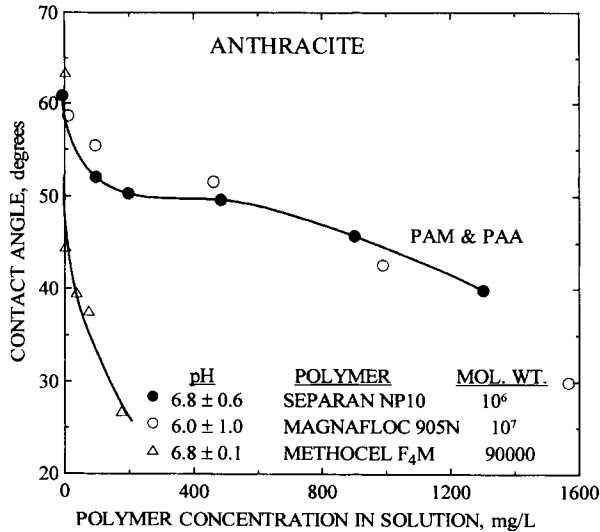
Fig. 5.43. Effect of polyacrylamide (PAM), polyacrylic acid (PAA) and hydroxypropyl cellulose (Methocel) on wettability of anthracite surface. (After Pradip and Fuerstenau [19].)

followed coal wettability in the presence of various polyelectrolytes through contact angle measurements. Some of their results are portrayed in Fig. 5.43. They claim that coal hydrophobicity in the presence of the tested polymers decreases in the order PEO > PAM > Methocel (Methocel is a trade name of hydroxypropyl methylcellulose) (see also Fig. 6.18).

Regarding polysaccharides, in his studies on the selective flocculation of a hematite/kaolinite mixture Weissenborn [126] found that amylopectin behaved as a flocculant whereas amylose was not a flocculant. While small amounts of amylose enhanced amylopectin performance, higher dosages diminished this performance. It is important to realize that since flocculants are very hydrophilic macromolecules, they will also depress coal flotation.

Polysaccharides have been used in the mineral industry for over six decades. The first patent for using starch in combination with lime was filled in 1928 [127] for the clarification of colliery effluents. The patents and publications that followed focused on the applications of polysaccharides primarily as: (i) depressants/flocculants of iron oxides from silicates; (ii) selective modifiers in the flotation of salt-type minerals (calcite, fluorite, etc.); (iii) depressants of inherently hydrophobic minerals.

It is obvious that the last application is directly related to the use of such compounds in coal flotation. Developments in this area are summarized in Table 5.11. These applications involve the use of polysaccharides to depress inherently hydrophobic solids and these applications suggest that polysaccharides possess a high affinity toward hydrophobic solids and render them hydrophilic. We and Fuerstenau [128] suggested that dextrin adsorbs on molybdenite through hydrophobic bonding and in many publications that followed a similar explanation was adopted.

Table 5.11
Developments in the use of polysaccharides in mineral processing

Application of starch, in combination with lime, for clarification of colliery effluent containing fine coal particles and clays	Patent filed in 1928; J.A.Kitchener, in The Scientific Basis of Flocculation (K.J. Ives, ed.) Sijthoff and Noordhoff, 1978
Application of starch to depress apatite in a cationic flotation of quartz	U.S. Patent, 1,914,695/1931
Application of starch in flocculation/flotation of hematite and quartz	Publications by Cooke, and Iwasaki and co-workers in the 1950's and 1960's, and later on by Colombo
Application of starch to depress flotation of salt-type minerals calcite, fluorite. etc.)	Somasundaran, 1969; Hanna and Somasundaran, 1976
Application of polysaccharides (e.g. dextrin, guar gum, carboxymethyl cellulose, etc.) to depress flotation of inherently hydrophobic minerals	U.S. Patents 2,070,076; 2,145,206; 2,211,686; Klassen, 1963; Wie and Fuerstenau, 1974; Rhodes, 1979; Steenberg and Harris, 1984
Application of dextrin in selective flotation of the chalcopyrite-pentlandite bulk concentrate	Since 1959 at Kotalahti mine in Finland
Depression of coal with dextrin and other polysaccharides	Klassen, 1963; Im and Aplan, 1981
Desulfurizing of coal by depressing it with dextrin in a two-stage reverse flotation of coal	U.S. Patent 3,807,557; K.J. Miller et al., 1970's; J.D. Miller et al, 1980's, K.J. Miller and A.W. Deurbrouck, 1982
Depression of graphite with the use of carboxymethyl cellulose (CMC). Desulfurizing flotation of coal with CMC	Solari et al, 1986; Laskowski et al.,1985
Depression of pyrite in coal flotation with polysaccharides and xanthated polysaccharides	Perry and Aplan, 1985
Mechanism of adsorption of polysaccharides onto solid surfaces, and in particular onto inherently hydrophobic solids	Liu and Laskowski, 1989; Nyamekye and Laskowski, 1991-1994, Subramanian et al. 1993-1999

Fig. 5.44 shows the data of Huang et al. [129]) on the adsorption of dextrin on coal, molybdenite, coal-pyrite and ore-pyrite. As Fig. 5.45 reveals, coal flotation is strongly depressed by dextrin, but not pyrite flotation [130]. Im and Aplan [131] demonstrated that dextrin is a superior coal depressant. This is likely to result from its molecular weight and branching. A good depressant is one that adsorbs strongly onto the coal surface and establishes a coating which repels air bubbles.

In 1986, Solari et al. [132] showed that while high-purity graphite adsorbed carboxymethyl cellulose (CMC) quite well (Fig. 5.46), the same graphite when further purified by leaching hardly adsorbed CMC at all. It was also found that the flotation of the original graphite was strongly depressed by CMC, but that the same CMC did not depress the purified graphite. These findings revealed the role of impurities (Fe, Ca, etc.) on a graphite surface as centers for CMC adsorption. The following tests carried out with dextrin and methylated silica revealed that neither hydrophilic quartz
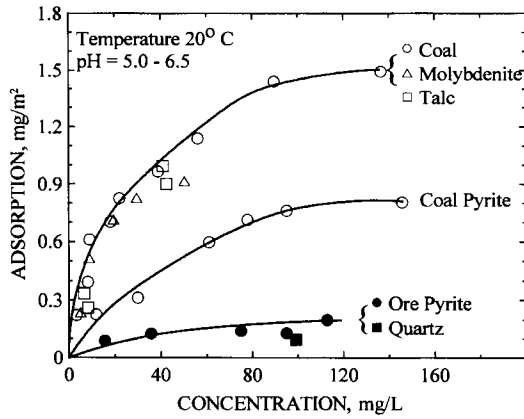
Fig. 5.44. Adsorption of dextrin on hydrophobic and hydrophilic solids at 20°C and pH 5–6.5. (After Miller et al. [130]; by permission of Gordon and Breach.)
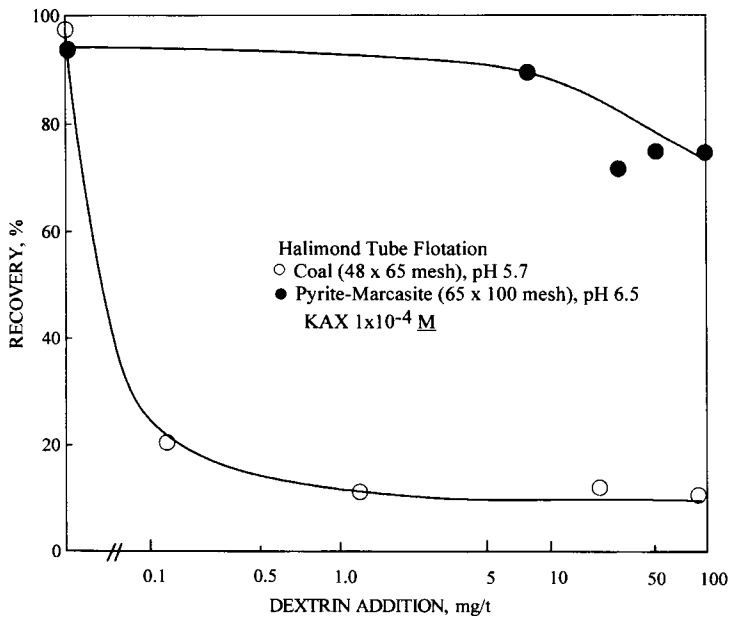
Fig. 5.45. Effect of dextrin addition on Hallimond tube flotation of coal and pyrite. (After Miller et al. [130]; by permission of Gordon and Breach.)

nor methylated hydrophobic quartz adsorbs dextrin [133,134]. Dextrin was, however, very well adsorbed by both hydrophilic and hydrophobic quartzes if they also contained some metallic adsorption centers (Figs. 5.47 and 5.48). Similar tests carried out with sulfides led to the discovery that the adsorption of dextrin on lead and nickel sulfides
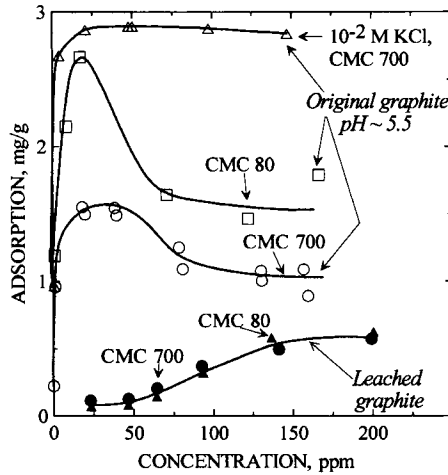
Fig. 5.46. Adsorption isotherms of carboxymethyl cellulose on original high-quality graphite and graphite purified further by leaching, pH 5.5, 25°C; 80 and 700 stand for molecular weight of carboxymethyl cellulose of 80,000 and 700,000, respectively. (After Solari et al. [132]; by permission of Gordon and Breach.)
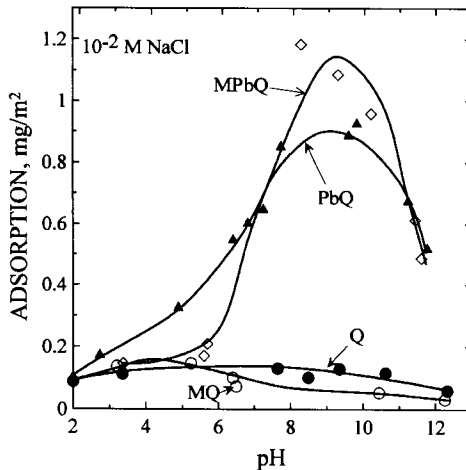
Fig. 5.47. Effect of pH on adsorption of dextrin on pure hydrophilic quartz (Q), quartz rendered hydrophobic by methylation (MQ), lead-coated hydrophilic quartz (PbQ) and hydrophobic methylated lead-coated quartz (MPbQ); initial concentration of dextrin was 50 ppm. (After Liu and Laskowski [133]; by permission of Elsevier Science.)

is strongly pH dependent, while the affinity of dextrin towards copper sulfides is much lower and is pH independent [135].

All these findings point to a strong interaction between dextrin macromolecules and solid surfaces which is chemical in nature. They also indicate that although surface hydrophobicity is not the primary factor, it does further enhance the interaction between
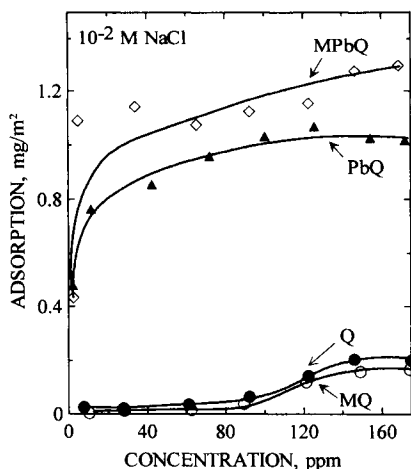
Fig. 5.48. Adsorption isotherm of dextrin on different quartz samples (symbols as in Fig. 47). (After Liu and Laskowski [133]; by permission of Elsevier Science.)

dextrin and mineral surfaces. In light of these observations it seems likely that a similar mechanism is involved in polysaccharide adsorption on coal surfaces. The hydrophobic matrix of coal with its numerous inorganic impurities and polar groups would be an excellent candidate for a strong interaction with polysaccharides.

There are several reports on the effect of humic acids on flotation. Wong and Laskowski [136] studied the effect of humic acids on the surface properties and flotation of graphite. Humic acids were found to adsorb in appreciable quantities onto a hydrophobic solid such as graphite, to increase the negative charge of graphite over the whole investigated pH range from 3 to 11, and to make the graphite surface hydrophilic.

Yarar and Leja [137] observed that oxidized coal, which floated poorly, produced intense coloration in the flotation pulp. These results agree remarkably with our Fig. 5.49 which shows the results of 4-min flotation tests on three different metallurgical coals. These flotation tests were performed using 900 g/t of kerosene and 100 g/t of MIBC [138]. On dry-ash-free basis, Oxide 13 coal (Fording mine, B.C.) contained 34.7 volatile matter and 65.3% FC, while Oxide 4 sample 21.6% VM and 88.4% FC, and ESMC sample (Quintette mine, B.C.) 21.1% VM and 88.9% FC. By following the procedure developed by Gray and Lowenhaupt [25,26], a very low transmittance was determined for Oxide 13 coal, and this correlates well with its poor flotation, while for ESMC coal, the transmittance was almost 100% and the coal floated well. Since this procedure determines the content of humic acids in coal, the relationship in Fig. 5.49 seems to imply that humic acids affect coal floatability very strongly.

In Fig. 5.50 the zeta potential is plotted against pH for the three tested coals, also in the presence of humic acids. As seen from Fig. 5.51, humic acids sharply reduce both the advancing and receding contact angles on coal. The effect of humic acids on the zeta potential of the same coals is shown in Fig. 5.52 [139]. There is no doubt that irrespective of the original coal surface properties, humic acids impart properties
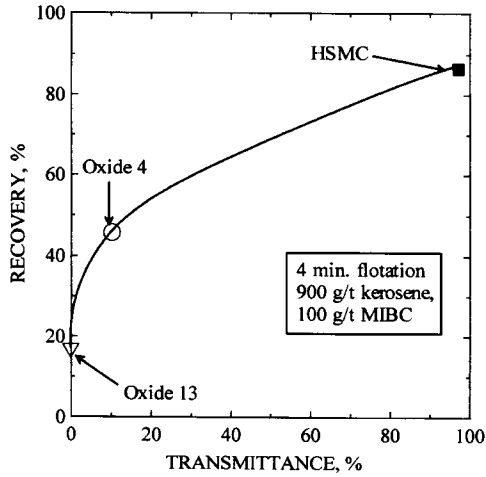
Fig. 5.49. Correlation between the batch flotation results and transmittance of the alkali-extract. (After Liu and Laskowski [138].)
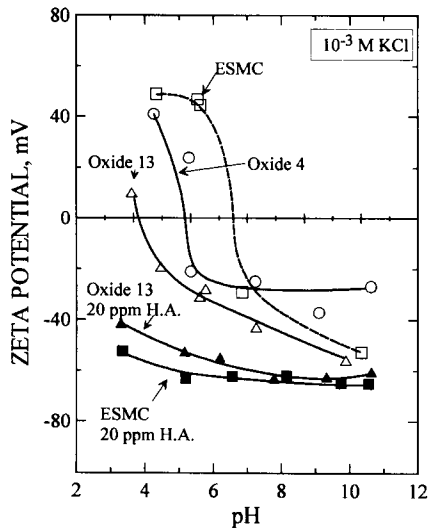
Fig. 5.50. Zeta potential–pH curves for freshly ground three bituminous coal samples. Two additional curves show the zeta potential–pH curves for the same coals in 20 ppm humic acid solutions. (After Liu and Laskowski [138].)

similar to those of low-rank coals to all coals. As Fig. 5.53 reveals, the effect of humic acids on coal zeta potentials is even stronger than that of carboxymethyl cellulose [140]. Humic acid also affects the zeta potential of oil droplets (Fig. 5.54). In separate tests this effect was found to be as pronounced as the effect of carboxymethyl cellulose on the zeta potential of kerosene droplets. All these effects are reflected in flotation tests,
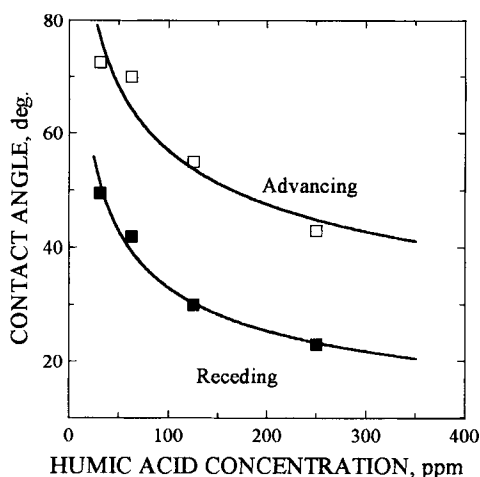
Fig. 5.51. Effect of humic acids on advancing and receding contact angles measured on a high-volatile bituminous coal. (After Pawlik et al. [139]; by permission of Gordon and Breach.)
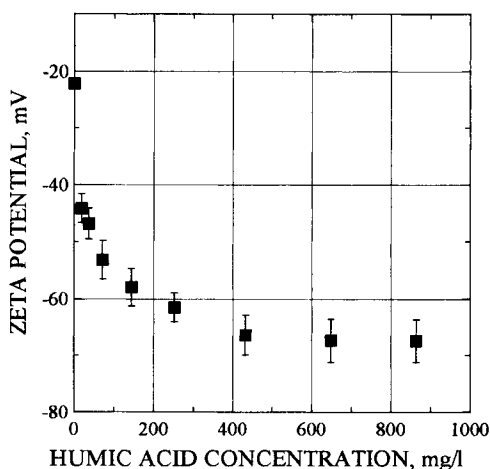
Fig. 5.52. Effect of humic acids on the zeta potential of high-volatile bituminous coal; pH 5.7–7.6. (After Pawlik et al. [139]; by permission of Gordon and Breach.)

which revealed that humic acids very strongly affect emulsion flotation with kerosene (Fig. 5.55) [141].

Figs. 5.56 and 5.57 show a series of concomitant tests on the effect of humic acids on the flotation of ESMC metallurgical coal with MIBC and kerosene. As these figures demonstrate, the effect of humic acids is particularly pronounced in acidic environments. Flotation with the addition of humic acid at pH 8 is almost as efficient as that without humic acid, but is more selective. It is noteworthy that Lai and Wen [142] also observed that humic acids do not depress coal in an alkaline environment.
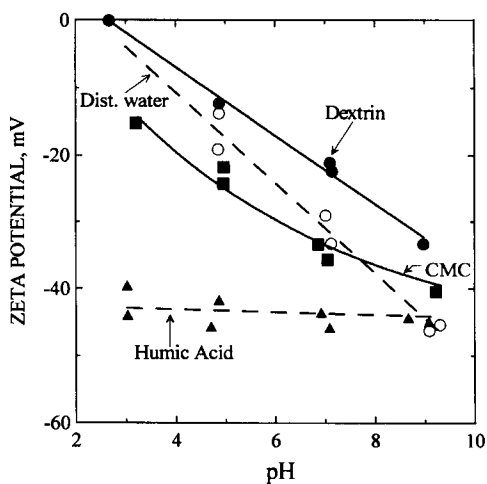
Fig. 5.53. Effect of pH and various modifiers at concentration of 20 ppm on zeta potential of Fording bituminous coal. (After Laskowski and Yu [140].)
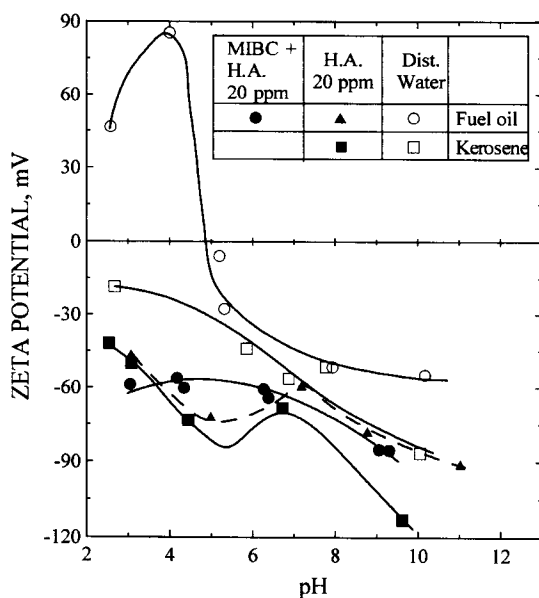
Fig. 5.54. Effect of pH and humic acids on the zeta potential of kerosene and fuel oil (4 : 1 No. 2 and No. 6 fuel oils) droplets. (After Laskowski and Yu [140].)

As has already been discussed, promoters are frequently used to aid in the flotation of difficult-to-treat coals. The contact angle of kerosene droplets (measured through aqueous phase) formed on a coal surface in aqueous solutions is clearly affected by 20 ppm of humic acid; these angles are about 90° in distilled water but drop almost
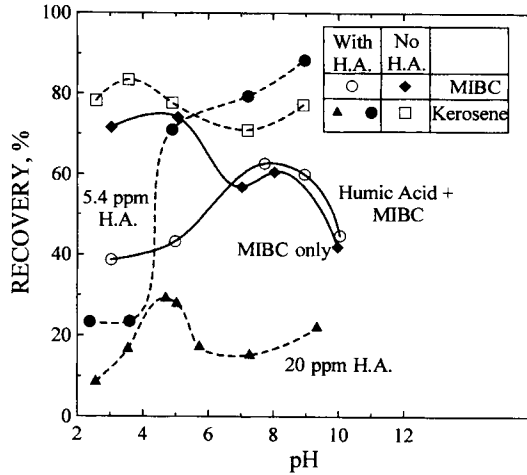
Fig. 5.55. Effect of pH and humic acids on flotation of Fording coal with kerosene and MIBC. Concentration of humic acid was 20 ppm unless otherwise specified. (After Laskowski et al. [141]; by permission of Gordon and Breach.)

to zero in the presence of humic acid at low pH values (Fig. 5.58 [3]). When 5% of the Dowell M-210 promoter was added to the kerosene, the contact angle jumped to more than 160°, indicating that kerosene with the promoter wetted the coal surface almost perfectly. In acidic solutions, where the M-210 promoter behaves as a strongly cationic surfactant, its presence eliminates the negative effect of humic acids, but not in alkaline solutions. In an alkaline environments, the coal surface is strongly negatively charged and the adsorption of anionic humic acid onto coal is apparently hindered.

As Fig. 5.49 demonstrates, humic acids can easily be extracted from coal. It is thus possible that when coal is first brought into contact with an alkaline solution which is later adjusted to more acidic values, the humic acids may precipitate onto the coal surface and depress its flotation. This was actually observed in tests where the coal was first conditioned in an alkaline solution and then the pulp was acidified prior to flotation [138].

Liu et al. [143] have recently reported the opposite effect. They observed that when the pH of the coal pulp is increased, some hydroxides may precipitate on the coal surface and so depress coal flotation.

5.3.6.2. Pyrite depression

Pyrite almost always appears in polymetallic sulfide ores. Since it is treated as a gangue which has to be depressed in the differential flotation of sulfides, its floatability has been extensively studied. It is common to depress it by carrying out flotation in an alkaline environment using lime. However, similar conditions do not seem to depress pyrite in the flotation of coal. This is one of the key observations which points to possible differences between ore-pyrite and coal-pyrite flotation properties. Of course, it
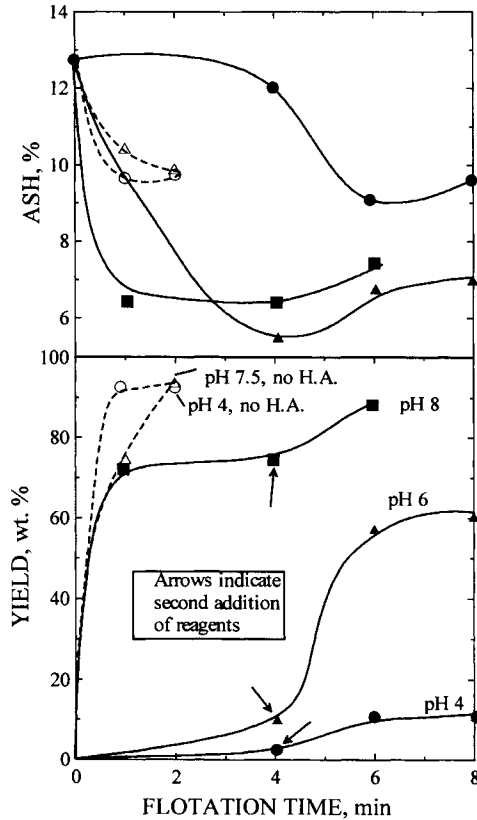
Fig. 5.56. Flotation of −0.212 mm Quintette East Seam Metallurgical Coal (ESMC) in the presence and absence of 2 kg/t of humic acids with 900 g/t of kerosene and 100 g/t of MIBC. (After Liu and Laskowski [138].)

is to be borne in mind that thio-collectors are used in the flotation of sulfide ores while coal is floated with the use of frother and oily collector. Because pyrite particles can enter the froth not only by true flotation, but also by entrainment, or when these particles are not perfectly liberated and contain some organic matter which makes them floatable, the subject is very controversial. It is known that some sulfides display so-called self-induced flotation in moderately oxidizing conditions [144], and this mechanism may also be responsible for the different behavior of coal-pyrite.

In general, because of their inability to form hydrogen bonds with water, sulfides are not strongly hydrophilic [145]. Based on the critical surface tension of wettability values, sulfides are classified as partially hydrophobic minerals [146].

Pyrite appears in coal not only in the form of individual crystals, but also as assemblies of crystals forming framboids [147]. It has been reported that coal-pyrites are characterized by higher porosity and higher reactivity than ore-pyrites [148–150]. The oxidation of pyrite leads to the formation of sulfur and/or iron polysulfides which
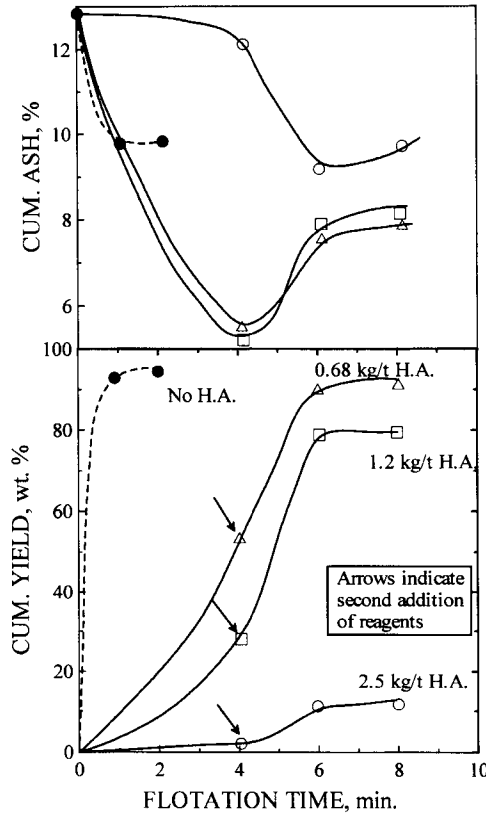
Fig. 5.57. Effect of stage addition of the reagents (kerosene and MIBC as in Fig. 55) on flotation of ESMC coal at pH 4.3 in the presence of humic acids. (After Liu and Laskowski [138].)

are responsible for increased hydrophobicity. While this increase in hydrophobicity is very moderate, it is apparently sufficient to make these minerals floatable in the presence of a frother and oily collector [151].

Heyes and Trahar [152] studied the self-induced flotation of pyrrhotite and pyrite. In their flotation experiments the pulp redox potential was controlled by the use of sodium dithionite and sodium hypochlorite. The collectorless flotation tests carried out versus the pulp potential revealed that while pyrrhotite displayed pronounced self-induced floatability which depended upon pulp potential, pyrite did not float at any potential. However, the same pyrite floated quite well when it was first subjected to the treatment with sodium sulfide and then to aeration.

Self-induced floatability of sulfides results from mild oxidation. In the case of pyrite, the first stage of oxidation is believed to involve the following anodic and cathodic reactions:

$$FeS_2 = Fe^{2+} + 2S^{\circ} + 2e \tag{5.27}$$

$$\tfrac{1}{2} + H_2O + 2e = 2OH^- \tag{5.28}$$
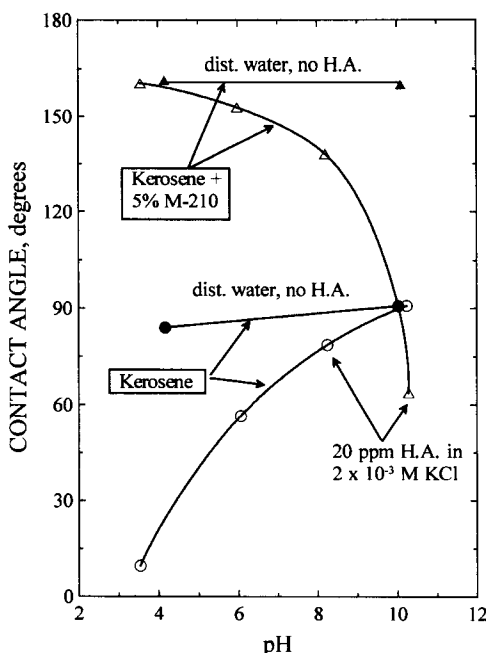
Fig. 5.58. Contact angles at droplets of kerosene (measured through aqueous phase) and kerosene containing 5% Dowell M-210 promoter on ESMC in water. (After Liu and Laskowski [138].)

with the overall reaction being

$$FeS_2 + \tfrac{1}{2}O_2 + H_2O = Fe^{2+} + 2S^\circ + 2OH^- \tag{5.29}$$

Since the $Fe(OH)_2$ that formed on the surface as a result of reaction 29 is thermodynamically unstable, it oxidizes further, and the overall reaction is usually written as follows:

$$FeS_2 + \tfrac{3}{2}O_2 + \tfrac{3}{2}H_2O = Fe^{3+} + 2S + 3OH^- \tag{5.30}$$

Singer and Stumm [153] are of the opinion that the oxidation of ferrous ions to ferric ions is the rate-controlling step in pyrite oxidation.

Yoon et al. [151] postulated that polysulfides (FeS_n) are formed on the surface rather than elemental sulfur (and are responsible for weakly hydrophobic surfaces):

$$nFeS_2 + \frac{n-2}{2}O_2 + (n-2)H_2O = (n-2)Fe^{2+} + 2FeS_n + 2(n-2)OH^- \tag{5.31}$$
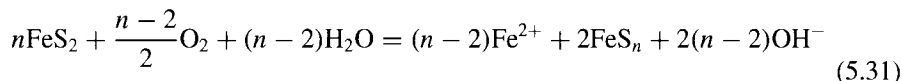
Native and induced floatability of coal- and ore-pyrite was recently re-examined in an interesting paper by Jiang et al. [154]. Fig. 5.59 shows their comparison of the floatability of ore-pyrite, coal-pyrite and coal using MIBC and fuel oil. While the floatability of ore-pyrite was only slightly improved by fuel oil, fine coal-pyrite floated much better in the presence of fuel oil. It has often been reported that coal-pyrite does not float very well with xanthate. As Jiang et al.'s results clarified, while ore-pyrite floats
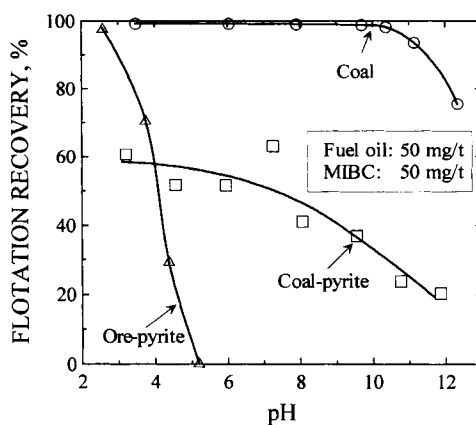
Fig. 5.59. Comparison of flotation recovery of fine coal, coal- and ore-pyrite as a function of pH using fuel oil and MIBC. Coal, -74 μm; coal- and ore-pyrite, -45 μm. (After Jiang et al. [154].)

very well with xanthate over a broad pH range, coal-pyrite floats with xanthate only in acidic pHs, and xanthate also enhances coal flotation. Since chemical analyses of their samples showed that the coal-pyrite contained 5.33% C, different flotation properties of the two tested pyrites were attributed to the presence of carbon in the coal-pyrite sample. Although this still remains open to doubt, the explanation advanced by Jiang et al. is very convincing. Kawatra et al.'s column flotation data [155], which indicate that in coal flotation pyrite reports to the froth products mostly as a result of entrainment or imperfect liberation, seem to support Jiang et al.'s view that pyrite floats because it contains some carbon (imperfect liberation).

Preparation of the coal-pyrite for the tests is not simple and a method was developed in some labs which provides the pyrite with some degree of hydrophobicity. This is achieved by conditioning pyrite in a sodium sulfide solution with the addition of a certain amount of HCl followed by aeration [32,156]. Such a procedure deposits a film of elemental sulfur on the pyrite surface which then exhibits some degree of hydrophobicity. It is drawn on the assumption that such a sample simulates coal-pyrite. This could be true only if coal-pyrite could undergo an oxidation process leading to the appearance of sulfur on its surface due to the electrochemical conditions prevailing in the coal flotation environment. Lai et al.'s [157] comparison of the flotation properties of ore-pyrite and coal-pyrite by floating these minerals with an undisclosed anionic fluorosurfactant in the presence of sodium hydrosulfide confirms that these two specimens behaved differently. While ore-pyrite floated under such conditions only in the acidic pH range, coal-pyrite floated in the alkaline pH range in good agreement with Fig. 5.59. But does this mean that coal pyrite floats along with coal because it carries sulfur on its surface resulting from oxidation? Is this hydrophobicity really due to the presence of sulfur and not carbon resulting from poor liberation? Is it possible that the presence of carbon on a coal-pyrite surface enhances its oxidation? Lai et al. [157] did report that coal-pyrite oxidized much faster than mineral pyrite. But since a frother and oily collector only are utilized in coal floatation, does it matter
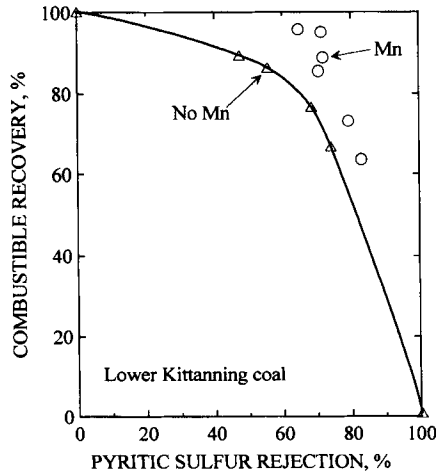
Fig. 5.60. Results of the laboratory microbubble column flotation tests conducted on the −0.15 mm Lower Kittanning coal sample: without Mn (△) and with 10 g of Mn mixed with 200 g of coal sample conditioned at 20% solids (○). (After Yoon et al. [160]; by permission of Gordon and Breach.)

whether coal-pyrite is hydrophobic due to the presence of sulfur or carbon on its surface?

Miller et al. [158,159] reported that conditioning of coal with a triple salt available under the trade name Oxone (du Pont), which contains potassium monopersulfate ($KHSO_5$) as an active ingredient, may activate coal flotation and depress pyrite. Monopersulfate is a strong oxidant and it seems that moderate oxidation of the coal surface with this reagent cleans the surface and makes it more hydrophobic. On the other hand, conditioning coal with this reagent prior to flotation improves pyrite rejection. The results imply that this is due to the oxidation of the hydrophobic species on the surface of pyrite. While improvement in flotation efficiency was found to vary with the coal sample, the improved pyrite rejection was quite general for all tested coals.

In a mixture containing both coal and pyrite particles there are two contradictory tendencies: in general, the oxidation of coal reduces its floatability, but at the same time it induces self-floatability of pyrite. Avoidance of the oxidation should then result in a very good flotation of coal and poor flotation of pyrite. Arnold and Aplan [35] reported that reducing agents such as dithionite, ferrous sulfate and sodium sulfide were effective in reducing the sulfur content in the flotation of the Upper Freeport seam coal. Yoon et al. [160] has recently shown that by galvanic coupling of pyrite with active metals such as zinc, manganese and aluminum, it is possible to lower the potential of pyrite to values that are low enough to prevent pyrite oxidation and to reduce the hydrophobic oxidation products that are already present on the surface. The galvanic coupling can effectively depress pyrite without adversely affecting the flotation of coal. Fig. 5.60 shows the results of flotation tests conducted in a 2-inch Microcel flotation column with −150 μm Lower Kittanning coal using MIBC and kerosene. The

grade–recovery curve was obtained for a 200 g coal sample; additional points indicate the experiments in which the sample of coal was conditioned with 10 g Mn powder at 20% solid concentration. As this figure reveals, the use of manganese powder shifted the combustible recovery vs. pyritic sulfur rejection curve toward the upper-hand corner, indicating that separation efficiency was substantially increased. These data additionally support the idea that coal-pyrite's improved floatability may result from the presence of sulfur (or polysulfides) on its surface. In light of Mulak's results [161] on the leaching of coal-pyrite under reducing conditions, it would be worth trying the use of metallic chromium in the galvanic coupling method.

5.4. References

[1] M.A. Eigeles, Fundamentals of Flotation of Non-Sulfide Minerals. Metallurgizdat, 1950 (in Russian).

[2] V.I. Klassen, Coal Flotation. Gosgortiekhizdat, Moscow, 1963 (in Russian).

[3] J.S. Laskowski, Oil assisted fine particle processing. In: J.S. Laskowski and J. Ralston (eds), Colloid Chemistry in Mineral Processing. Elsevier, Amsterdam, 1992, pp. 361–394.

[4] P.J. King, F. Morton and A. Sagarra, Chemistry and physics of petroleum. In: G.D. Hobson and W. Pohl (eds), Modern Petroleum Technology. Wiley, New York, 1973, pp. 186–219.

[5] V.A., Glembotski, G.M. Dimitrieva and M.M. Sorokin, Nonpolar Flotation Agents. Israel Program for Scientific Translations, Jerusalem, 1970.

[6] D.R. Woods and E. Diamadopoulos. In: D.T. Wasan, M.E. Ginn and D.O. Shah (eds), Surfactants in Chemical Process Engineering. Marcel Dekker, New York, 1988, pp. 369–539.

[7] P.D. Cratin, A quantitative characterization of pH-dependent systems. In: R. Ross (ed.), Chemistry and Physics of Interfaces II. Am. Chem. Soc., Washington, D.C., 1971, pp. 35–48.

[8] J.S. Laskowski, Frothers and frothing. In: J.S. Laskowski and E.T. Woodburn (eds), Frothing in Flotation II. Gordon and Breach, New York, 1998, pp. 1–49.

[9] E. Steenberg and P. Harris, Adsorption of carboxymethyl cellulose, guar gum, and starch onto talc, sulfides, oxides and salt-type minerals. South Afr. J. Chem., 37 (1984) 85.

[10] G.O. Aspinal, Polysaccharides. Perganon Press, New York, 1970.

[11] M.L. Wolfram and H.E. Khadem, Chemical evidence for structure of starch. In: R.L. Whistler and E.F. Paschall (eds), Starch: Chemistry and Technology. Academic Press, New York, 1965, pp. 251–278.

[12] R.H. Whistler and J.R. Daniel, Starch. In: J.I. Kroschwittz and M. Howe-Grant (eds), Kirk-Othmer Encyclopedia of Chemical Technology, 4th ed. Wiley, New York, 1992, Vol. 22, pp. 699–719.

[13] M.W. Rutenberg, Starch and its modifications. In: R.L. Davidson (ed.), Handbook of Water-Soluble Gums and Resins. McGraw Hill, New York, 1980, Chapter 22.

[14] G.V. Caesar, Dextrins and dextrinization. In: J.A. Radley (ed.), Starch and Its Derivatives. Chapman and Hall, London, 1968, pp. 282–299.

[15] A.H. Young, Fractionation of starch. In: E.L. Whistler, J.N. BeMiller and E.F. Paschall (eds), Starch: Chemistry and Technology. Academic Press, 2nd ed., 1984, pp. 249–283.

[16] K.J. Miller and A.F. Baker, Flotation of pyrite from coal. Tech. Progr. Rep. U.S. Bureau of Mines, 51 (1972).

[17] K.J. Miller, Flotation of pyrite from coal: pilot plant study. US Bureau of Mines Rep. Invest., 7822 (1973).

[18] J.S. Laskowski, M. Bustin, K.S. Moon and L.L. Sirois, Desulfurizing flotation of Eastern Canadian high-sulfur coal. In: Y.A. Attia (ed.), Processing and Utilization of High-Sulfur Coals I. Elsevier, Amsterdam, 1985, pp. 247–266.

[19] Pradip and D.W. Fuerstaneu, The effect of polymer adsorption on the wettability of coal. In: A.A. Attia (ed.), Flocculation in Biotechnology and Separation Systems. Elsevier, Amsterdam, 1987, pp. 95–106.

[20] R.W. Perry and F.F. Aplan, Polysaccharides and xanthated polysaccharides as pyrite depressants during coal flotation. In: Y.A. Attia (ed.), Processing and Utilization of High-Sulfur Coals I. Elsevier, Amsterdam, 1985, pp. 215–238.

[21] R.J. Good, M.K. Badgujar, T.L.H. Huang and S.N. Handur-Kulkarni, Hydrophilic colloids and the elimination of inorganic sulfur from coal: A study employing contact angle. Coll. Surf., 93 (1994) 39.

[22] J. Leja, Surface Chemistry of Froth Flotation. Plenum Press, New York, 1982, pp. 328–333.

[23] G.J. Lawson and D. Stewart, Coal humic acids. In: M.H.B. Hayes, P. MacCarthy, R.L. Malcolm and R.S. Swift (eds), Humic Substances II. Wiley, New York, 1989, pp. 641–688.

[24] N. Berkowitz, An Introduction to Coal Technology. Academic Press, New York, 1979, pp. 95–100.

[25] D.E. Lowenhaupt and R.J. Gray, The alkali-extraction tests as a reliable method of detecting oxidized metallurgical coal. Int. J. Coal Geol., 1 (1980) 63.

[26] R.J. Gray and D.E. Lowenhaupt, Aging and weathering. In: R. Klein and R. Wellek (eds), Sample Selection, Aging, and Reactivity of Coal. Wiley, New York, 1989, pp. 255–336.

[27] S.E. Manahan, R.E. Poulson, J.B. Green and D.S. Farrier, U.S. Dept. Energy, LETC/RI-78/5 (Sept. 1978).

[28] Y.A. Attia and J.A. Kitchener, Development of complexing polymers for the selective flocculation of copper minerals. Proc. 11th Int. Mineral Processing Congress, Universita di Cagliari, Cagliari, 1975, pp. 1233–1248.

[29] Y.A. Attia and D.W. Fuerstenau, Feasibility of cleaning high sulfur coal fines by selective flocculation. Proc. 14th Int. Mineral Processing Congress, Toronto, 1982, vol. 7, paper VII-4.

[30] Y.A. Attia, F. Bavarian and K.H. Driscoll, Use of polyxanthate dispersant for ultrafine pyrite removal from high sulfur cal by selective flocculation. Coal Preparation, 6 (1988) 35.

[31] F.J. Sotillo, D.W. Fuerstenau and G.H. Harris, Surface chemistry and rheology of Pittsburgh No. 8 coal–water slurry in the presence of a new pyrite depressant. Coal Preparation, 18 (1997) 151.

[32] T. Chmielewski and T.D. Wheelock, Thioglycolic acid as a flotation depressant for pyrite. In: P.R. Dugan, D.R. Quigley and Y.A. Attia (eds), Processing and Utilization of High-Sulfur Coals IV. Elsevier, Amsterdam, 1991, pp. 295–308.

[33] J. Drzymala and T.D. Wheelock, Effect of oxidation and thioglycolic acid on separation of coal and pyrite by selective oil agglomeration. Coal Preparation, 14, (1994) 1.

[34] Y. Ye, Y. Liu, J.D. Miller and M.C. Fuerstenau, Preliminary analysis of pyrite rejection during chemically modified fine coal flotation by conditioning with monopersulfate. In: R. Markuszewski and T.D. Wheelock (eds), Processing and Utilization of High-Sulfur Coals III. Elsevier, Amsterdam, 1990, pp. 159–170.

[35] B.J. Arnold and F.F. Aplan, The use of pyrite depressants to reduce the sulfur content of Upper Freeport coal. In: R. Markuszewski and T.D. Wheelock (eds), Processing and Utilization of High-Sulfur Coals III. Elsevier, Amsterdam, 1990, pp. 171–186.

[36] C.E. Capes, A.E. McIlhinney, A.F. Siriani and I.E. Puddington, Bacterial oxidation in upgrading pyritic coals. CIM Bull., 66 (1973) 88.

[37] R.J. Buttler, A.G. Kempton, R.D. Coleman and C.E. Capes, The effect of particle size and pH on the removal of pyrite from coal by conditioning with bacteria followed by oil agglomeration. Hydrometallurgy, 15 (1986) 325.

[38] M. Elzeky, F. Bavarian and Y.A. Attia, Feasibility of selected flocculation/froth flotation process for simultaneous deashing and desulfurization of high-sulfur coals. In: R. Markuszewski and T.D. Wheelock (eds), Processing and Utilization of High-Sulfur Coals III. Elsevier, Amsterdam, 1990, pp. 209–220.

[39] V.I. Klassen and V.A. Mokrousov, An introduction to the Theory of Flotation. Butterworths, London, 1963.

[40] J.S. Laskowski and J. Mielecki, Salt flotation of coals with a simultaneous use of organic agents. Przeglad Gorniczy, 20 (1964) 113 (in Polish).

[41] J.S. Laskowski and F. Weber, Influence of inorganic salts on coal flotation rate using water-insoluble oily collectors. Przeglad Gorniczy, 21 (1965) 296 (in Polish).

[42] J. Iskra and J.S. Laskowski, New possibilities for investigating air-oxidation of coal surfaces at low temperatures. Fuel, 46 (1967) 5.

[43] N.P. Finkelstein, Oil flotations — discussion. In: P. Somasundaran and N. Arbiter (eds), Beneficiation of Mineral Fines. AIME, 1979, pp. 331–340.

[44] C.E. Capes, Liquid phase agglomeration: process opportunities for economic and environmental challenges. In: K.V.S. Sastry and M.C. Fuerstenau (eds), Challenges in Mineral Processing. SME, Littleton, CO, 1989, pp. 237–252.

[45] C.E. Capes and R.J. Germain, Selective oil agglomeration in fine coal beneficiation, In: Y.A. Liu (ed.), Physical Cleaning of Coal. Marcel Dekker, New York, 1979, pp. 293–351.

[46] C.E. Capes, Oil agglomeration process principles and commercial application for fine coal cleaning. In: J.W. Leonard (ed.), Coal Preparation, 4th ed., AIME, 1979, pp. 105–116.

[47] D.W. Fuerstenau, Interfacial processes in mineral/water systems. Pure Appl. Chem., 24 (1970) 135.

[48] D.W. Fuerstenau and S. Chander, Thermodynamics of flotation. In: P. Somasundaran (ed.), Advances in Mineral Processing. SME, Littleton, CO, 1986, pp. 121–136.

[49] A.B. Taubman and L.P. Yanova, Certain features in the action mechanism of nonpolar flotation reagents in coal flotation. Russian Coll. Chem. J., 24 (1960) 69.

[50] D.J. Brown, V.R. Gray and A.W. Jackson, The spreading of oil on wet coal. J. Appl. Chem., 8 (1958) 752.

[51] Y.B. He and J.S. Laskowski, Contact angle measurements on discs compressed from fine coal. Coal Preparation, 10 (1992) 19.

[52] A.R. Burkin and J.V. Bramley, Flotation with insoluble reagents I. J. Appl. Chem., 11 (1961) 300.

[53] A.R. Burkin and J.V. Bramley, Flotation with insoluble reagents II. J. Appl. Chem., 13 (1963) 417.

[54] W.W. Wen and S.C. Sun, An electrokinetic study on the oil flotation of oxidized coal. Separation Sci., 16 (1981) 1491.

[55] J.S. Laskowski and J.D. Miller, New reagents in coal flotation. In: M.J. Jones and R. Oblatt (eds), Reagents in the Mineral Industry. IMM, London, 1984, pp. 145–154.

[56] S.H. Castro, R.M. Vurdela and J.S. Laskowski, The surface association and precipitation of surfactant species in alkaline dodecylamine hydrochloride solutions. Coll. Surf., 21 (1986) 87.

[57] J.S. Laskowski, The colloid chemistry and flotation properties of primary aliphatic amines. In: K.V.S. Sastry and M.C. Fuerstenau (eds), Challenges in Mineral Processing. SME, Littleton, CO, 1989, pp. 15–34.

[58] A. Zettlemoyer, M.P. Aronson and J.A. Lavelle, Spreading at the teflon/oil/water/air interfaces. J. Coll. Interf. Sci., 34 (1970) 545.

[59] V.I. Klassen and S.I. Krokhin, Contribution to the mechanism of action of flotation reagents. In: A. Roberts (ed.), Proceedings of the 6th Int. Mineral Processing Congress. Pergamon Press, Oxford, 1965, pp. 397–406.

[60] V.I. Klassen, Theory of apolar reagents action in flotation. In: I.N. Plaksing (ed.), Physicochemical Bases of the Action of Nonpolar Collectors in Flotation of Ores and Coal. Izdat. Nauka, Moscow, 1965, pp. 3–11 (in Russian).

[61] V.I. Melik-Gaykazian, Investigation of the apolar reagent mechanism of action in flotation of inherently hydrophobic and rendered hydrophobic particles. Izdat. Nauka, Moscow, 1965, pp. 22–49 (in Russian).

[62] N.S. Vlasova, V.I. Klassen and I.N. Plaksin, Investigation into the Action of Reagents in Flotation of Coals. Izdat. Akad. Nauk SSSR, Moscow, 1962 (in Russian).

[63] V.N. Petukhov and L.A. Popova, Investigation of flotation properties of 1,3-dioxane and its derivatives. Processing of Non-Metallic Ores — Trans. Kirov Ural Polytechnic Institute, 1976, No. 2, pp. 30–34 (in Russian).

[64] V.N. Petukhov and V.I. Lugovaya, Investigation of flotation properties of 1,3-dioxane derivatives in flotation of graphite. Processing of Non-Metallic Ores — Trans. Kirov Ural Polytechnic Institute, 1976, No. 2, pp. 40–43 (in Russian).

[65] G.H. Harris, J. Diao and D.W. Fuerstenau, Coal flotation with nonionic surfactants. SME Annual Meeting, Reno, NV, 1993, Preprint 93-241.

[66] G.H. Harris, J. Diao and D.W. Fuerstenau, Coal flotation with nonionic surfactants. Coal Preparation, 16 (1995) 135.

[67] R.M. Horsley and H.G. Smith, Principles of coal flotation. Fuel, 30 (1951) 54.

[68] T. Onlin and F.F. Aplan, Surface properties of coal as influenced by collectors. In: S.H. Ciang (ed.),

Proceedings of the Annual Tech. Conf. Filtration and Separation. Am. Filtration Soc., Pittsburgh, PA, 1989, pp. 37–44.

[69] F.F. Aplan, Coal properties dictate coal flotation strategies. Trans. AIME, 294 (1993) 83.

[70] R.B. Booth and W.L. Freyberger, Froth and frothing agents. In: D.W. Fuerstenau (ed.), Froth Flotation. AIME, New York, 1962, pp. 258–276.

[71] M. Lason, L. Czuchajowski and M. Zyla, A note on the sorption of methanol and water vapours on vitrains. Fuel, 39 (1960) 266.

[72] A.M. Al-Taweel, B. Delory, J. Wozniczek, M. Stefanski, N. Anderson and H.A. Hamza, Influence of the surface characteristics of coal on its floatability. Coll. Surf., 18 (1986) 9.

[73] N.Z. Frangiskos, C.C. Harris and A. Jowett, The adsorption of frothing agents on coals. Proc. 3rd Int. Congress Surface Active Substances, Koln, 1960.

[74] G.F. Eveson, S.G. Ward, F. Worthington, Froth flotation of low rank coal. J. Inst. Fuel, 29 (1956) 540.

[75] D.W. Fuerstenau and Pradip, Adsorption of frothers at coal/water interfaces. Coll. Surf., 4 (1982) 229.

[76] J.D. Miller, C.L. Lin and S.S. Chang, MIBC adsorption at the coal/water interface. Coll. Interf., 7 (1983) 351.

[77] H. Gan, S.P. Nadi and P.L. Walker, Nature of the porosity in American coals. Fuel, 51 (1972) 272.

[78] N.S. Vlasova, Modification of coal surface in flotation. In: Composition and Washability of Mineral Resources. Izd. Nauka, Moscow, 1978, pp. 84–88 (in Russian).

[79] J.R. Aston, J.E. Lane and T.W. Healy, The solution and interfacial chemistry of nonionic surfactants used in coal flotation. In: J.S. Laskowski (ed.), Frothing in Flotation. Gordon and Breach, New York, 1989, pp. 229–254.

[80] J.S. Laskowski and J.A. Kitchener, The hydrophilic — hydrophobic transition on silica. J. Coll. Interf. Sci., 29 (1969) 670.

[81] J.A. Gutierrez-Rodriguez and F.F. Aplan, The effect of oxygen on the hydrophobicity and floatability of coal. Coll. Surf., 12 (1984) 27.

[82] E. Malysa, K. Malysa and J. Czarnecki, A method of comparison of the frothing and collecting properties of frothers. Coll. Surf., 23 (1987) 29.

[83] K. Malysa, K. Lunkenheimer, R. Miller and C. Hartenstein, Surface elasticity and frothability of *n*-octanol and *n*-octanoic acid solutions. Coll. Surf., 3 (1981) 329.

[84] K. Malysa, Wet foams, properties and mechanism of stability. Adv. Coll. Interf. Sci., 40 (1992) 37.

[85] C. Sweet, J. van Hoogstraten, M. Harris and J.S. Laskowski, The effect of frothers on bubble size and frothability of aqueous solutions. In: J.A. Finch, S.R. Rao and I. Holubec (eds), Processing of Complex Ores — Proceedings of the 2nd UBC-McGill Int. Symp., IM Metal. Society, Montreal, 1997, pp. 235–246.

[86] T.A. Wheeler, Coal floats by itself — doesn't it? In: P.S. Mulukutla (ed.), Reagents for Better Metallurgy. SME, Littleton, CO, 1994, pp. 131–142.

[87] E. Hindmarch and P.L. Waters, Froth-flotation of coal. Trans. IMM, 111 (1952) 221.

[88] V.I. Klassen and V.A. Nevska, Flotation of coal with high content of clays. Coke Chem., 3 (1958) 15–18 (in Russian).

[89] V.I. Klassen and V.A. Nevska, Effect of frothing-collecting reagents on the flotation of coal with high slime content. Izv. Akad. Nauk SSSR, OTN — Metallurgy and Fuels, No. 6 (1960), pp. 168–172 (in Russian).

[90] V.I. Melik-Gaykazian, I.N. Plaksin and V.V. Voronchikhina, On the mechanism governing the interaction of apolar collectors with certain surfactants during froth flotation. Dokl. Akad. Nauk SSSR, 173 (1967) 883.

[91] N.S. Vlasova, Effect of oxygen functional groups on coal floatability. In: New Investigations in the Field of Beneficiation of Fine Coals and Ores. Izd. Nauka, Moscow, 1965, pp. 17–23 (in Russian).

[92] M. Agus, P. Carbini, R. Ciccu, M. Ghiani, F. Satta and C. Tilocca, The influence of coal properties on surface-based separation processes. In: W. Blaschke (ed.), New Trends in Coal Preparation Technologies and Equipment — Proceedings of the 12th Int. Coal Preparation Congress, Gordon and Breach, New York, 1996, pp. 571–578.

[93] M. Chander, H. Polat and B. Mohal, Flotation and wettability of a low-rank coal in the presence of surfactants. Miner. Metal. Process., 11 (1994) 55.

[94] A.R. Burkin and S.B. Soane, Flotation using insoluble liquids, adsorption and spreading processes. Proc. 3rd Congr. Surface Activity, Cologne, 1960, Vol. 4, p. 430.

[95] W.W. Wen and S.C. Sun, An electrokinetic study on the amine flotation of oxidized coal. Trans. AIME, 262 (1977) 174.

[96] J. Rubio and J.A. Kitchener, The mechanism of adsorption of polyethylene oxide flocculant on silica. J. Coll. Interf. Sci., 57 (1976) 132.

[97] R.J. Gochin, M. Lekili and H.L. Shergold, The mechanism of flocculation of coal particles by polyethyleneoxide. Coal Preparation, 2 (1985) 19.

[98] J. Sablik, The grade of metamorphism of Polish coals and their natural and activated floatability. Int. J. Miner. Process., 9 (1982) 245.

[99] K.H. Nimerick, S.K. Bowden and J.M. Carder, Froth conditioning — a proven approach to increase fine coal recovery. In: Coal Conference and Expo VI (Louisville, Kentucky, 1981), McGraw-Hill, New York, 1981, pp. 111–127.

[100] US Patent 4,211,642

[101] A. Watanabe, Electrochemistry of oil/water interface. In: E. Matijevic (ed.), Surface and Colloid Science. Plenum Press, New York, 1984, Vol. 13, p. 32.

[102] J.S. Laskowski, Coal flotation promoters and their mechanism of action. 191st Am. Chem. Soc. Meeting, New York, April 1986.

[103] J.S. Laskowski, Flotation of difficult-to-float coals. Proc. 10th Int. Coal Preparation Congress, CIM, Edmonton, 1986, Vol. 1, pp. 122–142.

[104] M.J. Scanlon, P.V. Avotins, S.S. Wang and P. Strydon, Flotation promoters improve fine coal recovery. World Coal (Feb. 1983) 54.

[105] R.O. Keys, Improvement in coal recovery through coarse coal flotation. 1st Annual Coal Prep. Conf., Lexington, March, 1984.

[106] A. Frumkin, On the phenomena of wetting and the adhesion of bubbles I. Zh. Fiz. Khim., 12 (1938) 337; A. Frumkin and A. Gorodetzkaya, Part II, Acta Physicochim. URSS, 9 (1938) 327.

[107] E.J.W. Verwey and J.Th.G. Overbeek, Theory of the Stability of Lyophobic Colloids. Elsevier, Amsterdam, 1948.

[108] B.V. Derjaguin, Theory of Stability of Colloids and Thin Films. Consultants Bureau, New York, 1989.

[109] R.M. Pashley, Interparticulate forces. In: J.S. Laskowski and J. Ralston (eds), Colloid Chemistry in Mineral Processing. Elsevier, Amsterdam, 1992, pp. 97–114.

[110] J. Isrealachvili and R. Pashley, The hydrophobic interaction is long range decaying exponentially with distance. Nature, 300 (1982) 341.

[111] N.V. Churaev, The relation between colloid stability and wetting. J. Coll. Interf. Sci., 172 (1995) 479.

[112] Z. Xu and R.H. Yoon, The role of hydrophobic interactions in coagulation. J. Coll. Interf. Sci., 132 (1989) 532.

[113] Z. Xu and R.H. Yoon, A study of hydrophobic coagulation. J. Coll. Interf. Sci., 134 (1990) 427.

[114] R.H. Yoon, D.H. Flinn and Y.I. Rabinovich, Hydrophobic interactions between dissimilar surfaces. J. Coll. Interf. Sci., 185 (1997) 363.

[115] J.S. Laskowski and J. Iskra, Role of capillary effects in bubble–particle collision in flotation. Trans. IMM, Sec. C, 79 (1970) 6.

[116] J.S. Laskowski, The relationship between floatability and hydrophobicity. In: P. Somasundaran (ed.), Advances in Mineral Processing. SME, Littleton, CO, 1986, pp. 189–208.

[117] F.M. Fowkes, Attractive forces at solid liquid interfaces. In: Wetting — Soc. Chem. Industry Monograph No. 25, Soc. Chem. Ind., London, 1967, pp. 3–30.

[118] J.S. Laskowski, Z. Xu and R.H. Yoon, Energy barrier in particle-to-bubble attachment and its effect on flotation kinetics. Mines et carrieres – Les Techniques, 74 (1992, No. 5) 95.

[119] D.W. Fuerstenau, J.M. Rosenbaum and J.S. Laskowski, Effect of surface functional groups on the flotation of coal. Coll. Surf., 8 (1983) 153.

[120] S. Kelebek, T. Salman and G.H. Smith, Interfacial phenomena in coal flotation systems. In: A.M. Al-Taweel (ed.), Coal: Phoenix of the 80s. Can. Soc. Chem. Eng., Halifax, NS, 1981, pp. 145–151.

[121] J.S. Laskowski and Z. Lupa, Coal surface properties in the light of flotation experiments. Archiwum Gornictwa, 11 (1966) 397 (in Polish).

[122] J.S. Laskowski, Flotation of Inherently Hydrophobic Minerals in Concentrated Solutions of Inorganic Salts. Trans. Silesian University of Technology, Mining, No. 16, Gliwice, 1966 (in Polish).

[123] S.C. Sun and R.E. Zimmerman, The mechanism of coarse coal and mineral froth flotations. Trans. AIME, 187 (1950) 616.

[124] G.A. Pikkat-Ordynsky and V.A. Ostry, Coal Flotation Technology. Izd. Nauka, Moscow 1972 (in Russian).

[125] B.M. Moudgil, Effect of polyacrylamide and polyethylene oxide polymers on coal flotation. Coll. Surf., 8 (1983) 225.

[126] P.K. Weissenborn, Selective Flocculation of Ultrafine Iron Ore. Ph.D. Thesis, Curtin University of Technology, Perth, 1993.

[127] J.A. Kitchener, Flocculation in mineral processing. In: K.J. Ives (ed.), The Scientific Basis of Flocculation. Sijthoff and Noordhoff, Alphen a/d Rijn, 1978, pp. 283–328.

[128] J.M. Wie and D.W. Fuerstenau, The effect of dextrin on surface properties and flotation of molybdenite. Int. J. Miner. Process., 1 (1974) 17.

[129] H.H. Huang, J.V. Calara and J.D. Miller, Adsorption reactions in the depression of coal by organic colloids. In: N. Li (ed.) Recent Developments in Separation Science. CRC Press, Baton Rouge, LA, 1978, Vol. 4, pp. 115–133.

[130] J.D. Miller, C.L. Lin and S.S. Chang, Coadsorption phenomena in the separation of pyrite from coal by reverse flotation. Coal Preparation, 1 (1984) 21.

[131] C.J. Im and F.F. Aplan, Depression of coal by starches and starch derivatives. In: A.R. Swanson (ed.), Proceedings of the 1st Australian Coal Preparation Conference. Coal Preparation Societies of N.S.W. and Queensland, Newcastle, 1981, pp. 183–203.

[132] J.A. Solari, A.C. de Araujo and J.S. Laskowski, The effect of carboxymethyl cellulose on the flotation and surface properties of graphite. Coal Preparation, 3 (1986) 15.

[133] Qi Liu and J.S. Laskowski, The role of metal hydroxides at mineral surfaces in dextrin adsorption, Part I. Int. J. Miner. Process., 26 (1989) 297.

[134] J.S. Laskowski, Q. Liu and N.J. Bolin, Polysaccharides in flotation of sulfides, Part I. Int. J. Miner. Process., 33 (1991) 223.

[135] J.S. Laskowski, S. Subramanian and G.A. Nyamekye, Polysaccharides — emerging non-toxic modifiers for differential flotation of sulfides. Proc. 18th Int. Mineral Processing Congress, Sydney, 1993, pp. 593–600.

[136] K. Wong and J.S. Laskowski, Effect of humic acid on the properties of graphite aqueous suspensions. Coll. Surf., 12 (1984) 317.

[137] B. Yarar and J. Leja, Flotation of weathered coal fines from USA and Western Canada. Proc. 9th Int. Coal Preparation Congress, New Delhi, 1982, Paper C5.

[138] Qi Liu and J.S. Laskowski, Effect of humic acids on coal flotation, Part II. The role of pH. SME Annual Meeting, Phoenix, AZ, 1988, Preprint 88-31.

[139] M. Pawlik, J.S. Laskowski and H. Liu, Effect of humic acids and coal surface properties on rheology of coal–water slurries. Coal Preparation, 18 (1997) 129.

[140] J.S. Laskowski and Z. Yu, The effect of humic acids on the emulsion flotation of inherently hydrophobic minerals. In: S. Castro and J. Alvarez (eds), Proceedings of the 4th Meeting of the Southern Hemisphere on Mineral Technology. University of Concepcion, 1994, Vol. 2, pp. 397–412.

[141] J.S. Laskowski, L.L. Sirois and K.S. Moon, Effect of humic acids on coal flotation, Part I. Coal flotation selectivity in the presence of humic acids. Coal Preparation, 3 (1986) 133.

[142] R.W. Lai and W.W. Wen, Effect of humic substances on the flotation response of coal. Coal Preparation, 7 (1989) 69.

[143] D. Liu, P. Somasundaran, T.V. Vasundewan and C.C. Harris, Role of pH and dissolved mineral species in Pittsburgh No. 8 coal flotation system. Int. J. Miner. Process., 41 (1994) 201.

[144] W.J. Trahar, The influence of pulp potential in sulfide flotation. In: M.H. Jones and J.T. Woodcock (eds), Principles of Mineral Flotation — The Wark Symposium Australas. IMM, 1984, pp. 117–136.

[145] N.P. Finkelstein, S.A. Allison, V.M. Lovell and B.V. Stewart, Natural and induced hydrophobicity in sulfide mineral systems. In: P. Somasundaran and R.B. Greves (eds), Advances in Interfacial Phenomena of Particulate/Solution/Gas Systems; Applications to Flotation Research. Am. Inst. Chem. Eng., 150, Vol. 71 (1975) 165–175.

[146] O. Ozcan, Classification of minerals according to their critical surface tension of wetting values. Int. J. Miner. Process., 34 (1992) 191.

[147] R.T. Greer, Coal microstructure and pyrite distribution. In: T.D. Wheelock (ed.), Coal Desulfurization — Chemical and Physical Methods. ACS Symp. Series 64, Am. Chem. Soc., Washington, D.C., 1977, pp. 1–15.

[148] W.F. Caley, S.G. Whiteway and I. Stewart, Variation of the reactivity of FeS_2 in Eastern Canadian coal as a function of morphology. Coal Preparation, 7 (1989) 37.

[149] J. Lekki and T. Chmielewski, The role of surface morphology in flotation of coal and mineral pyrite. In: R. Markuszewski and T.D. Wheelock (eds), Processing and Utilization of High-Sulfur Coals III. Elsevier, Amsterdam, 1990, pp. 145–158.

[150] D.P. Tao, P.E. Richardson, G.H. Luttrell and R.H. Yoon, An electrochemical investigation of surface reactions of coal- and mineral-pyrite in aqueous solutions. In: B.K. Parekh and J.G. Groppo (eds), Processing and Utilization of High-Sulfur Coals V. Elsevier, Amsterdam, 1993, pp. 219–236.

[151] R.H. Yoon, M.L. Lagno, G.H. Luttrell and J.A. Mielczarski, On the hydrophobicity of coal pyrite. In: P.R. Dugan, D.R. Quigley and Y.A. Attia (eds), Processing and Utilization of High-Sulfur Coals IV. Elsevier, Amsterdam, 1991, pp. 241–154.

[152] G.W. Heyes and W.J. Trahar, The flotation of pyrite and pyrrhotite in the absence of conventional collectors. In: P.E. Richardson, S. Srinivasan and R. Woods (eds), Electrochemistry in Mineral and Metal Processing. Electrochem. Soc., Pennigton, NJ, 1984, pp. 219–232.

[153] P.C. Singer and W. Stumm, Acidic mine drainage: the rate-determining step. Science, 167 (1970) 1121.

[154] C. Jiang, X.H. Wang, J.W. Leonard and B.K. Parekh, On the native and induced floatability of coal and pyrite. In: B.K. Parekh and J.G. Groppo (eds), Processing and Utilization of High-Sulfur Coals V. Elsevier, Amsterdam, 1993, pp. 171–188.

[155] S.K. Kawatra, T.C. Einsele and H. Johnson, Recovery of liberated pyrite in coal flotation: entrainment or hydrophobicity. In: P.R. Dugan, D.R. Quigley and Y.A. Attia (eds), Processing and Utilization of High-Sulfur Coals IV. Elsevier, Amsterdam, 1991, pp. 255–278.

[156] J. Drzymala, R. Markuszewski and T.D. Wheelock, Oil agglomeration of sulfurized pyrite. Miner. Eng., 4 (1991) 161.

[157] R.W. Lai, J.R. Diehl, R.W. Hammack and S.U.M. Khan, Comparative study of the surface properties and the reactivity of coal pyrite and mineral pyrite. Miner. Metal Process., 7 (1990) 43.

[158] J.D. Miller, Y. Ye and R. Jin, Improved pyrite rejection by chemically-modified fine coal flotation. Coal Preparation, 6 (1989) 151.

[159] Y. Ye, Y. Liu, J.D. Miller and M.C. Fuerstenau, Preliminary analysis of pyrite rejection during chemically modified fine coal flotation by conditioning with monopersulfate. In: R. Markuszewski and T.D. Wheelock (eds), Processing and Utilization of High-Sulfur Coals III. Elsevier, Amsterdam, 1990, pp. 159–170.

[160] R.H. Yoon, D.P. Tao, M.X. Lu, P.E. Richardson and G.H. Luttrell, Improving pyrite rejection by galvanic control. Coal Preparation, 18 (1997) 53.

[161] W. Mulak, Leaching of coal pyrite in acidic solutions under reductive conditions. In: W. Blaschke (ed.), New Trends in Coal Preparation Technologies and Equipment — Proc. 12th Int. Coal Preparation Congress. Gordon and Breach, New York, 1996, pp. 263–268.

This Page Intentionally Left Blank

Chapter 6

FLOTATION TECHNOLOGY

6.1. Introduction

As stated in the introduction to Chapter 5, coal flotation depends on coal's natural properties (wettability), the floatability acquired from the use of reagents, and particle size effects. Although the flotation of coal is less complicated than the flotation of ores (especially polymetallic sulfide ores), the list of parameters that affect it is still considerable. It is convenient to categorize these parameters into four groups: characteristics of coal, characteristics of pulp, application of reagents, flotation circuits and machines (these are discussed in Chapters 7 and 8)

6.2. Characteristics of coal

As Fig. 3.3 demonstrates, coal surface properties strongly depend on coal rank. Similarly, coal floatability depends on coal rank (Figs. 3.21, 3.22 and 3.23). While very hydrophobic bituminous coals float well using only a simple frother such as MIBC, different frothers, different combinations with collectors, and even the use of promoters may be required to float lower-rank coals. Coal oxidation also affects flotation and this effect is not that different from the effect of coal rank.

Freshly mined coals float better than coals that have been stored for a long time (e.g. in old tailing ponds) and this effect is generally attributed to oxidation. Because of the possible oxidation of the coal surface, testing of coal flotation also poses some problems. This subject has been studied by many researchers and several examples from these tests will be used here to discuss the problem.

In Fig. 6.1 [1], both the advancing and receding contact angles measured at an oil droplet in water (through water) are plotted versus the carbon/oxygen ratio. The data, as set forth in Fig. 6.1, clearly show that coal oxidation increases its hydrophilicity.

Fig. 6.2 [2] illustrates the effect of time of weathering on the flotation properties of three different coals (Illinois No. 6, Pittsburgh No. 8 and Upper Freeport). Two size fractions, −6.4 mm +0.6 mm, and −0.6 mm were either kept in inert conditions of argon or in oxidizing conditions of an exposed stockpile. The coarse coal fractions were dry ground before flotation below −0.6 mm, and both fractions were floated in a 2-1 Denver cell using dodecane as a collector, and MIBC frother. The Illinois No. 6 sample required 2.4 kg/t dodecane and 0.59 kg/t MIBC, Pittsburgh No. 8 was floated using 0.95 kg/t of dodecane and 0.2 kg/t MIBC, and the Upper Freeport required only 0.12 kg/t of dodecane and 0.13 kg/t MIBC.
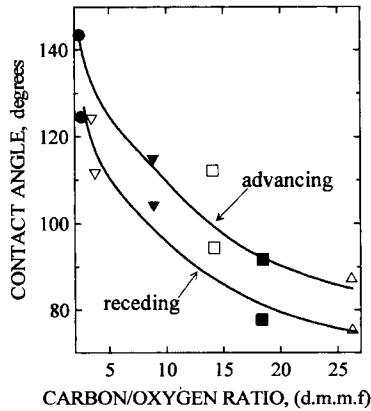
Fig. 6.1. Effect of carbon/oxygen ratio on wettability of coal discs compressed from fine coal. (After Crawford et al. [1]; by permission of Elsevier Science.) Please note that the reported contact angles were measured through the oil phase, hence: $\Theta_{water} = 180 - \Theta_{oil}$ (see Fig. 5.7).

As Fig. 6.2 demonstrates, the coarse coal ground just before the flotation experiment floated much better than the fine fraction. In the former case, a new surface was exposed during grinding and so the effect of oxidation was minimized. In the case of the fine coal kept under argon, the flotation response also slightly decayed with increasing weathering time indicating that the inerting process (purging the drum containing coal with argon) was not completely effective in preventing oxidation. The flotation properties of the fine coal exposed to the atmosphere deteriorated quite visibly after a few months of weathering. These results confirm without any doubt that oxidation affects coal flotation. They also indicate that in the case of the flotation tests taking place over a long period of time it is safe to use coarse coal which can then be crushed and ground immediately before the tests.

Since collection of samples from various seams and mines is not simple, and since such samples always vary in the content of ash, in order to test the effect of oxidation on flotation it is more convenient to oxidize coal samples in a lab and then study the effect of oxidation on wettability and flotation. The most obvious question which must be answered before carrying out such tests is how does one oxidize the coal selected for the tests. The most common method is to use dry oxidation in air at an elevated temperature, but wet oxidation with the use of various chemicals is also applied.

It is not clear whether coal oxidation under dry or under wet conditions in lab tests simulates coal which is oxidized under natural conditions. As pointed out by Somasundaran et al. [3], in most studies of gaseous oxidation the effect of heating was not isolated from the effect of oxidation. This is shown in Fig. 6.3. In these tests a -250 μm $+150$ μm high-volatile bituminous coal, which was oxidized dry either in a stream of nitrogen, in air or in an N_2–O_2 mixture, was floated using only MIBC. While heating in nitrogen improved flotation response, heating in air caused depression only at the higher temperature, and heating in the O_2–N_2 mixture always produced depression. The authors claim that the improved flotation after prolonged heating in nitrogen was probably due to the removal of surface moisture.
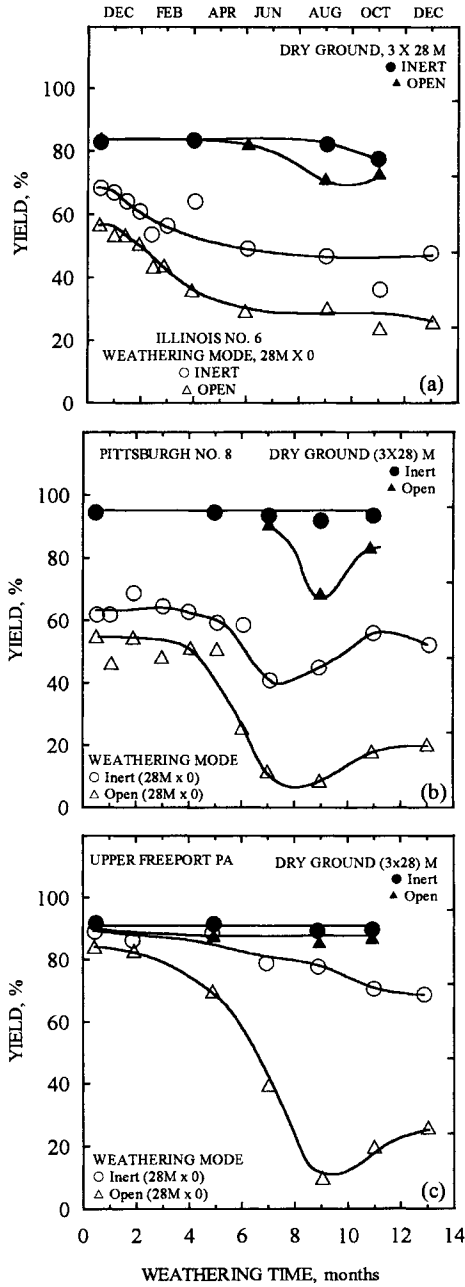
Fig. 6.2. Effect of weathering time and regrinding on the flotation yield of coals stored under inert and open modes: (a) Illinois No. 6, (b) Pittsburgh No. 8 and (c) Upper Freeport. (After Fuerstenau et al. [2]; by permission of Gordon and Breach.)
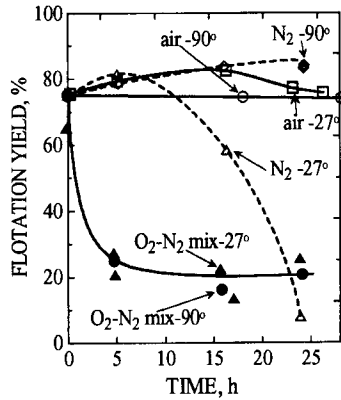
Fig. 6.3. Effect of time of oxidation under different conditions on flotation of a -250 μm $+150$ μm size fraction of a high volatile bituminous coal using only MIBC. (After Somasundaran et al. [3]; by permission of Elsevier Science.)
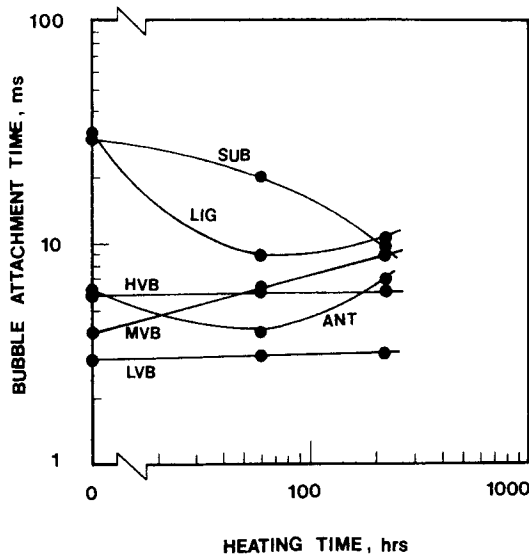
Fig. 6.4. Measured induction time for samples of six coals as a function of heating time (particle size -150 μm $+75$ μm). (After Ye et al. [4]; by permission of Gordon and Breach.)

Such effects were also examined by Ye et al. [4] who heated -150 μm $+75$ μm samples of coals varying in rank in air at 130°C. The wettability of the coal particles was characterized by induction time measurements (Fig. 6.4). While low-rank coals became more hydrophobic (induction time decreased) with time of treatment, higher-rank coals either did not respond to heating at 130°C or showed a slight increase in hydrophilicity. This reveals that the response to heating is also rank-dependent. Lignite subjected to heating floated much better. FTIR spectroscopy revealed the disappearance of phenolic groups from the lignite surface after heating at 130°C. As a result, the hydrophilicity

index based on FTIR spectroscopy dropped after such a treatment. As will be discussed in the last chapter of this book, such a high-temperature treatment is used in several processes to up-grade low-rank coals in the coal–water technology.

The oxidation of two samples of coal from the Adolfa coal seam in the Asturian Central Basin in Spain (from the underground Mosquitera mine, AUM sample), and from the open-pit Brana del Rio mine (ASM sample) was studied by Garcia et al. [5].

With the use of FTIR spectroscopy they detected some oxygen functional groups in the ASM sample, but not in the AUM sample. But while the AUM sample contained only pyrite and siderite, the ASM sample also contained basic iron hydro-oxides (goethite and lepidocrocite). After being oxidized in the laboratory, the coal was initially characterized by a high content of jarosite (basic iron sulfate), which with time was converted to hydro-oxides. The authors claim that the generation of sulfuric acid should lead to some alteration of clay minerals and may supply alkali cations. This is in line with Firth and Nicol [6], who found that oxidation of coal containing pyrite quickly affects its flotation, an effect which cannot be attributed to coal oxidation. They showed that coal flotation is influenced by the pyrite oxidation products and that this effect is particularly pronounced in the presence of clays. Firth and Nicol claim that at quantities of oxidized pyrites as small as 0.05%, the generated sulfuric acid reduces pH enough to release humic acids which in the acidic pH range react with clays and form hydrophobic entities. This explanation is based on a previous publication by Firth and Nicol [7] in which they took into account the organic oxidation products of coal and postulated the formation of clay–humic acid oleophobic complexes which cause the clay to become hydrophobic and to some extent floatable, especially in acidic pH ranges.This may have considerable practical significance for certain plants operating in acid pH ranges caused, for example, by pyrite oxidation.

Because it is not certain whether heating of coal produces surfaces oxidized to the same degree as coal particles oxidized under natural conditions, it is always better to use naturally oxidized coal samples, or samples of lower-rank coals; characterization of the surface oxidation either by titration of carboxylic and phenolic groups (total acidity) or with the use of FTIR spectroscopy should be used to quantify the degree of oxidation if oxidation under lab conditions is preferred.

Examples of such tests in which a few coal samples were oxidized in air at temperatures from 150°C to 244°C for 8 h are provided below [8]. Coal oxidation was characterized using the well established titration procedure (see papers [23], [24] and [42], [43] in Chapter 3), and coal surface wettability was characterized by determination of the critical wetting surface tension in methanol aqueous solutions, and by vacuum flotation tests in 0.5 M sodium chloride solutions. Fig. 6.5 shows the relationship between carboxylic group content and flotation, and between critical wetting surface tension and flotation. It was shown earlier that ionizable oxygen functional groups (e.g. phenolic and carboxylic groups) control coal wettability through the balance of hydrophobic/hydrophilic sites, and control flotation kinetics by their influence on surface charge [9]. For coal varying in oxidation degree there is a clear relationship between the oxygen functional groups' content and the critical wetting surface tension of coal.

The highest-rank coals are relatively unreactive. These coals have very little reactive hydrogen, are highly aromatic, and probably contain few reactive functional groups.
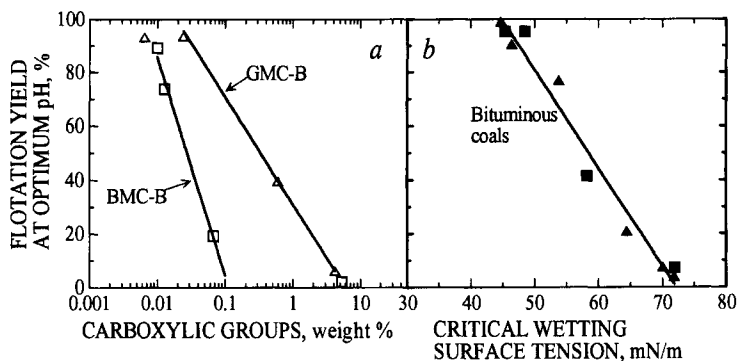
Fig. 6.5. Flotation response of two bituminous coals as a function of the content of the carboxylic groups (a), and the critical wetting surface tension (b). (After Fuerstenau et al. [8]; by permission of Gordon and Breach.)

One of the techniques used to study the structure of coal is oxidative degradation. While some oxidants preferentially oxidize the aliphatic portion of coal, there are also methods which were developed to oxidize the aromatic rings. Since the chemical composition of coal macerals differs, it is easy to imagine that various coal macerals respond differently when coal is subjected to oxidation. Miller and Ye [10] reported that resinite macerals, which are known to be much less aromatic than other macerals, can be selectively floated if coal is subjected to oxidation by preconditioning with ozone. Especially when coal is freshly wet ground and then conditioned with ozone, coal particles become strongly hydrophilic, while resin particles retain their hydrophobicity to a certain extent. Because extensive oxidation with ozone eventually depresses the resin, this indicates that the kinetics of oxidation is different for different coal petrographic constituents.

Coal flotation depends on coal petrographic composition and particle size as shown in Fig. 3.24 and Table 3.1. In one of our research projects [11] we concluded that the floatability of coal particles with a very low ash content visibly depends on coal petrographic composition. At ash contents exceeding 15%, the surface properties of tested coal particles were predominantly determined by mineral matter. Bennett et al. [12] found that the grains which consisted entirely of vitrinite, clarite, vitrinertinite or trimacerite had similar floatabilities provided that they had no visible mineral matter. Inertinite grains were slower floating than the grains of other maceral groups. In all cases the content of mineral matter clearly affected flotation behavior. This effect was found to be smaller for higher-rank (more hydrophobic) coals and is claimed to depend primarily on particle density which for coal increases with the mineral matter content.

Coal flotation depends not only on the mineral matter content but also on the mineralogical composition of the mineral matter associated with the coal. Because the mineralogy of gangue strongly affects particle size distributions it will be discussed in the following section dealing with the composition and properties of flotation pulp.

6.3. Characteristics of pulp

The flotation pulp properties are determined by solids content, particle size distributions, slimes content, water ionic strength and composition. Since water is recycled in modern plants (Fig. 1.5), and since many of these variables depend to a large extent on the composition of the gangue (mineral matter associated with coal), these indices may be pretty high (e.g. ionic strength, slimes content, etc.).

It is a common observation that while coarse coal particles in a flotation feed float selectively but at low recoveries, the finer particles float very well with high recoveries but poor selectivity. All flotation processes are sensitive to colloidal phenomena caused by very fine mineral particles referred to as slimes, and in some cases desliming prior to flotation is absolutely necessary (e.g. flotation of potash ores, flotation of phosphates, etc.). The term slimes is commonly applied to very fine mineral particles and there is no sharp size cut-off. In some publications particles finer than 10 μm are referred to as slimes, while some prefer to define slimes as particles finer than 30 μm. The latter number is based on flotation experiments which reveal that such fine particles remain suspended in the inter-bubble water and are recovered by entrainment [13,14]. Bustamante and Warren's results shown in Fig. 6.6 [15] illustrate it very well.

As Fig. 6.6 shows, the recoveries of the size fractions of high-volatile bituminous A coal correlate linearly with the weight of water collected with the froth product. The straight lines have the form $R = F + eW_{water}$, where R is the overall recovery of a given size fraction after 2 min flotation, F is the intercept of the extrapolated line on the mineral recovery axis, e (the slope in Fig. 6.6) is the entrainment factor, and W_{water} is the weight of water recovered in the concentrate in 2 min. If the intercept F is assumed to represent the recovery due to true flotation, and eW_{water} the recovery due to entrainment, then the contributions due to these two mechanisms can be separated [15]. It is clear from Fig. 6.6 that the entrainment factor (slope) increases with decreasing size, although most of the -74 μm fraction is still recovered by true flotation ($F = 50\%$). For
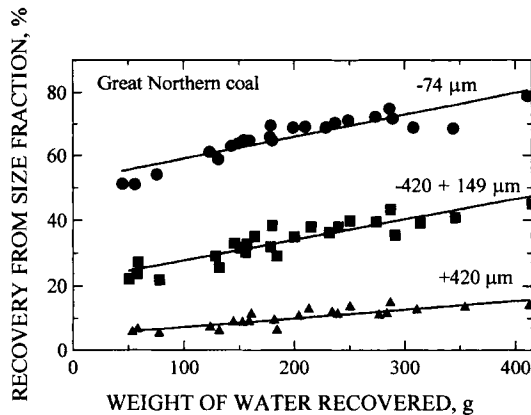
Fig. 6.6. Relation between the coal recovery and the weight of water recovered in the concentrate. (After Bustamante and Warren [15].)
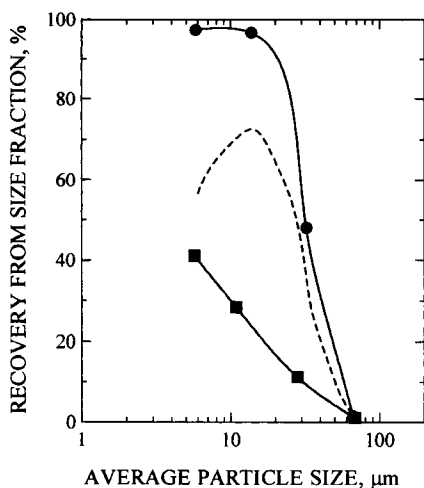
Fig. 6.7. Recovery of siderite as a function of particle size. Recovery without collector (•), recovery with collector (■), the difference curve (dotted line) estimates recovery due to "true flotation". (After Smith and Warren [16]; by permission of Gordon and Breach.)

coarser fractions the recovery resulting from true flotation are much lower (after 2 min flotation), but at the same time they are not affected by the amount of recovered water. They float "cleanly". The evidence presented in the discussed publications indicates that particles finer than 30 μm mainly report to the flotation froth products with inter-bubble water. This, of course, applies to flotation cells working with negative bias (see Chapter 8).

The effect of particle size on flotation is even better seen in Fig. 6.7 [14,16]. As this figure shows, particles below a certain critical size (grains below 30 μm equivalent quartz size [14]) report to the froth product mainly by entrainment; the amount entrained is proportional to the concentration of such particles in the feed [12]. For such fine particles, Kitchener coined the term "colloidal minerals" [17]. He distinguishes three classes of colloidal minerals: (A) naturally occurring clay minerals, such as kaolinite, illite, montmorillonite, which are intrinsically composed of very small particles (mainly 2 μm downwards); (B) the fines inevitably produced during the crushing and grinding in mineral beneficiation operations; and (C) the residues of leaching of crushed ores in metallurgical processes.

It is obvious that only the first class of colloidal minerals may play an important role in coal flotation circuits, and slimes resulting from a high content of clays in coal may strongly affect the flotation. First, since such high-ash particles report to the froth by entrainment, the ash content of the froth product will be high, but second, such slime particles are also known to affect the flotation of coarse coal particles. The effect is due to "slime coating" which will be illustrated by Jowett et al.'s results [18].

Fig. 6.8 depicts the wettability of a coal specimen. In the absence of any clays, coal is hydrophobic. The same coal in the presence of clay becomes hydrophilic due to the coating of the coal surface by hydrophilic clay particles (slime coating). However,
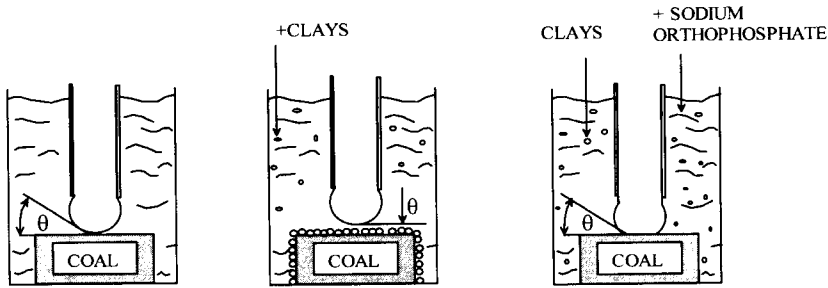
Fig. 6.8. Effect of clays and dispersants (phosphates) on wettability of coal surface in aqueous solution. (After Jowett et al. [18]; by permission of Elsevier Science.)
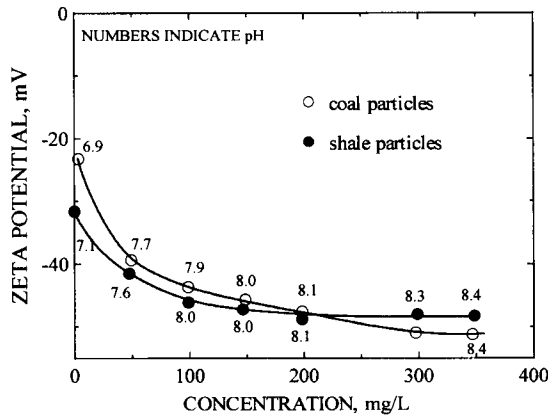
Fig. 6.9. Effect of sodium hydrogen phosphate on the zeta potential of coal and clay particles. (After Jowett et al. [18]; by permission of Elsevier Science.)

coal hydrophobicity can be restored by simply adding a dispersant. In electrokinetic measurements, both coal and clay particles were found to acquire more negative zeta potential values in 50–100 mg/l sodium hydrogen phosphate solution used as a dispersant (Fig. 6.9). Apparently, the acquired more negative values of electrokinetic potential are high enough to prevent clay particles from coagulating onto the coal surface. Therefore, the effect of clays on flotation can be eliminated by using dispersing agents, by desliming the feed, and by splitting the feed into coarse and fine fractions and floating them separately under proper physico-chemical conditions. Equipment choice may also help to reduce the deleterious effect of slimes. Flotation cells working with positive bias (flotation columns with wash water) definitely provide lower ash contents when floating high-clay coals.

The extraordinary reactivity of clays, and the ability of clayish slimes to affect flotation of other minerals, result from the crystallochemistry of alumino-silicates. The zeta potential of alumino-silicates, such as kaolinite, is a weighted mean of the various exposed faces. As a result of isomorphous replacement of the structural cations (i.e. of Al^{3+} for Si^{4+}), the faces of the thin kaolinite platelets are negatively charged. The

exposed edges of the broken platelets contain AlOH groups which have a pzc situated around pH 9.1. Thus, in the case of clays, the negatively charged basal surfaces may coexist with the edges which — depending on pH — are either positively (at pH < 9.1) or negatively (at pH > 9.1) charged. Obviously, such a composition makes it possible for clays to interact with many minerals and under very different conditions.

The effects of slimes on flotation have been studied by different groups of researchers. Firth and Nicol [7] claim that clays can depress coal flotation only in acidic pH ranges in the presence of humic acids. Arnold and Aplan [19] studied the effect of different clay minerals and concluded that whereas some of them may be very harmful (e.g. montmorillonite), the effect of some others (e.g. illite, kaolinite) is not so pronounced. According to them, coal flotation is better in tap water than in distilled water, and they also reported that the ions present in the pulp may neutralize the charge on the clay particles and so inhibit the formation of slime coatings. They found that increased additions of fuel oil collector reduce the depressing effect of clays, and that humic acids depress coal flotation irrespective of the presence of clays.

Fig. 6.7 implies that slime particles undergo mechanical entrainment; the true flotation is negligible for very fine particles. Fig. 6.7 also exhibits a maximum for particles in the 50–100 μm range (that also depends on solid density) and drops for coarse particles.

Bustamante and Warren [15] pointed out that the degree of hydrophobicity required to promote a high level of floatability increased with increasing particle size. The addition of collector (kerosene) had a similar effect to increasing rank, in that the more hydrophobic surfaces resulting from the abstraction of kerosene allowed larger particles to be floated, which extend the plateau in the recovery–size curves. The flotation curves plotted versus the particle density showed a very strong effect of particle density on flotation. This is not surprising since coal density is a function of mineral matter content, and higher density therefore translates into less hydrophobic surfaces. The effect of density is much more pronounced for lower-rank and less hydrophobic coals. These conclusions agree very well with those drawn by Bensley and Nicol [20], who pointed out that the inability to float coarse coal results from the inability to float coarse middlings material and that any attempt to increase the recovery of middlings material in a single-stage flotation circuit will almost certainly lead to selectivity problems (any modification which increases the recovery of coarse material will increase the recovery of lower-grade intermediate and fine size particles). For this reason, they suggest that this problem can only be overcome by splitting the flotation feed into fine and coarse streams and floating them separately under proper conditions. These proper conditions also include pulp density. Contrary to the conclusions by Bensley and Nicol [20], Klassen demonstrated [21] that while fine particles float very well at high pulp densities, coarse particles require much lower densities. It should be pointed out, however, that coal flotation in most cases is carried out at very low pulp densities (around 10% by weight). Nicol [22] summarized that with the advent of more sophisticated split feed circuits, the pulp density is controlled by the classifying hydrocyclone and may be 3–5% (hydrocyclone overflow, fine circuit) and 15–20% (cyclone underflow, coarse circuit).

The floatability of coarse coal particles can be improved by carrying out flotation with an upward flow of the pulp. The flotation of coarse coal fractions (−2 +1 mm,

−3 +2 mm and −4 +3 mm) in a short lab column (4 cm diameter, 30 cm height) was shown to proceed with quite good recoveries if the pulp flows upward [23,24]. The upward flow rate was selected on the basis of sedimentation experiments with coal and shale particles, and most experiments were carried out with a flow rate of 2.65 cm/s. The experiments conducted with a −4 +1 mm fraction of a low-volatile bituminous coal that contained 16.2% ash gave 90% combustible recovery at 7.5% ash in the clean product and 63% ash in the tailings. These results were obtained using 800 g/t fuel oil, with 40 mg/l of frother (aliphatic alcohols) at a 1.35 cm/s upward pulp flow rate.

6.4. The use of reagents under industrial conditions

Diffusion of molecules/ions of a water-soluble collector and their adsorption at the mineral/water interface renders mineral particles hydrophobic. This is an unlikely mechanism in the case of water-insoluble oily hydrocarbons. As discussed in Chapter 5, Section 3.1, the mode of action of the water-insoluble oily collectors is quite different. In such a case, the collector species can be transported towards mineral particles only in the form of oil droplets, and so the oil must first be dispersed (emulsified) in water and the droplets of oil must get attached to the mineral particles in order to facilitate the attachment of bubbles to mineral particles [21,25,26].

According to the IUPAC definition, "an emulsion is a dispersion of droplets of one liquid in another one with which it is incompletely miscible." In general, the diameter of the droplets exceeds 0.1 μm.

Fig. 6.10 shows aqueous and organic (oil) phases before and after the dispersion of oil in water. The latter is an emulsion of oil in water (O/W emulsion). Of course, it is also possible to emulsify water in oil (W/O emulsion).

The isothermal reversible work which has to be performed to disperse the oil phase in the aqueous phase (Fig. 6.10) equals

$$\Delta W = \gamma_{WO}(A_{II} - A_I) \tag{6.1}$$

where γ_{WO} stands for the water/oil interfacial tension, A_{II} is the water/oil interfacial area after emulsification, and A_I is the water/oil interfacial area before emulsification.
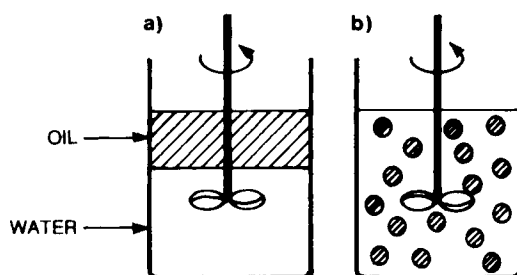
Fig. 6.10. Illustration of emulsification process: (a) two-phases system, (b) oil-in-water emulsion.
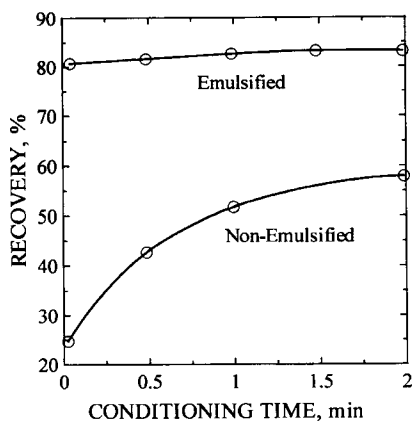
Fig. 6.11. Flotation of a bituminous coal with an ultrasonically emulsified collector as a function of conditioning time with reagents. Collector: 0.18 kg/t paraffin oil, 0.018 kg/t Span 40 and 0.018 kg/t Twen 40; frother: 0.04 kg/t pine oil. (After Sun et al. [28]; by permission of the American Institute of Mining, Metallurgical and Petroleum Engineers.)

Thus, the work performed to disperse one phase in another is needed to increase the interfacial area. Of course, this work can be reduced if the water/oil interfacial tension is low. If an emulsion is prepared by homogenizing two pure liquid components, the emulsion will be unstable and phase separation will generally be rapid. To prepare a reasonably stable emulsion, a third component — an emulsifying agent (emulsifier) — is required. It is then obvious that application of surfactants which adsorb at an oil/water interface and reduce the interfacial tension, facilitates emulsification and stabilizes the emulsion.

There are many simple emulsifying devices that can be employed to emulsify the oily collector prior to contacting it with coal particles. As indicated by Arbiter and Williams [27], it is more efficient to disperse oil in a concentrated stock solution with small specially designed equipment. If the droplets are initially coarse, the separation results are poorer and cannot be brought to the same level as those with a pre-emulsified reagent. This is also seen from Fig. 6.11, published by Sun et al. in 1955 [28]. This subject was heavily discussed in several papers presented at the first few International Coal Preparation Congresses.

My recent visits to some very new plants reveal that even today these problems are not always properly solved, so this subject resurfaces from time to time. One of the papers at the 8th International Coal Preparation Congress shows a new emulsifying device and the effect of emulsification on flotation results [29].

Since emulsification is not always practiced, and since conditioning tanks have been removed from many plants to save on energy, the collector is commonly added to the pulp stream. In the case of the flowsheet shown in Fig. 7.1, the collector is added either to the sump pump preceding the sieve bend, or under the sieve bend into the fine screening product that constitutes the flotation feed. With the former type of arrangement it is inevitable that some amount of the flotation collector is lost with the coarse particles removed on screens. One-stage addition of reagents causes very intense flotation in the

few first cells, with almost no flotation at all in the remaining cells in the bank [30]. Emulsification of an oily collector with some amount of a frother, and the addition of reagents in stages were shown to stabilize the bank with all cells working more evenly, with improved overall recovery, and with reduced ash content in the clean coal product.

Fig. 7.11 shows a flotation circuit which includes the various reagent preparation stages discussed previously with emulsification of an oily collector aided by some amount of frother (with the major part of the frother being directly supplied to various cells). This type of reagent feeding system may work with any flotation circuit (such as, for example, Fig. 7.10 [31]).

The effect of clays on coal flotation was discussed in the preceding chapter. It was mentioned that either desliming, the use of dispersing agents or the use of flotation columns should be considered to reduce the deleterious effect of slimes. Working with coal from Karaganda that was characterized by a high content of clays, Klassen and Nevskaya [21,32] found these slimes to strongly depress coal flotation. The use of dispersing agents was tested as one of the solutions, and the search for such agents resulted in the unexpected finding that higher alcohols also exhibit the ability to peptize clay suspensions; α-terpineol also exhibits such properties. The modified flowsheet, which includes the use of such higher alcohols as frother/clay dispersants, was found to dramatically improve flotation of this coal. The mechanism which leads to clay dispersion in the presence of higher alcohols is not clear. It is also possible that the presence of humic acids plays a part in such effects.

6.5. Desulfurizing flotation

The common objective of coal flotation is to reject ash from the clean product. However, in the case of high-sulfur coals the reduction of sulfur content in the clean coal product becomes more important.

As already discussed, there are three forms of sulfur in coal: organic, sulfatic (mostly gypsum), and pyritic; only pyritic sulfur (e.g. pyrite, marcasite) can be separated from coal in coal preparation plants. Coarse and well liberated pyrite is easily separated from coal by gravity methods. This may be difficult, however, if pyrite is finely disseminated in the coal.

It has been reported that coal-pyrite is very different in its surface and flotation properties from ore-pyrite. The coal pyrite is characterized by lower density, much larger specific surface areas, and greater reactivity. It oxidizes easily and dissolves to some extent in water.

In general, coal and pyrite can be separated either by depressing pyrite and floating coal, or by depressing coal and floating pyrite. The rejection of gangue (and thus also pyrite) can be improved by better circuitry and machinery.

Pyrite appears in all complex sulfide ores and it is known that its floatability can be inhibited in alkaline solutions, especially when lime is used to adjust the pH. However, these and other pyrite depressants (e.g. cyanides, SO_2, etc.), which are well established in the differential flotation of polymetallic sulfide ores, were not found to be very helpful in desulfurizing flotation of coal.

A simple solution to the problem of the desulfurizing flotation of coal has been advocated by Aplan. It is known as a grab-and-run process [33]. In the series of publications that followed, Aplan et al. [34,35] showed that under starvation conditions (quantity of reagents just sufficient to achieve 80% yield), flotation rates for coal particles are much greater than those for the pyrite. For particles above 75 μm, the flotation rates for coal particles are approximately 5- or 10-fold greater than those of the pyrite. For particles below 75 μm, the flotation rates of the coal are only 2- or 3-fold greater than those of the pyrite. In the early stages of flotation, not much mineral matter floats, and only 15–18% of the liberated pyrite in both of the studied coals (Lower Kittanning and Lower Freeport) floated in the first minute. This emphasizes the inherent disadvantage of using long flotation times.

According to Aplan, pyrite is best rejected during coal flotation by maintaining: (1) short flotation times; (2) gentle flotation conditions; (3) starvation frother and collector; (4) non-oily collector; (5) low aeration; (6) low impeller speeds; and (7) column flotation with wash water.

It should be pointed out, however, that the frother–collector system in coal flotation is dictated by coal rank and floatability, and the selected reagents for best coal flotation may also promote pyrite flotation. All tested pyrite depressants are firstly not very efficient, and secondly depress coal to some extent as well.

Fig. 6.12, which was obtained with a mixture of Lower Kittanning bituminous clean coal and pyrite-rich water-only cyclone reject, illustrates very well the effect of reagent dosage on the coal-pyrite flotation selectivity [35]. The lower the dosage of the reagents the better the selectivity. Hirt and Aplan [36] suggested that the selective flotation of coal from pyrite may be represented by the ratio of their respective flotation rate constants k_T / k_{SLP} (where k_T is the flotation rate of the total material floated, and k_{SLP} is the rate constant for liberated pyritic sulfur).

Perry and Aplan [37] found the higher amylose containing starch, Hylon VII, to be a superior polysaccharide for pyrite depression in either the xanthated or unxanthated form. They claim that if an OH group in a polysaccharide is replaced by another group (e.g. in carboxymethyl cellulose), it is an inferior depressant, whereas if it is replaced by another and more readily accessible OH group (e.g. in hydroxyethyl cellulose), it may produce a superior pyrite depressant. The β/*cis* configuration (e.g. in guars) is more strongly adsorbed onto pyrite than is the α/*trans* (starches) or β/*trans* (cellulose) form. However, the guars also seriously depress coal.

In our studies on the adsorption of polysaccharides on various solids we also tested carboxymethyl cellulose [38]. This reagent was used by Blaschke [39] and Hucko [40] in the selective flocculation of coal. In the process studied by Blaschke, coals were treated with doses of carboxymethyl cellulose (CMC) high enough to cause dispersion, and then were flocculated with anionic polyacrylamide (PAM). Since polyelectrolytes (e.g. carboxymethyl cellulose) with high molecular weight work as flocculants at lower concentrations, higher doses of carboxymethyl cellulose were required to disperse coal. Our tests with graphite revealed that CMC adsorbs onto it through interactions with some impurities on the graphite surface serving as adsorption centers. Graphite purified by leaching hardly adsorbed CMC at all. If CMC adsorbs onto coal via a similar mechanism then the density of adsorption probably varies with the amount of impurities
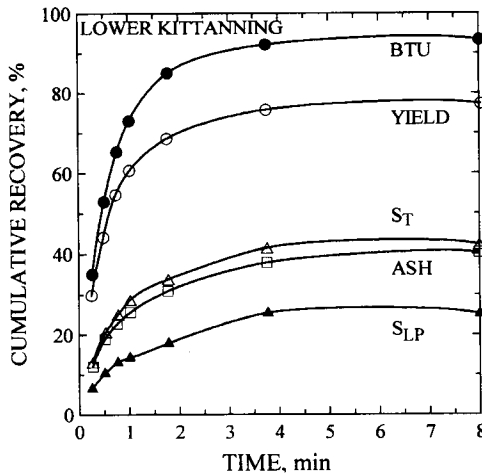
Fig. 6.12. Flotation of the various constituents of Lower Kittaning coal with 0.085 kg/t of MIBC. BTU stands for British thermal unit (BTU × 1.055 = kJ), YIELD stands for the percent clean coal yield, S_T stands for total sulfur in the floated coal, ASH stands for the ash content of the floated coal, and S_{LP} stands for the liberated pyritic sulfur content in the floated coal. (After Purcell and Aplan [35].)

on the coal surface. The fact that the subsequent use of PAM flocculates high ash fraction and leaves coal particles suspended in water may result from quite different phenomena. Since even "clean" coal particles contain a few percent of ash, CMC should adsorb on such particles quite well. This will make such particles hydrophilic. So, Blaschke's results [39] may indicate a better adsorption of CMC onto coal particles, and formation of the protective layers on such surfaces with PAM adsorbing preferably onto mineral particles.

CMC was also tested in the desulfurizing flotation of Eastern Canadian coal [41]. This highly volatile bituminous coal contained 2.76% pyritic sulfur and 3.7% total sulfur. The pyrite grain size distribution was studied using image analysis, and the extent of pyrite liberation in each sample was determined by point count analysis using standard coal petrographic techniques. It was found that pyrite particle size distribution in the raw coal was in part bimodal, with coarser pyrite (greater than 5 μm) consisting of massive subhedral to anhedral forms, and fine fractions consisting of framboidal pyrite (1 μm to 5 μm in size) and fine singular pyrite particles that range in size from less than 1 μm to 5 μm. The pyrite in most samples not crushed below 53 μm had a bimodal pyrite grain distribution which was inherited from the raw coal. Samples crushed below 53 μm generally had a unimodal distribution with a mode between 3 and 7 μm. The amount of liberated pyrite increased with increased grinding time. Wet grinding in a laboratory rod mill for 21 min provided materials 90% below 38 μm. However, even prolonged wet grinding (50 min) did not liberate the finest pyrite grains (less than 2 μm). The results of flotation tests carried out varying grinding time are shown in Fig. 6.13. The batch flotation tests included conditioning with 100 g/t of CMC (molecular weight of 80,000), then conditioning with 900 g/t of kerosene emulsified with 50 g/t of MIBC, and finally, an additional 50 g/t of MIBC more just before flotation. After 2 min of
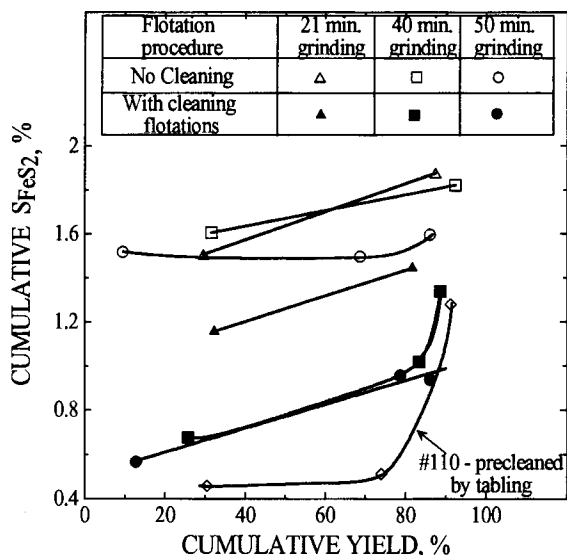
Fig. 6.13. Effect of grinding time on selectivity of flotation with CMC, kerosene and MIBC. Flotation conditions after 21 min grinding: 100 g/t CMC; stage addition of collector and frother: 900 g/t kerosene emulsified with 100 g/t MIBC, and 300 g/t of kerosene emulsified with 100 g/t of MIBC. Flotation conditions after 40 and 50 min grinding: 1800 g/t of kerosene emulsified with 200 g/t MIBC, and 600 g/t kerosene emulsified with 200 g/t MIBC. pH 8.9–9.1. (After Laskowski et al. [41].)

flotation, 300 g/t of kerosene emulsified with 50 g/t of MIBC was added again and then another 50 g/t of MIBC was added and flotation was continued for an additional 2 min. As Fig. 6.13 shows, flotation with the use of kerosene and CMC turned out to be amenable to cleaning. The selectivity was clearly improved after cleaning; the feed ground for 40 and 50 min required doubled amounts of reagents. Flotation conducted with feed ground for 40 min was no more selective than after 21 min grinding. However, cleaning changed this situation quite clearly and reduced the content of pyritic sulfur in the first concentrates to about 0.5%. Since the pyrite grain size distribution in the raw coal was found to be bi-modal, in the rational flowsheet, the coarse pyrite grains should be removed by gravity methods and only then should be followed by fine grinding and flotation of the precleaned coal. In the following tests the coal was crushed below 1 mm and classified into +0.075 mm and −0.075 mm size fractions. The −1 mm +0.075 mm fraction was first cleaned by tabling to reject coarse pyrite and then the table concentrate was wet ground for 40 min and combined with the −0.075 mm portion of the feed. As Fig. 6.13 demonstrates, the best results were obtained following this procedure.

   The exact molecular weight of the CMC used by Blaschke [39] is unknown, but since it was flocculating coal at low concentrations its molecular weight was likely to be high (above 10^6). Apparently, it was dispersing coal particles at high concentrations which were utilized. The flotation of such flocs would probably have been impossible. The molecular weight of the CMC utilized in our experiments was only 80,000, but adsorption of this CMC on graphite was not that different from the adsorption of CMC with a molecular weight of 700,000 [38]. There is no reason to assume that the 80,000

CMC did not adsorb onto coal. However, the limited data does not lend itself to ready analysis. With such fine grinding (90% below 38 μm) the entrainment should be quite high. The obviously superior results that were obtained with 100 g/t of CMC might also result from lower entrainment caused by better dispersion of coal particles. Although the flotation experiments indicate that CMC adsorption did not preclude kerosene emulsified with MIBC to interact with the coal, they do not necessarily indicate that hydrophilicity was imparted to the coal-pyrite by CMC.

Yoon et al. [42] reported that the hydrophobicity of pyrite is induced by initial oxidation which leads to the formation of iron polysulfides. Collectors and frothers may adsorb on a weakly hydrophobic pyrite and further improve its floatability. In agreement with these concepts, recent results by Yoon et al. [43] confirmed that in the presence of some metals (galvanic coupling) pyrite rejection in coal flotation may be improved (see Fig. 5.59).

In a series of papers Capes et al. [44–46] proposed a method for the desulfurization of coal which involves the treatment of a finely ground coal with *Thiobacillus ferrooxidans* followed by recovery of the coal by oil agglomeration.

It is known that pyrite can be removed from coal by bio-leaching with *Thiobacillus ferrooxidans*. Hoffman et al. [47] reported that 90% desulfurization can be achieved in 8 to 12 days by grinding below 74 μm. Of course, a process in which the changes generated by bacteria are limited only to the surface effects must be much cheaper.

The mechanism of the process has not yet been fully elucidated. It is possible that the substances produced by the culture during the adaptation period and the bacterial cells themselves act as wetting agents and render the pyrite surface hydrophilic. Butler et al. [45] claims that this mechanism does not involve pyrite oxidation. Other bacteria such as *Thiobacillus acidophilus* and *Escherichia coli* which do not oxidize pyrite worked even better.

In the flotation process with *Thiobacillus ferrooxidans* preconditioning, Dogan et al. [48] achieved pyrite removal after a conditioning time of 4 h. Atkins et al. [49] showed that the time of conditioning at pH 2 could be reduced to 2 min but they also observed that while floatability of the $-212 +106$ μm pyrite particles could be significantly suppressed by the bacterial treatment, the depression of the -106 μm pyrite particles was very limited.

To increase selectivity of pyrite rejection, and to reduce the time of conditioning with the bacteria as much as possible, Elzeky and Attia [50] studied the effect of the adaptation period of *Thiobacillus ferrooxidans*. The adaptation was carried out with 200 ml of activated bacteria, 50 g of -75 μm coal-pyrite, and 1000 ml of water. The pH was adjusted to 2.0 (H$_2$SO$_4$) and the bacteria were left to adapt and grow at 30°C with frequent stirring and aeration by bubbling over 2, 4 and 6 weeks. The bacterial solution obtained by filtration of the flask content was used for conditioning with coal pulp prior to flotation. In the flotation tests, 75 g of -75 μm wet ground coal was treated with 300 ml of the adapted bacterial solution, and distilled water was added to make up a 1.5-l volume. The pH of the slurry was adjusted to 2.0 with dilute sulfuric acid. The slurry was stirred and aerated over 5, 10, 15, 20, 25 and 30 min and was then left to settle, the solution was siphoned off, and tap water was used to re-slurry the collected solids to a total volume of 1.5 l for flotation tests. The pH of the slurry was adjusted with 1.0 M
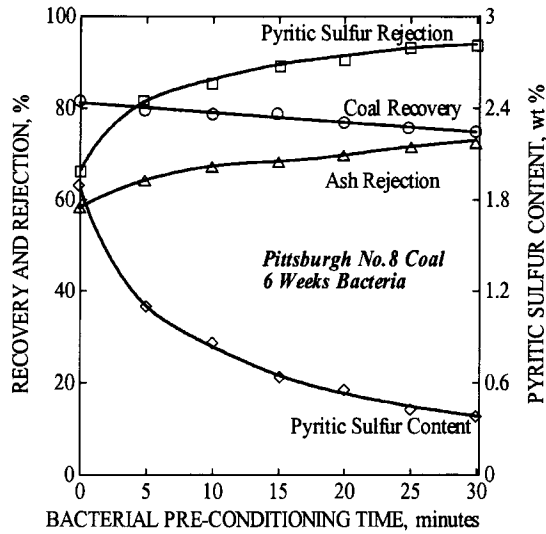
Fig. 6.14. Effect of bacterial pre-conditioning time on the flotation of Pittsburgh No. 8 coal with 6-weeks adapted bacteria. Reagents: 1.35 kg/t of the 1 : 2 blend of fuel oil No. 2 and MIBC. (After Elzeky and Attia [50]; by permission of Gordon and Breach.)
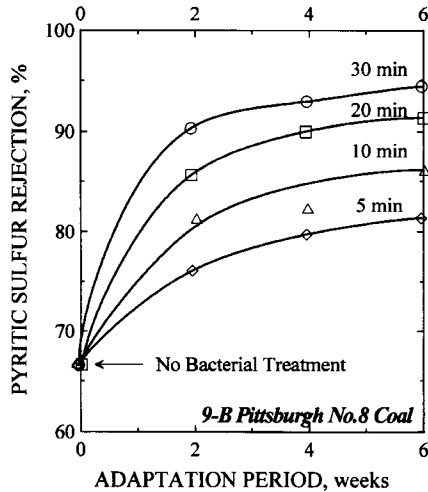
Fig. 6.15. The effect of adaptation period of *ferrooxidans* on the pyritic sulfur rejection at constant bacterial pre-conditioning time. (After Elzeky and Attia [50]; by permission of Gordon and Breach.)

KOH to the coal natural pH (i.e. 8.5 for Upper Freeport and 8.0 for Pittsburgh No. 8). A 1 : 2 blend of MIBC and fuel oil No. 2 was used in the flotation tests (0.79 kg/t for Upper Freeport coal and 1.35 kg/t for Pittsburgh No. 8 coal).

Examples of Elzeky and Attia's results [50] are shown in Figs. 6.14 and 6.15. Fig. 6.16 illustrates the effect of pre-conditioning time on the desulfurising flotation of
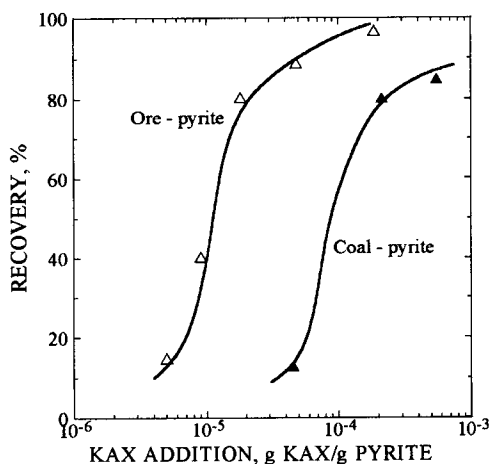
Fig. 6.16. Flotation recoveries of ore-pyrite and coal-pyrite. Conditions: Hallimond flotation tube, 2 g of 65 × 100 mesh material, pH 6.5. (After Miller and Deurbrouck [61]; by permission of Marcel Dekker Inc.)

Pittsburgh No. 8 coal with the use of bacteria that were adapted over a 6-week period. As seen, the bacteria only slightly reduce coal recovery and significantly improve pyrite rejection; this treatment reduced the pyritic sulfur content in the cleaned coal from about 1.9% down to about 0.5%. Elzeky and Attia concluded that the longer the adaptation period, the higher the pyrite removal and the shorter the bacterial pre-conditioning time. As Fig. 5.58 demonstrates, most pyritic sulfur rejection (81–90%) can be achieved in the first 10 min of bacterial pre-conditioning.

Wheelock and his co-workers [51,52] studied collectorless flotation of pyrite and sulfurized pyrite, and also the flotation of these pyrites in the presence of fuel oil. The pyrite did not float without sulfurization, but was floatable in the presence of fuel oil. Fan et al. [53] showed that oxidized pyrite, which responded to oil agglomeration with heptane only in acidic pH conditions, could also be agglomerated even at pH 9 if the amount of heptane was drastically increased. These results confirm that while the hydrophobicity of untreated pyrite may not be sufficient to support its flotation, such a pyrite may be floatable in the presence of fuel oil. These results also imply that sulfur reduction by oil agglomeration may be difficult.

As pointed out by Capes [54], conventional oil agglomeration (which is carried out with 10–20% addition of oil) is not selective towards pyrite. However, he points out that oil agglomeration with lower oil dosage results in improved selectivity (Figs. 9.3 and 9.4) with regard to pyrite rejection. The agglomeration at low oil levels is, however, very different from the conventional oil agglomeration process. In the conventional process, oil addition is sufficient to form large agglomerates which can then be recovered by screening. Capes claims that when very small amounts of oil are added, it is preferentially abstracted by the coal and not by the pyrite, which results in the formation of agglomerates which can be removed by flotation. This leaves oil-free pyrite in the tailings.

The Agloflot process developed at the Alberta Research Council [55,56] is an agglomerate flotation process in which a low amount of oil (0.5 to 3% of dry coal) is used for agglomeration prior to flotation. In a two-stage process the micro-agglomerates recovered by flotation are resuspended in fresh water, mixed for 1 min to release the entrapped mineral particles (pyrite) and are separated again by flotation. While the reduction in total sulfur for Illinois No. 6 coal was only up to 27% [56], the authors claim that the process may reduce 75 to 90% of pyritic sulfur. These data do not correlate very well with some flotation observations. For instance, as Fig. 5.55 shows, an increase in the amount of fuel oil in the flotation results in an increased content of pyritic sulfur in the froth product (the flotation doses are more then 10 times lower than 1% used in the oil agglomeration). These data may, perhaps, indicate that a high content of pyrite in the froth product from conventional coal flotation could be further reduced by cleaning flotation. Another option would be the use of depressants. For instance, thioglycollic acid was shown to be a good depressant in collectorless flotation of sulfurized pyrite (used as a model of coal-pyrite), and in the flotation of untreated pyrite with fuel oil [51,53].

Many coals require extremely fine grinding in order to achieve pyrite liberation [41,57]. Flotation of such a fine coal may pose a difficult problem. Selectivity of oil agglomeration is still an open question, and the use of conventional flocculants does not allow the recovery of flocs by flotation. Elzeky et al. [58], working with a mixture of Pittsburgh No. 8 seam coal and pyrite, both ground below 25 μm, used a hydrophobic flocculant, FA-7A (Calgon Corp.), to selectively aggregate the coal. Polyxanthate dispersant (PAAX) was applied as a pyrite dispersant/depressant. This interesting process is not very different from the agglomeration in which oil droplets agglomerate hydrophobic particles or the aggregation caused by hydrophobic bacteria [59,60], and is further discussed in Section 6.

Since the first option, namely flotation of coal and depression of pyrite has not been very successful, the second option of reverse flotation in which coal is depressed and pyrite is floated was also investigated. The second option turned out to be more successful and it is known as a "two-stage reverse flotation process".

The first stage of this process is conventional flotation, which takes advantage of the coal particles' natural floatability. During this stage coal is floated away from hydrophilic gangue (e.g. clays, shale, quartz, some pyrite) utilizing a conventional collector and frother. The second stage involves the flotation of pyrite particles remaining in the first stage concentrate using a thio-collector (amyl xanthate) after repulping the froth product with an organic depressant of coal (dextrin). The selectivity that can be achieved with the reverse flotation strategy is reflected by the sensitivity of the flotation response of both minerals to dextrin addition, as shown in Fig. 5.45.

Figs. 6.16 and 6.17 show the conditions for the flotation of pyrite in the second "reverse" stage [61]. As can be inferred from Fig. 6.17, higher doses of xanthate are needed for efficient flotation of coal-pyrite compared with those in the flotation of ore-pyrite.

An interesting fine-coal processing circuit which incorporates the MGS separator and a Microcell flotation column, and which was specially designed to desulfurize fine coal, is discussed in Chapter 7.
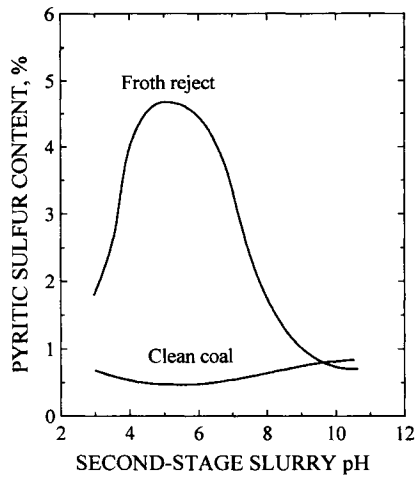
Fig. 6.17. Pyritic sulfur content of the products from the second stage of reverse flotation as a function of pH. (After Miller and Deurbrouck [61]; be permission of Marcel Dekker Inc.)

6.6. Flocculants in coal preparation

A fines treatment circuit includes four distinct unit operations: fine coal cleaning, clean coal dewatering, tailings dewatering and water clarification. An important part of the fine-coal processing module, the flotation circuit, does not treat a pulp prepared by grinding and classification, but treats fines arising from various stages of coal preparation. These streams may be coming from various beneficiation and solid/liquid separation operations, and because of the closure of water circuits (Fig. 1.5) may be exposed to various chemical additives.

To improve dewatering operations (e.g. thickening, filtration, etc.), the industry applies flocculating agents. These polyelectrolytes are highly hydrophilic, water-soluble polymers which, as discussed in Chapter 5, Section 3.6, are strong coal depressants. Obviously they are not compatible with flotation, and flotation collectors in particular [62]. This topic has not been extensively researched and some claims are quite conflicting. However, with the present trend towards higher flocculant levels for dewatering and the likelihood of flocculant build-up in recycle streams over time, this is a very important topic. It is claimed that some plants operating with high flocculant doses may give (high) flocculant returns to the flotation system in the order of 50 g/t. The doses of flocculants for dewatering in centrifuges and filters are an order of magnitude higher than are common in conventional thickeners/clarifiers [63].

Coal flotation is very strongly depressed by dextrin (Fig. 5.45). Fig. 5.43 indicates [64] that polymers used as flocculants impart different degrees of hydrophilicity to coal.

Pikkat-Ordynsky and Ostry [65], included some of the early Russian work in a chapter devoted entirely to the topic of flocculant effect on coal flotation. They claim that lab tests indicate that only 60–90% of the available polyacrylamide is adsorbed on coal tailings in one stage conditioning. Quoting various authors they conclude that almost all high molecular weight flocculants at a consumption of 20–30 g/t affect coal
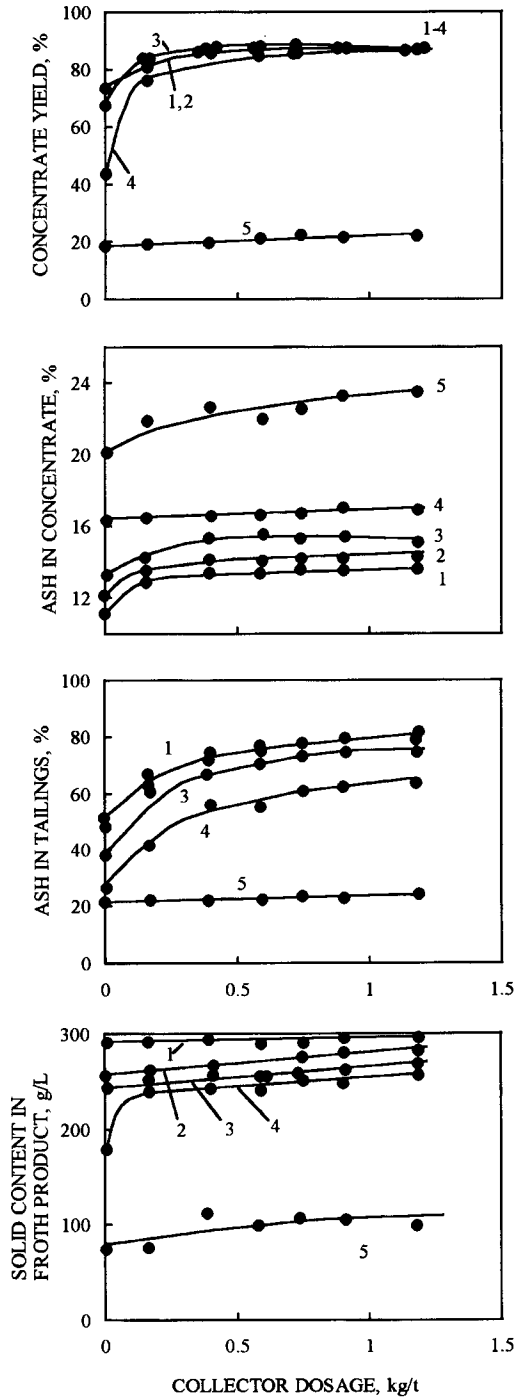
Fig. 6.18. Effect of AF-2 oily collector dosage on flotation of coal fines from Dzierzynsky mine as a function concentration of polyacrylamide. PAA concentrations: $1 = 0$; $2 = 5$ g/m^3; $3 = 20$ g/m^3; $4 = 80$ g/m^3; $5 = 150$ g/m^3. (After Pikkat-Ordynsky and Ostry [65].)

flotation. Many authors found that the commercial use of flocculants increased ash content in the flotation feed by 3–4%, increased consumption of collectors by 1.8–2.4 times, consumption of frothers by 1.2–1.7 times, and required lower pulp densities.

In one of the preparation plants, application of polyacrylamide (PAA) at 8–10 g/t to enhance water clarification resulted in an increased yield of −0.04 mm fraction in the flotation feed from 30 to 49%; ash content in the flotation feed also increased by 6%. These changes strongly affected the flotation process: kerosene consumption increased by 2.4 times (from 1060 to 2500 g/t) and frother consumption increased from 200 to 350 g/t. Both the yield of concentrate and the ash content of the tailings decreased. Throughput of the mechanical flotation machines decreased from 33 to 17 m^3/h (from 7 to 3.1 t/h).

As shown by some authors [65], at PAA dosages of 2–10 g/t there is no effect on flotation if pulps are diluted (100–180 g of solids per liter). At 10–100 g/t of PAA (or 1–10 g/m^3 of pulp at 100 g solids per liter) both concentrate yield and tailings ash content decrease. Higher molecular weight polyelectrolytes exhibit stronger depression. It was also observed that in the presence of some flocculants (e.g. polyethylene oxide) voluminous but very unstable froth was produced.

Fig. 6.18. illustrates the effect of PAA flocculant and of apolar collector (at 196 g/t of frother) on the flotation of bituminous coal in the lab flotation tests carried out in a 1.5-l batch cell at 150 g solids per liter [65]. While concentrate yield can be maintained at a high level by increased collector doses, an increased addition of PAA leads to increased clean coal ash content and decreased tailings ash content. These results agree reasonably well with those of Williams and Unlu [66]. They studied the effect of anionic flocculant (Superfloc A110 made by Cyanamid Corp., molecular weight of 4.7 × 10^6, and cationic flocculant (Superfloc C110 made Cyanamid Corp., molecular weight of 0.9 × 10^6 [67]) on batch flotation of anthracite with 0.9 kg/t of oily collector. Their results confirm
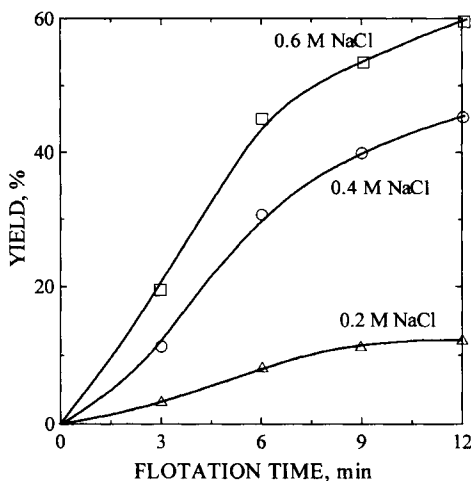
Fig. 6.19. Salt flotation of a high volatile bituminous coal (20.3% ash), size fraction: 100% below 0.75 mm. (After Laskowski and Mielecki [68].)

that in the presence of flocculants coal flotation is affected: recoveries decrease, clean coal ash increases and tailings ash decreases. Williams and Unlu [66] also observed that the yield of clean coal concentrate could be increased at very low doses of flocculant. This may indicate a beneficial effect of fine coal aggregation on flotation at doses of flocculant which do not yet affect coal wettability.

It is obvious that the use of totally hydrophobic flocculants, especially in thickeners that are ahead of flotation, could eliminate these problems (see Chapter 9, Section 3).

6.7. Salt flotation

The most obvious difference between salt flotation and conventional coal flotation is the rate; the rate of the salt flotation is much higher. This is clearly seen in Fig. 6.19
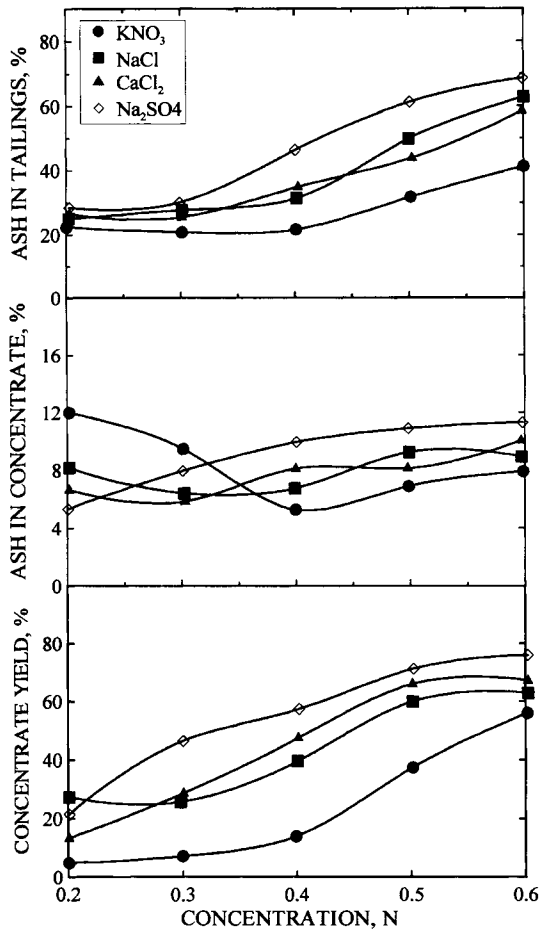
Fig. 6.20. Effect of concentration of various salts on salt flotation of a high volatile bituminous coal (as in Fig. 6.19) [68].
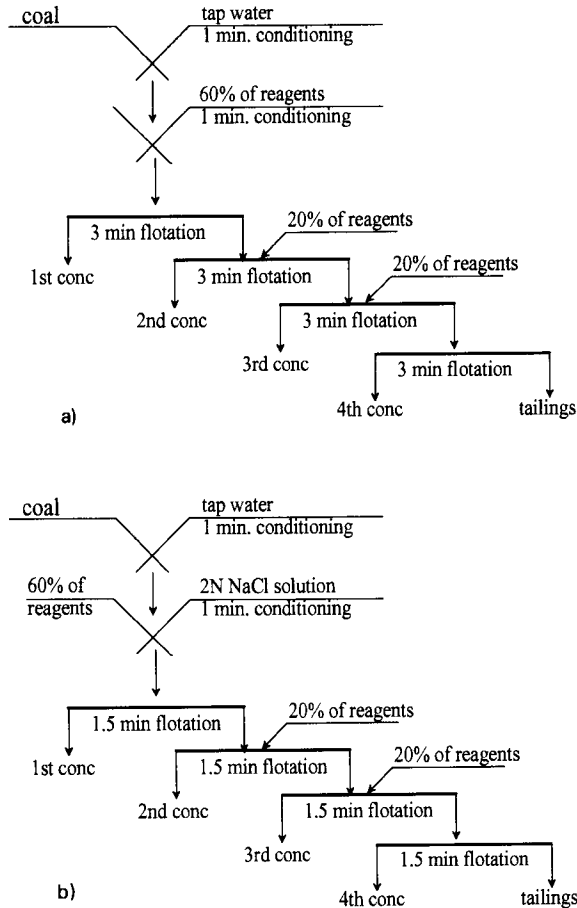
Fig. 6.21. Experimental procedures that were followed in the flotation tests (for results see Figs. 6.22 and 6.23). (a) The flotation procedure for the tests carried out with the use of oily collector. (b) The procedure of the tests in which both inorganic salts and oily collectors were utilized.

[68]. The figure shows the salt flotation test results for high-volatile B bituminous coal (20.3% ash) crushed below 0.75 mm. Much steeper kinetic curves obtained at increasing NaCl concentrations point to greatly improved kinetics.

Fig. 6.20 depicts the flotation curves for the same coal obtained in tests carried out at different concentrations of NaCl, KNO_3 and Na_2SO_4 and at a constant flotation time of 7 min. Comparison of these three salts reveals that the results with KNO_3 are the least satisfactory; even in 0.4 N solutions [1] the clean coal yield was only about 14% and started significantly increasing only in the 0.5–0.6 N range of concentrations. High ash contents in the froth product at very low KNO_3 concentrations indicates that

---

[1] N stands for the number of equivalents per liter of solution (normality). For instance, for NaCl N = M/1, for $CaCl_2$ N = M/2, for $AlCl_3$ N = M/3.
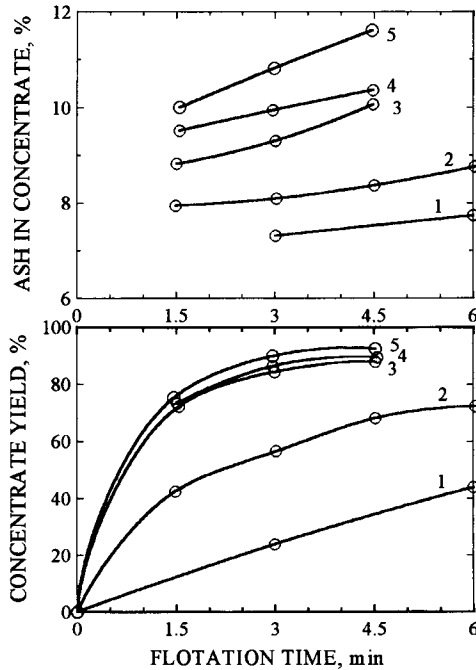
Fig. 6.22. Flotation of a high volatile bituminous coal with 400 g/t kerosene in NaCl solutions of varying concentration: 1 = tap water; 2 = 0.1 N NaCl; 3 = 0.2 N NaCl; 4 = 0.3 N NaCl; 5 =0.5 N NaCl. (After Laskowski and Weber [69].)

probably only fusinite was floating under such conditions. The results with NaCl were very different. At concentrations higher that 0.3 N the curve assumes "normal" shape and at 0.5 N the yield was 61.4% (9.7% ash) with 50.3% ash in the tailings. The most satisfactory was the flotation with Na_2SO_4. The yield vs. concentration curve has the expected shape as the ash content in the froth product increases proportionally to the yield. The 72.2% yield of clean coal (11.1% ash) at 61.1% ash content of the tailings obtained at a 0.5 N concentration of Na_2SO_4 is very good indeed.

The same coal was also used in tests with both kerosene and NaCl. The procedures of the flotation tests conducted in tap water with kerosene, and with kerosene and NaCl are shown in Fig. 6.21. An increase in kerosene addition slightly improves the recovery, but does not significantly change the flotation rate (Fig. 6.22). As Fig. 6.23 demonstrates, very different kinetic curves were obtained when both kerosene and NaCl were used simultaneously [69]; any increase in NaCl concentration was accompanied by a higher flotation rate.

Fig. 6.23 summarizes the results obtained under different conditions using NaCl and either kerosene or low phenol medium tar oil. An increase in the salt concentration up to 0.3 N is advantageous; exceeding this concentration only produces higher ash concentrates without any beneficial effects.

It is to be pointed out that the water pumped out from underground mines is very often characterized by a high content of NaCl. The use of such water for flotation
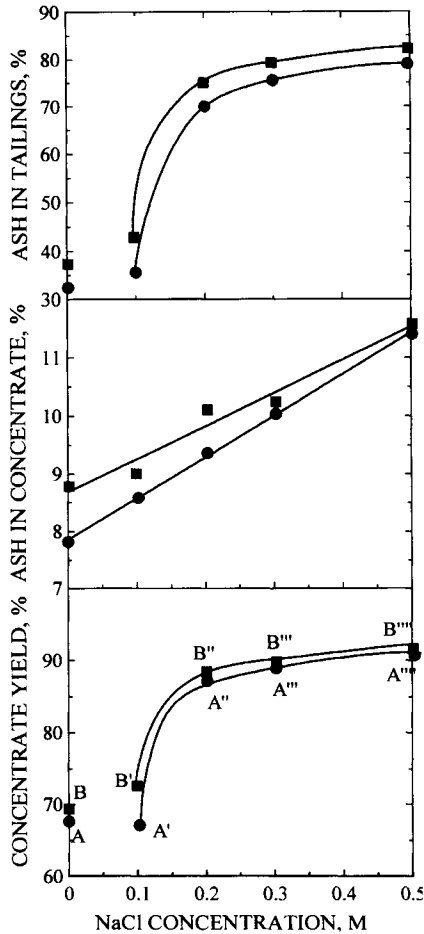
Fig. 6.23. Optimum results of the flotation experiments for a high volatile bituminous coal using 400 g/t of either low-phenol tar oil (A) or kerosene (B). A and B: results after 12 min of flotation in tap water; A' and B': results after 6 min of flotation in 0.1 N NaCl solution; A" and B": results after 6 min of flotation in 0.2 N NaCl solution; A''' and B''': results after 4.5 min of flotation in 0.2 N NaCl solution; A'''' and B'''': results after 4.5 min of flotation in 0.5 N NaCl solution. (After Laskowski and Weber [69].)

may significantly improve performance of the flotation circuit. It was also reported that fine-coal dewatering by filtration proceeds much better in salt solutions.

Although this subject has never been properly investigated, salt flotation was also reported to be very selective in desulfurizing flotation of fine coal.

6.8. References

[1] R.J. Crawford, D.W. Guy and D.E. Mainwaring, The influence of coal rank and mineral matter content on contact angle hysteresis. Fuel, 73 (1994) 742.

[2] D.W. Fuerstenau, J. Diao, J.S. Hansen, F. Sotillo and P. Somasundaran, Effect of weathering on the wetting behavior and flotation response of coal. In: W. Blaschke (ed.), New Trends in Coal Preparation Technologies and Equipment. Proc. 12th Int. Coal Preparation Congr., Gordon and Breach, London, 1996, pp. 747–754.

[3] P. Somasundaran, C.E. Roberts and R. Ramesh, Effects of oxidizing methods on the flotation of coal. Miner. Eng., 4 (1991) 43.

[4] Y. Ye, R. Jin and J.D. Miller, Thermal treatment of low-rank coal and its relationship to flotation performance. Coal Preparation, 6 (1988) 1.

[5] A.B. Garcia, S.R. Moinelo, M.R. Martinez-Tarazona and J.M.D. Tascon, Influence of weathering process on the flotation response of coal. Fuel, 70 (1991) 1391.

[6] B.A. Firth and S.K. Nicol, The effect of oxidised pyritic sulfur on coal flotation. Coal Preparation, 1 (1984) 53.

[7] B.A. Firth and S.K. Nicol, The influence of humic materials on the flotation of coal. Int. J. Miner. Process., 8 (1981) 239.

[8] D.W. Fuerstenau, G.C. Yang and J.S. Laskowski, Oxidation phenomena in coal flotation. Coal Preparation, 4 (1987) 161.

[9] D.W. Fuerstenau, J.M. Rosenbaum and J.S. Laskowski, Effect of surface functional groups on the flotation of coal. Coll. Surf., 8 (1983) 153.

[10] J.D. Miller and Y. Ye, Selective Flotation of fossil resin from Wasatch Plateau high-volatile bituminous coal. Miner. Metall. Process., 10 (1989) 87.

[11] M.E. Holuszko and J.S. Laskowski, Coal heterogeneity and its effect on coal floatability as derived from flotation tests in methanol solutions. In: J.S. Laskowski and G.W. Poling (eds), Processing of Hydrophobic Minerals and Fine Coal. Proc. 1st UBC-McGill Int. Symp., Metall. Soc. of CIM, Montreal, 1995, pp. 145–164.

[12] A.J.R. Bennett, H. Bustamante, A. Telfer and L.J. Warren, The floatability of vitrinite, inertinite and composite grains in coals of differing rank. In: R.L. Whitmore (ed.), Proceedings of the 2nd Australian Coal Preparation Conference. Coal Prep. Societies of New South Wales and Queensland, 1983, pp. 161–174.

[13] N.W. Johnson, D.J. McKee and A.J. Lynch, Flotation rates of non-sulfide minerals in chalcopyrite flotation processes. Trans. AIME, 256 (1974) 204.

[14] L.J. Warren, Determination of the contributions of true flotation and entrainment in batch flotation tests. Int. J. Miner. Process., 14 (1985) 33.

[15] H. Bustamante and L.J. Warren, Factors affecting the floatability of Australian bituminous coals. Proc. 15th Int. Mineral Processing Congr., Cannes, 1985, Vol. 2, pp. 232–243.

[16] P.G. Smith and L.J. Warren, Entrainment of particles into flotation froths. In: J.S. Laskowski (ed.), Frothing in Flotation. Gordon and Breach, London, 1989, pp. 123–146.

[17] J.A. Kitchener, Flocculation in mineral processing. In: K.J. Ives (ed.), The Scientific Basis of Flocculation. Sijthoff and Noordhoff, Alphen a/d Rijn, 1978, pp. 283–328.

[18] A. Jowett, H. El-Sinbawy and H.G. Smith, Slime coating of coal in flotation pulps. Fuel, 35 (1956) 303.

[19] B. Arnold and F. Aplan, The effect of clay slurries on coal flotation, Parts I and II. Int. J. Miner. Process., 17 (1986) 225.

[20] C.N. Bensley and S.K. Nicol, The effect of mechanical variables on the flotation of coarse coal. Coal Preparation, 1 (1985) 189.

[21] V.I. Klassen, Coal Flotation. Gosgortiekhizdat, Moscow, 1963 (in Russian).

[22] S.K. Nicol, Fine Coal Beneficiation. Australian Coal Prep. Society, 1992.

[23] J.S. Laskowski and M. Marchewicz, Flotation of coarse grains of coal. Przegl. Gorn., 25 (1969) 438 (in Polish).

[24] J.S. Laskowski and W. Bartoniek, Floto-gravity of coal. Przegl. Gorn. 26 (1970) 250 (in Polish).

[25] I.N. Plakisn (ed.), Physico-Chemical Fundamentals of the Action of Nonpolar Collectors in Flotation of Ores and Coal. Izdat. Nauka, Moscow, 1965 (in Russian).

[26] V.A. Glembotski, G.M. Dmitrieva and M.M. Sorokin, Nonpolar Flotation Agents. Israel Program for Scientific Translation, Jerusalem, 1970.

[27] N. Arbiter and E.K.C. Williams, Conditioning in oleic acid flotation. In: P. Somasundaran (ed.), Fine Particle Processing. AIME, New York, 1980, Vol. 1, pp. 802–831.

[28] S.C. Sun, L.Y. Tu and E. Ackerman, Mineral flotation with ultrasonically emulsified collecting reagents. Mining Eng., 7 (1955) 656.

[29] S.D. Dchendova, S.M. Stoev, M.S. Metodev and M.G. Radeva, Vibro-hydrodynamic emulsifying device. 8th Int. Coal Preparation Congr., Donetsk, 1979, Paper C-1.

[30] J.S. Laskowski and D. Romero, The use of reagents in coal flotation. In: J.S. Laskowski and G.W. Poling (eds), Processing of Hydrophobic Minerals and Fine Coal. Proc. 1st UBC-McGill Int. Symp, Metall. Soc. of CIM, Montreal, 1995, pp. 191–197.

[31] F. Dedek, G. Sebor, M. Barcal and V. Bortlik, Development of the theory and practice of coal flotation in the Czech Republic. 8th Int. Coal Preparation Congr., Donetsk, 1979, Paper C-7.

[32] V.I. Klassen and V.A. Nevskaya, Flotation of coal with high content of clayish slimes. Koks Khimia (1958) (3) 15 (in Russian).

[33] F.F. Aplan, Use of flotation process for desulfurization of coal. In: T.D. Wheelock (ed.), Coal Desulfurization — Chemical and Physical Methods. ACS Symp. Ser. 64, Washington, DC, 1977, pp. 70–81.

[34] T. J. Oslon and F.F. Aplan, The effect of frothing and collecting agents on the flotation of coal, pyrite and locked particles in a coal flotation system. In: Y.P. Chugh and R.D. Caudle (eds), Processing and Utilization of High-Sulfur Coals II. Elsevier, Amsterdam, 1987, pp. 71–82.

[35] R.J. Purcell and F.F. Aplan, Pyrite and ash depression during coal flotation by flotation rate, recovery and reagent control. In: P.R. Dugan, D.R. Quigley and Y.A. Attia (eds), Processing and Utilization of High-Sulfur Coals IV. Elsevier, Amsterdam, 1991, pp. 279–294.

[36] W.C. Hirt and F.F. Aplan, The influence of operating factors on coal recovery and pyritic sulfur rejection during coal flotation. In: P.R. Dugan, D.R. Quigley and Y.A. Attia (eds), Processing and Utilization of High-Sulfur Coals IV. Elsevier, Amsterdam, 1991, pp. 339–356.

[37] R.W. Perry and F.F. Aplan, Polysaccharides and xanthated polysaccharides as pyrite depressants during coal flotation. In: Y.A. Attia (ed.), Processing and Utilization of High-Sulfur Coals I. Elsevier, Amsterdam, 1985, pp. 215–238.

[38] J.A. Solari, A.C. de Araujo and J.S. Laskowski, The effect of carboxymethyl cellulose on the flotation and surface properties of graphite. Coal Preparation, 3 (1986) 15.

[39] Z. Blaschke, Beneficiation of coal fines by selective flocculation. Proc. 7th Int. Coal Preparation Congr., Sydney, 1976. Paper F2.

[40] R. Hucko, Beneficiation of coal by selective flocculation. A laboratory study. US Bureau of Mines, RI 8234, 1977.

[41] J.S. Laskowski, M. Bustin, K.S. Moon and L.L. Sirois, Desulfurizing flotation of Eastern Canadian high-sulfur coal. In: Y.A. Attia (ed.), Processing and Utilization of High-Sulfur Coals I. Elsevier, Amsterdam, 1985, pp. 247–266.

[42] R.H. Yoon, M.L. Lagno, G.H. Luttrell and J.A. Mielczarski, On the hydrophobicity of coal pyrite. In: P.R. Dugan, D.R. Quigley and Y.A. Attia (eds), Processing and Utilization of High-Sulfur Coals IV. Elsevier, Amsterdam, 1991, pp. 241–254.

[43] R.H. Yoon, D.P. Tao, M.X. Lu, P.E. Richardson and G.H. Luttrell, Improving pyrite rejection by galvanic control. Coal Preparation, 18 (1997) 53.

[44] C.E. Capes, A.E. McIlhinney, A.F. Siriani and I.E. Puddington, Bacterial oxidation in upgrading pyritic coals. CIM Bull., 66 (1973) 88.

[45] R.J. Buttler, A.G. Kempton, R.D. Coleman and C.E. Capes, The effect of particle size and pH on the removal of pyrite from coal by conditioning with bacteria followed by oil agglomeration. Hydrometallurgy, 15 (1986) 325.

[46] A.G. Kempton, N. Maneib, R.G.C. McCready and C.E. Capes, Removal of pyrite from coal by conditioning with *Thiobacillus ferrooxidans* followed by oil agglomeration. Hydrometallurgy, 5 (1980) 117.

[47] M.R. Hoffman, B.C. Faust, F.A. Panda, H.H. Kao and H.M. Tsuchija, Kinetics of the removal of non pyrite from coal by microbial catalysis. Appl. Environ. Microbiol., 42 (1981) 259.

[48] M.Z. Dogan, G. Ozboyoglu, C. Hicyilmaz, M. Sarikaya and G. Ozengiz, Bacterial leaching versus

bacterial conditioning and flotation in desulfurization of coal. Proc. 15th Int. Mineral Processing Congr., Cannes, 1985, Vol. 2, pp. 304–313.

[49] A.S. Atkins, E.W. Bridgwood, A.J. Davis and F.D. Pooley, A study of the suppression of pyritic sulfur in coal froth flotation by *Thiobacillus ferrooxidans*. Coal Preparation, 5 (1987) 1.

[50] M. Elzeky and Y.A. Attia, Coal slurries desulfurization by flotation using thiophilic bacteria for pyrite depression. Coal Preparation, 5 (1987) 15.

[51] T. Chmielewski and T.D. Wheelock, Thioglycolic acid as a flotation depressant for pyrite. In: P.R. Dugan, D.R. Quigley and Y.A. Attia (eds), Processing and Utilization of High-Sulfur Coals IV. Elsevier, Amsterdam, 1991, pp. 295–308.

[52] J. Drzymala, R. Markuszewski and T.D. Wheelock, Oil agglomeration of sulfurized pyrite. Miner. Eng., 4 (1991) 161.

[53] C.W. Fan, R. Markuszewski and T.D. Wheelock, Separation of coal/pyrite mixtures by agglomeration with heptane. In: R. Markuszewski and T.D. Wheelock (eds), Processing and Utilization of High-Sulfur Coals III. Elsevier, Amsterdam, 1990, pp. 265–278.

[54] C.E. Capes, Oil agglomeration process principles and commercial application for fine coal cleaning. In: J.W. Leonard (ed.), Coal Preparation. AIME, 1991, 5th ed., pp. 1020–1041.

[55] W. Pawlak, K. Szymocha, Y. Briker and B. Ignasiak, High-sulfur coal upgrading by improved oil agglomeration. In: R. Markuszewski and T.D. Wheelock (eds), Processing and Utilization of High-Sulfur Coals III. Elsevier, Amsterdam, 1990, pp. 279–288.

[56] Y. Briker, K. Szymocha, W. Pawlak, J. Kramer and B. Ignasiak, Feasibility of Aglofloat Process for deashing and desulfurization of high-sulfur coals. In: P.R. Dugan, D.R. Quigley and Y.A. Attia (eds), Processing and Utilization of High-Sulfur Coals IV. Elsevier, Amsterdam, 1991, pp. 353–374.

[57] W.A. Kneller and G.P. Maxwell, Size, shape and distribution of microscopic pyrite in selected Ohio coals. In: Y.A. Attia (ed.), Processing and Utilization of High-Sulfur Coals I. Elsevier, Amsterdam, 1985, pp. 41–66.

[58] M. Elzeky, F. Bavarian and Y.A. Attia, Feasibility of selective flocculation/froth flotation process for simultaneous deashing and desulfurization of high-0sulfur coals. In: R. Markuszewski and T.D. Wheelock (eds), Processing and Utilization of High-Sulfur Coals III. Elsevier, Amsterdam, 1990, pp. 209–220.

[59] M. Misra, R.W. Smith, J. Dubel and S. Chan, Selective flocculation of fine coal with hydrophobic *Mycobacterium phlei*. Miner. Metall. Process., 10 (1993) 20.

[60] A.M. Raichur, M. Misra, S.A. Davis and R.W. Smith, Flocculation of fine coal using synthetic and biologically derived flocculants. Miner. Metall. Process., 14 (1997) 22.

[61] K.J. Miller and A.W. Deurbrouck, Froth flotation to desulfurize coal. In: Y.A. Liu (ed.), Physical Cleaning of Coal. Marcel Dekker, New York, 1982, pp. 255–291.

[62] J.S. Laskowski and Z. Yu, Fine coal particle aggregation in coal preparation plant circuits. In: A.C. Partridge and I.R. Partridge (eds), Proceedings of the 13th International Coal Preparation Congress. Australian Coal Preparation Society, Brisbane, 1998, Vol. 2, pp. 591–599.

[63] Discussion to the paper by K.P. Williams and M. Unlu, Coal Preparation, 4 (1987) 130–132.

[64] Pradip and D.W. Fuerstenau, The effect of polymer adsorption on the wettability of coal. In: Y.A. Attia (ed.), Flocculation in Biotechnology and Separation Systems. Elsevier, Amsterdam, 1987, pp. 95–106.

[65] G.A. Pikkat-Ordynsky and V.A. Ostry, Technology of Coal Flotation. Izd. Nedra, Moscow, 1972 (in Russian).

[66] K.P. Williams and M. Unlu, Coal flotation in the presence of polymeric flocculants. Coal Preparation, 4 (1987) 109.

[67] K.P. Williams and M. Unlu, Streaming potential studies on anthracite in the presence of inorganic ions and polyelectrolytes. Coal Preparation, 3 (1987) 195.

[68] J.S. Laskowski and J. Mielecki, Salt flotation of coals with a simultaneous use of organic agents. Przegl. Gorn., 20 (1964) 113 (in Polish).

[69] J.S. Laskowski and F. Weber, Influence of inorganic salts on coal flotation rate using water-insoluble oily collectors. Przegl. Gorn., 21 (1965) 296 (in Polish).

Chapter 7

FINE-COAL MULTI-UNIT PROCESSING CIRCUITS

7.1. Flotation and gravity methods in fine-coal processing

Comparison of gravity-based washability curves with flotation results indicates that gravity-based processes are always more efficient [1], especially at treating coals with a significant yield of middlings. Because of bubble attachment to the hydrophobic (coal) portion of the particle, a particle containing as little as 5% coal may still report to the froth product. Therefore, for coal fines having a high middlings content, a high combustible recovery commonly results in high ash and sulfur levels in the flotation products.

In the case of high sulfur coals, one of the severe deficiencies of coal flotation is its limited ability to separate coal from pyrite. There are many possible reasons for such behavior of pyrite particles in coal flotation: (i) pyrite can become hydrophobic when superficially oxidized, making its separation from coal difficult, and (ii) composite particles containing small inclusions of pyrite (or coal) are readily floated. Because of large differences between coal and pyrite densities, the ability of gravity separation methods to separate these two solids is much better. Although the gravity methods are not very efficient in handling very fine particles, incorporation of gravity separators along with flotation into the fine-coal processing circuit is still the best solution.

Fig. 7.1 shows a fine-coal cleaning flowsheet typical for Canadian plants, which includes water-only cyclones (WOC) and sieve bends prior to flotation.

A water-only cyclone, which is a hydrocyclone with a short, wide-angle cone and a long vortex finder, is a simple separator with a low cost/high capacity ratio. The
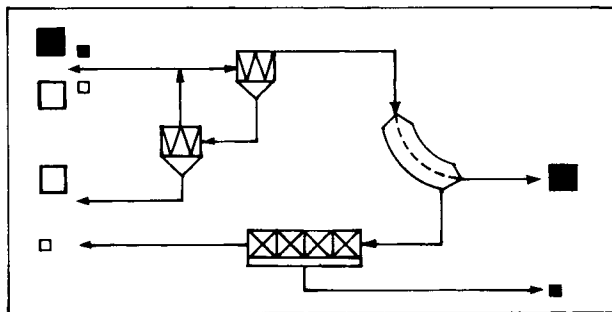
Fig. 7.1. Fine-coal cleaning circuit typical for Canadian coal preparation plants.
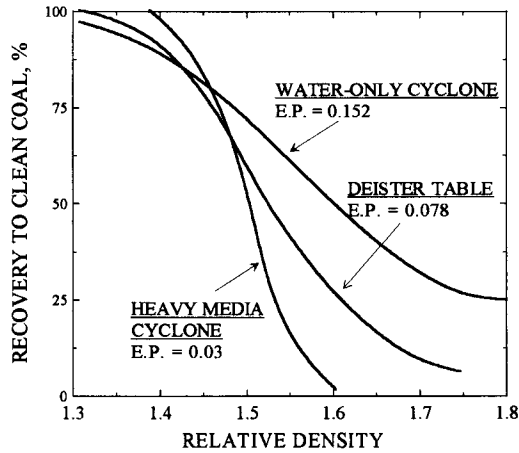
Fig. 7.2. Comparison of performance characteristics for water-only cyclone, concentrating table and dense-medium cyclone. (After O'Brien and Sharpeta [2].)

separation density (cutpoint density, d_{50}) can be controlled by varying the dimensions of the discharge orifices. The cleaned coal ash content can be reduced by decreasing the diameter of the vortex finder or by increasing the diameter of the apex spigot. Also, an increased solids content in the feed increases the cutpoint density. As Fig. 7.2 shows, a WOC is a poor separator with performance that cannot be compared to a dense-medium cyclone (DMC) or concentrating table [2]. Two-stage washing (shown in Fig. 7.1) significantly improves the performance. As generalized partition curves for a primary cyclone and a secondary cyclone and the overall partition curve for both stages indicate (Fig. 7.3), a two-stage combination is characterized by a steeper partition curve and hence lower E_p value [3].

As in all gravity separators, the separation efficiency of a WOC strongly depends on particle size (Fig. 1.4). As Fig. 7.4 demonstrates, for a two-stage WOC circuit the increase of the E_p values with decreasing particle size [4] is not as steep as in a one-stage application [5]. Also, the d_{50} increases with decreasing size of the cleaned coal, and varies from 1.5–1.6 for particles a few millimeters in size to more than 2 for particles approaching 0.1 mm. Typical results of cleaning in a two-stage WOC installation are shown in Fig. 7.5 [2]. The underflow configuration shown in Fig. 7.1 is superior [6].

Separation results in a WOC also depend on the cone angle. Suresh et al. [7] tested a 76-mm diam WOC fitted with different compound cones (the water-only cyclone which consists of three cone angle sections is known as Visman's Tricone). The cone angle of the first section was varied from 80° to 136° while the angles in the other two sections were kept contact (60° and 30°). For the tests in which the percentage of fines in the feed (−0.075 mm) was kept constant, an increase in the cone angle resulted in an increased separation density (d_{50}).

Another device which can handle fine coal particles is the spiral. Fig. 7.6 shows a combination of a classifying cyclone with a modern spiral (e.g. MDL-LD4 spiral)
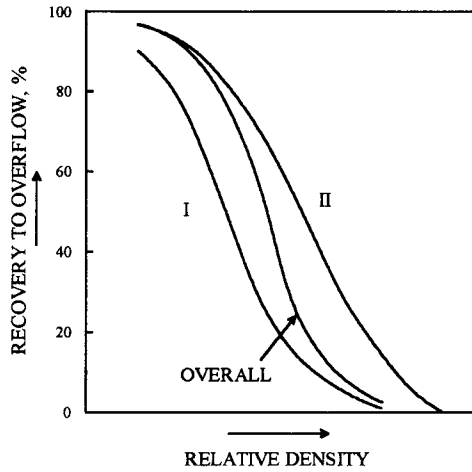
Fig. 7.3. Generalized partition curves for water-only cyclones: I = primary water-only cyclone; II = secondary water-only cyclone. Overall performance of the two-stage water-only cyclone circuit. (After O'Brien and Sharpeta [2].)
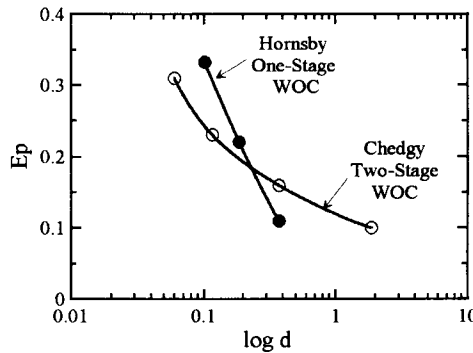
Fig. 7.4. Effect of particle size on separation efficiency of a one-stage water-only cyclone (after Hornsby et al. [5]; by permission of the Australian Coal Preparation Society) and a two-stage water-only cyclone circuit (after Chegdy [4]).

and flotation. This type of arrangement is typical for Australian plants; the WOC-spiral combination in which the spiral is used to "clean up" the reject stream from the WOC is quite popular in the eastern U.S.

It is known that coal finer than 0.075 mm is not beneficiated in a WOC; the separation efficiency of the spiral was also found to decrease sharply below about 0.125 mm [4]. For a given coal ash specification, the 200 mm WOC could be operated at approximately twice the solids capacity of the tested spirals [4]. Other studies confirmed appreciably higher cut points and poorer E_p values for the −0.125 mm particles [7]. Since the slime fraction follows water and reports to the clean coal product stream increasing its ash content, either spiral feed or spiral product must be deslimed. Comparison of a Vicker's

Plus 0.34 mm coal

First cut   Second cut

Coal
6.6% ash

D

Feed
14.2% ash   Feed
                                                   33.3% ash

D_0

D_1

D_2

Refuse
33.3%   Refuse
                                                   49.3% ash

Coal
7.9% ash
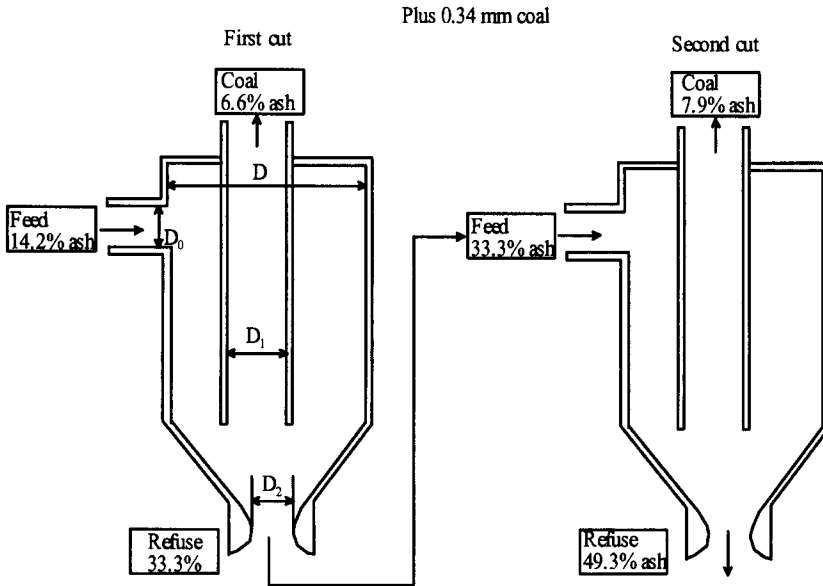
Fig. 7.5. Typical separation results in a two-stage water-only cyclone circuit. (After O'Brien and Sharpeta [2].)

spiral with a WOC gave a sharper separation for the spiral (E_p of 0.27 compared to 0.39 for the WOC at a 1.70 cut-point density) [8,9].

Figs. 7.1 and 7.6 show in a simplified way how heavy (gangue) and light (coal) particles behave depending on their sizes. In circuits incorporating gravity methods and flotation (Figs. 7.1 and 7.6), coarser particles are removed from the feed in the first-stage gravity separation prior to flotation. In the flotation circuit that incorporates classification between two flotation stages (Fig. 7.7, last example), fine coal is recovered first and the rejection of fine gangue in the classifying cyclone follows. Under such conditions the second-stage flotation can easily separate coarser coal from coarser gangue particles
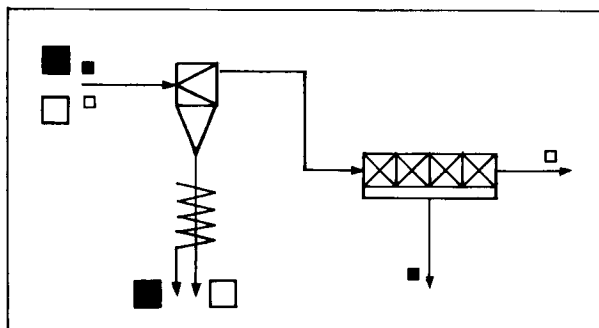
Fig. 7.6. Typical "Australian" fine-coal cleaning circuit.

FLOTATION CIRCUIT		YIELD %	PRODUCT ASH %	TAILINGS ASH %
Single stage flotation		59.6	11.6	27.0
Desliming		60.0	8.2	31.3
Two stage conditioning		51.0	13.0	23.5
Split feed flotation (sands/slime flotation)		65.0	12.8	28.6
Two stage reagant addition		79.6	11.0	43.6
Reflotation of classified tailings		81.0	9.9	58.0

Fig. 7.7. Effect of circuitry on flotation performance: F = feed stream; R = reagent addition points; P = product stream; T = tailings stream. (After Firth et al. [19]; by permission of Elsevier Science.)

provided that it has its own conditioning tank into which some additional reagents are supplied.

Southern Hemisphere coals are much more difficult to wash than coals from Europe and North America. The more difficult a coal is to wash, the more efficient the cleaning methods have to be. As shown in Fig. 7.2, a DMC is a superior separator. The selection of dense-medium separation methods for difficult-to-wash coals is then obvious, and incorporation of a DMC and flotation in a fine-coal cleaning circuit is another interesting proposition.

A two-stage dense-medium cyclone circuit was installed in the colliery situated near Witbank (South Africa) in 1971. The plant treated +0.5 mm feed and produced a 7% ash metallurgical concentrate and 15% ash middlings.

In 1975, the float–sink tests carried out with the −0.5 mm material from this colliery

showed that, at a cut point of about 1.48, a theoretical yield of 58% for a product ash of 7% should be obtained [10]. At this cut point, the yield of the ±0.1 near density material of about 40% indicated, however, that only dense-medium cyclones could be realistically considered. Van der Walt et al. [10] reported that remarkably sharp separations were achieved almost immediately in the 5 t/h dense-medium pilot plant while processing the −0.5 +0.075 mm coal and that there was no difficulty at all in obtaining a reasonable yield of 7% ash coal. They also observed that the main problem was magnetite. For good separation, the magnetite was to be ground finer than usual (to about 50% minus 10 μm) making magnetite recovery difficult.

The first commercial two-stage dense medium plant to process −0.5 mm +0.1 mm coal was built at Greenside Colliery (South Africa). The underflow from the first-stage DMC was diluted with water before being pumped to the second-stage DMC washing for separation into middlings and discard. As pointed out by the authors [10], the plant started up smoothly and produced the desired quality of products virtually from the outset.

More recent data indicate that the plant, which is still in operation, uses magnetite ground to 93% below 45 μm, and operates at an organic efficiency in excess of 90%. This compares favorably with the organic efficiency of about 80% reported for the South African spiral plants [11].

A very interesting development in this area took place in Australia. The original processing plant at the Curragh Mine utilized two-stage dense-medium cyclones to process a −32 +0.5 mm fraction of the feed. The −0.5 +0.075 mm fines were processed in conventional flotation cells to produce a coking coal concentrate, while the −0.075 mm material was discarded along with tailings. Since the flotation plant was needed to recover saleable coal from the sub 0.075 mm fraction, a second DMC circuit was added to treat the −0.5 +0.075 portion of the feed. The flowsheet of the Curragh Mine plant is shown in Fig. 7.8 [12,13].

It is to be pointed out that various pilot-plant trials of fine-coal cleaning in dense-medium cyclones indicated as early as in 1963 that higher inlet pressures and finer magnetite were better for separation [14]. Stoessner et al. [15] reported that in tests on cleaning the −0.6 +0.15 mm coal in a dense-medium cyclone at low separation densities (1.3 g/cm3) the sharpest partition curves were obtained for the finest magnetite. As has been demonstrated [16], only rheological measurements can clarify the complicated effects of magnetite particle size distribution and medium density on dense-medium separation.

The Curragh Mine results confirmed that magnetite particle size distribution is critical in maintaining medium stability and dense-medium cyclone performance. An important feature of the plant was the ability to control the magnetite size distribution. This was achieved by bleeding the reject drain medium out of the fine-coal circuit and replacing it with make-up medium taken from the coarse-coal dense-medium cyclone overflow return. These measures, along with improved Climaxx counter-rotational magnetic separators, provide a continuous replacement of coarse magnetite with fine magnetite and allows the fine-coal circuit magnetite size distribution to be maintained. Another important feature was a much higher inlet pressure. Dense-medium cyclones
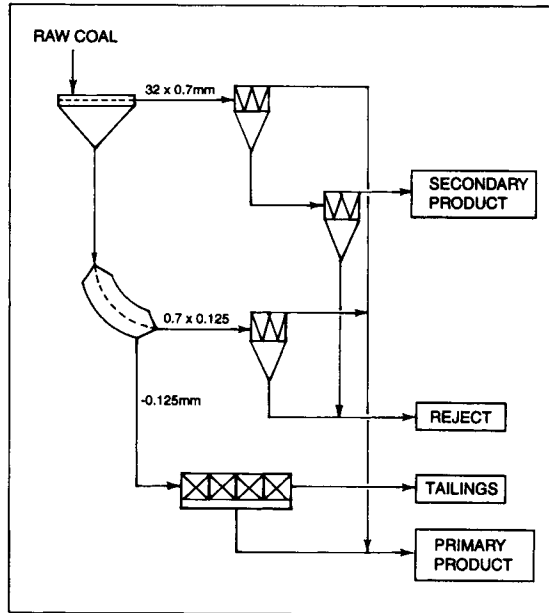
Fig. 7.8. Curragh mine coal preparation plant flowsheet. (After Kempnich et al. [12]; by permission of the Australian Coal Preparation Society.)

are low-pressure devices and traditionally work at a standard inlet pressure of

$$H = 9D\rho \tag{7.1}$$

(where D is the diameter of the cyclone, and ρ is the medium density) which for the Curragh mine DMC was about 45 kPa. An increase in the inlet pressure to 65 kPa improved the E_p in the $+0.25$ mm fraction, but the performance on the -0.25 mm material remained poor. However, a further increase in the inlet pressure to 120 kPa improved efficiency and from this point the overall target product ash of below 7% has been consistently maintained. Low E_p values of 0.04–0.05 were achievable on the $+0.25$ mm material and E_p values in the range of 0.1–0.11 were achievable on the -0.025 mm material. These separation efficiencies are obviously much better than the efficiencies of other separating devices.

7.2. Flotation circuits for difficult-to-float coals

The coal flotation process is based on differences in surface properties between hydrophobic coal particles and hydrophilic high-ash refuse. Coals of various rank have different chemical compositions and physical structures, and as a result their surface properties and floatability change with coalification. While metallurgical coals float easily and may only require a frother, flotation of lower-rank bituminous and subbituminous coals may be difficult. It is thus not surprising that fines of the latter

are usually not floated (type III plant, Figs. 1.1 and 1.8 show type V and type VI, respectively). With the use of thermal coal in the form of coal–water slurries, there is a growing tendency towards producing low-ash (and -sulfur) power generation coal.

Coal flotation circuits, up to the present time, have generally employed a single-stage reagent addition within, or prior to, a bank of flotation cells. However, with the need to treat poorly floating/lower-rank coals, this will have to change. Earlier work has shown that a substantial increase in coal yield can be obtained by collector emulsification and staged reagent addition.

Flotation results are affected by the petrographic composition of coal and the size of particles (Fig. 3.24 [17]). It is rather well established that coarse-coal particles start floating only when fine-coal particles are removed from the cell [18]. It is therefore also possible to improve flotation results by incorporating classification between the two stages of flotation to remove fine gangue particles from the rougher tailings after floating off fine coal particles and prior to floating coarser coal in the second stage (Fig. 7.7, last example).

In a paper by Firth et al. [19], an Australian coal with poor flotation characteristics was used to investigate a number of possible flotation circuits. These circuit configurations, which were simulated on a laboratory scale, are listed in Fig. 7.7.

The last circuit in Fig. 7.7 (reflotation of classified tailings) includes the classification of the tailings from rougher flotation with rejection of fine gangue prior to refloating the coarser material in the scavenger cells. This creates better conditions for flotation of coarse particles in the scavenger cells. In the flowsheet shown in Fig. 7.1 (typical for Canadian plants), the overflow from water-only cyclones (which contains fine and coarse coal and fine gangue particles) is screened to remove coarse coal prior to flotation. Both circuits recognize the problem: the particles in the $-0.5 +0.2$ mm range which float with difficulty under normal conditions. In the flowsheet shown in Fig. 7.1 these particles are removed from the flotation stream, and in the last circuit shown in Fig. 7.7, special conditions are created in the scavenger cells to improve the flotation of such particles. For a high-sulfur coal, the flowsheets in Figs. 7.1 and 7.6 that incorporate both flotation and gravity separation can be expected to perform better. In all these cases reagent emulsification and stage addition would further improve the overall results.

7.3. Advanced coal flotation circuits

Cleaning of rougher concentrates is a well established technique in the mineral industry for improving concentrate grade. Low-grade material which is initially floated in the rougher cells is rejected as tailings on subsequent refloats. This is possible because part of the solids in the rougher froth consists of slimes which enter the froth by entrainment. The concentration of slimes in the froth water is similar to that in the pulp from which the froth came. Thus by diluting the froth with clean water and refloating, the concentration of slime in the next froth will be reduced. Fig. 7.9 shows an example of cleaning taken from Nicol [20]. In coal preparation, the cost of any extra flotation capacity is usually considered to outweigh the advantage of a cleaner product. As Fig. 7.9 shows, the reduction in ash content in the final product is accompanied by

ROUGHER CELLS
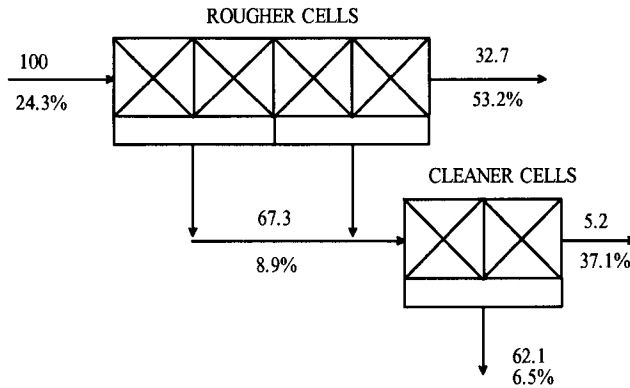
Fig. 7.9. Rougher–cleaner flotation in fine-coal processing. (After Nicol [20]; by permission of the Australian Coal Preparation Society.)
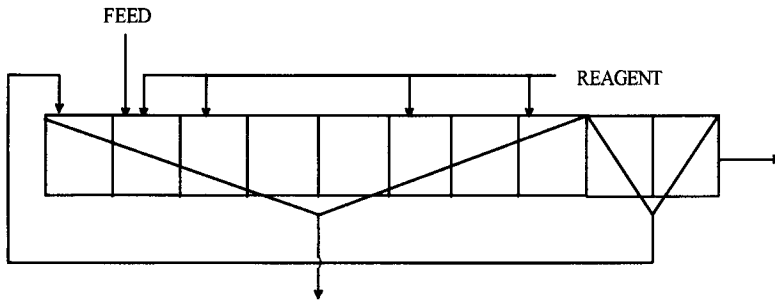
Fig. 7.10. Rougher–scavenger–cleaner flotation circuit in one of the coal preparation plants in the Czech Republic. (After Dedek et al. [21].)

the second by-product (tailings from cleaning); such a circuit may be justifiable only when a low-ash product is needed (e.g. for coal water fuels) and also when there is a market for the second product that is higher in ash.

Fig. 7.10 shows an interesting flotation circuit of one of the coal preparation plants in the Czech Republic [21]. Cells 2 to 8 work as roughers, and 9 to 10 as scavengers from which the concentrate is recirculated to cell 1 for cleaning. The circuit also involves stage addition of reagents as shown below.

The circuit in Fig. 7.11 includes both emulsification and stage addition of reagents. Emulsification of an oily collector is aided by some amount of frother; the major part of the frother is supplied directly to various cells. Of course, this type of arrangement can work with any previously discussed flowsheets.

A new multi-unit fine-coal cleaning circuit has been developed at the Center for Coal and Minerals Processing (CCMP at Virginia Tech, Blacksburg, Va.) [22]. The circuit consists of a Microcel flotation column and a Mozley Multi-Gravity flowing film separator (MGS). The Microcel column uses small air bubbles to improve the flotation recovery of fine coal, while the MGS utilizes centrifugal forces to enhance the gravity
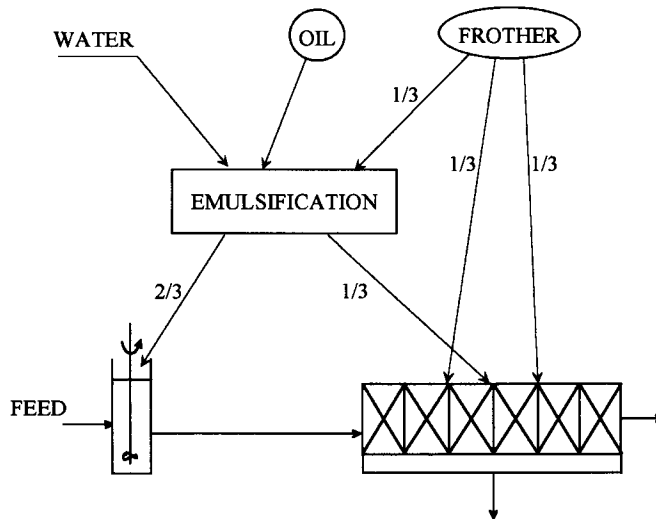
Fig. 7.11. A general concept showing a fine-coal flotation circuit with emulsification of oily collector and stage addition of reagents.

separation of fine pyrite. These two unit operations were compared by conducting laboratory tests using a -230 μm coal sample from the Illinois No. 5 seam.

The MGS was found to be very effective in rejecting particles containing a high-density component such as pyrite. Since Microcel is more efficient in rejecting fine clay particles, precleaning using the Microcel and then cleaning using the MGS produced good rejections of both pyrite and ash. These results suggest that the Microcel and MGS separators may be combined in a single circuit to maximize the rejection of both ash-forming minerals and pyrite.

The pilot plant tests were carried out at the Pittsburgh Energy Technology Center. The froth products from the Microcel unit were typically 6–8% lower in ash than the concentrates obtained using the MGS. This was attributed to the ability of column flotation to reject clay minerals which are too fine to be separated in a density-based separator. In contrast, the concentrates obtained using the MGS contained 0.5–0.7% less pyritic sulfur than those obtained by flotation. This confirms that the MGS is more efficient at rejecting coal-pyrite middlings than surface-based flotation techniques are.

The tests in which the froth product from the Microcel was passed through a foam-breaker and then processed in the MGS gave ash rejections slightly better than those obtained using the Microcel alone. The combination also gave pyritic sulfur rejections better than those obtained using the MGS alone. According to the authors [22], the major benefit of the combined Microcel/MGS circuit is that it allows high levels of pyrite sulfur rejection without fine grinding.

A number of fine-coal cleaning circuits that incorporate the so-called enhanced gravity separators and flotation have been studied over the last decade. The enhanced gravity separators based on using centrifugal force to enhance the separation of fine particles include: Multi-Gravity Separator (MDS), the Kelsey Centrifugal Jig [23], the

Falcon Concentrator [24–26], and the magnetite dense-medium Falcon Concentrator [27].

A new type of centrifugal jig, the Kelsey Centrifugal Jig, was developed by GeoLogics Pty Ltd Australia for processing of fine particles. Riley and Firth's results [23] showed that this jig is capable of cleaning fine coal (down to 0.038 mm) at relative densities as low as 1.6.

Another continuous separator that utilizes centrifugal forces to effectively treat fine particles is the Falcon Concentrator. The essential feature of this concentrator is a vertically aligned, open-top cylindrical bowl which is mounted on a revolvable shaft. The bowl speed can be adjusted so that up to 300 g of centrifugal force can be produced to cause deposition and stratification of the fine particles against the inside wall of a smooth centrifugal bowl. The coal slurry is continuously introduced at the bottom of the spinning bowl and is impelled to the wall of the bowl by an impeller, thereby causing stratification along the inclined lower section of the bowl (the migration zone). The strong force component normal to the wall is the concentrating gravity force that allows the hindered settling and stratification of the particles in the feed according to (i) density, and (ii) particle size. The weak driving component parallel to the wall of the bowl pushes the stratified material toward the top of the bowl. During the upward movement, heavy particles and coarse light particles continue to form a bed on the bowl surface with the heavy particles forming a layer nearest the wall. Because the upper part of the bowl (the retention zone) is parallel to the axis of rotation, the driving force component to push particles upward toward the top of the bowl is very weak; this tendency is further limited by the overflow lip with internal diameter smaller than the bowl diameter. The combination of the lack of a vertical force component and the presence of an overflow lip cause the heavy (pyrite and high-ash) particles to exit through a slot (around the circumference of the bowl) and light particles to move upward and overflow the lip of the bowl. These fine particles report as final product along with other particles that are too fine to be affected by the enhanced gravitational force. A 25-cm diameter unit (C10 Falcon Concentrator) [25] and a 100-cm diameter unit (C40 Falcon Concentrator) with a capacity of 75 t/h [26] have been tested by Honaker and his co-workers. For a −1 mm +0.075 mm coal the unit cleaned at $d_{50} = 1.6$ and $E_p = 0.12$. Processing of the +37 μm coal containing 14.1% ash and 3.49% sulfur gave the clean coal product with 6.3% ash and 1.94% sulfur at 92.4% coal recovery. On the basis of product ash content, the most effective separation was achieved by cleaning the −75 μm size fractions using a froth flotation while processing the +75 μm fractions in the Falcon Concentrator. On the basis of total sulfur reductions, the most efficient was the treatment of the +37 μm fractions in the Falcon Concentrator, and the −37 μm material by froth flotation [26]. Since the Falcon offers higher throughputs than other enhanced gravity separators at excellent separation performance, there is a good chance that this technology will eventually be commercialized.

Further improvements that have recently been reported [27] include the use of magnetite dense medium in a continuous C10 Falcon Concentrator. For −1 mm +44 μm easy-to-clean coal, the use of dense medium resulted in 8% increase in the clean coal yield compared to the standard use of water medium. For a difficult-to-clean coal, the yield of clean coal increased nearly by 20% at organic efficiency exceeding 90%.

The -1 mm $+44$ μm coal was processed at E_p values of less than 0.05 and at a low separation density $(d_{50} = 1.42)$.

7.4. References

[1] W.R. Forrest, G.T. Adel and R.H. Yoon, Characterizing coal flotation performance using release analysis. Coal Preparation, 14 (1994) 13.

[2] E.J. O'Brien and K.J. Sharpeta, Water-only cyclones: their function and performance. In: P. Merit (ed.), Coal Age Operating Handbook of Preparation. McGraw-Hill, New York, 1978, pp. 114–118.

[3] G. Ferrara, H.J. Ruft and A. Schena, Improvement of coal preparation by dynamic multistage dense medium process. Proc. 10th Int. Coal Preparation Congr., Edmonton, 1986, Vol. 1, pp. 9–27.

[4] D.L. Chedgy, Optimized preparation of fine coal. SME Annual Meeting, New York, 1986, Preprint 86–22.

[5] D.T. Hornsby, S.J. Watson and C.J. Clarkson, Fine coal cleaning by spiral and water washing cyclone. In: R.L. Whitmore (ed.), Procceedings of the 2nd Australian Coal Preparation Conference. Coal Preparation Societies of New South Wales and Queensland, Rockhampton, 1983, pp. 83–106.

[6] P.T. Luckie, Alternatives to surface chemical methods for fine coal processing. In: S.K. Mishra and R.R. Klimpel (eds), Fine Coal Processing. Noyes Publ., Park Ridge, NJ, 1987, pp. 205–224.

[7] N. Suresh, M. Vanangamudi and T.C. Rao, Effect of cone angle on separation characteristics of compound water-only cyclone. Miner. Metall. Process., 6 (1989) 130.

[8] W.G. Weale and A.R. Swanson, Some aspects of spiral plant design and operation. Proc. 5th Australian Coal Preparation Conf., Newcastle, 1991, pp. 98–110.

[9] W.G. Weale, L. Geczy, D. Johns and J. Moore, The role of water washing cyclone circuits in upgraded coal preparation plants at Newdell and Bayswater. In: J.J. Davis (ed.), Proceedings of the 6th Australian Coal Preparation Conference. Australian Coal Preparation Society, Mackay, 1993, pp. 60–85.

[10] P.J. van der Walt, L.M. Falcon and P.J.F. Fourie, Dense medium separation of minus 0.5 mm coal fines. In: A.R. Swanson (ed.), Proceedings of the 1st Australian Coal Preparation Conference, Coal Preparation Societies of New South Wales and Queensland, Newcastle, 1981, pp. 207–219.

[11] M.C. Harris and J.-P. Franzidis, A survey of fine coal treatment practice in South Africa. Colloq. Coal Processing, Utilisation and Control of Emissions, SAIMM, Mintek, 1995.

[12] R.J. Kempnich, S. van Barneveld and A. Luscan, Dense medium cyclones on fine coal — the Australian experience. In: J.J. Davis (ed.), Proceedings of the 6th Australian Coal Preparation Conference. Australian Coal Preparation Society, Mackay, 1993, pp. 272–288.

[13] R.J. Kempnich, S. van Barneveld and A. Lusan, Dense medium cyclones on fine coal — the Australian experience. In: W. Blaschke (ed.), New Trends in Coal Preparation Technologies and Equipment. Proc. 12th Int. Coal Preparation Congr. (Cracow, 1994), Gordon and Breach, New York, 1996, pp. 843–850.

[14] M.R. Geer and M. Sokaski, Cleaning Unisized fine coal in a DMC pilot plant. U.S. Bureau of Mines Report No. 6274, 1963.

[15] R.D. Stoessner, D.G. Chedgy and E.A. Zawadzki, Heavy medium cyclone cleaning 28 100 mesh raw coal. In: R.R. Klimpel and P.T. Luskie (eds), Industrial Practice of Fine Coal Processing. SME, Littleton, 1988, pp. 57–64.

[16] Y.B. He and J.S. Laskowski, Dense medium cyclone separation of fine particles, Parts I and II. Coal Preparation, 16 (1995) 1, 27.

[17] V.I. Klassen, Coal Flotation. Gosgortiekhizdat, Moscow, 1963 (in Russian).

[18] B.A. Firth, A.S. Swanson and S.K. Nicol, The influence of feed size distribution on the staged flotation of poorly floating coals. Proc. Australas. IMM, 267 (1978) 49.

[19] B.A. Firth, A.S. Swanson and S.K. Nicol, Flotation circuits for poorly floating coals. Int. J. Miner. Process., 5 (1979) 321.

[20] S.K. Nicol, Fine Coal Beneficiation. Australian Coal Preparation Society, Advanced Coal Preparation Monographs, Vol. IV, Part 9, 1992, pp. 107–108

[21] F. Dedek, G. Sebor, M. Barcal and V. Bortlik, Development of the theory and practice of coal flotation in Czech Republic. Proc. 8th Int. Coal Preparation Congr., Donetsk, 1979, Paper C-7.

[22] P. Venkatraman, G.H. Luttrell, R.H. Yoon, F.S. Knoll, W.S. Kow and M.J. Mankosa, Fine coal cleaning using the multi-gravity separator. In: S.K. Kawatra (ed.), High Efficiency Coal Preparation: An International Symposium. SME, 1995, pp. 109–117.

[23] D. Riley and B. Firth, Enhanced gravity separation. In: J.J. Davis (ed.), Proceddings of the 6th Australian Coal Preparation Conference. Australian Coal Preparation Society, Mackay, 1993, pp. 135–157.

[24] R.Q. Honaker, B.C. Paul, D. Wang and M. Huang, Application of centrifugal washing for fine-coal cleaning. Miner. Metall. Process., 8 (1995) 80.

[25] R.Q. Honaker, D. Wang and K. Ho, Application of the Falcon concentrator for fine coal cleaning. Miner. Eng., 9 (1996) 1143.

[26] R.Q. Honaker, High capacity fine coal cleaning using an enhanced gravity concentrator. Miner. Eng., 11 (1998) 1191.

[27] R.Q. Honaker, N. Singh and B. Govindarajan, Application of dense-medium in an enhanced gravity separator for fine coal cleaning. Miner. Eng., 13 (2000) 415.

This Page Intentionally Left Blank

Chapter 8

FLOTATION MACHINES

8.1. Introduction

Separation of minerals by flotation involves selective concentration of hydrophobic minerals in the froth. The selectivity is based on wettability differences of the treated minerals with only hydrophobic particles being able to attach to bubbles (Fig. 8.1). The process is accomplished in a flotation cell. The necessary conditions in the cells for the attachment are an effective distribution of particles and air bubbles throughout the cell volume, and the accompanying hydrodynamic conditions necessary for the collision and attachment to take place. However, very fine particles can also enter the froth by entrainment along with the pulp. Thus, the overall selectivity is determined by differences in the flotation rates with which different mineral particles are carried over to the final product.

As is now generally recognized, the froth flotation kinetics involve several mass transfer processes [1]: (i) selective transfer of material from the slurry to the froth

O   Bubbles

■   Hydrophobic mineral particles

□   Hydrophilic mineral particles
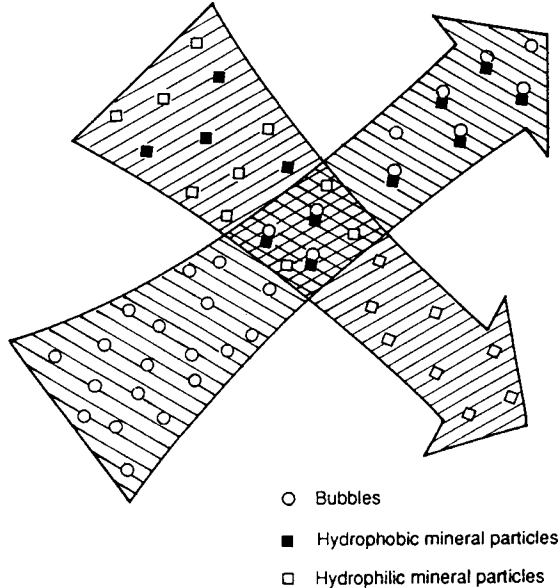
Fig. 8.1. Separation of hydrophobic from hydrophilic particles in flotation.

by particle–bubble attachment: (ii) non-selective transfer of material from the slurry to the froth by mechanical and hydraulic entrainment; (iii) return (both selective and non-selective) of material from the froth to the slurry through froth drainage; (iv) mechanically or hydraulically induced material transport from the froth over the cell lip into the concentrate products.

While (i) takes place in a pulp and is now referred to as collection zone kinetics, (ii), (iii) and (iv) involve the processes taking place in a froth.

8.1.1. Collection zone kinetics

Flotation kinetics resemble chemical kinetics [2]. The latter is concerned with interactions between atoms, molecules or ions. In the chemical reaction

$$A + B = C \tag{8.1}$$

in which one of the reactants is in such a large excess that its concentration practically does not change with time (e.g. when the solvent serves as one of the reactants), a first-order equation adequately describes the rate of the reaction.

In a flotation process, mineral particles collide with bubbles (Fig. 8.1); flotation kinetics thus deals with interactions between particles and bubbles. The particles are classified as floatable if they successfully attach to air bubbles and are removed with them from the pulp. So, in the reaction

$$\text{solid particle} + \text{bubble} = \text{particle–bubble aggregate} \tag{8.2}$$
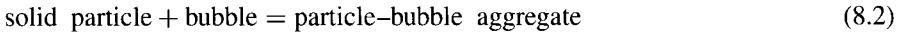
the rate of removal of the solid particles from a cell is second order with respect to the concentration of those particles and bubbles, but if it is assumed that the bubble surface is in excess, then the rate equation is reduced to the first-order relation (the assumptions made here also require that the particle–bubble aggregate is removed from the system once formed and this implies no drop-back from the froth). Commonly, the general rate equation is written as

$$-\frac{dC}{dt} = kC^n \tag{8.3}$$

where $n = 1$ (first-order reaction).

For solid particles concentration $C = C_0$ when $t = 0$, and integration leads to

$$C = C_0 e^{-kt} \tag{8.4}$$

where C is the floatable mineral concentration remaining in a cell at time t, and k is the flotation rate constant (dimensions of reciprocal time).

For graphical representation Eq. (8.4) is commonly written as

$$\ln \frac{C}{C_0} = -kt \tag{8.5}$$

and since recovery

$$R = \frac{C_0 - C}{C_0}$$
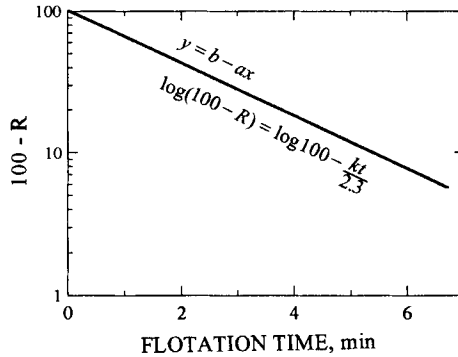
Fig. 8.2. Semi-log plot used to calculate the flotation rate constant.

Eq. (8.4) converts into

$$R = 1 = e^{-kt} \tag{8.6}$$

Letting R be R_∞ at $t = t_\infty$ it follows that: [1]

$$R = R_\infty(1 - e^{-kt}) \tag{8.7}$$

Eq. (8.6) results in a straight line if plotted on a semilog grid (Fig. 8.2). Using percent recovery Eq. (8.6) is equivalent to

$$\ln\left(\frac{100 - R}{100}\right) = -kt$$

or as shown in Fig. 8.2

$$\log(100 - R) = \log 100 - \frac{kt}{2.3}$$

Bogdanov et al. [4] conclude that since these equations were derived assuming an excess of air bubbles under the conditions of "inhibited flotation" [5], that is, the flotation in which the surface area of bubbles is not sufficiently large for the number of floatable particles, the amount floating at the beginning of the experiment will be lower than predicted. This will lead to changes in the value of the calculated constant k with time (according to Inoue et al. [6] this may lead to zero-order kinetics with the recovery rate being independent of the solid content present in the pulp). In the flotation kinetic equations, k is a complex function involving (among other things) particle and bubble sizes, reagent concentration, and flotation cell hydrodynamics. Although it is generally accepted that flotation recovery follows first-order kinetics [7], experimental evidence suggests that the order of the process may vary [4,8,9].

---

[1] As pointed out by Agar et al. [3], in laboratory batch flotation tests the rate equation is seldom exactly followed because of the difficulty of precisely assigning time zero (the time when the froth first flows over the lip of the cell). To overcome this difficulty, it was suggested to introduce the time lag correction:

$$R = R_\infty(1 - e^{-k(t+\phi)})$$

where ϕ is the lag time.

All equations discussed so far (Eqs. (8.1)–(8.7)) did not consider the effect of froth on the process and so they all apply only to the flotation collection zone. Flotation kinetic equations for the collection zone can also be derived by applying hydrodynamics to a particle–bubble encounter.

This can be obtained by putting

$$R = P_c \times P_a \times P_s \tag{8.8}$$

where chance of recovery R is the product of the probability of particle–bubble collision P_c, the probability of attachment P_a, and the probability of the formation of a stable particle–bubble aggregate P_s.

The collision probability is entirely determined by hydrodynamics and has attracted a great deal of attention [10–19]. Working with a very hydrophobic coal for which $P_a = 1$ could be assumed, Yoon and Luttrell [17] have demonstrated that for a first-order process the flotation rate constant

$$K = \frac{6 P Q_g}{\pi d_b D_c^2} \tag{8.9}$$

where P is the probability of collection (assuming $P_a = 1$ and $P_s = 1$, $P = P_c$), Q_g is the volumetric flow rate of gas (air), d_b is the bubble diameter and D_c is the cylindrical flotation cell diameter.

By putting [20]

$$J_g = \frac{Q_g}{A_c} \tag{8.10}$$

where J_g is the superficial gas rate, and A_c is the column cross-sectional area ($A_c = (\pi/4)D_c^2$) from Eq. (8.9) and Eq. (8.10) one can get Eq. (8.11) which was first derived by Jameson et al. [16]:

$$k = k_c = \frac{1.5 J_g P}{d_b} \tag{8.11}$$

Since the flotation rate constant is now rigorously used for the processes taking place in pulp only (collection zone), it is often denoted as k_c. This equation clearly states that the first-order rate constant depends on the superficial gas rate, on the probabilities of collision and attachment (which in turn depend on the size of the bubbles and particles, and on particle surface properties), and on bubble size.

There is a great deal of experimental evidence showing that the flotation rate constant is dependent on the air flow rate [21,22]. However, it was only recently demonstrated by Gorain et al. [23–25] and by O'Connor and Mills [26] how these relationships can be used in modeling flotation processes. As was shown, the flotation rate correlates poorly with bubble size; the correlation improves on going from bubble size to gas holdup and superficial gas velocity. Gas holdup (which is a measure of the amount of air per unit volume of pulp) does correlate better with k than does bubble size, but on its own does not correlate very well with k either. Of the three indicators of cell hydrodynamics investigated, the one which correlated best with the flotation rate was the superficial gas velocity. It is clear, however, that it is not the same whether there are a few large bubbles or thousands of small bubbles, and so the superficial gas velocity on its own cannot

properly describe these effects [25]. A term which incorporates both the superficial gas velocity and the bubble size (the Sauter mean bubble diameter) is the bubble surface area flux, S_b, which is defined as [20]

$$S_b = \frac{6 J_g}{d_{32}} \tag{8.12}$$

Commonly S_b is expressed in $m^2\ m^{-2}\ s^{-1}$ (m^2 bubble area per m^2 column area per seconde), J_g in m/s, and d_{32} in m.

The Sauter bubble diameter can be calculated from the bubble size as follows:

$$d_{32} = \frac{6V}{A} = \frac{6 \sum \frac{1}{6} \pi d_b^3}{\sum \pi d_b^2} = \frac{\sum d_b^3}{\sum d_b^2} \tag{8.13}$$

where d_b is the bubble size as measured, for example, using the UCT bubble sizer [27].

The most significant result obtained by Franzidis' team [25] is that a linear relationship exists between k and S_b which is independent of the impeller type. In order to obtain the same kinetics from different flotation machines for a particular ore, each machine must be manipulated with respect to its design and operating parameters (impeller speed, air flow rate) to produce the same bubble surface area flux. Dispersion of gas into bubbles is the heart of the flotation process irrespective of the type or design of flotation cell. If bubble surface area flux can be related to the flotation rate in mechanical cells, this should also be applicable to any other flotation cell (e.g. flotation columns) [2].

All commercial separations are carried out in continuous reactors, which means that any particle has a finite time to respond to the separating mechanism. To fully analyze the extent of processing in any continuous process, it is therefore necessary to know how long the material takes to proceed from the inlet to the outlet. To estimate these residence times it is necessary to know the flow patterns in the device. The patterns can be determined by injecting an impulse tracer of a conveniently detectable material into the flow device and following its emergence through the output streams [28].

The simplest type of flow pattern through a process is when all elements of the feed stream have an equal residence time t in the device; this is the so-called plug flow. It is believed that plug flow conditions prevail in a batch processing system (i.e. Eq. (8.6) and Eq. (8.7) hold for plug flow conditions).

In the case of perfect mixing, any input is immediately dispersed uniformly throughout the whole volume of the device. Some of the tracer leaves instantaneously, while some theoretically never leaves, so there is a distribution of residence time from zero to infinity. For the continuous flotation cell with perfect mixing, the residence time distribution $E(t)$ is given by [29]

$$E(t) = \frac{1}{\tau} e^{-t/\tau} \tag{8.14}$$

where the residence time (see Fig. 8.3)

---

[2] From Eq. (8.11) and Eq. (8.12) one gets $k = \frac{1}{4} P S_b$. While this relationship shows that k is linearly related to S_b, this should not be used to imply that doubling S_b will necessarily double k since P also seems to be dependent on some of the factors that influence S_b.
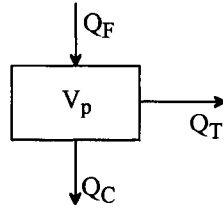
Fig. 8.3. Sketch of a single flotation cell showing nomenclature used in the text.

$$\tau = \frac{V_p}{Q_T} \tag{8.15}$$

So, for the case of a perfectly mixed cell Eq. (8.4) becomes

$$C = C_0 \int_0^\infty \exp(-kt)E(t)\,dt \tag{8.16}$$

This leads to Eqs. (8.17)–(8.20) which can be used to calculate the cumulative fractional recovery of a floatable component from N perfectly mixed cells [2,29]:

$$R_1 = \frac{k\tau}{1+k\tau} \tag{8.17}$$

$$R_2 = R_1(1-R_1) \tag{8.18}$$

$$R_3 = R_1(1-R_1)^2 \tag{8.19}$$

$$R_N = R_1(1-R_1)^{N-1} \tag{8.20}$$

So, total recovery from the bank of N cells is

$$R = R_1 + R_2 + \ldots R_N = 1 - (1+k\tau)^{-N} \tag{8.21}$$

It is to be pointed out that all the derived equations assume that all particles possess identical flotation properties ($k =$ const). If the particles are characterized by a continuous range of rate constants Eq. (8.16) further complicates things as discussed by Lynch et al. [29].

8.1.2. Effect of froth on flotation kinetics

As is clear from Fig. 8.4, the overall flotation rate constant — that is, the constant for the overall process accounting for both the collection zone and froth zone — depends on the froth thickness [1,21]. For the whole tested range of air flows the overall flotation rate constant decreases with the froth thickness. Of course, this results from the dropback of material from the froth to the slurry, which is responsible for additional upgrading in a froth layer; for froth thickness $h = 0$, $R_0 = R_c$, but $R_0 < R_c$ for $h \neq 0$ (where R_0 is the overall recovery, and R_c is the collection zone recovery).

The additional upgrading is very important in commercial froth flotation operations. Because of this phenomenon, plant froth varies in thickness depending on the desired
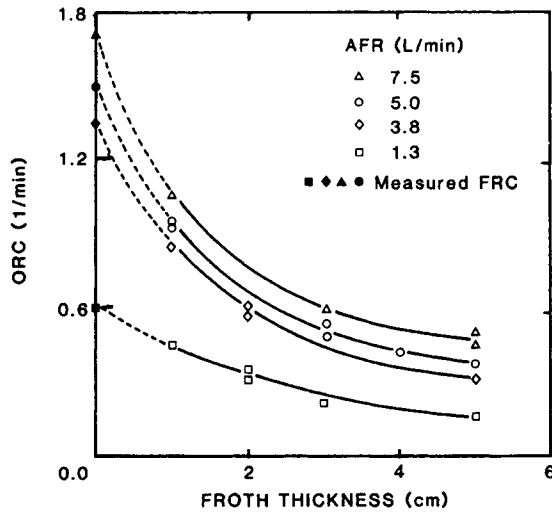
Fig. 8.4. Overall rate constant versus froth thickness at different air flow rates. (After Kaya and Laplante [21]; by permission of Gordon and Breach.)
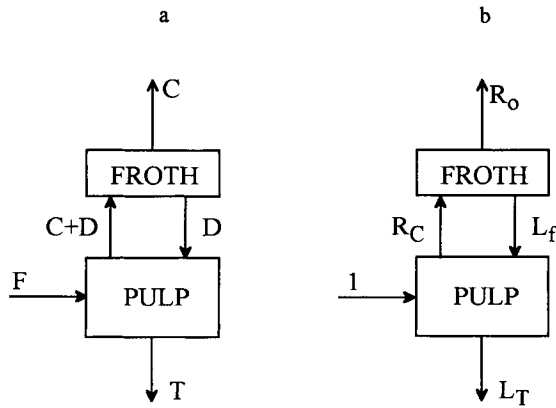
Fig. 8.5. Relationships between collection and froth zones.

objective. In cleaner stages in which the final froth product grade is important, thick froth is used. Since additional recovery is a major objective of scavenger flotation, thin froth is used to favor recovery. Rougher froth is a compromise between grade and recovery.

Fig. 8.5 explains the relationships in a two-phase flotation process. Falutsu and Doby [30] used a specially constructed flotation column to study the dropback.

If the same notation as in Fig. 8.5a is followed

$$F = C + T \tag{8.22}$$

Then

$$R_c = \frac{C + D}{C + T} \tag{8.23}$$

$$R_0 = \frac{C}{C + T} \tag{8.24}$$

Loss to tailings is

$$L_T = \frac{T}{C + T} \tag{8.25}$$

Dropback loss from froth is

$$L_f = R_c - R_0 = \frac{D}{C + T} \tag{8.26}$$

Following notations as in Fig. 8.5b, generally

$$R_c = R_0 + L_f \tag{8.27}$$

and at froth thickness $h = 0$, $L_f = 0$ and $R_c = R_o$.

Gorain et al. [31,32] have shown that for shallow froth

$$k_0 = k_c = P \times S_b \tag{8.28}$$

where P represents the floatability of the mineral.

However, for a thick froth this relationship deviates from linearity and so [33]

$$k_0 = P \times S_b \times R_f \tag{8.29}$$

where R_f is the so-called froth factor. As derived by Finch and Dobby [20], it is given by

$$R_f = \frac{k_0}{k_c} \tag{8.30}$$

Following the notations in Fig. 8.6, the following formula that also incorporates R_f can be derived for the column recovery [20]:

$$R_0 = \frac{R_c R_f}{R_c R_f + 1 - R_c} \tag{8.31}$$

when $R_f = 1$, $R_0 = R_c$.

8.2. Coal flotation versus mineral flotation

There are many important differences between coal flotation and mineral flotation. Fig. 8.7 shows simplified coal and ore flotation circuits. As this figure explains, unlike in ore flotation, the coal flotation plant does not treat a pulp prepared by grinding and classification, but treats "slurry", which is a pulp containing fines arising from various stages of coal preparation. The fines sent to the coal flotation section come from different unit operations and may be exposed to the environment and to various

$$R_f R_c$$

CLEANING
ZONE

$$R_c$$

$$R_c(1-R_f)$$

1   F=X

COLLECTION
ZONE

Column Recovery

$$R_{col} = \frac{R_f R_c}{R_f R_c + (1-R_c)}$$

$$1-R_c$$
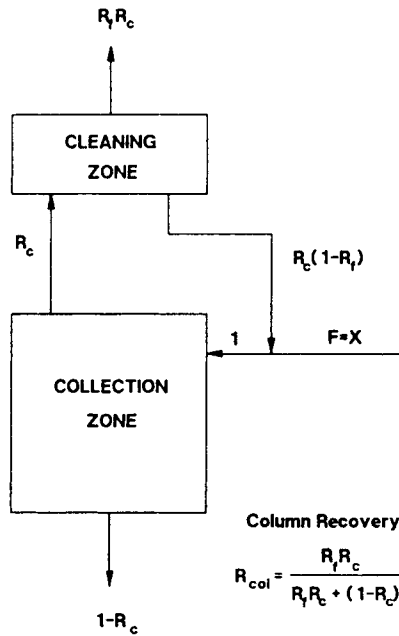
Fig. 8.6. Conceptual configuration of collection and froth zones in flotation column. (After Finch and Doby [20]; by permission of Elsevier Science.)

a   b

ROM COAL   REJECT

ROM ORE

SCREENING   COARSE   GRAVITY
                                SEPARATION

CRUSHING

WATER   INTERMEDIATE

GRINDING   FINES

CLASSIFICATION   GRAVITY
   +   −   SEPARATION

FLOTATION   FLOTATION

CONC.   TAILS   CLEAN
                                                 COAL
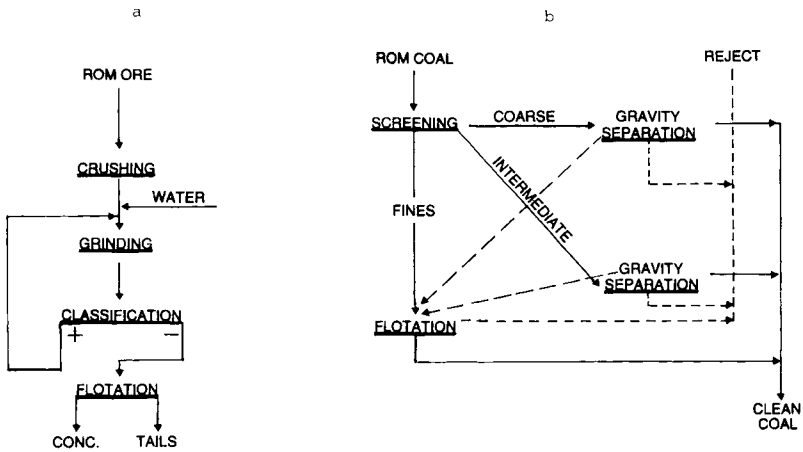
Fig. 8.7. Simplified flowsheets of mineral processing plant (a) and coal preparation plant (b).

chemical reagents for quite a long time prior to flotation. According to Klassen [34], the most important and most obvious feature that distinguishes coal flotation from all other ore flotation systems is a high yield of easily floatable coal particles.

The major differences between coal and sulfide ore flotation are set out in a simplified form in Table 8.1. In spite of these differences, as put Aplan [35] it, the basic coal froth

Table 8.1
Major features of coal and sulfide ore flotation systems

Factor	Coal flotation	Ore flotation
Properties of floatable component	Low-density (1.5 g/cm^3) hydrophobic	High-density (3–5 g/cm^3) hydrophilic
Reagents	Water-insoluble oily collectors and frothers	Water-soluble ionic collectors; various modifiers and frothers
Froth product yield (%)	70–80	Not higher than about 10%
Particle size	Below 0.5 mm	Below about 0.15 mm
Flotation feed source	Fines from ROM coal obtained by classification	Prepared by grinding ore down to liberation size

flotation technology was derived from its ore flotation sibling. It is obvious then that direct transfer of ore flotation technology and machines to coal processing plants must have created serious problems, and this probably explains why coal flotation technology lagged far behind the technology of ore flotation.

Since coal particles are characterized by low density and high natural hydrophobicity (and the yield of such particles in the coal flotation feed is very high), the flotation machine utilized to float coal should be characterized primarily by a high bubble surface area flux (S_b), and also by the ability to handle large volumes of froth product. The use of flotation cells developed for ore flotation that were designed to handle high pulp volumes but low yields of the froth products at long retention times did not fit such an application very well.

8.3. Classification of flotation machines

Many different flotation machines are available. The machine classification systems may be based on different factors. In the most common approach, the machines are classified as "mechanical", which are clearly the most common, and "non-mechanical". The former use impellers, while the latter do not. In mechanical machines, the impellers may be required to (i) circulate the pulp and suspend solid particles, (ii) draw in adequate quantities of air and disperse it into fine bubbles, and (iii) provide sufficient mixing of the air and solid particle streams (subaeration, or self-aerating machines), or in addition to (i) and (iii) may only disperse the air supplied from the external blower into fine bubbles (supercharged, or pneumo-mechanical machines). While cell-to-cell arrangement in a bank is characteristic for the subaeration cells, the open-flow design is common for the supercharged machines.

The non-mechanical machines include first of all the pneumatic machines which rely on compressed air to agitate the pulp. Another non-mechanical type is the "air precipitation machine" [36] in which bubbles of air precipitate from solution. This can be achieved either by decreasing pressure above the pulp (vacuum machines), or by oversaturating the pulp with pressurized air which is then released. The former takes

place in the vacuum machines which were used in the past in England (Elmore design [37]), while the latter mechanism is claimed to play a leading role in the air-lift flotation machine [34,38] which is also a very good example of the class of flotation machines termed reactor/separator machines by Finch [39]. The precipitation of bubbles directly onto hydrophobic solids is likely to play an important role in many other types of flotation machines as well.

While the mechanical machines are still the most common, the use of the flotation columns has been rapidly growing. In the classification adopted in this book, they will be listed in the class of "pneumatic machines".

In the froth separation the feed is introduced directly into the froth phase and these machines will be discussed separately. In Nicol's book [40] such a cell is referred to as a sprayflot cell.

As observed by Klassen and Mokrousov [36], "air is the working element in a flotation system" and the classification of flotation machines should be based on aeration processes. The most recent publications all confirm that the extent of pulp aeration determines the quality of flotation machines and their overall performance. Identification of the bubble area flux as a primary factor determining flotation performance adds weigh to such statements [25]. However, this information is not yet always available.

Fig. 8.8 shows the estimate of the bubble area flux, S_b, for different flotation machines [41]. As this figure indicates, the batch flotation cells used in labs produce low S_b values, mainly because these devices can only handle low J_g and generate bubble sizes greater than 1.2 mm. Because of the low bubble area flux in the lab cells as compared with commercial units, scaling up the cells is not an easy task. Flotation columns can handle greater superficial gas velocities, J_g, but also produce quite large bubbles. These conclusions were used by the authors to build the High Bubble Surface
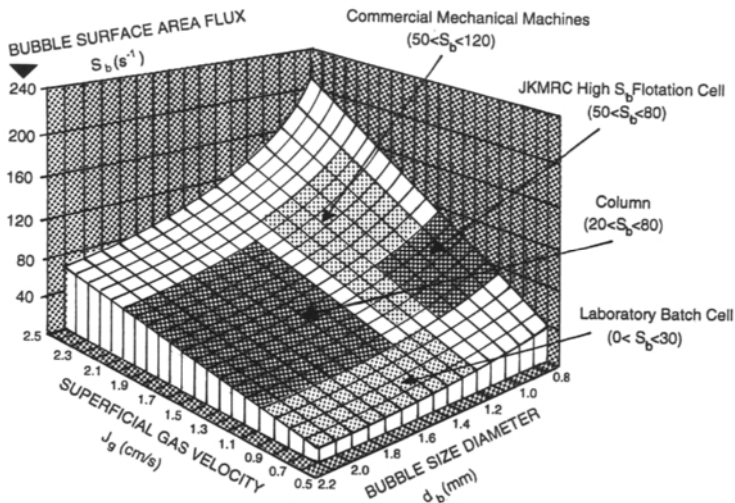
Fig. 8.8. Diagram of S_b–J_g–d_b for different flotation machines. (After Vera et al. [41]; by permission of Elsevier Science.)

Area Flux Flotation Cell (HSbFC) which can be better used in the scale-up projects. Since such information is lacking in most cases, the machines will be reviewed in a traditional way.

8.3.1. Mechanical flotation machines

In the mechanical cells the feed can be introduced directly to the impeller zone from the side as in a Denver Sub-A subaeration machine (Fig. 8.9) or from below as in WEMCO (1 + 1) cell (Fig. 8.10).

As discussed in detail by Degner [42], in the WEMCO cell, a centrally located paddle-wheel type impeller (Fig. 8.10) generates a rotating pulp vortex which extends between two stationary elements: the sandpipe located at the top of the cell, and the draft tube located at the bottom of the cell. The hydraulic action of this rotating vortex is to develop an internal cavity vacuum while simultaneously circulating the pulp from the bottom of the cell through the draft tube into the rotor region. The suction developed in the vortex core draws air into the central region of the rotor which is mixed with the pulp circulated from the bottom to the cell. The three-phase mixture of liquid,
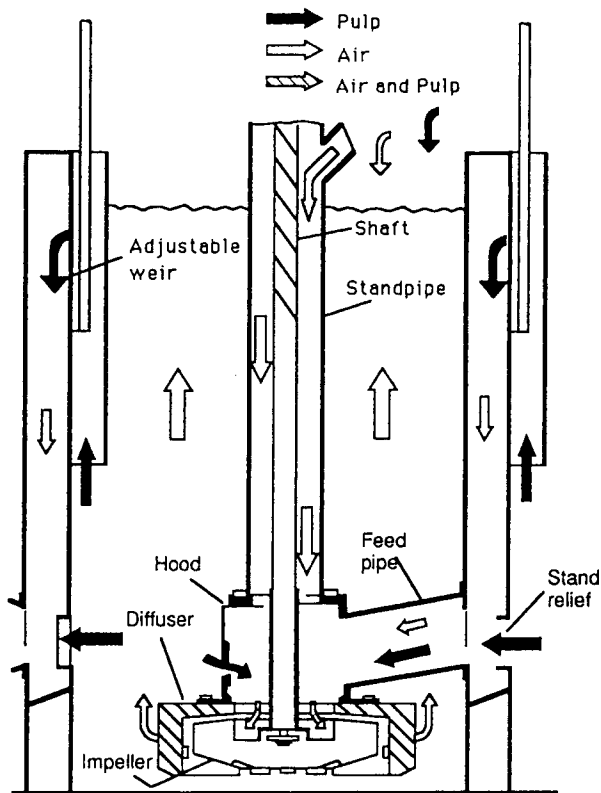
Fig. 8.9. Denver Sub-A subaeration flotation cell.
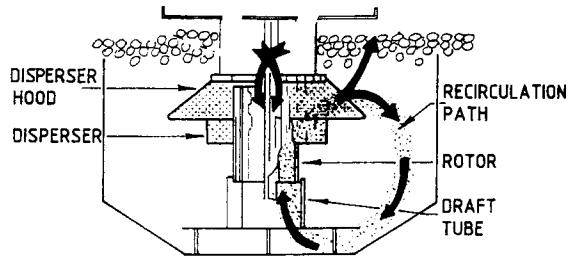
Fig. 8.10. The Wemco 1 + 1 flotation cell. (After Degner [42].)

air, and solids leaves the rotor in a tangential direction, and is turned to a dominantly radial direction as it passes through the holes in the dispenser. The combination of the mixing of air with pulp in the rotor and the turning of the three-phase material through the disperser serves to mix the air-solids at a high intensity, thereby producing the conditions for physical contact between the gas bubbles and the solid particles. The disperser also acts as an internal tank baffle, reducing the vortex action of the pulp in the cell itself, and also reducing the agitation level within the rotor region to a much lower level in the relatively quiescent separation zone outside the disperser. A hood is provided above the disperser, and this element acts to improve the surface stability of the froth.

The key operating parameters which influence the air and pulp circulation levels in a WEMCO flotation machine are the rotor size, speed, and submergence in the pulp. Tests carried out [43] over a 9.5-month period on flotation of a coarse phosphate fraction (29%, +35 mesh) in a large No. 120 size (5 m³) WEMCO cell revealed that both the rotor speed and its submergence had to be increased. These changes resulted in a higher cell power intensity and higher pulp circulation while maintaining essentially the same airflow.

Fig. 8.11 shows the Denver D-R impeller mechanism used in supercharged cells; a cell-to-cell bank and an open-flow bank are schematically shown in Fig. 8.12. In the open-flow bank a feed box is used at the head, with pulp flow by gravity and end tailings discharge over adjustable weirs.

The size of flotation machines has been dramatically increasing [44]. For example, the size of the cells WEMCO offers increased to 42.5 m³ (and even 85 m³). Other manufacturers such as Galigher, Humbold Wedag, Maxwell, Minemet, Outokumpu, Svedala, etc. also offer large cells. This is driven by a reduction in unit costs. Wiegel and Lawver discussed this trend in 1986 [45]. Their comments were based on the application of large cells to phosphate flotation, and these comments may be quite relevant to coal flotation since there are many important similarities between coal flotation and phosphate flotation.

Phosphate flotation plants handle quite coarse fractions, the yield of the froth product may be as high as 50%, and water insoluble oily collectors are also utilized. Based on observations made with regard to 8.5 m³ cells, they claim that in order to obtain the desired phosphate recovery, the selectivity was to be sacrificed when compared to smaller 2.8 m³ cells (they claim that the 1.4 m³ cells were even better than 2.8 m³ cells
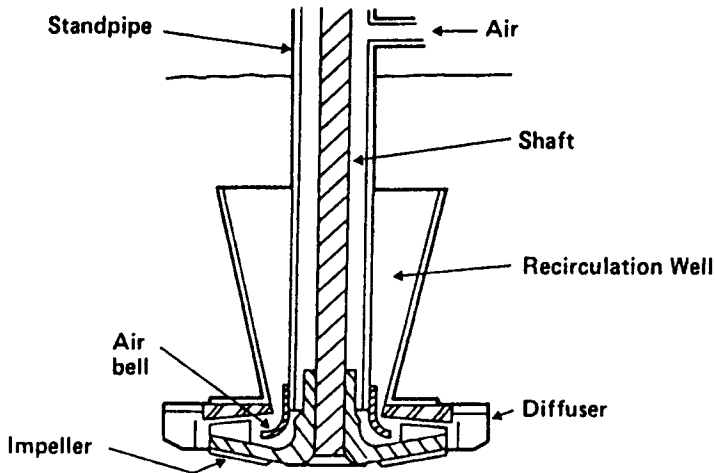
Fig. 8.11. Denver D-R impeller mechanism.
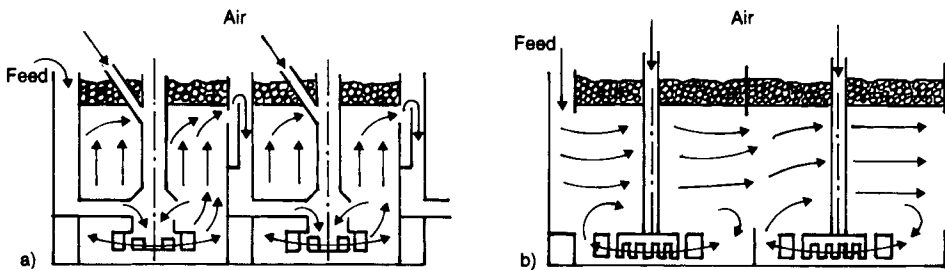
Fig. 8.12. Cell-to-cell and open-flow banks of flotation machines.

for such applications). As an explanation for inferior results, they indicate that there are problems with discharging large quantities of froth product from large cells; they also indicate that shallower and smaller-volume cells provide a better opportunity to carry large phosphate particles with bubbles.

The WEMCO/Leeds flotation column has a mechanical impeller to which air is supplied under pressure. Therefore, following the classification adopted in this book this machine will be classified as a supercharged mechanical machine rather than a flotation column. The dimensions of the WEMCO/Leeds cell are far from the common column length-to-diameter (L/D) ratio. Indeed, the WEMCO/Leeds cell closely resembles the overall configuration of a conventional mechanical machine [46] and its only column-like feature is the use of wash water.

The original design of this cell (Leeds Flotation Column) was based on the Dell's release analysis concept [47]; the idea was to arrange cleaner and recleaner cells in a manner that would simulate the release analysis procedure. The inverted version of such an arrangement is shown in Fig. 8.13. The cleaning and recleaning zones are placed directly above the rougher zone and they are separated from each other by movable

CONCENTRATE
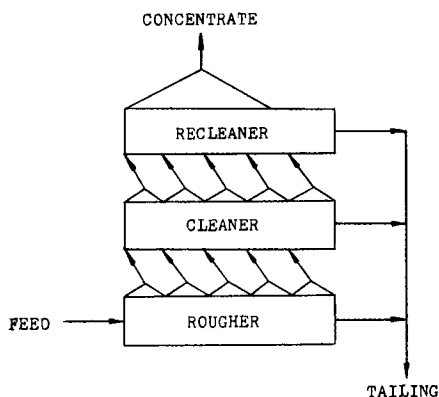
Fig. 8.13. Inversion of the Dell's release analysis concept. (After Dell and Jenkins [47].)
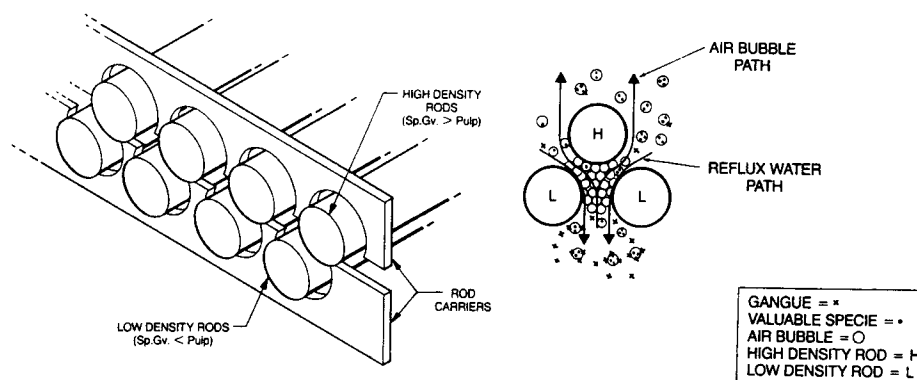
Fig. 8.14. Wemco/Leeds cell rod carrier concept (a) and the cell beneficiation mechanism (b). (After Degner and Sabey [46]; by permission of the American Institute of Mining, Metallurgical and Petroleum Engineers.)

barriers which are designed so as to allow bubbles to collect underneath as a distinct froth layer, but to pass through when the thickness of the layer exceeds a certain value. The major function of the barriers is to strip off any weakly adhering gangue particles from rising loaded bubbles. In each barrier set, the top rods have a density slightly greater than that of water while the lower row has a density slightly less than that of water. This results in a continuous movement of the barriers as suggested in Fig. 8.14.

The plant tests demonstrated that in comparison with conventional mechanical cells the WEMCO/Leeds cells produced a higher grade at comparable combustible recovery [46]. The benefits associated with the installation of the WEMCO/Leeds cells were also claimed to include a 10% reduction in plant floor space and the elimination of the need for classification prior to flotation.

8.3.2. Pneumatic flotation cells

Since pneumatic cells do not have impellers, they need a different type of sparger. Mixing, which is necessary to suspend mineral particles, is provided by a stream of rising bubbles. In older types of pneumatic cells, fine bubbles were produced by pumping compressed air through porous material. While in principle very simple these early cells had many maintenance problems [48].

An entirely different concept was employed in the Davcra cell (Fig. 8.15). This novelty was very different from the other designs and some elements of this design can be seen in many later developments (for instance in the JKMRC cell [41]). In this cell, the impeller was replaced by a feed pump and nozzle. Air and feed slurry are injected into the cell through a cyclone type of sparger and the energy of the aerated pulp jet is dissipated against a vertical baffle. The dispersion of air and the collection of particles by bubbles is claimed to occur in the highly agitated region of the tank. The pulp flows over the baffle into a quiescent separation region. This machine was ahead of its time as the two functions in this cell, namely particle–bubble collision and attachment, and the separation of the particle–bubble aggregates from the slurry, were to a large extent separated.

In the Heyl-Patterson-Miller cell the cyclone type spargers are placed in an open-flow type tank [49,50]. In such spargers the air is dispersed by the shearing forces of the created hydraulic vortex.

Similar aerators to those used in the Heyl-Patterson cells seem also to be utilized in the large FLOKOB cells [51].

In the jet cell described by Klassen [34], the feed (at a pressure of 3 atm) is pumped through a venturi type of injector in which negative pressure is formed drawing in air that is then vigorously mixed with the pulp in a mixing compartment. The aerated pulp is forced to the separating cell. In some applications the reagents were directly supplied into the mixing compartment as shown in Fig. 8.16. According to Klassen, the aeration degree of such machines was in the range of 1 m^3 of air per 1 m^3 of pulp.
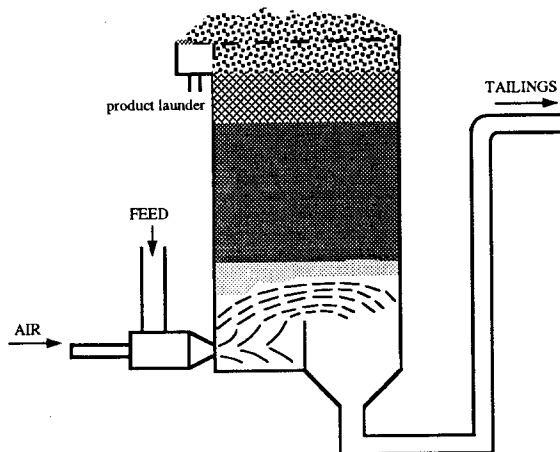
Fig. 8.15. The Davcra flotation cell.
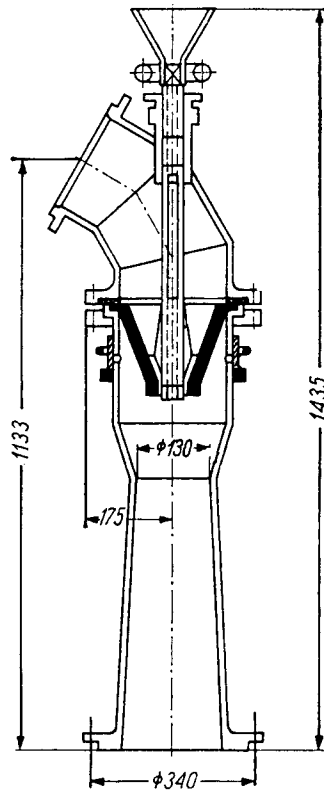
Fig. 8.16. The aerating injector. (After Klassen [34].)

The aerating jet described by Antipenko et al. [52] (Fig. 8.17) employs similar principles. The use of a shaping device in the center of the aerator seems to serve the same purpose as Davcra's vertical baffle. A 12-m^3 cell requires 2–4 such aerating jets. The specific throughput of the cell is in the range of 9–10 m^3 h^{-1} m^{-3}.

The aerating devices employed in Chinese XPM-8 and XPM-16 machines [53] (the volume of the latter is 16 m^3) resemble the aerating jet shown in Fig. 8.17. Four such aerating mechanisms are arranged radially in each XPM-8 cell. One circulating pump for every two cells draws part of the pulp from the adjacent cell in the XPM-8, whereas the XPM-16 uses one pump per cell. As described by Wu and Ma [53], in some Chinese coal preparation plants the impellers in old subaeration machines were replaced by the XPM-8 mechanisms (two per cell), and the cells were changed into an open-flow type. This change increased the unit capacity of the modified cells from 7.7 m^3 h^{-1} m^{-3} to 12.8 m^3 h^{-1} m^{-3}.

Flotation columns. Fine gangue particles enter the froth with pulp water by entrainment and their concentration in the froth water is similar to that in the pulp. Hence, by diluting the froth product with clean water and refloating, the gangue content in the subsequent froth product is reduced. Practically, the selectivity is improved by refloating
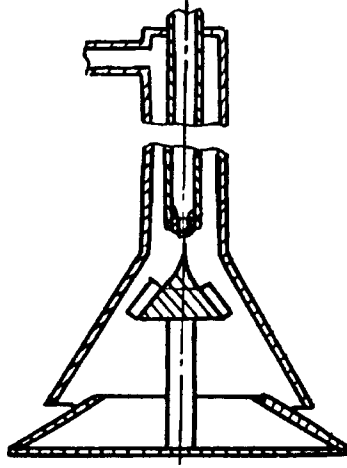
Fig. 8.17. The aerating jet. (After Antipenko et al. [52]; by permission of Gordon and Breach.)

the rougher concentrate in cleaning flotation. In the Canadian flotation column, selectivity is further enhanced by the use of washing water. To some extent both rougher and cleaning stages are then accomplished in the same unit.

A schematic of the Canadian column is shown in Fig. 8.18. The most characteristic feature of this device is its height of 9–15 m with a diameter ranging from 0.5 to 3 m [20]. Other features that distinguish the column from other machines are the counter-current feeding arrangement, use of wash water, and bubble generation system. Canadian Process Technologies (CPT) claim to have installed over 200 diverse industrial flotation columns. CPT jointly with Eriez developed the CoalPro column to meet the special requirements of coal producers.

An efficient air sparging system must be capable of producing small, uniformly sized bubbles at a desired aeration rate. Small bubbles can improve flotation kinetics [17], and more importantly, finer bubbles provide higher bubble surface area flux (Eq. (8.12)). There are two general types of spargers: internal and external bubble generators. The former are fabricated from filter cloth, perforated rubber, porous metal or ceramic tubes. Fig. 8.19 shows the USBM/Cominco jet type sparger, and the Minnovex variable gap sparger [39]. Single orifice gas spargers (SparJet and SlamJet spargers) are offered by the Canadian Process Technologies. A porous sparger (e.g. Mott sparger) is shown in Fig. 8.20. Perhaps the best known example of column with external spargers is the Microcel column, which uses a static in-line mixer [54] (Fig. 8.21). In this system, dispersion is achieved by using a centrifugal pump to circulate a portion of the flotation pulp from the lower section of the column. Controlled amounts of air and frother are introduced into the pulp just ahead of the mixers.

An important advantage of the external spargers is that they are externally mounted on the column, thus allowing easy replacement without interrupting the column operation.
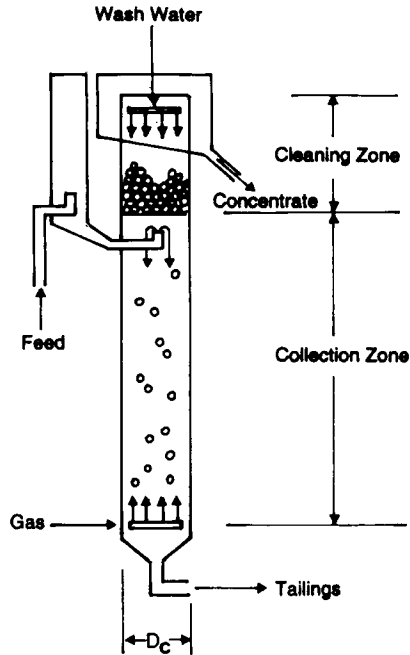
Fig. 8.18. Schematic of Canadian flotation column.

Another important feature of the column is the use of wash water. Spraying the froth in mechanical cells to enhance secondary upgrading in the froth layer was discussed by Klassen and Mokrousov [36] and was fully analyzed by Pikkat-Ordynsky and Ostry [55]. They claim that spraying water over the first cells (in which flotation is very intense) is very effective, but it may be detrimental in subsequent cells in which coarse particles finally start floating. While spraying the froth with water in mechanical cells is not common, the use of wash water became common in columns. Fig. 8.22 shows typical water flow patterns in conventional mechanical cells (without spraying water) and in columns. While the pulp water along with fine gangue particles is carried over to the froth in conventional cells, the use of wash water added counter-currently to the flow of particle-laden air bubbles prevents the pulp water from reporting to the froth product.

To discuss the mass balances as shown in Fig. 8.22 let

$$Q_F = Q_{Fw} + Q_{Fs}$$

$$Q_C = Q_{Cw} + Q_{Cs} \tag{8.32}$$

$$Q_T = Q_{Tw} + Q_{Ts}$$

where Q is the volumetric flow rate, and the subscripts F, C and T stand for feed, concentrate and tailings, and the subscripts w and s stand for water and solids.

The bias rate is commonly defined as the net downward flow of water through the froth [20]. In superficial velocity terms dividing volumetric flow rate by A_c (see
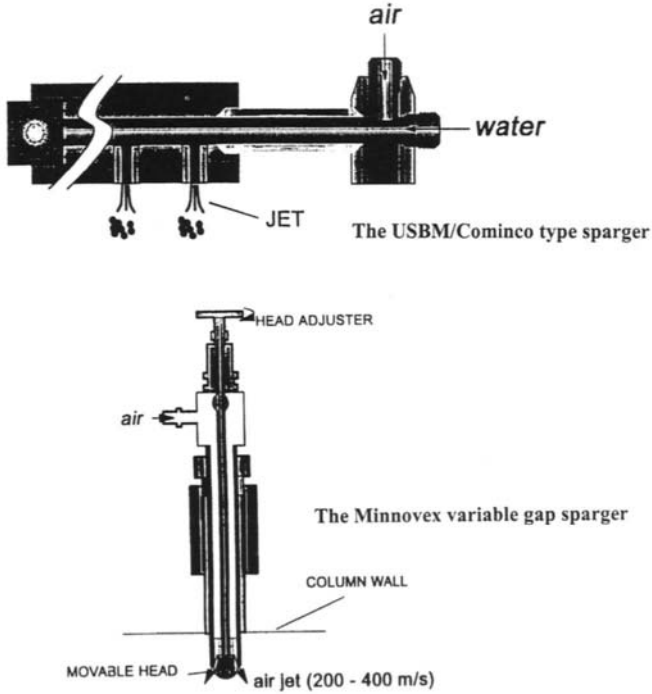
Fig. 8.19. UBSM/Cominco sparger (a), and the Minnovex variable gap sparger (b). (After Finch [39]; by permission of Elsevier Science.)
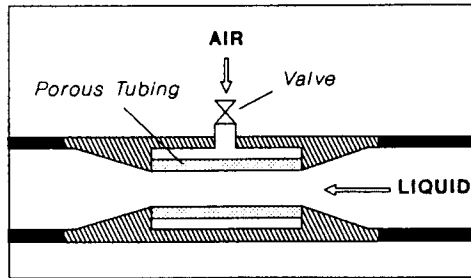
Fig. 8.20. Porous sparger.

Eq. (8.10)) one can write:

$$J_F = J_{Fw} + J_{Fs}$$
$$J_C = J_{Cw} + J_{Cs} \qquad (8.33)$$
$$J_T = J_{Tw} + J_{Ts}$$

By definition

$$J_{bias} = J_{Tw} - J_{Fw} \qquad (8.34)$$
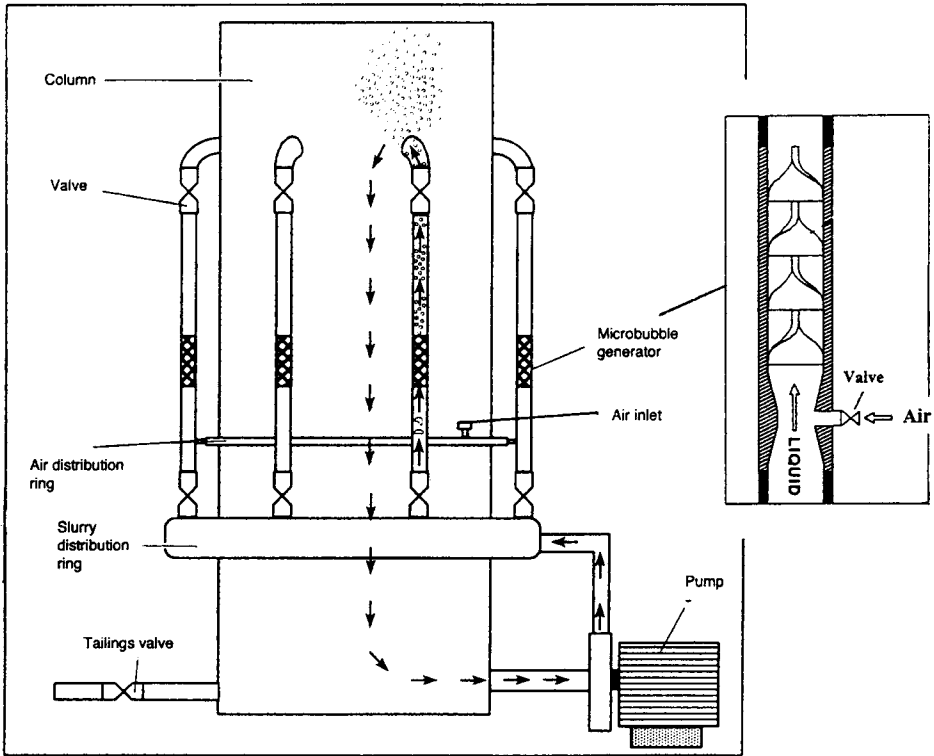
Fig. 8.21. The Microcell static in-line mixer air sparging system, and a single in-line static mixer.

A. MECHANICAL CELL

B. COUNTERCURRENT COLUMN
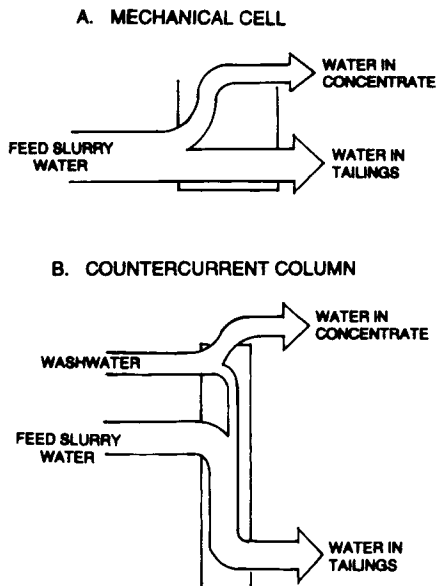
Fig. 8.22. Distribution of water flow in mechanical cell (a) and in counter-current column (b).

and since

$$J_{Fw} = J_{Cw} + J_{Tw} \tag{8.35}$$

therefore

$$J_{bias} < 0 \tag{8.36}$$

So, the mechanical cells without wash water work with a positive bias rate (which indicates an upward flow of water to the froth product).

In a column with wash water

$$J_{Ww} + J_{Fw} = J_{Cw} + J_{Tw} \tag{8.37}$$

and so

$$J_{bias} = J_{Tw} - J_{Fw} = J_{Ww} - J_{Cw} \tag{8.38}$$

and if $J_{Ww} > J_{Cw}$

$$J_{bias} > 0 \tag{8.39}$$

Then, the main difference between a mechanical cell and a column is that because of the positive bias, pulp water does not enter the froth product in the column. Since pulp water carries all types of fine gangue particles (slimes), this improves the grade of the final product.

As discussed by Luttrell and Yoon [56], the design of the wash water distributor can significantly affect column performance since it may impose some undesirable mixing. Also, since the center of the froth in large-diameter columns often drains excessively and becomes immobile, a special construction of the distributor may be beneficial. Fig. 8.23d shows a multi-level distributor patented by Virginia Tech. This system allows for independent control of water flow to different concentric areas of the froth.

As shown in Fig. 8.24, mechanical cells with very turbulent and very quiescent zones in the same tank are characterized by mutually conflicting requirements which limit their performance. The mechanical cells are considered to be perfect mixers, while the columns are believed to be characterized by plug flow conditions. Rice and Littlefield [57] demonstrated, however, that the columns are also characterized by a turbulent mixing region near the sparger and quiescent mixing conditions in the upper part of the column.

According to Mankosa et al. [58], an increase in either column diameter or gas flow rate results in an increase in mixing (i.e. decrease of Peclet number). When the column L/D_c aspect ratio was increased from $11:1$ to $20:1$, prevailing plug-flow conditions were observed. This, however, may be impractical since typical plant installations have L/D ratios around 2 to $3:1$.[3] Because lab columns have much larger L/D ratios than the industrial columns, their scale-up is a difficult task.

It is generally believed [59] that columns require significantly less floor space (but a higher foundation loading), less electrical power (since they do not have impellers), and

---

[3] For instance, Canadian Process Technologies Inc. has installed the CoalPro units with the following dimensions: 3.66 m diam. by 9.0 m h (CWF Italia, Sardinia, Italy), 4.27 m diam. by 8.5 m h (Coastal Coal, Kingwood, USA), 3.96 m diam. by 7.3 m h (Massey, Power Montain, USA), and 3.05 m diam. by 8.5 m h (Tampa Electric, Clintwood, USA).
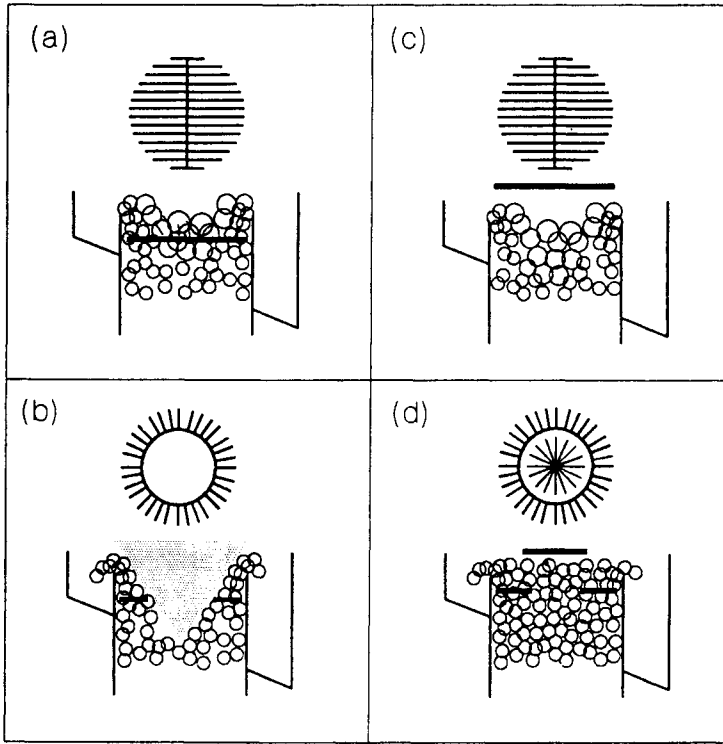
Fig. 8.23. Schematic diagram of various wash water distribution systems. (After Luttrell and Yoon [56]; by permission of the American Institute of Mining, Metallurgical and Petroleum Engineers.)
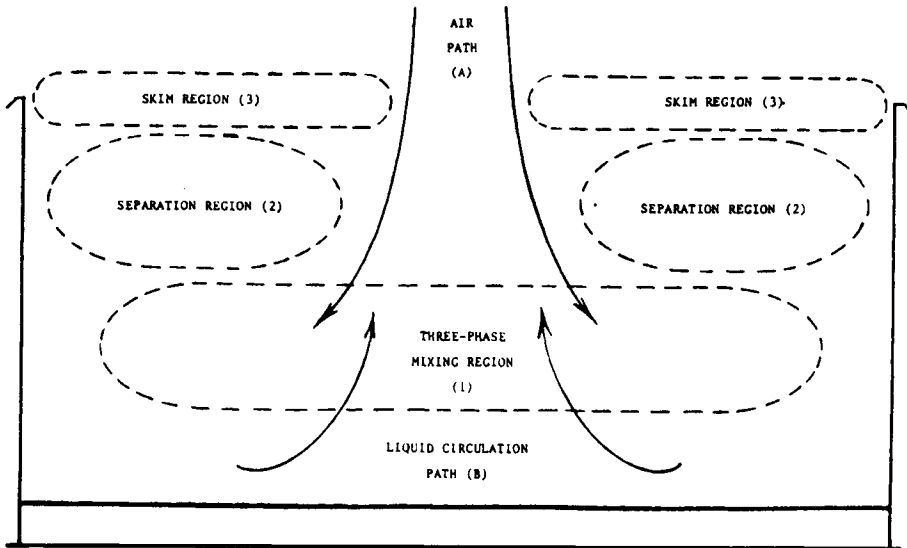
Fig. 8.24. Hydrodynamic characteristics of mechanical flotation cell.

less maintenance, since cell bodies do not show any wear. Also, low wear is observed with gas spargers, and they are inexpensive and easy to replace. However the economic analyses offered by Luttrell et al. [60] indicate that the equipment capital cost for a column cell installation is significantly higher than that for a conventional bank of the same capacity. The cost differential can be greatly reduced through the application of very large-diameter columns. For the case study examined in Luttrell et al.'s paper [60], the installation of columns of 3.0 m diameter was approximately twice as costly as its conventional counterpart. This difference was reduced to approximately 1/3 when compared to an installation of 4.25 m diameter columns. Although this represents a significant cost difference, the additional revenues generated by the column circuit may still make columns more attractive. For the case under consideration, the column circuit provided more that a 5% yield increase at the same concentrate ash. Also, columns may offer secondary benefits which are not widely recognized. Since the use of wash water eliminates ultrafine clay slimes from the froth product, the clean coal products obtained using columns often exhibit improved dewatering characteristics.

A very illustrative example of pilot-plant and full-scale commercial testing with columns at the Reverside plant was provided by Nicol et al. [61]. The Reverside plant was producing a 9.8% ash prime coking coal. The −0.5 mm fraction was processed in conventional flotation cells after desliming at about 0.075 mm; the −0.075 mm fraction (110–120 t/h) was discarded to the tailings thickener. The ash content of this stream could range from 38–44% up to 50–55%, depending on the mining sequence. A 4.3 m × 0.1 m pilot column with feed entering 3 m above the tailings was used to test the process. Fig. 8.25 summarizes the results. Without wash water, the ash content was in the range of 18–21% for frother dosages above 15 g/t of water. The ash content could be reduced by decreasing the frother dosage below 12 g/t, but the reduction was still insufficient. Based on pulp volume, the residence time was 2.7–3.2 min and the feed was treated at a superficial velocity of 1.9–2.3 cm/s (feed volumetric rate per column cross-sectional area). The results could, however, be dramatically improved with wash
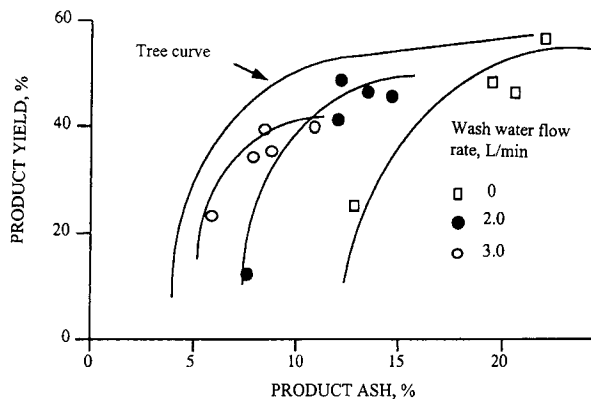
Fig. 8.25. Effect of froth spraying on product ash. (After Nicol et al. [61]; by permission of the American Institute of Mining, Metallurgical and Petroleum Engineers.)

water (Fig. 8.25). Based on these results it was decided to build a full-scale unit treating 175 m^3/h. For a feed superficial velocity of 2.1 cm/s, it was calculated that the column diameter should be 1.7 m. For a 2.6-min residence time in the recovery section of the column, the distance between the air spargers and the froth/pulp interface should thus be 3.35 m. With a 0.5 m froth and 0.1 m froth overflow weir, the overall designed column height was 5.5 m. These dimensions give a column L/D_c ratio of 3.2. After some tests a 3-m extension was added (the total height was then 8.5 m).

The column performed very well and concentrates with a 9–10% ash content at 70–80% combustible recovery were obtained. With a feed rate of 180 m^3/h, and the wash water increased up to 24.4 m^3/h the concentrate ash content decreased from 10.7 down to 8.0% at a combustible recovery of about 73%. These results were obtained at the following reagent dosages: 1–1.5 kg/t of collector and 15–20 g of frother per ton of water. The aim for a full column installation within the plant was the annual production of 150,000 t/year of concentrate and this turned out to be quite possible.

The example quoted after Nicol et al. [61] shows the scale-up procedure which was adopted to build a full-scale industrial unit. Since there are no well established methods to scale up columns, this material may be very useful.

Deister Flotair columns also utilize external bubble generators. In the Deister Air Generator, compressed air is supplied through a microporous tube with pressurized water flowing at a high velocity along the inner porous tube surface. This shears off air bubbles as they emerge from the porous surface. The aerated stream is discharged directly to the inside of the column. Examples of full-scale 2.4-m diameter Flotaire columns and smaller 0.8-m units which were used to float coarse coal ($-0.6 +0.2$ mm), were provided by Christophersen and Jonaitis [62].

The multisectional columns were described by Rubinstein and his colleagues [52,63]. Such a pilot-scale unit with counter-current and co-current sections is shown in Fig. 8.26. While easy to float fines are recovered in the first compartment, more difficult to float particles (e.g. coarser particles) have a better chance to be recovered in the subsequent co-current compartment. A 100-m^3 two-section industrial unit was built in 1994 [63].

In general, the ratio of the cross-sectional area to the volume (also referred to as the specific surface area) is small for columns. For units with $L = 9$ to 15 m and $D_c = 0.5$ to 3 m, the specific surface area varies from 0.05 to 0.1 m^2/m^3. For mechanical cells, these numbers are much larger, 0.4–2.2 m^2/m^3 [56]. Comparison of these numbers merits an additional comment.

At a given bubble surface area flux, S_b, and bubble loading, there is a certain mass rate of solids that can be carried by bubbles:

$$C_r = K d_p \rho_p S_b \qquad (8.40)$$

where C_r is the carrying rate, and d_p and ρ_p are the particle size and particle–bubble aggregate density, respectively. The units are mass of solids per unit time per unit column cross-sectional area. The practical measure of the maximum carrying rate for a given set of conditions is called the *carrying capacity*, C_a [20].

Following Espinoza-Gomez et al.'s [64] suggestions, Eq. (8.40) was written as follows [65]:

$$C_a = \alpha d_{80} \rho_p \qquad (8.41)$$
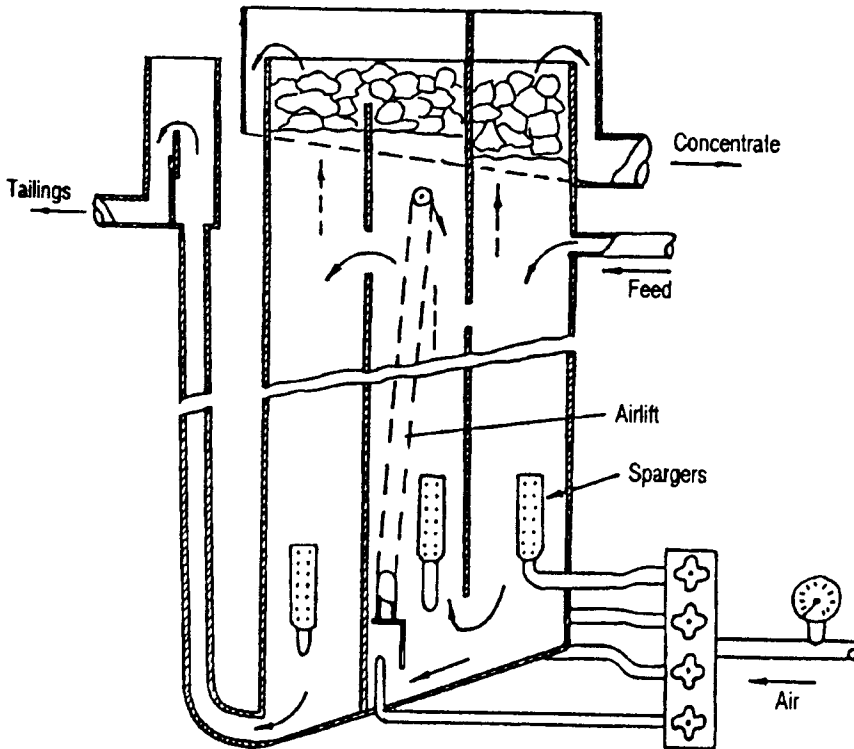
Fig. 8.26. Multisectional flotation column. (After Rubinstein [63]; by permission of the Gordon and Breach.)

where d_{80} is the size at which 80% of the concentrate by mass passes, expressed in μm. The parameter α was found to be 0.068 for small 50 mm in diameter columns, 0.05 for larger columns of up to 1.0 m in diameter, and 0.035 for columns greater than 2.0 m in diameter.

The carrying capacity is never discussed along with conventional cells, but it cannot be ignored for columns. This results from a very limited column-specific surface area. To obtain the same throughput, a column must be capable of achieving a carrying capacity more than an order of magnitude higher than a conventional cell. How can this be accomplished? As comparison of the recoveries calculated from Eq. (8.6) (plug flow) and Eq. (8.17) (perfectly mixed) demonstrates, a cell characterized by plug flow conditions shows better performance (Fig. 8.27). So, the throughput can be increased by increasing the Peclet number (for plug flow conditions Pe $= \infty$) and by increasing k which is a function of S_b (Eq. (8.11) and Eq. (8.12)). However, the Peclet number is also a function of the L/D_c ratio [56] and for larger cells with lower L/D_c ratio the flow pattern in nth cells is somewhere between the two extremes: perfectly mixed and plug flow conditions.

As concluded by Espinoza-Gomez et al. [64], the carrying capacity is most likely rate limiting when a large fraction of solids is to be recovered from the feed. This is
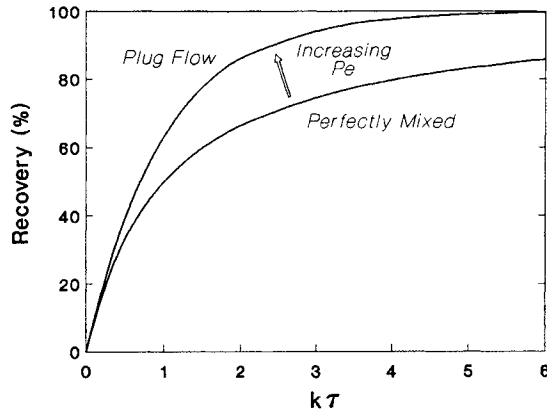
Fig. 8.27. Predicted recovery as a function of $k\tau$ for plug flow and perfectly mixed flotation cells. (After Luttrell and Yoon [56]; by permission of the American Institute of Mining, Metallurgical and Petroleum Engineers.)

exactly the case of coal flotation, where the yield of froth product may be as high as 70–80%. To cope with the high yield of floatable particles, the solids content in the feed is commonly kept below 10% by weight. (According to the study conducted by Olson [66], the flotation feed density in the sixteen visited coal preparation plants in North America varied from 2.9 to 8.8%). Using a pilot-scale column ($L = 2$ m, $D_c = 5.3$ cm) and working with a coal pulp density of 10%, Stonestreet and Franzidis [67] found that the carrying capacity was reached at a feed rate of 1.35 t h^{-1} m^{-2} (Fig. 8.28). Since in such a tall column, plug flow conditions can be expected, the only improvement in carrying capacity could be achieved by increasing S_b , or P (determined by particle hydrophobicity). For the Middle Fork coal, Davis et al [68] found that the carrying capacity of the column was 1.6 t h^{-1} m^{-2}. (According to Luttrell et al. [60] the full-scale columns in the coal industry operate at carrying capacity in the range of 0.9 to 1.9 t
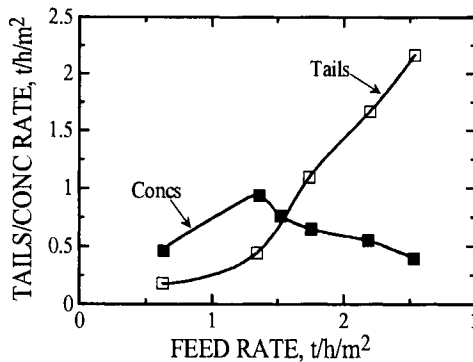
Fig. 8.28. Determination of column carrying capacity. (After Stonestreet and Franzidis [67]; by permission of Elsevier Science.)

h^{-1} m^{-2}.) As was pointed out, the limiting factor in the design of the column flotation circuit for the Middle Fork facility was the concentrate carrying capacity. The column diameter was calculated from the expression

$$D_c = \sqrt{\frac{4\gamma_c M_f}{\pi C_a}} \tag{8.42}$$

where γ_c is the anticipated concentrate yield, and M_f is the mass flow rate of feed. [4]

It is well known [29] that in coal flotation the early froth in the first cells frequently becomes immobile. This reduces the flow of the froth product to the launder, and hence, overloading has an important effect on the rate of flotation. Froth paddles (and other more efficient skimming devices [34]) are utilized to overcome froth immobility. In the larger columns the center of the froth often becomes immobile and special wash water distribution systems have been designed to minimize such effects [56]. In general, for larger cells it is obvious that the froth collection also depends on froth horizontal transport. Ameluxen [69] claims that Eq. (8.41) holds quite well for small and intermediates size columns ($D_c < 1.2$ m) where the ratio of the lip length to the surface area is large. However, a particle that surfaces needs to find its way to the overflow lip; during this trajectory, it is impeding the surfacing of other particles, thus becoming a hindrance to the process. The importance of such phenomena can be expected to increase with increasing column diameter. With the solids flux to the pulp–froth interface higher than the rate of the froth product removal (the situation which is very likely in coal flotation), the problem will be accentuated. To account for such effects in scale-up procedures, Ameluxen [69] introduced the lip loading capacity which expresses the transport rate of the concentrate per unit lip length, and showed that for some sulfide flotation systems, the lip loading plotted versus cell diameter reaches limiting values. The parameter a (Eq. (8.41)) decreases with increasing cell diameter precisely due to froth transport limitations. The lip loading constrains may require a larger column diameter, or the incorporation of internal launders. This agrees very well with the trend of designing the mechanical cells treating coal with larger surface to volume ratios.

There is not enough data to evaluate the importance of the lip loading parameter in coal flotation systems but it is likely to be significant.

8.3.3. Contactor/separator machines

Mechanical flotation cells (Fig. 8.24) are characterized by mutually conflicting requirements; namely in the same vessel: (i) a high-intensity mixing zone, (ii) a relatively quiescent separation zone, and (iii) a stable pulp–froth interface zone.

Such conflicting hydrodynamic requirements are easily accommodated in the narrow and tall columns in which a concentration gradient along a column's height results in high recoveries in the lower portion of the column, while maintaining high removal rates in the upper regions. However, in industrial units axial mixing adversely affects column

---

[4] Useful information on the effect of L on recovery was provided by Parekh et al. [70].

performance. Since mixing is mostly determined by gas holdup and thus also by frother concentration [71], it can only be reduced by judicial selection of sparger type and size, and proper selection of gas and liquid superficial velocities. Horizontal baffles are also used to minimize axial mixing in large columns [72,73].

As the discussion above reveals, particle–bubble collision and attachment, and the separation of particle–bubble aggregates from the pulp cannot be entirely separated in the flotation cells that have so far been discussed. By placing mechanical cells in series in banks and by selecting proper conditions for columns, the effect of mixing (which is inherent to the first function) on the second function can be reduced, but it cannot be entirely eliminated. A different type of flotation cell which will be discussed in this section was developed to separate these two functions, i.e. the contactor and the separator are separate.

The aerolift centrifugal flotation machine is shown in Fig. 8.29 after Klassen [36]. (Elyashevitch and Pushkarenko [38] also provide some details.) Reagents are introduced to the pipe through which the pulp flows 20 m down under gravity. On the other side of the lower part of the U-turn, compressed air is injected through the aerolift (aerator) (Fig. 8.29c) and transports the pulp 24 m up to the centrifugal separating vessel (Fig. 8.29b). Because air must be supplied under a pressure high enough to overcome the hydrostatic head of 24 m of pulp, a large amount of air dissolves in the pulp. The pressure in the aerated pulp decreases as it rises up the supplying pipe (distributor) toward the separating vessel, and this facilitates precipitation of bubbles directly on hydrophobic particles. So, two processes take place in this portion of the distributor:
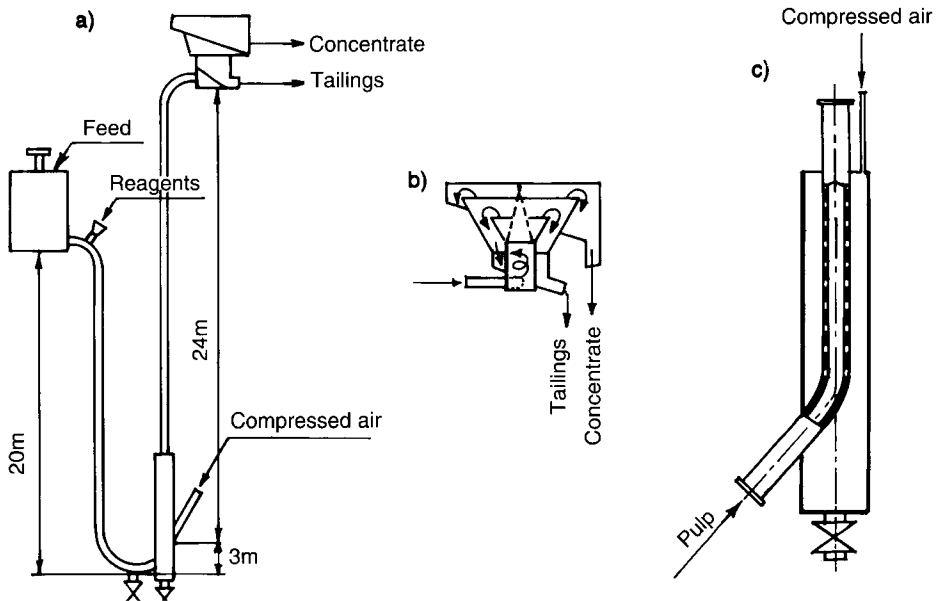
Fig. 8.29. Example of an early contactor/separator flotation machine. (After Klassen [34].)

microbubbles precipitate directly on the surface of hydrophobic particles and at the same time the solid particles collide with co-currently transported bubbles. The presence of microbubbles on the hydrophobic particles facilitates the attachment of the hydrophobic particles to bubbles and as a result the flotation kinetics is improved [36]. The tests revealed the following concentrations of air in the pulp at different distances from the aerator: 29 cm^3/l (0.1 m), 20.3 cm^3/l (1.1 m), 16.5 cm^3/l (5.0 m), 13.0 cm^3/l (9.0 m). These numbers confirm that the air evolves from the pulp as it rises up toward the separating cell. Shimoizaka and Matsuoka's [74] results on fine coal flotation in a Denver batch cell, also after pressurizing the pulp for 5 min under a pressure of 343 kPa, clearly confirm a very significant improvement after pressurization. The results obtained after pressurizing the pulp were superior in all cases.

In the aerolift machine, the aerated pulp enters the separating vessel tangentially and separation of the loaded bubbles from the slurry is further facilitated by centrifugal forces.

Both Klassen [36] and Elyashevitch and Pushkarenko [38] conclude that the aero-lift flotation machine provides better metallurgical results and higher specific throughput (2–2.5 t h^{-1} m^{-3}) than mechanical machines.

In the pneumatic cells developed by Bahr et al. [75–77], the two functions of flotation machines are separated. The EKOF pneumatic cell which evolved from this research [77] is now available in two versions with either a tangential inlet of the aerated slurry to the separating vessel, or a vertical inlet. These machines are now utilized by coal industries in many countries [78]. The Jameson cell also uses the vertically mounted aerator, referred to as downcomer (Fig. 8.30). Technical literature abounds with descriptions of this device [65,79–82].

As Jameson pointed out [79], in flotation columns (which may be up to 13 m high) the froth depth is usually less than 1 m and thus the rest of its volume is occupied by liquid. But since the washed and well-drained froth is the most important region of the column, it should be possible to further improve column efficiency by reducing the volume occupied by the liquid. Comparison of Fig. 8.18 with Fig. 8.30 reveals that the much smaller volume (height) of the Jameson cell is indeed the most important difference between these two.[5] Unlike the Canadian column, the Jameson cell is a co-current device. The feed is (slurry with reagents) pumped through a fixed diameter orifice which draws in air at the top of the downcomer. The downcomer is sized so that the bubbles created by the plunging jet are carried downward, but at the same time the downward pulp velocity is sufficiently low to allow bubbles to rise relative to flow to create a mixture of high gas content [65]. Although the residence time in the downcomer is only 5–10 s, the intensive mixing coupled with the high void fraction in the liquid suffices to provide high flotation rates. Low values of the superficial gas velocity (calculated by dividing the downcomer air rate (cm^3/s) by the cross-sectional area (cm^2) of the riser part of the cell) of $J_g = 0.4$ to 0.8 cm/s are employed in cleaning applications, and high J_g values (1.0 to 2.0 cm/s) are employed in roughing and scavenging applications. J_g values typically range from 0.8 to 1.4 cm/s for coal applications. Jameson cells generally operate with a volumetric

---

[5] Mohanty and Honaker [83] claim that the volume of the separating cell can be further reduced.
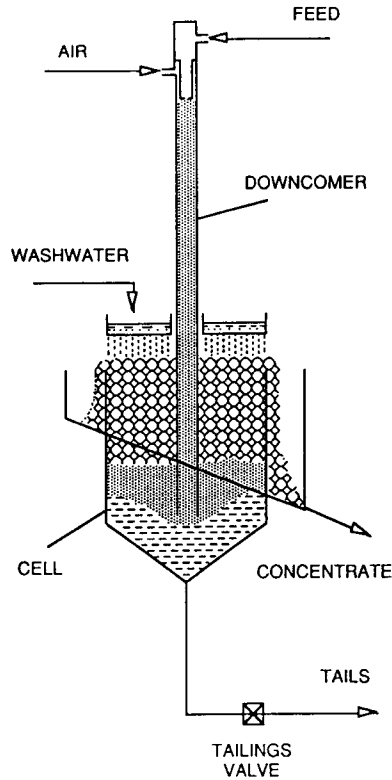
Fig. 8.30. Layout of a single-downcomer Jameson cell.

air/feed ratio of 0.3–0.9. The required frother concentrations vary from 5 to 25 ppm.

The large units ($L = 3.5$ m, $D_c = 1.5$ m) installed at the Newlands Coal Pty produced 9–11% ash concentrates, and 45–60% ash tailings at greater than 85% combustible recovery [80] from a feed containing 19–20% ash. The list and detailed description of full-scale Jameson cell installations in six Australian coal preparation plants can be found in the paper by Dawson et al [84].

Initial applications of the Jameson cell in coal flotation have concentrated on −0.1 mm fine coal. Atkinson et al. claim [81] that subsequent tests proved that the cell efficiently floats coarse coal up to 0.5 mm as well.

The concentrate carrying capacity in all Jameson cell applications has been shown to be in the same range as for conventional columns [81]. In order to calculate the carrying capacity of the Jameson cell, Honaker et al. [85] derived an improved expression and demonstrated that J_g has a significant impact on the carrying capacity of the Jameson cell. However, according to Eq. (8.40), higher carrying capacity can be achieved by increasing gas rate or decreasing bubble size. Too large a gas rate or too small a bubble size will result in either (i) column gas flooding, (ii) loss of positive bias, or (iii) sparger

MUSHROOM

FROTH LAUNDER

CALMING REGION

POROUS WALL

air

FEED

FROTH

TAILS

FEED SLURRY FORMS INVERTED VORTEX IN THIS REGION
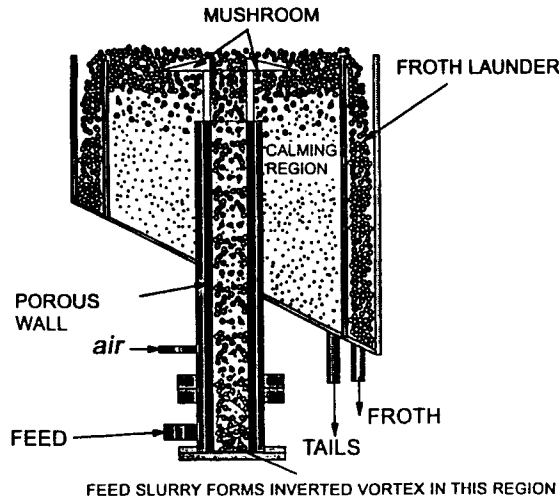
Fig. 8.31. Centrofloat high rate cell.

burping. There are, therefore, the practical values of J_g/d_b that determine the maximum carrying capacity at which columns are operated.

Atkinson et al [82] tested the effect of solids content in the feed in the range of up to 10% and found that in this range the concentrate production increased with feed percent solids. Among the tested operating parameters Mohanty and Honaker [83] concluded that the frother concentration was the most important for the separation efficiency of the Jameson cell.

Interesting results were reported by Honaker et al. [85] who floated different samples of North American coals in lab, pilot-scale and full-scale Jameson cells. They claim that in the case of ultrafine feeds a rougher–scavenger circuit is much better, while rougher-only flotation may be sufficient for the treatment of relatively coarse samples.

Fig. 8.31 shows a distinctly simple and interesting Centrofloat High Rate Cell. In this cell, feed is pumped in tangentially, the swirling motion is set, and as the feed travels upward it shears off the bubbles when they are forced through a porous wall. Due to the centrifugal forces, the bubbles migrate towards the center of the vortex while high-density gangue particles are forced away from the froth core to the outer layers. The high-ash pulp phase exits the mashrum below the froth layer and exits as a tailing stream. The sparging device in this cell has similarities to that in the air sparged hydrocyclone developed by Miller and his co-workers [86,87]. The Centrofloat cell was promising large throughputs and simple construction and the first report was enthusiastic [88], but the devil is in detail and the following report claimed unsolved scale-up problems [89].

A further refinement of the contactor/separator flotation machines is the new TurboFlotation device. The TurboFlotation system is shown in Fig. 8.32 [90]. The slurry is pumped through a static mixer at which point both collector and frother are also introduced. A jet mixer is used to inject compressed air into the pulp stream, and an
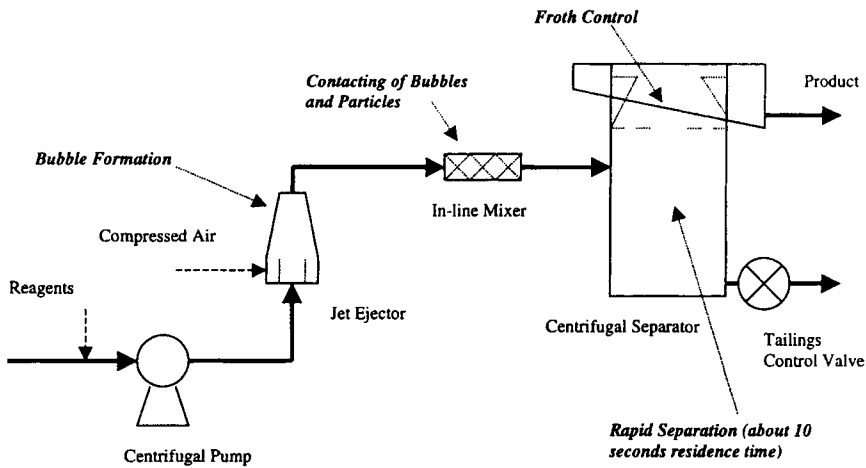
Fig. 8.32. TurboFlotation system. (After Ofori and Firth [90]; by permission of the Australian Coal Preparation Society.)

in-line mixer is employed to further increase the collision frequency of the co-currently flowing solid particles and air bubbles. The aerated slurry is injected tangentially into a cylindrical separator. This interesting technology has a good chance of succeeding if it scales up well from the demonstration 30-cm diameter unit that is being tested.

It is of interest to point out that newly developed cells use many similar elements. Both the High Bubble Surface Area Flux Flotation Cell [41] and the TurboFlotation [90] cell utilize static mixers which are also used in the Microcell. The centrifugal separator that was utilized in the Russian aerolift machine also appears in the TurbFlotation system. The attractive concept of utilizing centrifugal forces in the separating vessel was also an important part of the Centrofloat High Float Cell. While this idea is unarguably attractive this design apparently poses difficult scale-up problems which makes the outcome hard to predict.

8.3.4. Froth separation

In the report presented at the 10th International Mineral Processing Congress in 1973, Malinovsky et al. [91] described a froth separation process. In this process the pulp is fed onto a low-mobility froth. The maximum size of the particles that can be efficiently treated under such conditions is claimed to be at least two times larger than the top size of the particles treated by conventional froth flotation.

As already discussed, by assuming that the thick froth layer was the most important part of the column flotation system, Jameson was able to significantly reduce the volume of his cell in comparison with the Canadian flotation column. In the froth separators this idea is pushed to the extreme, and the froth is practically the only phase of significance in this process.

The tests revealed [92] a good correlation between the contact angle hysteresis (difference between advancing and receding contact angles) and the recovery of coarse

particles in this process. The three-phase (solid–liquid–gas) line becomes pinned on a heterogeneous surface [93]; this effect is responsible for holding the particles on the froth surface and the effect will increase with increasing values of contact angle hysteresis. Since only the particles that are held up by the froth and do not sink through it are finally recovered as a concentrate, it is easy to understand that the hysteresis can indeed play a very significant role in such a process. The reagents that are utilized should make mineral particles very hydrophobic, and increased contact angle hysteresis is particularly beneficial [92]. The feed in this process must be evenly distributed on top of the froth and additional aeration in this zone is needed to counteract the effect of the feed addition on the froth stability.

The rate of the process is claimed to be 5 to 10 times faster than the rate of conventional froth flotation. However, the fundamentals of this process have not been sufficiently studied and Rubinstein et al. [92] concluded that this has hindered the broader application of this technology.

Schultz et al. [94], in their search for a process to beneficiate oil shales, tested a flotation column as a froth separator and provided very encouraging data.

8.4. References

[1] A.R. Laplante, M. Kaya and H.W. Smith, The effect of froth on flotation kinetics — a mass transfer approach. In: J.S. Laskowski (ed.), Frothing in Flotation. Gordon and Breach, London, 1989, pp. 147–168.

[2] N. Arbiter and C.C. Harris, Flotation kinetics. In: D.W. Fuerstenau (ed.), Froth Flotation — 50th Anniversary Volume. AIME, 1962, pp. 215–246.

[3] G.E. Agar, R. Stratton-Crawley and T.J. Bruce, Optimizing the design of flotation circuits. Bull. CIM, 73, 824 (1980) 173.

[4] O.S. Bogdanov, A.K. Podnek, V.J. Khayman and N.A. Yanis, Theoretical and technological problems of flotation. Trans. Mekhanobr., Leningrad, 124 (1959).

[5] H.S. Tomlinson and M.G. Fleming, Flotation rate studies. In: A. Roberts (ed.), Proceedings of the 6th International Mineral Processing Congress. Pergamon, London, 1965, pp. 563–579.

[6] T. Inoue, M. Nonaka and T. Imaisumi, Flotation kinetics — its macro and micro structure. In: P. Somasundaran (ed.), Advances in Mineral Processing. SME, Littleton, CO, 1986, pp. 209–228.

[7] C.H. G. Bushell, Kinetics of flotation. Trans. SME/AIME, 223 (1962) 266.

[8] N. Arbiter, Flotation rates and flotation efficiency. Trans AIME, 190 (1951) 791.

[9] N. Ahmed and G.J. Jameson, Flotation kinetics. In: J.S. Laskowski (ed.), Frothing in Flotation. Gordon and Breach, London, 1989, pp. 77–100.

[10] K.L. Sutherland, Kinetics of the flotation process. J. Phys. Chem., 52 (1948) 394.

[11] L.R. Flint and W.J. Howarth, The collision efficiency of small particles with spherical air bubbles. Chem. Eng. Sci., 26 (1971) 1155.

[12] D. Reay and G.A. Ratcliff, Removal of fine particles from water by dispersed air flotation: effects of bubble size and particle size on collection efficiency. Can. J. Chem. Eng., 51 (1975) 481.

[13] J.F. Anfruns and J.A. Kitchener, Rate of capture of small particles in flotation. Trans. IMM, 86C (1977) 9.

[14] H.J. Schulze, Physico-Chemical Elementary Processes in Flotation. Elsevier, Amsterdam, 1984.

[15] G.L. Collins and G.J. Jameson, Experiments on the flotation of the fine particles — the influence of particle size and charge. Chem. Eng. Sci., 31 (1976) 985.

[16] G.J. Jameson, S. Nam and M. Moo Young, Physical factors affecting recovery rates in flotation. Miner. Sci. Eng., 9 (1977) 103.

[17] R.H. Yoon and G.H. Luttrell, The effect of bubble size on fine coal flotation. Coal Preparation, 2 (1986) 179.

[18] R.H. Yoon and G.H. Luttrell, The effect of bubble size on fine particle flotation. In: J.S. Laskowski (ed.), Frothing in Flotation. Gordon and Breach, London, 1989, pp. 101–122.

[19] R.H. Yoon, G.H. Luttrell, G.T. Adel and M.J. Mankosa, Recent advances in fine coal flotation. In: S. Chander and R.R. Klimpel (eds), Advances in Coal and Mineral Processing Using Flotation. SME, Littleton, CO, 1989, pp. 211–218.

[20] J.A. Finch and G.S. Doby, Column Flotation. Pergamon, London, 1990.

[21] M. Kaya and A.R. Laplante, Investigation of batch and continuous flotation kinetics in a modified Denver laboratory cell. Can. Metall. Q., 25 (1986) 1.

[22] M. Xu, P. Quinn and R. Stratton-Crawley, A feed aerated flotation column. Modeling and scale-up. Miner. Eng., 9 (1996) 655.

[23] B.K. Gorain, E.V. Manlaping and J.P. Franzidis, The effect gas dispersion properties on the kinetics of flotation. In: C.O. Gomez and J.A. Finch (eds), Column '96. Metall. Soc. CIM, Montreal, 1996, pp. 299–313.

[24] B.K.Gorain, F. Burges, J.P. Franzidis and E.V. Manlaping, Bubble surface area flux — a new criterion for flotation scale-up. In: Sixth Mill Operator's Conference (Madang, Papua New Guinea, Oct. 1997). Australian Institute of Mining and Metallurgy, 1997, pp. 141–148.

[25] B.K. Gorain, J.P. Franzidis and E.V. Manlaping, Studies on impeller type, impeller seed and air flow rate in an industrial scale flotation cell, Part 4. Effect of bubble surface area flux on flotation performance. Miner. Eng., 10 (1997) 367.

[26] C.T. O'Connor and P.J.T. Mills, The influence of bubble size on scale-up of column flotation cells. Miner. Eng., 8 (1995) 1185.

[27] C.T. O'Connor, E.W. Randall and C.M. Goodall, Measurements of the effect of physical and chemical variables on bubble size. Int. J. Miner. Process., 28 (1990) 139.

[28] E.G. Kelly and D.J. Spottiswood, Introduction to Mineral Processing. Wiley, New York, 1982.

[29] A.J. Lynch, N.W. Johnson, E.V. Manlaping and C.G. Thorne, Mineral and Coal Flotation Circuits. Elsevier, Amsterdam, 1981.

[30] M. Falutsu and G.S. Doby, Direct measurement of froth drop back and collection zone recovery in a laboratory flotation column. Miner. Eng., 2 (1989) 377.

[31] B.K. Gorain, T.J. Napier-Munn, J.P. Franzidis and E.V. Manlaping, Studies on impeller type, impeller speed and air flow rate in an industrial scale flotation cell, 5. Validation of k–Sb relationship and effect of froth depth. Miner. Eng., 11, (1998) 615.

[32] B.K.Gorain, M.C. Harris, J.P. Franzidis and E.V. Manlaping, The effect of froth residence time on the kinetics of flotation. Miner. Eng., 11 (1998) 627.

[33] Z.T. Mathe, M.C. Harris, C.T. O'Connor and J.P. Franzidis, Review of froth modelling in steady state flotation systems. Miner. Eng., 11 (1998) 397.

[34] V.I. Klassen, Coal Flotation. Gosgortiekhizdat, Moscow, 1962.

[35] F. F. Aplan, The historical development of coal flotation in the United States. In: B.K. Parkeh and J.D. Miller (eds), Advances in Flotation Technology. SME, Littleton, CO, 1999, pp. 269–288.

[36] V.I. Klassen and V.A. Mokrousov, An Introduction to the Theory of Flotation. Butterworths, London, 1963.

[37] J.L. Lewis, Present flotation practice in the coal industry in the United Kingdom. Q. Colo. School Mines, 56 (1961) No. 3, 333.

[38] M.G. Elyashevitch and J.I. Pushkarenko, Experience of Coal Flotation. Gosgortiekhizdat, Moscow, 1960 (in Russian).

[39] J.A. Finch, Column flotation. Miner. Eng., 8 (1995) 587.

[40] S.K. Nicol, Fine Coal Beneficiation. Advanced Coal Preparation Monograph Series, Australian Coal Prep. Soc., 1992, Vol. IV, Part 9.

[41] M.A. Vera, J.P. Franzidis and E.V. Manlaping, The JKMRC high bubble surface area flux flotation cell. Miner. Eng., 12 (1999) 477.

[42] V.R. Degner, Design considerations in large flotation machine developments. 14th Int. Miner. Process. Congr., Toronto, 1982, Session 6, Paper VI-8.

[43] U.K. Custred, V.R. Degner and E.W. Long, Recent advances in coarse particle recovery utilizing large-capacity flotation machines. Trans. SME/AIME, 258 (1975) 324.

[44] R.R. Klimpel, Mechanical flotation machines for the treatment of fine coal. In: S.K. Mishra and R.R. Klimpel (eds), Fine Coal Processing. Noyes Publ., Park Ridge, NJ, 1987, pp. 136–159.

[45] R.L. Wiegel and J.E. Lawver, Reducing theory to practice in mineral processing. In: P. Somasundaran (ed.), Advances in Mineral Processing. SME, Littleton, CO, 1986, pp. 685–694.

[46] V.R. Degner and J.B. Sabey, WEMCO/LEEDS flotation column development. In: K.V.S. Sastery (ed.), Column Flotation '88. SME, Littleton, CO, 1988, pp. 267–279.

[47] C.C. Dell and B.W. Jenkins, The Leeds flotation column. Proc. 7th Int. Coal Preparation Congr., Sydney, 1976, paper J-3.

[48] A.M. Gaudin, Flotation. McGraw-Hill, 1957.

[49] W.E. Bearce, The Cyclo-Cell. Colliery Guardian, 206 (5319) (1963) 377.

[50] R.R. Klimpel, Mechanical flotation machines for treatment of fine coal. In: S.K. Mishra and R.R. Klimpel (eds), Fine Coal Processing. Noyes Publ., Park Ridge, NJ, 1987, pp. 136–159.

[51] R. Brzezina and J. Sablik, The "FLOKOB" column flotation machine. In: W. Blaschke (ed.), New Trends in Coal Preparation and Equipment — Proceedings of the 12th International Coal Preparation Congress. Gordon and Breach, London, 1996, pp. 779–786.

[52] L.A. Antipenko, Y.B. Rubinstein, L.P. Ilueshenko and L.P. Kravchenko, New Generation of Flotation Equipment. Gordon and Breach, London, 1996, pp. 461–468.

[53] D. Wu and L. Ma, XPM-Series jet flotation machine. In: A.C. Partridge and I.R. Partridge (eds), Proceedings of the 13th International Coal Preparation Congress. Australian Coal Prep. Soc., Brisbane, 1998, Vol. 2, pp. 737–745.

[54] I. Brake, G. Eldridge, G. Luttrell and R.H. Yoon, The design of industrial Microcel sparging systems. In: C.O. Gomez and J.A. Finch (eds), Column '96. Metall. Soc. CIM, Montreal, 1996, pp. 13–23.

[55] G.A. Pikkat-Ordynsky and V.A. Ostry, Technology of Coal Flotation. Izd. Nauka, Moscow, 1972.

[56] G.H. Luttrell and R.H. Yoon, Column flotation — a review. In: H.El-Shall, B.M. Moudgil and R. Wiegel (eds), Beneficiation of Phosphate: Theory and Practice. SME, Littleton, CO, 1993, pp. 361–369.

[57] R.G. Rice and M.A. Littlefield, Dispersion coefficients for ideal bubbly flow in truly vertical bubble columns. Chem. Eng. Sci., 42 (1987) 2045.

[58] M.J. Mankosa, G.H. Luttrell, G.T. Adel and R.H. Yoon, A study of axial mixing in column flotation. Int. J. Miner. Process., 35 (1992) 51.

[59] J.T. Furey, Integrating columns into existing plants.In: C.O. Gomez and J.A. Finch (eds), Column '96. Met. Soc. CIM, Montreal, 1996, pp. 147–160.

[60] G.H. Luttrell, J.N. Kohmuench, F.L. Stanley and V.L. Davis, Technical and economic considerations in the design of column flotation circuits for the coal industry. SME Annual Meeting, Denver, 1999, Preprint No. 99-166.

[61] S.K. Nicol, T. Roberts, C.N. Bensley, G.W. Kidd and R. Lamb, Column flotation of ultrafine coal: experience at BHP-Utah Coal Limited's Riverside Mine. In: K.V.S. Sastry (ed.), Column Flotation '88. SME, Littleton, CO, 1988, pp. 7–11.

[62] J.A. Christophersen and A.J. Jonaitis, Deister Flotaire column flotation cell plant experience. In: S. Chander and R.R. Klimpel (eds), Advances in Coal and Mineral Processing Using Flotation. SME, Littleton, CO, 1989, pp. 113–119.

[63] J.B. Rubinstein, Column Flotation — Process, Designs and Practices. Gordon and Breach, London, 1995.

[64] R. Espinoza-Gomez, J. Yianatos and J. Finch, Carrying capacity limitations in flotation columns. In: K.V.S. Sastry (ed.), Column Flotation '88. SME, Littleton, CO, 1988, pp. 143–148.

[65] G.M. Evans, B.W. Atkinson and G.J. Jameson, The Jameson Cell. In: K.A. Matis (ed.), Flotation Science and Engineering. Marcel Dekker, New York, 1995, pp. 331–363.

[66] T.J. Olson, How to get higher recoveries via improved flotation. Coal Min. Process., 20 (June 1983) 60.

[67] P. Stonestreet and J.-P. Franzidis, Development of the Reverse Coal Flotation Process: application to column cell. Miner. Eng., 5 (1992) 1041.

[68] V.L. Davis, P.J. Bethell, F.L. Stanley and G.H. Luttrell, Plant practices in fine coal column flotation. In:

S.K. Kawatra (ed.), High Efficiency Coal Preparation: An International Symposium. SME, Littleton, CO, 1995, pp. 237–246.

[69] R.L. Ameluxen, Lip loading considerations in flotation columns. In: G.E. Agar, B.J. Huls and D.B. Hudyma (eds), Column '91. Sudbury, 1991, Vol. 2, pp. 661–672.

[70] B.K. Parekh, J.G. Groppo, W.F. Stotts and A.E. Bland, Recovery of fine coal from preparation plant refuse using column flotation. In: K.V.S. Sastry (ed.), Column Flotation '88. SME, Littleton, CO, 1988, pp. 227–233.

[71] A.M. Al-Taweel, A.M. Ramadan, M.R. Moharam, T.A. Hassan and S.M. El Mofty, Reducing axial mixing in flotation columns. In: S.K. Kawatra (ed.), High Efficiency Coal Preparation: An International Symposium. SME, Littleton, CO, 1995, pp. 271–281.

[72] S.K. Kawatra and T.C. Eisele, Use of horizontal baffles to reduce axial mixing in coal flotation columns. In: W. Blaschke (ed.), New Trends in Coal Preparation and Equipment — Proceedings of the 12th International Coal Preparation Congress. Gordon and Breach, London, 1996, pp. 87–794.

[73] D.B. Woodruff, S.A. Heley, S. Pringle and G. Budge, The installation of an EIMCO pyramid column flotation system at RJB Mining Gascoigne Wood Mine UK.In: A.C. Partridge and I.R. Partridge (eds), Proceedings of the 13th International Coal Preparation Congress. Australian Coal Prep. Soc., Brisbane, 1998, Vol. 1, pp. 417–426.

[74] J. Shimoizaka and I. Matsuoka, Applicability of air-dissolved flotation for separation of ultrafine mineral particles. Proc. 14th Int. Miner. Process. Congr., Toronto, 1982, Paper IV-11.

[75] A. Bahr, H. Ludke and F.W. Mehrhoff, The development and introduction of a new coal flotation cell. Proc. 14th Int. Miner. Process. Congr., Toronto, 1982, Paper VII-5.

[76] A. Bahr, K. Legner, H. Ludke and F.W. Mehrhoff, 5 Years of operational experience with pneumatic flotation in coal preparation. Aufbereitungs-Technik, 1 (1987) 1.

[77] R. Imhof, S. Hofmeister and J.V. Brown, EKOF pneumatic flotation experience and developments. In: J. Smitham (ed.). Proceedings of the 7th Australian Coal Preparation Conference. Australian Coal Prep. Soc., Mudgee, 1995, pp. 145–157.

[78] B. Bogenschneider, R. Janitschek, R.G. Jung, H.C. Haarmann, R. Lotzien and J. Schwerdtfeger, Pneumatic flotation: an alternative to conventional mechanical flotation machines? In: A.C. Partridge and I.R. Partridge (eds), Proceedings of the 13th International Coal Preparation Conference. Australian Coal Prep. Soc., Brisbane, 1998, Vol. 1, pp. 427–435.

[79] G.J. Jameson, A new Concept in flotation column design. In: K.S.V. Sastry (ed.), Column Flotation '88. SME, Littleton, CO, 1988, pp. 281–285.

[80] G.J. Jameson, M. Goffinet and D. Hughes, Operating experiences with Jameson Cells at Newlands Coal Pty Ltd., Queensland. In: P.J. Lean (ed.), Proceedings of the 5th Australian Coal Preparation Conference. Australian Coal Prep. Soc., Newcastle, 1991, pp. 146–158.

[81] B. Atkinson, C. Conway and G. J. Jameson, Fundamentals of Jameson Cell operation including size–yield response. In: J.J. Davis (ed.), Proceedings of the 6th Australian Coal Preparation Conference. Australian Coal Prep. Soc., Mackay, 1993, pp. 401–417.

[82] B.W. Atkinson, C.J. Conway and G.J. Jameson, High-efficiency flotation of coarse and fine coal. In: S.K. Kawatra (ed.), High Efficiency Coal Preparation: An International Symposium. SME, Littleton, CO, 1995, pp. 283–293.

[83] M.K. Mohanty and R.Q. Honaker, Performance optimization of Jameson flotation technology for fine coal cleaning. Miner. Eng., 12 (1999) 367.

[84] W.J. Dawson, G.F. Yannoulis, B.W. Atkinson and G.J. Jameson, Application of the Jameson Cell in the Australian Coal Industry. In: C.O. Gomez and J.A. Finch (eds), Column '96. Metall. Soc. Sci. CIM, Montreal, 1996, pp. 233–246.

[85] R.Q. Honaker, A. Patwardhan, M.K. Mohanty and K.U. Bhaskar, Fine coal cleaning using the Jameson Cell: the North American experience. In: B.K. Parekh and J.D. Miller (eds), Advances in Flotation Technology. SME, Littleton, CO, 1999, pp. 331–341.

[86] Y. Ye, S. Gopalakrishnan, E. Pacquet and J.D. Miller, Development of the air-sparge hydrocyclone. In: K.S.V. Sastry (ed.), Column Flotation '88. SME, Littleton, CO, 1988, pp. 305–313.

[87] S. Gopalakrishnan, Y. Ye and J.D. Miller, Dimensionless analysis of process variables in air-sparged hydrocyclone flotation of fine coal. Coal Preparation, 9 (1991) 169.

[88] I. Brake, J. Graham, R. Madden and R. Drummond, Centrifloat pilot scale trials at Goonyella Coal

Preparation Plant. In: J.J. Davis (ed.), Proceedings of the 6th Australian Coal Preparation Conference. Australian Coal Prep. Soc., Mackay, 1993, pp. 384–400.

[89] R.G. Stone, I.R. Brake and G. Eldridge, Development of a new column flotation circuit for Peak Downs Coal Preparation Plant. In: J. Smitham (ed.), Proceedings of the 7th Australian Coal Preparation Conference. Australian Coal Prep. Soc., Mudgee, 1995, pp. 145– 157.

[90] P.K. Ofori and B.A. Firth, Turboflotation for fine coal. In: A.C. Partridge and I.R. Partridge (eds.), Proceedings of the 13th International Coal Preparation Congress. Australian Coal Prep. Soc., Brisbane, 1998, Vol. 2, pp. 746–755.

[91] V.A. Malinovsky, N.V. Matveenko, O.M. Knaus, Y.P. Uvarov, N.N. Teterina and N.N. Boiko, Technology of froth separation and its industrial application. In: M.J. Jones (ed.), Proceedings of the 10th International Mineral Processing Congress. Inst. Min. Metall., London, 1974, pp. 717–727.

[92] J.B. Rubinstein, V.I. Melik-Gaikazyan, N.V. Matveenko and S.B. Leonov, Froth Separation and Column Flotation. Izd. Nedra, Moscow, 1989.

[93] J. Drelich, Instability of the three-phase contact region and its effect on contact angle relaxation. J. Adhesion Sci. Technol., 13 (1999) 1437.

[94] C.W. Schultz, R.K. Mehta and J.B. Bates, The flotation column as a froth separator. Mining Eng., Dec. (1991) 1449.

Chapter 9

PARTICLE SIZE ENLARGEMENT

9.1. Introduction

Separation results depend on the degree of liberation, so size reduction which improves the degree of liberation should be beneficial to separation results. However, large quantities of coal fines generated during mining and processing pose serious problems. Conventional methods of coal cleaning are not very efficient in dealing with fine particles, and the finer the particles are the more difficult the solid/liquid separation in downstream processing stages is. Thermal drying always poses a danger of spontaneous combustion and the problems are not over when the particles are finally dry. The handling, transportation, and storage of dry fine coal particles is always difficult. Since coal density is very low, fine coal particles easily become airborne and this results in dusting. Along with possible self-combustion and freezing over winter months, all this is a constant source of annoyance. Such operational, environmental, transportational and handling problems resulting from fine sizes of the treated particles can only be circumvented by particle size enlargement. Several methods are available: flocculation is utilized to improve both thickening and filtration, and agglomeration methods that create a coarser granular material [1,2] are utilized to improve handleability of the final products.

In solid/liquid separation unit operations, the most common is bridging flocculation using polymeric agents (flocculants). The cluster-type flocs formed in this process occupy a large volume. At high dosages of flocculants and additional rolling or tumbling, the flocs can be further compacted into agglomerate-like sludges (pellet flocculation) [3–5]. In liquid-phase agglomeration, known in coal preparation as oil agglomeration, an immiscible liquid (oil) pulls hydrophobic (coal) particles suspended in water into agglomerates under highly energetic agitation. The resulting agglomerates are dense and spherical [1,2]. Since oil droplets get attached only to hydrophobic particles (see Eq. 5.20), the process is selective and is used in the beneficiation of fine coal [6,7]. Recently, a new hydrophobic agglomeration process has been developed. Rather than using oil as the agglomeration agent, the process uses a newly developed class of latex-type flocculants which — unlike common flocculants — are totally hydrophobic [8].

Agglomeration methods also include pelletization and briquetting in which dry fine particles can be processed into larger bodies (pellets or briquettes).

9.2. Oil agglomeration

As discussed in Section 5.3.1, in oil-assisted separation processes a water-insoluble oil is utilized either to improve the attachment of hydrophobic particles to bubbles (emulsion flotation), to improve flotation of very fine particles by increasing their size (agglomerate flotation), or to increase the size of fine particles to an extent which allows for the separation of the agglomerates by screening (oil agglomeration).

As with emulsion flotation, oil agglomeration of coal relies on differences in the surface properties of hydrophobic coal particles and hydrophilic inorganic gangue. In this process, oil droplets attach to the hydrophobic particles and when such particles collide with each other the oil droplets attached to hydrophobic particles merge and bring the particles into larger agglomerates as shown in Fig. 5.4. Of course, this is only possible if the hydrocarbons that are utilized (oil) are immiscible with water and if they selectively wet hydrophobic (coal) particles.

Oils do not spread spontaneously on coal when it is immersed in water (Section 5.3.1.2). In the thermodynamic analysis of the wetting and bridging of individual solid particles by oil in water, Jacques et al. [9] found that formation of the bridges (Fig. 9.1a) is more likely than the formation of films of oil around hydrophobic particles suspended
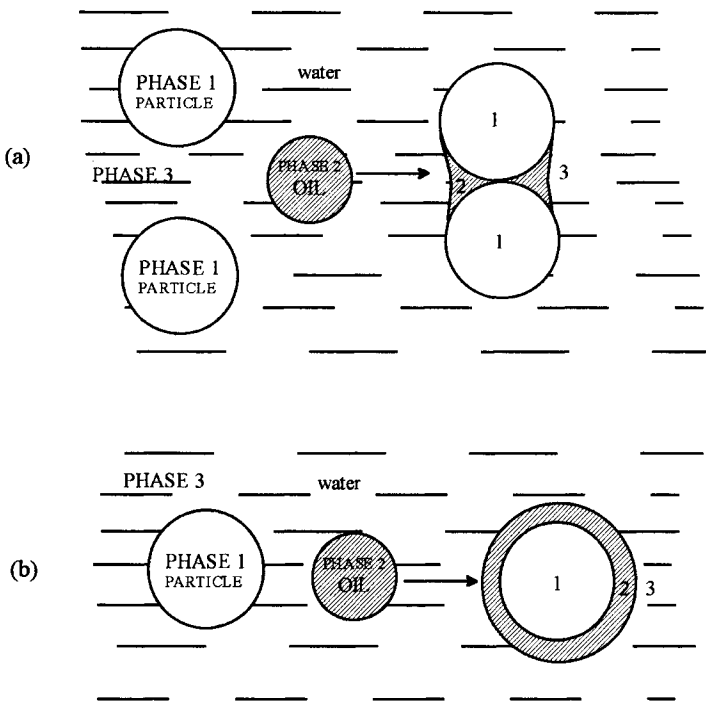
Fig. 9.1. Schematic model of formation of oil bridges between hydrophobic particles dispersed in water (a), and oil spreading (b). (After Jacques et al. [9]; by permission of the American Institute of Chemical Engineers.)
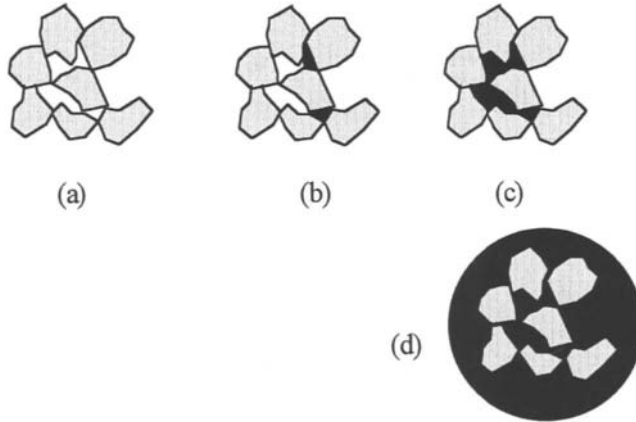
Fig. 9.2. Oil distribution on moist agglomerates: (a) pendular state; (b) funicular state; (c) capillary state; (d) oil droplets with particles inside or at its surface.

in water. Since the surface of coal is a patchwork assembly (see Section 3.5) which consists of areas of organic matter, mineral matter and pores that display various contact angles, while hydrocarbon liquid bridges are formed between hydrophobic parts of coal particles, water will form similar bridges between hydrophilic spots on coal particles in the agglomerates [10].

Three major factors control oil agglomeration [11,12]: (a) the solid wettability; (b) the amount of bridging oil; and (c) the type and intensity of conditioning.

As shown in Fig. 9.2, the amount of agglomerating oil is critical. At low oil levels, discrete lens-shaped rings are formed at the points of contact of the particles (Fig. 9.2a). At higher doses, the oil rings begin to coalesce and form a continuous network (the funicular state, Fig. 9.2b). The interparticle space becomes filled with oil when the capillary state prevails (Fig. 9.2c). At higher that 10% oil consumption, spherical agglomerates of a few mm in size are formed.

The effect of oil characteristics is interrelated with the hydrodynamics of the system. It was commonly held that more viscous, "heavier" oils were less efficient agglomerants; these oils were, however, shown to yield excellent coal recoveries under the more intense mixing conditions needed to disperse the oil in water [6,11].

Only very hydrophobic particles can be agglomerated with oil. Tests with alumina particles carried out by Kavouridis et al. [13] confirmed that agglomeration took place only over the pH range and sodium dodecyl sulfate concentrations where the contact angle on alumina at the water/oil interface was greater than 90° (contact angle measured through aqueous phase, see Fig. 5.7). Light oils efficiently agglomerate bituminous coals which (as shown in Figs. 3.2 and 3.3) are very hydrophobic, but not lower-rank coals. However, lower-rank coals can be agglomerated with heavy oils. This observation reveals the effect of coal surface properties and organic phase composition on the overall agglomeration results.

As discussed in Section 5.2.1, the chemical composition of crude oil distillation fractions changes with distillation temperature. The heavier fractions contain paraffins

of high molecular weight, polycyclic compounds, condensed polyaromatics, and sulfur-, nitrogen-, and oxygen-containing compounds. Fuel oil No. 6 was shown to be a better collector for lower-rank/oxidized coals, and Fig. 5.12 confirms that the droplets of such an oil suspended in water have quite different properties from those of fuel oil No. 2. In line with such findings it was reported that subbituminous coals could be agglomerated with heavy refinery residues [14]. This was further confirmed by Carbini et al. [15] and Blaschke [16]. Blaschke showed that oil agglomeration of lower-rank coals could be improved by adding aromatic hydrocarbons to fuel oil No. 2.

Keller and Bury [10] observed a linear relationship between ash content in the agglomerated clean coal product and the oil/water interfacial tension; the ash content was higher for hydrocarbons within the 30–40 mJ/m^2 interfacial tension range, and decreased for oils with higher interfacial tensions with water. This agrees perfectly with the line of reasoning adopted in this book. The interfacial tensions between saturated aliphatic hydrocarbons and water slightly exceeds 50 mJ/m^2. Any deviation from this value indicates the presence of polar compounds which can interact with water not only via dispersion forces but by hydrogen bonding as well. Aromatic hydrocarbons also interact with water via pi-bonding and as a result values of their interfacial tensions with water are about 15 mJ/m^2 lower. The hydrocarbons which contain polar groups that can interact with water via hydrogen bonds are characterized by very small values of interfacial tension. Droplets of pure paraffinic hydrocarbons attach only to hydrophobic particles, while the interactions between droplets of the oils containing polar compounds and solid particles can obviously include specific chemical interactions as well. Therefore, droplets of the oils containing polar compounds can also attach to the high-ash coal particles. This translates into higher yields of the agglomerated product and higher ash contents. In the process developed at the Energy and Environmental Research Center (EERC) a low-rank coal is first cleaned by leaching with nitric acid and the clean product is recovered by oil agglomeration [17]. The most suitable oils for agglomeration of low-rank coals under low-shear mixing conditions were the crude phenol/tar oil mixture and the commercial cresylic acid-based oils.

The use of vegetable oils was also studied. Garcia et al. [18] reported that Spanish anthracites could be agglomerated with sunflower and soybean oils. The water/oil interfacial tensions for these oils were 21.2 and 26.5 mJ/m^2, respectively. While 80–90% combustible recoveries were reported in these experiments at oil doses of up to 20%, the selectivity at such high oil dosages was poor.

Various oil agglomeration processes have been reviewed by Mehrotra et al. [19]. These include: Trent, Convertol, NRCC (National Research Council of Canada), Shell, Olifloc, CRFI (Central Fuel Research Institute in Dhanbad, India) and BHP (Broken Hill Proprietary, Australia) processes. In the process developed at the National Research Council in Ottawa [11], the light-oil addition and high-intensity conditioning produces micro-agglomerates and this is followed by the addition of heavy oil and low-intensity conditioning to produce a handleable product that can be recovered by screening. An early flowsheet developed in the 1970s is given in Fig. 9.3. In the first agglomeration stage employing high-intensity blenders, a light oil is preferred [20]. The micro-agglomerates are dewatered on a screen and then pelletized in a disc or drum pelletizer. An additional amount of cheaper oil is used as a binder at this stage to produce sufficiently
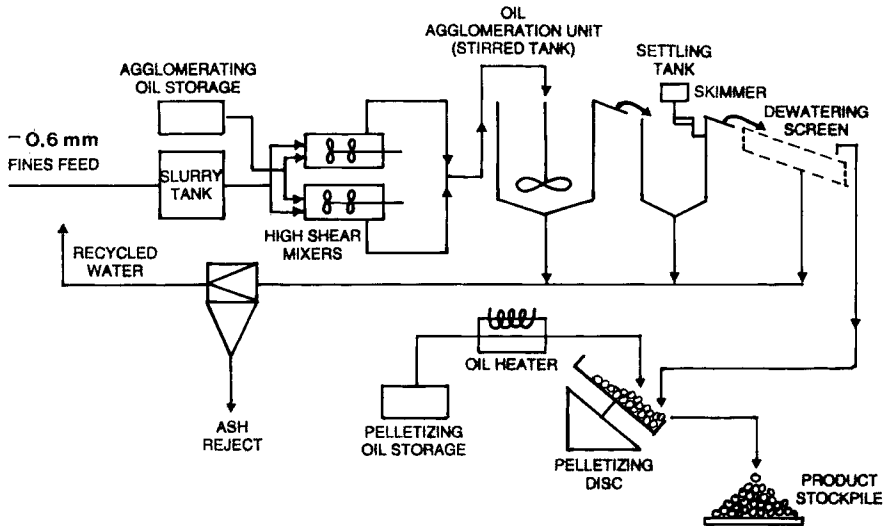
Fig. 9.3. A flowsheet of the NRCC process; in this process oil and coal are contacted in high-sheer mixers and oil-agglomerated coal is further pelletized in a disc unit.
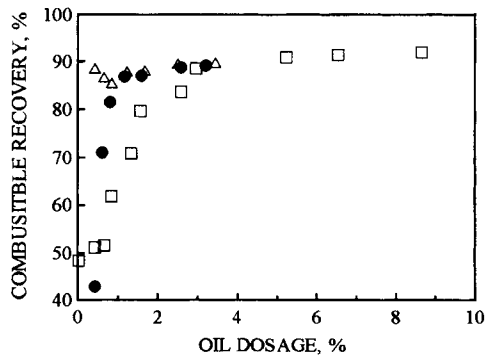
Fig. 9.4. Low oil agglomeration effects on combustible recovery. Different graphic symbols represent coals from different mines. (After Capes [11]; by permission of the American Institute of Mining, Metallurgical and Petroleum Engineers.)

strong pellets. In the more recent developments [11], the amount of oil was reduced down to a few percent and this provides better selectivity as demonstrated by Figs. 9.4 and 9.5. In these more recent flowsheets, the high-intensity mixing is followed by a low-intensity mixing which enables the coal–oil agglomerates to enlarge and strengthen. The agglomerated slurry is then passed to a Vor-Siv screen. The recovered agglomerates are then dewatered in a screen bowl centrifuge. In a final stage, the agglomerates are further enlarged by pelletization. In this later modification, some micro-agglomerates which pass through the Vor-Siv are recovered by skimming in a process resembling flotation.
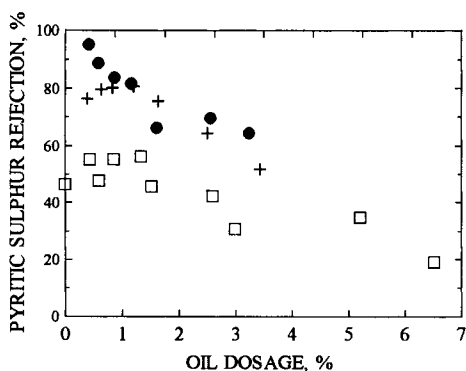
Fig. 9.5. Low oil agglomeration effects on pyritic sulfur rejection. (After Capes [11]; by permission of the American Institute of Mining, Metallurgical and Petroleum Engineers.)

As discussed by Bensley et al. [21], most oil agglomeration data have been obtained with the use of high-speed mixers (>10,000 rpm). Therefore, one obvious drawback of such a process is high energy input. However, energy savings may be obtained by the efficient emulsification of the oil phase prior to its addition to the pulp. Prior oil emulsification is a characteristic feature of the BHP process. Also, Zhang and Wheelock [22] reported a sharply enhanced rate of agglomeration when hexadecane agglomerant was emulsified. The use of surfactants in the emulsification of an oil phase, as shown in Fig. 9.6 [23,24], may also reduce the oil dosage required to obtain high combustible recoveries. Fig. 9.6 also includes the results obtained with the use of UBC-1 latex (the agglomeration with totally hydrophobic flocculants will be discussed in Section 9.3.3). The addition of surfactants reduces the oil/water interfacial tension and facilitates the dispersion of oil in water. While the median size of the kerosene droplets emulsified in a high-speed blender was 20 μm, the size dropped to about 2 μm with addition of the surfactants [24,25]. The use of either anionic or cationic surfactants entirely changes the electrokinetic characteristics of the oil droplets and, consequently, kerosene cationic emulsions can efficiently agglomerate oxidized coal particles. This was shown in experiments with two different bituminous coal samples whose proximate analyzes are set out in Table 9.1. The total acidity of these samples after demineralization was 0.04 meg/g for the F-4 sample, and 1.22 meg/g for the F-13 sample [26]. The equilibrium moisture content of the demineralized samples was 0.94% for F-4 and 4.59% for F-13. These values indicate that the F-13 sample was oxidized and should be

Table 9.1
Proximate analyses of coal samples

Sample	Ash (%)	Moisture (%)	Volatile matter (%)	Fixed carbon (FC^{dmmf}, %)
Ford-4	8.4	0.71	19.74	78.3
Ford-13	9.4	2.84	22.43	74.4
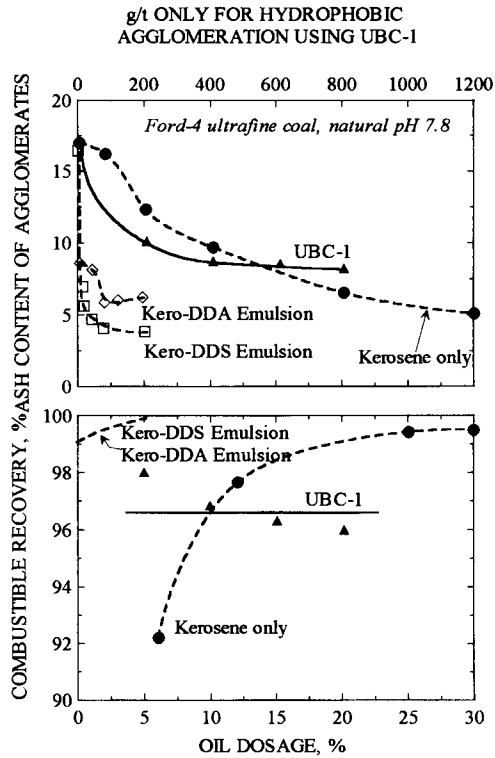
Fig. 9.6. Comparison of oil agglomeration using emulsified oil with conventional agglomeration and hydrophobic agglomeration using UBC-1 latex. Test conditions: 100 ppm and 300 ppm of sodium hexametaphosphate in oil agglomeration and hydrophobic agglomeration, respectively; stirring of 20,000 rpm in oil agglomeration and 300 rpm in hydrophobic agglomeration. (After Laskowski and Yu [23]; by permission of the Australian Coal Preparation Society.)

fairly hydrophilic. Wettability by water, characterized by contact angle measurements on polished specimens, was $\Theta_{adv} \approx 80°$ and $\Theta_{rec} \approx 50°$ for the F-4 sample, and $\Theta_{adv} \approx 45°$ and $\Theta_{rec} \approx 25°$ for the F-13 sample [27]. Sessile drop measurements carried out with very fine coal compressed into pellets gave contact angles exceeding 110° for the F-4 sample and 20° for the F-13 sample [28]. Because of the porosity of the pellets, these are apparent contact angle values. In the case of a hydrophobic sample, such an apparent contact angle value is expected to be larger than that measured on the polished specimen, but it should be smaller for the hydrophilic sample.

The two coal samples were ground below 0.5 mm and were either agglomerated using kerosene, flocculated with polyacrylamide flocculant, or were agglomerated using FR-7A latex (FR-7A totally hydrophobic flocculant was described by Attia et al. [29,30]). The agglomeration results, as characterized by vacuum filtration, are shown in Figs. 9.7 and 9.8 [25]. A large variety of additives, a cationic kerosene emulsified with dodecyl amine (kero–DDA), an anionic kerosene emulsified with sodium dodecyl sulfate (kero–DDA), a hydrophobic latex (FR-7A), as well as polyacrylamide flocculant
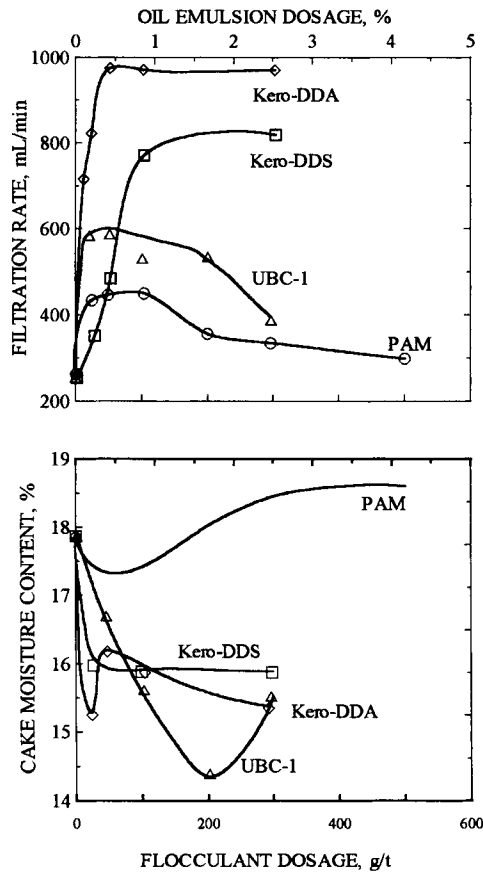
Fig. 9.7. Vacuum filtration of −0.5 mm Ford-4 coal that was agglomerated either using emulsified kerosene or hydrophobic agglomerant. Kero–DDA, cationic emulsion of kerosene prepared from kerosene containing 1% of dodecylamine; Kero–DDS, anionic emulsion of kerosene prepared from kerosene containing 1% of sodium dodecyl sulfate; PAM, polyacrylamide with molecular weight of 6×10^6; UBC-1 hydrophobic latex. (After Laskowski and Yu [25], by permission of Elsevier Science.)

(PAM) all aggregate the F-4 hydrophobic coal particles as judged from the remarkable improvement in the filtration rates (Fig. 9.7). In the case of the hydrophilic F-13 sample, only Kero–DDA and PAM aggregate the coal particles (Fig. 9.8). Obviously, positively charged kerosene droplets of kero–DDA emulsion can efficiently agglomerate the negatively charged particles of F-13 oxidized coals. An extension of the above argument suggests that such coal particles should not be agglomerated by negatively charged droplets of Kero–DDS emulsion, and this accords very well with the experimental data.

These results show that the use of appropriate surfactants to enhance emulsification of the oil utilized in oil agglomeration cannot only reduce the consumption of the oil but can also improve oil agglomeration of less hydrophobic lower-rank and/or oxidized coals. Additions of small amounts of alcohols can also be beneficial. Labuschange
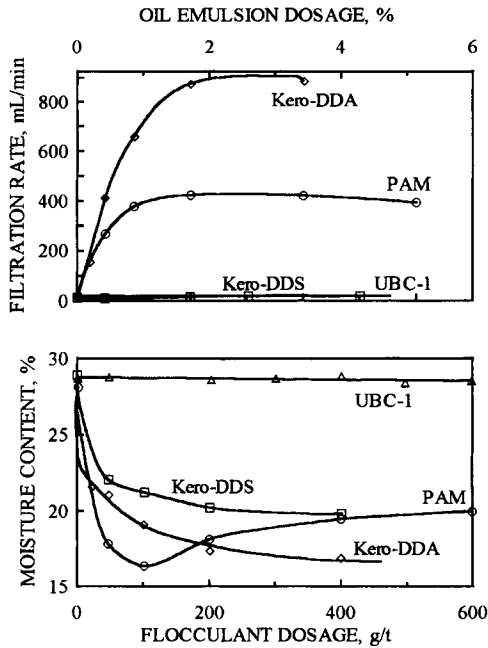
Fig. 9.8. Vacuum filtration of −0.5 mm Ford-13 coal that was either agglomerated or flocculated (as in Fig. 7). (After Laskowski and Yu [25]; by permission of Elsevier Science.)

[31] showed that the agglomerating ability of an oil towards hydrophilic coal could be improved by adding a small amount of alcohol to the oil. Good et al. [32] described and patented an improved oil agglomeration process in which octanol was added to decane to increase coal hydrophobicity (see Fig. 5.24) and Amioca starch was used to depress pyrite. All this gives credence to the conclusion that different technical products referred to as oils may exhibit quite different agglomerating abilities.

In the "T-process", finely ground coal is agglomerated using pentane [33]. The most interesting aspect of this is that the pentane is recovered by vaporation/condensation for reuse in the process leaving the clean coal for utilization either as a slurry or as dry pellets. The continuous pilot plant tests demonstrated combustible recoveries in excess of 95%, but also rather high losses of pentane. This process was rated very highly in comparison with other oil agglomeration methods [34], but the losses of pentane were very high in continuous tests.

New light was shed on the mechanism of oil agglomeration by a series of papers by Wheelock and co-workers [35–37] on an interesting effect of air present in the system upon oil agglomeration. The new experimental data reveals that the agglomeration process of a moderately hydrophobic coal with heptane is triggered by a small amount of air present as a separate phase. The rate of agglomeration increases as more air is added to the system or as the amount of agglomerant or agitation increases. In the presence of air, compact, nearly spherical agglomerates are formed, while only
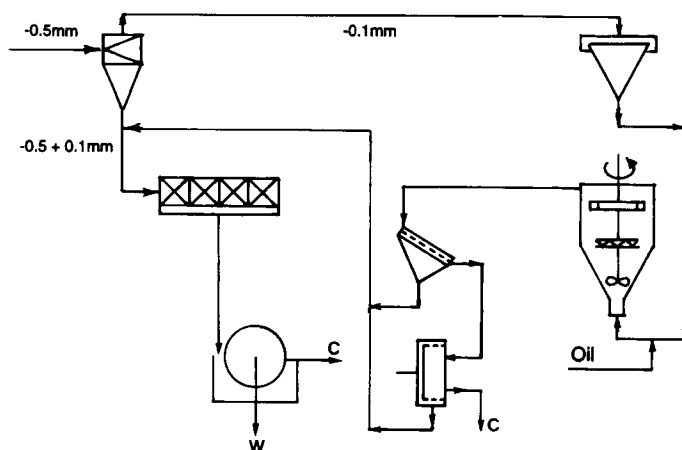
Fig. 9.9. Flowsheet of the Oilfloc test set-up in the Monopol Dressing Plant, of Ruhrkohle AG. (After Bogenschneider and Jasulaitis [40].)

small flocs and flake-like agglomerates are produced without air. More air is required at a higher solids content, and less air is required at a higher stirring speed. Oil agglomeration experiments in a system providing only a moderate shear rate proved it necessary to have air present [38]. One general criticism of the oil agglomeration process has been that it requires high energy inputs. Wheelock et al.'s results will likely attract a good deal of interest as they seem to indicate how such a high energy requirement could be reduced. From this point of view, the idea of agglomerating fine coal during pipelining with inexpensive bitumen/heavy oil additives is even more attractive [39]. This process combines hydraulic transportation of fine coal over long distances with simultaneous beneficiation, and it is undoubtedly economically viable.

One of the important benefits of an oil agglomeration process is its ability to replace conventional dewatering and drying. The flowsheet of the Oilfloc process (Fig. 9.9) illustrates it very well [40]. In this process, classifying hydrocyclones are used to split the flotation feed into −0.1 mm and +0.1 mm fractions. The former is processed by oil agglomeration while the latter goes to flotation. The Oilfloc process offers a means for avoiding thermal drying. The flotation concentrate obtained when floating coarser feed dewatered by vacuum filtration contains 2% less moisture and the oil agglomeration of the fine fraction produces 6–8% ash clean coal product. It is worth noting that such a process can dramatically improve handleability of the final products (see Section 10.2).

The most frequent goal of fine-coal dewatering is to improve handling, and to prevent freezing, sticking in bins, or leaking from cars. At the other extreme, dust caused by fine-coal handling is a loss, a nuisance, and an air pollution concern. Oil agglomeration can provide a free-flowing, non-freezing and dust-free product. This aspect of oil agglomeration is of particular value when the proportion of fines in the clean-coal products is high.

An economic evaluation of the oil agglomeration process for coal cleaning compared to the possible alternative of using a flotation–filtration–thermal drying flowsheet was

reported by Mehrotra et al. [41]. The capital costs for oil agglomeration are expected to be cheaper than the alternative treatment. The analysis established that oil agglomeration can be economical only if one accounts for (a) the increased recovery of combustible matter, (b) the increased calorific value of the coal due to the added oil, and (c) the added benefits of product handling which are: its dust-free nature, non-freezing characteristics, lower capital costs and the elimination of thermal drying. Full-scale oil agglomeration plants commissioned at two New South Wales mine sites demonstrate that fine coal can be economically recovered from coal preparation plant tailings by oil agglomeration [42]. The fine coal recovered is combined with the main product stream from both plants as a saleable product.

9.3. Flocculation

Fine solid particles dispersed in water can be aggregated in different ways. Reduction of the interparticle electrical repulsion either by adjusting surface potential (via concentration of potential-determining ions) or by collapsing the diffuse double layers by raising the ionic strength changes the balance between the attractive van der Waals and electric repulsive forces and brings about the coagulation.

9.3.1. Coagulation

This process is dealt with by the classical DLVO theory of colloids stability which takes into account van der Waals (attractive) forces and electrical forces. The presence of an electrical charge on interacting solid particles results in the formation of electrical double layers around such particles. The overlap of such layers when two particles approach each other results in repulsion. The results of Pugh and Kitchener [43] and Pugh [44] are used here to illustrate coagulation either by adjustment of the potential-determining ions, or by changing the ionic strength.

The -0.2 $+0.05$ μm fractions of finely ground quartz and hematite were used in these experiments. Fig. 9.10 shows the electrokinetic potential of these two samples plotted vs. pH (i.e. versus the concentration of potential-determining ions). The stability of the single-mineral suspensions was studied at 2.2 wt.% solids, while the suspensions of two mineral mixtures were studied at 1.1 wt.% solids of each mineral. While the quartz suspension was stable over a broad pH range (from 3 to 13), the hematite suspension was stable in both the acidic and alkaline pH ranges with rapid coagulation in the 5–7 pH range (Fig. 9.11). As comparison with Fig. 9.10 demonstrates, the suspensions were stable when the zeta potential values of the tested mineral particles were high, but were unstable and coagulated in the vicinity of the iso-electric points (at which zeta potential values are equal to zero). Since above pH 6.5 both quartz and hematite particles are negatively charged, it was possible to achieve selective coagulation around this narrow pH window. The hematite particles are only slightly negatively charged in the 6.5–7 pH range and slowly coagulate, while strongly negative quartz particles (see Fig. 9.10) are perfectly stable. Of course, both coagulate vigorously in acidic solutions since quartz particles are charged negatively and hematite is charged positively over
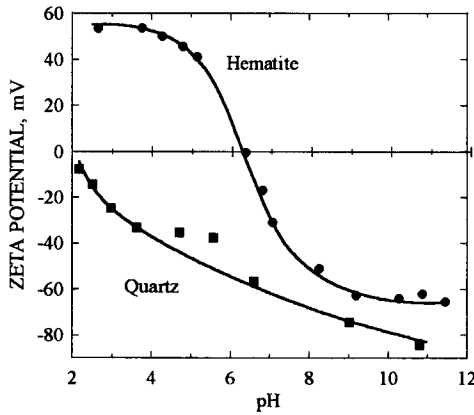
Fig. 9.10. Electrokinetic potential of fine quartz and hematite particles. (After Pugh [44]; by permission of Steinkopff Publishers.)
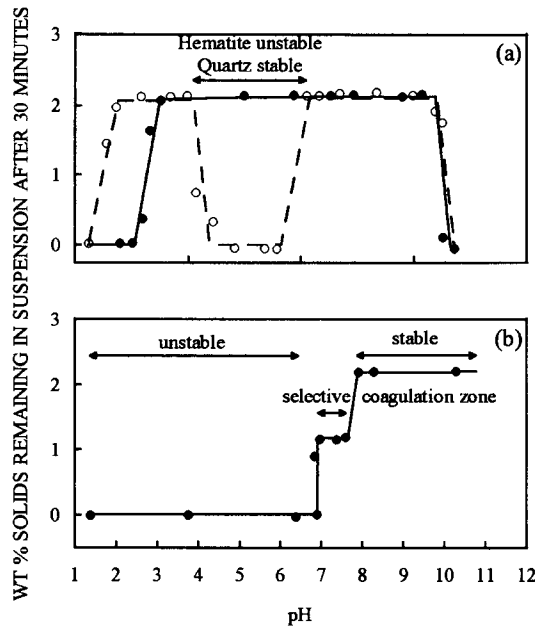
Fig. 9.11. The stability regions without addition of electrolyte: (a) hematite suspensions (○) and quartz suspension (●); (b) 1 : 1 hematite/quartz suspension. (After Pugh and Kitchener [43]; by permission of Academic Press.)

this pH range, and thus the electrical forces between the interacting particles are also attractive.

As Fig. 9.12 illustrates, coagulation can also be achieved by increasing the ionic strength using any simple electrolyte. These experiments were carried out at pH 9,
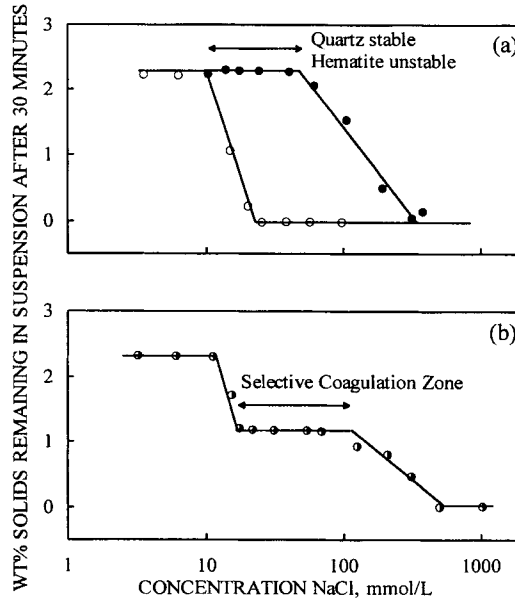
Fig. 9.12. The stability regions over a range of NaCl concentrations of: (a) hematite suspension (○) and quartz suspension (●); (b) 1 : 1 hematite/quartz suspension at pH 9 (After Pugh and Kitchener [43]; by permission of Academic Press.)

and as can be seen from Fig. 9.10, both quartz and hematite particles are negatively charged at pH 9. A mixture of such particles at this pH is perfectly stable (Fig. 9.11). However, upon increasing the electrolyte concentration, the double layers are compressed. Hematite starts coagulating first, and over a concentration range from 20 to 100 mmole NaCl/liter, selective coagulation is possible. At higher NaCl concentrations both minerals eventually coagulate.

The same can be deduced from Fig. 9.13, which shows the rheological behavior of a highly concentrated aqueous suspension of ZrO_2 (57 wt.%) [45,46]. The high yield stress values observed over pH 7–9 (i.e. around the iso-electric-point for ZrO_2) indicate the coagulation of ZrO_2 particles in this pH range which form the network of aggregated particles.

The results of the discussed experiments can easily be explained by the DLVO theory. Whenever the surface potential of the interacting particles is reduced, the repulsive electrical forces operating between the particles fall off and at a given point are overcome by the attractive van der Waals forces. This leads to coagulation. The results of Fig. 9.14 [47,48] are entirely different; as this figure reveals, the zeta potential–pH curves for both tested coals are approximately identical, but their coagulation is different. While the oxidized coal sample coagulates within the pH range close to the i.e.p., the fresh hydrophobic coal coagulates over a broad pH range irrespective of the zeta potential values. It is obvious that strong electrical repulsion is in this case compensated for by some additional strong attractive forces. These are the so-called hydrophobic forces.
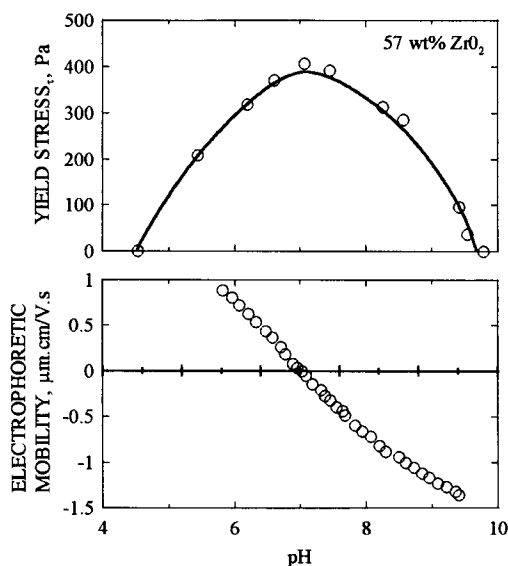
Fig. 9.13. Effect of pH on the yield stress of concentrated suspensions of ZrO_2 and the electrophoretic mobility of ZrO_2 particles (adapted from Leong et al. [45]; by permission of Elsevier Science.)

Recently modified DLVO theory also includes structural forces [49]. For hydrophilic surfaces these are hydration repulsive forces, whereas for hydrophobic surfaces these are strongly attractive hydrophobic forces. According to Churaev [50], the former should be considered for interactions between particles thoroughly wetted by water (contact angles smaller than 20°), whereas for contact angles larger than 40°, the structural forces become strongly attractive. In Fig. 9.15, various interaction terms in the modified DLVO theory are plotted as a function of the separation distance between two highly hydrophobic particles at the critical pH of coagulation. According to Yoon et al. [51], there is a functional relationship between the hydrophobic force and the contact angle. These results explain the frequently observed tendency of fine hydrophobic coal particles to aggregate.

9.3.2. Bridging flocculation

The main function of polymeric flocculants in mineral processing is to produce large and strong flocs. Polymeric flocculants are hydrophilic colloids with high molecular weight, they are soluble in water because solvation of the polar (ionic and non-ionic) groups is strong enough to overcome the van der Waals cohesive forces between the polymer segments.

It is generally accepted that polymers used as flocculants aggregate suspensions of fine particles by a bridging mechanism [52–54]. Bridging is considered to be a consequence of the adsorption of the segments of the flocculant macromolecules onto the surfaces of more than one particle. Such bridging links the particles into loose flocs.
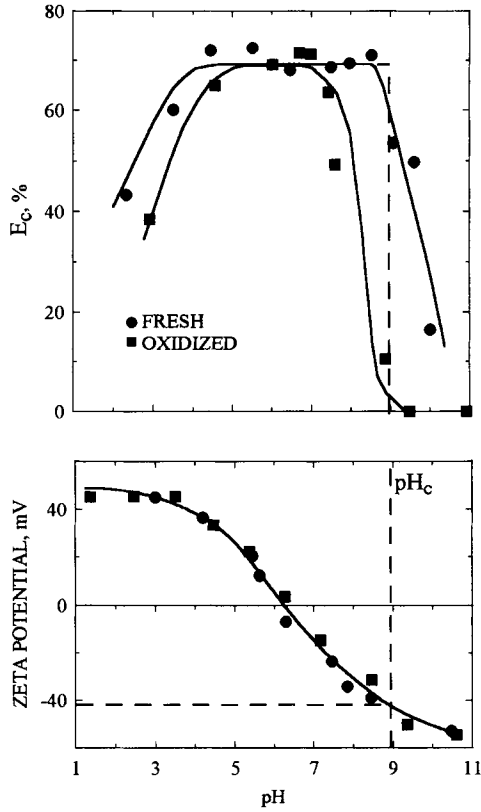
Fig. 9.14. Effect of pH on coagulation and zeta potential of fresh (●) and oxidized (■) (140°C) coal samples. (After Xu and Yoon [47]; by permission of Academic Press.)
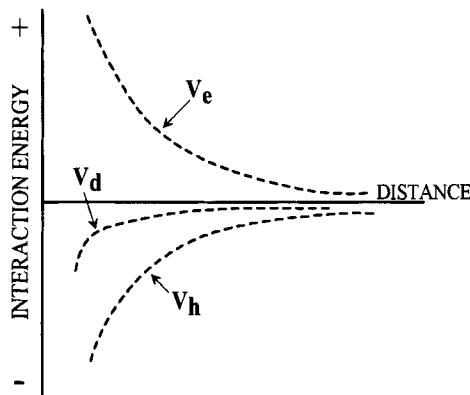
Fig. 9.15. Electrostatic (V_e), dispersion (V_d) and hydrophobic (V_h) terms in the energy of interaction between two very hydrophobic solid particles plotted vs. distance between the interacting particles.

The polymers used in flocculation can be classified into coagulants, which are highly charged, cationic polyelectrolytes with molecular weights in the 50,000 to 10^6 range, and flocculants with molecular weights up to 20×10^6 (since most naturally occurring particles are negatively charged in water, cationic polymers that act by neutralizing electrical charge of solid particles are commonly used as coagulants).

Adsorption of the polymer is generally necessary for flocculation to occur (not in depletion flocculation which will not be discussed here). It is important, however, to realize that adsorption and flocculation are not separate sequential processes, but occur simultaneously [55]. There is general agreement as to the basic mechanism involved in the process; the optimum flocculation occurs at flocculant dosages corresponding to a particle coverage that is significantly less than complete. Incomplete surface coverage ensures that there is sufficient unoccupied surface available on each particle for the adsorption of segments of the flocculant chains during collision of the particles [56].

As pointed out by Kitchener [57], the merit of modern polymeric flocculants is their ability to produce larger, stronger flocs than those obtained by coagulation. Theoretically, the flocculants may be applied either after destabilizing of the suspension via coagulation, or without prior destabilization:

(a) Stable suspension $\rightarrow$ coagulation $\rightarrow$ flocculant addition $\rightarrow$ flocculation
(b) Stable suspension $\rightarrow$ flocculant addition $\rightarrow$ flocculation

It is known that flocculants are not very effective for treating stable suspensions and so the first option, which involves prior destabilization by coagulation, is always better [57–59].

Electrokinetic studies on blackwater solids revealed that the particles are negatively charged from pH 2 to 11 [60]. The solids appear to be coagulated at pH less than about 9, but are quite stable between pH 9 and 11. In this pH range, flocculation was found to be very difficult. Gochin et al. [61] reported that the addition of NaCl at pH 9.4, in an amount which alone did not produce coagulation, markedly improved the flocculation of fine coal with PEO.

The most effective flocculation, at the least required dosage, occurs close to the zero point of charge where adsorption is generally at a minimum. This apparent paradox was discussed by Hogg [55]. At the point of zero charge, particles are already coagulated to some extent so the surface area available for polymer adsorption is reduced relative to that of the dispersed primary particles. The addition of polymer causes further flocculation and further reduction in available surface area. Thus, only a small amount of polymer is needed to provide sufficient coverage of the external surface for bridging to occur. So, while adsorption induces flocculation, flocculation actually inhibits adsorption. Since larger particles receive more polymer (per particle) than the finer material, when polymer is added to stable fine suspensions the overall result is the development of a bimodal particle/floc size distribution consisting of large flocs as well as dispersed primary particles. Only at higher polymer dosages can the residual primary particles be incorporated into the flocs [55].

For a polymeric flocculant to induce bridging flocculation, it is necessary for its macromolecules not only to adsorb on the surface of the particles, but also for loops of the adsorbed chains to extend further into the dispersing medium. This requires the

expansion of the loops of the flocculant to span at least the distance over which the electrostatic repulsion between particles is operative. This distance is of the order equal to the sum of thickness of the electrical double layers surrounding the interacting solid particles. The extension of polymer molecules increases not only with molecular weight but also with increasing electrical charge of the macromolecules. At low ionic strength, screening of the charges on the chains is limited and the polymer adopts an extended configuration which makes bridging more likely. At high ionic strength, screening of the charge produces a more compact configuration, thus reducing the chance of bridging. However, increasing the electrolyte concentration also results in reduction of the range of interparticle repulsion and hence compact chains could still bridge the particles. At high electrolyte concentrations, adsorption of polyelectrolytes is enhanced and this also increases the likelihood of bridging [62].

The configuration of the polymers in solution (and at interfaces) depends on the polymer–solvent (in our case, water) interaction energy. This is expressed by the Flory–Huggins chain–solvent interaction parameter, χ.

As has been pointed out, the bridging takes place at flocculant dosages corresponding to a particle surface coverage that is significantly less than complete. At higher concentrations, the polymers stabilize suspensions by the mechanism referred to as steric stabilization. This may only happen in good solvent conditions (i.e. $\chi < 0.5$; $\chi = 0.5$ is referred to as the theta-condition, which determines the onset of attraction). Khan and his colleagues [63] showed that the steric potential created by the adsorbed polymer is given by

$$\frac{V_{\text{steric}}}{kT} \propto \left(\tfrac{1}{2} - \chi\right)$$

The change of sign of the interaction potential, V_{steric}, from positive to negative indicates transition from repulsion to attraction. Such a change depends only on the value of the χ parameter. So, in order to stabilize particles (positive V_{steric}), the medium must be a good solvent for the polymer chains, which means that χ should be $<1/2$. Alternatively, in poor solvents $\chi > 1/2$, causing particles to flocculate due to attractive interactions between the adsorbed chains which prefer the chain–chain interactions to chain–water interactions. It is thus obvious that such interactions in sterically stabilized suspensions may bring about flocculation at electrolyte concentrations that are sufficiently high to affect the solvency of the medium for the flocculant. The flocculation of sterically stabilized suspensions which is induced by the reduction of solvency is referred to as incipient flocculation [62]. Many suspensions exhibit flocculation upon addition of a non-solvent to the aqueous polymer solution whereby the chains reach their theta-condition. Many authors have found good correlation between the onset of attraction (flocculation) and the θ-point [64]. This indicates that the behavior of common flocculants may be quite different at high electrolyte concentrations (e.g. in brine in processing of potash ores, and in seawater, but also in highly salted waters pumped out of some underground mines).

Hogg et al. [65] showed that the appropriate choice of flocculants is determined primarily by chemical factors (mineral composition, solution chemistry, etc.), but the performance of the flocculant depends more on physical variables, such as agitation

intensity and the rate of flocculant addition. Different mixing/polymer addition conditions may result in very different floc sizes and settling rates [66,67]. The developed experimental procedure includes addition of the flocculant to a vigorously agitated suspension; however, the agitation should be immediately stopped after addition of the reagent. Flocculant performance is also claimed to depend on the concentration of the polymer solution that is added to the mineral suspension [65]. It was shown that a very substantial increase in the initial settling rate can be achieved by reducing the concentration of the polymer stock solution.

The vast majority of commercial flocculants are based on partially hydrolysed polyacrylamide:

$$(-CH_2-CH-)_m(-CH_2-CH-)_n$$
$$CONH_2 COO^-Na^+$$
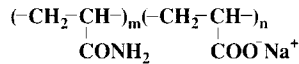
Polyacrylamides can also be obtained by co-polymerization of acrylamide and acrylic acid. As a result of hydrolysis even "non-ionic" polyacrylamides contain some anionic groups. This is expressed as "the degree of anionicity" (the degree of anionicity of completely hydrolysed polyacrylamide is 100%, so it is a polyacrylic acid).

Another important group of flocculants in the processing of fine coal is polyethylene oxide, $(-CH_2CH_2O-)_n$. Cationic polyelectrolytes such as co-polymers of acrylamide and quaternary ammonium compounds are also available (e.g. Poly-DADMAC). Naturally occurring materials such as polysaccharides (e.g. carboxymethyl cellulose, starch, guar gum, etc.) have also been used as flocculants. According to Kitchener [68], the first use of flocculants involved the application of starch in combination with lime for the clarification of a coal mine's effluent (a patent was filed in 1928).

The effectiveness of polymers as flocculants depends on their molecular weight, the sign of their charge (e.g. anionic or cationic) and the relative charge density. Depending on molecular weight, the same compounds can operate as dispersants (e.g. dextrin, low molecular weight) or flocculants (e.g. starch, high molecular weight). Low molecular weight copolymers of polyacrylate type are manufactured as dispersants (e.g. Cataflot manufactured by Pierrefitte-Auby Co., Dispex manufactured by Allied Colloids, etc.). While the charge density of the polymers which contain weakly ionic groups (e.g. carboxylic, amine, etc.) depends on pH, polyelectrolytes with strongly ionized groups (e.g. sulfonate, quaternary ammonium, etc.) are less sensitive to pH. The information on the chemical composition and molecular weight of commercial flocculants is usually hard to obtain and this makes interpretation of the experimental results very difficult in most cases [69].

The principal application of the flocculation process in coal preparation lies in the areas of solid/liquid separation and waste water treatment. This, first of all, involves treatment of flotation tailings, and consequently, it is determined more by the behavior of the associated minerals (clays, quartz, dolomite, etc.) than the coal. Polymeric flocculants were found to adsorb strongly onto coal, however, and thus the coal particles can consume up to ten times as much polymer per unit surface area as the mineral constituents and this contributes to overall reagent consumption [70]. Brookes et al. [71]
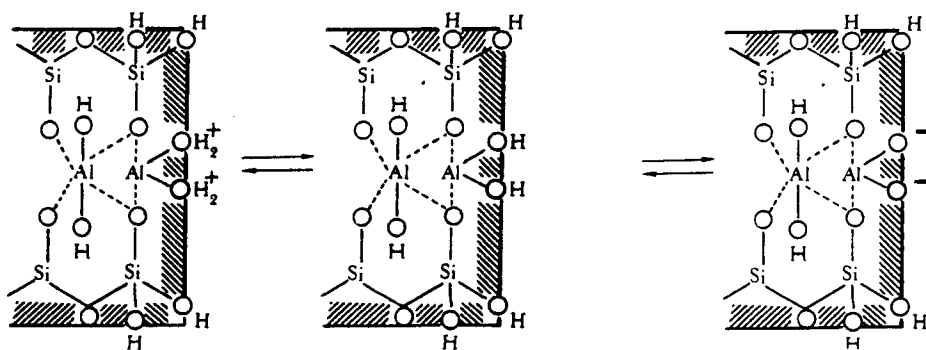
Fig. 9.16. Origin of electrical charge at the clay particle edge.

attributed the observed flocculation selectivity (when working with mixtures of coal and shale) to the preferential adsorption of flocculant onto coal over shale.

It has been reported that among clays the most common in "blackwater" are illite and kaolinite. In aqueous systems under normal conditions, particles of such minerals as well as particles of other common coal constituents (quartz, dolomite, calcite, etc.) are negatively charged. However, it must be borne in mind that due to their crystallo-chemical composition, clays have very peculiar anisotropic surface properties. A montmorillonite clay is a 2 : 1 layer mineral composed of an octahedral alumina sheet sandwiched between two silica sheets. As a result of isomorphous substitution of some silicon atoms for aluminum, the face surface carries a negative electrical charge while $=Al(OH)$ groups at the edges are either positively or negatively charged depending on pH (Fig. 9.16). Tests with different polyacrylamides show that such polymers primarily adsorb onto clays via hydrogen bonds [72]. It is also interesting to recall that Carty et al. [73] have recently pointed out that kaolinite is a 1 : 1 sheet silicate composed of a silicate tetrahedral layer and an alumina octahedral layer. Below pH 9 this would thus result in plate-like particles with "top" and "bottom" surfaces carrying different electrical charges. It is then obvious that the interactions between polymer chains and such particles will be site-specific.

Recent data indicate that the best flocculants for the Syncrude clays were moderately anionic high molecular weight polyacrylamides (optimum around 20–30% anionicity) [74]. Hamza et al. [75] reported that slightly anionic polyacrylamides were the best for enhancing the settling rate of fine coal.

Since flocculants are either used to enhance solids settling rates to maximize thickener capacity, to enhance dewatering by filtration, or to improve water clarification, various tests are utilized. They include measurements of solids settling rate, supernatant turbidity, sediment density, or filtration characteristics [76]. The recommended flocculation procedure involves the use of a standard mixing system that consists of a cylindrical tank with four baffles which is agitated by a six-bladed impeller. Polymer solution should be added below the surface to the agitated suspension at a controlled rate for a short time (e.g. 10 s). Agitation should cease immediately after polymer addition to monitor the settling rate and supernatant turbidity.
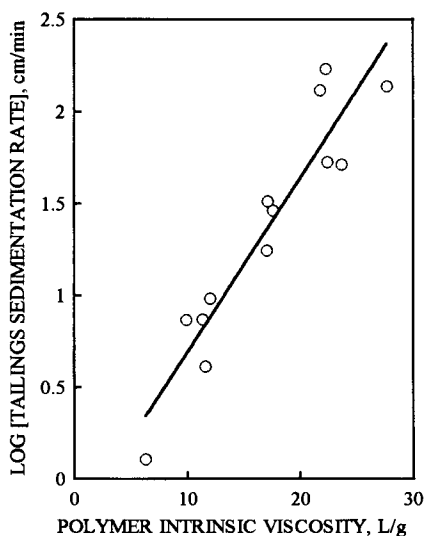
Fig. 9.17. Effect of polyacrylamide intrinsic viscosity on the sedimentation rate of flocculated tailings (polymers with various anionicities, 0–100%). (After Henderson and Wheatley [77]; by permission of Gordon and Breach.)

The molecular weight of flocculants is commonly characterized through viscosity measurements. This is based on the Mark–Houwink equation:

$$[\eta] = kM^a$$

where $[\eta]$ is the intrinsic viscosity of the polymer solution (has units of reciprocal concentration), M is molecular weight, and k and a are constants.

Strictly speaking, this equation should only be used for polymers with varying molecular weight and the same chemical composition, but this is rarely the case. After Henderson and Wheatley [77] Fig. 9.17 shows the effect of polyacrylamide intrinsic viscosity on the sedimentation rate of flocculated tailings for polyacrylamides with varying anionicities. Similar results showing how the solid content in centrate drops after centrifugation of coal tailings flocculated with polyacrylamides of 40% anionicity were published by Field [78]. Fig. 9.18 shows the relationship between the solids content of the tailings and the flocculant dose required to produce the measured settling rate [77]. The tailings were flocculated with the polyacrylamide polymer (intrinsic viscosity of 22, and anionicity degree of 30%).

Of course, the flocculation results are also affected by particle size distribution. As small particles have a very large surface area, the flocculant requirement increases with decreasing particle size. The flocculant dosage is proportional to particle surface area [77,79]. Moudgil et al. [80] tested polyacrylic acid with molecular weights varying from 1800 to 4,000,000 and found a strong correlation between flocculation of apatite particles of a given size and the molecular weight of the polymer. Coarser particles required higher molecular weight flocculants.

Large flocs are generally characterized by low densities and low compressibility.
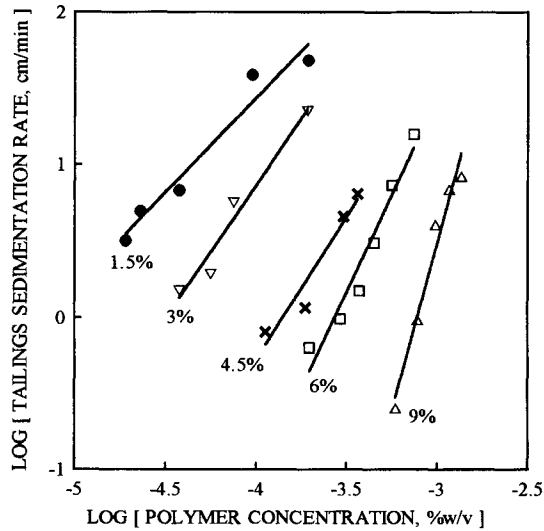
Fig. 9.18. Effect of solids content (in tailings) and flocculation on the sedimentation rate (30% anionic polyacrylamide). (After Henderson and Wheatley [77]; by permission of Gordon and Breach.)

An increase in the molecular weight of a flocculant has been reported to increase the filtration cake yield, but also to increase the moisture content [81]. A greater degree of moisture reduction can be achieved with lower molecular weight flocculants.

Comparative flocculation studies carried out with different coals and different flocculants revealed that the flocculation results depend not only on the type of flocculant but also on the coal surface properties. Palmes and Laskowski [82] reported that whereas hydrophobic F-4 coal (see Table 9.1) could be flocculated with all the tested flocculants (PAM, FR-7A hydrophobic latex, and F1029-D semi-hydrophobic flocculant[1]), the F-13 hydrophilic sample was only flocculated by PAM. The results shown in Fig. 9.19 confirm these findings [23]. As these results demonstrate, the UBC-1 hydrophobic latex flocculated only hydrophobic coal, polyacrylamide (PAM) flocculated both tested coal samples, while polyethylene oxide (PEO) worked very well with F-4 coal, but was not very efficient with the oxidized F-13 sample. The results obtained with the PEO and F1026-D flocculants turned out to be very similar. Gochin et al. [61] studied adsorption of a high molecular weight PEO onto coal, and they also studied coal flocculation. They concluded that PEO was a good flocculant for unoxidized coal over a broad pH range (from 2 to 10), but that it would not flocculate oxidized coal under any circumstances. These findings are consistent with our own (Fig. 9.19).

PEO is an interesting flocculant. It was extensively studied by Rubio and Kitchener [83,84]. They demonstrated that the presence of isolated –SiOH silanol groups on the otherwise hydrophobic matrix favors its adsorption on solid surfaces. The flocculation

---

[1] According to Attia [91], this is a copolymer of acrylamide (85%), sodium acrylate (5%) and ester of acrylic acid with 2-ethylhexyl (10%).
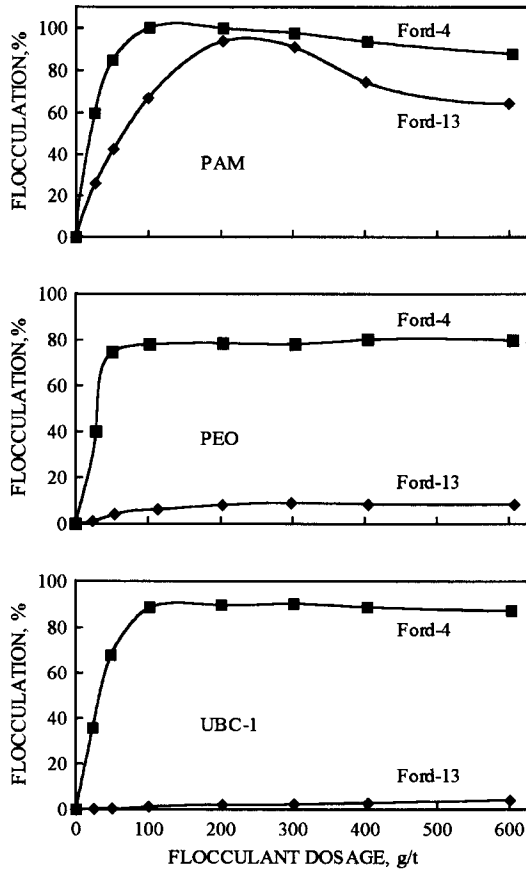
Fig. 9.19. Effect of flocculant dosage and coal wettability on aggregation of ultrafine (−0.045 mm) coal at pH 6.8. (After Laskowski and Yu [23]; by permission of the Australian Coal Preparation Society.)

of hydrophobic minerals with PEO was found to be very effective [85]. The use of PEO made it possible to selectively flocculate the minerals rendered hydrophobic with xanthates from quartz, calcite and dolomite [85]. These results seem to suggest that PEO can be classified as a semi-hydrophobic flocculant and thus its presence in the process water in coal flotation circuits should be less harmful to flotation than the presence of other more hydrophilic flocculants. Direct flotation tests seem to corroborate such conclusions [86]. In line with these ideas, Vigdergauz et al. [87] reported that combination of kerosene and PEO leads to improved flocculation at very low dosages of PEO.

Scheiner [88–90] showed that PEO can be successfully applied in dewatering coal–clay waste from coal preparation plants. This line of research follows earlier publications by Kitchener in which the idea of "sensitization" was developed. Wright and Kitchener [58] found that montmorillonite clay slurry can be put into a filterable condition by a combination of coagulant (e.g. Mg^{2+} salts) and polymeric flocculant (PEO). Their

results strongly indicated the need for prior coagulation before efficient bridging by flocculant can occur.

Scheiner et al.[89] postulated that PEO, a polymer with repeating $-CH_2CH_2O-$ groups interacts with the surface of clay minerals through a water bridge whose strength is influenced by the exchange ion. For this to happen, mechanical energy has to be applied (e.g. through shaking or tumbling) (see also [90]). Large flocs formed from fine particles when high molecular weight polymers are applied have low density. According to Szczypa et al. [5], such flocculated coal fines contain about 60% water and compaction by proper handling may further decrease water content by about 10–15%. In the process developed by Scheiner and his colleagues, the compacted flocs formed when high molecular weight PEO and lime are utilized can be separated and further dewatered on sieve bends. Lime is added up to pH 9 or higher and the PEO dosage required to get optimum results varied from 50 to 150 g/t. Interestingly, the dewatered material does not reslurry when contacted with water such as rainfall [90]. This, by the way, confirms the semi-hydrophobicity of PEO.

In sedimentation/clarification operations, clarification problems are common in the presence of ultrafine clays. While high molecular weight flocculants are very effective in producing large flocs, they are not efficient for treating stable suspensions. According to Hogg [55], the fine primary particles receive little polymer and tend to remain in a dispersed state. Low turbidity can be achieved by first applying coagulants (e.g. low molecular cationic polymers, or inorganic salts of Fe^{3+}, Al^{3+}, Ca^{2+}, Mg^{2+}, etc.) along with controlled agitation which is then followed by the addition of a high molecular weight flocculant. In practice, this often involves the addition of a cationic polymer to tail boxes of froth flotation cells, and the addition of flocculant to the thickener feedwell. Ordering the addition of polymers in this way can augment the action of bridging flocculants as shown in Fig. 9.20 [78]. These results demonstrate that the addition sequence is an important consideration in situations where the combination of bridging flocculation and coagulation are utilized. Kaiser and Latsch [92] claim that the addition of an anionic flocculant (40% anionicity, 14×10^6 molecular weight) followed by the addition of cationic flocculant ($6–12 \times 10^6$ molecular weight) can improve both sedimentation/clarification and filtration.

In pressure filtration the most effective aids are mid-range anionic flocculants of medium to high molecular weight. Improvements in the testing procedures that resulted from the CIBA studies [93] in which it was shown that the main difference between the lab tests and plant application was in mixing, led to the development of the TwinTec dewatering system. This is an encapsulated two-component filtration additive that contains both anionic and cationic flocculant with the slow release of the second component.

Other synergistic effects have also been reported. Engler et al. [94] demonstrated that there is a strong synergistic effect between the coal and mineral matter constituents of the blackwater to produce a flocculated sludge of higher solids than was possible by using either of the parent constituents alone. In the flocculation experiments in which the flocculated sludge was further dewatered on a screen, solids recovery was very high if the blackwater contained both coal and mineral matter, but was poor for coal only. The highest solids content in the compacted pellets was obtained at about 50% mineral matter in the sludge.
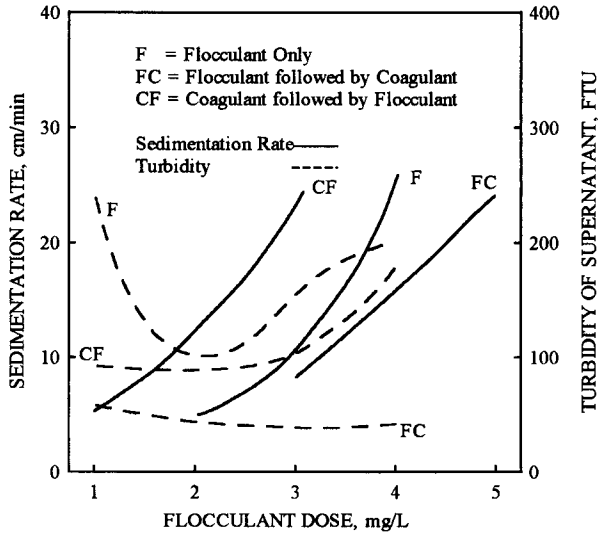
Fig. 9.20. Typical trends obtained in the treatment of coal tailings using a combined anionic flocculant/cationic coagulant system at a constant coagulant dose. (After Field [78]; by permission of Gordon and Breach.)

Loo and Smitham (as quoted by A.G. Walters [95]) showed that poor clarity in flocculation tests involving kaolin clays can be caused by the presence of humic acids which are naturally occurring anionic polyelectrolytes. There are reports which indicate that the presence of such anionic compounds in aqueous systems interferes with the use of cationic flocculants [96].

A few reports have been published on selective flocculation of coal as a means of separating coal from gangue particles. Blaschke reported [97] some selectivity in tests with carboxymethyl cellulose utilized as a dispersant followed by the use of polyacrylamide flocculant. The process was further studied by Hucko [98] who tested various dispersing agents. A non-ionic polyacrylamide with a molecular weight of about 4 million was found to be more selective than other flocculants, and sodium hexametaphosphate was the best dispersant. Interesting results were reported by Attia [91] with the use of F1029-D, a semi-hydrophobic flocculant. The most selective seem to be the totally hydrophobic flocculants, which are discussed in the following chapter.

9.3.3. Hydrophobic agglomeration with totally hydrophobic flocculants

Fig. 9.6 shows the results of oil agglomeration, and agglomeration with the use of UBC-1 hydrophobic agglomerant. Such hydrophobic agglomerants are often referred to as totally hydrophobic flocculants [99].

The use of polystyrene latices as selective flocculants was described by Lyadov [100] and Littlefair and Lowe [101]. According to Vigdergauz et al. [87], the first patent, which was filed in 1980, involved a butadiene–styrene latex. The totally hydrophobic

flocculant, FR-7A, described by Attia et al. [29], apparently belongs to the same group of hydrophobic latex agglomerants.

The latices are produced by emulsion polymerization with the use of an appropriate surfactant (emulsifier for the monomer) whose molecules become permanently incorporated and appear at the latex/water interface. The latex particles are therefore characterized by "hairiness" [102].

The use of latex-type agglomerants (totally hydrophobic flocculants) will be illustrated by the results obtained with the FR-7A and UBC-1 latices [8,23,103].

The FR-7A latex tested by Attia et al. [29,30] was provided by the Calgon Corporation, Pittsburgh; UBC-1 was developed in the Department of Mining and Mineral Process Engineering, University of British Columbia [8]. The average particle size of the FR-7A latex ranged from 0.06 to 0.1 μm, while the average size of the UBC-1 latex was about 0.5 μm. Electrophoretic experiments revealed that both were negatively charged over broad pH ranges (see Fig. 9.21). The films obtained by evaporating these latices turned out to be very hydrophobic, with water-advanced contact angles being about 60° in both cases.

The results of the flocculation tests that were carried out following the procedure used previously [82] are shown in Fig. 9.21. As seen, particles of the F-13 sample are not aggregated over the entire pH range tested. As is obvious, in the case of the hydrophilic F-13 coal, the aggregation does not depend on the coal surface charge, and even below pH 4 where this coal is charged positively the aggregation does not take place. On the other hand, the F-4 coal is aggregated over a broad pH range from 3 to 9 and the aggregation efficiency decays sharply only when the pH exceeds 10. Even over the pH range 7–9, over which both the latex and coal particles are charged negatively, the aggregation is quite efficient. These results correlate very well with those of Xu and Yoon (Fig. 9.14) as both seem to result from the hydrophobic interactions.

Fig. 9.22 shows the results of the tests in which abstraction of the UBC-1 latex particles onto the F-4 coal and silica particles was determined over a broad pH range. In these tests the −500 μm +45 μm size fraction of either F-4 coal or silica were conditioned with the UBC-1 latex, and following the procedure from the paper by Yu and Attia [104] turbidity was used to determine the residual concentration of the latex in the solution. As Fig. 9.22 reveals, at a pH of 10.3, the abstraction of the latex is already much lower and this correlates very well with the flocculation results (Fig. 9.21). The abstraction data confirm that the particles of UBC-1 latex do not attach to silica even at low pH values (4.1). This substantiates the conclusion that it is the hydrophobic interaction which plays the decisive role in these phenomena.

Figs. 9.23–9.25 show beneficiation of 1 : 1 mixtures of ultrafine (−25 μm) F-4 coal and silica, and F-4 coal and kaolin clay mixtures. The aggregated product was recovered on a 400 mesh screen. The one-stage separation procedure provided very good results indeed, and combustible recoveries were around 85% even in the case of 1 : 1 coal–kaolin mixtures. The selectivity could be further improved, as shown in Fig. 9.26, by selecting an appropriate dispersing agent.

The tests with a raw F-4 coal (17% ash) showed that the clean product (8% ash) could be obtained at over 95% recovery of combustible matter in a one stage separation using UBC-1 latex (Fig. 9.27).
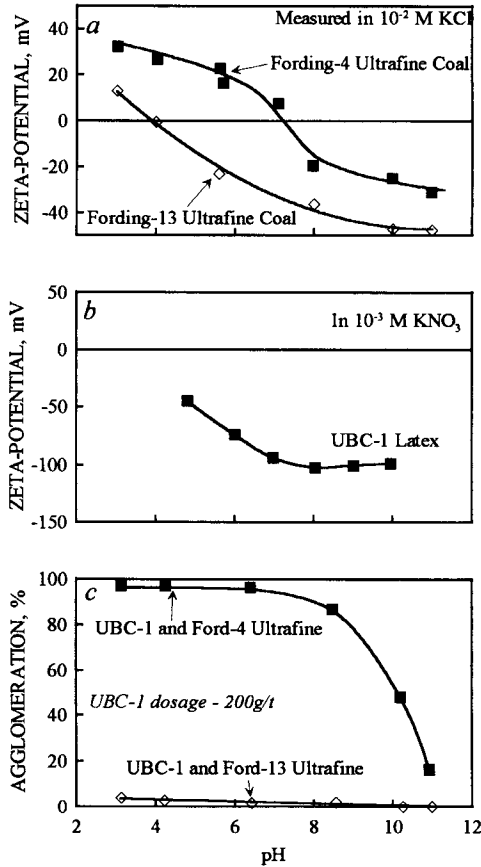
Fig. 9.21. Effect of pH on zeta potential of two bituminous coals (a), zeta potential of UBC-1 hydrophobic latex (b) and on hydrophobic agglomeration of these ultrafine coals with UBC-1 hydrophobic agglomerant (c) (After Yu [103].)

Latices are very convenient for direct use after dilution with water and do not require troublesome dissolution procedures typical for high molecular weight polymeric flocculants. The use of latices in fine-coal filtration should not lead to increased moisture content. By the way, the effect of both UBC-1 and FR-7A on coal wettability was studied directly by contact angle measurements [103] and these tests confirmed that the contact angle decreased in the presence of PAM while it increased in the presence of both tested latices. Overdosing resulted in stabilization of coal suspensions in the case of PAM but not in the case of UBC-1 [8,100]. These results demonstrate the fundamental differences in the properties of the adsorbed layers formed on the surface of the coal particles when these different flocculants are used. In line with these observations, the vacuum filtration tests shown in Fig. 9.7 demonstrate that the use of FR-7A latex (identical results were obtained with the UBC-1) not only increases filtration rate but also decreases the moisture content in the filtration cake. Since latices do not interact
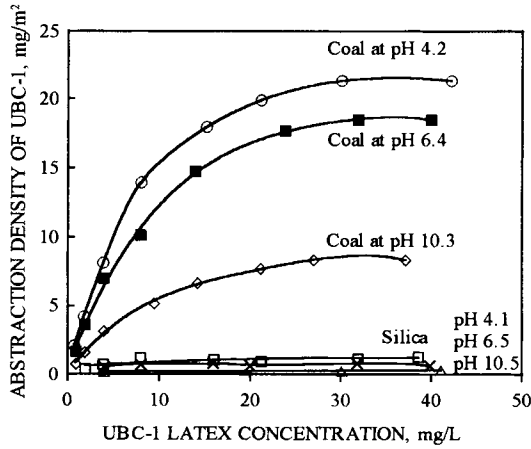
Fig. 9.22. Abstraction of UBC-1 latex by −500 μm +45 μm F-4 coal and silica particles at different pH values. (After Yu [103].)
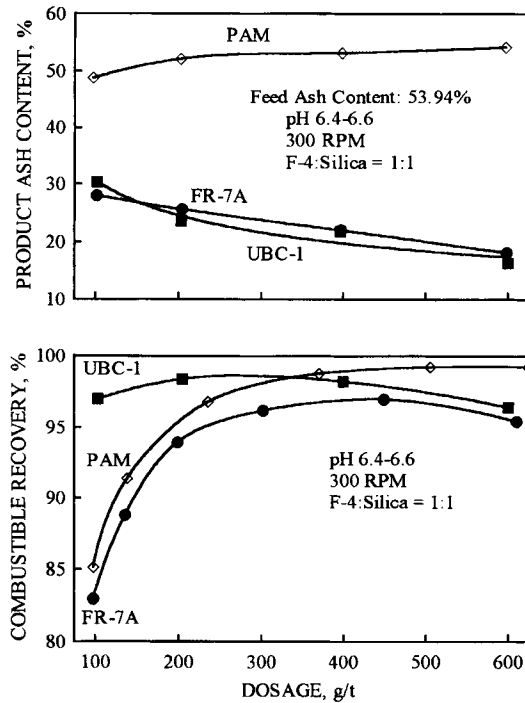
Fig. 9.23. Beneficiation of a 1:1 F-4 coal/silica mixture (particle size below 25 μm) in a selective flocculation using different reagents: polyacrylamide (PAM) and two hydrophobic agglomerants (FR-7A and UBC-1). (After Laskowski et al. [8]; by permission of Canadian Institute of Mining, Metallurgical and Petroleum Engineers.)
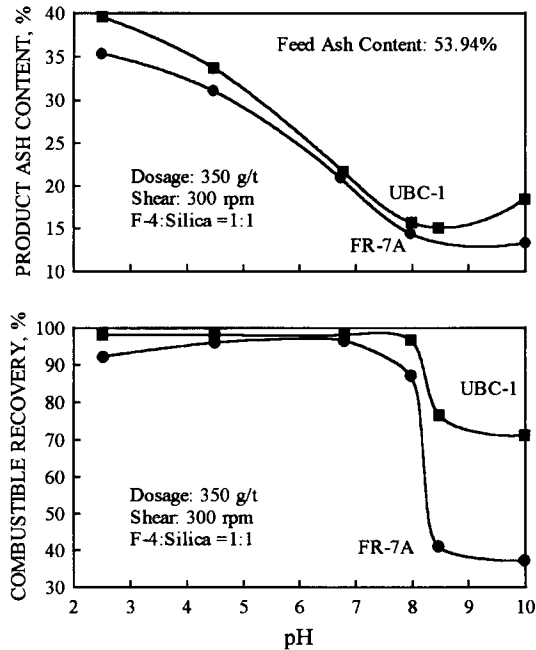
Fig. 9.24. Effect of pH on the beneficiation of 1 : 1 F-4 coal/silica mixture (particle size below 25 μm) using two hydrophobic agglomerants. (After Laskowski et al. [8]; by permission of Canadian Institute of Mining, Metallurgical and Petroleum Engineers.)

with the hydrophilic F-13 sample, they neither affect the filtration rate nor the moisture content in tests with this coal (Fig. 9.8).

Contact angles measured on hematite discs confirmed the hydrophilic nature of the adsorbed film of polyacrylic acid (PAA), and as Gebhardt and Fuerstenau showed [105], only at very low concentrations of PAA could the flotation of fine hematite with sodium dodecylsulfonate be improved. Since latex agglomerants are hydrophobic, they are compatible with flotation reagents. Therefore, the use of hydrophobic latices in flotation does not impose such limits. Rubinstein et al. [106] reported that in the flotation of a −0.074 mm fine coal, the use of 100 g/t of latex agglomerant along with kerosene and MIBC increased the concentrate yield by 4%, and tailings ash content by 9% (up to 73%). A beneficial effect of latex agglomerant on coal flotation was also reported by Vidgergauz et al. [87]. Since molybdenite belongs to the same group of inherently hydrophobic solids as coal, the UBC-1 was also found to improve flotation of fine molybdenite [107].

It is to be pointed out that size enlargement can be achieved with the aid of quite different additives. Flocculants are the most common. However, these polyelectrolytes are highly hydrophilic polymers so they strongly depress coal flotation [108] (see Section 6.5). The results discussed in this book demonstrate that in the case of hydrophobic bituminous coals, and especially flotation concentrates, the use of latices should be seriously considered. Since dewatering of fine particles is not difficult
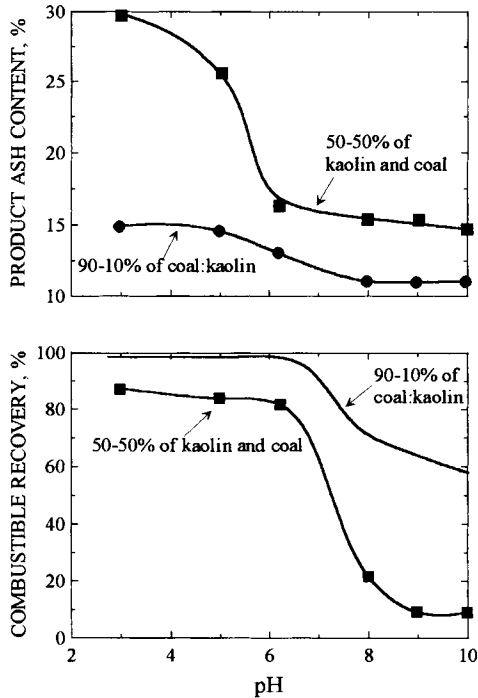
Fig. 9.25. Effect of pH on beneficiation of F-4 coal/kaolin 90:10% and 50:50% mixtures using UBC-1 hydrophobic agglomerant. 350 g/t of UBC-1, 320 rpm stirring. (After Laskowski et al. [8]; by permission of Canadian Institute of Mining, Metallurgical and Petroleum Engineers.).

when such particles are hydrophobic, there is no reason to again make these products hydrophilic in the final dewatering stages with the use of common flocculants. Wen et al. [109] confirmed these conclusions with a series of fine-coal filtration tests using asphalt–water emulsions.

Misra et al. [110] and Raichur et al. [111] described the use of the bacterium *Mycobacterium phlei*, and the biomass obtained by sonication of such bacteria, as selective flocculants for coal. The bacterium was shown to be hydrophobic and to carry a negative electrical charge due to the presence of carboxylic groups. This interesting agglomerant is then very similar to the described latices and should be classified into the same group of hydrophobic agglomerants.

9.4. Pelletization

Pelletization is the process of forming nearly spherical pellets by tumbling moist particulate feed (with or without the addition of a binder) in such devices as discs, drums or cones. The process is extensively utilized in the processing of iron ores and may involve pelletization of concentrates or raw iron ore [112]. In iron ore processing
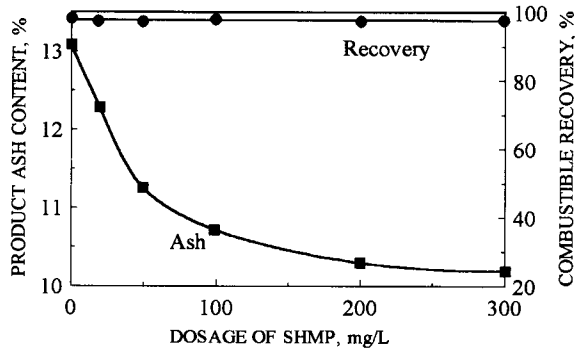
Fig. 9.26. Effect of sodium hexametaphosphate on hydrophobic agglomeration of 90 : 10% mixture of F-4 coal and kaolin with UBC-1 hydrophobic agglomerant. UBC-1 dosage 400 g/t, pH 6.2, stirring 320 rpm. (After Laskowski et al. [8]; by permission of Canadian Institute of Mining, Metallurgical and Petroleum Engineers.)
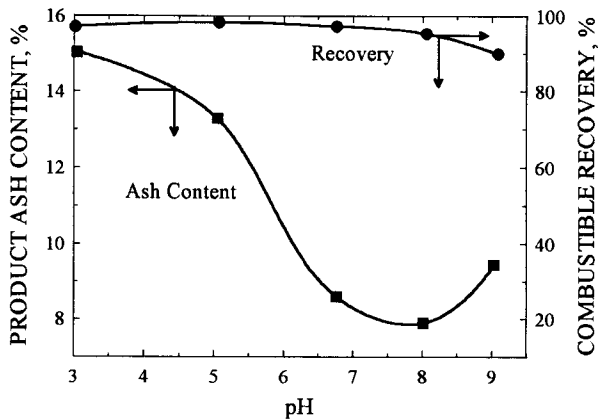
Fig. 9.27. Effect of pH on beneficiation of finely ground F-4 coal by hydrophobic agglomeration. UBC-1 dosage 350 g/t, stirring 320 rpm. (After Laskowski et al. [8]; by permission of Canadian Institute of Mining, Metallurgical and Petroleum Engineers.)

the pelletization consists of two distinct steps: (1) preparation of so-called green pellets (balls) with uniform mineralogical composition, size distribution and high porosity; and (2) firing the green pellets to increase their strength for subsequent handling.

Coal preparation plants rely mainly on gravity separation techniques and in the past the coarse products constituted the main saleable products. Introduction of new separation methods such as flotation resulted in a wide utilization of fine size fractions as well. This in turn has resulted in a considerable increase in the amount of fine clean coal products which pose severe storage, transportation and pollution problems. One possible method by which these problems can be reduced is pelletization of fine coal.

As reported in literature [113], the addition of a few percent of water to a dry fine coal can substantially increase its bulk density. This indicates that in the presence of water
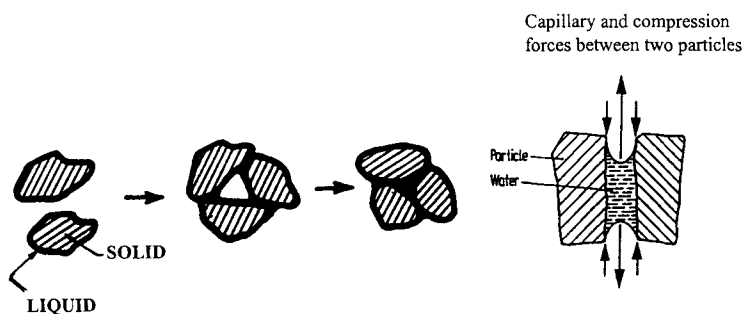
Fig. 9.28. Schematic representation of the formation of nuclei through reduction in the total air–water interface.

droplets some sort of consolidation takes place in the bed of fine dry particles. Such a process is further intensified by tumbling the particles in a disc or drum (pelletization).

The process is controlled by capillary phenomena and the driving potential for the pelletization is the lowering of the total surface free energy of the system through a reduction of the effective air–water interfacial area. As shown by Kapur and Fuerstenau [114] and Sastry and Fuerstenau [115], the kinetics of the pellet formation proceed through three stages: the formation of nuclei agglomerates, the transitional stage, and the ball growth stage. The rolling action of the drum brings the individual particles into proximity with each other so that the physical forces become operative and cause the particles to rearrange so that surface tension reduction can bring about nuclei formation via the bridges of wetting liquid. In the agglomeration of granular materials by capillary forces, the wettability of the agglomerated particles by the applied liquid plays an important role [116].

Because of the heterogeneity of coal surface (Fig. 3.1) water does not spread onto coal surface and does not form a film. This is a controversial topic, however, and for particles immersed in water for very long it is likely that they look as shown in Fig. 9.28. Once the liquid bridges are formed between contacting particles the capillary forces become responsible for bonding.

Fig. 9.29 shows a coal pelletizing circuit with a pelletizing disc [117].

Only a limited number of research results on pelletization of fine coal are available and Sastry and Fuerstenau's EPRI report [118] is probably the most valuable source of information in this area. Some results from this report will be used to illustrate the principles.

Since the primary reason for pelletizing fine coal is to minimize problems encountered during drying, handling, storage, and transportation, fine coal below 0.6 mm (28 mesh) that may derive either from ROM coal, or from gravity or flotation circuits (e.g. as filtration cake) is a typical candidate for pelletization.

Sastry and Fuerstenau [118] found that it is possible to pelletize coals of different ranks and widely different size distributions (Rive et al. [119] reported that even coal as coarse as 1.2 mm could be pelletized provided that it contained at least 50% of minus 74 μm material). The pellet size distribution is not influenced by the operating
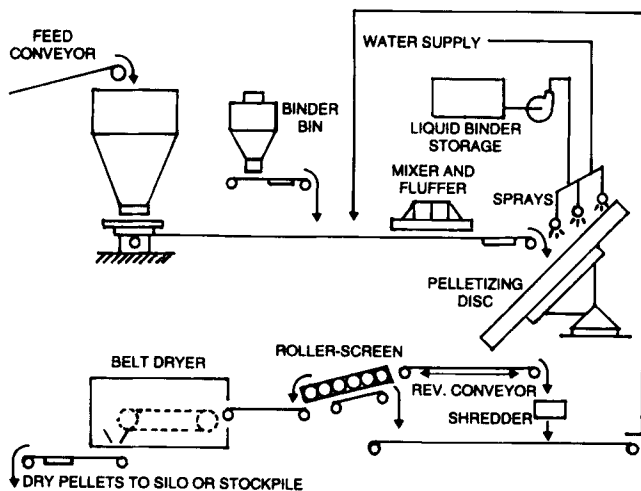
Fig. 9.29. Flowsheet of a coal-pelletizing circuit showing a pelletizing disc; a pelletizing drum can be installed instead of a disc. (After Sastry and Mehrotra [117].)
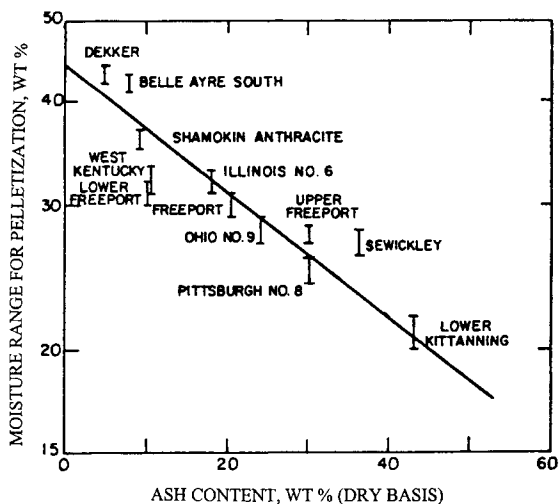
Fig. 9.30. Influence of the ash content (dry basis) of coal samples on their moisture requirements for pelletization. (After Sastry and Fuerstenau [118].)

conditions and type of coal sample [120], but the rate of the process is governed by the operating conditions and the type of coal fines. The rate of pellet growth is strongly affected by the amount of feed moisture. The amount of moisture required to pelletize is different for different coal samples and was found to be determined by the ash content. Figs. 9.29 and 9.30 show the pelletization results obtained with different samples of raw coal, pre-cleaned coal, and two samples of flotation concentrates. The
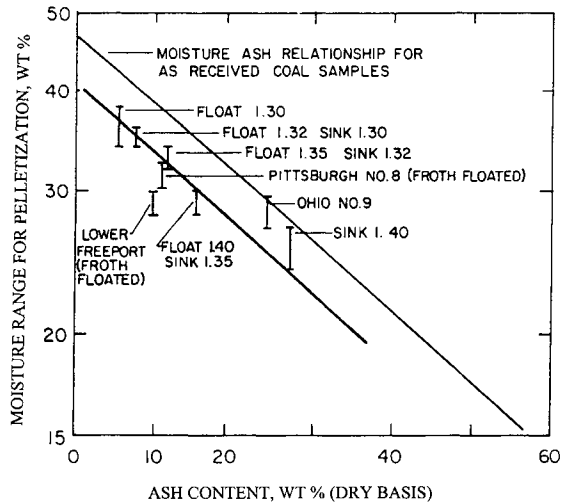
Fig. 9.31. Dependence of the moisture required for pelletization on the ash content and coal cleaning. (After Sastry and Fuerstenau [118].)

coal fines for these experiments were prepared by stage-crushing in a jaw crusher and dry grinding in a laboratory ball mill. Two hundred gram batches of the dry coal fines utilized in the pelletization experiments were premixed with the desired amount of distilled water (10 min) to prepare a moist feed. The moist feed was then placed in a 150-mm length by 225-mm diameter pelletizing drum, enclosed in a humidified chamber, and tumbled at a rotational speed of 40 rpm. At the end of each experiment, a portion of the pellets were used for determining their moisture content and compressive strength.

As Figs. 9.30 and 9.31 demonstrate, pelletization of fine coal is possible only within a narrow range of moisture additions. Outside the range, the coal fines are either too dry to agglomerate or too wet and form lumpy and weak agglomerates. Ash content was found to be the most significant property that determines moisture requirements for pelletization. The rate of growth of the pellets was found to decrease with increasing fineness of feed (the reverse trend was observed for lignite).

In Fig. 9.32, Sastry and Fuerstenau's data are plotted versus the fixed carbon content calculated on the dry-mineral-matter-free basis (Parrs' formula, mineral matter = 1.1 × % ash + 0.1 × % sulfur, was used to calculate the mineral matter content). Lignite, anthracite, and the samples containing more than 30% ash were excluded from the plot. The plot shows quite a good correlation with the fixed carbon content and it can then be hypothesized that the pelletization depends on the coal surface wettability. The plot also shows the fraction of surface that is pore-area-calculated with the use of the formula derived by Keller [121] (pore area fraction $= 2.642 \times 10^{-3}$ C% $- 0.4689$ C% $+ 20.818$, FC^{dmmf} was used instead of C% to estimate the porosity). Since only the water droplets present on the surface of coal particles, and not the moisture that penetrates into the pores, participates in the pelletization process, it is reasonable to expect that the coals
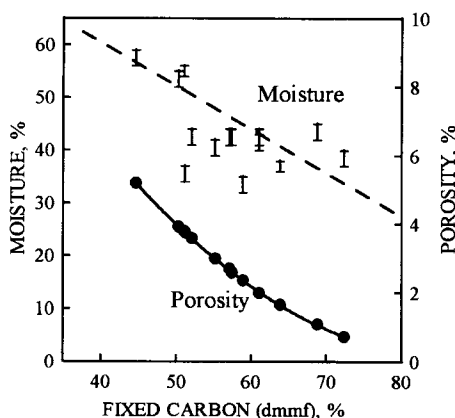
Fig. 9.32. The same data as shown in Figs. 30 and 31 plotted vs. fixed carbon content (see text for explanation).

with higher porosity will require more water for successful pelletization. This, of course, is only true for the solids which are not very hydrophobic, since for very hydrophobic solids water will not be drawn into the pores by capillary forces. However, comparison with Fig. 3.2 confirms that the samples used in the discussed pelletization experiments were indeed quite hydrophilic.

Sastry and Fuerstenau's report [118] also brings information on the effect of binders on fine-coal pelletization. The dry compressive strength of the pellets produced without a binder is within 1–10 kg strength. Pellet strength was found to decrease with decreasing ash and sulfur content. Corn starch was found to be a very good binder in that it improves the compressive strength of the pellets by several hundred percent; however, such pellets exhibit poor resistance to moisture penetration. On the other hand, asphalt emulsion, which was found not to improve pellet qualities much, renders pellets waterproof. The pellets produced with 1% by weight of corn starch that were subsequently sprayed with asphalt emulsion produced strong pellets which were also water resistant.

Wen et al. [122] described the use of a coal-derived humic acid as a binder in fine-coal pelletization. The pellets were dried at a temperature from 80°C to 191°C and the tests revealed that the pellet-drying temperature was the most critical parameter. For a one hour drying time, drying temperatures above 120°C produced water-resistant pellets with good compressive strength; a half hour drying required temperatures exceeding 140°C.

As Figs. 9.30 and 9.31 reveal, the pelletization of fine coal is possible only within a narrow range of moisture addition. For clean coal with an ash content in the range from 5 to 15%, the percent moisture required for pelletization is around 30–35%. It is then obvious that the pelletizing method should be the most economical means for treating coal filter cake [123]. The moisture content of filter cake as it is discharged from a vacuum filter is around 25%, thus eliminating the need for drying.

9.5. Briquetting

Pressure agglomeration is probably the best known size enlargement method. All particulate matter can be agglomerated by pressure agglomeration equipment and there is a great variety of pressure agglomeration methods [124–127]. The roll-type briquetting machine (or "Belgian" press) was developed in the last half of the 19th century to agglomerate fine coal; in the coal industry, this method is referred to as briquetting. Two groups of briquetting processes can be distinguished: binderless briquetting and briquetting with the addition of binders.

Before the advent of pulverized fuel systems, coal was sold by size with the coarsest fraction used as premium domestic fuel and medium sizes used for industrial purposes. The fines, sometimes referred to as "slack", constituted a relatively worthless byproduct. This led to the development of coal briquetting technology. For instance, by briquetting, lignite is converted from a friable material with a high water content (up to 60%) into a hard compact material which has a higher calorific value (Germany has been the largest producer of briquettes from brown coal). The use of briquetting declined after the Second World War. However, the increased mechanization of mines resulted in a higher production of coal fines, and the development of briquetted smokeless fuel and formed coke again generated interest in coal briquetting [128]. In some geographic areas, the demand for lamp solid fuel (which in a domestic use can be combusted with a higher efficiency) continuously increases and so creates a favorable situation for new developments in the area of briquetting [129–131].

The purpose for coal briquetting is three-fold: (a) to convert troublesome coal fines into a more easily handled and attractive fuel whose transportation does not pose environmental problems; (b) to increase the calorific value of the smokeless fuel made from low-rank coals by partial carbonization; and (c) to permit the production of metallurgical cokes from non-coking coals (formed coke).

The briquetted product should satisfy several conditions: it should be of uniform quality and size, it should be hard and resistant to mechanical stresses and water, and it should have satisfactory combustion properties. A sound operation first demands careful control over the composition of the feed material and secondly a briquetting process in which adequate cohesion of the briquetted material is ensured by careful selection of the conditions (and a binder) under which the mixture is compressed. If the raw material is relatively soft (e.g. lignite), an alternative is provided by the possibility of briquetting the coal without a binder, relying on the fact that it will plastically deform under sufficiently high pressures. Elimination of a binder demands even more stringent control over the briquetting conditions than are necessitated in conventional briquetting with the use of a binder [132].

A consequence of the short range of surface forces is that significant cohesion between adjacent particles can only be induced if the particles are brought into intimate contact with each other. The cohesion strength should then be directly determined by the degree of compaction and the elastic constants of the material. An increase in temperature and pressure are therefore beneficial. The compaction also depends on the particle size distribution of the raw material, and the optimum particle size distribution must be equal to that distribution which yields maximum packing density [132]. Another

complex variable is related to the presence of film-forming material on the surfaces of the briquetted particles. Such films act as a lubricant that enable particles to rearrange themselves more quickly and efficiently, and they also reinforce solid–liquid cohesional interactions through capillary forces. In the case of dry feed, any increase in pressure and temperature increase briquette strength by causing more extensive plastic deformation of the solid particles.

In binderless briquetting, the moisture content of the raw coal is a very important factor which determines briquette strength; conversely, in briquetting with binders, the presence of moisture has a very deleterious effect.

Iyengar [133] and Iyengar et al. [134] reported that briquettes of maximum strength were obtained at all pressures at an optimum moisture content, which is characteristic of the coal. This characteristic moisture content corresponds to the air-dried moisture content at 60% relative humidity and 40°C. For lignites, the best briquette strength was obtained at about 16% moisture [133]. When the compressive strengths of various briquettes prepared from coals of different ranks at their respective air-dried moisture content are compared, the minimum strength is observed with coals of 81 to 83% carbon content. Interestingly, the content of carboxylic groups in coal practically drops down to zero for coals with 81–83% carbon. Fundamental investigations on Indian lignites showed that these coals are characterized by a high content of phenolic and carboxylic functional groups which can form hydrogen bonds. It was also observed that non-polar liquids like benzene did not increase the strength of these briquettes. Blocking these groups by acetylation considerably reduced the strength of the briquettes.

Recently published results confirm that it is possible to produce briquettes with a sufficiently high compression strength from brown coals by reducing the moisture content to an optimal range and by applying high pressures [135]. In the briquetting of German brown coals the optimum moisture content of the briquettes lies between 12 and 18% [124]. But since these coals are not hydrophobic the resulting products are not hydrophobic either, and the water-resistance of the briquettes is not very good. It was reported that the addition of 20% fine coke to the coal made the final product not only mechanically strong, but also water-resistant [135].

In the past, binderless briquetting was considered possible only with low-rank coals containing less than 75% carbon on a dry, ash-free basis [132]. Therefore, the use of binders in briquetting was a common practice.

Theoretically, the potential range of additives available for briquetting is very wide. The additive should posses adequate adhesive properties and it should be a solid at room temperature, but it should also be sufficiently fluid at moderately elevated temperatures to permit its easy introduction into the briquetting raw material. The additives should be water-insoluble, weather-resistant and cheap. Briquette strength is determined by (a) coal nature and particle size, (b) the distribution of binder in the coal, and (c) the strength of the bond between the individual coal particles and the binding material [132]. When a briquette is stressed to rupture, failure will as a rule occur by separation along the solid/binder interface rather than by fracture across individual coal particles [136]. Obviously, the binder–coal adhesion plays a very important role. The most common binders were coal tar pitches (the residue left when coal-tar is distilled), and bitumens (material derived from petroleum oil as a distillation residue). Addition of such products

not only binds fine coal particles together, but in the case of low-rank coals, this may also increase the calorific value of the final product. Many other substances have also been tested including inorganic compounds that increase ash content such as cement and sodium silicate. Organic binders in most cases are not weatherproof. Sulfite lye and sulfite pitch produce briquettes of high strength, but the binder increases sulfur content and has a low resistance to water [124].

Komarek's early research indicated that a high pressure, high temperature briquetting process may produce good briquettes without binders if the moisture could be removed. This led to the conclusion that drying is the single most important factor in the successful manufacture of binderless briquettes. Several new binderless briquetting processes are carried out at sufficiently high temperatures to dry and partially devolatilize the coal. The released tars then act as a binder [129,130,137] and obviously wet coal surfaces very well. Thus, this type of a "binder" is not that different from conventional binders that include coal tar pitch and asphalt.

The technology was found to be especially attractive for binderless briquetting of subbituminous coals. Such coals from the western states of the USA contain 25–30% moisture with a calorific value between 19.5 and 21 MJ/kg. The process requires thermal drying and also requires processing of the resultant product so that it remains stable (not subject to spontaneous combustion) and handleable (not subject to degradation). It was found that the coal particle size distribution determines the final moisture content. In the KKS process [128], the coal is ground below 25 mm and its further degradation is achieved by subjecting it to a thermal shock at 700°C. The temperature of the dry feed that is briquetted varies from 100–110°C for low-rank coals to 300°C for a bituminous filter cake. The calorific value of the briquettes is in the range from 25.5 to 29.0 MJ/kg. Further development of this binderless briquetting process was discussed by Kalb et al. [137] in the paper they presented to the 13th Int. Coal Preparation Congress.

Also, in the thermo-briquetting process described by Golovin et al. [130], lignites are subjected to pressure at the temperature at which coal devolatilization begins. The process involves rapid heating of the coal at 200°C followed by pressing it at 380–400°C. The devolatilization products provide sufficient binding, and the obtained briquettes are characterized by good strength, high calorific value (over 25 MJ/kg) and water-resistance. Since the coal is partially devolatilized, the briquettes produce less smoke when burned.

Komarek's research also prompted CSIRO in Australia to study low-temperature binderless briquetting [138]. The compressive strength of the briquettes showed a strong correlation with the Hardgrove Grindability Index of the coal. Coal particle size was found to have only a marginal effect on low-temperature binderless briquetting. Microscopic examination of the briquettes revealed that vitrinite macerals undergo massive deformation under pressure to the point where evidence of the original grain is completely lost. The process requires drying the coal down to below 5% moisture and low-temperature briquetting (at temperatures of up to 200°C).

The re-emergence of the briquetting process as an important particle size enlargement method was also fueled by the growth of the iron and steel industry and the consequently increased demands for metallurgical coke. This increased demand requires the use of
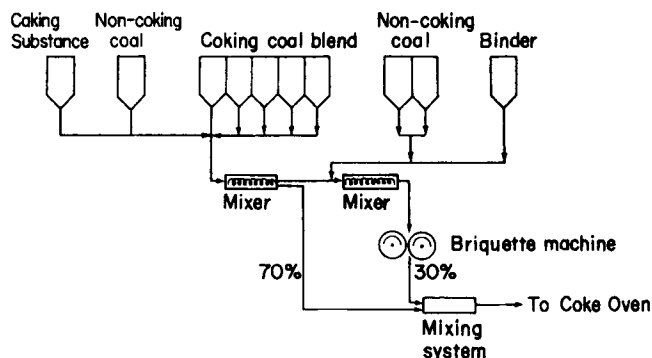
Fig. 9.33. The use of briquetted non-coking coal in the formed coke production. (After Sugasawa et al. [140]; by permission of the American Institute of Mining, Metallurgical and Petroleum Engineers.)

coking coals whose reserves are limited. For instance, Germany does not have enough coking coals, and Japan, which relies on imported coking coals more than any other country, needed a new coke-making technology.

In the coke-making process, it is customary to blend different coals before carbonization in order to produce the desired type of coke. Densification of the blend was found to improve the quality of the coke. Formed coke is made from briquetted weakly coking coals (or even from non-coking coals) which otherwise could not be used to make a metallurgical coke [139].

A simplified flowheet of one of the briquette charging methods developed in Japan is shown in Fig. 9.33 [140]. The percentage of non-coking coals in the blend reaches 25–30%, and in the DKS process a mixture of 70–90% of non-coking coals and up to 20% of coking coals with 10% pitch binder is briquetted at 90°C, followed by carbonization of the briquettes in an oven. Blast furnace tests confirmed that the quality of the DKS formed coke was equal to that of conventional coke.

9.6. References

[1] C.E. Capes, A.E. McIlhinney and A.F. Sirianni, Agglomeration from liquid suspensions — research and applications. In: K.V.S. Sastry (ed.), Agglomeration '77. AIME, 1977, Vol. 2, pp. 910–929.

[2] C.E. Capes and K. Darcovich, Size enlargement. In: Kirk-Othmer Encyclopedia of Chemical Technology, 4th ed. Wiley, New York, 1997, Vol. 22, pp. 222–255.

[3] M. Yusa, Mechanism of pelletizing flocculation. Int. J. Miner. Process., 4 (1977) 293.

[4] J. Szczypa, J. Neczaj-Hruzewicz, W. Janusz and R. Sprycha, New technique for coal fines dewatering. In: P. Somasundaran (ed.), Fine Particles Processing. SME, Littleton, CO, 1980, Vol. 2, pp. 1676–1686.

[5] J. Szczypa, R. Sprycha and W. Janusz, Agglomeration of flocculated fines — a competitive method for coal slimes dewatering. Coal Preparation, 1 (1985) 251.

[6] C.E. Capes and R.J. Germain, Selective oil agglomeration in fine coal beneficiation. In: Y.A. Liu (ed.), Fine Coal Beneficiation. Marcel Dekker, New York, 1982, pp. 293–351.

[7] J.S. Laskowski, Oil assisted fine particle processing. In: J.S. Laskowski and J. Ralston (eds), Colloid Chemistry in Mineral Processing. Elsevier, Amsterdam, 1992, pp. 361–394.

[8] J.S. Laskowski, Z. Yu and Y. Zhan, Hydrophobic agglomeration of fine coal. In: J.S. Laskowski and G.W. Poling (eds), Processing of Hydrophobic Minerals and Fine Coal. Proc. 1st UBC-McGill Int. Symp., Metall. Soc. of CIM, Montreal, 1995, pp. 245–258.

[9] M.T. Jacques, A.D. Hovarongkura and J.D. Henry, Feasibility of separation processes in liquid–solid systems: free energy and stability analysis. AIChE J., 25 (1979) 160.

[10] D.V. Keller and W. Bury, An investigation of a separation process involving liquid–water–coal systems. Coll. Surf., 22 (1987) 37.

[11] C.E. Capes, Oil agglomeration process, principles and commercial application for fine coal cleaning. In: J.W. Leonard and B.C. Hardringe (eds), Coal Preparation, 5th ed. SME, Littleton, CO, 1991, pp. 1020–1041.

[12] C.E. Capes, Liquid phase agglomeration: process opportunities for economic and environmental challenges. In: K.V.S. Sastry and M.C. Fuerstenau (eds), Challenges in Mineral Processing. SME, Littleton, CO, 1989, pp. 237–252.

[13] C.B. Kavouridis, H.L. Shergold and P. Ayers, Agglomeration of particles in an aqueous suspension by an immiscible liquid. Trans. IMM, Sect. C, 90 (1981) 53.

[14] W. Pawlak, A. Turak and B. Ignasiak, Selective agglomeration of low rank bituminous and subbituminous coals. In: C.E. Capes (ed.), Proceedings of the 4th International Symposium on Agglomeration. AIME Iron and Steel Society, Toronto, ON, 1985, pp. 907–916.

[15] P. Carbini, R. Ciccu, M. Ghiani and F. Satta, Flotation of low-rank coal using mixtures of commercial oils. In: Proceedings of the 11th International Coal Preparation Congress. Mining and Materials Processing Institute of Japan, Tokyo, 1990, pp. 293–298.

[16] Z. Blaschke, Influence of the carbon content, kind of gangue and of diesel oil on the results of coal beneficiation by oil agglomeration. In: Proceedings of the 11th International Coal Preparation Congress. Mining and Materials Processing Institute of Japan, Tokyo, 1990, pp. 257–260.

[17] M.A. Musich, R.A. Dewall and R.C. Timpe, Oil agglomeration of low-rank coals. In: Proceedings of the 8th Annual Coal Preparation, Utilization and environmental Control Contractors Conference. DOE/PETC, Pittsburgh, PA, 1992, pp. 62–67.

[18] A.B. Garcia, M.R. Martinez-Tarazona and J.M.G. Vega, Cleaning of Spanish high-rank coals by agglomeration with vegetable oils. Fuel, 75 (1996) 885.

[19] V.P. Mehrotra, K.V.S. Sastry and B.W. Morey, Review of oil agglomeration techniques for processing of fine coals. Int. J. Miner. Process., 11 (1983) 175.

[20] C.E. Capes, A.E. McIlhinney, R.E. McKeever and L. Messer, Application of spherical agglomeration to coal preparation. In: Proceedings of the Symposium on Pellets and Granules. Aust. Int. Miner. Metall., Newcastle, Oct. 1976, Paper H9.

[21] C.N. Bensley, A.R. Swanson and S.K. Nicol, The effect of emulsification on the selective agglomeration of fine coal. Int. J. Mineral. Process., 4 (1977) 173.

[22] F. Zhang and T.D. Wheelock, Kinetics of a gas-promoted oil agglomeration process. Coal Preparation, 18 (1997) 69.

[23] J.S. Laskowski and Z. Yu, Fine coal particle agglomeration in coal preparation plant circuits. In: A.C. Partridge and I.R. Partridge (eds), Proceedings of the 13th International Coal Preparation Congress. Australian Coal Preparation Society, Brisbane, 1998, Vol. 2, pp. 591–599.

[24] Z. Yu and J.S. Laskowski, The effects of surfactants on oil agglomeration and filtration of fine coal. In: S.R.S. Sastri, S. Mohanty and B.K. Mohapatra (eds), Proceedings of the International Symposium on Beneficiation, Agglomeration and Environment. Regional Res. Lab, Bhubaneswar, 1999, pp. 115–132.

[25] J.S. Laskowski and Z. Yu, Oil agglomeration and its effect on beneficiation and filtration of low rank/oxidized coals. Int. J. Miner. Process., 58 (2000) 237.

[26] J.S. Laskowski, Y.B. He and Y. Zhan, Coal wettability and its correlation with floatability. SME Annual Meeting, Phoenix, AZ, 1992, Preprint 92-125.

[27] M. Pawlik, J.S. Laskowski and H. Liu, Effect of humic acids and coal surface properties on rheology of coal–water slurries. Coal Preparation, 12 (1998) 129.

[28] Y.B. He and J.S. Laskowski, Contact angle measurements on discs compressed from fine coal. Coal Preparation, 10 (1992) 19.

[29] Y.A. Attia, S. Yu and S. Vecci, Selective flocculation cleaning of Upper Freeport coal with a totally

hydrophobic flocculant. In: Y.A. Attia (ed.), Flocculation in Biotechnology and Separation Systems. Elsevier, Amsterdam, 1987, pp. 547–564.

[30] Y.A. Attia and S. Yu, Production of super-clean coal slurries from the high-sulfur coals by selective flocculation. In: Y.P. Chugh and R.D. Caudle (eds), Processing and Utilization of High-Sulfur Coals II. Elsevier, Amsterdam, 1987, pp. 402–412.

[31] B.C.J. Labuschange, Influence of oil consumption, pH and temperature on the selective agglomeration of coal. ICHEME, 5th Int. Symp. Agglomeration, Brighton, 1987, pp. 505–514.

[32] R.J. Good, M.K. Badgujar, T.L.H. Huang and S.N. Handur-Kulkarni, Hydrophilic colloids and the elimination of inorganic sulfur from coal: a study employing contact angle measurements. Coll. Surf., 93 (1994) 39.

[33] D.V. Keller and W.M. Bury, The demineralization of coal using selective agglomeration by the T-Process. Coal Preparation, 8 (1990) 1.

[34] R.E. Hucko, R.P. Killmayer and P.S. Jacobsen, Selective agglomeration: an interlaboratory test program. Miner. Metall. Process., 7 (1990) 74.

[35] J. Drzymala, R. Markuszewski and T.D. Wheelock, Influence of air on oil agglomeration of carbonaceous solids in aqueous suspensions. Int. J. Miner. Process., 18 (1986) 227.

[36] G. Milana, A. Vettar and T.D. Wheelock, Air-promoted oil agglomeration of moderately hydrophobic coals, Part I. Coal Preparation, 18 (1997) 17.

[37] J. Drzymala and T.D. Wheelock, Air-promoted oil agglomeration of moderately hydrophobic coals, Part II. Coal Preparation, 18 (1997) 37.

[38] G. Milana, A. Vettor and T.D. Wheelock, Oil agglomeration of coal at a moderate shear rate. Proc. 9th Int. Pittsburgh Coal Conf., Pittsburgh, PA, 1992, pp. 50–55.

[39] J. Janiak, W. Pawlak, K. Szymocha, B. Ignasiak and C.M. Rodkiewicz, Selective agglomeration during pipelining of slurries. Coal Preparation, 1 (1985) 155.

[40] B. Bogenschneider and W.A. Jasulaitis, The Oilfloc Process for the dewatering and cleaning of ultra-fine slurries in coal preparation. Proc. Inst. Briquetting and Agglomeration, Vol. 15, Montreal, 1977, pp. 13–24.

[41] V.P. Mehrotra, K.V.S. Sastry and B.W. Morey, Oil agglomeration offers technical and economical advantages. Min. Eng., 32 (1980) 1230.

[42] J. Donnelly, B. Cooney, I. Hoare, B. Waugh, R. Robinson and R. McCollough, Development of a full scale selective oil agglomeration plant. In: A.C. Partridge and I.R. Partridge (eds), Proceedings of the 13th International Coal Preparation Congress. Australian Coal Preparation Society, Brisbane, 1998, Vol. 2, pp. 703–712.

[43] R.J. Pugh and J.A. Kitchener, Experimental confirmation of selective coagulation in mixed colloidal systems. J. Coll. Interf. Sci., 38 (1972) 657.

[44] R.J. Pugh, Selective coagulation in quartz–hematite and quartz–rutile suspensions. Coll. Polym. Sci., 252 (1974) 400.

[45] Y.K. Leong, P.J. Scales, T.W. Healy and D.V. Boger, Interparticle forces arising from adsorbed polyelectrolytes in colloidal suspensions. Coll. Surf., A95 (1995) 43.

[46] P.J. Scales, T.W. Healy and D.V. Boger, The role of surface forces in the control of the rheology of particulate fluids. In: S.P. Mehrotra and S. Shekhar (eds.), Mineral Processing, Recent Advances and Trends. Allied Publishers, New Delhi, 1995, pp. 105–117.

[47] Z. Xu and R.H. Yoon, The role of hydrophobic interactions in coagulation. J. Coll. Interf. Sci., 132 (1989) 532.

[48] Z. Xu and R.H. Yoon, A study of hydrophobic coagulation. J. Coll. Interf. Sci., 134 (1990) 427.

[49] N.V. Churaev and B.V. Deryaguin, Inclusion of structural forces in the theory of stability of colloids and films. J. Coll. Interf. Sci., 103 (1985) 542.

[50] N.V. Churaev, The relation between colloid stability and wetting. J. Coll. Interf. Sci., 172 (1995) 479.

[51] R.H. Yoon, D.H. Finn and Y.I. Rabinovich, Hydrophobic interactions between dissimilar surfaces. J. Coll. Interf. Sci., 185 (1997) 363.

[52] R.A. Ruehrvein and D.W. Ward, Mechanism of clay-aggregation by polyelectrolytes. Soil Sci., 73 (1952) 485.

[53] A.S. Michaels and O. Morelos, Polyelectrolyte adsorption by kaolinite. Ind. Eng. Chem., 47 (1955) 1801.

[54] R.H. Smellie and V.K. La Mer, Flocculation, subsidence and filtration of phosphate slimes. J. Coll. Sci., 23 (1958) 589.

[55] R. Hogg, Polymer adsorption and flocculation. In: J.S. Laskowski (ed.), Polymers in Mineral Processing. Proc. 3rd UBC-McGill Int. Symp., Metall. Soc. CIM, Montreal, 1999, pp. 3–18.

[56] R. Hogg, Collision efficiency factors for polymer flocculation. J. Coll. Interf. Sci., 102 (1984) 232.

[57] J.A. Kitchener, Principles of action of polymeric flocculants. Br. Polym. J., 4 (1972) 217.

[58] H.J.L. Wright and J.A. Kitchener, The problem of dewatering clay slurries: factors controlling filterability. J. Coll. Interf. Sci., 56 (1976) 57.

[59] D.T. Ray and R. Hogg, Polymer adsorption in flocculating suspensions. Proc. Annu. Tech. Conf. Filtration and Separation, Am. Filtration Soc., Kingwood, 1989, pp. 145–150.

[60] P.A. Rey and F.F. Aplan, Characterization and flocculation of coal preparation plant blackwater. In: B.K. Parekh and J.G. Groppo (eds), Processing and Utilization of High-Sulfur Coals V. Elsevier, Amsterdam, 1993, pp. 119–138.

[61] R.J. Gochin, M. Lekili and H.L. Shergold, The mechanism of flocculation of coal particles by polyelectrolytes. Coal Preparation, 2 (1985) 19.

[62] Th.F. Tadros, Correlation of viscoelastic properties of stable and flocculated suspensions with their interparticle interactions. Adv. Coll. Interf. Sci., 68 (1996) 97.

[63] S.R. Raghavan, J. Hou, G.L. Baker and S.A. Khan, Colloidal interactions between particles with tethered non-polar chains dispersed in polar media: direct correlation between dynamic rheology and interaction parameters. Personal information, 1999.

[64] D.H. Napper, Polymeric Stabilization of Colloidal Dispersions. Academic Press, New York, 1983.

[65] R. Hogg, P. Bunnual and H. Suharyono, Chemical and physical variables in polymer-induced flocculation. Miner. Metall. Process., 10 (1993) 81.

[66] R.O. Keyes and R. Hogg, Mixing problems in polymer flocculation. AIChE Symposium Series, No. 190, Vol. 75, 1979, pp. 63–72.

[67] R. Hogg, R.C. Klimpel and D.T. Ray, Growth and structure of agglomerates in flocculation processes. Proc. 4th Int. Symp. Agglomeration, Toronto, ON, 1985, pp. 581–588.

[68] J.A. Kitchener, Flocculation in mineral processing. In: K.J. Ives (ed.), The Scientific Basis of Flocculation. Sijthoff and Noordhoff, Alphen a/d Rijn, 1978, pp. 283–328.

[69] D.W. Rogers and G.W. Poling, Compositions and performance characteristics of some commercial polyacrylamide flocculants. CIM Bull., 71 (793) (1978) 152.

[70] R. Hogg, Flocculation problems in the coal industry. In: P. Somasundaran (ed.), Fine Particles Processing. SME, Littleton, CO, 1980, Vol. 2, pp. 990–999.

[71] H.N. Brookes, M.J. Littlefair, L. Spencer and A.A. Abdelrahman, The selective flocculation of coal/shale mixtures using commercial and modified polyacrylamide polymers. 14th Int. Mineral Processing Congr., Toronto, ON, 1982, paper 7.1.

[72] C. McConnell Boykin and R.Y. Lochhead, Determining the nature of clay/polymer interactions. American Chemical Society Meeting, Boston, August 24–27, 1998.

[73] W.M. McCarty, K.R. Rossington and B.S. Sundlof, Rheology of aqueous suspensions of clay and alumina. Eng. Found. Conf. Rheology in the Mineral Industry II, Hawaii, March 14–19, 1999.

[74] Y. Xu and G. Cymerman, Flocculation of fine oil sand tails. In: J.S. Laskowski (ed.), The Use of Polymers in Mineral Processing. Proc. 3rd UBC-McGill Int. Symp. Fundamentals of Mineral Processing, Metall. Soc. CIM, Montreal, ON, 1999, pp. 591–604.

[75] H.A. Hamza, A.W. Mo and R. Frenette, Chemical reagents for mechanical dewatering. In: R.R. Klimpel and P.T. Luckie (eds), Industrial Practice of Fine Coal Processing. SME, Littleton, CO, 1988, pp. 231–237.

[76] R. Hogg, Coal preparation wastewater and fine refuse treatment. In: S.K. Mishra and R.R. Klimpel (eds), Fine Coal Processing. Noyes Publications, Park Ridge, NJ, 1987, pp. 269–293.

[77] J.M. Henderson and A.D. Wheatley, Factors affecting the efficient flocculation of tailings by polyacrylamides. Coal Preparation, 4 (1987) 1.

[78] J.D. Field, Some developments associated with flocculants during the last decade. Coal Preparation, 4 (1987) 79.

[79] J.R. Macdonald, S.A. Mays, E. Gallagher and J.E. Lewis, A mathematical description of factors affecting settling rates of slurries. In: R.L. Whitmore (ed.), Proceedings of the 2nd Australian Coal

Preparation Conference. Coal Preparation Societies of N.S.W. and Queensland, Brisbane, 1993, pp. 397–420.

[80] B.J. Moudgil, S. Behl and T.S. Prakash, Effect of particle size in flocculation. J. Coll. Interf. Sci., 158 (1993) 511.

[81] S.K. Mishra, Dewatering of fine coal. In: S.K. Mishra and R.R. Klimpel (eds), Fine Coal Processing. Noyes Publications, Park Ridge, NJ, 1987, pp. 225–268.

[82] J.R. Palmes and J.S. Laskowski, Effect of the properties of coal surface and flocculant type on the flocculation of fine coal. Miner. Metall. Process., 10 (1993) 218.

[83] J. Rubio and J.A. Kitchener, The mechanism of adsorption of polyethylene oxide flocculant on silica. J. Coll. Interf. Sci., 57 (1976) 132.

[84] J. Rubio and J.A. Kitchener, New basis for selective flocculation of mineral slimes. Trans. IMM, Sect. C, 86 (1977) 97C.

[85] J. Rubio, The flocculation properties of polyethylene oxide. Coll. Surf., 3 (1981) 79.

[86] B.J. Moudgil, Effect of polyacrylamide and polyethylene oxide polymers on coal flotation. Coll. Surf., 8 (1983) 225.

[87] V.E. Vigdergauz, E.A. Schrader, S.A. Stepanov, V.L. Kusnetsov and E.A. Antonova, Selective flocculation of coal and sulfide minerals by the emulsions of synthetic polymers. In: J.S. Laskowski (ed.), Polymers in Mineral Processing. Proc. 3rd UBC-McGill Int. Symp., Metall. Soc. CIM, Montreal, 1999, pp. 265–280.

[88] P.M. Brown and B.J. Scheiner, Dewatering of coal–clay waste slurries from preparation plants. US Bureau of Mines Rep. Invest., No. 8824 (1983).

[89] B.J. Scheiner and D.A. Stanley, Flocculation of fine particles with polyethylene oxide: a proposed mechanism. Trans. SME/AIME, 280 (1985) 2115.

[90] B.J. Scheiner, Screen dewatering of coal–clay waste from preparation plants. Coal Preparation, 17 (1996) 39.

[91] Y.A. Attia, Cleaning and desulfurization of coal suspensions by selective flocculation. In: Y.A. Attia: Processing and Utilization of High-Sulfur Coals I. Elsevier, Amsterdam, 1985, pp. 267–285.

[92] M. Kaiser and H. Latsch, Enhancement of the efficiency of polymeric flocculants in dewatering and clarification. In: W. Blaschke (ed.), New Trends in Coal Preparation Technologies and Equipment. Proc. 12th Int. Coal Preparation Congress, Gordon and Breach, New York, 1996, pp. 493–500.

[93] P. McColl and I.J. Flanagan, The Twintac advanced dewatering system for the solid–liquid separation of coal tailings. In: J.S. Laskowski (ed.), Polymers in Mineral Processing. Proc. 3rd UBC-McGill Int. Symp., Metall. Soc. CIM, Montreal, 1999, pp. 579–589.

[94] M.J. Engler, R. Hogg and F.F. Aplan, The flocculation and dewatering of coal preparation plant blackwater. In: P.J. Lean (ed.), Proceedings of the 5th Australian Coal Preparation Conference. Australian Coal Preparation Society, Newcastle, NSW, 1991, pp. 181–197.

[95] A.G. Waters, Clarification and Thickening. Australian Coal Preparation Society, Newcastle, NSW, 1992, Vol. V, Part 12.

[96] N. Narkis and M. Rebhun, The mechanism of flocculation processes in the presence of humic substances. J. Am. Water Works Assoc., 67 (1975) 101.

[97] Z. Blaschke, Beneficiation of coal fines by selective flocculation. Proc. 7th Int. Coal Preparation Congress, Sydney, 1976, paper F-2.

[98] R. Hucko, Beneficiation of coal by selective flocculation. A laboratory study. US Bureau of Mines Rep. Invest., No. 8234 (1977).

[99] Y.A. Attia, Flocculation. In: J.S. Laskowski and J. Ralston (eds), Colloid Chemistry in Mineral Processing. Elsevier, Amsterdam, 1992, pp. 277–308.

[100] V.V. Lyadov et al., Selective flocculation of coal slurries using latexes. USSR Coke Chem., 9 (1979) 12 (English transl.).

[101] M.J. Littlefair and N.R.S. Lowe, On the selective flocculation using polystyrene latex. Int. J. Mineral. Process., 17 (1986) 187.

[102] T.G.M. van de Ven, T. Dabros and J. Czarnecki, Flexible bonds between latex particles and solid surface. J. Coll. Interf. Sci., 93 (1983) 580.

[103] Zhimin Yu, Flocculation, Hydrophobic Agglomeration and Filtration of Ultrafine Coal. Ph.D. Thesis, University of British Columbia, Vancouver, 1998.

[104] S. Yu and Y.A. Attia, Thermodynamics of adsorption of a hydrophobic polymeric flocculant on coal, pyrite and shale minerals. In: J. Hanna and Y.A. Attia (eds), Advances in Fine Particles Processing. Elsevier, Amsterdam, 1990, pp. 299–310.

[105] J.E. Gebhardt and D.W. Fuerstenau, Flotation behavior of hematite fines flocculated with polyacrylic acid. Miner. Metall. Process., 3 (1986) 164.

[106] J.B. Rubinstein, A.E. Molchanov, V.A. Chanturia and A.I. Guzenko, Possibilities of raising the rate of fine coal flotation. In: J.S. Laskowski and G.W. Poling (eds), Processing of Hydrophobic Minerals and Fine Coal. Proc. 1st UBC-McGill Int. Symp., Metall. Soc. CIM, Montreal, 1995, pp. 165–178.

[107] S.H. Castro, R. Stocker and J.S. Laskowski, The effect of hydrophobic agglomerant on the flotation of fine molybdenite particles. In: H. Hoberg and H. Blottnitz (eds), Proceedings of the 20th International Mineral Processing Congress. GMDB, Aachen, 1997, Vol. 3, pp. 559–569.

[108] G.A. Pikkat-Ordynsky and V.A. Ostry, Technology of Coal Flotation. Izd. Nauka, Moscow, 1972 (in Russian).

[109] W.W. Wen, R.P. Killmeyer, B.R. Utz and R.E. Hucko, Simultaneous fine coal dewatering and reconstitution via the US Department of Energy's in situ cake hardening process. In: W. Blaschke (ed.), New Trends in Coal Preparation Technologies and Equipment. Proc. 12th Int. Coal Preparation Congress, Gordon and Breach, New York, 1996, pp. 107–114.

[110] M. Misra, R.W. Smith, J. Dubel and S. Chen, Selective flocculation of fine coal with hydrophobic *Mycobacterium phlei*. Miner. Metall. Process., 10 (1993) 20.

[111] A.M. Raichur, M. Misra, S.A. Davis and R.W. Smith, Flocculation of fine coal using synthetic and biologically derived flocculants. Miner. Metall. Process., 14 (1997) 22.

[112] K. Meyer, Pelletizing of Iron Ores. Springer, Berlin, 1980.

[113] J.W. Leonard and D.A. Newman, Volumetric efficiency and the potential for increased productivity in underground haulage: a discussion of plans and concepts. Min. Eng., 41 (1989) 1202.

[114] P.C. Kapur and D.W. Fuerstenau, Size distributions and kinetic relationship in the nuclei region of wet pelletization. Ind. Eng. Chem., Process Design Dev., 5 (1966) 5.

[115] K.V.S. Sastry and D.W. Fuerstenau, Kinetic and process analysis of the agglomeration of particulate materials by green pelletization. In: K.V.S. Sastry (ed.), Agglomeration '77. SME, Littleton, CO, 1977, Vol. 1, pp. 381–402.

[116] H. Schubert, Capillary forces — modelling and application in particulate technology. Aufbereitungs-Technik, 1 (1984) 39.

[117] K.V.S. Sastry and V.P. Mehrotra, Pelletization of coal fines: state-of-the-art. 3rd Int. Symp. Partikel Technologie, Nurnberg, 1981, Vol. 2, pp. H36–H51.

[118] K.V.S. Sastry and D.W. Fuerstenau, Pelletization of Fine Coals. EPRI CS-2198 Research Project 1030-1, 1982.

[119] W.J. Riva, H.P. Hudson, J.E. Landon and J.H. Walsh, Coal pelletizing studies for the vertical shaft carbonization process. CIM Bull., 57 (1964) 52.

[120] V.P. Mehrotra, Pelletization of Coal Fines — Kinetic and Strength Aspects. Ph.D. Thesis, University of California, Berkeley, 1980.

[121] D.V. Keller, The contact angle of water on coal. Coll. Surf., 22 (1987) 21.

[122] W.W. Wen, P.D. Bergman and A.W. Deurbrouck, A humic acid binder for pelletizing of fine coal. Proc. 10th Int. Coal Preparation Congr., Edmonton, ON, 1986, Vol. 2, pp. 120–131.

[123] C.A. Holley and J.M. Antonetti, Agglomeration of coal fines. Proc. Inst. Briquetting and Agglomeration, Montreal, 1977, Vol. 15, pp. 1–12.

[124] D.C. Rhys Jones, Briquetting. In: H.H. Lowry (ed.), Chemistry of Coal Utilization — Suppl. Volume. Wiley, New York, 1963, pp. 675–753.

[125] K.R. Komarek and J.E. Browning, Briquetting. Chem. Eng., Dec. 4 (1967) 154.

[126] W.B. Pietsch, Pressure agglomeration — state of the art. In: K.V.S. Sastry (ed.), Agglomeration 77. SME, Littleton, CO, 1977, Vol. 1, pp. 649–677.

[127] W.B. Pietsch, Large roller briquetting machines in coke production. Aufbereitungs-Technik, 1 (1984) 29.

[128] P.V. Tucker, G.B. Bosworth and G.W. Kalb, New developments in coal briquetting technology. In: W. Blaschke (ed.), New Trends in Coal Preparation Technologies and Equipment. Proc. 12th Int. Coal Preparation Congr., Gordon and Breach, New York, 1996, pp. 389–397.

[129] G.S. Golovin, A.P. Fomin, O.G. Patepenko, Y.V. Ivanov and I.K. Nekhoroshy, Industrial introduction of thermal methods of Kansk-Achinsk brown coal preparation. In: W. Blaschke (ed.), New Trends in Coal Preparation Technologies and Equipment. Proc. 12th Int. Coal Preparation Congr., Gordon and Breach, New York, 1996, pp. 399–402.

[130] G.S. Golovin, I.K. Nekhoroshy, A.P. Fomin and V.N. Applae, Thermal moulding of brown coals and peat to produce environmentally safe fuel briquettes. In: A.C. Partridge and I.R. Partridge (eds), Proceedings of the 13th International Coal Preparation Congress. Australian Coal Preparation Society, Brisbane 1998, Vol. 2, pp. 681–691.

[131] K.A. Kini, Coal utilization research in India and abroad. In: S. Sanga Raja Rao (ed.), Coal Preparation and Use. Balkema, Rotterdam, 1982, pp. 231–236.

[132] N. Berkowitz, Fundamental aspects of coal briquetting. Proc. 3rd Biennial Briquetting Conf., University of Wyoming, Banff, 1953, pp. 3–23.

[133] M.S. Iyengar, The problem of briquetting slack coal in India. Proc. 6th Biennial Briquetting Conf., Glacier Park, MO, 1959, pp. 20–29.

[134] M.S. Iyengar, T.A. Subramanian, A. Ghosal and A. Lahiri, Binderless briquetting of coals. J. Inst. Fuel, 31 (1958) 108.

[135] J. Lukac, Briquetting of hard brown coal without a binding agent. In: W. Blaschke (ed.), New Trends in Coal Preparation Technologies and Equipment. Proc. 12th Int. Coal Preparation Congr., Gordon and Breach, New York, 1996, pp. 385–388.

[136] D.P. Agrawal and N. Berkowitz, On the wetting of coal surfaces by carbonaceous binders. Proc. 9th Biennial Briquetting Conf., Denver, 1965, pp. 104–114.

[137] G.W. Kalb, R.P. Whitt and A. Boire, Binderless briquetting of bituminous coal. In: A.C. Partridge and I.R. Partridge (eds), Proceedings of the 13th International Coal Preparation Congress. Australian Coal Preparation Society, Brisbane, 1998, Vol. 2, pp. 703–712.

[138] K. Clark, R. Meakins and M. Attalla, An economic approach to agglomeration using new briquetting technology. In: J. Smitham (ed.), Proceedings of the 7th Australian Coal Preparation Conference. Australian Coal Preparation Society, Brisbane, 1995, pp. 277–298.

[139] M.O. Holowaty, R.G. Phelps, W. DuBroff and G.L. Landsly, Coal carbonization. In: R.A. Meyers (ed.), Coal Handbook. Marcel Dekker, New York, 1981, pp. 435–492.

[140] K. Sugasawa, Y. Sunami, T. Kanoh and M. Tsuyuguchi, The utilization of non-coking coal for metallurgical coke manufacture. In: K.V.S. Sastry (ed.), Agglomeration '77. AIME, 1977, Vol. 2, pp. 955–969.

Chapter 10

FINE-COAL UTILIZATION

10.1. Utilization of thermal coals and metallurgical coals

The value of coal for utilization is determined by coal rank, impurities (moisture, ash, sulfur, some trace elements, etc.), and particle size.

As far as utilization is concerned, coals fall more or less distinctly into three groups: thermal (steam), metallurgical (coking) and conversion coals. In some publications a fourth group that involves coals used in making active carbon and electrodes is also included [1] (Fig. 10.1).

The thermal coals are used as fuel either for direct heating or for the production of hot water and steam for power generation. The metallurgical coals are utilized as a raw material to make coke needed in blast-furnace operations and foundries. The term coking refers to a carbonization process where a bituminous coal is heated to drive off the volatile matter and leave a porous solid residue with a significantly higher carbon content. Conversion coals are used as feedstock in the production of gaseous and/or liquid fuels derived from coal. At present this form of utilization represents jointly a small proportion of total coal utilization. According to some projections, 30% of US coal production will be utilized in synfuel plants by 2060 [2].

The quality of fuel is first of all determined by its heating value and by the properties of the combustion products: solid residue (ash) and airborne emissions. While in the
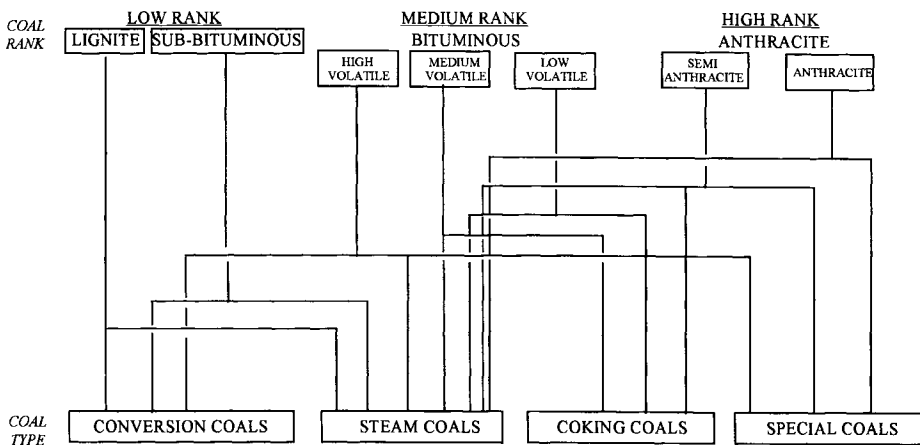
Fig. 10.1. Relationship between coal rank and coal utilization. (After Osborne [1]; by permission of Kluwer Academic Publishers.)

case of ash its handleability during combustion is an important factor, in the case of flue gas, the primary factor is the environmental impact. Therefore, while it is obvious that the heating value is of primary importance, the impurities — especially sulfur — play an increasingly important role in determining the value of the thermal coal.

Thermal coals do not appear as such in coal classification systems (Fig. 2.4). Since the reserves of good metallurgical coals are limited and their value is much higher than that of thermal coals, all coals that can be used as a component in the blend to make a coke are utilized in the coke-making process. That defines thermal coals as those which are not used for coke-making. In the American coal classification system these will include subbituminous coals, lignites and also anthracites (see Fig. 10.1). An anthracite is a hard, free-burning, smokeless coal of low-volatile matter and high heating value.

Because of the differences in utilization of thermal and metallurgical coals, the objectives of their cleaning are different. While in the case of thermal coals the primary objective of the cleaning is to increase coal calorific value and to reduce shipping costs by rejecting inorganic rock and separating troublesome impurities (e.g. sulfur), the primary objective of cleaning the metallurgical coal is a reduction of its ash content to maintain optimum ratio of reactives to inerts in the feed to a coke-making plant. However, since low-sulfur coke increases iron production in a blast-furnace operation, reduction of the coal sulfur content is also important in cleaning metallurgical coals. So, in practice, for both thermal coals and metallurgical coals the primary objective of their cleaning is rejection of inorganic rock and sulfur. As already discussed, this becomes more efficient when the feed to the cleaning operation contains liberated particles. However, liberation can only be achieved by size reduction and so it also increases the yield of fines in the final product. The presence of fines heavily affects coal handleability as is discussed in the following section.

Whereas steaming or coking are the most important coal applications today, coal conversion into gaseous or liquid fuels may become more important in this century. The Sasol One plant was built in South Africa to establish a technology for reducing South Africa's dependence on imported oil. Its significance is in proving that the World War II technology utilized in Germany could be improved, scaled up, and implemented for use in the modern era. As a result of the oil crisis in 1973 and soaring oil prices, the Sasol Two plant was built based on experience with Sasol One. By the end of 1981 Sasol Three was completed. The Sasol plants are now producing about 40% of South Africa's liquid fuel requirements.

Only one mine, the Bosjespruit mine, supplies coal to both Sasol Two and Sasol Three plants (the mine is only about 1.5 km from Sasol Two site). Because of the use of Lurgi Mark IV gasifiers which require rather coarse coal, the coal preparation was planned to minimize the amount of coal fines. The coal preparation involves only breaking and crushing, and the wet-screening to remove a −3 mm fraction. The coal utilized in the Sasol Two and Sasol Three technology contains 22.5% ash, 5.5% moisture and 25% volatile matter. The coal fines (up to 30% of the total production) are utilized for power generation [3]. According to the Scientific Encyclopedia (quoted after Reed [2]), the South African syncrude plants are converting a poor grade of coal into an acceptable grade of crude oil at an efficiency of approximately 62%.

10.2. Fine-coal handleability

Although there is no widely accepted rigorous definition of handleability, the handling coal characteristics often referred to as handleability, define whether a coal has the ability to flow unhindered through the processing and transportation systems [4–6]. A thermal coal blend must be consistent with respect to its composition (e.g. calorific value, moisture, ash and sulfur contents, etc.) to produce regular burn in steam boilers.

Consistency of coking properties will be required for metallurgical coals. Such blends are also, however, required to pass through a handling system without causing blockages and hold-ups. When coal passes through the transportation route without difficulties and blockages it is said to be of good handleability.

Coal preparation plants produce a range of products, commonly offered as blends of various size fractions. Such blends may also include the filter cake, the product which is known to contain more than 20% moisture. The presence of such a product in the blend often results in handleability problems encountered at power stations, or at various stages of transportation. Table 10.1 provides an example of a power station blend known to exhibit poor flow characteristics [4].

While the short-term solution might be the exclusion of part of the filter cake from the blend, the long-term solution must consider process improvements that would also allow for utilization of the fine clean coal products. The long-term solution may involve further drying of the filter cake or its reconstitution to guarantee its inclusion into any saleable product. In order to find a proper solution a standardized test that could be used to evaluate the handleability of the final product is needed. In the 60s, British Coal developed the Durham cone test and the Jenike shear test. While the former, a simple test that can easily be performed, provides some experimental indices, the latter is a scientifically sound method that can be used to evaluate rheology of granular matter.

In a simple Durham cone test, 10 kg of the coal sample is vibrated in the cone for 30 s after which the coal is allowed to gravitate through the aperture of the base of the hopper. The time taken by the whole of the sample to discharge from the Durham cone is measured.

In Fig. 10.2, the handleability index for a −25 mm +0 mm UK coal is plotted against the moisture content after Vickers [7]. As these results reveal, handleability dramatically

Table 10.1
A power station blend known to exhibit poor flow characteristics [4]

Component	Total moisture (%)	Total ash (%)
25% Dry fines	5.09	41.27
45% Clean coal	7.69	3.71
7% Large middlings	4.02	9.36
15% Small middlings	9.63	21.7
8% Filter cake	22.43	11.96
Total ash of the blend (%)		17.81
Total moisture of the blend (%)		8.12
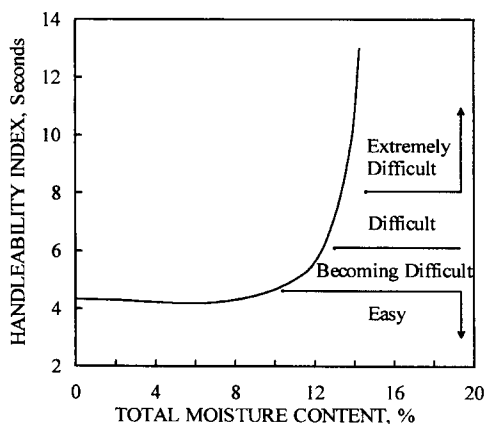
Fig. 10.2. Typical handleability curve for −25 mm fine UK coal using Durham cone results (After Vickers [7].)
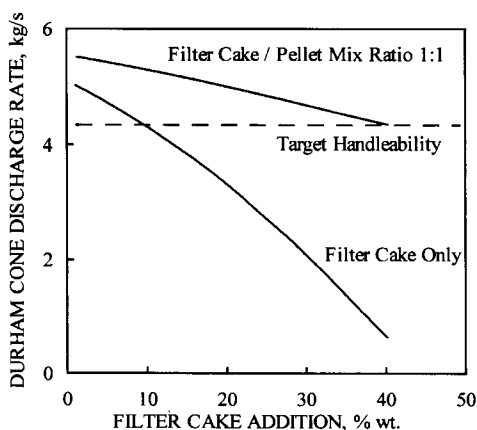
Fig. 10.3. Durham cone discharge rate for varying percentages of filter cake addition to the power station blend. (After Jones [4]; by permission of the Mining and Materials Processing Institute of Japan.)

deteriorates when the moisture content exceeds a given value (for this particular coal it is about 11%).

One of the examples discussed by Jones [4] is given in Fig. 10.3. To improve the handleability of the clean coal blend that had to include also the filter cake of high moisture content, the filter cake product was pelletized. As Fig. 10.3 shows, the filter cake addition in excess of 8% of the total blend placed the blend handleability below the target level and into the problem zone. By adding the minus 0.5 coal fines in equal parts of filter cake and coal pellets the handleability drastically improved.

The results of measurements with the use of the Durham cone (Figs. 10.2 and 10.3) are simply expressed as the time it takes for flow out of the cone. More recent reports
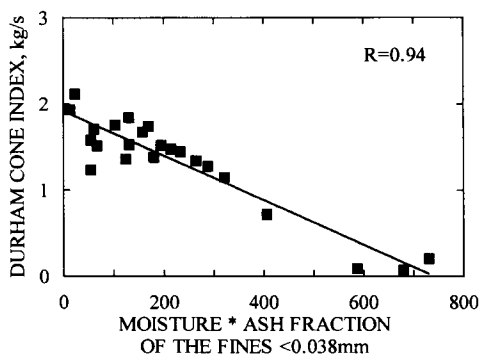
Fig. 10.4. Durham Cone Index versus moisture ash fraction of the fines (After Brown [6] and Vickers [7].)

point out that the Durham cone tests, while simple and fast, are not very reproducible. In the tests described by Brown et al. [8], the measurements are repeated eight times for each sample with the longest and shortest times discarded and the remaining six averaged and expressed as the Durham cone Index given by

$$DCI = 10 : \text{Average time (kg/s)} \qquad (10.1)$$

Correlation between the Durham Cone Index and total moisture content, DCI and sample ash content, DCI and percent yield of the -0.038 mm fraction, DCI and ash content of the -0.038 mm fraction were poor. A good correlation was only found between DCI and the product of the sample moisture content and fines ash fraction [3,4] (Fig. 10.4). The fines ash fraction is given by:

$$\frac{\gamma_{0.038} \, Ash_{0.038}}{100 \, Ash_{whole}} \qquad (10.2)$$

where $\gamma_{0.038}$ is the wt.% yield of the -0.038 mm size fraction, $Ash_{0.038}$ is the ash content in the -0.038 mm material, and Ash_{whole} is the ash content in the whole sample.

In a very recent publication on this subject, additional tests were carried out with the use of the Handleability Monitor [9,10] (from the research program developed at the University of Nottingham), and the simple correlation (Fig. 10.4) was further questioned. The extrusion through used in these tests was used to determine the maximum pressure (bar) versus time of ram extension (s), and the maximum pressure and the maximum gradient of the line were determined from the plots. These results show poor handling for the low-average maximum pressures (AMP), followed by progressively good handling, borderline handling and poor handling as the AMP increases. Generally, coal blends producing an AMP of less than 10 bar had high moisture contents. The blends acted more as fluids and hence their handling was classed as poor. Such coals have to be blended with a better handling coal to produce a blend with acceptable handling characteristics. The good handling coals produced the next lowest AMP's. These coals could be introduced into the coal handling plant at line capacity without causing blockages or stoppages. The borderline handleability samples were considered by the operator to be those that on the basis of a visual inspection
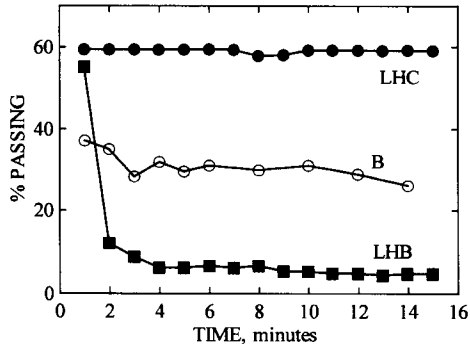
Fig. 10.5. Screening experiments to assess coal handleability for three different coals. (After Blondin et al.
[11]; by permission of the American Institute of Mining, Metallurgical and Petroleum Engineers.)

might cause blockages in the handling system. The poor handling coal blends, which
had the highest AMP's, were generally ones that had a very low or high moisture
content, but did not act as a "fluid". They also usually contained a large quantity of
fines (finer than 0.038 mm). Surprisingly, coals with a significant proportion of coarse
particles could also be described as exhibiting poor handling. This was ascribed as being
due to the large particles bridging together over an aperture preventing the free flow of
solids. The project identified the samples with borderline handleability as those of the
greatest concern to the operators. These samples' handling category cannot be easily
identified.

The handleability index, which is based on the Average Maximum Pressure deter-
mined experimentally using a new handleability monitor, is able to identify unhandleable
samples with a higher AMP than the handleability index for the plant. Such an index
can then be incorporated into a specification for the purchase of coal.

It is obvious that the coal handleability must to a large extent depend on coal surface
properties and that the discussed experimental results only considered the effect of
"mechanical" variables (e.g. particle size, yield of the finest size fraction, etc.), and ash
content. Blondin et al. [11] claim that dry screening at a low screen aperture (e.g. 6
mm) can be considered a good tool for assessing fine-coal handleability. Because of
plugging, coals that are difficult to handle are also difficult to screen. Fig. 10.5 shows
screening results for three coal samples differing widely in handleability. LHB coal
blinded the screen and after two minutes of screening only a limited amount of coal
could pass through the screen. The LHC coal, which is very easy to handle, contains
37.1% volatile matter (dry basis), 7.1% ash (dry basis), 14.1% moisture in a −4 mm
size fraction and 43% yield of the −2 mm fraction. Coal B with intermediate handling
characteristics contains 26.5 volatile matter (dry basis), 11.7% ash (dry basis), 7.7%
of moisture in a −4 mm fraction and 35% yield of the −2 mm fraction. The LHB
coal, which was very difficult to handle, contained 24.5% volatile matter (dry basis),
45.9% ash (dry basis), 14.4% moisture in a −4 mm fraction, and 45% yield of the
−2 mm fraction. So the LHB coal has a much higher ash content than the other two
coal samples, and the highest yield of the −2 mm fraction in the whole sample. The
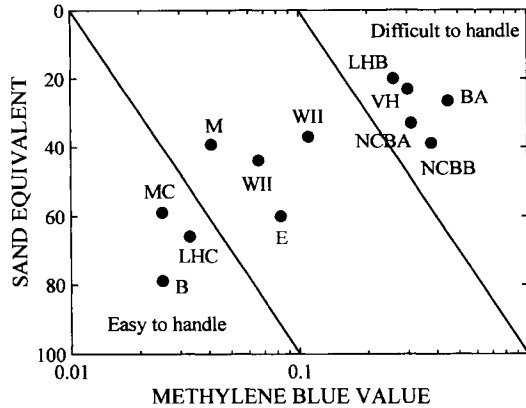
Fig. 10.6. Coal handleability classification. (After Blondin et al. [11]; by permission of the American Institute of Mining, Metallurgical and Petroleum Engineers.)

methylene blue test which was developed to determine the content of clays in the tested samples indicated the high clay content in the LHB coal, and low clay contents in the LHC and B coals.

To further evaluate the handleability of the tested coals, the sedimentation test was used (French Standards NF 15598) in which a 200 g sample of coal is placed in a cylinder with water and dispersant. After a given time, the sample which contains only coarse particles gives a high sand equivalent (all particles settle leaving clear supernatant), while in the samples containing also very fine "colloidal" particles, the sand equivalent is lower. For the three discussed coals the sand equivalents were as follows: 65.8% for LHC coal, 78.8% for B coal and 19.9% for LHB coal. Both the sand equivalent and the methylene blue value were used to classify coal handleability as shown in Fig. 10.6. [11]. The samples in the upper right hand corner are very difficult to handle, while the lower left hand corner corresponds to easy to handle coals.

As the results of tests developed by French researchers illustrate [8], coal handleability depends not only on coal particle size, the content of the finest fractions and the ash content, but also on the mineralogical composition of the mineral matter. Since coal interaction with water and coal surface wettability is determined by coal rank and coal ash content, it is obvious that the rank, ash content as well as clays content must be primarily responsible for coal handleability. These parameters affect the behavior of fine-coal samples, their screening and pelletization and they should also determine coal handleability. Existing research programs are likely to confirm such predictions [12].

More complete characterization of the flow properties of powdered solid samples can only be provided by full rheological tests. While several recent publications offer interesting solutions to the experimental problems posed by such measurements, such methods at this stage can only be used to study very fine solid particles [13].

10.2.1. Superabsorbents

As the tests specifically developed to evaluate fine-coal handleability show, coal moisture content is one of the most important parameters that determine coal flowing properties. Thus, the most radical way of improving such properties of fine-coal samples is moisture reduction. As discussed in Chapter 8, this can be achieved by the use of high molecular weight polymers (flocculants) which improve both thickening and filtration. Recent years have brought publications on an entirely new way of using high molecular weight polymers in the dewatering of fine particles. They are also referred to as handleability aids [14,15].

Studies on handleability of the fine moist products led to an unusual transfer of technology of "superabsorbents" from the medical and agricultural industries to mineral processing applications. The superabsorbents are high molecular weight, cross-linked, water-insoluble polymers which can absorb several tens to several hundreds of times their own weight of water. An example of the dewatering system which illustrates the way in which such products are utilized is shown in Fig. 10.7 [16]. In this case a rotating drum is used to contact the wet cake (41% moisture) with certain amount of the polymer. After 30 minutes of mixing the swollen polymer is then separated from the dry coal particles (4.8% moisture) by screening. Obviously, the polymer selected for such an experiment must be water-insoluble.

Fig. 10.8 shows linear and cross-linked polymer macromolecules [15]. Fig. 10.8a depicts a copolymer of acrylic acid with acrylamide (common flocculant). The formation of methylene bridges in the polymer shown in Fig. 10.8b makes it insoluble in water. Despite the presence of amide and acrylate groups which are highly polar and impart a strong tendency towards solubility in water, the resultant polymer particle will no longer dissolve but merely absorb large quantities of water and swell to form a non-sticky gel.
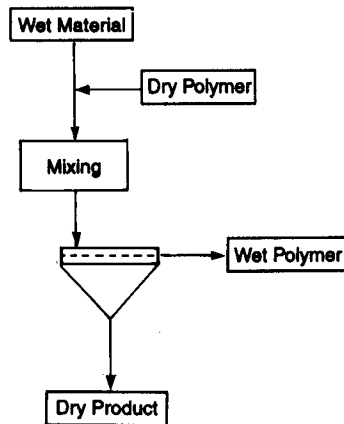
Fig. 10.7. An example of dewatering with the use of superabsorbents. (After Masuda and Iwata [16]; by permission of Elsevier Science.)
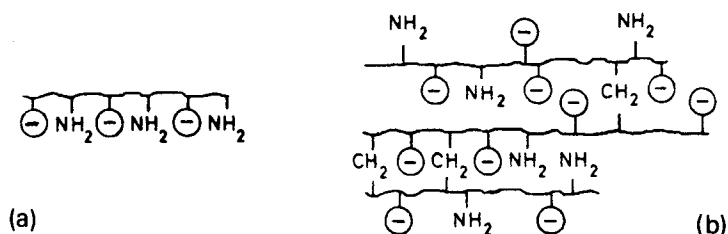
Fig. 10.8. Representation of linear (a) and cross-linked (b) polyacrylamides. (After Moody [15]; by permission of The Institution of Mining and Metallurgy.)

The most efficient superabsorbents are capable of absorbing very rapidly up to 500 times their own weight of pure water. The "drying" effect strongly depends on water quality and decreases with increasing concentration of dissolved salts in water, and so the dose of polymer in processing the filtration cake may vary from 1 to 5 kg/t of material treated [15]. Different polymers were developed for soft and hard waters (hard water is characterized by a high content of Ca^{2+} and Mg^{2+}). The overall effect also depends on the polymer particle size [17].

As was pointed out, in the plant application of the superabsorbents the most important factor is effective mixing of the polymer with moist material. The data tabulated in Table 10.2 illustrate the effect of the filter-cake addition to the fine-coal clean product on the handleability of the blend. The handleability of the blend characterized by the Durham cone test is very much improved by treating the filter cake with superabsorbents [14,15].

Fig. 10.9 shows the effect of coal particle size and time of mixing with the polymer in a rotating drum on the dewatering of fine coal with an initial moisture content of 41% [16]. The polymer particle size was in the range from 0.59 to 1.20 mm and the relative weight of polymer to the treated material was 1%. As Fig. 10.9 demonstrates, the moisture was removed in approximately 10 min.

A critical issue in the application of superabsorbents for dewatering of fine coal is the ability to regenerate the used polymer so that it can be recycled. Dzinomwa and Wood [17] identified some suitable techniques for regeneration of the used polymer.

Table 10.2
Improvement in flow rate through Durham cone of fine-coal filter cake after treatment with 0.3 kg/t superabsorbent polymer [15]

Ratio of washed smalls to filter cake	Flow rate (kg/s)	
	Untreated filter cake	Treated filter cake
0	1.35	1.32
6 : 1	1.17	1.38
5 : 1	0.87	1.46
4 : 1	0.77	1.49
3 : 1	0.54	1.49
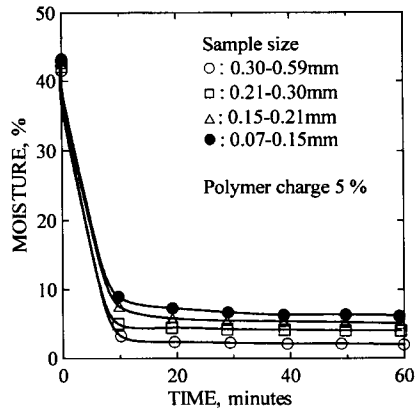
Fig. 10.9. Effect of coal particle size on dewatering of Datung coal with the use of a superabsorbent. (After Masuda and Iwata [16]; by permission of Elsevier Science.)

The available information is clearly sufficient to conclude that the moisture content of fine coal (e.g. filter cake, etc.) can be significantly reduced with the use of superabsorbents. Important steps in this technology are the mixing of fine coal and superabsorbents in order to transfer moisture from the former to the latter, separation of the dried coal from wet superabsorbent by screening, and regeneration of the polymer for recycling. The estimates have shown that the costs associated with this process are comparable to, if not significantly less than, those of thermal drying [17].

Another option in fine-coal utilization that avoids drying is the seam-to-steam strategy (Fig. 1.7). In this technology, instead of drying a filter cake, this moist material is converted into a coal–water slurry. Since this technology eliminates the need for drying, it not only cuts down on a number of dewatering unit operations, but also minimizes problems associated with transportation of fine coal in a dry state. These problems include spontaneous combustion.

10.3. Spontaneous combustion of coal

Spontaneous combustion results from self-heating of coal, the surface phenomenon which depends on coal surface properties and coal particle size; in general, the finer the particles, the greater the tendency for the coal to self-heating.

It is a common observation that stored coal tends to heat up when exposed to rain after a sunny period, or when placed on a dry pile while wet. This is consistent with the research results which identify coal oxidation, heat of wetting and condensation, and oxidation of pyrite as the main exothermic reactions that raise the temperature of a coal pile.

As discussed in Section 3.2, the wetting of a coal surface results from interactions between the coal surface and water molecules. While bituminous coals, and especially medium- and low-volatile matter bituminous coals, are very hydrophobic (Figs. 3.2

and 3.3), lower-rank coals are much less hydrophobic. The low-rank coals contain a considerable amount of oxygen (Fig. 3.4), and a good correlation between water sorption on coal and its content of oxygen is well established (Section 3.3). As Fuller's results show (see Fig. 3.57) [18], the heat of immersion varies markedly with coal rank. Due to a much higher content of oxygen and a more open and loose structure, the heat evolution on wetting exhibits a 10-fold increase for lower-rank coals.

Various aspects of coal spontaneous combustion have been widely studied and there are many papers on this subject. This chapter is mostly based on Tony Walters' endeavors which started when he was with P.T. Kaltim Prima Coal in Indonesia on the waters sailed by Joseph Conrad. The barque "Palestine", on which Conrad signed as 2nd Mate in 1881, transported coal from Newcastle to Bangkok, caught fire and exploded not far from Sumatra. Tony's research of Joseph Conrad's knowledge of the spontaneous combustion resulted in an unusually "readable" technical paper [19,20].

Both the wetting of dry coal by water and the condensation of water when coal is in contact with humid air release a substantial amount of heat, which raises the temperature of a coal pile. This is especially significant if the coal has been previously dried so that all the surface moisture has been removed. Since the rates of organic chemical reactions double for every 10°C rise, and since the reaction between coal and oxygen is also exothermic, this further speeds up the rise in temperature. Once higher temperatures are reached, the rate of oxidation and subsequent heat generation increases dramatically, as shown in Fig. 10.10, until ignition occurs.

Calorimetric studies show that due to polarity of minerals (SiO_2, Al_2O_3, $CaCO_3$, etc.), the heat of wetting of coal by water is greater for the mineral-rich fractions and it is widely accepted that the high ash levels in the coal contribute to spontaneous combustion. Barve and Mahadevan [21] found a good correlation between the susceptibility of coals to spontaneous combustion and moisture and ash contents.

Since the reactivity of coal petrographic constituents varies, the coal petrographic
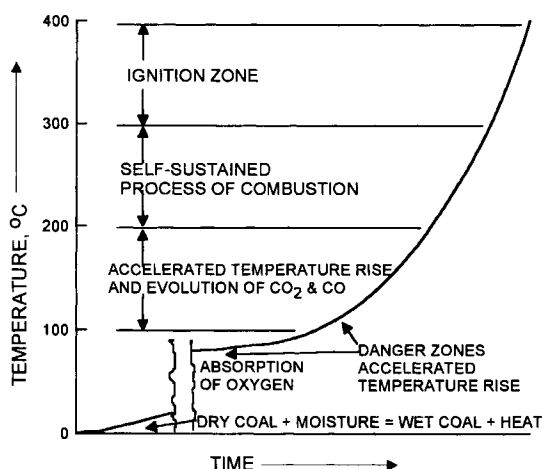
Fig. 10.10. Temperature rise in a coal pile with time.

composition also affects spontaneous combustion. The tendency to spontaneous combustion decreases with increasing content of inertinite.

Several empirical equations have been derived to predict the susceptibility of coal to spontaneous combustion. While the calculation of the Indian Institute of Technology's B-M Liability Index is based on coal moisture and ash contents [21], the US Bureau of Mines SHT Index is calculated from the dry-ash-free oxygen content [22], and the BHP Australia's maximum temperature rise (ΔT) produced by a coal sample under controlled oxidizing conditions is calculated from dry-mineral-matter-free carbon and oxygen contents [23,24]. Comparison of these different predictive equations for the "Conrad" coals gave very similar results; especially strong correlation was observed between the SHT and ΔT indices [19].

Any increase in mass of the coal pile augments the self-heating. Since coal is a poor heat conductor, the heat generated will result in higher temperatures at the center of the pile. The larger the pile, the higher will be the internal temperature, and therefore it is generally recommended that the stockpile be no higher than 5 m.

10.4. Coal–water slurries

Typically, coal which has been mined and cleaned in a coal preparation plant is shipped either to a power generation plant (thermal coals) or to a coke-making plant (metallurgical coals). Comparison of the flowheets of refineries with those of coal preparation plants reveals that while the former are highly "condensed" and confined, the latter need large areas for dry sample storage, handling and transportation, and pose all sorts of environmental problems (dusting, spontaneous ignition, etc.). So what is it that makes these two operations so different? Well, the former handle liquids which are pumped through multitudes of pipes but are stored in closed tanks, while the latter handle dry solid material for which storage and loading requires large areas. The problems further multiply when the solid material is in the form of fine particles.

Coal–water slurries, CWS (also referred to as coal–water fuels, CWF, or coal–water mixtures, CWM) are highly loaded suspensions of fine coal in water. Since these are mixtures of coal and water, CWS is free from some of the major problems of solid coal, such as dusting and spontaneous combustion during storage and transportation. Unlike solid coal, CWS is a liquid, so it does not require large handling facilities. Utilization of a fine coal in the form of CWS also simplifies the fine-coal preparation circuit in that it does not need deep dewatering and drying. The fine coal in a filter cake is directly converted into CWS and is pipelined to a power-generating plant where it is burned like a heavy oil; the coarse coal does not have to be blended with the troublesome fines and so its handling is improved as well.

Although this topic has been extensively studied and comprehensive reviews have been written [25,26], many reports that are traditionally presented at various conferences are not readily available.

Several coal–slurry fuels made of combinations of various liquids and coal have been described in technical literature. These include: coal–oil mixtures, coal–oil–water mixtures, coal–methanol mixtures, coal–methanol–water mixtures, and coal–
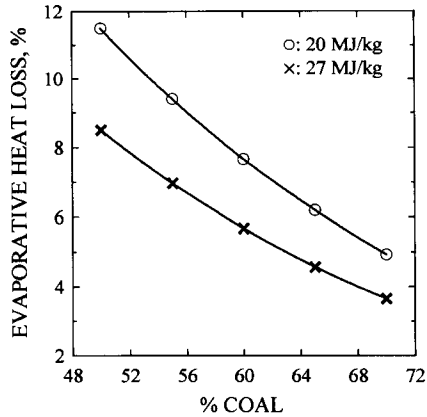
Fig. 10.11. Effect of coal content in CWS and coal heating value on evaporative heat loss during combustion of CWS.

water mixtures. In spite of the fact that some of these possess favorable combustion characteristics, coal–water fuels have attracted the most attention.

Since coal–water slurry is utilized as a fuel to generate power, its calorific value is an important factor. Because of the loss of energy on water evaporation (latent heat of vaporization for water is about 2300 kJ/kg) the presence of water in coal–water slurry reduces its heating value. For instance, for one kilogram of CWS containing 60% of bituminous high-volatile coal with a heating value of 27 MJ/kg, the simplified calculation gives:

$$\frac{\text{Evaporation loss}}{\text{Combustion heat}} \times 100 = \frac{0.4 \times 2.3}{0.6 \times 27} \times 100 = 5.68\% \qquad (10.3)$$

Of course, the evaporative heat loss can be reduced by increasing coal content in the coal–water slurry as shown for two coals in Fig. 10.11. For a highly loaded CWS with 70% coal the minimum evaporative heat loss will be about 3.65% for high-volatile bituminous coal (27 MJ/kg), and 4.9% for a subbituminous coal (20 MJ/kg). However, the most important requirement for the coal–water fuels is that they must be pumpable. Consequently, the risen problem can be stated as follows: what are the factors which can minimize viscosity at a given solids concentration? Or, how can the solids concentration be increased without raising viscosity above an acceptable level?

10.4.1. Viscosity of suspensions

Fig. 10.12 shows a liquid with viscosity η sandwiched between two parallel plates of area A. If a force F_x parallel to the x direction is applied to one of these plates, the plate will move in the x direction. Assuming that the liquid layers which are in contact with the plates possess the same velocities as the plates and that the velocities of the intervening layers change linearly with distance as shown in Fig. 10.12 (laminar flow),
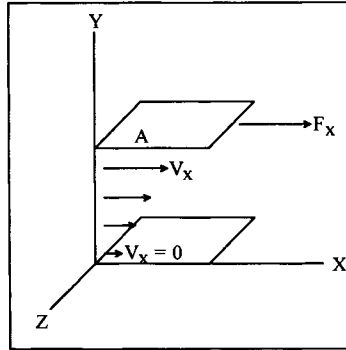
Fig. 10.12. Illustration of the relationship between applied force per unit area and fluid flow.
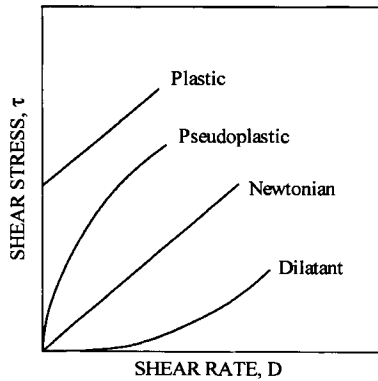
Fig. 10.13. Rheological curves for Newtonian and several non-Newtonian liquids.

Newton's law of viscosity applies

$$\tau = \frac{F}{A} = \eta \frac{d\upsilon_x}{dy} \tag{10.4}$$

The viscous forces act parallel to fixed surfaces (not perpendicular like pressure) and they are referred to as shear stress, τ (units Pascal, $Pa = 1\ N/m^2$). For a Newtonian fluid, the shear stress plotted versus shear rate, $d\upsilon/dy$ (units of reciprocal time), gives a straight line of zero intercept and slope equaling η. Non-Newtonian fluids exhibit nonlinear plots (Fig. 10.13). The viscosity is a factor of proportionality in Eq. (10.4); the more viscous a liquid is, the larger will be the forces and the rate of energy deposition in a flowing liquid for any shear rate. η has units of mass $\times$ time^{-1} $\times$ length^{-1}. In cgs units, $1\ g\ s^{-1}\ cm^{-1}$ is defined as 1 poise. At room temperature, pure water has a viscosity of about 0.01 P (or 1 cP), or 10^{-3} Pa s.

$$1\ P = 1\ dyne \frac{s}{cm^2} = 0.1\ N \frac{s}{m^2} = 0.1\ Pa\ s$$
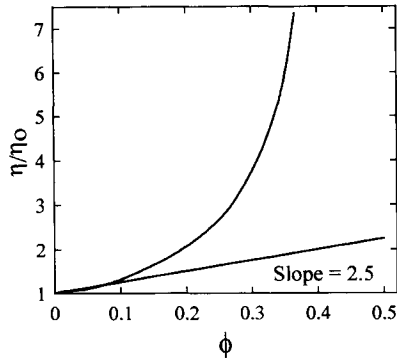
Fig. 10.14. Effect of volume fraction of glass spheres ($R = 6.5 \times 10^{-3}$ cm) on relative viscosity of the aqueous suspension of glass spheres. (After Vand [27]; by permission of Academic Press.)

For a dilute suspension of solid rigid spheres Einstein derived the following equation:

$$\frac{\eta}{\eta_0} = 1 + 2.5\phi \tag{10.5}$$

where η_0 is the viscosity of the continuous phase (solvent), and ϕ is the volume fraction occupied by the spherical particles; η/η_0 is also referred to as relative viscosity, η_r.

Vand's viscosity data [27,28] for a suspension of glass spheres ($d = 130$ μm) when η/η_0 is plotted vs. ϕ gives a straight line of slope 2.5 and intercept 1 (Fig. 10.14).

Einstein's equation was derived for extremely dilute suspensions when interactions between particles can be ignored. Several attempts have been made to extend the range of its applicability by introducing higher-order terms in ϕ:

$$\frac{\eta}{\eta_0} = A + B\phi + C\phi^2 + \tag{10.6}$$

As the concentration of a suspension goes to zero, its viscosity must go to that of the continuous phase (medium), therefore $A = 1$, $B = 2.5$ (Einstein), and $C = 7.349$ was given by Vand [27], and $C = 6.2$ by Batchelor [29] (values of C as large as 15 were reported).

Viscosity measurements are reported in many different forms. These include: (1) relative viscosity $\eta_r = \eta/\eta_0$; (2) specific viscosity $\eta_{sp} = \eta_r - 1$; (3) reduced viscosity $\eta_{red} = \eta_{sp}/c$; and (4) the limit of the reduced viscosity at zero concentration called intrinsic viscosity $[\eta] = \lim \eta_{red}$ as $c \to 0$. The units of intrinsic and reduced viscosities are reciprocal concentration. In suspension rheology, concentrations are expressed as volume fractions, $c = \phi$, and $[\eta]$ is dimensionless since the phase volume is also dimensionless.

In Einstein's derivation, a dispersion of rigid spheres in which the particles are sufficiently far apart to make interactions impossible was considered. In fact, Einstein's equation does not include the effects of particle size. In the measurements involving mineral suspensions at solids concentrations far exceeding the applicability range of Einstein's equation ($\phi > 0.1$), the effect of particle size is usually clearly seen. Examples of Berghofer's data [30] for aqueous suspensions of magnetite clearly demonstrate
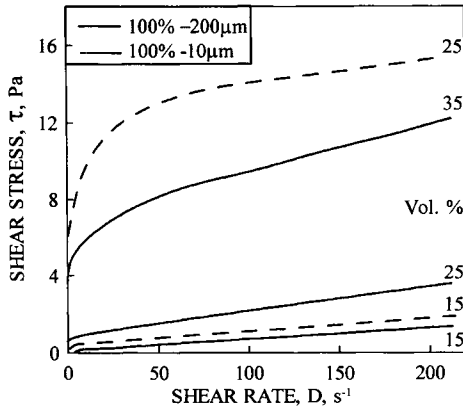
Fig. 10.15. Effect of particle size and volumetric content of magnetite on the rheological curves of aqueous suspensions of fine magnetite. (After Berghofer [30].)

this effect (Fig. 10.15). For low solids content (15% by volume), the viscosities of both the very fine and coarse suspensions are almost identical. However, with a further increase in the solids content, even though a 25% magnetite suspension with particles 100% below 200 μm still behaves nearly like a perfectly Newtonian fluid, the 25% suspension with particles 100% below 10 μm is clearly non-Newtonian. To describe this latter case it is common to use the Bingham equation derived for plastic systems.

$$\tau = \tau_B + \eta_{pl} D \tag{10.7}$$

where τ is the shear stress, τ_B is the Bingham yield stress, η_{pl} is the plastic viscosity, and D is the shear rate.

For the pseudoplastic systems, the yield stress, τ_B, can be obtained by extrapolating to $D \to 0$ (Fig. 10.16). Since for this case the shear stress is not proportional to the shear rate, the so-called apparent viscosity (η_a) (defined as the ratio of shear stress to shear rate at a given shear rate) is calculated. Such a viscosity is a function of the shear rate for pseudoplastic systems (see Fig. 10.17), and since it decreases with shear rate such systems are also referred to as shear-thinning.
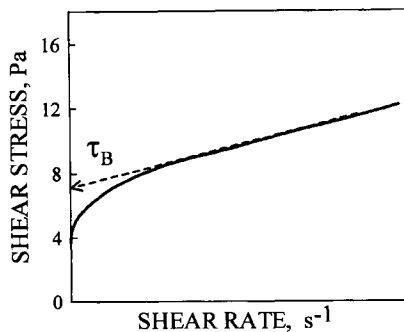
Fig. 10.16. Pseudoplastic systems and graphical extrapolation to find the Bingham yield stress.
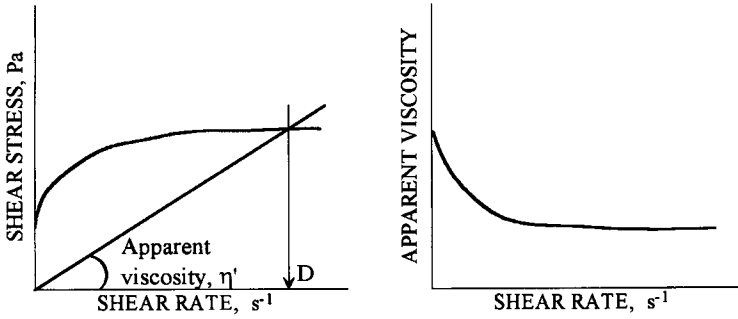
Fig. 10.17. Apparent viscosity vs. shear rate for shear-thinning systems.

As measurements on highly loaded suspensions indicate, with increasing solids content (1) the viscosity rapidly increases (the finer the particles the more pronounced the viscosity increase), (2) such systems exhibit progressively more non-Newtonian behavior.

Fidleris and Whitmore [31] found that (1) if the size ratio (small to fine) $R_{12} \leq$ 1 : 10 the large spherical particles sedimenting through a suspension of fine particles encountered the same resistance to motion as when (2) they passed through a pure liquid of the same viscosity and density as the suspension. Based on this information, Farris [32] showed that many rheological measurements carried out with monosized spherical suspensions can be represented by the curve shown in Fig. 10.18, but that the viscosity–solid content relationship can be progressively shifted towards higher solids concentrations by decreasing the R_{12} ratio in bimodal suspensions.

The influence of particle concentration on the viscosity of the concentrated suspensions is best determined in relation to the maximum packing fraction. At solids content
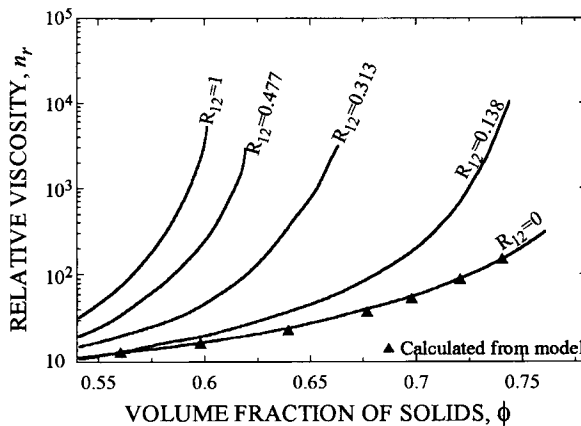
Fig. 10.18. Measured and calculated relative viscosity for a bimodal suspension with varying fine-to-coarse particle size ratio, R_{12}. Volume fraction of fine spheres is 25%. (After Farris [32]; by permission of the American Institute of Physics.)
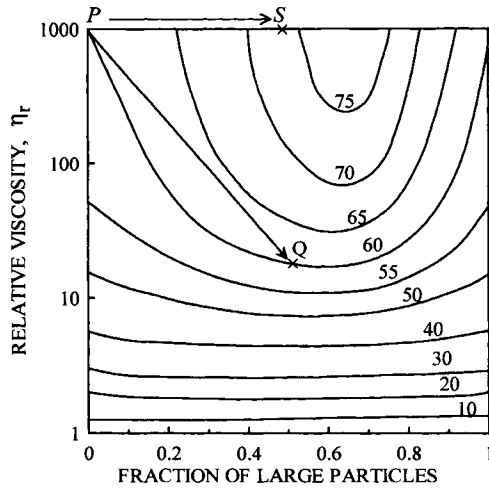
Fig. 10.19. Relative viscosity of a bimodal suspension containing coarse and fine particles (with small-to-fine particle size ratio of 1 : 5) plotted versus total solid phase volume for different coarse-to-fine ratios. $P \rightarrow Q$ illustrates the 50-fold reduction in viscosity when a 60% v/v suspension is changed from a mono- to a bi-modal (50/50) mixture. $P \rightarrow S$ illustrates the 15% increase in phase volume possible for the same viscosity when a suspension is changed from mono- to bi-modal. (After Barnes et al. [33]; by permission of Elsevier Science.)

close to the maximum packing fraction (ϕ_m) at which particles form a continuous three-dimensional network, the viscosity tends to infinity (the maximum packing fraction for hexagonally packed monodisperse spheres is 0.74). The utility of this approach is in the fact that it takes into account the effect of particle size distribution and particle shape, since they both control the maximum packing fraction.

The Krieger–Dougherty equation is

$$\frac{\eta}{\eta_0} = \left(1 - \frac{\phi}{\phi_m}\right)^{-[\eta]\phi_m} \tag{10.8}$$

The important conclusion resulting from this equation is that the relative viscosity can be significantly reduced by increasing ϕ_m. Fig. 10.19 shows the relative viscosity of a suspension with a bimodal particle size distribution in which the ratio of sizes of coarse-to-fine particles is 5 : 1, plotted in accordance with Eq. (10.8) [33]. Several important conclusions are evident from this figure. The effect of particle size distribution becomes very pronounced at higher than 50% by volume solids content, and the large reduction in viscosity is seen near a fraction of 0.6 of large particles. $P \rightarrow Q$ illustrates the 50-fold reduction in viscosity when 60% v/v suspension is changed from mono- to a 50/50 bimodal mixture. $P \rightarrow S$ illustrates the 15% increase in volumetric solids content when a suspension is changed from mono- to bi-modal.

Since coal content in coal–water slurry is the most important factor determining CWS's utility, the effect of the coal particle size distribution and coal surface properties on the rheology of CWS will be discussed in detail next.
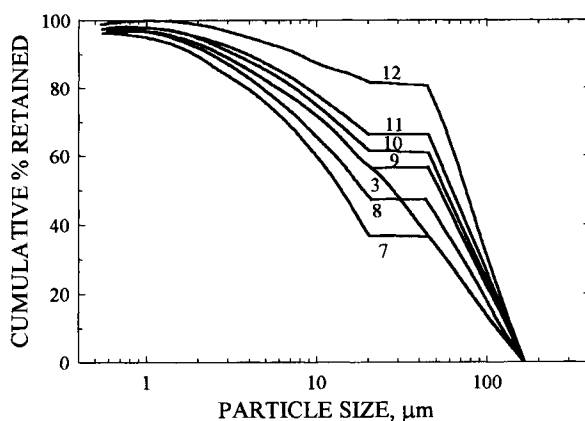
Fig. 10.20. Particle size distribution of a family of bimodal particle samples derived from the continuous reference curve No. 3. (After Ferrini et al. [34].)

10.4.2. Effect of coal particle size distribution on rheology of CWS

The top particle size in coal–water slurry is determined by boiler requirements; on the other hand, the size and the yield of the finest fractions is determined by CWS viscosity and the grinding cost. Because of the burning process limitations, it is usually assumed that the top size cannot exceed 300 μm with a particle size distribution of 70–80% below 75 μm. With these limits in mind, Ferrini et al. [34] showed how the coal particle size distribution can be optimized with regards to viscosity of the highly loaded CWS.

Curve 3 in Fig. 10.20 shows the particle size distribution of the coal sample prepared by grinding. The bimodal suspensions were prepared by screening −20 μm and +45 μm size fractions from this sample and mixing them at different ratios. The particle size distributions of such samples are also included in Fig. 10.20. The rheological curves for the 72% by wt. coal–water slurries prepared from these samples are given in Fig. 10.21. As can be seen, samples 10, 9 and 11 have much lower viscosities than sample 3. Fig. 10.22 demonstrates that changes in viscosity with particle size distribution are quite dramatic. Fig. 10.23 shows the effect of coal content on rheology of the three selected samples in which the top size was either 160 or 300 μm. The increase in top size allows higher loading to be obtained for both the continuous and bimodal samples. An increase in top size increases the ratio of the average coarse to fine particle size and this, in accordance with the theory of packing [32], reduces viscosity.

As Ferrini et al.'s [34] results clearly demonstrate, a highly loaded CWS can only be obtained by properly adjusting the coal particle size distribution. The beneficial effects which can be obtained by manipulating the particle size distribution are considerable, and therefore, grinding and selection of optimum particle size distribution is an important aspect in all CWS-patented technologies.

Optimization of the maximum packing fraction, and consequently the rheological behavior of a bimodal coal–water slurry, involves particle size, particle size distribution and particle shape. The shape can be defined from the measurements of the sphericity.
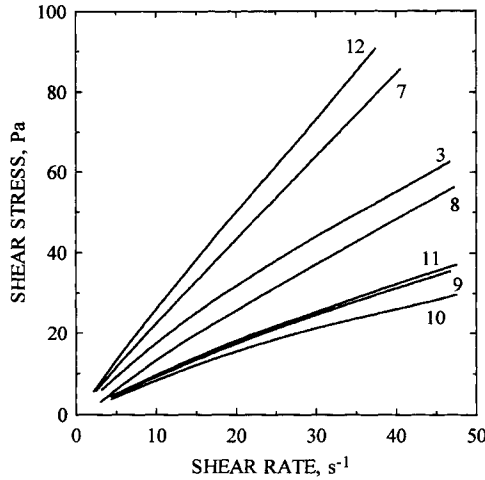
Fig. 10.21. Rheological curves for CWS containing 72% of coal by wt. prepared from the samples whose particle size distribution is shown in Fig. 20. (After Ferrini et al. [34].)
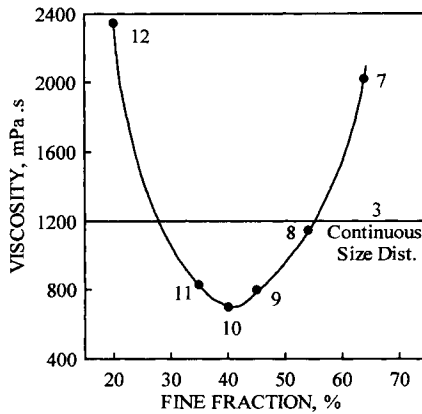
Fig. 10.22. Effect of a -20 μm fraction content on viscosity of bimodal coal–water slurries at constant overall coal content (72% by wt.). (After Ferrini et al. [34].)

Chryss and Bhattacharya [35] assumed the sphericity to be constant for a given material and used the Krieger–Dougherty equation modified for a bimodal particle system to predict the viscous minimum. Usui [36] demonstrated that the particle sphericity depends on particle size, measured the sphericity for different size fractions and showed how this information can be used to predict the maximum packing volume fraction, as well as the slurry viscosity.

The Rosin–Rammler–Bennett distribution usually describes coal particle size distribution quite well.

$$F(d) = 1001 - \exp[(-d/d_{63.2})^m] \qquad (10.9)$$

where $F(d)$ is the cumulative percent passing on size d, $d_{63.2}$ is the size modulus ($d_{63.2}$ is
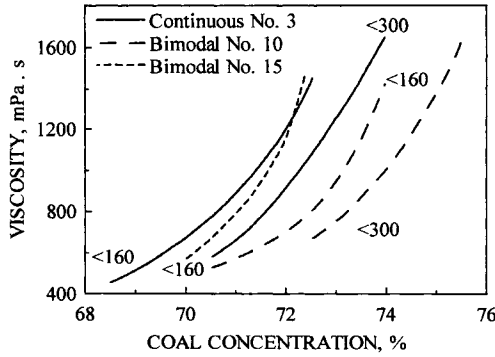
Fig. 10.23. Effect of coal content on rheology of the three selected samples with the top size of either 160 μm or 300 μm. (After Ferrini et al. [34].)
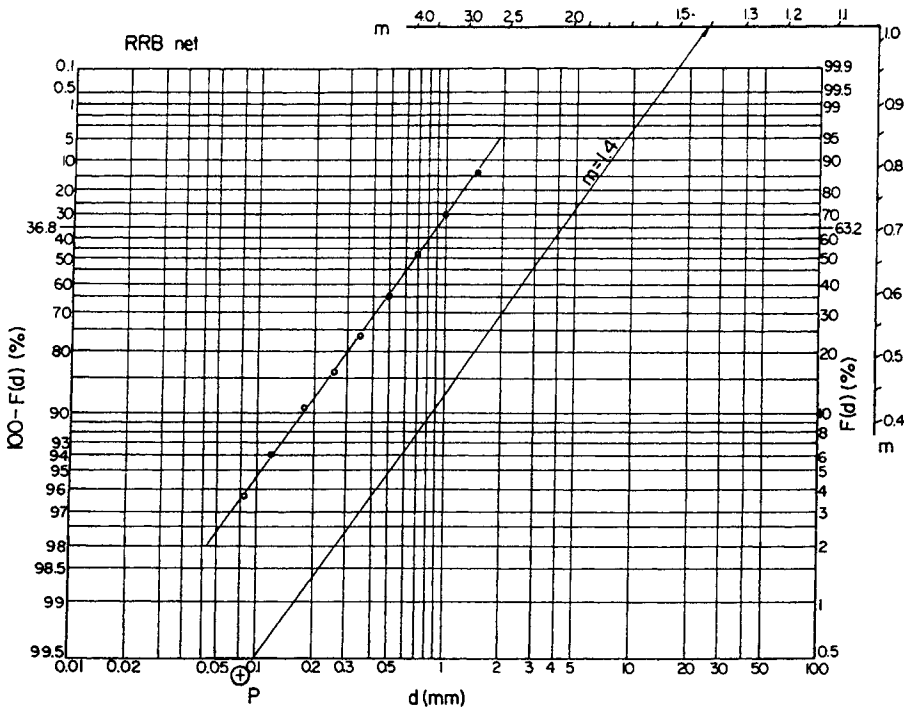
Fig. 10.24. Example of Rosin–Rammler–Bennett net with additional scales.

that aperture through which 63.2% of the sample would pass), and m is the distribution modulus (the slope of the curve on the RRB graph paper). An example of the RRB plot is shown in Fig. 10.24. With diminishing value of the distribution modulus (m), the line representing the distribution becomes less steep and that translates into larger differences between the sizes of fine and coarse particles in the sample. While maximum packing fractions for uniform spherical particles with cubical, orthorhombic, tetragonal,
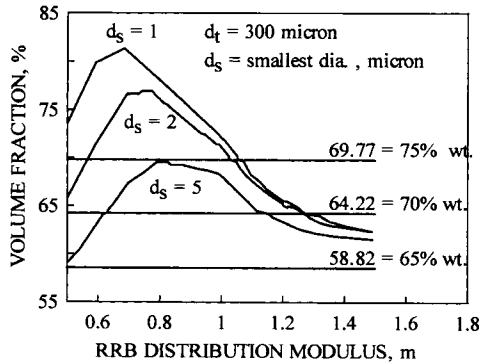
Fig. 10.25. Relationship between the RRB modulus "m" and particle volume concentration (After Zhang et al. [37].)

pyramidal (face-centered cubic) and tetrahedral (close-packed hexagonal) arrangements are 0.5236, 0.6045, 0.6980, 0.7405 and 0.7405, respectively, the maximum packing fraction increases with increasing polydispersity. If the sample contains fine and coarse particles, smaller particles fill in the interstitial space between the large particles, thus increasing ϕ_m, the maximum attainable solids volume fraction.

Chinese authors [37,38] analyzed the packing efficiency for coal samples characterized by the RRB distributions. For the top particle size of 300 μm, and minimum sizes of 1, 2, 5 or 20 μm, Fig. 10.25 shows the calculated relationship between particle packing and the distribution modulus m. Three horizontal lines represent coal concentrations of 65%, 70 and 75% by wt. Letting the coal density be 1.3 g/cm^3 this corresponds to 58.82%, 64.22% and 69.77% by volume. As this figure demonstrates, the range of the acceptable "m" values widens with decreasing size of the smallest particles.

The authors of these calculations point out that the Chinese experience indicates that if a fine coal is unsuitable in its as-received form for CWS preparation, in most cases this is due to low content of ultra-fine particles.

Grinding is a very expensive process. Small changes in the fine-particle processing circuits as shown in Fig. 10.26 can produce a clean coal product characterized by
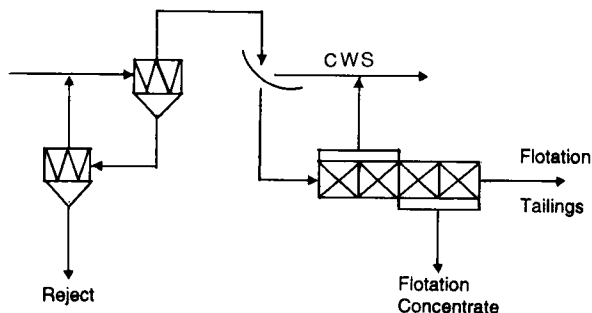
Fig. 10.26. Fine-coal cleaning circuit that includes two stages of water-only cyclones, sieve bends and a bank of flotation cells. (After Laskowski [39]; by permission of Gordon and Breach.)

a bimodal particle size distribution [39]. This is based on a well proven observation that fine coal floats mostly in the first cells while coarse coal particles start floating only in the following cells when fine particles have already been removed (see Fig. 3.24). Mixing the product from the first cell(s) with that collected from the last cell(s) will give a material with a bimodal size distribution. In the case of the "Canadian" fine-coal processing circuits in which coarse coal particles are recovered by screening the overflow coming out of the second stage of water-only cyclones, the bimodal character of the final product can further be enhanced by using the coarse fraction recovered on the screen. While this type of "adjustment" in the circuit can make the size distribution more bimodal, additional changes will be needed to fully optimize the flotation circuit with regards to CWS, as will be discussed later.

10.4.3. Effect of coal surface properties on rheology of CWS

In an attempt to explain the differences in rheological properties of coal–water slurries prepared from various coals, Kaji et al. [40] tested CWS prepared from 15 different coals. They found that coal surface wettability, which is related to the O/C atomic ratio in coal and can also be characterized by equilibrium moisture content, greatly affects the rheology of CWS. In line with these findings, Igarashi et al. [41] indicated that there is a good correlation between the CWS's apparent viscosity (at 126.7 s^{-1}), measured at 65% wt. solids content, and coal equilibrium moisture content. All these correlations were further developed by Seki et al. [42] into the final form as known today. These correlations are critical towards an understanding of the effect of coal surface properties (coal type) on the rheology of highly loaded coal–water slurries. They indicate that the maximum packing density of fine coal varies not only with particle size distribution but also, as postulated by many researchers (see for example [43]), with coal surface properties, or with the interaction between particles. As shown in Fig. 9.14, hydrophobic solid particles suspended in water are likely to coagulate due to strong hydrophobic attractive forces, and any aggregation of primary particles into larger aggregates reduces the maximum packing density.

Bituminous coals contain less than 10% moisture but the moisture content in subbituminous coals may be as high as 40%; the moisture in lignites may even reach 60%. Since moisture content depends strongly on the conditions under which the sample is stored, it is always advisable to treat such numbers with caution. For a sample equilibrated with an atmosphere of 96–97% relative humidity at 30°C, the moisture is referred to as equilibrium moisture content (see Section 3.3). Since some amount of "lubricating" water is always needed in a highly loaded suspension, it is obvious that the total amount of water in the coal–water slurry will be very different for a high-rank bituminous coal and a low-rank coal. If, say, 30% of the lubricating water is needed for the suspension to exhibit a certain degree of fluidity then in the case of "dry" bituminous coal containing 10% moisture, the total amount of water in the coal–water slurry will be 40% (and, hence, the coal content will be 60%). The same calculation for the case of subbituminous coal containing 40% moisture will give 70% as a total water content in the coal–water slurry. In the latter case the content of coal in the coal–water slurry will

therefore be only 30%. The difference in heating values for such two coal–water slurries will be huge.

As Seki et al. [42] put it, the free water content in CWS is given by:

$$M_f = 100 - C_c \left(1 + \frac{M_e}{100}\right) \tag{10.10}$$

where M_f is the free water in CWS, C_c is the dry coal content in CWS, and M_e is the coal equilibrium moisture content (in Seki et al.'s work measured at 80% humidity and 20°C).

So, obviously, for a highly loaded CWS (C_c in Eq. (10.10)) the free water content will sharply decrease if the coal moisture content is high. Since some amount of water must be present between particles to "lubricate" movement and reduce viscosity, the free water content for a coal with a high content of equilibrium moisture only can be maintained by reducing the coal content in CWS.

In Fig. 10.27 apparent viscosities (measured at 100 s^{-1}) of the coal–water slurries prepared from six different coals are plotted against coal content. In all cases 1% (on dry coal basis) of the same non-ionic additive was utilized. Several conclusions are evident from these curves. First, the experimentally measured apparent viscosity dramatically increases at a given solids content, and, second, this limiting solids content is different for different coals. Since particle size distributions of these samples were similar the conclusion is that the rheology of CWS also depends on coal surface properties. Fig. 10.28 shows the same experimental points plotted versus free water content. Obviously, the viscosity decreases with increasing content of the free water,

Coal	Under 74 μm Particle Size, %	Additive, % Concentration	Equilibrium Moisture Content, %
× Coal H	78	1.0	1.4
○ Coal G	81	1.0	2.4
◇ Coal E	80	1.0	3.3
△ Coal C	79	1.0	3.3
◇ Coal A	81	1.0	4.9
⊕ Coal D	76	1.0	5.6
● Coal F	77	1.0	8.6
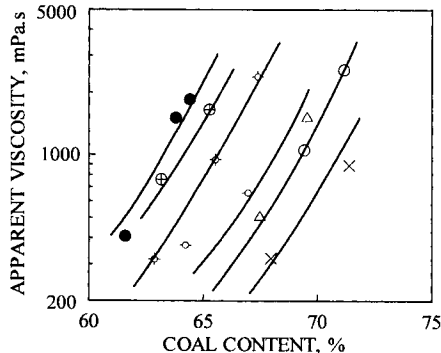
Fig. 10.27. Relation between apparent viscosity and coal content in CWS for different coals. Non-ionic additive 1% on dry coal basis. (After Seki et al. [42].)
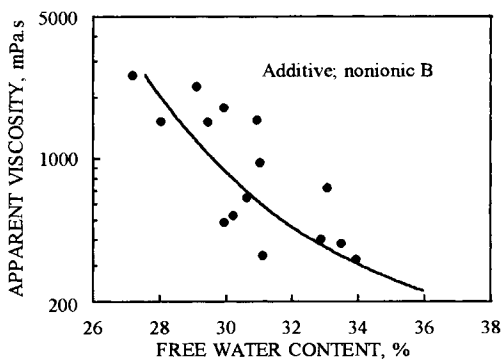
Fig. 10.28. Relation between apparent viscosity and free water content in the tested CWS. Non-ionic additive 1% on dry coal basis. (After Seki et al. [42].)
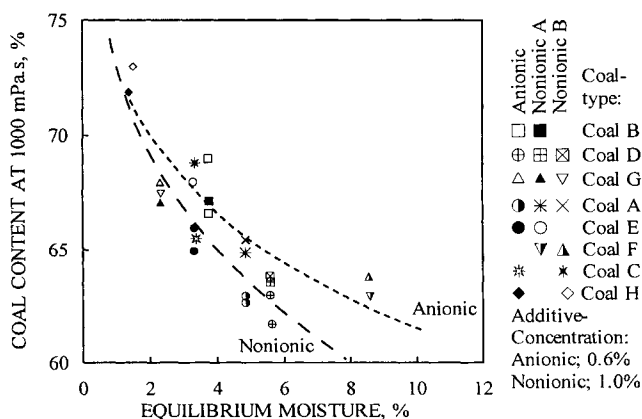
Fig. 10.29. Relation between coal content in CWS at 1000 mPa s and coal equilibrium moisture. (After Seki et al. [42].)

that is, with decreasing solids content. The coal content in the coal–water slurries at an apparent viscosity of 1000 mPa s is plotted in Fig. 10.29; the two curves were obtained with non-ionic and anionic dispersants.

As these results demonstrate, the rheological properties of coal–water slurries prepared from different coals characterized by similar RRB particle size distributions can clearly be correlated with the coal moisture content. Schwartz' results [44] entirely support these conclusions. The relationship between the CWS viscosity and coal moisture content can be used to estimate the slurryability (maximum coal content in the CWS) at an acceptable viscosity.

Higashitani et al.'s results [45] confirmed these correlations further. Fig. 10.30 shows the relationship between reduced slurry viscosity (η/η^*) and reduced coal concentration (C_c/C_c^*), where η^* is 0.5 Pa s and C_c^* is C_c at $\eta = \eta^*$. A very good correlation obtained for different tested coal samples implies that C_c^* is an appropriate parameter for evaluating the effect of coal properties on the CWS rheology. These results were
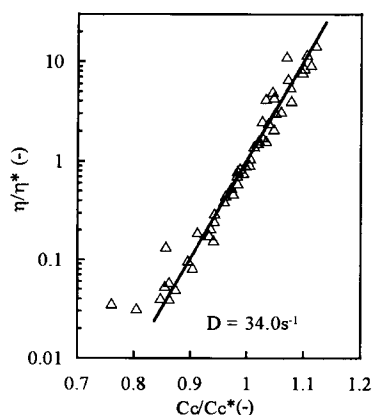
Fig. 10.30. Correlation between reduced apparent viscosity of CWS and reduced solid concentration for different coals. (After Higashitani et al. [45]; by permission of the Mining and Materials Processing Institute of Japan.)
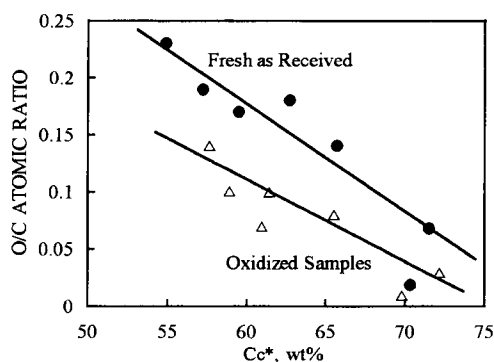
Fig. 10.31. Correlation between O/C ratio in the tested coals and C_c^*. Two different correlations were obtained for fresh coal samples and oxidized samples. (After Higashitani et al. [45]; by permission of the Mining and Materials Processing Institute of Japan.)

obtained for the coal–water slurries prepared from the coal samples that contained 70% of a −200 mesh size fraction and 30% of a −50 +200 mesh fraction. The anionic surfactant, a sodium salt of naphthalene formaldehyde sulfonate with a molecular weight of 2750, was utilized in all the tests.

Fig. 10.31 shows the correlation between the O/C ratio in the tested coals and C_c^*. These correlations are quite good but they are different for the original coal samples (dots) and the oxidized samples (circles). These samples were oxidized in air at 120°C for either 10 or 30 days. However, all the data points converge on a single straight line when plotted versus equilibrium moisture content (Fig. 10.32), hence giving credence to Seki et al.'s correlation (Fig. 10.29).

It is of interest to inspect the relationship between the sedimentation volume and C_c^* (Fig. 10.33) that was also provided by Higashitani et al. [45]. The sedimentation volume was evaluated by the ratio, V_s, of original to final sediment height in 50 cm³ cylinders
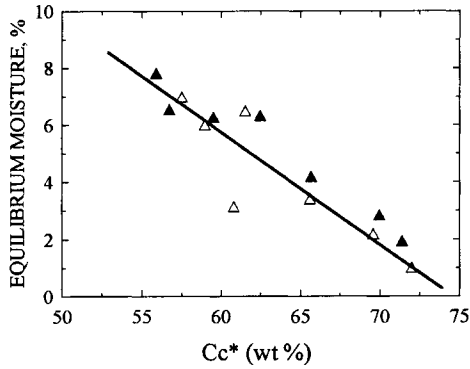
Fig. 10.32. Correlation between C_c^* and coal moisture content for CWS prepared from different fresh and oxidized coal samples. (After Higashitani et al. [45]; by permission of the Mining and Materials Processing Institute of Japan.)
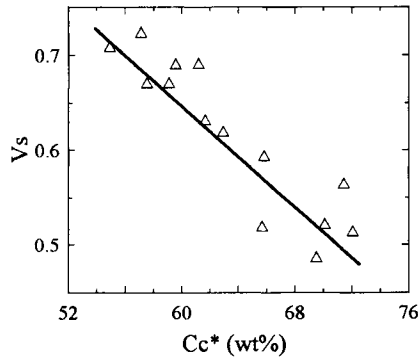
Fig. 10.33. Correlation between coal concentration in CWS at $\eta' = 0.5$ Pa s and sediment volume ratio, V_s. (After Hihashitani et al. [45]; by permission of the Mining and Materials Processing Institute of Japan.)

after 7 days at 30°C. Since the sediment volume depends directly on aggregation of the particles (see Fig. 10.33), a good correlation between the sediment volume and C_c^* suggests that the CWS loading limit (slurryability) is determined by the aggregation degree of coal particles. The maximum loading of those slurries in which coal particles aggregate are not high and this is indicative of the role the particle–particle interactions play in determining the properties of coal–water slurries.

The limiting solids content is commonly referred to as "slurryability". Dooher et al. [46] defined slurryability as follows:

$$S_0 = \frac{\phi_m^{exp}}{\phi_m^{th}} \tag{10.11}$$

where S_0 is the slurryability, ϕ_m^{exp} is the maximum volume concentration of coal in a slurry that would yield a rheologically acceptable slurry at a typical pumping shear rate of 100 s^{-1}, and ϕ_m^{th} is the maximum volume of coal particles, treated as a distribution of spheres with diameters equal to the particle size distribution of a specific coal feed.

As a point of reference for non-interacting glass beads, $S_0 = 1$. Due to interparticle interactions, for coal, $S_0 < 1$. This again points to particle–particle interactions which, depending on the particle surface properties and liquid phase composition, may lead to aggregation, as a very important parameter.

10.4.4. Additives in the preparation of CWS

Coal–water slurries must be pumpable and this requirement translates into sufficiently low viscosity. But coal–water slurries may be stored in tanks over a long period of time, and thus they must also exhibit sufficient sedimentation stability. Different additives are commonly required to reduce viscosity and to increase stability. Fig. 10.34, reproduced from Atlas et al. [47], will be used here to discuss these effects further.

First, it must be borne in mind that the properties of coal–water slurries are very different from the properties of the disperse systems commonly dealt with by colloid chemistry. The most obvious difference is the solids content. While in a very dilute disperse system any aggregation between particles results in a loss of stability and fast sedimentation, in a heavily loaded suspension the aggregation may prevent particles from settling and so it may stabilize the system. But aggregation creates a network of interacting particles and this will sharply increase viscosity. Therefore, it is obvious that particles in CWS must be properly dispersed to reduce viscosity, and to increase
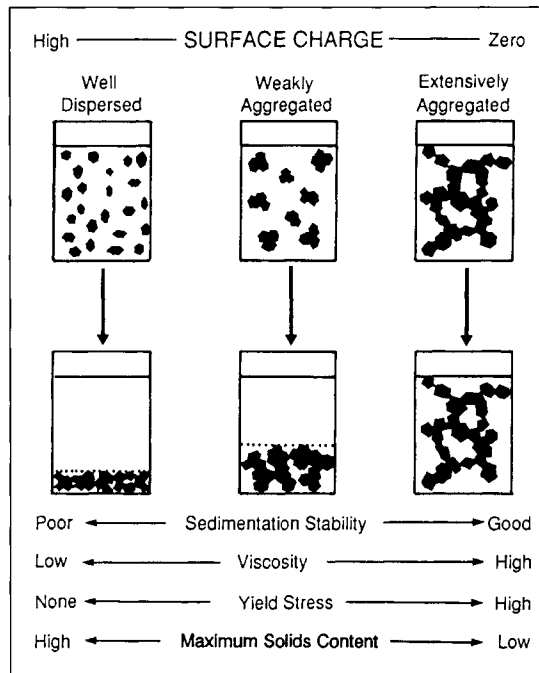
Fig. 10.34. Illustration of concentrated suspensions showing that at a given solids content the volume of sediment depends on particle aggregation. (After Laskowski and Parfitt [47]; by permission of Marcel Dekker Inc.)

the maximum packing density. Dispersants are used for this reason. But since CWS must also be stable, some weak aggregation will also be required, and this is achieved with the use of polyelectrolytes. While the addition of the later is needed to improve sedimentation stability, it may also increase the viscosity.

10.4.4.1. Dispersants

As discussed in Chapter 3, coal is a highly heterogeneous solid. It can be visualized as a hydrophobic matrix, whose wettability varies with coal rank, with some hydrophilic sites spread on it (Fig. 3.1). It is likely that the adsorbed surfactant molecules such as ethoxylated nonyl phenol orient at a coal–water interface as shown in Fig. 10.35 [48]. At low concentrations the molecules of this compound adsorb with polyethylene oxide (PEO) chains on the hydrophilic sites of the coal surface, leaving the hydrophobic alkyl chains pointing towards the bulk solution. This initially increases coal hydrophobicity as seen in Fig. 10.36 [48]. As this figure reveals, the values of the absolute shear modulus (viscoelastic measurements) increase for low surfactant concentrations corresponding to about one third of the saturation adsorption; this is likely due to aggregation of the coal particles. Further surfactant adsorption occurs with the alkyl groups on the hydrophobic positions of the particle surface, and may lead to multilayer adsorption (see also [49]). At this point the surface becomes hydrophilic, which is essential for preventing initially hydrophobic particles from aggregation. Apparently it is not enough to provide some amount of lubricating water to reduce the viscosity of coal concentrated suspension; this water can form stable layers separating coal particles only if these particles are sufficiently hydrophilic. Before discussing it further let us first point out that the results of Fig. 10.36 are perfectly in line with Chander et al.'s [50] data shown in Fig. 10.37. These results explain why
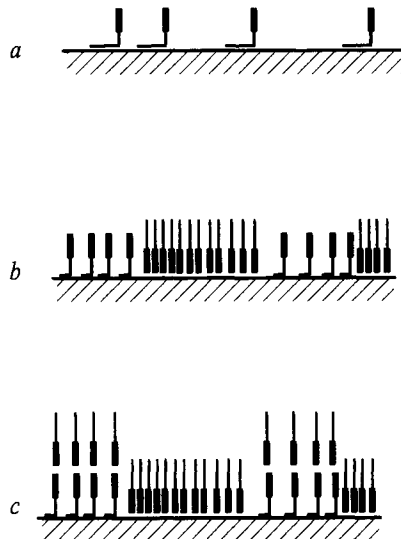
Fig. 10.35. Schematic diagram of the effect of concentration on adsorption on a non-ionic dispersant on a coal surface. (After Taylor et al. [48]; by permission of Elsevier Science.)
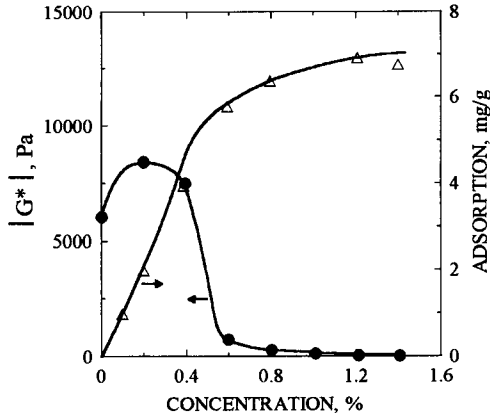
Fig. 10.36. Effect of concentration of non-ionic ethoxylated surfactant on adsorption on coal, and absolute shear modulus ($|G^*|$ at $v = 0.1$ Hz). (After Taylor et al. [48]; by permission of Elsevier Science.)
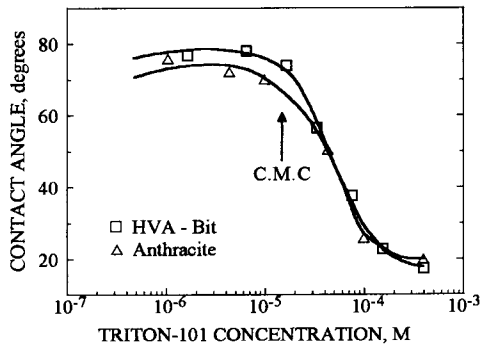
Fig. 10.37. Wettability of high-volatile bituminous coal and anthracite in aqueous solutions of Triton N-101. After Chander et al. [50]; by permission of Elsevier Science.)

low concentration of some surfactants may be beneficial in flotation, whereas high concentrations are required when surfactants are used as viscosity reducers in CWS technology.

Fig. 10.38 depicts the effect of surfactant concentration on the viscosity of the coal–water slurry [45]. Viscosity is clearly reduced but only at high concentrations of the dispersant. Obviously, there exists a critical concentration above which the viscosity cannot be reduced further. This implies, as pointed out by Higashitani et al. [45], that the saturated adsorption of the dispersant is a necessary condition for reaching low viscosity and this is perfectly in line with Figs. 10.35–10.37.

As discussed in Section 5.3.6, humic acids impart to a coal surface properties that are similar to those of low-rank coals (see Figs. 5.50 and 5.51). In Fig. 10.39, advancing and receding contact angles on two different coals are plotted against humic acid concentration [51]. Since humic acids are anionic polyelectrolytes that contain both carboxylic and phenolic groups, coal acquires negative electrical charge in their
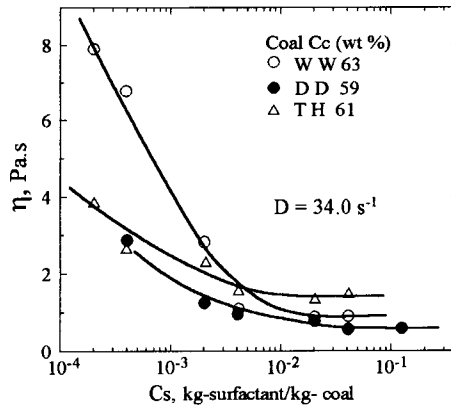
Fig. 10.38. Effect of concentration of sodium salt of naphthalene formaldehyde sulfonate on CWS apparent viscosity at 34 s^{-1}. Symbols WW, DD and TH stand for different coal samples. (After Higashitani et al. [45]; by permission of the Mining and Materials Processing Institute of Japan.)
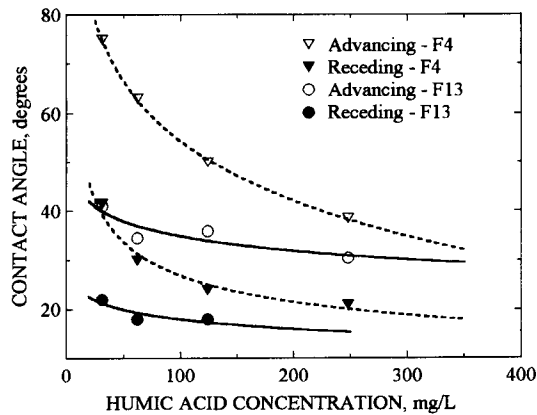
Fig. 10.39. Effect of humic acid concentration on advancing and receding contact angles on F-4 and F-13 bituminous coals. (After Pawlik et al. [51]; by permission of Gordon and Breach.)

presence (Fig. 10.40). In support of this concept it is worth recalling Fig. 3.2, which shows that bituminous coals are characterized by inherent hydrophobicity, and, as discussed in Section 9.3.1, strong hydrophobic interactions lead to coagulation of hydrophobic particles (see Figs. 9.13 and 9.14). In the presence of humic acids coal surfaces acquire negative electrical charge and are rendered hydrophilic; this should lead to the dispersion of coal suspensions. Fig. 10.41a shows the effect of solids content on the rheology of coal–water slurries prepared from the F-4 coal, and Fig. 10.41b shows the rheology of the same suspensions in the presence of humic acid (0.8%). While the rheological curves obtained without the addition of humic acids are very non-Newtonian and exhibit high yield stress values (Fig. 10.41a), the curves in Fig. 10.41b are nearly Newtonian. They do not exhibit any yield stress even at a very high solids content. The relationship between the yield stress and the contact angle values plotted versus humic
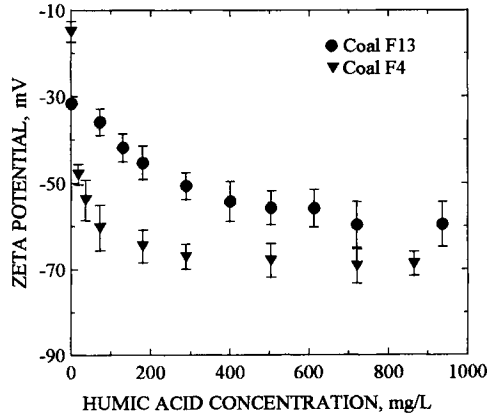
Fig. 10.40. Effect of humic acid on zeta potential of F-4 and F-13 coal samples; pH ranges: 5.8–7.8. (After Pawlik et al. [51]; by permission of Gordon and Breach.)
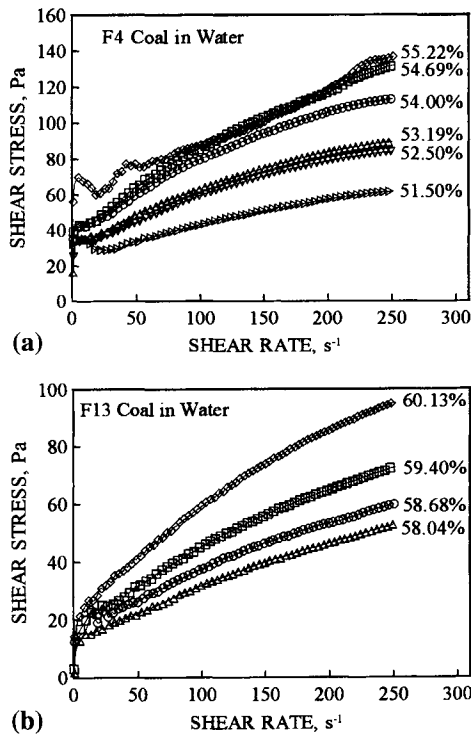
Fig. 10.41. Effect of coal content on rheological curves for CWS prepared from F-4 coal (a) and F-13 coal (b). Coal particle size distributions in terms of RRB are given by $d_{63.2} = 50$ μm and $m = 1.35$. (After Pawlik et al. [51]; by permission of Gordon and Breach.)
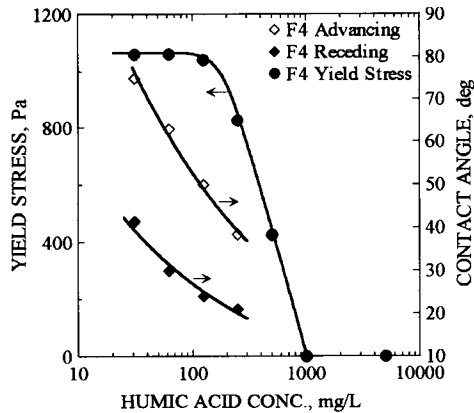
Fig. 10.42. Effect of humic acid on contact angles and on the yield stress of 65% (wt.) CWS prepared from F-4 coal. (After Pawlik and Laskowski [52]; by permission of Canadian Institute of Mining, Metallurgical and Petroleum Engineers.)

acid concentration, set out in Fig. 10.42 [52], illustrates these effects very clearly. In summary, this relationship is another way of showing the same effect which in Fig. 9.14 was characterized by the percentage of coagulating particles. Since coagulation occurs when attractive forces between particles prevail over repulsive forces, the aggregating particles form a network and this results in an increased yield stress on the rheological curve (see Fig. 9.13). Rheological measurements on coal–water slurries indicate that the likelihood of this type of aggregation in aqueous suspensions of fine coal is always substantial. Without additives, the apparent viscosity for a hydrophobic bituminous coal (F-4) measured at a shear rate of 100 s^{-1} reaches high values for relatively low coal content; much higher solids contents at the same viscosities can be achieved with the oxidized coal (F-13) (Fig. 10.43), and this is indicative of a higher degree of aggregation in the suspension of very hydrophobic particles. It is noteworthy that the viscosities plotted versus coal content converge on the same curve when humic acid is used as dispersant. The effect of humic acids on the rheology of a hydrophilic coal (Fig. 10.43) is insignificant since, due to oxidation, such a surface is already negatively charged and rich in humic acids. Interestingly, it has been reported that CWS produced from lower-rank coals may have acceptable viscosity even without any additives [38]. Grimanis and Breault [53] reported that the lower-rank CWS were inherently more stable. Wyodak, a low-rank subbituminous coal, required no dispersant at all.

Plots such as Fig. 10.43 are even more dramatic if the yield stress instead of viscosity is plotted versus solids content (Fig. 10.44). The Casson yield stress in Fig. 10.44 was calculated from the Casson equation:

$$\tau^{1/2} = \tau_c^{1/2} + (\eta_c D)^{1/2} \tag{10.12}$$

where τ is the shear stress at shear rate D, and τ_c and η_c are the Casson yield stress and Casson viscosity, respectively.

Fig. 10.42 provides a general explanation of the effect of the additives that are utilized to reduce CWS viscosity. Such additives operate by rendering coal particles hydrophilic.
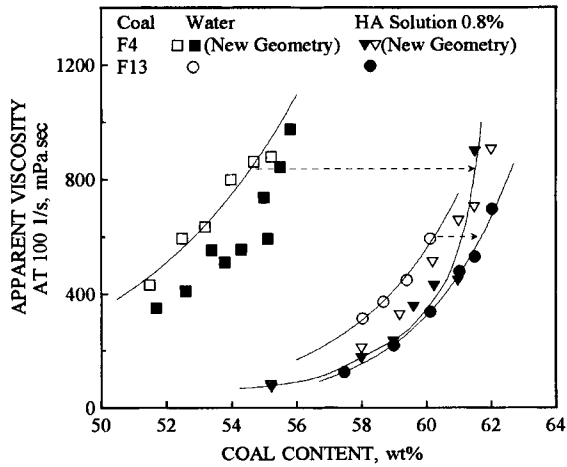
Fig. 10.43. Apparent viscosity of CWS at 100 s^{-1} for both water and 0.8% humic acid solution as a function of coal concentration. (After Pawlik et al. [51]; by permission of Gordon and Breach.)
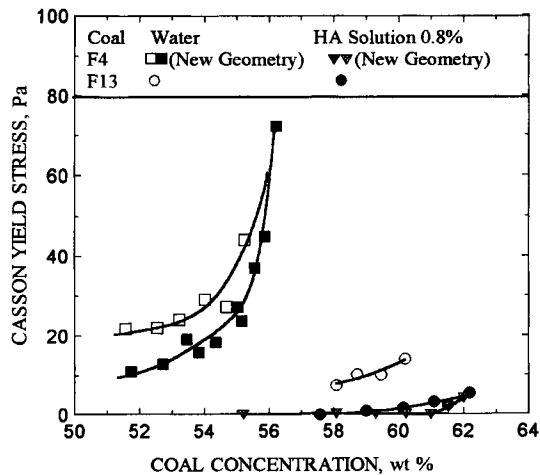
Fig. 10.44. Effect of coal content in CWS (as in Fig. 42) and humic acid on the Casson yield stress for F-4 and F-13 coals. (After Pawlik et al. [51]; by permission of Gordon and Breach.)

Since most naturally occurring particles are negatively charged in water, only non-ionic and anionic additives can be utilized (by neutralizing the charge, the cationic additives operate as coagulants). While the non-ionic additives can stabilize CWS only by steric effects, adsorption of an anionic additive also imparts negative charge to coal particles, and thus in such a case both electrostatic and steric stabilization can play a role.

Trochet-Mignard et al. [54] have systematically studied the effect of a series of non-ionic surfactants (Synperonic NPE) on rheology of CWS. The selected surfactants contained the same hydrophobic chain, nonyl phenol with 13 moles propylene oxide, and varying hydrophilic chain length. The hydrophilic polyoxyethylene (PEO) chain
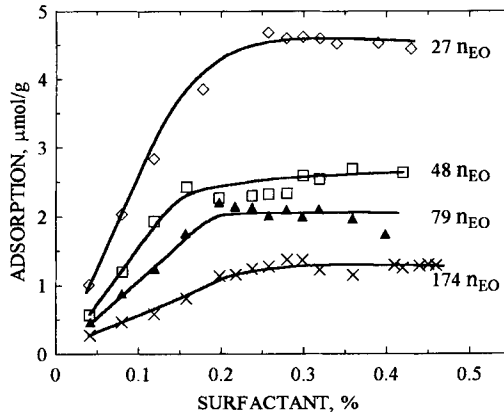
Fig. 10.45. Adsorption isotherms for Synperonic NPE surfactants onto coal. (After Trochet-Mignard et al. [54]; by permission of Elsevier Science.)

contained between 27 and 174 EO units. The adsorption results are shown in Fig. 10.45. The figure reveals a clear decrease in the adsorption values as the PEO chain length of the surfactant increases. In the absence of additives, viscoelastic measurements confirmed a rapid increase of the absolute shear modulus (G^*) as the volume fraction of coal exceeded 0.4. In the presence of surfactants, the increase in G^* occurred at higher ϕ values. A critical volume fraction, ϕ_{cr}, defined as the solid volume fraction at which there is a rapid increase in G^*, was the highest for the surfactant with 48 EO units per molecule. The authors postulated that while the surfactant containing the shortest PEO chain gave the highest adsorption value, and was probably the most strongly adsorbed, in this case the thickness of the adsorbed layer in the order of 6–7 nm was apparently not able to eliminate the attraction minimum on the energy–distance curve. With such a minimum, weak coagulation was likely to be significant. By increasing the PEO chain length to 48 units, the thickness of the adsorbed layer might increase sufficiently to cause a significant reduction in the minimum depth. A further increase in the PEO chain length to 79 and 174 units results in stronger chain–solvent interaction, thus weakening the adsorption of the molecules on the coal surface. These results indicate that to obtain maximum loading of CWS, one has to choose a surfactant molecule with optimum composition of hydrophilic and hydrophobic chains.

Tadros et al. [55] studied block copolymers of the ABA type. In such molecules the B chain should adsorb strongly onto the coal surface (anchoring chain) whereas the A chain(s) should be strongly hydrated in water. The studied Synperonic PE block copolymers contain PEO–PPO–PEO chains (PEO stands for ethylene oxide and PPO for propylene oxide chains, respectively). All four tested copolymers contained 55 propylene oxide units, and 4, 25, 37 or 147 EO groups. The efficiency of the tested compounds as viscosity-reducing additives for CWS prepared from a high-volatile A bituminous coal increased with increasing number of EO units in the molecule.

Yoshihara [56] studied various copolymers and found that the graft copolymers of polyacrylate with a side chain of polystyrenesulfonate (M.W. of 12,000) exhibit high

affinity towards the coal surface and good dispersing ability. Saeki et al. [57,58] claim that sodium salt of condensation product of formalin and naphthalene sulfonic acid with a molecular weight of 1000 was the most efficient dispersing agent for the upgraded low-rank Indonesian (Banjarsari) coal.

Sodium polystyrene sulfonate (PSS) has been commercially used in Japan as an additive in manufacturing CWS. The results of systematic tests with the use of PSS and NSF (sodium naphthalene sulfonate formaldehyde condensate) were published by Hara et al. [59]. The tests were carried out with bituminous coal that contained: 4.2% equilibrium moisture, 34.8% volatile matter and 8.6% ash, with the analytical content of carbon being 75.6% (dry ash-free basis). The tests revealed that PSS was a better dispersant from NSF. Minimum apparent viscosities (at 100 s^{-1}) were obtained at 0.4–0.5% addition of PSS and this corresponded well with the maximum effect of the additive on the zeta potential at this concentration. Fig. 10.46 shows the effect of PSS molecular weight on the apparent viscosity of the tested CWS. A clear minimum was observed at a molecular weight ranging from 15,000 to 20,000. Also, electrokinetic measurements plotted versus PSS molecular weight displayed maximum negative values in this molecular weight range. It is noteworthy that the adsorption of PSS increases with the molecular weight but this does not correlate well with the optimum viscosities around 15,000–20,000 molecular weight.

As summarized by Botsaris and Glazman [26], many different compounds were tested as additives to reduce CWS viscosity. Unfortunately, many reports did not provide sufficient detail to fully analyze these data. In general, the CWS stabilized with non-ionic additives are not sensitive to the concentration of electrolytes [60], but those stabilized with anionic additives are. However, the slurries stabilized by non-ionic
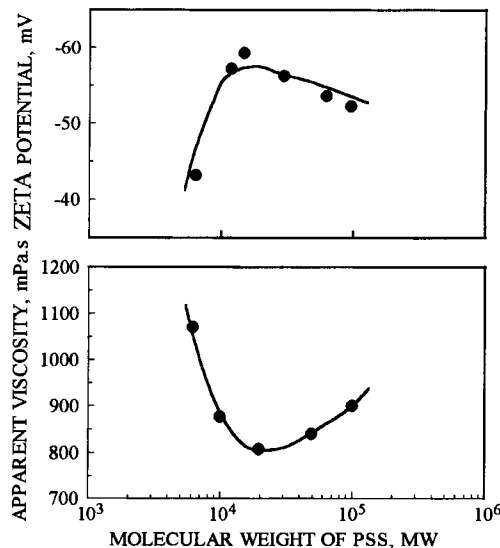
Fig. 10.46. Effect of molecular weight of sodium polystyrene sulfonate on zeta potential of coal particles and apparent viscosity of the tested CWS. (After Hara et al. [59].)

additives are sensitive to changes in temperature and may aggregate on increasing temperature.

10.4.4.2. Additives stabilizing against settling (anti-settling additives)

Coal–water slurries are made of relatively coarse particles. Such particles tend to settle under gravity and, when stabilized either sterically or electrostatically against aggregation, the repulsive forces allow them to roll over each other and form a compact sediment which may be difficult to redisperse. Since CWS can be stored in tanks over a considerable period of time, such a system must also be stabilized against settling. As Fig. 10.34 explains, this can be achieved by weak flocculation.

Fig. 10.47 shows the effect of the anti-settling additive on apparent rheology of CWS [61]. As shown, the sample that contains only the dispersing additive initially exhibits lower viscosity. However, this changes with the time of storage, and the sample that is also stabilized against settling finally exhibits lower viscosity.

Since CWS are very concentrated aqueous suspensions they are not transparent and this makes the use of simple optical methods to characterize CWS stability impossible.

Fig. 10.48 shows the rod penetration test setup described by Usui et al. [62]. This test is designed to find the layer of the compact sediment deposited at the bottom of the cylinder. The sensing device, a rod of 3 mm in diameter, has a small disc (10 mm in diameter and 1 mm thick) attached to the tip of the rod. The total weight of the rod is 30 g. The setup can be utilized to measure both the soft sediment and the hard sediment. The rod penetrates CWS at a speed of 12 mm/s and it stops when the tip gets in contact with the soft sediment. The device is switched on again after tapping the rod lightly with a finger and it stops when the tip gets in contact with the hard sediment. This, as discussed in Usui et al.'s paper [68], can be used to characterize the sedimentation stability of CWS by following the deposition of the sediment at the bottom of the measuring device. Some more sophisticated methods are also available [63,64].
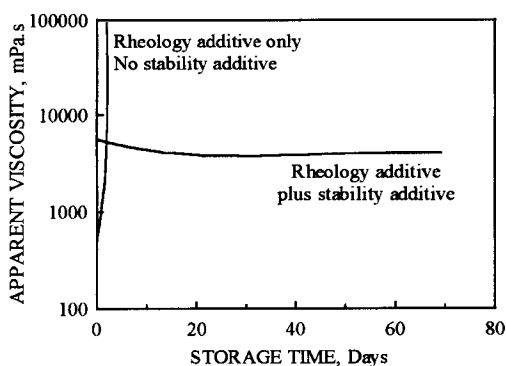
Fig. 10.47. Effect of storage time on properties of CWS prepared only with viscosity reducing additive (dispersant), or with both viscosity reducing and stabilizing additives. (After Pommier et al. [61]; by permission of the American Institute of Mining, Metallurgical and Petroleum Engineers.)
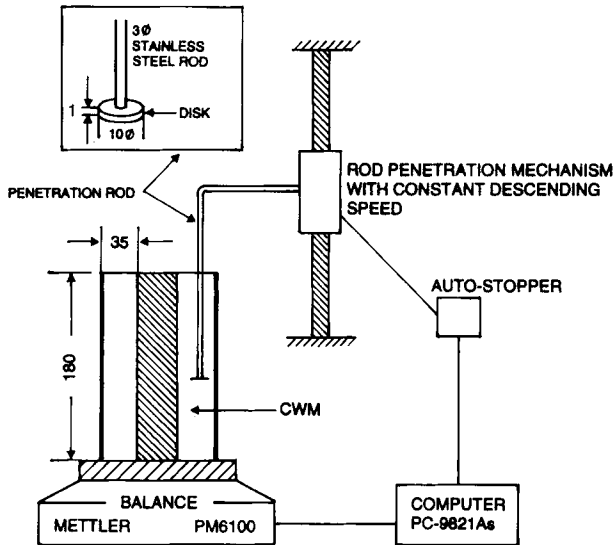
Fig. 10.48. Rod penetration test equipment. (After Usui et al. [62]; by permission of Gordon and Breach.)

Among the tested anti-settling additives guar gums were recognized as being very effective (e.g. Rhamsan gum S-194). These natural polysaccharides have a molecular weight in the range of a few million and they exhibit properties of weak flocculants.

10.4.5. CWS from low-rank coals

There are many deposits of subbituminous coals and lignites which can easily be recovered by strip mining. Very often these coals constitute a very attractive "clean" energy source as they may contain 0.2% sulfur and 8% ash (e.g. Alaskan low-rank coals). However, the high inherent moisture content of these coals and their low heating value on an "as mined" basis (that is a low specific energy) compromise the economics for rail haulage. Consequently, most low-rank coals are consumed by electric utilities located near mine sites.

In an effort to upgrade coal and produce a transportable fuel, several dewatering processes have been developed. Almost all of the coal inherent moisture content can be removed by thermal drying; the final moisture content achieved in the product is dependent on particle size and residence time. However, since low-rank coals depreciate due to shrinkage and loss of structural elasticity when they are dried in hot gases, the dried product is dusty and is subject to spontaneous combustion. When the dried coal is slurried in water, a significant portion of the coal moisture removed during drying is reabsorbed onto coal particles. Such slurries have only slightly higher energy densities than similar slurries made from raw coals, usually less than 11.6 MJ/kg [65]. To minimize moisture reabsorption, the dried coal can be coated with a fuel oil or can be briquetted.

A variety of methods of thermal dewatering of LRCs have been investigated by the University of North Dakota Energy Research Center [65–68] and at the Mineral

Industry Research Laboratory of the University of Alaska, Fairbanks [69]. A low-rank coal–water fuel plant with a capacity of 120 t/d, constructed at the University of Alaska, Fairbanks, is planned to start commercial-scale testing soon [70].

In a hydrothermal treatment, coal is subjected to a temperature of up to 400°C in the presence of water in an autoclave. When coal is heated, first it starts losing its volatile matter. In a hot-water drying process (HWD), coal is heated under pressure in water. Under such conditions, evolved tars remain on the coal surface and plug micropore entrances. For instance, the surface area of the Indian Head lignite after HWD decreased to 98 m²/g, almost half of the raw lignite [66]. It was found that the process temperature is the most important variable. The effect of particle size in the tested range from 6.4 down to 0.6 was insignificant. The results shown for a subbituminous coal C from No. 4 seam of Usibelli Coal Mine, Alaska, confirm the very strong effect of temperature on the process: equilibrium moisture content decreases from 25% down to 9.5%, and calorific value increases from 27.3 MJ/kg to almost 31 MJ/kg when the process temperature is increased from 275°C to 325°C [69] (Fig. 10.49). As these results clearly demonstrate, the treatment leads to the reduction of the oxygen content in coal (carbon content increases) and this translates into a more hydrophobic surface. Ohki et al. [71] used FTIR spectroscopy and in an elegant paper discussed their results obtained with an Indonesian low-rank coal, Adaro (proximate analysis: 16.42% moisture, 45.6% volatile matter,
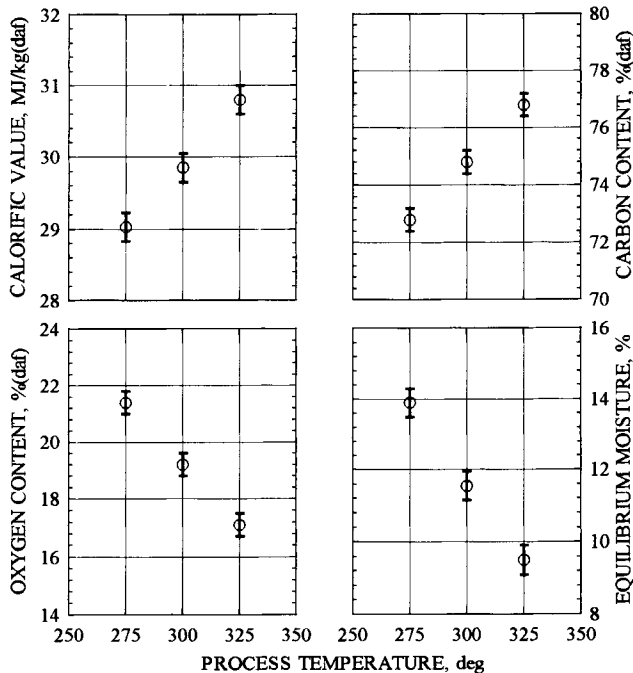
Fig. 10.49. Parameters of hot-water drying products versus process temperature. Data are mean values averaged over residence times and error bars represent the 95% family confidence intervals of the mean using the Benferroni method. (After Walsh et al. [69]; by permission of Gordon and Breach.)
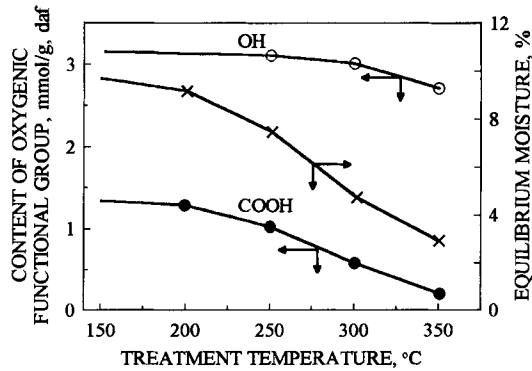
Fig. 10.50. Effect of process temperature on content of carboxylic and phenolic groups, and equilibrium moisture in the HWD products. (After Ohki et al. [71]; by permission of Gordon and Breach.)

1.24% ash, 36.74 fixed carbon on as-received basis). As Fig. 10.50 implies, the reduction of oxygen content in the LRC in the HWD process mostly results from a decomposition of carboxylic groups. Oxygen content reduction is concomitant to the equilibrium moisture content reduction and this translates into a more hydrophobic surface after the treatment. Since only low-rank coals have a significant amount of carboxylic groups, this also explains that this process is particularly appropriate for processing low-rank coals.

Fig. 10.51 illustrates the effect of hot-water drying on the rheological curves of coal–water slurries prepared from two lignites and one subbituminous coal [65] (the temperature was 430°C, the treatment was completed after 15 min). As seen, the 60% CWS loading was quite possible with the hydrothermally treated lignites. The authors also observed that the hot-water-dried lignite slurries showed natural stability with little or no settling after an extended period of time.
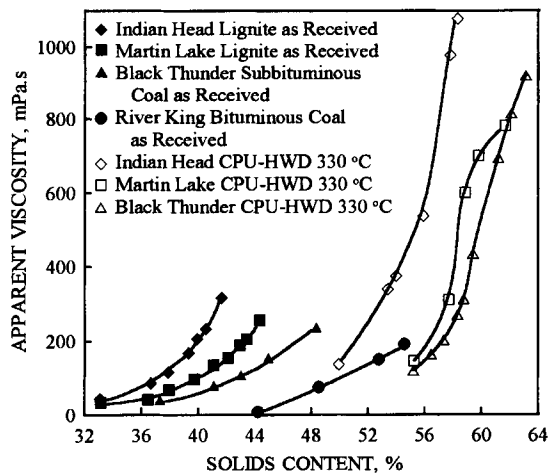
Fig. 10.51. Effect of hot-water drying (at 430°C for 15 min) on the rheological curves of CWS prepared from two lignites and one subbituminous coal. (After Potas et al. [65]; by permission Gordon and Breach.)
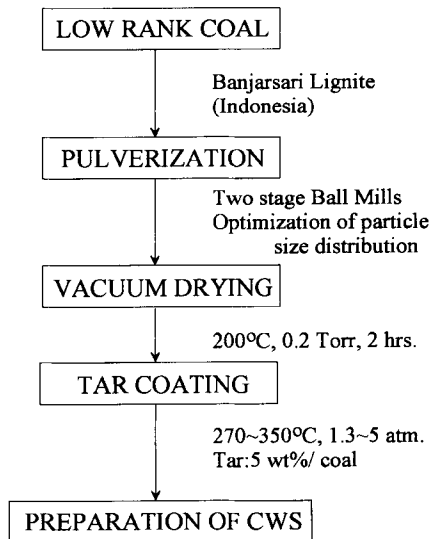
Fig. 10.52. Schematic flowsheet of the vacuum drying/tar coating upgrading process (After Usui et al. [73]; by permission of Gordon and Breach.)

Many deposits of low-rank coals with very low sulfur and ash contents are available in many parts of the world, and since the prices of these coals are much lower than those of bituminous coals, the coal–water slurry technology would be particularly attractive if such fuels could be prepared from low-rank coals. Usui et al. [72,73] developed a new technology in which a low-rank coal is first subjected to vacuum drying and then is coated with tar. A schematic flowsheet of the process is given in Fig. 10.52. Proximate analyses of the Banjarsari lignite from Indonesia are set out in Table 10.3. The raw coal contains 0.55% sulfur, and as shown in Table 10.3, 20.6% of moisture. The raw coal was pulverized in a two-stage grinding process in a ball mill. The coarser product from the first stage of grinding was mixed with the second-stage finer-grinding product at a ratio of 85% coarse to 15% of fines. In the vacuum drying

Table 10.3
Proximate and ultimate analyses of the Banjarsari coal prior to and after upgrading [73]

	Moisture (wt.%)	Ash (wt.%)	Volatile matter (wt.%)	Fixed carbon (wt.%)	Heating value (kcal/kg)	
Raw coal (as received)	20.6	5.8	38.2	35.4	4650	
Upgraded coal (air-dried base)	2.1	8.9	31.9	59.2	6380	
(Dry basis)	Carbon (wt.%)	Ash (wt.%)	Hydrogen (wt.%)	Oxygen (wt.%)	Nitrogen (wt.%)	Sulfur (wt.%)
Raw coal	63.5	7.4	4.1	23.3	1.1	0.55
Upgraded coal	70.7	8.9	3.6	15	1.3	0.48

stage the coal was heated up to 200°C while maintaining vacuum of 0.2 Torr. This was followed by an addition of 5% of tar (based on dry coal mass) and then it is heated up to 270–300°C at a rate of 5°C/min. During this stage the tar evaporates and coats dried coal particles. As Table 10.3 reveals, the Banjarsari lignite upgraded by this method contained only 2.1% moisture. The feasibility study showed that this method is economically viable and that it may further reduce the cost of the utilization of low-rank coals [73].

10.4.6. Effect of beneficiation on CWS

As discussed in Chapter 3, coal is a very heterogeneous organic rock in which organic matter has inclusions of mineral matter. Since mineral matter is hydrophilic, its removal in coal cleaning operations renders the cleaning product more hydrophobic. Hydrophobic particles suspended in water tend to aggregate due to hydrophobic attractive forces (see Section 9.3.1), and thus the product of the cleaning is even more likely to aggregate. Different beneficiation methods are used to clean coal. Very fine particles are cleaned by flotation. The reagents used in flotation make coal particles even more hydrophobic. Since the collectors utilized in coal flotation include oily hydrocarbons which are insoluble in water, the tendency of fine coal particles to aggregate is further augmented in the presence of such reagents (exactly the same additives are utilized in the oil agglomeration of fine coal). It is thus obvious that the fact that coal beneficiation produces a more homogeneous product with a lower content of inorganic impurities (ash), it has a positive effect on CWS preparation (of course, it also reduces the environmental impact of burning coal in power generating plants). However, producing coal that is "contaminated" with flotation reagents, and especially with oily hydrocarbons which tend to agglomerate fine coal particles, has a negative effect on CWS preparation [39]. As already discussed, the dispersing agents used to reduce the viscosity of CWS operate by making coal particles hydrophilic. Therefore, the presence of flotation collectors in the fine clean coal product that were used to make coal particles more hydrophobic must have some negative effect on CWS preparation. As a matter of fact this was observed by Walters [74]. Walters reported that while CWS could be prepared from raw coal using a less expensive anionic dispersant, non-ionic additives were necessary to prepare CWS from the flotation concentrate. This may result from the need to solubilize the oil droplets attached to the coal surface, and apparently non-ionic additives are more efficient at doing this.

One of the most important parameters that control the rheological properties of CWS is coal particle size distribution. Wang et al. [38] reported that Chinese experience showed that if a coal fines were unsuitable in its as-received form for CWS preparation, in most cases this was due to low content of ultra-fines. As discussed in Section 3.7, coarse coal particles start floating only when the fines are removed from the feed. It should then be possible to modify the fine-coal cleaning circuit as shown in Fig. 39 [39]. Such a circuit should provide the clean coal product with a bimodal particle size distribution that would be much more suitable for the preparation of CWS.

10.5. References

[1] D.G. Osborne, Coal Preparation Technology. Graham and Trotman, London, 1988, Vol. 1, Chapter 1.
[2] C.B. Reed, The Coal Era in the United States. Ann Arbor Science, 1981.
[3] P.F. Mako and W.A. Samuel, The Sasol approach to liquid fuels from coal via the Fischer–Tropsch reaction. In: R.A. Meyers (ed.), Handbook of Synfuels Technology. McGraw-Hill, New York, 1984, Chapter 2.
[4] G.S. Jones, Some solutions to the problem of handling wet coal fines. Proc. 11th Int. Coal Preparation Congr., Mining and Materials Processing Institute of Japan, Tokyo, 1990, pp. 1–12.
[5] G.J. Brown, D.S. Creasey and N.J. Miles, Coal handleability — a good or a bad coal? Particle–Particle Syst. Charact., 13 (1996) 260.
[6] D.W. Brown, Factors affecting the handleability of coals and its measurement. Coal Int. (July 1997) 147.
[7] F. Vickers, The treatment of fine coal. Colliery Guardian, 230 (1982) 359.
[8] D.W. Brown, B.P. Atkin, N.J. Miles and D.S. Creasey, Getting a handle on coal. Mine Quarry, 25 (8) (1996) 34.
[9] D.W. Brown, B.P. Atkin, N.J. Miles and D.S. Creasey, Determination of the handleability of a coal blend using an extrusion trough. Fuel, 76 (1997) 1183.
[10] D.W. Brown, Coal Handleability. SME Annual Meeting, Salt Lake City, March, 2000.
[11] J. Blondin, M. Girardeau and M. Nomine, Two simple tests for the assessment of wet fine coal handleability. In: R.R. Klimpel and P.T. Luckie (eds), Industrial Practice of Fine Coal Processing. SME, Littleton, CO, 1988, pp. 253–255.
[12] B.J. Arnold, C.D. Harrison and R.A. Lohnes, Coal handleability — addressing the concerns of the electric utility industry. Min. Eng. (Jan. 1992) 84.
[13] A. Barois-Cazenave, P. Marchal, V. Falk and L. Choplin, Experimental study of powder rheological behaviour. Powder Technol., 103 (1999) 58.
[14] T.K. Hunter, Real and apparent dewatering of mineral concentrates and tailings. In: P.A. Dowd (ed.), Mineral Processing in the United Kingdom. Inst. Miner. Metall., Leeds, 1989, pp. 207–223.
[15] G.M. Moody, Role of polyacrylamides and related products in treatment of mineral processing effluent. Trans. IMM, Sect. C, 99 (1990) C136.
[16] K. Masuda and H. Iwata, Dewatering of particulate materials utilizing highly water-absorptive polymer. Powder Technol., 63 (1990) 113.
[17] G.P.T. Dzinomwa and C.J. Wood, Superabsorbent polymers for the dewatering of fine coal. Proc. 7th Australian Coal Preparation Conf., Australian Coal Preparation Society, Mudgee, 1995, pp. 200–218.
[18] E.L. Fuller, Structure and chemistry of coals: calorimetric analyses. J. Coll. Interf. Sci., 5 (1980) 577.
[19] A.D. Walters, Joseph Conrad and the spontaneous combustion of coal, Part I. Coal Preparation, 17 (1996) 147.
[20] A.D. Walters, Joseph Conrad and the spontaneous combustion of coal, Part II. Coal Preparation, 17 (1996) 167.
[21] S.D. Barve and V. Mahadevan, Prediction of spontaneous heating liability of Indian coal based on proximate constituents. 12th Int. Coal Preparation Congress, Cracow, May, 1994.
[22] A.C. Smith and C.P. Lazzara, Spontaneous combustion studies of U.S. coals. U.S. Bureau of Mines Report RI 9079, 1994.
[23] N.T. Moxon and S.B. Richardson, Development of a calorimeter to measure the self-heating characteristics of coal. Coal Preparation, 2 (1985) 79.
[24] N.T. Moxon and S.B. Richardson, Development of a self heating index for coal. Coal Preparation, 2 (1985) 91.
[25] G. Papachristodoulou and O. Trass, Coal slurry fuel technology. Can. J. Chem. Eng., 65 (1987) 177.
[26] G.D. Botsaris and Y.M. Glazman, Stability and rheology of coal slurries. In: G.D. Botsaris and Y.M. Glazman (eds), Interfacial Phenomena in Coal Technology. Marcel Dekker, New York, 1989, pp. 199–277.
[27] V. Vand, Viscosity of solutions and suspensions, Part II. J. Phys. Coll. Chem., 52 (1948) 300.
[28] P.C. Hiemenz, Principles of Colloid and Surface Chemistry. Marcel Dekker, New York, 1977, Chapter 2.

[29] G.K. Batchelor, The effect of Brownian motion on the bulk stress in a suspension of spherical particles. J. Fluid Mech., 83 (1977) 97.

[30] W. Berghofer, Konsistenz und Schwertrubeaufbereitung. Bergbauwissenschaften, 6 (20) (1959) 493; 6 (22) (1959) 533.

[31] V. Fidleris and R.L. Whitmore, The physical interaction of spherical particles in suspensions. Rheol. Acta, 1 (1961) 573.

[32] R.J. Farris, Prediction of the viscosity of multimodal suspensions from unimodal viscosity data. Trans. Soc. Rheol., 12 (1968) 281.

[33] H.A. Barnes, J.F. Hutton and K. Walters, An Introduction to Rheology. Elsevier, Amsterdam, 1989.

[34] F. Ferrini, V. Battarra, E. Donati and C. Piccinini, Optimization of particle grading for high concentration coal slurry. 9th Int. Conf. Hydraulic Transport of Solids in Pipes, Rome, 1984, Paper B2.

[35] A.G. Chryss and S.N. Bhattacharya, Maximum packing concentration of coal water mixtures. Coal Preparation, 21 (1999) 83.

[36] H. Usui, Non-Newtonian viscosity of dense slurries prepared by non-spherical particles. 8th Nisshin Eng. Particle Technol. Int. Sem. Suspension Rheology, Fundamentals and Application to Industrial Processing, Kobe, December 5–7, 1999.

[37] Zhang Rong-Zeng, Zeng Fang, Hu Kun-Mu and Gao Ming-Qiu, Research on CWM preparation techniques with Chinese coals. Proc. 6th Int. Symp. Coal Slurry Combustion and Technology, Orlando, FL, 1984, pp. 234–239.

[38] Zuna Wang, Rongzeng Zhang, Zhiwei Jiang and Shixin Jiang, Preparation of coal–water fuels from coal preparation plant fines. In: J.J. Davis (ed.), Proceedings of the 6th Australian Coal Preparation Conference. Australian Coal Preparation Society, Mackay, 1993, pp. 418–427.

[39] J.S. Laskowski, Does it matter how coals are cleaned for CWS? Coal Preparation, 21 (1999) 105.

[40] R. Kaji, Y. Muranaka, K. Otsuka, Y. Hishinuma, T. Kawamura, M. Murata, Y. Takahashi, Y. Arikawa, H. Kikkawa, T. Igarashi and H. Higuchi, Effects of coal type, surfactant, and coal cleaning on the rheological properties of coal water mixture. Proc. 5th Int. Symp. Coal Slurry Combustion and Technology, Tampa, FL, 1983, Vol. 1, pp. 151–175.

[41] T. Igarashi, N. Kiso, Y. Hayasaki, T. Ogata, K. Fukuhara and S. Yamazaki, Effects of weathering of coals on slurryabilities. 6th Int. Symp. Coal Slurry Combustion and Technology, Orlando, FL, 1984, pp. 283–303.

[42] M. Seki, K. Kiyama and J. Nishino, Effects of coal property and additive on the rheological characteristics of coal–water mixtures. 7th Int. Symp. Coal Slurry Fuels Preparation and Utilization, New Orleans, 1985, pp. 136–145.

[43] G.D. Botsaris and K.N. Astill, Effect of the interaction between particles on the viscosity of coal–water slurries. 6th Int. Symp. Coal Slurry Combustion and Technology, Orlando, FL, 1984, pp. 304–312.

[44] E. Schwartz, K. Stork and S.C. Crema, Physical properties of coal surfaces and their interaction with stabilizers. Proc. 7th Int. Symp. Coal Slurry Fuels Preparation and Utilization, New Orleans, 1985, pp. 41–49.

[45] K. Higashitani, T. Umemoto, Y. Kashiwabara and H. Ito, Mechanism of viscosity reduction of highly loaded coal water slurry. Proc. 11th Int. Coal Preparation Congress, Mining and Materials Processing Institute of Japan, Tokyo, 1990, pp. 323–326.

[46] J. Dooher, N. Malicki, J. Trudden and W. Weber, Phenomenological modeling of the rheological properties of coal suspensions. Proc. 17th Int. Conf. Coal Utilization and Slurry Technologies, Clearwater, 1992, pp. 49–58.

[47] J.S. Laskowski and G.D. Parfitt, Electrokinetics of coal–water suspensions. In: G.D. Botsaris and Y.M. Glazman (eds), Interfacial Phenomena in Coal Technology. Marcel Dekker, New York, 1989, p. 322.

[48] P. Taylor, W. Liang, G. Bognolo and Th.F. Tadros, Concentrated coal–water suspensions containing non-ionic surfactants and polyelectrolytes. Coll. Surf., 61 (1991) 147.

[49] J.S. Clunie and B.Y. Ingram, Adsorption of nonionic surfactants. In: G.D. Parfitt and C.H. Rochester (eds), Adsorption from Solution at the Solid/Liquid Interface. Academic Press, Orlando, FL, 1983, pp. 105–152.

[50] S. Chander, B.R. Mohal and F.F. Aplan, Wetting behavior of coal in the presence of some nonionic surfactants. Coll. Surf., 26 (1987) 205.

[51] M. Pawlik, J.S. Laskowski and H. Liu, Effect of humic acids and coal surface properties on rheology of coal–water slurries. Coal Preparation, 18 (1997) 129.

[52] M. Pawlik and J.S. Laskowski, Evaluation of flocculants and dispersants through rheological tests. In: J.S. Laskowski (ed.), Polymers in Mineral Processing. Proc. 3rd UBC-McGill Int. Symp., Metall. Soc. CIM, Montreal, 1999, pp. 541–556.

[53] M.P. Grimanis and R.W. Breault, Effect of coal type and beneficiation process on storage and handling. Proc. 17th Int. Conf. Coal Utilization and Slurry Technology, Clearwater, 1992, pp. 19–30.

[54] L. Trochet-Mignard, P. Taylor, G. Bognolo and Th.F. Tadros, Concentrated coal–water suspensions containing nonionic surfactants and polyelectrolytes, Part 2. Coll. Surf., 95 (1995) 37.

[55] Th.F. Tadros, P. Taylor and G. Bognolo, Influence of addition of a polyelectrolyte, nonionic polymers, and their mixtures on the rheology of coal/water suspensions. Langmuir, 11 (1995) 4678.

[56] H. Yoshihara, Graft copolymers as dispersants for CWM. Coal Preparation, 21 (1999) 93.

[57] T. Saeki, T. Tatsukawa and H. Usui, Preparation techniques of coal water mixtures with upgraded low rank coals. Coal Preparation, 21 (1999) 161.

[58] T. Saeki, S. Yamamoto and M. Ogawa, Dispersing and stabilizing additives for coal water mixtures with an upgraded low rank coal. In: J.S. Laskowski (ed.), Polymers in Mineral Processing. Proc. 3rd UBC-McGill Int. Symp., Metall. Soc. CIM, Montreal, 1999, pp. 557–577.

[59] S. Hara, H. Arai, H. Sugawara, T. Ukigai, E. Yoshida and J. Ogawa, Development of additives for concentrated coal–water mixture. Proc. 17th Int. Conf. Coal Utilization and Slurry Technologies, Clearwater, 1992, pp. 71–82.

[60] R. Kaji, Y. Muranaka, K. Otsuka and Y. Hishinuma, Effect of ions on the rheology of CWM. Proc. 7th Int. Symp. Coal Slurry Fuels Preparation and Utilization, New Orleans, 1985, pp. 16–23.

[61] L. Pommier, T. Frankiewicz and W. Weissberger, Coal water slurry fuels — an overview. Miner. Metall. Process., 1 (1984) 62.

[62] H. Usui, T. Saeki, K. Hayashi and T. Tamura, Sedimentation stability and rheology of coal water slurries. Coal Preparation, 18 (1997) 201.

[63] A.M. Al Taweel, H.A. Farag, O. Fadaly and G.D.M. Mackay, A method for determining the settling behavior of dense suspensions. Can. J. Chem. Eng., 61 (1983) 534.

[64] S.J.R. Simons, R.A. Williams and C.G. Xie, A sedimentation analyser suitable for opaque dispersions. In: R.A. Williams and N.C. de Jaeger (eds), Advances in Measurements and Control of Colloid Processes. Butterworths, London, 1991, pp. 107–121.

[65] T.A. Potas, R.E. Sears, D.J. Maas, G.G. Baker and W.G. Willson, Preparation of hydrothermally treated LRC/water fuel slurries. Chem. Eng. Commun., 44 (1986) 133.

[66] W.G. Willson, S.A. Farnum, G.G. Baker and G.H. Quentin, Low-rank coal slurries for gasification. Fuel Process. Technol., 15 (1987) 157.

[67] G.A. Wiltsee, D.J. Maas, T.K. Hammond and R.M. Goodman, Low-rank coal/water fuels. 3rd USA–Korea Joint Workshop Coal Utilization Technology, Pittsburgh, PA, Oct. 1986.

[68] P.D. Rao, D.E. Walsh, W.G. Willson and Y.L. Li, Dehydration of Alaska's low-rank coals by hydrothermal treatment. Miner. Metall. Process., 9 (1992) 41.

[69] D.E. Walsh, H.C. Owens and P.D. Rao, A study of non-evaporative hot water drying of an Alaskan low-rank coal. Coal Preparation, 13 (1993) 115.

[70] N. Hashimoto, CWM: its past, present and future. Coal Preparation, 21 (1999) 3.

[71] A. Ohki, X.F. Xie, T. Nakajima, T. Itahara and S. Maeda, Change in properties and combustion characteristics of an Indonesian low-rank coal due to hydrothermal treatment. Coal Preparation, 21 (1999) 23.

[72] H. Usui, T. Tatsukawa, T. Saeki and K. Katagiri, Rheology of low rank coal slurries prepared by an upgrading process. Coal Preparation, 18 (1997) 119.

[73] H. Usui, T. Tatsukawa, T. Saeki and K. Katagiri, Upgrading of low rank coal by a combined process of vacuum drying and tar coating. Coal Preparation, 21 (1999) 71.

[74] A. Walters, Chemical effects of beneficiation on coal–water fuel properties. Proc. 8th Int. Symp. Coal Slurry Fuels Preparation and Utilization, Orlando, FL, 1986, pp. 222–225.

This Page Intentionally Left Blank

Appendix

Graphical symbols used in this book in drawing coal
preparation plant flowsheets (IOO 561)
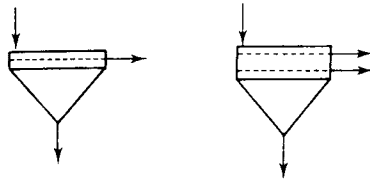
Single-deck and double-deck vibrating screens
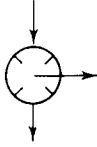
Bradford breaker

Classifying cyclone

a *or* *b*
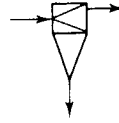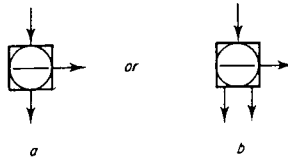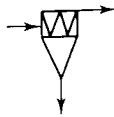
Dense-medium bath

Dense-medium cyclone
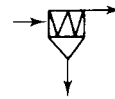
Water-only cyclone
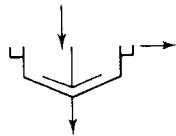
Thickener

Pump sump

Spiral

Concentrating table

a   b

Jig

a   b
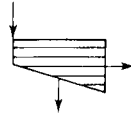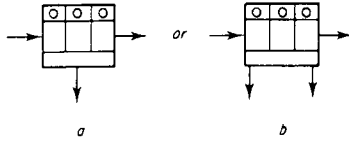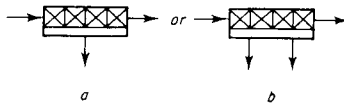
Froth flotation cells
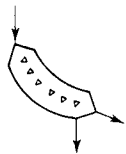
Sieve bend
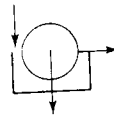
Vacuum drum filter

This Page Intentionally Left Blank

Subject Index

ERRATUM

Page 5, line 15 from bottom, not "41 Pa·s" but "1 Pa·s"

Page 32, equation 3.2 should read:

$$W_{SL} = W_{SL}^{LW} + W_{SL}^{AB}$$

and equation 3.3:

$$W_{SL}^{LW} = W_{SL}^{d} = 2(\gamma_{l}^{d} + \gamma_{s}^{d})^{1/2}$$

Page 181, line 11 from bottom: "... droplet in water (through water) are plotted..." should read "...droplet in water (see caption of Fig. 6.1 for explanation) are plotted..."

Page 188, caption of Fig. 6.7, it should read "Recovery without collector (■), recovery with collector (●)."

Page 246, line 5, not "positive" but "negative bias".

This Page Intentionally Left Blank